UNIVERSITATEA
DE MEDICINĂ ȘI FARMACIE
„VICTOR BABEȘ“ DIN TIMIȘOARA

NANOAPPLICATIONS IN DENTAL MEDICINE

Tareq Hajaj, Andreea Codruța Novac, Carina Sonia Neagu, Ioana Moldovan, Daria Negruț, Florina Titihazan, Flavius-Didier-François Miron, Borislav Dușan Caplar, Marius Mihai Țogoe, Cristian Zaharia, Emanuela Lidia Petrescu, Daniela Maria Pop, Meda-Lavinia Negruțiu, Mihai Romînu, Iulian Vasile Antoniac, Cosmin Sinescu

HIPPOCRATE

Editura „Victor Babeş”

Timişoara, 2024

Editura „Victor Babeş”

Piaţa Eftimie Murgu nr. 2, cam. 316, 300041 Timişoara

Tel./Fax 0256 495 210

e-mail: evb@umft.ro

www.umft.ro/ro/organizare-evb/

Director general: Prof. univ. dr. Sorin Ursoniu

Colecţia: HIPPOCRATE

Referent ştiinţific: Prof. univ. dr. Andrei Motoc

© 2024 Toate drepturile asupra acestei ediţii sunt rezervate.

Reproducerea parţială sau integrală a textului, pe orice suport, fără acordul scris al autorilor este interzisă şi se va sancţiona conform legilor în vigoare.

ISBN 978-606-786-381-9

Table of contents

1. General Knowledge of Nanomedicine 15

1.1. Short History 15

1.2. Nanomedicine: Principles, Properties, and Regulatory Issues 15

1.2.1. Definition 15

1.2.2. Size 16

1.2.3. Particle Size Distribution 17

1.2.4. Surface Area 17

1.2.5. Dynamic Behavior of Nanomaterials and Applications in Nanomedicine 17

1.2.6. Physicochemical Characterization 18

1.2.6.1. Counting Methods 19

1.2.6.2. Fractionation Methods 19

1.2.6.3. Ensemble Methods 19

1.2.6.4. Integral Methods 19

1.2.6.5. Process Control—Understanding the Critical Manufacturing Steps 19

1.2.6.6. Biocompatibility and Nanotoxicology 21

1.2.6.7. Evaluation Methods 21

1.2.6.8. Nanotoxicological Classification System 22

1.2.6.9. Scale-Up and Reproducibility 24

1.3. Nanomedicines and Nanosimilars 24

1.4. Market Access and Pharmacoeconomics 25

1.5. Conclusion and Prospects 25

1.6. Quiz 1 27

References 29

2. Nanorobotic Systems for Therapeutic and Diagnostic Applications 30

2.1. Concept of Controlled Drug Delivery Systems 31

2.2. Overview of the MRI Drug Delivery System Architecture 32

2.2.1. Nanocapsule 33

2.2.1.1. The nanocarrier. 33

2.2.1.2. Magnetic nanoparticles as actuating elements 34

2.2.1.3. Area Surface functionalization as a sensing element 34

2.2.1.4. Drug molecules 34

2.2.2. MRI Propulsion System 34

2.2.2.1. Main magnet 34

2.2.2.2. Gradient coils 34

2.2.2.3. Radio frequency coils 34

2.2.2.4. Computer system 34

2.2.3. MRI Tracking Unit 35

2.2.4. System Controller 35
2.2.4.1. Real-time navigation algorithm 35
2.2.4.2. Graphical user interface 35
2.3. Nanocarrier Technologies 35
2.3.1. Liposome Nanoparticles 36
2.3.2. Copolymer Micelles 36
2.3.3. Quantum Dots 37
2.3.4. Metallic Nanoshells 37
2.3.5. Gold Nanoparticles 38
2.3.6. Carbon Nanotubes 39
2.4. Nanoparticle Functionalization for sensing purpose 39
2.4.1. Targeting Mechanisms: Functionalization with Biomolecules to Increase Specificity 39
2.4.2. Mechanism of Evading Recognition by the Reticuloendothelial System: Functionalization of Nanocarriers with Copolymers for Enhanced Biodistribution 39
2.4.3. Triggered-Release Mechanisms: Functionalization of Nanocarriers with Copolymers Containing Stimuli-Responsive Functionalities 39
2.5. MRI-Based Propulsion, Tracking and Control 40
2.5.1. Magnetic Propulsion and Steering 40
2.5.2. Imaging and Tracking in MRI Scanners 42
2.6. Discussion 43
2.7. Conclusions 44
2.8. Quiz 2. 45
References 47
3. Applications of nanotechnology in dental medicine 49
3.1. Novel nanomaterials 49
3.1.1. Nanocomposites 50
3.1.2. Nanofilled Resin-modified Glass Ionomer 50
3.1.3. Nanosolution 50
3.1.4. Nano-optimized Moldable Ceramics 50
3.1.5. Impression Material 51
3.2. Dental Biomimetics 51
3.3. Nanorobotics - Local Anesthesia 51
3.4. Dental Hypersensitivity 52
3.5. Orthodontic Treatment 52
3.6. Nanorobotic Dentifrice (Dentifrobots) 53
3.7. Nanoencapsulation 53
3.8. Materials to induce Bone Growth 54
3.9. Nanoneedles 54
3.10. Nanotweezers 54

3.11. Nanomaterials for Periodontal Drug Delivery **54**
3.12. Photodynamic Therapy **55**
3.13. Implants **55**
3.14. Nanomaterials for Healing of Wounds **55**
3.15. Bionic Mandible **55**
3.13. Safety Aspects of Nanotechnology **56**
3.14. Conclusion **56**
3.15. Quiz 3. **58**
References **60**
4. Nanotechnology in dental materials **61**
4.1. Nanoparticles **61**
4.1.1. Metallic Nanoparticles **61**
4.1.1.1. Silver Nanoparticles (AgNPs) **61**
4.1.1.2. Gold Nanoparticles (AuNPs) **62**
4.1.1.3. Copper Nanoparticles (CuNPs) **62**
4.1.2. Metal Oxide Nanoparticles **62**
4.1.2.1. Zinc Oxide Nanoparticles (ZnO NPs) **62**
4.1.2.2. Titanium Dioxide-Based Nanoparticles (TiO_2NPs) **63**
4.1.2.3. Zirconium dioxide Nanoparticles (ZrO_2NPs) **63**
4.1.2.4. Aluminium Oxide Nanoparticles (Al_2O_3 NP) **63**
4.1.2.5. Silicon dioxide Nanoparticles (SiO_2 NPs) **64**
4.1.3 Unconventional Nanoparticles in Dentistry **64**
4.1.3.1. Nano Diamonds **64**
4.1.3.2. Quantum Dots **64**
4.1.3.3. NanoShells **65**
4.1.3.4. Quaternary ammonium methacrylate (QAM) Nanoparticles **65**
4.1.3.5. Quaternary ammonium polyethyleneimine (QPEI) Nano-particles **65**
4.1.3.6. Amorphous Calcium Phosphate Nanoparticles (ACPNP) **65**
4.2. Nanotube Based Nanomaterials **65**
4.2.1. Carbon Nano-tube (CNT) **65**
4.2.2. Halloysite Nano-tube (HNT) **66**
4.3. Nanoplatelets based nanomaterials **66**
4.3.1. Graphene oxide nanoplatelets **66**
4.4. The toxicity aspect of nanomaterials in dentistry **66**
4.5. Dental Materials **67**
4.5.1. Adhesives **72**
4.6. Conclusion **74**
4.7. Quiz 4. **75**
References **77**

5. Nanotechnology in Prosthodontics **81**
5.1. 3D-Printed Nanocomposite Denture-Base Resins **82**
5.1.1. Effect of ZrO_2 Nanoparticles on the Mechanical and Surface Properties In Vitro **82**
5.1.1.1. Nanocomposites Mixture Preparation **83**
5.1.1.2. Specimen's Preparation **83**
5.1.1.3. Results **84**
5.1.1.4. Discussions **87**
5.1.1.5. Conclusions **88**
5.1.2. The effect of incorporating TiO_2 nanoparticles on the growth of Candida albicans **89**
5.1.2.1. Resin Material and TiO_2 NPs **89**
5.1.2.2. Cells Cultures Preparations **90**
5.1.2.3. Results **91**
5.1.2.4. Conclusions **93**
5.1.3 Unconventional Nanoparticles in Dentistry Assessment of the mechanical properties of PMMA/Silica/Zirconia. Nanocomposite as a denture base material **93**
5.1.3.1. Materials and Methods **94**
5.1.3.2. Results **95**
5.1.3.3. Conclusions **96**
5.2. Characterization of dental prosthesis based on nano-fluorapatite glass-ceramic fabricated by shell sintering technology **96**
5.2.1. Introduction **96**
5.2.2. Materials and Methods **99**
5.2.3. Results and Discussions **102**
5.2.4. Conclusions **107**
5.3. Reduced wear of enamel with novel fine and nano-scale leucite glass-ceramics **107**
5.3.1. Introduction **107**
5.3.2. Materials and Methods **108**
5.3.3. Results **109**
5.3.4. Discussions **109**
5.3.5. Conclusions **111**
5.4. Evaluation of shear bond strength of a novel nano-zirconia and veneering ceramics **112**
5.4.1. Experimental procedure **112**
5.4.2. Conclusions **114**
5.5. Quiz 5. **115**
References **117**
6. Nanotechnology in Tissular Engineering **119**
6.1. Nanohydroxyapatite in dentistry: A comprehensive review **119**
6.1.1. Applications of Nanohydroxyapatite in dentistry **119**
6.1.1.1. Implantology **120**

6.1.1.2. Bleaching and dentinal hypersensitivity 121
6.1.1.3. Nano-hydroxyapatite in dental caries prevention 121
6.1.1.4. Nanohydroxyapatite in Glass Ionomer Cement (GIC) 123
6.1.1.5. Nanohydroxyapatite in dental composite 123
6.1.1.6. Application of Nanohydroxyapatite in orthodontics 123
6.1.1.7. Nanohydroxyapatite in Periodontal Tissue Regeneration 124
6.2. Scaffold design and stem cells for tooth regeneration 124
6.2.1. Introduction 125
6.2.2. Scaffolds for teeth tissue engineering: Biological polymer scaffolds 126
6.2.2.1. Collagen 127
6.2.2.2. Chitosan 128
6.2.2.3. Silk protein 128
6.2.2.4. Alginate 129
6.2.2.5. Hyaluronic acid and its derivatives 130
6.2.2.6. Peptide 130
6.2.3. Scaffolds for teeth tissue engineering: Ceramic Scaffolds 130
6.3. New technology in scaffold processing 131
6.3.1. Electrospinning technique 131
6.3.2. Rapid prototyping technology 132
6.3.3. Supercritical fluid-gassing process 134
6.3.4. Self-assembling technology 135
6.3.5. Artificial polymer scaffolds 135
6.4. Challenges in optimizing 3D scaffold for dentin-pulp complex regeneration 136
6.4.1. Introduction 137
6.4.2. Materials and Methods 137
6.4.3. Results 139
6.4.4. Discussions 145
6.5. New Challenges and Prospective Applications of Three-Dimensional Bioactive Polymeric Hydrogels in Oral and Craniofacial Tissue Engineering 147
6.5.1. Bio Scaffolds for Dental and Osseous Tissue Engineering 148
6.5.2. Pre-Requisites of Hydrogels for Dental and Osseous Regeneration 149
6.5.2.1. Cytotoxicity 150
6.5.2.2. Biological Responses 150
6.5.2.3. Mechanical Characteristics 151
6.5.2.4. Degradation 151
6.5.3. Classification of Hydrogels 151
6.5.4. Chemical Structure of Polymeric Hydrogels 152
6.5.4.1. Natural Polymers 152
6.5.4.2. Synthetic Polymers 159

6.5.4.3. Hybrid Polymeric Hydrogels 162
6.6. Application of dental stem cells in three-dimensional tissue regeneration 165
6.6.1. DPSCs (dental pulp stem cells) 169
6.6.2. SHED (stem cells from human exfoliated deciduous teeth) cells 170
6.6.3. PDLSCs (periodontal ligament stem cells) 170
6.6.4. SCAP (stem cells from apical papilla) 171
6.6.5. Dental Follicle Progenitor Cells (DFPCs) 172
6.6.6. CLINICAL APPLICATIONS OF DENTAL STEM CELLS 172
6.7. Resorbable Membranes for Guided Bone Regeneration: Critical Features, Potentials, and Limitations 172
6.7.1. Barrier Membranes 175
6.7.2. Natural Resorbable Membranes 176
6.7.2.1. Collagen 177
6.7.2.2. Chitosan 180
6.7.2.3. Silk Fibroin 181
6.7.3. Synthetic Resorbable Membranes 182
6.7.3.1. PLA 182
6.7.3.2. PGA 184
6.7.3.3. PLGA 184
6.7.3.4. PDO 185
6.7.3.5. PCL 186
6.7.3.6. PEG 187
6.7.4. Bioactive Composite Membranes 187
6.7.4.1. Biocompatibility 188
6.7.4.2. Mechanical Stability 189
6.7.5. Antibacterial Activity 195
6.7.6. Cell Proliferation Enhancement 197
6.8. Quiz 6. 201
References 203
7. Nanotechnology in Orthodontics 204
7.1. Orthodontic Elastomeric Ligatures 204
7.2. Orthodontic Power Chains 205
7.3. Orthodontic Bands 205
7.4. Orthodontic Miniscrews 206
7.5. Prevention of Dental Caries and Control of Oral Biofilm 207
7.6. Coated Orthodontic Archwires 208
7.7. Nanomaterials Application in Orthodontics 208
7.7.1. Nano-Coatings in Orthodontic Archwires 209
7.7.1.1. Nano Coatings Reducing Friction on Orthodontic Archwires 209

7.7.1.2. Delivering Nanoparticles from an Elastomeric Ligature 210
7.7.1.3. Shape Memory Polymers (SMP) in Orthodontics 210
7.7.1.4. Control of Oral Biofilms during Orthodontic Treatment 210
7.7.2. Bracket Materials 211
7.7.3. Nanomaterials in Orthodontics 214
7.7.3.1. Silver Nanoparticles (AgNPs) Coating 215
7.7.3.2. Chitosan 216
7.7.3.3. Copper Oxide 216
7.7.3.4. Nitrogen-Doped Titanium Dioxide (N-Doped TiO2) Brackets 217
7.7.3.5. Zinc Oxide (ZnO) 217
7.7.4. Relationship between the Orthodontic Arch and Bracket Materials 217
7.7.5. Microbial Colonization Associated with Different Kinds of FOAs. 218
7.7.6. Introduction of Nanofillers or NP (Silver, TiO2) to Orthodontic Adhesives 219
7.7.7. Nanomaterials in Orthodontics and Their Use in the Nearest Future 220
7.7.8. Materials in Orthodontics and Their Use in the Nearest Future 220
7.7.9. Conclusions 221
7.8. Quiz 7. 222
References 224
8. Nanoparticles for Oral Cancer Diagnosis and Therapy 225
8.1. Liposomes for Oral Cancer Diagnosis and Therapy 226
8.1.1. Liposomes for Oral Cancer Diagnosis 226
8.1.2. Liposomes for Oral Cancer Therapy 227
8.2. Dendrimers for Oral Cancer Diagnosis and Therapy 228
8.2.1. Dendrimers for Oral Cancer Diagnosis 229
8.2.2. Dendrimers for Oral Cancer Therapy 230
8.3. Orthodontic Miniscrews Gold Nanoparticles for Oral Cancer Diagnosis and Therapy 230
8.3.1. Gold Nanoparticles for Oral Cancer Diagnosis 231
8.3.2. Gold Nanoparticles for Oral Cancer Therapy 232
8.4. Magnetic Nanoparticles for Oral Cancer Diagnosis and Therapy 233
8.4.1. Magnetic Nanoparticles for Oral Cancer Diagnosis 234
8.4.2. Magnetic Nanoparticles for Oral Cancer Therapy 234
8.5. Quantum Dots for Oral Cancer Diagnosis and Therapy 235
8.5.1. Quantum Dots for Oral Cancer Diagnosis 235
8.5.2. Quantum Dots for Oral Cancer Therapy 237
8.6. Polymeric Nanoparticles for Oral Cancer Diagnosis and Therapy 237
8.6.1. Polymeric Nanoparticles for Oral Cancer Diagnosis 238
8.6.2. Polymeric Nanoparticles for Oral Cancer Therapy 239
8.7. Other Nanoparticles 240
8.8. Conclusions 240

8.9. Nanotechnology in Oral Cavity Carcinoma: Recent Trends and Treatment Opportunities 241
8.9.1. Cancer Nanotechnology 241
8.9.2. Diagnostic Procedures 242
8.9.3. Treatment Opportunities 244
8.9.3.1. Ongoing Clinical Trials 245
8.9.3.2. Sentinel Lymph Node Analysis 245
8.9.3.3. Photodynamic Therapy 248
8.9.4. Conclusions 250
8.9.5. Direction for Future Research 250
8.10. Quiz 8. 252
References 254
9. Nanodiagnostic 257
9.1. Nanotechnology in diagnosis of a number of diseases 257
9.1.1. Detection of disease genes 260
9.1.2. Detection of single nucleotide polymorphisms 260
9.1.2.1. Glucose monitoring in vivo by nanosensors 260
9.1.2.2. Nanotechnology and Diagnosis of infectious disease 261
9.1.2.3. Diagnosis of tuberculosis based on BioMEMS 261
9.1.2.4. Nanotechnology and cardiovascular diseases 262
9.1.3. Nanotechnology for clinical laboratory diagnostics – salient points 262
9.1.4. Insight of nano diagnostics 263
9.2. Outlook of various diagnostics and nanodiagnostic techniques for COVID-19 263
9.2.1. Introduction 264
9.2.2. Diagnostic techniques for COVID-19 266
9.2.2.1. Reverse-transcription polymerase chain reaction (RT-PCR) 266
9.2.2.2. Chest computerized tomography scan (CT scan) 267
9.2.2.3. X-ray imaging 268
9.2.2.4. Magnetic resonance imaging (MRI) scanning 268
9.2.2.5. Genome sequencing 268
9.2.2.6. Microarray technique 269
9.2.2.7. Biosensors 269
9.2.2.7.1. Clustered regularly interspaced short palindromic repeats (CRISPR)-based devices 270
9.2.2.7.2. Lateral flow assay/immunoassay (LFA/LFIA) 270
9.2.2.7.3. Enzyme-linked immunosorbent assay (ELISA) 271
9.2.2.7.4. Other biosensors 273
9.2.2.8.1. Loop-mediated isothermal amplification (LAMP) 273
9.2.2.8.2. Rolling circle amplification (RCA) 274
9.2.2.8.3. Circle-to-circle amplification (C2CA) 275

9.2.2.9. Intelligence-based techniques 276
9.2.3. Nanodiagnostic techniques for COVID-19 detection 276
9.2.3.1. Nanosensors 277
9.2.3.2. Nanodiagnostic-based LFA devices for COVID-19 279
9.2.3.3. Advantages and disadvantages of nanodiagnostic devices 280
9.2.4. Future perspectives 280
9.3. Quiz 9. 282
References 284
10. Nanoapplications in endodontics 285
10.1.1. Introduction 285
10.1.2. Antibacterial Nanoparticles 285
10.1.3. Bacterial Biofilms as the Therapeutic Target for Antimicrobials 286
10.1.3.1. Endodontic Biofilms 288
10.1.4. Antimicrobials in Root Canal Therapy 288
10.1.5. Classification and Types of Antibacterial Nanoparticles 289
10.1.5.1. Chitosan Nanoparticles 291
10.1.5.2. Bioactive Glass Nanoparticles 291
10.1.5.3. Silver Nanoparticles 293
10.1.5.4. Nanoparticle-Incorporated Root Canal Sealers 294
10.1.5.5. Nanoparticle Functionalization 295
10.1.5.6. Nanoparticle Modification for Antimicrobial Photodynamic Therapy 297
10.1.6. Concluding Remarks 297
10.1.7. Photodynamic therapy 298
10.2. Nanomaterials in endodontic instruments 298
10.3. Root canal sealers 298
10.4. Pulp repair and regeneration 299
10.4.1. Organic nanoparticles 300
10.4.1.1. Graphene 300
10.4.1.2. Chitosan Nanoparticles (Cs-NPs) 300
10.4.1.3. Poly (lactic) co-glycolic acid (PLGA) 301
10.4.2. Non-organic nanoparticles 301
10.4.2.1. Bioactive glass 301
10.4.2.2. Mesoporous calcium silicate 301
10.4.2.3. Hydroxyapatite nanoparticles 302
10.4.3. Metal nanoparticles 302
10.4.3.1. Silver nanoparticles (AgNP's) 302
10.4.3.2. Silica nanoparticles 303
10.4.4. Metal oxide nanoparticles 303
10.4.4.1. Iron compound (FeOx) 303

10.4.4.2. Magnesium halogen-containing nanoparticles 304
10.4.4.3. Zinc oxide nanoparticles (ZnONP) 304
10.4.4.4. Magnesium oxide and Calcium oxide (MgO and CaO) nanoparticles 304
10.4.4.5. Cuprum oxide (CuO) nanoparticles 304
10.4.4.6. Titanium dioxide (TiO2) nanoparticles 305
10.4.5. Possible perils of endodontic nanotechnology 305
10.5. Conclusions 305
10.6. Quiz 10 306
References 308
11. Nanoapplications in Preventive Dentistry 312
11.1. Repair of enamel by using hydroxyapatite nanoparticles as the building blocks 312
11.1.1. Results and discussion 313
11.1.2. Conclusions 315
11.2. Dentin Remineralization 316
11.3. Enamel Remineralization 321
11.4. Recent Advances in Dental Hard Tissue Remineralization 331
11.4.1. Fluoride 332
11.4.2. Fluoride-containing Dentifrices 333
11.4.3. Calcium Phosphate Compounds 333
11.4.4. β-TCP 333
11.4.5. Functionalized TCP 334
11.4.6. Dicalcium Phosphate Dihydrate (DCPD) 334
11.4.7. ACP 334
11.4.8. ACP-filled Composites 335
11.4.9. CPP–ACP 335
11.4.10. Bioactive Materials 335
11.4.11. 45S5 BG 336
11.4.12. Nanomaterials 336
11.4.13. Calcium Fluoride Nanoparticles 336
11.4.14. Calcium Phosphate-based Nanomaterials 336
11.4.15. β-TCP (Ca3(PO4)2) 336
11.4.16. NanoHAP Particles 337
11.4.17. ACP Nanoparticles 337
11.4.18. Nanobioactive Glass Materials 338
11.4.19. Xylitol 338
11.4.20. Biomimetic Remineralization of the Dentin and Enamel 338
11.4.21. Polydopamines 338
11.4.22. PA 339
11.4.23. Self-assembling Peptide 339

11.4.24. Electric Field-induced Remineralization 339
11.4.25. Polyamide 339
11.4.26. Theobromine 340
11.4.27. Arginine Bicarbonate 340
11.4.28. Conclusion 340
11.5. Dental plaque-inspired versatile nanosystem for caries prevention and tooth restoration 341
11.5.1. Introduction 341
11.5.2. Process description 342
11.5.2.1. Synthesis of polymer nanocarriers 343
11.5.2.2. Characterization of polymers 344
11.5.2.3. In vitro drug loading and release 345
11.5.2.4. Adsorbability of PMs@NaF-SAP on human enamel samples 345
11.5.2.5. In vitro antibacterial and antibiofilm experiments 346
11.5.2.6. PMs@NaF-SAP demineralization and remineralization assay 347
11.5.2.7. Cytotoxicity assay in vitro 347
11.5.2.8. In vivo study 348
11.5.3. Conclusions 351
11.6. Quiz 11. 354
References 356
12. Nanoapplications in Odontotheraphy 358
12.1. Nanoparticles in Glass Ionomer Materials 358
12.1.1. Experimental Materials 359
12.1.2. Commercial Alternatives 359
12.2. Application of Nanoparticles in Resin-Based Materials 361
12.2.1. Dentin Bonding Systems 361
12.2.2. Restorative Composite Resins, Sealants and Luting Systems 364
12.2.2.1. Commercial Alternatives 365
12.2.3. Indirect Restorative Systems 365
12.3. Dental Adhesive Interfaces Reinforced with Magnetic Nanoparticles 366
12.3.1. Materials and Methods 366
12.3.2. Results 369
12.3.2.1. Optical Microscopy Analysis 369
12.3.2.2. Micro-CT Analysis 370
12.3.3. Conclusions 374
12.4. Quiz 12. 376
References 378
13. Nanoapplications in Periodontal Management 384
13.1. Periodontal disease and their pathogenesis 385
13.2. Current biological approaches for periodontal therapy 386

13.3. The role of biomaterials in periodontal therapy and regeneration 388
13.4. Advanced biomaterials developed for periodontal disease treatment 388
13.4.1. Hydrogels 390
13.4.1.1. Natural Hydrogels 391
13.4.1.2. Synthetic hydrogels 391
13. 4.2. Micro/nanoparticles 392
13.4.3. Films 393
13.4.4. Micro/nanofibers 393
13.5. Biological properties of purpose-driven biomaterials 394
13.5.1. Biocompatibility and biodegradability 394
13.5.2. Immunogenicity 394
13.6. Clinical strategies using purpose-driven biomaterials 395
13.6.1. Injectable delivery 395
13.6.2. Delivery with solid scaffolds 396
13.7. Challenges and future prospects 397
13.8. Quiz 13. 399
References 401
14. Nanorobots in Medicine and Dentistry 402
14.1. Multiple fabrication techniques for micro/nanorobots 403
14.2. Smart motion control and intelligent collective behavior of micro/nanorobots 405
14.2. 1. Designs of collective behavior of micro/nanorobots 405
14.3. Applications of collective behavior of micro/nanorobots 408
14.4. Advanced function integration of micro/nanorobots 410
14.5. Cell-level biomedical applications of micro/nanorobots 411
14.6. Dental Applications 412
14.6.1. Maintenance of Oral Hygiene 413
14.6.2. Cavity Preparations and Restorations 414
14.6.3. Mobile Nanobots for Prevention of Root Canal Treatment Failure 415
14.7. Quiz 14. 423
References 425

1. General Knowledge of Nanomedicine

The concept of nanoparticles in biomedicine first appeared in literature in the late 1970s, leading to the publication of over 10,000 papers each year on the topic. However, the specific term "Nanomedicine" did not come into common usage until the beginning of the 21st century. By 2005, there were still less than 30 published papers that used this term. A notable surge in interest occurred over the following decade, with the Web of Science cataloging more than 1,000 articles on Nanomedicine in 2015 alone. This marked a tenfold increase in research output compared to earlier years, which featured significantly fewer studies on the use of nanoparticles in medical applications.

1.1. Short History

The European Science Foundation's forward Look Nanomedicine defines Nanomedicine as the utilization of nano-sized tools for disease diagnosis, prevention, and treatment, aiming to enhance our understanding of the complex pathophysiology of diseases with the ultimate goal of improving quality of life [1]. This interdisciplinary field encompasses three main areas of nanotechnology: drug delivery, imaging agents and diagnosis. It utilizes nanoparticles in the 1–1000 nm range, bioships produced through both "top-down" and "bottom-up" approaches, and polymer therapeutics [2, 3]. The relatively new term "theragnostic" refers to the combined application of diagnostics and therapy using the same nanopharmaceutical [4, 5].

Nanomedicine's historical roots can be traced back to the use of colloidal gold in ancient times [6, 7]. Modern foundations of the field were laid by pioneers such as Metchnikov and Ehrlich, who were awarded the Nobel Prize for Medicine in 1908 for their groundbreaking work on phagocytosis [8] and specific cell diagnostics and therapy [9], respectively. The last three decades of the 20th century marked significant advancements in Nanomedicine, characterized by the development of liposomes [10, 11], DNA-drug complexes [12], polymer-drug conjugates [13], antibody-drug conjugates [14], polymer nanocapsules [15, 16, 17], polymer-protein conjugates [18], albumin-drug conjugates [19], block-copolymer micelles [20], anti-arthritis gold nanoparticles [21], and anti-microbial silver nanoparticles [22]. These innovations have been crucial in enhancing the solubility of drugs in aqueous solutions, directing drugs to specific targets, and controlling the timing and rate of drug release [23].

One of the primary challenges faced is the non-specificity and poor water solubility of most drugs. Nanocarriers have been engineered to address these issues by first solubilizing drugs in aqueous media, serving as nanovectors, and controlling drug release. Although many nanocarriers facilitate oral drug delivery, their ability to translocate across barriers, such as the gastrointestinal tract, lung, and blood-brain barriers, is often limited, resulting in a transfer of less than 1% of the drug to the target organ [24, 25]. Consequently, there is an ongoing need for improvement.

The development of nanovector-drug assemblies is focused on optimizing the benefit/risk ratio, requiring extensive assessment through prolonged in vitro and in vivo studies, along with numerous clinical trials [26, 27]. Detailed characterization of nanomaterials is essential for conducting biological assays. These evaluations include investigations into antigenicity, immunotoxicity, complement activation, as well as studies on pharmacokinetics, biodistribution, and the rates of drug release [28].

1.2. Nanomedicine: Principles, Properties, and Regulatory Issues

1.2.1. Definition

Under the European Commission's recommendation, a nanomaterial is identified as natural, incidental, or manufactured material containing particles, whether unbound or aggregated, with at least one external dimension in the 1–100 nm range for a minimum of 50% of the particles, based on number size distribution. This threshold may adjust to between 1 and 50% under specific concerns related to environmental, health, safety, or competitiveness. Additionally, structures like fullerenes, graphene flakes, and single-wall carbon nanotubes with dimensions below 1 nm, or materials with a surface area over 60 m^2/cm^3, are classified as nanomaterials (Commission Recommendation, 2011). This definition is pivotal within the EU's legislative and regulatory frameworks, guiding the development of drug products.

The European Medicines Agency (EMA) describes nanomedicines as intentionally engineered systems for clinical use, with at least one component at the nanoscale. These systems should have reproducible properties and features designed specifically for their intended nanotechnological application, including administration route and dosage, to harness the clinical benefits of nano-engineering like targeted organ/tissue distribution (Ossa, 2014).

Conversely, the Food and Drug Administration (FDA) in the U.S. has not defined terms such as "nanotechnology," "nanomaterial," or "nanoscale." Instead, it aligns with broader material engineering definitions, considering materials with at least one dimension between approximately 1 nm to 100 nm as nanoscale. The FDA emphasizes that the evaluation of nanotechnology products should account for unique properties and behaviors that could impact safety, effectiveness, and public health, reflecting the current scientific and technical understanding of these materials (Guidance for Industry, FDA, 2014). Key indicators for identifying nanomaterials include size, particle size distribution (PSD), and surface area (Commission Recommendation, 2011; Bleeker et al., 2013; Boverhof et al., 2015).

1.2.2. Size

The crucial factor to consider when defining nanomaterials is their size, as it is applicable across a broad range of materials. Traditionally, the size range falls between 1 to 100 nm. However, setting a definitive limit is challenging, as there is no distinct boundary at 100 nm where the physicochemical and biological characteristics of materials undergo an abrupt change. It has been acknowledged that additional properties beyond size should be factored into the classification of a substance as a nanomaterial (Lövestam et al., 2010; Commission Recommendation, 2011; Bleeker et al., 2013; Boverhof et al., 2015). In pharmaceutical manufacturing, nanomaterials are typically created using either a top-down or bottom-up approach. The top-down method involves breaking down a bulk material into smaller pieces or forms using mechanical or chemical means. On the other hand, the bottom-up method begins at the atomic or molecular level, where precursor particles grow in size through chemical reactions (Luther, 2004; Oberdörster, 2010; Boverhof et al., 2015). These methodologies result in the formation of various particle types, including primary particles, aggregates, and agglomerates, as illustrated in Figure 1.1.

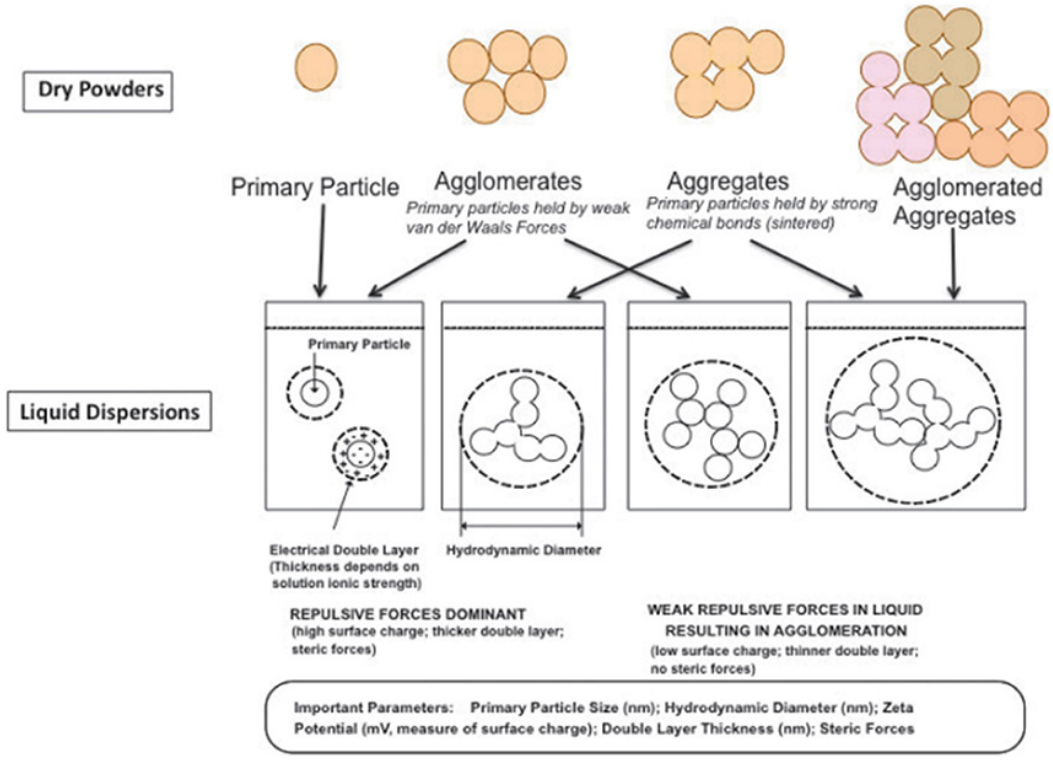


Figure 1.1. A schematic representation of the different particle forms encountered in nanomaterial manufacturing: primary particles, aggregates, and agglomerates, offering a visual distinction between these forms [1].

The respective definitions are as follows (sic):

- A "particle" is defined as a small piece of matter with clear physical boundaries (Oberdörster, 2010; Commission Recommendation, 2011).
- An "aggregate" is a particle made up of strongly bound or fused particles, with an external surface area that may be smaller than the combined surface areas of the individual particles (Oberdörster, 2010; Commission Recommendation, 2011).

- An "agglomerate" consists of loosely bound particles or aggregates, where the total external surface area is roughly equivalent to the sum of the surface areas of the individual components (Oberdörster, 2010; Commission Recommendation, 2011).

Given these definitions, it's clear why aggregates and agglomerates are considered when evaluating nanomaterials. These forms may retain characteristics of their constituent unbound particles and have the capability to disintegrate back into nanoscale components (Lövestam et al., 2010; Boverhof et al., 2015). Additionally, the establishment of a lower size limit helps to distinguish between atoms and molecules, which are not classified as particles, and actual particulate forms (Lövestam et al., 2010).

1.2.3. Particle Size Distribution

The Particle Size Distribution (PSD) is a vital factor widely used in identifying nanomaterials, as it captures the range of size variations within a sample. It's important to determine the PSD because nanomaterials are typically polydisperse, meaning they consist of particles of various sizes (Commission Recommendation, 2011; Bleeker et al., 2013; Boverhof et al., 2015). This variability in particle size is a key characteristic that helps define and categorize nanomaterials in scientific and regulatory contexts.

1.2.4. Surface Area

The measurement of surface area by volume is a critical relational parameter, required under specific regulatory circumstances. According to the established guidelines, a material is classified as a nanomaterial if its surface area by volume exceeds 60 m2/cm3. Nevertheless, it's crucial to recognize that the particle size distribution (PSD) is the primary determining factor. For example, a material might still be identified as a nanomaterial based on its PSD, even if its surface area by volume does not reach the threshold of 60 m2/cm3 (Commission Recommendation, 2011; Bleeker et al., 2013; Boverhof et al., 2015). This indicates that while surface area by volume is an important metric, PSD often has priority in defining nanomaterial status.

1.2.5. Dynamic Behavior of Nanomaterials and Applications in Nanomedicine

Nanomaterials find applications in nanomedicine for medical purposes across three primary areas: diagnosis (nanodiagnosis), controlled drug delivery (nanotherapy), and regenerative medicine. A burgeoning field known as theragnostic, which integrates diagnostics and therapy in the same system, is emerging as a promising approach holding both diagnostic/imaging agents and medicine. Nanomedicine is pioneering new approaches for diagnosis and treatment, meeting previously unaddressed medical needs by combining potent yet toxic molecules. This integration leverages multiple mechanisms of action to enhance effectiveness while minimizing the required dosage and toxicity. Additionally, nanomedicine offers targeted drug delivery, controlled release, and site-specific administration. These capabilities facilitate the preferential distribution of therapeutic agents within the body, such as in cancer-affected areas, and enhance the transport of drugs across biological barriers (Chan, 2006; Méndez-Rojas et al., 2009; Zhang et al., 2012; Ossa, 2014). This strategic approach to drug delivery is designed to maximize therapeutic benefits while reducing adverse side effects.

These advancements are due to the inherent properties of nanomaterials that provide numerous benefits in pharmaceutical development. The small size of nanomaterials results in a high specific surface area to volume ratio, which increases the surface energy of the particles and enhances their reactivity. When nanomaterials come into contact with biological fluids, they often adsorb biomolecules like proteins and lipids, creating a layer known as the "corona" on the surface of colloidal nanoparticles. This phenomenon has been documented by researchers such as Pino et al. in 2014. This corona's composition depends on the entry point into the body and the specific fluid encountered, with dynamic changes occurring as the nanoparticle transitions between biological compartments (Pearson et al., 2014; Louro, 2018).

Moreover, nanomaterials exhibit tunable magnetic, optical and electrical properties through electron confinement. The engineering of nanomaterials facilitates variations in their size, shape,

chemical composition, and surface characteristics. These modifications allow them to interact with specific biological targets, as described by Oberdörster et al. in 2005 and Kim et al. in 2010. Securing a positive biological result requires careful particle design and a comprehensive understanding of how nanomaterials interact with biological systems.

This understanding is essential for two main reasons. Firstly, it pertains to the physiological and pathological characteristics of diseases, where molecular processes occur at the nanoscale, involving factors like mutated genes, misfolded proteins, and infections. Enhanced knowledge of these processes enables the strategic design of engineered nanomaterials to specifically target desired locations within the body (Kim et al., 2010; Albanese et al., 2012). Secondly, it involves the interaction between nanomaterial surfaces and biological environments in fluids. Characterizing the biomolecules corona is crucial for understanding how the nanomaterial-cell interaction influences biological responses. This interaction is dynamic, involving exchanges between nanomaterial surfaces and biological components such as proteins, membranes, phospholipids, vesicles, and organelles.

The physicochemical characteristics of the biointerface are crucial in shaping cellular signaling pathways, kinetics, and transport mechanisms. A deeper understanding of these properties provides critical insights for the design of nanomaterials, guiding their development for enhanced efficacy and targeted therapeutic applications (Kim et al., 2010; Nel et al., 2009; Monopoli et al., 2012; Albanese et al., 2012).

1.2.6. Physicochemical Characterization

Characterizing nanomedicine is essential for understanding its behavior within the human body and aiding in process control and safety evaluation. Yet, reaching an agreement on the necessary parameters for accurate and comprehensive characterization remains a complex challenge. Employing internationally standardized methodologies and reference materials is crucial for aligning various perspectives in this field (Lin et al., 2014; Zhao and Chen, 2016).

It is recommended that characterization of nanomaterials be conducted at different stages of their lifecycle, from design through to performance evaluations in vitro and in vivo. Interactions with biological systems and the effects of sample preparation or extraction might alter some properties of the nanomaterials, affecting measurement outcomes. Thus, determining both in vivo and in vitro physicochemical properties is critical to assess potential risks (Lin et al., 2014; Zhao and Chen, 2016).

The Organization for Economic Co-operation and Development (OECD), in collaboration with the International Organization for Standardization, has established a Working Party on Manufactured Nanomaterials to provide scientific guidance on nanomaterials' safe usage, focusing on physicochemical characterization and metrology. Although there is no set list of essential parameters, some foundational characteristics include particle size, shape, size distribution, aggregation and agglomeration states, crystal structure, specific surface area, porosity, chemical composition, surface chemistry, charge, photocatalytic activity, zeta potential, water solubility, dissolution rate/kinetics, and dustiness (McCall et al., 2013; Lin et al., 2014).

In chemical composition, nanomaterials may be classified as organic, inorganic, crystalline, or amorphous and can exist as single particles, aggregates, or agglomerates, and may be dispersed in various matrices to form suspensions, emulsions, nanolayers, or films (Luther, 2004).

Regarding dimensions, nanomaterials may appear as particles, quantum dots, or hollow spheres if all three dimensions are below 100 nm. If two dimensions are below 100 nm, they may form tubes, fibers, or wires, and with one dimension below 100 nm, they can manifest as films, coatings, or multilayers (Luther, 2004).

Several analytical techniques are available for assessing these parameters, categorized into methods such as counting, ensemble, separation, and integral techniques (Linsinger et al., 2012; Contado, 2015).

1.2.6.1. Counting Methods

Counting methods are essential for distinguishing the individual particles that make up a nanomaterial, allowing for the measurement of their sizes and the visualization of their shapes. Microscopy techniques are commonly employed for particle visualization, with several variations being used depending on specific requirements. Examples include Transmission Electron Microscopy (TEM), High-Resolution TEM, Scanning Electron Microscopy (SEM), cryo-SEM, Atomic Force Microscopy, and Particle Tracking Analysis. A significant limitation of these methods has been their need for high-vacuum conditions, which can lead to sample dehydration. However, innovations like cryo-SEM have been developed to mitigate this issue by preserving the sample's hydration state under vacuum conditions (Linsinger et al., 2012; Contado, 2015; Hodoroaba and Mielke, 2015).

1.2.6.2. Fractionation Methods

Methods in this category generally involve a two-step process for sample treatment: initially, separating particles into a monodisperse fraction, and subsequently, detecting each of these fractions. Techniques such as Field-Flow Fractionation (FFF), Analytical Centrifugation (AC), and Differential Electrical Mobility Analysis are commonly used for these purposes. FFF includes a range of methods that separate particles based on the force field applied, while AC separates particles through the process of centrifugal sedimentation (Linsinger et al., 2012; Contado, 2015; Hodoroaba and Mielke, 2015).

1.2.6.3. Ensemble Methods

Ensemble methods are instrumental in determining intensity-weighted particle sizes by analyzing how the measured signal changes over time, thereby providing the size distribution of particles from a combined signal. Techniques such as Dynamic Light Scattering (DLS), Small-angle X-ray Scattering (SAXS), and X-ray Diffraction (XRD) are commonly employed. Both DLS and Quasi-Elastic Light Scattering (QELS) utilize the Brownian motion of particles in the sample to measure particle sizes. Conversely, XRD is a valuable technique that provides insights into the chemical composition, crystal structure, and physical properties of materials (Linsinger et al., 2012; Contado, 2015; Hodoroaba and Mielke, 2015).

1.2.6.4. Integral Methods

Integral methods are utilized to measure a comprehensive property of a particle, and are primarily used to determine the specific surface area. The Brunauer-Emmett-Teller (BET) method is a key technique in this category, which relies on the adsorption of an inert gas onto the surface of the nanomaterial to calculate its surface area (Linsinger et al., 2012; Contado, 2015; Hodoroaba and Mielke, 2015).

Another important technique within integral methods is electrophoretic light scattering (ELS), which is used to determine the zeta potential of particles. Zeta potential is an indicator of the overall charge that particles acquire in a specific medium. ELS measures the electrophoretic mobility of particles in a dispersion, based on electrophoresis principles (Linsinger et al., 2012).

Table 1 summarizes the main methods used for the characterization of nanomaterials, providing details on the operational principles, the physicochemical parameters they analyze, and their respective limitations.

1.2.6.5. Process Control—Understanding the Critical Manufacturing Steps

In pharmaceutical development, effectively controlling the manufacturing process presents a considerable challenge. It involves identifying critical parameters and selecting appropriate technologies for their analysis, crucial for ensuring the quality and safety of new medications (Gaspar, 2010; Gaspar et al., 2014; Sainz et al., 2015). This necessity has prompted the adoption of innovative methodologies, spurred by advances in pharmaceutical technology and heightened regulatory focus on medication quality and safety.

One prominent approach is Quality-by-Design (QbD), which is supported by Process Analytical Technologies (PAT). QbD is recognized for its systematic evaluation and control of nanomedicine production processes (FDA, 2004; Gaspar, 2010; Gaspar et al., 2014; Sainz et al., 2015; European Medicines Agency, 2017). The approach involves identifying Quality Attributes (QA), which are the chemical, physical, or biological properties that should be measured and controlled within certain limits to ensure product quality. Critical Quality Attributes (CQA) are those properties sensitive to changes during manufacturing, where variability might affect the product's quality and safety. Managing these attributes and their related process parameters is essential (Verma et al., 2009; Riley and Li, 2011; Bastogne, 2017; European Medicines Agency, 2017).

QbD emphasizes integrating quality into the product from the outset, rather than merely testing for it post-production. This method involves a deep understanding of the product's intended therapeutic role, its pharmacological, pharmacokinetic, and toxicological profiles, and its chemical and physical characteristics. It also includes an understanding of formulation processes, packaging, and manufacturing design. This approach shifts the focus towards a comprehensive analysis of how characteristics and parameters interact during formulation and processing, aiming to establish robust manufacturing processes that secure the quality of nanomedicines (FDA, 2014).

Furthermore, the FDA defines Process Analytical Technologies (PAT) as systems designed to design, analyze, and control manufacturing through real-time measurements of critical quality and performance attributes of raw and in-process materials. The aim of employing PAT is to guarantee the quality of the final product. PAT tools are used to analyze critical attributes and enhance understanding of the manufacturing process, facilitating improved control and optimization (Verma et al., 2009; Riley and Li, 2011; FDA, 2014; Bastogne, 2017; European Medicines Agency, 2017).

Method	Operation principle	Physicochemical parameters analyzed	Limitations
Transmission Electron Microscopy	An electron beam interacts and passes through the sample and the scattered electrons are focused to create an image.	Particle size and size distribution; Shape; Agglomeration; Aggregation; Crystal structure.	Operation in high-vacuum; Only applied for solid samples; Time consuming and expensive; Complex sample preparation.
Scanning Electron Microscopy	An electron beam interacts with the sample but the beam pass over the sample due to the secondary electrons ejected from the surface by inelastic scattering occurs the creation of the image.	Particle size and size distribution; Shape; Agglomeration; Aggregation; Crystal structure.	Operate in High-Vacuum; Time consuming and expensive; Solid and conductive materials; Complex sample preparation.
Atomic Force Microscopy	A scanning probe moves over the surface of the sample and detects the surface topography by the forces measured from the interaction between both surfaces.	Particle size and size distribution; Shape; Agglomeration; Aggregation; Surface properties.	Samples must adhere to a substrate or be dispersed on it; Time consuming.
Particle Tracking Analysis	The sample is placed in a dark background and then it is illuminated by an intense laser light. The scattered light and the movement of particles under Brownian motion is measured through a sensitive camera on the optical microscope.	Particle size and size distribution; Agglomeration; Aggregation.	The sample must be a suspension; Less sensitive if the particles distances are small.
Field-Flow Fractionation	The separation of the particles occurs according to the differences in their mobility induced by a laminar flow field and an interaction with a second perpendicularly field force.	Particle size distribution.	Complex algorithm to extract size distribution; Particles in agglomerates or aggregates are not determined.
Differential Mobility Electrical Analysis	The particle samples pass through an electric field and according to their electrical mobility (their charge) separation occurs.	Particle size and size distribution.	Only aerosol samples; Samples need to be charged.
Dynamic Light Scattering	The hydrodynamic diameter is determined through the measurement of the fluctuations of the scattered light caused by the particles Brownian motion in the suspension by Stokes-Einstein equation.	Particle size and size distribution.	Only applied for suspension; Bad resolution for polydisperse samples.

X-ray Diffraction	A X-ray beam passes through the sample and interacts with the repeated planes of atoms. Atoms organized in a crystalline structure will diffract the beam. Through Bragg's Law the distance between the planes of atoms is calculated.	Particle Size; Shape; Structure for crystalline materials.	Only applied for crystalline materials.
Brunauer Emmet Teller	This technique is based on the physical adsorption of an inert gas (N2 or Ar) at the surface of the particles at low temperature. By the number of adsorbed molecules on the surface, the surface area is calculated.	Specific surface area; Porosity.	Only applied for dry samples.

Figure 1.1. Some of the principal methods for the characterization of the nanomaterials, operation principle, physicochemical parameters analyzed, and respective limitations [1].

1.2.6.6. Biocompatibility and Nanotoxicology

Biocompatibility is a crucial aspect in the development of drug delivery systems, defined as the ability of a material to perform effectively in a specific application without eliciting any undesirable responses from the host organism (Williams, 2003; Keck and Müller, 2013). To ensure safety, pre-clinical evaluation of nanomaterials requires thorough biocompatibility testing, which typically involves a combination of in vivo studies and targeted in vitro assays. Without demonstrable biocompatibility, the potential benefits of nanosystems could lead to toxicological concerns.

Regulatory agencies, alongside entities in the pharmaceutical industry, government, and academia, are actively working to establish specific guidelines for the risk assessment of nanomaterials (Hussain et al., 2015). Despite efforts to standardize safety evaluation procedures, nanomaterials are often treated similarly to conventional chemicals, resulting in a lack of clear regulatory guidelines and standardized testing protocols. To address these gaps, various initiatives such as scientific opinions, guidelines, European regulations, and OECD guidelines have been developed to enhance the safety assessment of nanomaterials (Juillerat-Jeanneret et al., 2015).

Understanding how nanomaterials interact with biological systems is essential for evaluating exposure, hazards, and potential risks. The behavior of nanoparticles in the body—including their pharmacokinetics and distribution—is influenced by their surface physicochemical properties, shape, and size. For example, 10 nm nanoparticles tend to distribute across various organs, whereas larger particles are predominantly found in specific organs such as the spleen, liver, and blood (De Jong et al., 2008; Adabi et al., 2017).

The surface characteristics of nanoparticles also affect their organ distribution through interactions with serum proteins, which can influence cellular uptake. A biocompatible material should not provoke any immune response, and the adsorption pattern of body proteins on nanoparticles can affect their potential to trigger such responses (Keck et al., 2013).

The clearance of nanoparticles from the body depends on their size and surface properties. Smaller nanoparticles (less than 20–30 nm) are typically cleared quickly through renal excretion, while larger particles (over 200 nm) are predominantly processed by the mononuclear phagocytic system in the liver, spleen, and bone marrow (Moghimi et al., 2001; Adabi et al., 2017). The emerging field of nanotoxicology focuses on studying the effects of nanomaterials as they interact with biological systems, highlighting the need for comprehensive toxicological evaluations to ensure the safety of nanotechnologies (Donaldson et al., 2004; Oberdörster, 2010; Fadeel, 2013).

1.2.6.7. Evaluation Methods

The evaluation of potential toxic effects from nanomaterials is often linked to their ability to trigger recognized molecular responses within cells. Nanomaterials have the capacity to disrupt redox system balance, leading to the generation of reactive oxygen species (ROS), including hydroxyl radicals, superoxide anions, and hydrogen peroxide. While cells naturally generate reactive oxygen species (ROS) as a part of their metabolic processes, exposure to nanomaterials can lead to an increase in ROS production. Cells defend themselves through mechanisms involving reduced glutathione, superoxide dismutase, glutathione peroxidase, and catalase. However, increased ROS can deplete

glutathione, compromising the cell's ability to neutralize free radicals. This situation induces oxidative stress and interacts with cell membrane fatty acids, potentially compromising cell viability. Disruption of cell membranes, inflammatory responses involving upregulated transcription factors, and various biological reactions can trigger cell apoptosis or necrosis, leading to specific physiological outcomes (Arora et al., 2012; Nel et al., 2006; Azhdarzadeh et al., 2015).

In recent years, there has been an exponential increase in scientific publications on the toxicological effects of nanomaterials. However, concerns arise due to variations in experimental protocols, lack of standard nanomaterials for reference, and the use of doses that may not be applicable in biological systems, making results incomparable. To enable accurate comparisons, precise and comprehensive physicochemical characterization is essential, forming the basis for risk assessment guidelines. Nanomaterials with the same composition can display different biological activities due to subtle differences in surface charge, size, or shape, which influence their cellular interactions and accumulation within the human body (Sayes and Warheit, 2009). Sayes and Warheit (2009) proposed a three-phase model for characterizing nanomaterials: the primary phase assesses the native, dry state of the nanomaterial; the secondary phase examines nanomaterials in a wet state, such as in solutions or suspensions; and the tertiary phase focuses on in vitro and in vivo interactions with biological systems. However, in vivo studies using animal models pose practical, ethical, and financial challenges and may not always provide results that are directly applicable to humans. Alternatively, in vitro studies using cell lines or primary cells offer a more affordable and straightforward approach, though they often fail to mimic the complex interactions occurring within the human body, potentially leading to inaccurate predictions of human responses to nanomaterial exposure (Kroll et al., 2009; Fadeel et al., 2013b).

In silico nanotoxicology, which uses computational tools and biostatistical methods, presents a promising substitute for traditional in vitro assays. These computational approaches can analyze a wide range of nanomaterials, integrate various endpoints and pathways, and deliver rapid results while avoiding ethical issues. Quantitative structure-activity relationship models (QSAR) are among these computational tools, based on the premise that the toxicity and cellular fate of nanomaterials can be predicted by their physicochemical properties. These in silico methods represent a significant advancement in predicting nanomaterial behavior, offering a valuable resource for developing safer nanotechnology applications. QSAR aims to identify characteristics leading to toxicity, allowing for alterations to reduce toxicity. Toxigenomics, combining genomics and nanotoxicology, is another emerging area aiming to identify alterations in genes, proteins, and metabolite expressions in response to nanomaterial exposure (Winkler et al., 2013; Warheit, 2008; Raunio, 2011; Oksel et al., 2015; Rusyn et al., 2012; Fadeel et al., 2013a; Rusyn and Daston, 2010;).

1.2.6.8. Nanotoxicological Classification System

Several risk assessment methodologies for nanomaterials have been developed over the years. Among them, the DF4nanoGrouping framework stands out as a functionality-driven approach for grouping nanomaterials based on their intrinsic properties, system-dependent properties, and toxicological effects (Arts et al., 2014, 2016). This framework divides nanomaterials into four main groups, with possible subgroups: (1) soluble nanomaterials, (2) biopersistent high aspect ratio nanomaterials, (3) passive nanomaterials that exhibit no significant biological effects, and (4) active nanomaterials that display specific toxic properties related to their surfaces. The DF4nanoGrouping framework promotes a stepwise evaluation of nanomaterial properties and effects, incorporating increasing levels of biological complexity. Its effectiveness has been demonstrated in case studies involving diverse nanomaterials like carbonaceous materials, metal oxides, metal sulfates, amorphous silica, and organic pigments—all with primary particle sizes under 100 nm. This framework not only aids in the grouping and targeted testing of nanomaterials but also supports the collection of comprehensive data necessary for risk assessments, and it encourages the adoption of non-animal testing methods (Landsiedel et al., 2017). More recently, the DF4nanoGrouping has evolved to include three structure-activity relationship classification decision tree models. These models identify key structural features responsible for surface activity, such as size, specific surface area, and the quantum-mechanical calculated property "lowest unoccupied molecular orbital," using a limited set

of descriptors for intrinsic oxidative potential, protein carbonylation, and no observed adverse effect concentration (Gajewicz et al., 2018). Additionally, Keck and Müller proposed a nanotoxicological classification system (NCS), depicted in Figure 1.2., that categorizes nanomaterials into four classes based on their size and biodegradability (Müller et al., 2011; Keck and Müller, 2013). This system helps to further differentiate nanomaterials based on critical environmental and health-related properties.

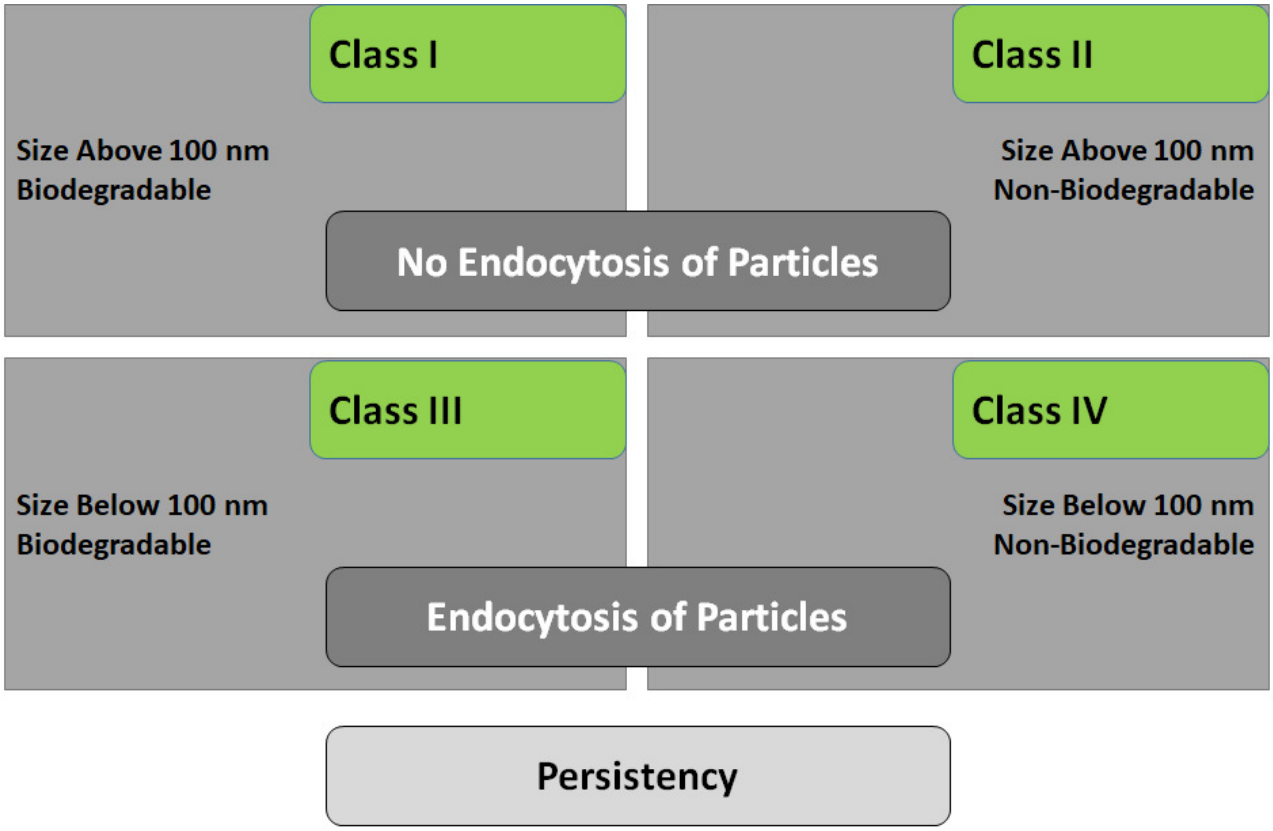


Figure 1.2. Nanotoxicological classification [1].

The size of nanomaterials significantly influences their behavior and associated risks. As nanomaterials decrease in size, their solubility often increases, particularly for materials that are typically poorly soluble. Smaller nanomaterials are also more likely to adhere to membrane surfaces. Furthermore, the size of nanomaterials affects their interaction with immune cells; nanomaterials larger than 100 nm are typically internalized only by macrophages, whereas those smaller than 100 nm can be taken up by virtually any cell type through endocytosis, leading to potentially higher toxicity risks (Müller et al., 2011; Keck & Müller, 2013).

Biodegradability is another vital factor in pharmaceutical applications. Biodegradable nanomaterials can be processed and eliminated by the human body, allowing the immune system to recover normal function post-elimination. Conversely, non-biodegradable nanomaterials may persist within the body indefinitely, potentially disrupting normal immune functions (Müller et al., 2011; Keck & Müller, 2013).

Moreover, the route of administration and surface biocompatibility are crucial determinants of nanomaterial toxicity. The risk associated with nanomaterials varies depending on the method of application, such as dermal versus intravenous. Surface biocompatibility is defined by physicochemical properties and is crucial regardless of size or biodegradability. Non-biocompatible surfaces may trigger immune responses by adsorbing proteins like opsonins, even if the nanomaterial falls into NCS class I. This distinction leads to further classification into eight subclasses, ranging from I-B (biocompatible) to IV-NB (non-biocompatible) (Müller et al., 2011; Keck & Müller, 2013).

While the Nanomaterial Classification Scheme (NCS) offers a framework for assessing nanoparticle risks, additional factors are essential for a comprehensive understanding of nanotoxicity.

Broad strategies that integrate toxicology, risk assessment modeling, and multicriteria decision analysis tools are also being explored to enhance the evaluation of nanomaterial safety (Rycroft et al., 2018).

1.2.6.9. Scale-Up and Reproducibility

The scale-up and reproducibility of nanomedicines pose significant challenges in pharmaceutical development. Many nanomedicines fail to meet these requirements, preventing their introduction into the pharmaceutical market (Agrahari and Hiremath, 2017).

Traditional manufacturing processes are not inherently designed for creating three-dimensional medicines at the nanometer scale. Nanomedicine manufacturing involves both top-down and bottom-up approaches, incorporating multiple steps such as homogenization, sonication, milling, emulsification, and, in some cases, the use of organic solvents and subsequent evaporation. While it is relatively easy to control and optimize formulations on a small scale, challenges arise when attempting to scale up production. Slight variations during large-scale manufacturing can lead to critical changes in the physicochemical characteristics, jeopardizing the quality, safety, and therapeutic outcomes of nanomedicines. Establishing acceptable limits for Critical Quality Attributes (CQA) is crucial, requiring identification and analysis at the small scale to understand how the manufacturing process influences these parameters and facilitate the transition to larger scales. A comprehensive understanding of critical steps and analytical tools developed for small-scale production greatly aids the introduction of large-scale manufacturing (Desai, 2012; Kaur et al., 2014; Agrahari and Hiremath, 2017).

Reproducibility is another key requirement for bringing medicines to the pharmaceutical market. It involves ensuring consistency in physicochemical characterization and therapeutic efficacy across different batches. Specific ranges for variations between batches are defined, and any slight changes in the manufacturing process can potentially compromise CQA, leading to inter-batch variations. Achieving reproducibility is essential for maintaining the quality and efficacy of nanomedicines (Desai, 2012; Kaur et al., 2014; Agrahari and Hiremath, 2017).

1.3. Nanomedicines and Nanosimilars

The approval process for nanomedicines is governed by a traditional benefit/risk analysis framework. A notable challenge emerges with the introduction of follow-on nanomedicines upon the expiration of patents for reference medicines (Ehmann et al., 2013; Tinkle et al., 2014).

Nanomedicines are classified into two main types: biological and non-biological. Biological nanomedicines are derived from biological sources, whereas non-biological nanomedicines, also known as non-biological complex drugs (NBCDs), consist of various synthetic structures (Tinkle et al., 2014; Hussaarts et al., 2017; Mühlebach, 2018). The market entry of generic versions necessitates extensive analysis that goes beyond simply measuring plasma concentrations. For both biological and non-biological nanomedicines, a thorough stepwise comparison of bioequivalence, safety, quality, and efficacy relative to the reference medicine is essential to establish their therapeutic equivalence and interchangeability (Astier et al., 2017).

Regulatory guidelines for biological nanomedicines are provided by the European Medicines Agency (EMA), which has set forth specific protocols for follow-on biological nanomedicines, including recommendations for comparative quality assessments and non-clinical and clinical studies (Mühlebach et al., 2015).

The regulatory framework for follow-on NBCDs is still evolving. The industry frequently seeks scientific advice, and the EMA approaches each case individually. In some instances, the regulatory framework for NBCDs borrows from that of biologicals, especially when considering their shared features like the inability to fully characterize their structures and the dependence of the in vivo activity on the manufacturing process. Like biologicals, comparability for NBCDs must be demonstrated throughout their lifecycle. For certain NBCD groups, such as liposomes, glatiramoids, and iron carbohydrate complexes, draft regulatory guidelines are in place, which help regulatory

bodies formulate comprehensive regulatory frameworks for different NBCD families (Schellekens et al., 2014).

The EMA has also published reflection papers tailored to specific types of nanomedicines, such as those with surface coatings, intravenous liposomal formulations, block copolymer micelles, and iron-based nano-colloidal medicines. These documents provide developers with guidance for preparing marketing authorization applications and address general issues related to the complexities of nanosystems. They also offer critical information for the pharmaceutical development, non-clinical, and early clinical studies of these nanomedicines. Topics covered include particle characteristics that can affect kinetic parameters, toxicity, and other factors like the physicochemical nature of coatings, their uniformity and stability, bio-distribution, and intracellular fate (European Medicines Agency, 2011, 2013a, b, c).

1.4. Market Access and Pharmacoeconomics

After obtaining marketing authorization, the introduction of nanomedicines into clinical practice across European Union (EU) countries encounters challenges related to the distinct pricing and reimbursement decisions made by each member state (Sainz et al., 2015). This variance can impact the accessibility of these innovative treatments.

To streamline patient access to medicines, the comprehensive process of Health Technology Assessment (HTA) has been established. HTA generates crucial information regarding a medicine's safety, effectiveness, and cost-effectiveness. This information aids health and policy decision-makers in evaluating the overall value of new treatments and making informed healthcare choices (Sainz et al., 2015).

Pharmacoeconomic studies are integral to the commercialization phase of nanomedicines. These studies assess the social and economic impact of new medicines by examining their added therapeutic value. Important metrics in these studies include quality-adjusted life years (QALYs) and the potential to reduce hospitalizations, providing a quantifiable measure of the health benefits relative to the costs (Sainz et al., 2015).

To facilitate the integration of new medicines into clinical practice and to ensure patient access to innovative treatments, the European Network for Health Technology Assessment (EUnetHTA) was established. EUnetHTA aims to harmonize the HTA processes across Europe, providing decisive, appropriate, and transparent information to support the assessments made in EU countries.

Currently, EUnetHTA is engaged in Joint Action 3, which is set to run until 2020. The primary focus of this initiative is "to define and implement a sustainable model for the scientific and technical cooperation on Health Technology Assessment (HTA) in Europe." This effort seeks to strengthen collaboration and enhance cooperation among EU member states in the field of HTA, aiming to optimize the integration of new medical technologies in a manner that is equitable and efficient.

1.5. Conclusion and Prospects

The advancement of research in nanomedicine has significantly contributed to the reformulation of existing medicines and the development of new ones. Nanotechnology has enabled modifications in toxicity, solubility, and bioavailability profiles of medicines.

While numerous applications of nanomedicine have been translated into clinical practice, there is still a considerable regulatory journey ahead. Challenges in the regulation and adoption of nanomedicines are manifold, primarily due to the absence of a universally accepted definition of nanomedicines, the vast diversity in the types and structures of medicinal products, and the continuous innovation leading to increasingly complex nanostructured designs. These sophisticated designs necessitate a deep understanding of pharmacokinetic and pharmacodynamic properties, introducing further complexities into the regulatory environment.

In response to these challenges, the European Medicines Agency (EMA) has formed an expert group on nanomedicines, composed of members from academia and the European regulatory network. This group's mission is to provide scientific guidance, develop or revise regulatory

guidelines, and facilitate international collaboration. For developers of nanomedicines, obtaining early advice from regulators is crucial to successfully navigate this complex regulatory landscape.

Another significant challenge lies in demonstrating the equivalence of complex drug products, particularly when establishing bioequivalence for generic versions of nanomedicines. This requires a detailed, stepwise approach that ideally should be driven by consensus, ensuring that all regulatory requirements are met comprehensively.

As science and technology continue to advance, the pharmaceutical market is expected to see an increase in medicines based on nanotechnology. Therefore, establishing robust guidelines for the development and evaluation of nanomedicines is essential. These guidelines need to be harmonized across different regulatory agencies to support informed and rational decision-making on scientific, regulatory, financial, and market access issues. Such harmonization is key to facilitating the integration of innovative nanomedicines into the market while ensuring safety and efficacy.

1.6. Quiz 1

1*. What dimensions classify a material as a nanomaterial according to the European Commission recommendation?

a). 1-50 nm
b). 1-100 nm
c). 1-200 nm
d). 1-500 nm
e). 1-1000 nm

2. What are the three main areas of application for nanomaterials in nanomedicine?

a). Diagnosis (nanodiagnosis)
b). Controlled drug delivery (nanotherapy)
c). Regenerative medicine
d). Cosmetic enhancement
e). Food preservation

3. Which of the following methods are used for the physicochemical characterization of nanomaterials?

a). Dynamic Light Scattering (DLS)
b). Transmission Electron Microscopy (TEM)
c). Field-Flow Fractionation (FFF)
d). Gas Chromatography
e). High-Performance Liquid Chromatography (HPLC)

4*. What does the Quality-by-Design (QbD) approach emphasize in nanomedicine manufacturing?

a). Ensuring nanomedicine quality through post-production testing
b). Focusing on achieving the highest possible nanoparticle size
c). Identifying and controlling critical parameters during manufacturing
d). Minimizing the need for regulatory oversight
e). Speeding up the production process regardless of quality concerns

5. Which factors influence the distribution of nanoparticles in the body?

a). Surface physicochemical characteristics
b). Particle shape
c). Particle size
d). Material composition
e). Ambient temperature fluctuations

6. The main groups of nanomaterials are:

a.) active nanomaterials
b.) passive nanomaterials
c.) passive materials with obvious biological effects
d.) soluble nanomaterials
e.) biopersistent low aspect ratio nanomaterials

7*. According to Keck and Müller class IV (NCS) has the following size:

a.) above 100 nm Biodegradable
b.) below 100 nm Non-Biodegradable
c.) above 100 nm Non-Biodegradable
d.) below 100 nm Non-Biodegradable, no Endocytosis of Particles
e.) below 100 nm Biodegradable, Endocythosis of Particles

8. The following sentences are true:
a.) Nanonmedicines can be broadly categorized into biological and non-biological products
b.) Biological nanomedicines are not derived from biological sources
c.) Non-biological nanomedicine are reffered to as non-biologica complex drugs
d.) For both biological and non-biological nanomedicines, a comprehensive analysis is necessary
e.) Non-biological nanomedicines consists of identical synthetic structures

9. Cells defend themselves through mechanisms involving:
a.) reduced glutathione
b.) manganese superoxide
c.) superoxide dismutase
d.) glutathione peroxidase
e.) catalase

10. Nanomedicine manufacturing involves both top-down and bottom-up approaches, incorporating multiple steps such as:
a.) homogenization
b.) in most cases subsequent evaporation
c.) sonication
d.) the use of inorganic solvents
e.) emulsification

References

[1]. European Science Foundation Forward Look Nanomedicine: An EMRC Consensus Opinion 2005. [(accessed on 21 December 2015)]. Available online :http://www.esf.org
[2]. Peer D., Karp J.M., Hong S., Farokhzad O.C., Margalit R., Langer R. Nanocarriers as an emerging platform for cancer therapy. Nat. Nanotechnol. 2007;2:751–760. doi: 10.1038/nnano.2007.387.
[3]. Duncan R. Polymer conjugates as anticancer nanomedicines. Nat. Rev. Cancer. 2006;6:688–701. doi: 10.1038/nrc1958.
[4]. Picard F.J., Bergeron M.J. Rapid theranostic in infectious diseases. Drug Discov. Today. 2002;7:1092–1101. doi: 10.1016/S1359-6446(02)02497-2.
[5]. Bardhan R., Lal S., Joshi A., Halas N.J. Theranosctic Shells: From Probe Design to Imaging and Treatment of Cancer. Acc. Chem. Res. 2011;44:936–946. doi: 10.1021/ar200023x.
[6]. Anconi F.Panacae Aurea-Auro Potabile. Bibliopolio Frobeniano; Hamburg, Germany: 1618.
[7]. Macker P.-J. Dictionnaire de Chymie. Lacombe; Paris, France: 1766.
[8]. Cooper E.L. From Darwin and Metchnikoff to Burnet and Beyond. Contrib. Microbiol. 2008;15:1–11.
[9]. Ehrlich P. Address in pathology. On chemiotherapy. Delivered before the 17th International Congress of Medicine. Br. Med. J. 1913;16:353–359. doi: 10.1136/bmj.2.2746.353.
[10]. Gregoriadis G., Leathwood P.D., Ryman B.E. Enzyme entrapment in liposomes. FEBS Lett. 1971;14:95–99. doi: 10.1016/0014-5793(71)80109-6.
[11]. Bangham A.D. Lipid bilayers and biomembranes. Annu. Rev. Biochem. 1972;41:753–776. doi: 10.1146/annurev.bi.41.070172.003541.
[12]. Cornu G., Michaux J.L., Sokal G., Trouet A. Daunorubicin-DNA: Further clinical trials in acute non-lymphoblastic leukemia. Eur. J. Cancer. 1974;10:695–700. doi: 10.1016/0014-2964(74)90106-6.
[13]. Ringsdorf H. Structure and properties of pharmacologically active polymers. J. Polym. Sci. Polym. Symp. 1975;51:135–153. doi: 10.1002/polc.5070510111.
[14]. Hurwitz E., Levy R., Maron R., Wilchek M., Arnon R., Sela M. The covalent binding of daunomycin and adriamycin to antibodies, with retention of both drug and antibody activities. Cancer Res. 1975;35:1175–1181.
[15]. Kreuter J., Speiser P.P. In vitro studies of poly(methyl methacrylate) adjuvants. J. Pharm. Sci. 1976;65:1624–1627. doi: 10.1002/jps.2600651115.
[16]. Couvreur P., Tulkens P., Roland M., Trouet A., Speiser P. Nanocapsules: A new type of lysosomotropic carrier. FEBS Lett. 1977;84:323–326. doi: 10.1016/0014-5793(77)80717-5.
[17]. Duncan R., Kopecek J. Soluble synthetic polymers as potential drug carriers. Adv. Polym. Sci. 1984;57:51–101.
[18]. Davis F.F. The origin of pegnology. Adv. Drug Deliv. Rev. 2002;54:457–458. doi: 10.1016/S0169-409X(02)00021-2.
[19]. Trouet A., Masquelier M., Baurain R., Deprez-de Campeneere D. A covalent linkage between daunorubicin and proteins that is stable in serum and reversible by lysosomal hydrolases, as required for a lysosomotropic drug-carrier conjugate: *In vitro* and *in vivo* studies. Proc. Natl. Acad. Sci. USA. 1982;79:626–629. doi: 10.1073/pnas.79.2.626.
[20]. Gros L., Ringsdorf H., Schupp H. Polymeric antitumour agents on a molecular and cellular level. Angew. Chem. Int. Ed. 1981;20:301–323. doi: 10.1002/anie.198103051.
[21]. Dequeker J., Verdickt W., Gevers G., Vanschoubroek K. Longterm experience with oral gold in rheumatoid arthritis and psoriatic arthritis. Clin. Rheumatol. 1984;3(Suppl. 1):67–74. doi: 10.1007/BF03342624.
[22]. Duncan R., Gaspar R. Nanomedicines under the microscope. Mol. Pharm. 2011;8:2101–2141. doi: 10.1021/mp200394t.
[23]. Duncan R., Gaspar R. Nanomedicines under the microscope. Mol. Pharm. 2011;8:2101–2141. doi: 10.1021/mp200394t.
[24]. Garcia-Garcia E., Andrieux K., Gil S., Couvreur P. Colloidal carriers and blood-brain barrier (BBB) translocation: A way to deliver drugs to the brain? *Int. J. Pharm.* 2005;298:274–292. doi: 10.1016/j.ijpharm.2005.03.031.
[25]. Wiwattanapatapee R., Carreno-Gomez B., Malik N., Duncan R. Anionic PAMAM dendrimers rapidly cross adult rat intestine *in vitro*: A potential oral delivery system. *Pharm. Res.* 2000;17:991–998. doi: 10.1023/A:1007587523543.
[26]. Boczkowski J., Hoet P. What's new in nanotoxicology? Implications for public health from a brief review of the 2008 literature. *Nanotoxicology.* 2010;4:1–14. doi: 10.3109/17435390903428844.
[27]. Astruc D. Research Avenues on Dendrimers towards Molecular Biology: From Biomimetism to Medicinal Engineering. *C. R. Acad. Sci.* 1996;322:757–766.
[28]. Szebeni J. Complement activation-related pseudoallergy: A new class of drug-induced acute immune toxicity. *Toxicology.* 2005;216:106–121. doi: 10.1016/j.tox.2005.07.023.

2. Nanorobotic Systems for Therapeutic and Diagnostic Applications

Nanorobotic drug delivery systems represent an innovative approach to targeted drug delivery within the human body. These systems leverage nanoscale machines guided by magnetic resonance imaging (MRI) scanners, with the aim of achieving enhanced rates of therapeutic and diagnostic success compared to traditional methods. This review provides an overview of the current state of this emerging field.

Nanorobots, in the context of medical applications, are defined as controllable machines at the nanometer scale. They consist of nanoscale components and can algorithmically respond to input forces and information. The inspiration for nanorobotics in medicine often draws from the natural function of antibodies, which the body employs to combat or repair diseased cells. Nanoparticles, due to their size similarity to human cells, serve as the fundamental building blocks of nanorobotic systems.

The integration of nanorobotic drug delivery systems with MRI guidance holds promise for precise and targeted drug delivery. This technology opens avenues for improved therapeutic outcomes and diagnostic capabilities. As research in this field advances, it is expected to contribute significantly to the evolution of medical treatments and diagnostics.

The review highlights the potential of nanorobotic drug delivery systems for achieving precise and controllable treatment at the cellular and subcellular levels within the human body. The size range of 30–300 nm is identified as critical for interactions with cells and circulation through the vasculature system [1, 2, 3, 4]. The incorporation of functionalities for sensing, targeting specific cells, and releasing drug molecules upon receiving triggering signals could revolutionize medical diagnosis and treatment for various diseases, including neoplasms, hepatitis, and diabetes [5, 6, 7, 8, 9, 10, 11, 12].

While nanoparticles and nanovesicle technologies have shown promise for diagnostic and therapeutic purposes, their systemic circulation limits targeting capabilities. To enhance targeting, guidance techniques are proposed, involving the integration of sensing and actuation mechanisms on nanocarriers. Magnetic nanoparticles, both micro- and nanoscale, have been explored for controlled locomotion within the vasculature [13, 14, 15, 16, 17]. The review emphasizes the importance of closed-loop nanoparticle localization systems, particularly those guided by magnetic resonance imaging (MRI) devices [18, 19, 20, 21, 22].

The MRI approach is favored due to its noninvasiveness, simultaneous actuation and tracking capabilities, accurate localization, and widespread availability in hospitals. Research in this field has focused on utilizing clinical MRI to navigate magnetic microparticles and agglomerates but has not extensively explored functionalized nanocarriers designed for diagnostic or therapeutic purposes [23, 24, 25, 26, 27, 28, 29, 30].

The integration of nanorobotic drug delivery systems with MRI guidance holds significant potential for advancing targeted drug delivery with minimized side effects. However, the review points out that further research is needed, especially in the application of closed-loop control to functionalized nanocarriers, to realize the full potential of this innovative approach in medicine [31, 32, 33, 34, 35, 36, 37, 38, 39].

The systematic approach towards MRI-based guidance of nanoscale, functionalized robotic capsules started in 2008 as part of the European Commission's Nanoactuators and Nanosensors for Medical Applications (NANOMA) project. The central concept of this MRI-guided nanorobotic system is to leverage an MRI scanner to apply an external driving force to nanoparticles, guiding them to a localized target and keeping them retained there. The control law determines the direction and magnitude of the forces applied to the nanoparticles, with feedback on their endovascular position obtained by processing the MRI data.

This innovative approach involves navigation techniques combined with chemical modifications of the nanoparticles' surfaces. The goal is to achieve more localized and controlled treatments, as well as controlled mechanisms for drug release. By integrating nanoscale robotic capsules with MRI guidance, this approach aims to revolutionize medical treatments by providing a high degree of precision and control at the cellular and subcellular levels within the human body.

The development of an MRI-based nanorobotic drug delivery system involves various technologies and disciplines, as illustrated in Figure 2.1. While the concept of an MRI-guided nanorobotic system is still in the early research stages, many of the individual modules required for this complex system have been developed, and their functionality has reached a sufficient level of maturity. The primary challenge lies in the integration of these individual modules to realize the MRI-based guidance of nanoscale robotic capsules.

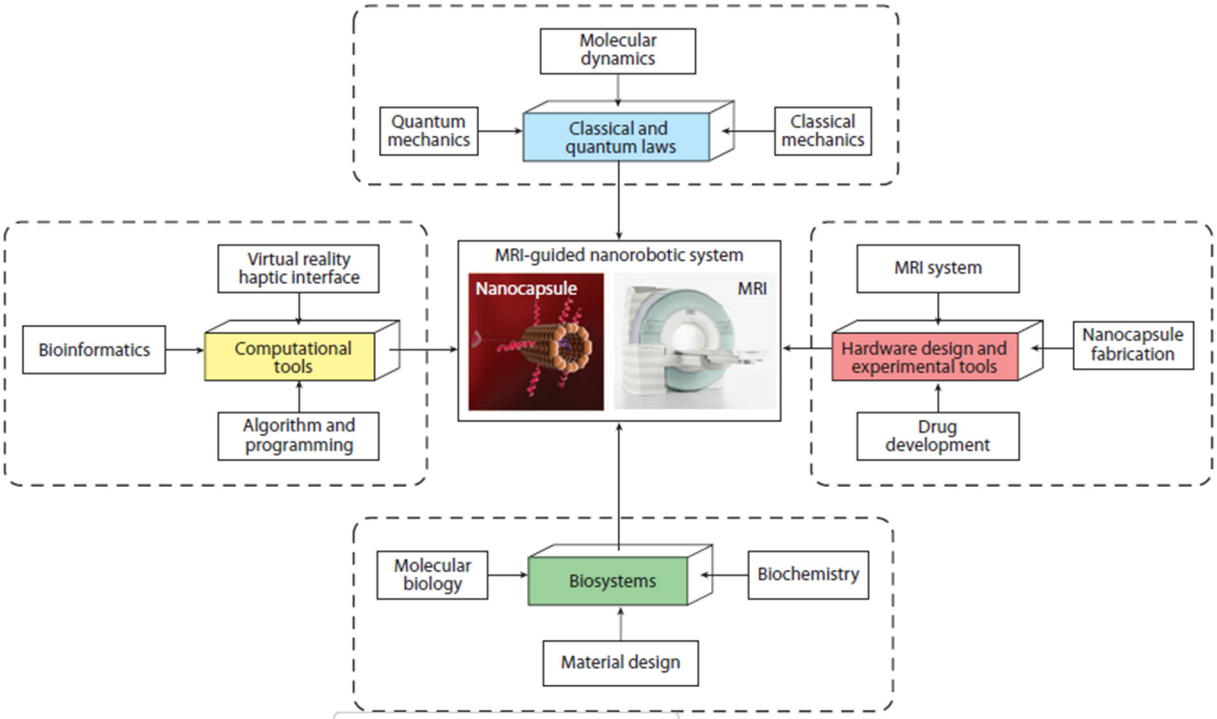


Figure 2.1. Magnetic resonance imaging (MRI)-based nanorobotic system: a multidisciplinary field. Scientific domains associated with the field of MRI-based nanorobotics are shown [1].

The main objectives of this review are to emphasize the significance of an MRI-based nanorobotic drug delivery system, outline its key components, provide an overview of current activities in this field, and discuss the challenges that need to be addressed in the near future.

2.1. Concept of Controlled Drug Delivery Systems

The goal of controlled drug delivery systems (DDSs) is to administer drugs at the right place, concentration, and duration, maintaining drug concentrations within a therapeutic window – the range between minimal therapeutic effect and toxicity. The body's natural processes often result in systemic distribution, leading to drug exposure in unnecessary organs and tissues, potentially causing side effects.

Two types of control in drug release can be achieved: temporal control and distribution control. Temporal control involves mechanisms that match the rate of drug release with the rate of drug elimination, maintaining drug concentrations within the therapeutic window over time. This is often achieved through controlled release mechanisms, such as polymer capsules.

Distribution control, on the other hand, focuses on targeting and releasing drugs specifically at the site of activity within the body. This type of control aims to increase drug dosage while minimizing side effects on healthy tissues. Various targeting mechanisms have been proposed for distribution control (Figure 2.2.).

MRI-guided drug delivery is an example of an active targeting mechanism that provides simultaneous propulsion and imaging capabilities. This allows real-time feedback control of the targeting process, enabling high-precision distribution control of the drug at the intended site, as opposed to systemic distribution that could lead to side effects in healthy tissues. The integration of

MRI into drug delivery systems holds promise for improving therapeutic efficiency while minimizing adverse effects [40, 41].

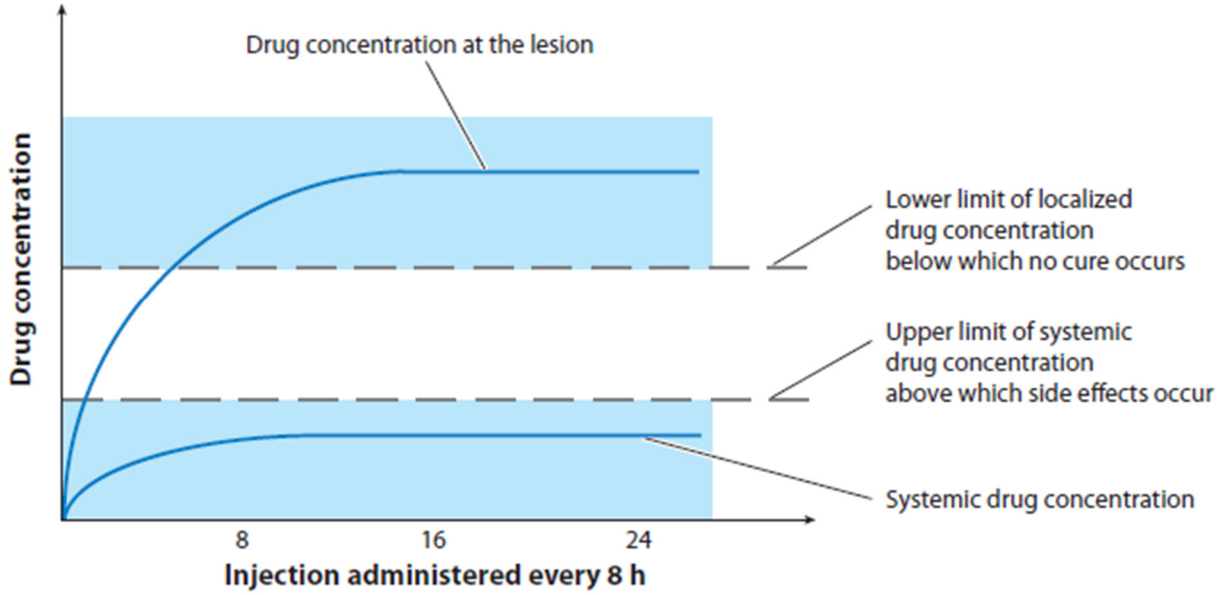


Figure 2.2. Distribution control of drug concentration [40].

2.2. Overview of the MRI Drug Delivery System Architecture

The general structure of the MRI-based nanorobotic system is illustrated in Figure 2.3. The key components crucial to the architecture of the MRI-guided nanorobotic system are elaborated upon below.

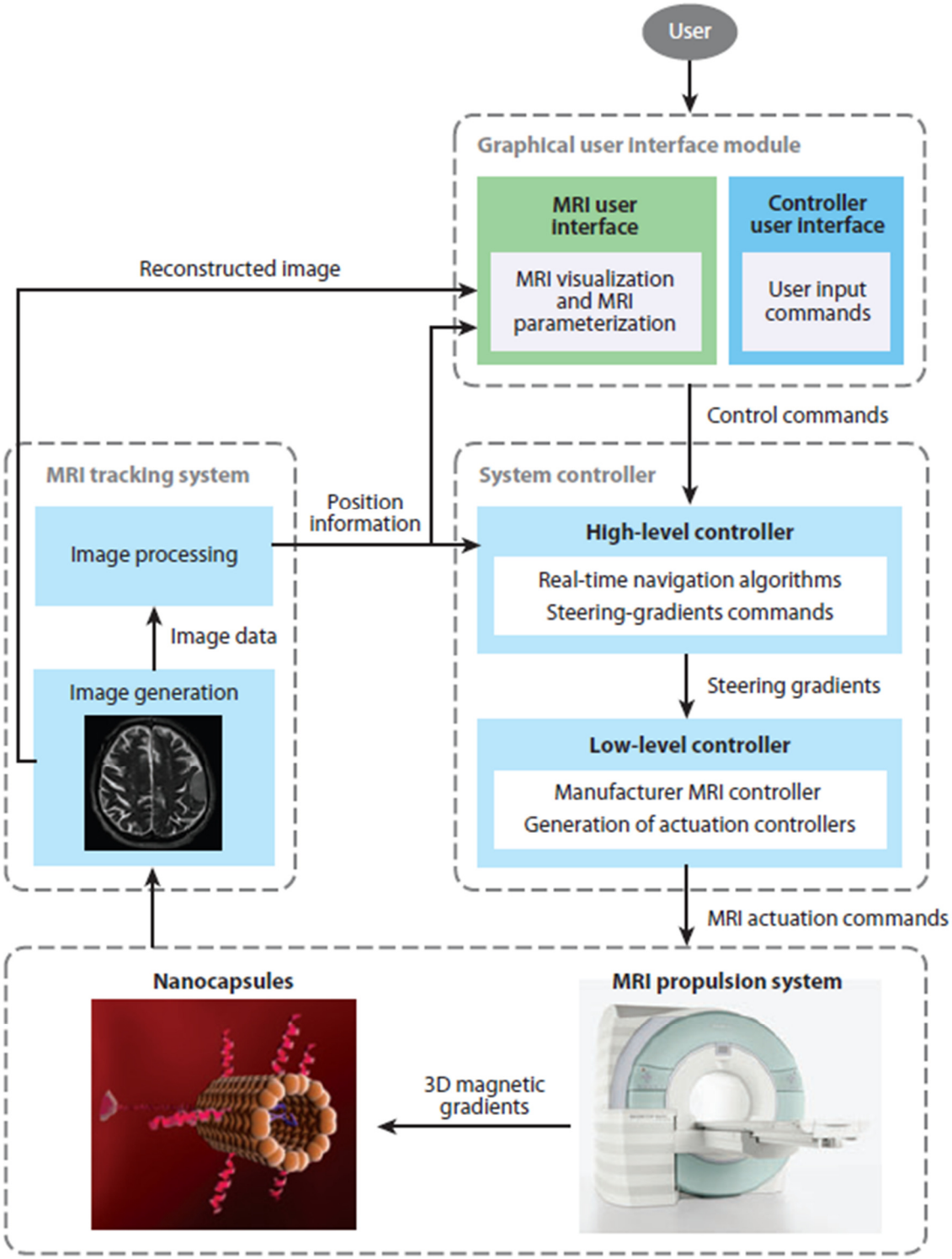


Fig. 2.3. MRI-guided nanorobotic system architecture [41].

2.2.1. Nanocapsule

The nanocapsule stands out as the most crucial subsystem within the architecture of the MRI-based nanorobotic system. Its constituent elements include the following.

2.2.1.1. The nanocarrier.

The nanocarrier forms the central body of the nanocapsules, performing dual functions: (a) acting as a vesicle for accommodating drug molecules and (b) serving as a framework to which

biomolecules and polymer chains are affixed to ensure solubility, biocompatibility, and prolonged circulation.

2.2.1.2. Magnetic nanoparticles as actuating elements

These mechanisms are accountable for generating propulsion forces and torques on the nanocapsules. Actuating elements typically consist of magnetic nanoparticles, either encapsulated within or attached to the carrier. Through the utilization of MRI field gradients, these elements induce magnetic forces and torques, thereby functioning as the propulsion mechanism for the nanocapsules.

2.2.1.3. Area Surface functionalization as a sensing element

This mechanism functions to perceive the status of the environment surrounding the nanocapsules. Sensing elements, often based on biomolecules, have diverse roles, including detecting and targeting specific molecules, initiating drug release mechanisms, and preventing immunogenic reactions.

2.2.1.4. Drug molecules

In therapeutic applications, the nanocapsules are loaded with drug molecules. Depending on the chemical process used for loading, the drug may be encapsulated in the hollow space of a vesicle or chemically attached on the surface of the carrier.

2.2.2. MRI Propulsion System

Each MRI installation will include at least the following main hardware building blocks. Their functionality is shared by both the propulsion system and the tracking system.

2.2.2.1. Main magnet

The static magnetic field is a crucial and costly component of an MRI system. A field strength of 0.5 T can be attained using permanent magnets. Higher field strengths require superconducting electromagnets, with liquid helium commonly used as the coolant to maintain superconducting properties.

2.2.2.2. Gradient coils

An MRI system requires three gradient-coil-system arrangements. These gradient coils play a dual role in both propulsion and tracking. In the context of propulsion, the gradient coils produce gradient fields. When combined with the magnetic properties of nanoparticles attached to or encapsulated in the nanocarrier, these fields induce the forces and torques needed to propel the nanocapsules.

2.2.2.3. Radio frequency coils

These coils function as both receivers and transmitters for radio frequency (RF) signals. They handle tasks like exciting refocusing pulses or processing response signals generated by nuclear magnetic resonance. In a standard MRI installation, there is an integrated RF coil system, and additional installation-specific coils may be employed for specialized examinations, such as those focused on the hand or knee.

2.2.2.4. Computer system

A distributed computer system is essential for overseeing all components of the MRI system. It manages tasks such as image reconstruction and control of gradient fields and RF coils.

2.2.3. MRI Tracking Unit

In the tracking scenario, the previously mentioned gradient coils are utilized for spatial encoding of the magnetic resonance signals and echo formation. These signals undergo processing through a tracking software module, comprising both MRI image reconstruction software and image processing software. The primary role of this module is to estimate the position and accumulation of the nanocapsules within the human vasculature, tissues, and organs. The image processing software operates in close temporal proximity to image generation to minimize communication latencies and delays, ensuring rapid controller reaction.

2.2.4. System Controller

2.2.4.1. Real-time navigation algorithm

The high-level controller subsystem, responsible for endovascular navigation, is realized by integrating real-time navigation algorithms with the MRI propulsion system and tracking events. This navigation algorithm is harmonized through the development of proprietary control modules integrated into the clinical MRI system. Achieving optimal navigation performance involves careful trade-offs in parameters such as refresh rate, duty cycle of the propulsion gradients, and repetition time of the tracking sequence. The robust implementation of controllers with plug-in architectures, requiring no modification of the clinical MRI hardware, is essential for automatic and stable trajectory tracking. The controller design process should account for various perturbations to ensure effectiveness.

2.2.4.2. Graphical user interface

This module serves as the interface between the MRI machine and the human operator, incorporating tools for input command prompts, 3D visualization, and process supervision. The underlying concept of the in vivo MRI guidance system revolves around the utilization of the MRI system's gradient coils for both imaging and propulsion. Achieving an effective interventional platform involves a software-based upgrade of a clinical MRI system, offering a cost-effective solution. At any given moment, only one function—either imaging or guidance—can be applied, yet both can be executed through the same MRI interface. While there hasn't been an in vivo demonstration of a complete MRI-guided nanorobotic system, substantial work has been conducted to establish the feasibility of several component modules. The following sections delve into the state of the art for various crucial modules in the development of MRI-guided nanorobotic systems.

2.3. Nanocarrier Technologies

The potential applications of nanoparticles in medicine, both as therapeutic and diagnostic agents, are extensive. Nanoparticle-based therapeutics hold significant promise in overcoming the limitations of traditional therapeutics, addressing issues like poor solubility and lack of target specificity. While only a few nanoparticle-based therapeutics have received approval from the U.S. Food and Drug Administration and entered the market, they are already making an impact on medicine and offering transformative possibilities for healthcare.

Researchers have developed optimized nanoparticles to enhance pharmacokinetics, improving factors such as absorption, distribution, metabolism, and excretion within the organism. These optimized nanoparticles aim to achieve more effective therapeutic activity while minimizing side effects. Critical properties of nanocarriers include biocompatibility, solubility, metabolic stability, and cellular permeability. Additionally, certain nanoparticles exhibit unique optical properties, making them suitable not only for therapeutic purposes but also for bioimaging applications. The subsequent section provides a brief overview of various nanoparticle technologies, each of which could serve as the carrier module in an MRI-guided nanorobotic system.

2.3.1. Liposome Nanoparticles

Liposomes stand out as prominent drug delivery carriers in cancer treatment. Their utilization offers significant advantages, leading to a substantial enhancement in antitumor efficacy when compared to free drugs or standard chemotherapy regimens. Liposomal formulations are currently employed as drug carriers for various drug classes, including antiviral, antifungal, antimicrobial, antitubercular drugs, vaccines, and gene therapeutics. A liposome is a nanometer-sized vesicle with a lipid-based bilayer membrane, typically measuring less than 400 nm. The bilayer consists of phospholipids arranged with hydrophilic heads (attracting water) and hydrophobic hydrocarbon tails (repelling water), forming a spherical vesicle as illustrated in Figure 2.4.

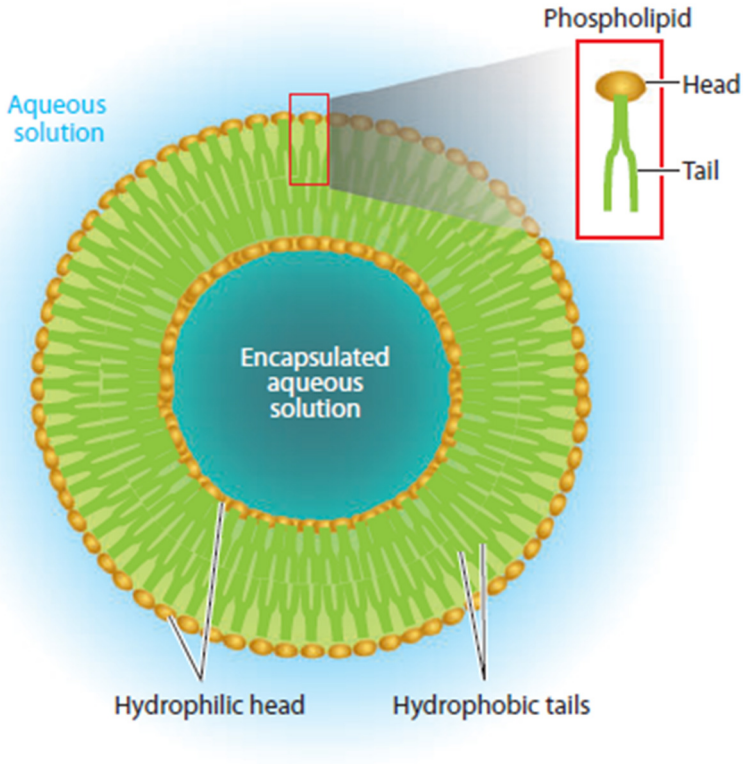


Figure 2.4. Liposome formulated by phospholipids. This is a lipid-based vesicle of nanometer size (typically less than 400 nm). Its bilayer membrane is made of two layers of phospholipids, which are molecules that have hydrophilic heads (which attract water) and hydrophobic hydrocarbon tails (which repel water), orderly arranged [41].

This vesicle encapsulates an aqueous drug core, providing protection against hydrolysis and enzymatic degradation.

2.3.2. Copolymer Micelles

Copolymer micelles have emerged as noteworthy nanocarriers for delivering low-mass drugs, proteins, genes, and imaging agents. These micelles form through the self-assembly of amphiphilic-block copolymers or graft copolymers in aqueous solutions, showcasing a distinctive core-shell architecture. The core of the micelle creates a hollow space that encapsulates water-insoluble drugs or diagnostic agents, providing effective protection against hydrolysis and enzymatic degradation. This core-shell structure allows for prolonged blood circulation times. The hydrophilic shell surrounding the micelle forms a brush-like corona (depicted in Figure 2.5.), contributing to the stabilization of the micelle in aqueous dispersion.

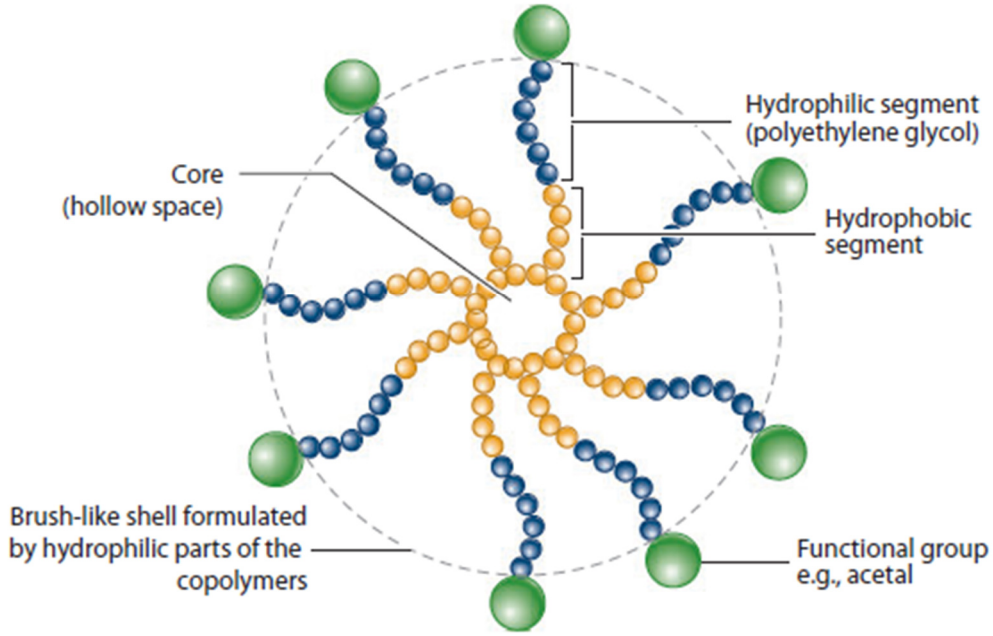


Figure 2.5. Copolymer micelle structure. A copolymer micelle is characterized by a unique core-shell architecture. The hollow core may encapsulate drugs, metal, quantum dots, or the like, depending on the application: drug delivery or diagnosis.

2.3.3. Quantum Dots

Quantum dots (QDs) represent a novel class of semiconductor nanocrystals with extensive potential across various applications in cancer research, management, and treatment. They serve as innovative fluorescent probes for biomolecular and cellular imaging. In the realm of drug delivery, Gao et al. [47] reported promising outcomes by modifying original cadmium selenide QDs. The addition of an impermeable polymer coating prevented the leakage of highly toxic cadmium ions and facilitated the chemical attachment of tumor-targeting molecules [7, 48, 49]. Uncoated or non-polymer-protected quantum dots can be unstable when exposed to ultraviolet radiation, leading to the release of toxic cadmium. However, appropriately coated QDs have demonstrated minimal toxicity to cells and animals, exhibiting no adverse effects on cell division or ATP production [48, 50].

2.3.4. Metallic Nanoshells

Metallic nanoshells refer to colloidal nanoparticles featuring a thin metallic layer forming core-shell structures. Gold and silver are among the frequently employed metals for synthesizing metallic nanoshells. The core of these nanoshells comprises polymers like Teflon or Latex nanosize spheres, although alternatives such as alumina, silica, or titanium dioxide can also be utilized. The optical properties of nanoshells hinge on the plasmon-mediated conversion of electrical energy into light. In medical applications, metallic nanoshells find common use in gene diagnostics, bioimaging, cancer imaging, and intracellular analysis (52, 53). Additionally, research has reported successful drug and gene delivery leveraging metallic nanoshells, as demonstrated by the work of Halas and colleagues (54).

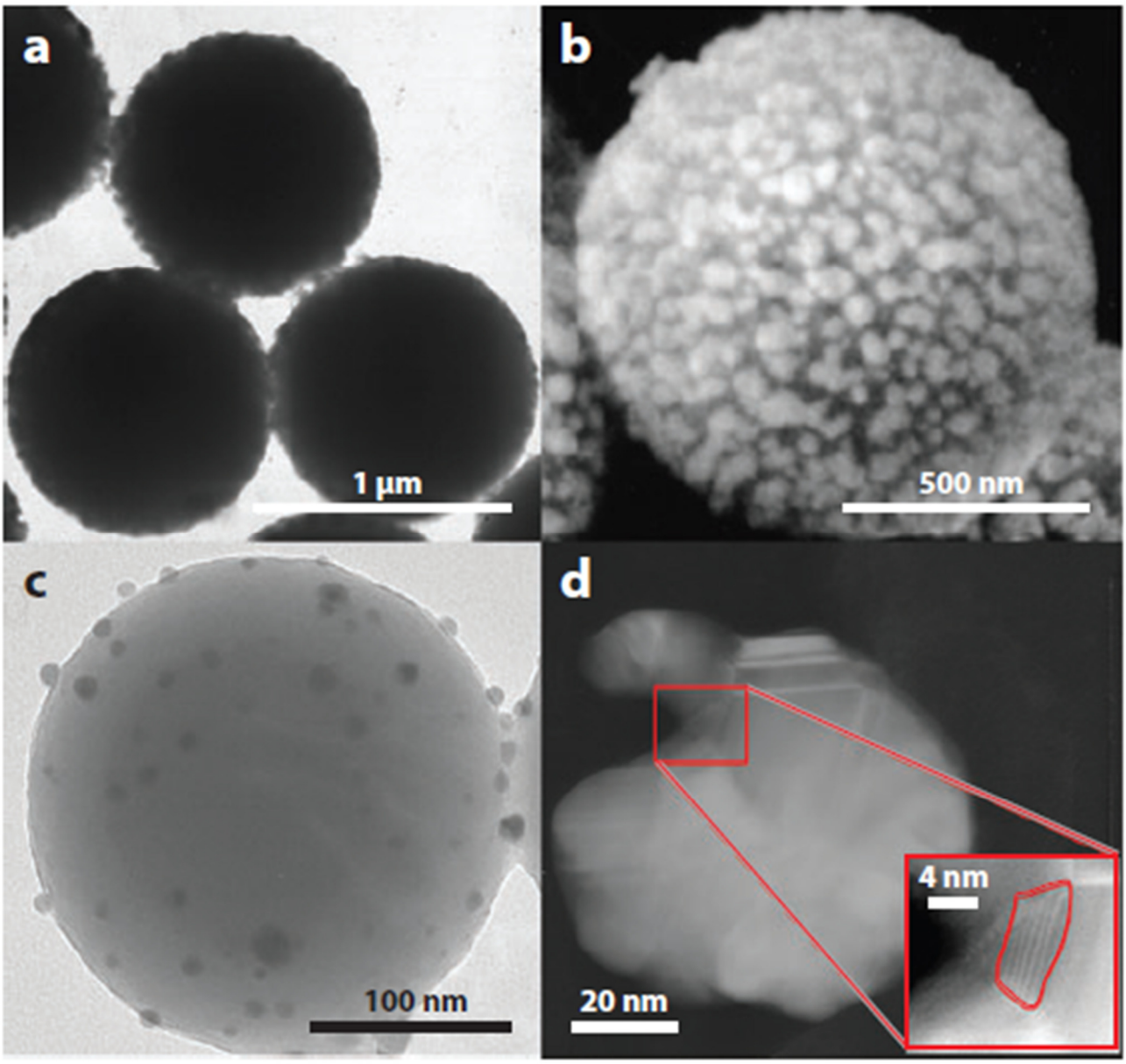


Figure 2.6. Silver nanoshells observed by a scanning electron microscope and transmission electron microscope. (a) Transmission electron microscopy (TEM) image of a 1-µm silica sphere coated with 20 nm of monocrystalline silver. (b) Scanning electron microscopy (SEM) image of a sphere from the same batch. (c) TEM image of a 250-nm sphere, with a 5–10-nm silver seed decorating the surface. (d) High-resolution TEM image of a polycrystalline silver grain. Reproduced by permission of the Journal of Colloid and Interface Science.

Figure 2.6 presents images obtained via scanning electron microscopy (SEM) and transmission electron microscopy (TEM), illustrating silver nanoshells. These imaging techniques provide detailed visualizations of the nanostructures, highlighting their unique physical properties and morphology.

2.3.5. Gold Nanoparticles

Colloidal gold or gold nanoparticles, utilized in biological applications since 1971, exhibit versatile properties extensively explored across various industries, from electronics to medicine. Typically ranging from 10 nm to 40 nm in size, these nanoparticles are characterized by robust light absorption, photostability, low toxicity, ease of conjugation to antibodies or proteins, and adjustable optical features. The optical properties stem from surface plasmon resonance, with nanogold demonstrating significantly higher absorption in cancer cells compared to normal cells. Additionally, gold nanoparticles have found application in controlled drug delivery, releasing drug molecules upon exposure to specific wavelengths of infrared light.

2.3.6. Carbon Nanotubes

Carbon nanotubes (CNTs) offer potential as nanocarriers due to their desirable dimensions and exceptional mechanical, thermal, and electrical properties. These hexagonal carbon atom networks boast a large aspect ratio (10–1,000), a terapascal-scale Young's modulus, remarkable elasticity, minimal interlayer friction, and excellent field-emission properties. CNTs come in single, double, or multiwall variations, with open or closed ends, and can be bonded together for increased functionality and extended mechanical properties. They also have the capability to incorporate magnetic nanoparticles, although achieving high-yield fabrication remains a challenge. While concerns persist regarding CNTs' biocompatibility, ongoing research indicates no apparent toxicity or negative health effects associated with their use.

2.4. Nanoparticle Functionalization for sensing purpose

The properties of many nanoparticles, as mentioned earlier, can be improved through proper nanoparticle functionalization. This involves chemically modifying the surface of a nanoparticle to achieve specific desired properties. Robotic nanocapsules undergo chemical processing not only to enhance stability, solubility, and biocompatibility but also to gain the ability to sense the environment surrounding the nanocapsule. Functionalization techniques encompass targeting mechanisms, strategies to evade immunogenic reactions, and triggered-release mechanisms, as outlined below.

2.4.1. Targeting Mechanisms: Functionalization with Biomolecules to Increase Specificity

Targeting specific cell types involves attaching specific molecules to the carrier's surface, thereby enhancing binding and interactions with antigens or receptors expressed on the target cell populations. Various vector molecules, such as antibodies, lectins, peptides, hormones, folate, and vitamins, are employed for recognizing specific tumors. For instance, monoclonal antibodies can be affixed to drug carriers to facilitate targeted drug release to tumor cells. Akerman et al. demonstrated specific targeting of vessels by using Quantum Dots (QDs) conjugated to peptides specific for blood or lymphatic vessels.

2.4.2. Mechanism of Evading Recognition by the Reticuloendothelial System: Functionalization of Nanocarriers with Copolymers for Enhanced Biodistribution

Avoiding immunogenic reactions, which involve the biorecognition and rejection of the nanocarrier by the immune system, is crucial for reducing clearance rates and achieving prolonged drug circulation time. The most well-known surface modifier for preventing immunogenic reactions is polyethylene glycol (PEG).

2.4.3. Triggered-Release Mechanisms: Functionalization of Nanocarriers with Copolymers Containing Stimuli-Responsive Functionalities

A triggered-release mechanism is a crucial functionalization property for drug delivery systems (DDSs). It allows the nanocapsules to actively participate, enabling the controlled activation of drug release, in contrast to conventional DDSs where the release is predetermined by the encapsulation material. Environmental changes, such as pH variations, temperature fluctuations, and optical or acoustic stimuli, can trigger the release of drug molecules.

The concept of a multifunctionalized drug-loaded nanocarrier is schematically depicted in Figure 2.7. The preparation of multifunctional magnetopolymeric nanohybrids poses a significant challenge and remains a subject of ongoing research. Issues related to biocompatibility and system stability become more crucial when the nanocarrier is loaded with drugs and further modified by antibodies to enhance targeting capabilities. Another key challenge is the development of high-quality, high-yield fabrication techniques for multifunctionalized drug-loaded nanocapsules.

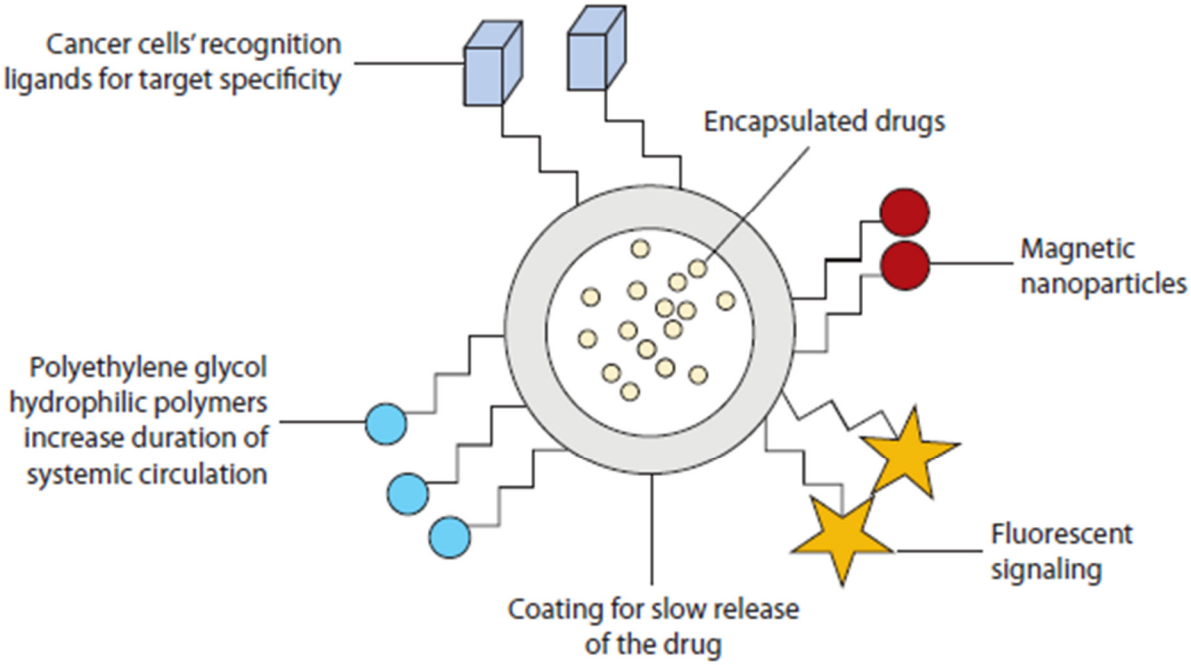


Figure 2.7. Multifunctionalized drug-loaded nanoparticle. The preparation of multifunctional, magnetopolymeric nanohybrids constitutes a major challenge and is a subject of ongoing research.

2.5. MRI-Based Propulsion, Tracking and Control

Demonstrating the controllable propulsion, tracking, and navigation of a nanocarrier with magnetic nanoparticles inside an MRI scanner is crucial. This section explores the latest developments in this area of study.

2.5.1. Magnetic Propulsion and Steering

In Carpi & Pappone, a magnetic navigation system from Stereotaxis Inc. was employed to propel a millimeter-sized endoscopic robotic capsule. Other studies, such as those by Maxwell and Helmholtz coil fields, also utilized magnetic propulsion and steering for microparticles, inducing the magnetic torque and force of a microrobot independently. Various concepts of magnetic propulsion include biomimetic robots using flagella, imitating the motion of eukaryotic bacteria, or attaching a magnetic bead to a helical nanocoil, imitating the motion of prokaryotic bacteria. Another concept involves magnetotactic bacteria, which are actuated through embedded or attached ferromagnetic material.

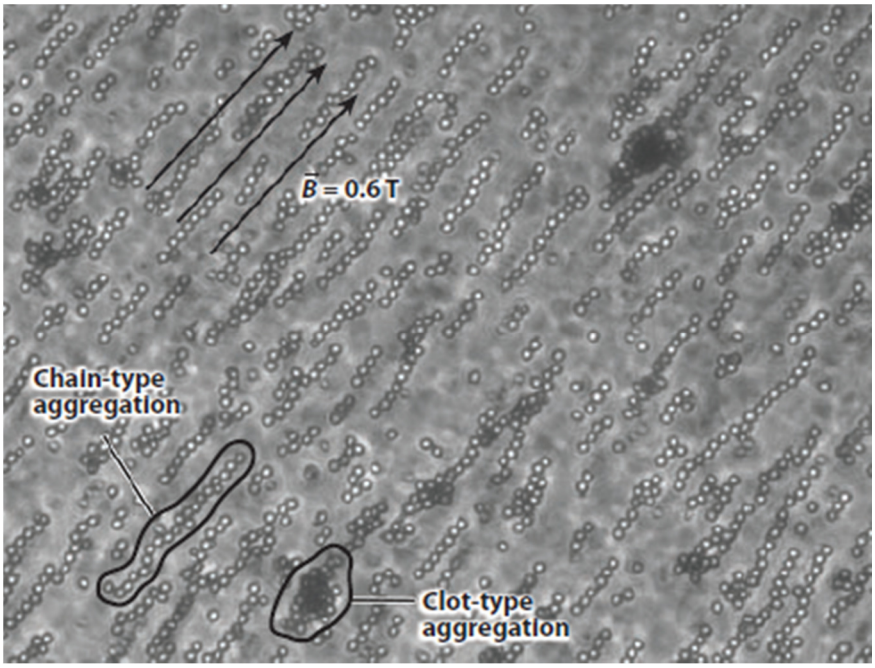


Fig. 2.8. Aggregation of superparamagnetic particles. The particle magnitude is 5 μm. The aggregation shape is chain-type or clot-type and has an average length of 60 μm. _B, magnetic field.

Demonstrating the use of magnetic gradients provided by a clinical MRI scanner to pull microparticles has been achieved at millimeter and micrometer scales, with the development of low-level multiplexed controllers and observers. In vivo experiments have been conducted on a living animal, although blood flow had been stopped using a balloon catheter. However, significant technical challenges arise as the particle size reduces to the nanoscale. Magnetic forces used for propulsion are volumetric, while the drag force is dependent on the particles' area. Consequently, propulsion with current MRI scanners is well-suited for particles up to a few dozen micrometers in radius. At lower scales, the required gradients exceed those generated by clinical MRI scanners. Research groups are exploring methods to increase magnetic forces acting on particles, such as using additional coils to supply higher gradients [24].

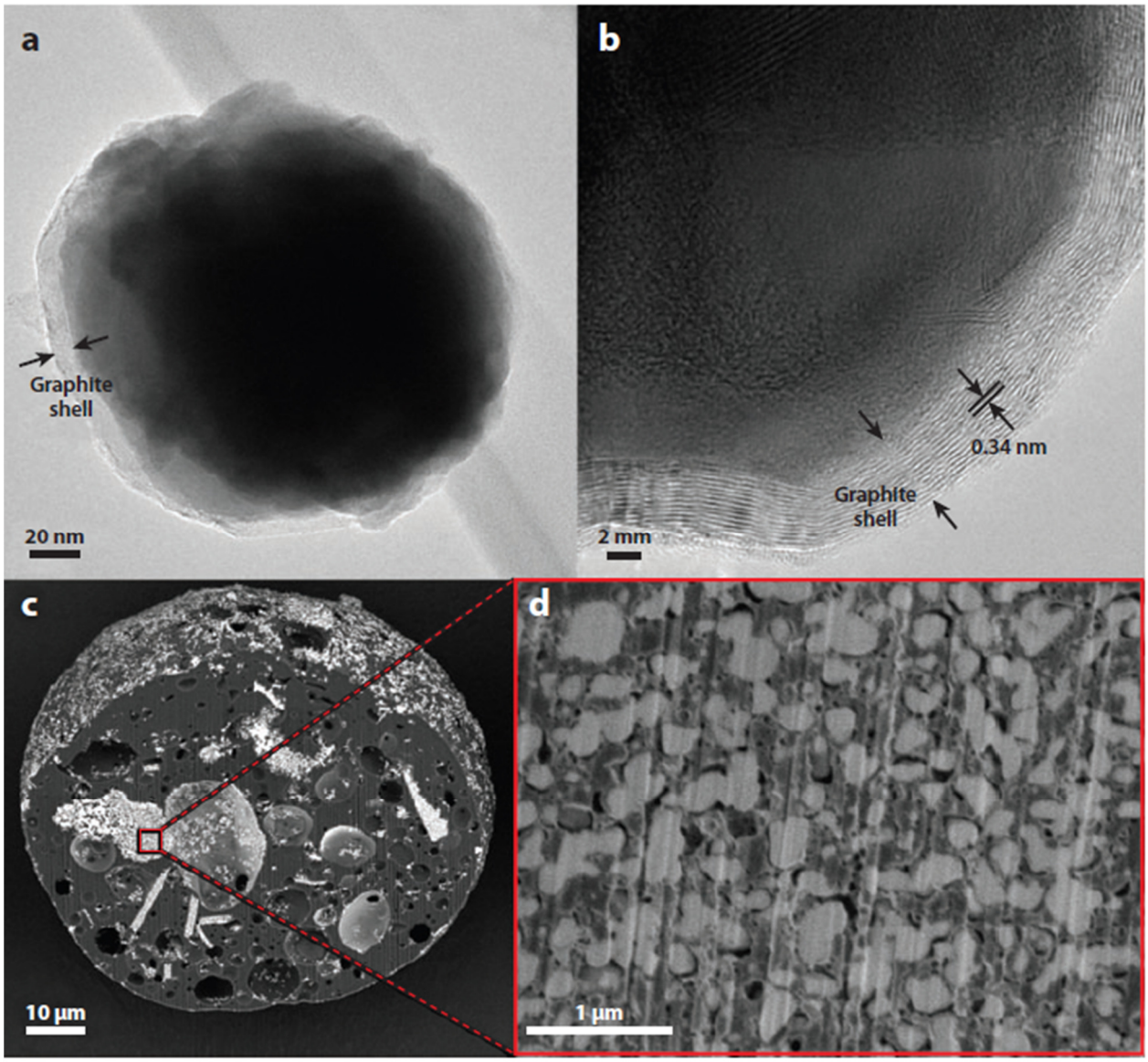


Figure 2.9. (a) TEM of a FeCo nanoparticle. (b) TEM image of the graphite shell of a FeCo nanoparticle. (c) SEM image of the cross section of a FeCo–PLGA microparticle (many nanoparticles are embedded in the PLGA). (d) FeCo nanoparticle distribution in the PLGA microparticle. Nanoparticles are shown in white, PLGA in gray, and the pores in back. PLGA, poly(lactic-co-glycolic) acid; SEM, scanning electron microscopy; TEM, transmission electron microscopy.

Additionally, MRI systems upgraded with additional gradient steering coils have been investigated to enhance standard MRI gradient amplitudes (100–500 mT). Another promising approach is leveraging the aggregation properties of magnetic micro- and nanoparticles, increasing the magnetic volume and resulting in a larger ratio of magnetic forces over drag forces (Figure 2.8.). A third approach involves encapsulating drug molecules and magnetic nanoparticles into larger, biodegradable polymer microcarriers, steering them in blood vessels near the tumor using additional gradient coils, and embolizing the surrounding capillaries. The embolized polymer carriers biodegrade, releasing therapeutic agents directed into the tumor. A combination of these approaches is anticipated to maximize targeting efficiency (figure 2.9.).

2.5.2. Imaging and Tracking in MRI Scanners

Hydrogen atoms, constituting a major component of water, are abundant in the human body, and various tissues can be distinguished based on hydrogen density and stability. MRI relies on exciting these atoms and allowing them to relax to equilibrium, thereby creating a map of their distribution and properties to generate an image of the body tissues in the observed slice. Clinical MRI involves four main steps. First, a permanent magnet generates a strong and uniform magnetic

field to align the spin magnetic moment of hydrogen nuclei (protons) along this field. Second, pulsing RF coils at Larmor frequency excite polarized protons, inducing resonance absorption. Third, RF excitation stops, and protons relax to their equilibrium state, producing a free induction decay (FID) signal in the RF coil. Simultaneously, gradient coils are used to select the observed slice during polarization and perform phase shift/frequency encoding during the readout, yielding 2D position encoding within the slice. Fourth, the slice image is obtained by applying inverse Fourier transforms to the measured FID signal.

The precision of an MRI system is closely tied to the uniformity and strength of the main magnet, influencing the signal-to-noise ratio. The speed and strength of the gradient coils, determined by their duty cycle, also impact precision and scanning speed. Utilizing MRI for 3D image guidance in endovascular procedures is highly valuable. Endovascular navigation is facilitated by integrating propulsion and tracking events through time multiplexing. The same equipment inducing motion in nanorobots can be used for localization by combining imaging/tracking procedures for precise navigation of an untethered interventional nanorobot. However, a drawback of MRI localization is the limited choice of materials for microrobot fabrication, as ferromagnetic objects can cause image artifacts. Efforts to enhance MRI sensitivity focus on developing new magnetic core materials and improving nanoparticle size or clustering. Shape control in nanoparticle research is emerging as a theme to influence biological behavior and electromagnetic properties. Localizing swarms of nanoparticles in an MRI system has been achieved using contrast agents, and nanoworms, elongated assemblies of nanoparticles, have shown enhanced magnetic relaxivity in MRI. Besides the trade-off between refresh rate and duty cycle of propulsion gradients, the repetition time of the tracking sequence is another consideration during imaging and tracking sequences. Fast and robust image processing algorithms remain key areas for future research.

2.6. Discussion

MRI DDSs (Drug Delivery Systems) present a promising avenue for targeted therapeutic agent delivery via intravascular routes. An advantageous feature is the use of three linearly independent, time-varying magnetic gradients, enabling precise targeting of deep-seated lesions within the human body—an accomplishment not feasible with static permanent magnets. The utilization of MRI enhances targeting accuracy and drug capture efficiency due to its trajectory tracking capabilities. Moreover, the widespread availability of MRI installations in hospitals worldwide makes this approach cost-effective.

However, challenges persist in the research on DDSs utilizing clinical MRI, particularly in achieving efficient real-time propulsion and position detection of nano- or microparticles. A significant hurdle lies in the disproportionate scaling of magnetic forces over drag forces, particularly in nanoscale dimensions. Magnetic gradients generated by MRI scanners are limited by factors such as the maximum permissible current in gradient coils and biological constraints preventing the application of high-magnitude and high-frequency magnetic gradients on human subjects.

Researchers are addressing these challenges through three primary approaches. Firstly, efforts are underway to enhance MRI gradient coils without significant cost implications. Secondly, strategies involve increasing the magnetic volume of therapeutic agents, either through aggregation techniques or encapsulation in biodegradable polymers. The third avenue explores novel magnetic materials with superior properties compared to traditional superparamagnetic nanoparticles, though challenges in biocompatibility testing and fabrication techniques must be addressed.

Additional challenges arise from the imaging system's limitations, including the need for high-frame-rate feedback with sufficient resolution for reliable robot control. Real-time control of nanocapsules requires fast acquisition and processing, necessitating the development of imaging processing software that operates in close proximity to image generation to minimize communication latencies.

Key issues in functionalizing drug-loaded nanocarriers involve using biomolecules, copolymers, and superparamagnetic nanoparticles while meeting stability, biodistribution, and biocompatibility criteria. The fabrication of nanocapsules, particularly those utilizing Carbon

Nanotubes (CNTs), faces challenges in systematic high-quality, high-yield production for drug containment. The potential toxic effects of CNTs and their suitability for biomedical applications are subjects of ongoing debate.

Despite these challenges, rapid technological and scientific advancements in MRI, nanocapsule fabrication, and nanorobotic manipulation suggest that critical components of a fully functional MRI DDS will soon reach technological maturity.

2.7. Conclusions

This review introduces the innovative concept of utilizing an MRI scanner to guide nanorobotic capsules within the human vasculature for drug delivery applications. The successful implementation of this MRI-based Drug Delivery System (DDS) holds the promise of significantly enhancing therapeutic efficiency while reducing side effects on healthy tissues. The system architecture of the MRI DDS encompasses functionalized drug-loaded nanocapsules, an MRI propulsion module, an MRI tracking module, a controller, and a user interface. Although a fully functional MRI DDS is yet to be developed, its realization poses unique challenges due to extreme scaling effects and the integration of diverse technologies with stringent requirements.

Despite these challenges, recent breakthroughs in nanoparticle manipulation, MRI technology, nanocapsules fabrication, and magnetic materials have brought critical components of the system architecture to a sufficient level of technological maturity. As a result, this nanorobotic concept stands at the threshold of becoming a reality. Ongoing advancements suggest that the development of a fully functional MRI DDS is imminent, offering a transformative approach to drug delivery with potential implications for improved therapeutic outcomes and minimized adverse effects on healthy tissues.

2.8. Quiz 2.

1. What is the primary inspiration for nanorobotics in medicine?
a). Antibodies
b). MRI scanners
c). Nanoparticles
d). MRI – guided drug delivery
e). Stem cells

2. What is the size range identified as critical for interactions with cells and circulation through the vasculature system?
a). 100-500 nm
b). 500-1000 nm
c). 30-300 nm
d). 1-10 micrometers
e). 10-50 micrometers

3. Which technique is proposed to enhance targeting capabilities of nanoparticles and nanovesicles?
a). Ultrasound imaging
b). MRI guidance
c). PET scanning
d). CT scanning
e). X-ray imaging

4. Which component serves as the interface between the MRI machine and the human operator?
a). Nanocarrier
b). Real-time navigation algorithm
c). Graphical user interface
d). MRI Propulsion System
e). Patient s medical history database

5. What is the primary role of the MRI tracking unit?
a). To estimate the position and accumulation of the nanocapsules
b). To generate magnetic forces and torques on the nanocapsules
c). To encapsulate drug molecules within the nanocapsules
d). To stabilize the micelles in aqueos dispersion
e). To monitor blood flow in real-time

6. Gold nanoparticles:
a.) Typically range from 100 nm to 140 nm
b.) Are characterized by photostability, high toxicity and robust light absorption
c.) Are also called colloidal gold
d.) Have found application in controlled drug delivery
e.) Were utilized in biological applications since 1981

7. Carbon nanotubes:
a.) Offer potential as nanocarriers due to their poor mechanical, thermal and electrical properties
b.) Have remarkable elasticity
c.) Have maximal interlayer friction

d.) Have excellent field- emission properties
e.) Come in single, double, or multiwall variations

8. Triggered-release mechanism:
a.) Is a crucial functionalization property for drug delivery systems
b.) It allows the nanocapsules to passively participate
c.) Environmental changes, such as pH variations, temperature fluctuations can trigger the release of drug molecules
d.) Enable the controlled activation of drug release
e.) Issues related to biocompatibility and system stability become more crucial when the nanocarrier is not loaded with drugs

9. Imaging and tracking MRI Scanners:
a.) Clinical MRI involves four main steps
b.) The precision of an MRI system is closely tied to the uniformity and strength of the main magnet
c.) The speed and strength of the gradient coils, determined by their duty cycle, do not impact precision and scanning speed
d.) Utilizing MRI for 3D image guidance in endovascular procedures is highly valuable
e.) Endovascular navigation is facilitated by integrating propulsion and tracking events through time multiplexing

10. MRI DDSs (Drug Delivery Systems):
a.) Do not present a promising avenue for targeted therapeutic agent delivery
b.) An advantageous feature is the use of four linearly independent
c.) The utilization of MRI enhances targeting accuracy and drug capture efficiency
d.) The widespread availability of MRI installations in hospitals worldwide makes this approach cost-effective
e.) Challenges persist in the research on DDSs utilizing clinical MRI, particularly in achieving unefficient real-time propulsion.

References

[1]. Ummat A, Dubey A, Mavroidis C. 2006. Bio-nanorobotics: a field inspired by nature. In Biomimetics: Biologically Inspired Technologies, ed. Y Bar-Cohen, pp. 201–28. Boca Raton, FL: CRC/Taylor & Francis
[2]. Berry CC, Curtis ASG. 2003. Functionalization of magnetic nanoparticles for applications in biomedicine. J. Phys. D 36:R198–206.
[3]. Hede S, Huilgol N. 2006. Nano: the new nemesis of cancer. J. Cancer Res. Ther. 2:186–95.
[4]. Gupta RB, Kompella UB. 2006. Nanoparticle Technology for Drug Delivery. New York: Taylor & Francis.
[5]. Bawa R. 2008. Nanoparticle-based therapeutics in humans: a survey. Nanotechnol. Law Bus. 5:135–55.
[6]. Bhushan B, ed. 2004. Handbook of Nanotechnology. Heidelberg: Springer-Verlag.
[7]. Cuenca AG, JiangH,Hochwald SN,DelanoM,CanceWG,Grobmyer SR. 2006. Emerging implications of nanotechnology on cancer diagnostics and therapeutics. Cancer 1:459–66.
[8]. Kingsley JD, Dou H, Morehead J, Rabinow B, Gendelman HE, Destache CJ. 2006. Nanotechnology: a focus on nanoparticles as a drug delivery system. J. Neuroimmune Pharmacol. 1:340–50.
[9]. Kiparissides C, Kammona O. 2008. Nanotechnology advances in controlled drug delivery systems. Phys. Status Solidi C 5:3828–33.
[10]. Langer R. 2001. Drug delivery: drugs on target. Science 293:58–59.
[11]. Orive G, Hernandez RM, Gascon AR, Pedraz JL. 2005. Micro and nano drug delivery system in cancer therapy. Cancer Ther. 3:131–38.
[12]. Sengupta S, Eavarone D, Capila I, Zhao G, Watson N, et al. 2005. Temporal targeting of tumour cells and neovasculature with a nanoscale delivery system. Nat. Lett. 436:568–72.
[13]. Uhrich K, Cannizaro S, Langer R, Shakeseff K. 1999. Polymeric systems for controlled drug release. Chem. Rev. 99:3181–98.
[14]. Arruebo M, Fernandez-Pacheco R, Ibarra MR, Santamaria J. 2007. Review: magnetic nanoparticles for drug delivery. Nano Today 2:22–32
[15]. Dobson J. 2006. Magnetic micro- and nano-particle-based targeting for drug and gene delivery. Nanomedicine 1:31–37.
[16]. Misra RDK. 2008. Magnetic nanoparticle carrier for targeted drug delivery: perspective, outlook and design. Mater. Sci. Technol. 24:1011–19.
[17]. Pankhurst QA, Connolly J, Jones SK, Dobson J. 2003. Applications of magnetic nanoparticles in biomedicine. J. Phys. D 36:R167–81.
[18]. Gillies GT, Ritter RC, Broaddus WC, Grady MS, Howard MA, McNeil RG. 1994. Magnetic manipulation instrumentation for medical physics research. Rev. Sci. Instrum. 65:533–62.
[19]. Alexiou C, Jurgons R, Seliger C, Brunke O, Iro H, Odenbach S. 2007. Delivery of superparamagnetic nanoparticles for local chemotherapy after intraarterial infusion and magnetic drug targeting. Anticancer Res. 27:2019–22.
[20]. Grief AD, Richardson G. 2005. Mathematical modeling ofmagnetically targeted drug delivery. J. Magn. Magn. Mater. 293:455–63.
[21]. Quate EG, Wika KG, Lawson MA, Gillies GT, Ritter RC, et al. 1991. Goniometric motion controller for the superconducting coil in a magnetic stereotaxis system. IEEE Trans. Biomed. Eng. 38:899–905.
[22]. Takeda S-I, Mishima F, Fujimoto S, Izumi Y, Nishijima S. 2006. Development of magnetically targeted drug delivery system using superconducting magnet. J. Magn. Magn. Mater. 311:367–71.
[23]. Abbott JJ, Ergeneman O, Kummer MP, Hirt AM, Nelson BJ. 2007. Modeling magnetic torque and force for controlled manipulation of soft-magnetic bodies. IEEE Trans. Robot. 23:1247–52.
[24]. Yesin KB, Vollmers K,Nelson BJ. 2006. Modeling and control of untethered biomicrorobots in a fluidic environment using electromagnetic fields. Int. J. Robot. Res. 25:527–36.
[25]. Abbott JJ, Peyer KE, Lagomarsino MC, Zhang L, Dong L, et al. 2009. How should microrobots swim? Int. J. Robot. Res. 28:1434–47
[26]. Martel S, Felfoul O, Mathieu J-B, Chanu A, Tamaz S, et al. 2009. MRI-based medical nanorobotic platform for the control of magnetic nanoparticles and flagellated bacteria for target interventions in human capillaries. Int. J. Robot. Res. 28:1169–82
[27]. Martel S, Mathieu J-B, Felfoul O, Chanu A, Aboussouan E, et al. 2008. A computer-assisted protocol for endovascular target interventions using a clinical MRI system for controlling untethered microdevices and future nanorobots. Comput. Aided Surg. 13:340–52.
[28]. Mathieu J-B, Beaudoin G, Martel S. 2006. Method of propulsion of a ferromagnetic core in the cardiovascular system through magnetic gradients generated by an MRI system. IEEE Trans. Biomed. Eng. 53:292–99.
[29]. Mathieu J-B, Martel S. 2007. Magnetic microparticle steering within the constraints of an MRI system: proof of concept of a novel targeting approach. Biomed. Microdevices 9:801–8.
[30]. Mathieu J-B, Martel S, Yahia LH, Soulez G, Beaudoin G. 2003. MRI systems as a mean of propulsion for a microdevice in blood vessels. Presented at IEEE Eng. Med. Biol. Soc., 25th, Cancun, Mexico.
[31]. Rosengart AJ, Kaminski MD, Chen H, Caviness PL, Ebner AD, Ritter JA. 2005. Magnetizable implants

and functionalized magnetic carriers: a novel approach for noninvasive yet targeted drug delivery. J. Magn. Magn. Mater. 293:633–38.
[32]. Yellen BB, Forbes ZG, Halverson DS, Fridman G, Barbee KA, et al. 2005. Targeted drug delivery to magnetic implants. J. Magn. Magn. Mater. 293:647–54.
[33]. Dreyfus R, Beaudry J, RoperML, FermigierM, Stone HA, Bibette J. 2005. Microscopic artificial swimmers. Nature 437:862–65.
[34]. Behkam B, Sitti M. 2006. Design methodology for biomimetic propulsion of miniature swimming robots. ASME J. Dyn. Syst. Meas. Control 128:36–43.
[35]. Behkam B, Sitti M. 2007. Bacterial flagella-based propulsion and on/off motion control of microscale objects. Appl. Phys. Lett. 90:1–3.
[36]. LeeH, Purdon AM, Chu V, Westervelt RM. 2004. Controlled assembly of magnetic nanoparticles from magnetotactic bacteria using microelectromagnets arrays. Nano Lett. 4:995–98.
[37]. Martel S, Mohammadi M, Felfoul O, Lu Z, Pouponneau P. 2009. Flagellated magnetotactic bacteria as controlled MRI-trackable propulsion and steering systems for medical nanorobots operating in the human microvasculature. Int. J. Robot. Res. 28:571–82.
[38]. Mathieu J-B, Martel S. 2007. In vivo validation of a propulsion method for untethered medical microrobots using a clinical magnetic resonance imaging system. Proc. IEEE/RSJ Int. Conf. Intell. Robots Syst., San Diego, Calif., pp. 502–8. Red Hook, NY: Curran Associates.
[39]. Darton NJ, Sederman AJ, Ionescu A, Ducati C, Darton RC, et al. 2008. Manipulation and tracking of superparamagnetic nanoparticles using MRI. Nanotechnology 19:395102
[40]. Bar J, Herbst RS, Onn A. 2009. Targeted drug delivery strategies to treat lung metastasis. Expert Opin. Drug Deliv. 6:1003–16.
[41]. Torchilin V. 2010. Passive and active drug targeting: drug delivery to tumors as an example. Handb. Exp. Pharmacol. 197:3–53.
[42]. Immordino ML, Dosio F, Cattel L. 2006. Stealth liposomes: review of the basic science, rationale, and clinical applications, existing and potential. Int. J. Nanomed. 1:297–315.
[43]. Bontha S, Kabanov A, Brovnich T. 2006. Polymer micelles with cross-linked ionic cores for delivery of anticancer drugs. J. Controll. Release 114:163–74.
[44]. Kwon GS, Kataoka K. 1995. Block copolymer micelles as long-circulating drug vehicles. Adv. Drug Deliv. Rev. 16:295–309.
[45]. BruchezMJ, Moronne M, Gin P,Weiss S, Alivisatos A. 1998. Semiconductor nanocrystals as fluorescent biological labels. Science 281:2013–16.
[46]. Seydel C. 2003. Quantum dots get wet. Science 300:80–81.
[47]. Gao X, Cui Y, Levnson RM, Chung LWK, Nie S. 2004. In vivo cancer targeting and imaging with semiconductor quantum dots. Nat. Biotechnol. 22:969–76.
[48]. Derfus A, Chan W, Bjatia S. 2004. Probing the cytotoxicity of semiconductor quantum dots. Nano Lett. 4:11–18.
[49]. Vo-Dinh T, ed. 2007. Nanotechnology in Biology and Medicine: Methods, Devices, and Applications. Boca Raton, FL: CRC/Taylor & Francis.
[50]. Hobbs S, Monsky W, Yuan F. 1998. Regulation of transport pathways in tumor vessels: role of tumor type and microenvironment. Proc. Natl. Acad. Sci. USA 95:4607–12.

3. Applications of nanotechnology in dental medicine

Nanodentistry represents a significant advancement in dental science and technology, focusing on the diagnosis, treatment, and prevention of oral and dental diseases using nanostructured materials. This field utilizes a variety of cutting-edge dental products, from implants to oral hygiene products, which benefit from the properties at the nanoscale. Techniques like Atomic Force Microscopy (AFM) and Optical Interferometry are employed to explore dental issues such as the characterization of dental enamel, oral bacteria, biofilms, and the interaction of surface proteins with biomechanical and nanomechanical properties of bacterial adhesions.

Recent developments in Nanodentistry are revolutionizing the field, including the use of saliva exosomes for diagnostics and the creation of biocompatible, antimicrobial dental implants. Although still in its formative stages, Nanodentistry promises to make dental procedures minimally invasive, enhancing the patient experience by making dental care more patient-friendly. Increasing patient awareness and education about these advancements is vital to help individuals understand their treatment options and the potential benefits of nanotechnology in dental care.

At the nanoscale, detailed examination of dental structures and surfaces offers profound insights into their structure, function, and physiological relationships, crucial for a deeper understanding of oral health and disease. Nanocharacterization tools are pivotal in studying oral diseases at molecular and cellular levels, which is essential for developing preventive strategies. These nano-enabled technologies offer superior methods to evaluate disease onset or progression, identify therapeutic targets, and design dental materials and implants that are more biocompatible and resistant to microbes.

Furthermore, advanced nanocharacterization technologies are essential in understanding the physiochemical mechanisms that enhance the biocompatibility and osseointegration of dental implants. By adopting nanoscale perspectives, researchers and clinicians can achieve a more comprehensive understanding of dental health, leading to the development of better diagnostic tools and treatment modalities for oral diseases. This holistic approach not only promises to improve dental care but also to transform the general perception of dentistry, ultimately benefiting patients' overall experiences.

3.1. Novel nanomaterials

Nanomaterials play a crucial role in modern dentistry, offering a diverse range of structures such as nanoparticles, nanoclusters, nanocrystals, nanotubes, nanofibers, nanowires, nanorods, and nanofilms. The fabrication of these nanomaterials involves various advanced technologies including electrospinning, phase separation, self-assembly, thin film deposition, chemical vapor deposition (CVD), chemical etching, nano-imprinting, and photolithography. These techniques allow for the creation of both ordered and random nanotopographies, enabling precise control over the properties of the nanomaterials [1].

In the realm of resin-based composite (RBC) ceramic restorative systems, there is a trend towards reducing the size of nanoparticles to better replicate the actual structure of natural dental tissues [2]. These nano composite systems, typically ranging from 1 nm to 100 nm, are designed to improve adhesion and create stable, natural interfaces between the tooth's mineralized tissues and advanced restorative materials [3]. Efforts are underway to enhance the formulations of interfacial silanes that coat and bond inorganic fillers within RBC matrices, with developments such as nanohybrid resins, nanofillers, and nanoadhesives that demonstrate superior mechanical, physical, and chemical properties.

Ormocer, an innovative material based on organically modified ceramics, is synthesized through sol-gel processes utilizing components such as silicones, organic polymers, and ceramic glasses [4]. Used frequently in dental composites, Ormocer technology incorporates nanoparticle fillers like ZnO2 to improve the performance of nanocomposite restorative systems.

Silver nanoparticles are gaining popularity as dental filling agents due to their unique properties, which include resistance to wear and their antibacterial and antifungal capabilities, making them highly beneficial for restorative dentistry [5]. Additionally, nanorods that mimic the structure of enamel rods are being used to better replicate the natural composition of teeth. Hydroxyapatite (HA) nanorods, with their enamel prism-like structure and self-assembly capabilities, are particularly effective in creating a realistic artificial approximation of tooth enamel [6]. These advancements highlight the transformative impact of nanotechnology in enhancing dental materials and treatments.

3.1.1. Nanocomposites

Discrete nanoparticles, when non-agglomerated and uniformly distributed within resins or coatings, lead to the creation of high-performance nanocomposites. In this application, the nanofiller used typically consists of aluminosilicate powder with an average particle size of 80 nm and a 1:4 molar ratio of alumina to silica. Additionally, this type of nanofiller has a refractive index of 1.508, aligning well with the optical properties required for dental applications.

The benefits of employing non-agglomerated discrete nanoparticles in resins or coatings are manifold. These nanocomposites exhibit enhanced hardness and flexible strength, which are critical for durability and wear resistance in dental applications. The modulus of elasticity is improved, which enhances the material's ability to endure stress without permanent deformation. From an aesthetic standpoint, these materials offer increased translucency and appealing esthetics, crucial for applications like dental veneers and crowns. They also boast excellent color density, high polish, and polish retention, features that contribute to their visual appeal and longevity in a clinical setting. Moreover, these nanocomposites are appreciated for their excellent handling properties, making them easier to work with during dental procedures. This combination of mechanical and aesthetic attributes makes non-agglomerated discrete nanoparticles an ideal choice for enhancing the performance and appearance of dental resins and coatings.

3.1.2. Nanofilled Resin-modified Glass Ionomer

A new nanofilled Resin-Modified Glass Ionomer (RMGI) restorative material has been introduced for the restoration of primary teeth and small cavities in permanent teeth. This material is based on a previous RMGI with a simplified dispensing and mixing system (paste/paste), requiring a priming step but no separate conditioning step.

The primary curing mechanism for this material is light activation, and there is no redox or self-curing during the setting process. Besides its user-friendliness, a significant innovation in this material is the incorporation of nanotechnology. This allows for a highly packed filler composition (69%), with approximately two-thirds of the fillers being nanofillers.

3.1.3. Nanosolution

Nanosolutions offer unique and dispersible nanoparticles that can be incorporated into various solvents, paints, and polymers, ensuring homogeneous dispersion. In the context of bonding agents, nanotechnology ensures the uniform mixing of adhesives with perfect consistency in every application. Additionally, nanoparticles have been employed as sterilizing solutions, taking the form of nanosized emulsified oil droplets that actively target and combat pathogens.

3.1.4. Nano-optimized Moldable Ceramics

Nanofillers contribute to improved polishing ability and reduced wear.

Nanopigments play a role in adjusting the shade of the restoration to match the surrounding teeth, creating a chameleon effect.

Nanomodifiers enhance the stability of the material and prevent it from sticking to instruments.

3.1.5. Impression Material

Recent advancements in impression materials have been driven by the integration of nanotechnology. Specifically, the incorporation of nanofillers into vinylpolysiloxanes has led to the development of a novel siloxane-based impression material. This innovative composition demonstrates enhanced fluidity, improved hydrophilic characteristics, and heightened precision in capturing fine details.

3.2. Dental Biomimetics

The advancement of nanorestorative technologies in dental structures presents compelling opportunities for leveraging nanotechnology to emulate natural biological processes, particularly those observed in biomimetics, such as dental enamel formation. The potential for cost-effective desktop manufacturing systems could revolutionize dental treatments by enabling the production of new teeth within the operational and financial boundaries of a standard dental appointment, thereby making full dentition replacement therapies viable.

Chen and colleagues have pioneered the use of nanotechnology to replicate the natural biomineralization process involved in the formation of dental enamel. They accomplished this by synthesizing highly organized microarchitectural units, which consist of nanorod-like calcium hydroxyapatite crystals aligned in a roughly parallel orientation [7].

3.3. Nanorobotics - Local Anesthesia

Micron-sized active analgesic dental robots, suspended in a colloidal solution applied to the patient's gingiva, navigate to the pulp through the gingival sulcus, lamina propria, and dentinal tubules. The deployment of nanorobots in dentistry involves intricate navigation that leverages a suite of environmental and positional cues—chemical gradients, temperature variations, and specific locational signals—all coordinated by an integrated nanocomputer under the dentist's supervision. These nanorobots traverse a path approximately 10 mm long from the tooth's surface to its pulp at a velocity of 100 μm/s, completing the journey in about 100 seconds.

Upon reaching the pulp chamber, these analgesic nanorobots, now interfacing with nerve-impulse pathways, can be precisely controlled via a handheld device operated by the dentist. This control allows for the targeted numbing of any specified tooth almost instantaneously. Following dental treatment, the dentist commands the nanorobots to reinstate full sensation, cease control over nerve signaling, and retract from the tooth using their entry routes, before being safely aspirated out [8].

Nanorobotic analgesics offer significant benefits including enhanced patient comfort, elimination of needle-based procedures, precise control over pain management, quick and reversible effects, and a reduction in potential side effects and complications (Fig. 3.1).



Figure 3.1. Nanorobots in local anesthetic solution.

3.4. Dental Hypersensitivity

In the case of natural hypersensitive teeth, there is an eightfold increase in the surface density of dentinal tubules and their diameter is twice as large compared to nonsensitive teeth. Reconstructive dental nanorobots, utilizing native biological materials, have the potential to selectively and precisely occlude specific tubules within minutes, providing patients with a rapid and permanent cure [9, 10, 11, 12].

Upon reaching the dentin, nanorobots enter dentinal tubular holes, which are typically 1 to 4 μm in diameter, and proceed toward the pulp. The guidance of nanorobots through this journey is orchestrated by a combination of chemical gradients, temperature differentials, and positional navigation—all controlled by the onboard nanocomputer under the dentist's direction. The pathways for nanorobots to travel from dentin to pulp can vary due to different tubular branching patterns, posing a significant challenge to navigation. Assuming a total path length of about 10 mm from the tooth surface to the pulp and a modest travel speed of approximately 100 μm/second, nanorobots can complete the journey into the pulp chamber in roughly 100 seconds. The presence of natural cells, in constant motion around and inside the teeth, including human gingival, pulpal fibroblasts, cementoblasts, odontoblasts, and bacteria within dentinal tubules, along with lymphocytes within the pulp or lamina propria, suggests that such a journey is feasible for cell-sized nanorobots with similar mobility.

3.5. Orthodontic Treatment

In orthodontic practice, the movement of teeth along an archwire is counteracted by frictional forces, which can complicate treatment by causing anchor loss and root resorption if the applied forces are too high. A significant reduction in this friction has been achieved by Katz through the application of a coating of inorganic fullerene-like tungsten disulfide nanoparticles (IFWS2) on the orthodontic wires. These nanoparticles are celebrated for their exceptional properties in dry lubrication, facilitating smoother movement of the teeth during adjustments [13].

Looking to the future, the implementation of orthodontic nanorobots presents an exciting frontier. These nanorobots could directly alter periodontal structures such as the gingivae, periodontal ligament, cementum, and alveolar bone. This advanced technology could significantly speed up orthodontic procedures, allowing for teeth to be straightened, rotated, or repositioned vertically within

mere minutes to hours—a stark contrast to traditional methods like molar uprighting, which can take weeks or months to accomplish the same results (Fig. 3.2).



Figure 3.2. Orthodontic nanorobots

3.6. Nanorobotic Dentifrice (Dentifrobots)

The prospect of a mouthwash infused with smart nanorobots presents an intriguing possibility for oral health. These nanorobots could potentially identify and eliminate pathogenic bacteria, promoting the growth of healthy flora in the mouth. Moreover, they might detect particles of food, plaque, or tartar, lifting them from the teeth for easy rinsing. As these nanorobots would be suspended in liquid and capable of swimming, they could access surfaces beyond the reach of toothbrush bristles or traditional floss.

These dentifrobots, ranging from 1 to 10 microns in size and moving at speeds of 1 to 10 microns per second, would be cost-effective, purely mechanical devices. The dentifrobots would be engineered to shut down harmlessly in case of accidental ingestion and equipped with precise occlusal avoidance algorithms. With the right settings, these dentifrobots could detect and eradicate harmful bacteria residing in plaque and various oral regions, fostering the growth of beneficial oral microflora. Additionally, they could provide a continuous defense against halitosis, addressing bacterial putrefaction—a central process in oral malodor. With such daily dental care available from an early age, the conventional issues of tooth decay and gingival disease could become obsolete [14, 15].

3.7. Nanoencapsulation

The Southwest Research Institute (SWRI) has pioneered targeted release systems utilizing nanocapsules across various domains, including innovative vaccines, antibiotics, and drug delivery methods aimed at minimizing adverse effects. Prospective future applications may encompass specialized nanoparticles tailored to target oral tissues, particularly those originating from the periodontium. SWRI has also introduced additional products, such as protective gear and filtration masks incorporating antipathogenic nanoemulsions and nanoparticles. Furthermore, SWRI has contributed to the advancement of medical adjuncts for rapid healing, including biodegradable nanofibers acting as a platform for hemostatic agents, wound dressings featuring silk nanofibers, and

wound dressings incorporating nanocrystalline silver particles (ActicoatTM, UK) endowed with antimicrobial attributes.

Moreover, SWRI has been actively engaged in the development of nanocarriers targeting bones. These carriers, utilizing calcium phosphate biomaterials, offer a malleable paste capable of conforming to and integrating with host bone structures, thereby facilitating the proliferation of cartilage and bone cells.

3.8. Materials to induce Bone Growth

Nanotechnology aims to replicate the natural nanostructure of bone, which is a composite of organic compounds (mainly collagen) reinforced with inorganic ions, such as hydroxyapatite (HA). Nanobone, for example, utilizes the principle that smaller particle sizes result in larger surface areas, promoting a loose microstructure with nanopores between nanocrystallites. This structure, along with micrometer-sized pores, creates a rough surface at the biomaterial-cell boundary, crucial for rapid cell growth. The interconnected pores retain blood plasma containing essential proteins.

Several hydroxyapatite nanoparticles used for treating bone defects include:

- Ostium (Osartis GmbH, Germany) HA
- VITOSSO (Orthovita, Inc, USA) HA + TCP
- NanOSSTM (Angstrom Medica, USA) HA.

A new nanobioactive glass, developed in concentrations less than 4 mg/ml, has shown biocompatibility with gingival fibroblasts in vitro. Additionally, a calcium sulfate-based nanocomposite, BoneGen-TR, has been formulated by Dr. Ricci. This composite resorbs more slowly and consistently regenerates bone, making it suitable for filling small voids in post-extraction sockets and periodontal bone defects.

3.9. Nanoneedles

Scientists have achieved precise surgical operations on specific living cells using nanoneedles, which are nanosized stainless steel needles a few billionths of a meter wide. These nanoneedles enable cell surgery on a microscopic scale, allowing for intricate procedures at the cellular level. Nanoneedles can be utilized to deliver molecules, including nucleic acids, proteins, or other chemicals, to the nucleus of cells. The key advantage of this method is the ability to target very specific locations within the nucleus. The trade name for these nanoneedles is Sandvik Bioline, RK 91TM needles, developed by AB Sandvik in Sweden.

3.10. Nanotweezers

The Nanohand research group in Denmark has developed nanotweezers, a technology capable of both imaging and manipulating nanosized objects. This innovation holds the potential to make cell surgery feasible in the near future. The nanotweezers are part of ongoing dental research focused on single particle surveillance and manipulation using laser nanotweezer technology. These nanotweezers consist of two wires tapered consecutively through a nanopipette while being kept electrically isolated. The development of nanotools, including nanotweezers, nanobearings, and nano-oscillators, represents a significant advancement in the manipulation of nanoscale objects.

3.11. Nanomaterials for Periodontal Drug Delivery

Nanomaterials are extensively explored for controlled drug release, including hollow spheres, core-shell structures, nanotubes, and nanocomposites. Controlled drug release involves incorporating drugs into nanospheres made of biodegradable polymers, allowing for timed release as the nanospheres degrade. This approach facilitates site-specific drug delivery. Triclosan-loaded nanoparticles, prepared with poly (d, l-lactide-co-glycolide), poly (d, l-lactide), and cellulose acetate phthalate, have demonstrated effectiveness in reducing inflammation. Tetracycline incorporated into microspheres, as seen in products like Arestin, enables local drug delivery into periodontal pockets.

Additionally, a nanostructured 8.5% doxycycline gel has shown efficacy in preserving periodontal surfaces in experimental periodontal disease in rats.

3.12. Photodynamic Therapy

Antimicrobial Photodynamic Therapy (aPDT) is a novel treatment method designed for the removal of infectious pathogens using a combination of a photosensitizer and light of a specific wavelength. For instance, toluidine blue, with a wavelength of about 600 nm, is used as a photosensitizer. In recent developments, methylene blue, another photosensitizer, has been encapsulated within poly (D,L lactide-co-glycolide) (PLGA) nanoparticles, measuring approximately 150-200 nm in diameter. This encapsulation offers a novel nanoplatform design for improved drug delivery and enhanced photodestruction of oral biofilms. Another photosensitizer, indocyanine green (ICG), loaded into nanospheres with an 805 nm wavelength low-level diode laser irradiation, has demonstrated an aPDT-like effect. This may have potential applications in photodynamic periodontal therapy.

3.13. Implants

The utilization of nanotechnologies is on the rise for surface alterations of dental implants, aiming to improve characteristics like chemistry and roughness. These enhancements are pivotal in attaining and sustaining long-term stability within bone tissue. The primary objective is to foster direct bone-to-implant contact to facilitate biomechanical anchorage, rather than the encapsulation of fibrous tissue. Recent developments in nanostructured implant coatings include:

1. Nanostructured Diamond: These coatings exhibit ultra-high hardness, improved toughness compared to conventional microcrystalline diamond, low friction, and good adhesion to titanium alloys.
2. Nanostructured Hydroxyapatite Coatings: Nanostructured processing is applied to hydroxyapatite coatings to achieve desired mechanical characteristics and enhanced surface reactivity. This has been found to increase osteoblast adhesion, proliferation, and mineralization.
3. Nanostructured Metalloceramic Coatings: These coatings provide a continuous variation from a nanocrystalline metallic bond at the interface to a hard-ceramic bond on the surface.

Various nanostructured materials, including ceramics, carbon fibers, polymers, metals, and composites, are employed to enhance osteoblast adhesion and calcium/phosphate mineral deposition. Some studies suggest that nanophase ZnO and TiO2 may reduce bacterial adhesion and enhance osteoblast functions, contributing to the efficacy of orthopedic implants.

3.14. Nanomaterials for Healing of Wounds

Located in Wakefield, USA, Nucryst has pioneered a wound-healing material, commonly employed in specialized burn treatment facilities across America. This innovative dressing integrates nanocrystalline silver, renowned for its antimicrobial properties. It effectively combats approximately 150 varieties of fungi and bacteria, encompassing various antibiotic-resistant strains.

Additionally, some companies have incorporated nanoparticles into plastic materials to impart biocidal properties. This innovation is particularly valuable for devices implanted inside the body, where maintaining a sterile environment is crucial.

3.15. Bionic Mandible

The concept of a bionic mandible involves reconstructing the entire mandible to function and provide sensation similar to a normal mandible. This idea draws inspiration from the development of bionic limbs, such as the first bionic arm constructed for Sullivan by Todd Kuiken and his team. Nanotechnology-enabled robotic myoelectric prosthetic limbs have played a role in advancing the field of bionics, allowing for more sophisticated and functional artificial limbs. The application of

nanotechnology in bionics holds promise for creating advanced prosthetic devices that closely mimic the capabilities of natural body parts.

3.13. Safety Aspects of Nanotechnology

The use of nanomaterials and nanotechnologies in various applications has indeed led to significant health and healthcare advances. However, it is crucial to acknowledge and address potential side effects and health risks associated with their use. Some of the main health risks related to nanomaterials and nanotechnologies include:

1. Cytotoxicity: Some nanoparticles have been found to be cytotoxic, meaning they can cause damage to cells. Increased surface area of certain nanoparticles may contribute to their heightened toxicity.
2. Translocation to Undesired Cells: Nanoparticles may translocate to unintended cells or tissues in the body, potentially leading to adverse effects.
3. Acute and Chronic Toxicity: Exposure to certain nanomaterials has been associated with both acute and chronic toxicity, which can have varying effects on different organs and biological systems.
4. Unpredictable and Indeterminate Safety Concerns: The safety of certain nanomaterials and their long-term effects are still not fully understood, leading to unpredictable safety concerns.
5. Environmental Impact: Nanomaterials may pose environmental risks, and their long-term impact on ecosystems is an area of concern.
6. Non-Biocompatibility: Some nanoparticles may not be biocompatible, meaning they may not interact well with biological systems and may elicit immune responses.

Carbon nanotubes, metals, and metallic oxide nanoparticles are examples of nanomaterials that have been studied for their potential health risks. It is essential to note that the field is still evolving, and ongoing research is necessary to better understand the potential risks associated with nanotechnology.

Regulatory agencies such as the FDA, EPA, and others are working to establish guidelines and regulations for the safe use of nanomaterials. Standardization of nanotechnology-based products, thorough characterization, safety assessments, and consideration of environmental impact are critical components of responsible development and use of nanotechnologies.

In the context of medical nanorobots, there is a mention of materials used, including nonpyrogenic materials like bulk Teflon, carbon powder, and monocrystal sapphire, as well as pyrogenic materials like alumina, silica, copper, and zinc. The discussion emphasizes the importance of understanding and mitigating potential health risks associated with nanorobots.

In conclusion, while the benefits of nanotechnology are significant, ongoing research and regulatory efforts are necessary to ensure the safe and responsible use of nanomaterials and nanotechnologies in various applications.

3.14. Conclusion

The passage highlights the transformative impact of nanotechnology on various aspects of dental practice. Key points include:

1. Changes in Traditional Approaches: New science and technologies, particularly nanotechnology, are influencing all facets of dental practice. These changes extend to diagnostics, risk assessment, prevention, and various procedures.
2. Major Impact on Restorative Dentistry: Nanotechnology, especially through nanostructures like nanoparticles, nanotubes, nanorods, etc., has significantly impacted restorative dentistry. It has enhanced established clinical resin-based composite (RBC) systems.
3. Role of Nanocomposites and Nanomaterials: Nanocomposites and nanomaterials are anticipated to play a significant role in material development for the dental trade, contributing to the improvement of dental materials.

4. Enhancements in Diagnosis and Treatment: Nanotechnology has improved the understanding of the pathophysiologic basis of diseases, leading to refinements in diagnosis and more efficient treatment and preventive properties.
5. Potential of Nanodentistry: Nanodentistry, involving the use of nanomaterials, biotechnology (including tissue engineering and gene therapy), and dental nanorobotics, has the potential to preserve complete oral health.
6. Future Core Technology in Dentistry: The passage suggests that nanotechnology is expected to evolve into the core technology underlying dentistry, pointing to its increasing importance in shaping the future of dental practices.
7. Importance of Open Sharing and Research: Success in the future development of nanotechnology in dentistry is emphasized to require open sharing of ideas and research findings, testing, and open discussions among professionals.
8. Exciting Future Applications: The passage concludes with an optimistic view, expressing that the future will be amazing, and the potential applications of nanotechnology in dentistry will be limited only by imagination.

In summary, the passage highlights the ongoing and potential future impacts of nanotechnology on dentistry, emphasizing advancements in materials, diagnostics, treatment, and the overall improvement of oral health through nanodentistry.

3.15. Quiz 3.

1.Which of the following are examples of nanomaterials used in dentistry?
a). Silver nanoparticles
b). Enamel prism-like nanorods
c). Iron nanoparticles
d). Gold nanoparticles
e). Titanium dioxide nanoparticles

2. What advantages do nanorobotic analgesics offer in dental procedures?
a). Increased patient comfort and reduced anxiety
b). Fully reversible action
c). Avoidance of most side effects and complications
d). Rapid onset of action
e). Long-lasting effects

3. What applications does nanoencapsulation have in dental medicine?
a). Targeted release systems for drug delivery
b). Targeting oral tissues
c). Treatment of bone defects
d). Improvement of enamel strength
e). Prevention of dental caries

4. Which materials are used to induce bone growth in dentistry?
a). Hydroxyapatite nanoparticles
b). Nanobone
c). Calcium sulfate-based nanocomposite
d). Titanium nanoparticles
e). Zirconium nanoparticles

5. What are the benefits of using nanotechnology in orthodontic treatment?
a). Reduction in friction
b). Rapid and painless tooth movement
c). Improved selectivity and controllability of treatment
d). Avoidance of root resorption
e). Enhanced stability of orthodontic appliances

6. What hydroxyapatite nanoparticles are used for treating bone defects?
a.) Ostium (Osartis GmbH, Germany) HA
b.) Ostium (Osartis GmbH, Germany) HA + TCP
c.) VITOSSO (Orthovita, Inc, USA) HA + TCP
d.) NanOSSTM (Angstrom Medica, USA) HA
e.) NanOSSTM (Angstrom Medica, USA) HA + TCP

7. Nanoneedles:
a.) Are nanosized stainless steel needles a few billionths of a centimeter wide
b.) Enable cell surgery on a microscopic scale
c.) Can be utilized to deliver molecules, but not nucleic acids
d.) The key advantage of this method is the ability to target very specific locations within the nucleus
e.) The trade name for these nanoneedles is Sandvik Bioline, RK 91TM needles

8. What recent developments do nanostructured implant coatings include?
a.) Nanostructured diamond
b.) Nanostructured hydroxyapatite coatings
c.) Nanostrucutred hydroxyapatite diamond
d.) Unstructured coatings
e.) Nanostructured metalloceramic coatings

9. Which of the following affirmations are true?
a.) The concept of a bionic mandible involves reconstructing the entire mandible to function and provide sensation similar to a normal mandible
b.) This idea draws inspiration from the development of bionic limbs
c.) The application of nanotechnology in bionics holds promise for creating advanced prosthetic devices that closely mimic the capabilities of natural body parts
d.) Nanotechnology-enabled robotic myoelectric prosthetic limbs have played a role in advancing the field of bionics, allowing for more simple and functional artificial limbs
e.) The concept of a bionic mandible involves reconstructing just a part of the mandible

10. Some of the main health risks related to nanomaterials and nanotechnologies include:
a.) Biocompatibility
b.) Predictable safety concearns
c.) Translocation to desired cells
d.) Cytotoxicity
e.) Acute and chronic toxicity

References

[1]. Chen VJ, Ma PX. Nano□fibrous poly (L□lactic acid) scaffolds with interconnected spherical macropores. Biomaterials 2004;25:2065□73.
[2]. Saunders SA. Current practicality of nanotechnology in dentistry. Part 1: Focus on nanocomposite restoration and biomimetcs. J Clin Cosm Invest Dent 2009;1:47□61.
[3]. Terry DA. Direct applications of a nanocomposite resin system: Part 1. The evolution of contemporary composite materials. Pract Proced Aesthet Dent 2004;16:417□22.
[4]. Moszner N, Salz U. New developments of polymeric dental composites. Prog Polym Sci 001;26:535□76.
[5]. Garcia□Contreras R, Augeta□Figueoroa C, Mejija Rabalcava C, Jimenez□Martinez R, Cuevas Gujardo S, Sanchez□Reyna PA, et al. Perspectives for the use of silver nanoparticles in dental practice. Int Dent J 2011;61:297□301.
[6]. Chen H, Clarkson BH, Sun K, Mansfield JF. Self□assembly of synthetic hydroxyapatite nanorods into an enamel prism□like structure. J Colloid Interface Sci 2005;288:97□103.
[7]. Mallanagouda Patil, Dhoom Singh Mehta. Future impact of nanotechnology on medicine and dentistry. J Ind Soc Periodontol 2008;12(2):34-40.
[8]. Mjör IA, Nordahl I. The density and branching of dentinal tubules in human teeth. Arch Oral Biol 996;41(5):401-412.
[9]. Freitas RA Jr. Nanodentistry. J Am Dent Assoc 2000;131(11): 1559-1566.
[10]. Kong LX, Peng Z, Li SD, Bartold PM. Nanotechnology and its role in the management of periodontal diseases. Periodontol 2000. 2006;40:184-196.
[11]. Mjör IA, Nordahl I. The density and branching of dentinal tubules in human teeth. Arch Oral Biol 1996;41(5):401-412.
[12]. Freitas RA. Jr. Exploratory design in medical nanotechnology: A mechanical artificial red cell. Artificial Cells Blood Substitute Immobile Biotechnology. 1998;26:30-32.
[13]. Freitas RA. Jr. Exploratory design in medical nanotechnology: A mechanical artificial red cell. Artificial Cells Blood Substitute Immobile Biotechnology. 1998;26:30-32.
[14]. Shwetarnbari S. Nanorobots in Dentistry. (Online) (cited 2006 August 29). Available at: www.dharwadhubli.com.
[15]. Saravana Kumar R, Vijayalakshmi R. Nanotechnology in Dentistry. Ind J Dent Res 2006;17(2):62-65.

4. Nanotechnology in dental materials

Restorative dentistry is dedicated to the diagnosis and management of conditions affecting teeth and their supporting structures. Advanced techniques play a crucial role in repairing and replacing damaged tooth structures, restoring tooth function, and enhancing overall aesthetics [1].

Nanotechnology has emerged as a significant contributor to the manufacturing of biocompatible and non-toxic dental restorative materials, including Glass Ionomer Cement (GIC), dental composites, dental implants, and endodontic materials [2]. In recent years, resin-based dental restorative materials have experienced notable advancements. The incorporation of nanoparticles into the resin matrix of dental composites has proven beneficial, leading to improvements in mechanical properties, reduced polymerization shrinkage, increased abrasion resistance, and enhanced surface hardness [3, 4]. A recent study demonstrated that adding fluoro-aluminosilicate glass nanoparticles to GIC resulted in enhanced mechanical and aesthetic properties [5]. Additionally, Nanoionomers like Ketac™ Nano from 3M ESPE have been introduced for clinical use [6].

Nanomaterials can be categorized in diverse ways, considering their application and composition. In this context, the classification is based on their shape and composition. Nanomaterials with distinct shapes fall into categories such as Nanoparticles, Nanotubes, and Nanoplatelets.

4.1. Nanoparticles

Nanomaterials based on nanoparticles encompass both conventional and unconventional types. Conventional nanoparticles comprise metallic NPs and metal oxides NPs, which have been extensively researched for various applications over the decades.

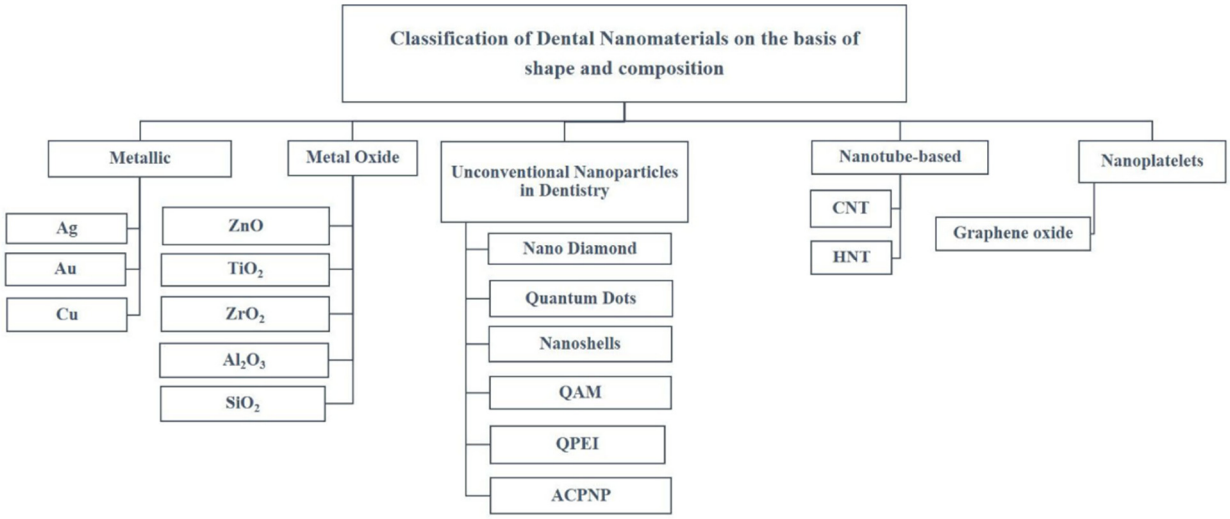


Figure 4.1. Classification of Dental Nanomaterials on the bases of shape and composition.

Unconventional nanoparticles, such as nano diamonds, nanoshells, and quantum dots, represent innovative fillers for advanced dental materials. These unconventional NPs offer versatility and can be easily modified to suit specific applications (Figure 4.1.).

4.1.1. Metallic Nanoparticles

Metallic nanoparticles are produced through processes that involve reducing larger particles to smaller ones, achieving sizes on the nanoscale. These metal nanoparticles exhibit enhanced antibacterial activity in comparison to traditional metals. This heightened antibacterial effectiveness has become a focal point in dental research, emphasizing the potential applications and benefits of metallic nanoparticles in dentistry.

4.1.1.1. Silver Nanoparticles (AgNPs)

Silver has been known for its antibacterial properties for centuries, and recent research has expanded its applications in therapeutics through nanotechnology. The mechanism of action involves

silver ions inactivating enzymes, leading to the failure of DNA replication and subsequent cell death in microorganisms [7]. This antibacterial potential of silver can be harnessed in dental materials [8].

In recent publications, silver nanoparticles (AgNPs) have demonstrated high antibacterial efficacy as fillers in dental restorative materials [9]. They not only provide excellent antibacterial properties but also contribute to better aesthetic outcomes without compromising the mechanical properties of the dental composite. Studies have shown that incorporating AgNPs in dental composites can reduce lactic acid formation and biofilm growth on teeth, thereby preventing secondary caries [10]. AgNPs have also been employed in endodontic sealers, showing high antibacterial efficiency [11].

Researchers have explored the dual-action properties of AgNPs when combined with other bioactive agents, aiming for remineralization coupled with antibacterial effects [12]. In dental composites, the incorporation of AgNPs has resulted in a significant increase in strength along with antibacterial activity [13]. Studies using AgNP-containing gels have shown notable antibacterial activity against biofilms at low concentrations, outperforming commercially available dental composite products in terms of mechanical properties such as flexural strength and elastic modulus [14].

4.1.1.2. Gold Nanoparticles (AuNPs)

Gold has long captivated researchers due to its inert and biocompatible nature, coupled with its antibacterial properties. In recent studies, gold nanoparticles (AuNPs) have emerged as potential carriers for nano drug delivery in cancer treatment and diagnosis [15]. Various gold nanostructures, including nanospheres and nanorods, have been synthesized for applications such as photothermal agents, contrast agents, and drug delivery carriers [16].

Heo et al. reported on the surface immobilization of titanium dental implants with AuNPs, utilizing these nanocomposites as osteoinductive agents. This surface modification promotes the rapid formation of bone around dental implants, supporting nascent bone formation. AuNPs exhibit lower toxicity compared to other metal nanoparticles and offer diverse synthesis methods, including chemical functionalization. The versatility of gold nanoparticles makes them promising candidates for enhancing dental implant performance and bone regeneration [17].

4.1.1.3. Copper Nanoparticles (CuNPs)

Copper is an essential element for the metabolism of both animal and plant cells, serving as a trace component present in nearly all organisms. It plays a crucial role in over 30 types of proteins. Copper nanoparticles (CuNPs) generate hydroxyl radicals that disrupt the cell membrane of microorganisms, leading to leakage and cell death. CuNPs attach to carboxylic and amine groups on the microorganism surface, inducing alterations that destabilize cell membranes and result in cell death [18].

The presence of copper ions induces the generation of free radicals capable of altering DNA replication and protein synthesis in microorganisms. Recent reports highlight the antimicrobial activity of CuNPs against S. mutans when added to dental adhesives [19]. This addition prevents the degradation of the adhesive interface without compromising the mechanical properties of the formulations. Metal nanoparticles with antimicrobial properties, such as copper, hold promise for future applications in treating dental diseases by combating bacteria and microorganisms [20].

4.1.2. Metal Oxide Nanoparticles

Metal oxide nanoparticles refer to oxides of metal particles that exhibit increased stability in their oxide form. In recent years, there has been extensive research on the potential role of metal oxide nanoparticles as antimicrobial agents and fillers in dentistry.

4.1.2.1. Zinc Oxide Nanoparticles (ZnO NPs)

Zinc exhibits effective antibacterial activity at the nanoscale, and its efficiency in this regard significantly increases. When a Zinc ion interacts with the bacterial cell membrane, it binds to proteins

and lipids, inducing an osmotic imbalance that enhances membrane permeability and leads to cell death [21]. Zinc nanoparticles generate oxygen radicals and Zn2+ ions, intensifying oxidative stress and inhibiting the growth of microorganisms [22]. Studies on cell lines, such as human embryonic lung fibroblasts (HELF) and gastric epithelial cell lines (GES-1), have shown that ZnO nanoparticles have less cytotoxic effects, which can be further enhanced when administered with ascorbic acid [23]. Research, such as that conducted by Kasraei et al., has demonstrated the significant antibacterial activity of dental composite resins containing ZnO nanoparticles and AgNPs against Streptococcus mutans and Lactobacillus [24]. Additionally, Wang et al. have shown the positive impact of small amounts of cellulose nanocrystal/ZnO NPs combination nanohybrids on the mechanical and antibacterial properties of dental resin composites [25]. The incorporation of ZnO nanoparticles in various dental materials holds promise for harnessing their antibacterial properties [26].

4.1.2.2. Titanium Dioxide-Based Nanoparticles (TiO_2NPs)

Titanium alloys are widely utilized in dentistry due to their exceptional properties, including high strength, corrosion resistance, and biocompatibility [27, 28]. When exposed to ultraviolet (UV) rays, Titanium Dioxide (TiO2) generates reactive oxygen radicals (H2O2 and OH−), creating an osmotic imbalance in microorganisms and disrupting their phosphorylation, ultimately leading to bacterial cell lysis [29]. Previous reports have indicated that high concentrations of TiO2 nanoparticles can induce inflammatory responses in human gingival fibroblasts [30]. GIC modification with TiO2 demonstrates moderate biocompatibility on Oral Squamous Cell Carcinoma Cell Lines [31]. The incorporation of TiO2 nanoparticles into composite resins has exhibited significant antibacterial activity, resulting in reduced colony counts of Streptococcus mutans and Streptococcus sanguinis [32]. Nanoscale modification of the Titanium surface, achieved through a chemical etching technique, has shown improved results in terms of the proliferation of murine preosteoblastic cells in vitro compared to rough and smooth surfaces of pure titanium [33, 34]. Further research and investigations are still necessary to explore the potential future oral applications of TiO_2.

4.1.2.3. Zirconium dioxide Nanoparticles (ZrO_2NPs)

Zirconium dioxide (ZrO_2) has been a crucial component in the production of dental materials for an extended period. Referred to as "ceramic steel," zirconia exhibits superior toughness, strength, fatigue resistance, excellent wear resistance, and biocompatibility. Its properties closely resemble those of natural teeth, ensuring better aesthetics.

Zirconia nanoparticles can be generated using techniques such as laser vaporization, producing nanoparticles ranging from 20 to 50 nm in size [35]. Zirconia's biocompatibility, osseo-conductivity, and ability to reduce plaque accumulation make it an ideal choice for manufacturing dental implants and coating materials for dental prostheses. ZrO_2NP can serve as a filler to reinforce the polymethyl methacrylate (PMMA) matrix, enhancing mechanical properties [36].

Zirconia-based ceramics exhibit superior strength and bending resistance compared to alumina ceramics [37]. When used as a filler in dental nanocomposites, ZrO_2NP improves mechanical properties, aesthetics, and radiopacity. Dental composites incorporating zirconia nanoparticles demonstrate enhanced fracture toughness [38]. The addition of ZrO_2NP to glass ionomer cement (GIC) restorative cement improves compressive strength and reduces cracks within the cement matrix [39]. ZrO_2NPs, when added to the manufacturing of dental dentures, contribute to high strength, color stability, and low electrical and thermal conductivity [40].

4.1.2.4. Aluminium Oxide Nanoparticles (Al_2O_3 NP)

Aluminium oxide nanoparticles (Al_2O_3 NPs) can be synthesized using various methods, including wet-chemical synthesis, mechanical ball milling, laser ablation, exploding wire, and the solution of reduction and decomposition processes. Due to their high reactivity to moisture, heat, and sunlight, safety precautions are essential for handling this material. Al_2O_3 NPs should be stored in a vacuum, in a cool and dry environment.

Alumina ceramics, exemplifying the use of aluminium oxide, exhibit superior aesthetics, polished surfaces, wear resistance, hardness, and high biocompatibility with surrounding oral tissues.

The addition of Al_2O_3 NPs to dental materials lacking in mechanical strength can significantly enhance toughness. For instance, Polymethylmethacrylate (PMMA), which has drawbacks such as low flexural strength and impact strength, shows improved mechanical and thermal properties, as well as reduced water absorption and solubility when Al_2O_3 NPs are incorporated into its matrix [41, 42].

In orthodontics, an orthodontic bracket made of polysulfone incorporated with alumina nanoparticles was introduced in 2012 by UC3M. This bracket exhibits high strength, reduced mechanical resistance, and friction [43].

4.1.2.5. Silicon dioxide Nanoparticles (SiO_2 NPs)

Silicon dioxide nanoparticles (SiO_2 NPs) are utilized as fillers in dental restorative materials to enhance their mechanical properties. In general dentistry, fine silica powder is employed as a polishing agent to smooth tooth surfaces, preventing the accumulation of food and plaque. Silicon dioxide, commonly known as silica, is an oxide of silicon with the chemical formula SiO_2, frequently found in nature as quartz. SiO_2 NPs have gained prominence in various biomedical and dental applications, offering benefits such as size, surface area, biocompatibility, low toxicity, low density, and adsorption capacity.

In dentistry, silica nanoparticles play a crucial role, and their mesoporous form can serve as a blocking agent for dentinal tubules, helping alleviate hypersensitivity upon exposure [44]. Silica nanoparticles, when combined with hydroxyapatite nanoparticles, have been tested on fully demineralized dentin, demonstrating a localized increase in the concentration of calcium phosphate compounds and the restoration of mineral volume in dentin infiltrated with silica NPs [45, 46].

4.1.3 Unconventional Nanoparticles in Dentistry

The development of advanced dental nano-materials involves the fabrication of new nanoparticles to harness unique properties. Key challenges in this field include creating robust, non-toxic, and antibacterial materials, and nanotechnology provides a platform to explore diverse nanoparticles for dental applications. Various approaches for nanoparticle integration in dental materials have been implemented, depending on the specific properties of the particles. Researchers are actively exploring ways to leverage nanotechnology to enhance the properties and performance of dental materials.

4.1.3.1. Nano Diamonds

Diamond is renowned as the hardest natural material on Earth. Nano diamonds (ND) are extremely small diamonds, typically with sizes below 100 nm. Their exceptional surface and chemical properties make them excellent candidates for use as fillers in the fabrication of dental nanocomposites [47]. In recent developments, amoxicillin-loaded nano diamond Guttapercha composite (NDGP-AMC) has been created and tested for its applicability in root canal treatments, showing promising results [48]. The incorporation of nano diamonds into PMMA has demonstrated an overall improvement in the performance of fixed interim dental prostheses [49]. Nano diamonds hold significant potential for various applications in restorative dentistry.

4.1.3.2. Quantum Dots

Quantum dots are semi-conductive nanoparticles, including materials such as lead sulfide, zinc sulfide, and indium sulfide, capable of emitting light based on the intensity and wavelength of the incident light [50]. Moreover, their semi-conductive properties can be altered by external factors such as a magnetic field or light exposure. These nanoparticles can serve as nanocarriers for drugs or genes, offering potential therapeutic applications [51].

The distinctive optical properties of quantum dots make them valuable for cancer treatment when conjugated with photosensitizers and targeting agents. This enables their use in both diagnostic imaging and therapeutic interventions. By coating them with specific substances, their binding to cancer cells can be enhanced. Upon attachment, exposing them to UV light triggers light emission,

facilitating the detection of oral cancers [52]. Consequently, quantum dots hold promise for the treatment of head and neck diseases through drug delivery and correction of genetic defects, potentially contributing to the prevention of oral cancer [53].

4.1.3.3. NanoShells

NanoShells consist of a dielectric core and a thin metal coating [54]. In dentistry, NanoShells offer various therapeutic applications. The metal coating on NanoShells can be utilized to destroy oral cancer cells by exposing them to infrared light, generating intense heat around the NanoShells and leading to cell death [55]. This approach holds potential for therapeutic applications such as ligaturing vessels to control internal bleeding, promoting wound healing, and reducing angiogenesis. Such therapeutic methods could be instrumental in minimizing blood loss in trauma cases, thereby preserving nearby vital tissues. Additionally, NanoShells loaded with antibodies, proteins, or other cell-targeting agents can be employed for targeted drug delivery [56].

4.1.3.4. Quaternary ammonium methacrylate (QAM) Nanoparticles

Quaternary ammonium methacrylate nanoparticles can serve as fillers for restorative dental materials due to their antibacterial efficacy. The antibacterial mechanism involves inducing cytoplasmic leakage in the microorganism cell wall, leading to cell death. QAM resins and bacterial cell walls have oppositely charged surfaces, facilitating ionic adhesion that disrupts the electric balance in the cell membrane, increasing osmotic pressure and ultimately causing cell death [57]. An interesting feature of QAM resins is their ability to inhibit 3D biofilms [58]. Due to their bactericidal properties, QAM increases stress conditions, triggering apoptosis in bacteria. QAM resins have also demonstrated effective bond strength with restorative dental adhesive materials, making them potentially valuable for the development of advanced dental adhesive restorative materials [59].

4.1.3.5. Quaternary ammonium polyethyleneimine (QPEI) Nano-particles

Endodontic sealers with antibacterial properties can be highly beneficial in combating root canal infections. Quaternary polyethylenimine nanoparticles (QPEINPs) have been employed as fillers in commercially available endodontic sealers, such as Guttaflow, Epiphany, and AH Plus, for their antibacterial effects [60]. The incorporation of QPEI NPs in resin composites has demonstrated potent antibacterial activity without significantly compromising the mechanical properties [61]. Additionally, the addition of QPEI NPs provides stability and high antibacterial efficacy without generating any undesirable by-products.

4.1.3.6. Amorphous Calcium Phosphate Nanoparticles (ACPNP)

Remineralization of affected dentin or enamel can have a positive impact on oral health. The addition of mineralizing agents in restorative materials proves to be beneficial for restoration [62]. When dealing with deep carious lesions, a minimally invasive technique is typically employed to protect the pulp and preserve tooth structure [63, 64]. The incorporation of nanoparticles in restorative dental materials serves a dual purpose by providing antibacterial effects and facilitating the remineralization of decayed teeth. In dental composites, nanoparticles of amorphous calcium phosphate release calcium and phosphate ions around the restoration during acidic conditions, helping to maintain pH levels [65].

4.2. Nanotube Based Nanomaterials

4.2.1. Carbon Nano-tube (CNT)

Carbon nanotubes (CNTs) exhibit excellent mechanical and electronic properties, making them a promising reinforcing filler in dental composites [66, 67]. Single-walled carbon nanotubes (SWCNTs), seamless cylinders composed of a layer of graphene, have attracted significant attention in research [68]. The use of SWCNTs as fillers in dental resins has demonstrated satisfactory results, contributing to high flexural strength [69]. CNTs also show potential for use as a coating material on titanium dental implants [70]. Previous studies have explored CNTs for drug delivery in anti-cancer

applications, exhibiting considerable results in in vitro and in vivo studies, particularly with epidermal growth factor (EGF) [71].

CNTs and carbon nanofibrils have been utilized as reinforcing fillers in various nanomaterials to enhance their mechanical properties [72]. Cooper et al. prepared composites with different quantities of CNTs or carbon nanofibrils incorporated into a polymethyl methacrylate (PMMA) matrix using a dry powder mixing method. The results demonstrated an increase in the mechanical properties of composites, including high impact strength [73]. Additionally, An et al. fabricated alumina-CNT composites through a hot-pressing technique, revealing a significant reduction in wear and a substantial enhancement in mechanical properties [74].

4.2.2. Halloysite Nano-tube (HNT)

Clay-based nanomaterials, specifically Halloysite Nanotubes (HNTs), present a promising alternative as dental fillers and nano drug delivery agents in dentistry. HNTs possess a nanotubular structure with dimensions in the nanometer scale, showcasing a natural milky white color, high strength, and elastic modulus, making them an ideal choice for dental composite fabrication [75]. Furthermore, HNTs can be loaded with antibiotic agents, creating a nano-filler with the capacity to inhibit the formation of oral biofilm, thereby preventing the development of secondary dental caries [76, 77].

4.3. Nanoplatelets based nanomaterials

Nanoplatelet-based nanomaterials utilize nanosheets or flakes of nanoplatelets, with graphene being a prominent example in this category. Graphene oxide nanoplatelets are specifically employed in dentistry due to their unique properties.

4.3.1. Graphene oxide nanoplatelets

Graphene, consisting of a single layer of carbon atoms arranged in a hexagonal honeycomb lattice, possesses unique material characteristics [78]. The incorporation of graphene nano-powder into dental materials has opened up new opportunities for manufacturing dental nanomaterials [79].

Graphene, used as a nano-filler in dental nanocomposites, has demonstrated a significant increase in mechanical properties [80]. Numerous studies have highlighted the antibacterial properties of graphene-based materials, suggesting that their incorporation into dental materials can serve a dual purpose as a filler and an antibacterial agent [81, 82, 83].

Graphene-based nanoplatelets have exhibited strong antibacterial activity against Streptococcus mutans, indicating their potential as key antibacterial agents for dental materials [84]. In tissue engineering, materials with minimal cytotoxic effects on healthy tissues are essential.

A recent study reported that graphene oxide (GO) combined with fibroin had no adverse effects on periodontal ligament stem cells (PDLSCs), suggesting that GO-based tissue scaffolds hold great potential in regenerative dentistry [85].

Graphene oxide (GO) coated Ti (GO-Ti) membranes have demonstrated significant effects in stimulating osteogenic differentiation, superior bioactivity, and enhanced new bone formation without inflammatory responses [86]. GO-based substrates have facilitated dental pulp stem cell (DPSC) attachment and proliferation, showcasing the high biocompatibility of graphene [87].

Graphene emerges as a promising nanomaterial to enhance the performance of dental materials, and its derivatives can be employed as high-performance coating materials for dental implants.

4.4. The toxicity aspect of nanomaterials in dentistry

Nanoparticles are currently employed in various dental applications, including dental composites, root canal sealers, preventive drugs for oral diseases, prostheses, and teeth implantation. They play a crucial role in carrying oral fluids or drugs, maintaining oral hygiene, preventing oral diseases such as cancer, and contributing to the restoration of oral health care to a significant extent.

However, the use of nanomaterials in dentistry is a subject of debate due to concerns about their toxicity.

Several types of nanoparticles, including metal nanoparticles like Gold, Silver, and metal oxide nanoparticles such as TiO_2 and Fe_2O_3, have been explored for different dental applications. In a recent study, Gold nanoparticles coated on dental implants exhibited notable osteoinductive properties and were found to be non-toxic to MG-63 cell lines [88]. Silver nanoparticles are renowned for their antimicrobial properties, and in another study, silver nanoparticles coated with a capping agent were determined to be noncytotoxic on human gingival fibroblast cells (HGF-1) [89]. In a recent study, silver nanoparticles immobilized on Halloysite nanotubes were used for fabricating dental resin composites and were found to be non-cytotoxic on NIH 3T3 cell lines (mouse embryonic fibroblast cells) [90]. Metal oxide nanoparticles like TiO2 and Fe2O3 have been incorporated into PMMA resins in past studies and were found to be highly biocompatible, reducing the adherence of Candida albicans cells [91]. Moreover, chitosan nanoparticles have been incorporated as root canal sealers to prolong their antibacterial activity [92].

By carefully controlling the relative proportion of nanoparticles in dental materials, it is possible to make them more patient-friendlier for dental applications. However, ongoing research efforts are crucial to fully understand the use of nanomaterials and their potential deleterious effects on human health.

4.5. Dental Materials

The development of new dental restorative materials must meet several key requirements, including:

1. Lack of toxicity;
2. Inhibition of bacterial growth;
3. Effective separation from the oral environment, especially when placed beneath dental structures;
4. Ability to repair damaged tooth structures;
5. Mechanical properties similar to dental structures;
6. Capability for restoring tooth shape;
7. Aesthetic appearance.

Dental restorative materials can be categorized based on their chemical structures:

1. Resin composite;
2. Polyacid-modified resin composite;
3. Glass ionomer cements;
4. Resin-modified glass ionomer cement.

They can also be classified according to the filler particles used:

1. Macrofill;
2. Microfill;
3. Hybrid;
4. Midifill;
5. Minifill;
6. Nanofill (as shown in Figure 4.2.)[93, 94].

The integration of nanofillers into dental materials brings new possibilities to enhance the mechanical properties of composite materials. Researchers are actively working on developing fillers that can improve various characteristics of composite materials, including shrinkage profile, flexural strength, tensile strength, microhardness, toughness, and resistance to wear. Achieving optimal properties is crucial for the successful clinical use of composites.

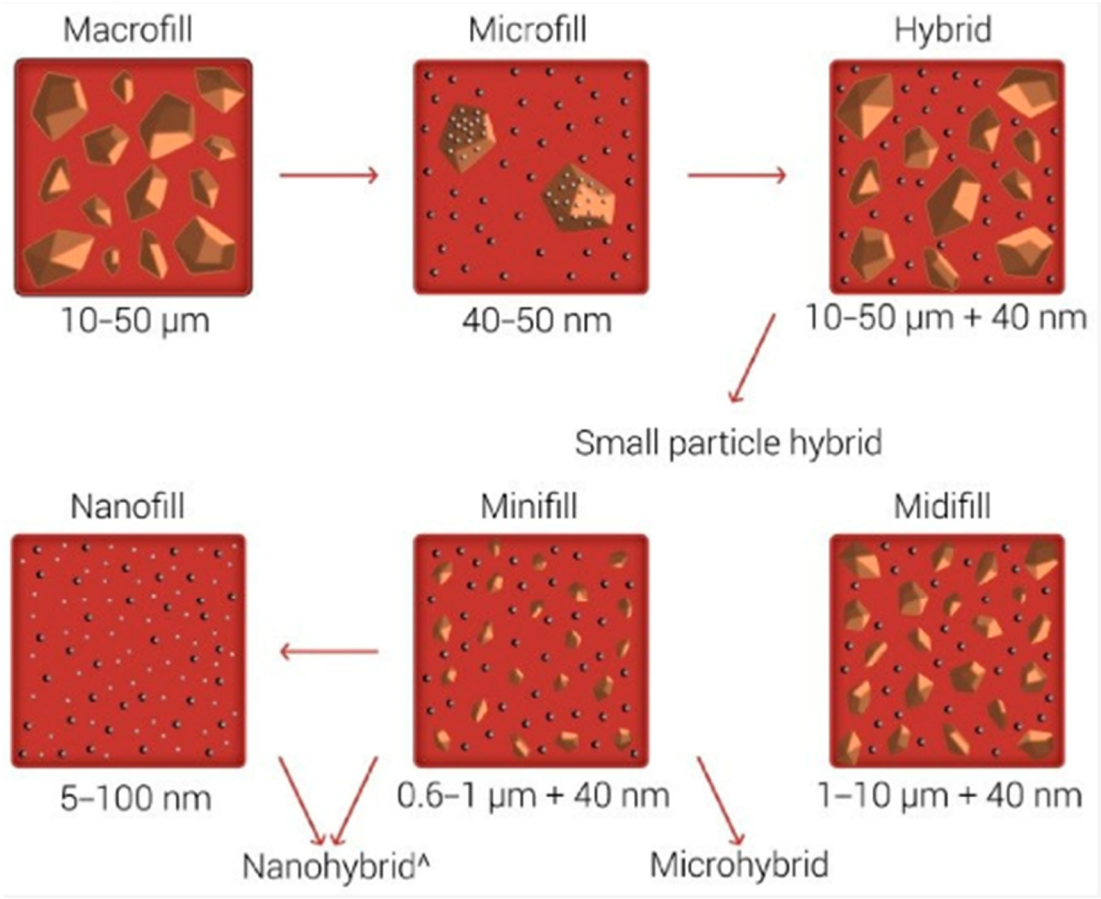
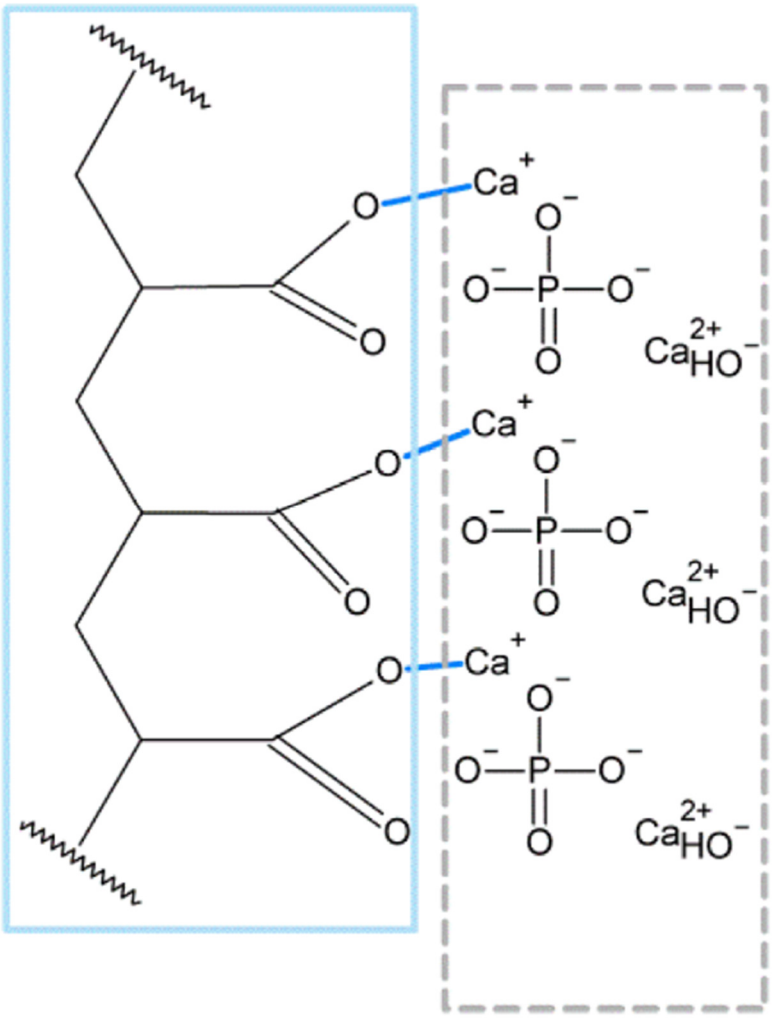


Figure 4.2. The segmentation of dental composite fillers [93, 94] is based on the work originally published by Ferracane in Dental Materials, with permission from Elsevier, in 2011.

Intelligent composites, incorporating nanofillers, boast distinctive capabilities such as the potential to remineralize dental structures and hinder the growth of bacterial plaque. Certain formulations of these composites even demonstrate mechanical properties surpassing those of natural dentine or enamel. The efficacy of dental restorations hinges on their adhesion to tooth structures. In clinical practice, two primary strategies are employed: direct bonding of the restoration to the tooth and restoration via adhesive substances (bond) to enhance adhesive toughness. Research has delved into the adhesion strength of nanofilled resin-modified glass ionomer seals compared to their non-nanofilled counterparts. It was discovered that the bonding mechanism of nano-modified seals to dentin/enamel closely resembles that of non-nanofilled resin-modified glass ionomer. This mechanism entails the formation of a polycarboxylate bond between the polycarboxylic acid of the nano-modified seal and the calcium ions from hydroxyapatite, through a micro-mechanical interlocking process. Although it was anticipated that nanofilled glass ionomer would exhibit higher bonding strength owing to the reaction of nanofilled particles with dentin/enamel structures, the bonding strength was surprisingly found to be comparable for both types of glass ionomers [95, 96] (Figure 4.3.).


Ca+
O
O
O

In comparison, a commercially available nanocomposite achieved a flexural strength of approximately 70 MPa and an elastic modulus of 7 GPa.

The data obtained from this study suggest the high potential usability of the newly designed restorative material in preventing the formation of secondary caries at the seal-tooth contact surface [97].

Addressing secondary caries involves not only enhancing the remineralization process but also integrating antibacterial nanoagents into composites. Nano zinc oxide (n-ZnO) and nano silver particles (n-Ag) have garnered attention for their antibacterial properties. While the precise mechanisms of action are not fully elucidated, it is believed that silver ions disrupt bacterial cell walls and plasma membranes, leading to cell demise. Conversely, n-ZnO interacts with reactive oxygen species, altering cell membrane functions, while zinc ions impede bacterial enzymes.

Despite the well-established antibacterial activity of n-ZnO and n-Ag, incorporating these materials into composites poses scientific challenges. Studies have explored the impact of novel nanocomposites on bacterial viability and seal mechanical properties. Composites containing anodic porous alumina (APA), n-Ag, and bis-GMA and TEGDMA as a matrix have demonstrated promising potential for controlled n-Ag release. Another investigation replaced fillers with nano silver particles coated with oleic acid, showcasing robust antibacterial effects and enhanced mechanical properties.

However, the subdued esthetic appeal of n-Ag composites due to color absorption has prompted researchers to investigate antibacterial effects through n-ZnO. A composite with varying concentrations of n-ZnO exhibited potent antibacterial effects against S. mutans. Increasing the n-ZnO content did not significantly alter its antibacterial activity. Importantly, the composite maintained its mechanical properties at levels comparable to the unfilled reference, suggesting that n-ZnO can function as a nanofill in commercially available dental composites with notable antibacterial activity.

Fluorides are recognized for their ability to inhibit bacterial growth and enhance tooth structure remineralization. A novel composite incorporating nanofillers comprising a combination of fluoride and hydroxyapatite (FHA) has been developed. The mechanical characteristics of this composite surpassed those of the control, with the highest flexural strength and modulus observed for the composite with 0.2 wt.% FHA content. Immersion tests revealed fluoride release, achieving concentrations sufficient to hinder enamel demineralization after 21 days of immersion [98, 99, 100, 101].

Improving the mechanical properties of dental restorative materials, particularly composites, is a key focus of research. Polymerization shrinkage, a phenomenon that induces stress in healthy tooth structures, often resulting in pain symptoms, poses a considerable challenge associated with composites. Fillers and, more recently, nanofillers have been introduced to enhance the mechanical properties of composites. Various studies have explored the use of nanofillers, including clay, silica, and other nanoparticles, to address this issue (Figure 4.4).

1. Clay Nanofillers:
   - Fuller's Earth (FE), a nanofiber-shaped inorganic material, was used as a nanofiller in composites. The addition of 0.72 wt.% of FE improved flexural strength, flexural modulus, and work-of-fracture (WOF), which is crucial for cervical restorations.
   - Polymer montmorillonite (MMT), composed of sheets with approximately 1 nm thickness, did not show improvement in mechanical characteristics and exhibited higher water sorption than the unfilled composite.
2. Silica Nanofillers:
   - Hybrid composites incorporating porous diatomite and Aerosil OX-50 particles showed improved mechanical properties when compared to those with only nano-silica. The composite with a mass diatomite to nano-silica ratio of 21:49 demonstrated high flexural strength, elastic modulus, Vickers microhardness, and compressive strength.
   - Thermal sintering of nano-silica particles resulted in secondary particles with improved dispersion in the composite, leading to higher flexural strength and a smoother surface profile.

3. Carbon Nanotubes (SWCNTs):
   - Silane-modified single-walled carbon nanotubes (SWCNTs), coated with nano-SiO2, were introduced into a composite matrix. This integration resulted in a nanofilled composite with exceptional mechanical properties, notably featuring a significantly elevated flexural strength compared to the reference material.
4. Cellulose Nanofillers:
   - Cellulose nanocrystals and cellulose microfibers, used as fillers in glass ionomer cement, showed improved mechanical properties. Cellulose nanocrystals, in particular, led to a considerable enhancement in all studied mechanical properties.
5. Color Stability and Esthetics:
   - Nanofillers, especially silica nanoparticles, demonstrated a stabilizing effect on the color of composites, with nanofilled composites showing better color stability compared to those filled with micro-sized glass particles.
   - Titanium dioxide nanoparticles (TiO2) in the size range of 300–400 nm were found to impact the color of the seal.

In conclusion, the incorporation of nanofillers in dental composites has shown promise in improving mechanical properties, color stability, and esthetics. However, challenges such as proper dispersion and potential changes in color need to be addressed for the optimal use of nanofillers in dental restorative materials [102].

Name	Manufacturer	Flexural Strength [MPa]	Flexural Modulus [GPa]
Z250	Filtek	136.40	11.53
Hybrid resin composite	TPH	119.15	4.90
Artglass	Heraeus Kulzer	114.00	13.00
Concept	Ivoclar	109.00	15.00
Compomer	Dyract	91.49	6.17
Resin modified glass ionomer	Vitremer	39.36	5.57
Glass ionomer	Ketac-Bond	17.02	5.20

Figure 4.4. Flexural strength and modulus of various commercial dental restorative materials.

Biocompatibility and toxicity are crucial considerations in the evaluation of dental restorative materials, especially concerning eluted substances. The eluted mixture from these materials consists of various components, including unpolymerized starting materials such as monomers, initiators, fillers, and others. The toxicity of methacrylate monomers, commonly used in dental materials, has been studied, with bis-GMA being found toxic at a concentration of 0.25 mM, while HEMA, TEGDMA, and MMA showed no toxicity at concentrations up to 10 mM.

The insertion of silver nanoparticles into composites, such as Tetric flow®, showed a correlation between the release profiles of monomers and the increasing amount of silver nanoparticles. The release of monomers increased with a higher concentration of nanofillers, attributed to increased unpolymerized monomers and decreased polymerization yield due to the interaction of photons with silver particles. Additionally, nanosilver's reaction with the photoinitiator was suggested to result in complex formation.

Research investigating the correlation between the degree of conversion (DC) and elution profiles for nano-hybrid materials, such as Venus® Diamond, Tetric Evo Ceram®, and Filtek™ Supreme XTE, revealed an inverse relationship between DC and the quantity of substances eluted. Additionally, the influence of time on the release of composite ingredients was examined, indicating no substantial concentration or composition variances with different irradiation durations.

Nanofillers have contributed to the wear resistance of dental restorative materials. Nanocomposites, such as Filtek Supreme® and Esthet X®, exhibited high resistance to abrasive wear, with filler size playing a role in wear susceptibility. Larger fillers with a lower surface area-to-volume ratio were associated with a fragile interaction between fillers and the polymer network, contributing to decreased mechanical properties.

In vivo studies on wear resistance during brushing revealed that Seal & Protect, a nanofilled dental material, demonstrated the highest resistance to abrasion, attributed to the size and shape of the composite filler. Irregular-shaped particles were found to be more resistant to wear than spherical ones, emphasizing the importance of filler characteristics.

Concerns about the potential inhalation of nanodust during shaping (grinding or polishing) of dental composites led to investigations on whether polishing or grinding generates nanodust. The results indicated that released dust particles during these procedures were smaller than 500 nm, with particles below 100 nm also detected. To mitigate the potential health impact on dental personnel, the use of water-cooling during polishing and wearing masks with filters for small particles were suggested [103].

4.5.1. Adhesives

The dental adhesive system is a crucial component in restorative dentistry, particularly for achieving better seal adhesion to tooth structures, especially dentin. Seal adhesion is a key parameter that influences the durability of the seal in restorative dental procedures. The dental adhesive system typically comprises three main components: etchants, primer, and adhesive.

1. Etchants: Etchants play a fundamental role in the dental adhesive system. They are designed to dissolve the mineral surface of the tooth, simultaneously forming a demineralized collagen network in dentin. This demineralization allows the penetration of the primer into the tooth structure. Etchants are typically strong acids with a pH range of 1–2.
2. Primer: The primer is responsible for forming a bifunctional layer that connects the hydrophilic tooth structures with the hydrophobic adhesive. The structure of the primer generally includes three main components:
   - Methacrylate group: This group is connected to the composites.
   - Spacer group: The spacer group provides flexibility to the linker.
   - Reactive group: The reactive group forms a strong bond with dentin.

   The primer's role is to create a stable and durable connection between the tooth structure and the adhesive, facilitating the subsequent bonding of the adhesive to dentin.
3. Adhesive: The adhesive, often a monomer, connects to the primer under curing light. This bonding process fills the interfibrillar space of the collagen network in dentin. The adhesive forms a hybrid layer that serves as the foundation for the composite seal.

There are two main types of dental adhesive systems based on the number of steps involved in the application process:

- Etch-and-rinse systems: These systems typically involve 2–3 steps, including the application of an etchant, followed by a primer, and then the adhesive.
- Self-etch systems: These systems combine the etching, priming, and adhesive application into a single step, simplifying the process.

The choice between etch-and-rinse and self-etch systems depends on various factors, including the specific clinical situation, the substrate being treated, and the preferences of the clinician. Each dental restoration system possesses its own set of advantages and considerations, and the selection is typically guided by the specific requirements of the restoration procedure.

The bond stability of glass ionomer cements, crucial in restorative dentistry, has been a subject of recent study. Researchers, including Calvo et al., investigated three commercial glass ionomer cements: Ketac™ Molar Easymix, Vitremer, and Ketac™ Nano Light-Curing. The study primarily centered on bond strength, and the materials underwent an aging process that involved immersion in water. The microtensile bond strength (μTBS) was evaluated immediately after curing and again after a storage period of 2 years in water.

The study revealed that the highest bond strength was initially observed for Ketac™ Nano, with Vitremer exhibiting the highest bond strength after 2 years of storage. In the bonding mechanism of glass ionomer cements, a chemical bond forms between polycarboxylic acids and hydroxyapatite. The resin modifies this mechanism through chemical and micromechanical adhesion, resulting in strong bond strength immediately after curing. However, with time, fillers are released during storage, leading to a reduction in micromechanical interactions. The incorporation of nanofillers, as seen in Ketac™ Nano, showed fewer disruptions in adhesion strength due to their high surface-to-volume ratio.

Addressing secondary caries formation, researchers explored the incorporation of antibacterial agents into restorative primers. An antibacterial primer, containing 12-methacryloyloxydodecylpyridinium bromide (MDPB) and nano silver particles (n-Ag), exhibited strong inhibition of bacterial growth, particularly against Streptococcus spp. and S. mutans. This primer demonstrated a synergistic antibacterial effect, and its antibacterial potential did not compromise bond strength.

In the context of re-mineralization, nanoamorphous calcium phosphate (NACP) was introduced into the primer and adhesive material. The modified adhesive system, augmented with nano silver particles (n-Ag) for antibacterial treatment, did not affect dental bond strength. However, it demonstrated considerable antibacterial efficacy, notably reducing the total colony-forming units (CFU) of microorganisms and S. mutans, alongside decreased metabolic activity and lactic acid production. Improving adhesive systems, a modified adhesive system containing zinc oxide (ZnO) nanoparticles and $ZnCl_2$ demonstrated high bond stability after storage, along with increased hardness. The addition of n-ZnO particles was associated with the replacement of calcium ions with zinc ions in apatite crystals, contributing to the increased hardness (Figure 4.5.).

In summary, recent studies have focused on enhancing bond stability, antibacterial properties, and re-mineralization potential in dental restorative materials, showing promising results for the development of improved and multifunctional dental adhesives [104].

To enhance bond strength in dental adhesives, researchers have explored various nanofillers. Lohbauer et al. investigated zirconia nanoparticles (ZrO2) obtained through laser vaporization, resulting in spherically shaped nanoparticles of approximately 20–50 nm size. The reduced agglomeration tendency of these particles, attributed to only one point of Van der Waals interaction, contributed to the improved bond strength. The study utilized the commercial adhesive system Adper Scotchbond Multi-Purpose (SBMP), with the addition of zirconia nanofillers into either the primer or adhesive solution. Microtensile bond strength (μTBS) increased with higher nanofiller concentrations up to 20% weight. Notably, at 20% weight of nanofiller in the adhesive solution, a significant difference in μTBS favored the nanofilled primer. Transmission electron microscopy (TEM) micrographs revealed that zirconia fillers added to the primer accumulated on the surface, while addition to the adhesive solution resulted in dispersion, ultimately reinforcing the interface surface of the bond system.

The same research team investigated the influence of SiO2-BaO glass filler (180/500 nm size, irregular shape) on the mechanical properties of a bond system. Compared to an unfilled bond, the addition of nanofillers up to 10% weight led to increased tensile strength, elastic modulus, and μTBS. However, agglomeration of nanofillers was observed, attributed to their irregular shape.

In addressing dental pulp exposure, Yoshida et al. proposed an adhesive material for direct pulp capping based on Super-bond (SB) with incorporated nano hydroxyapatite. The material, particularly with 30% nano-component, demonstrated promising results in a rat pulp exposure model, leading to dentin reconstruction with dentin tubules. However, the study highlighted the challenge of pulp contamination with bacteria as a major obstacle to full recovery.

These findings indicate the ongoing exploration of nanofillers for improving bond strength and developing restorative materials for specific dental applications, including direct pulp capping.

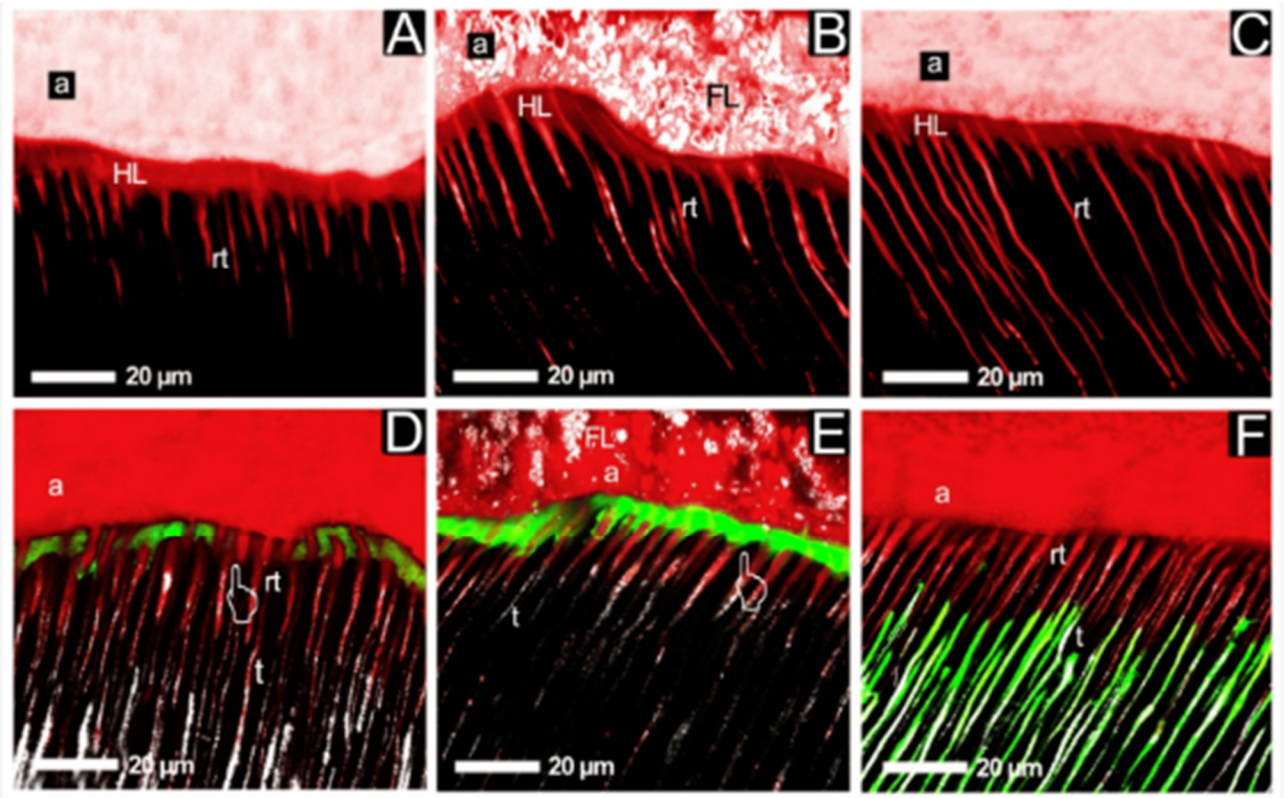


Figure 4.5. Single confocal images of the resin–dentin interfaces were captured after 24 hours of storage in artificial body fluid. The images depict the interfaces created using the SB control and SB modified with either ZnO nanoparticles or ZnCl2. In image (A), the reference SB is shown, while image (B) displays SB modified with nano-ZnO particles containing reflective filler. Image (C) depicts SB modified with ZnCl2. In images (D), (E), and (F), fluorescein nanoleakage is indicated by the finger, with (D) representing the reference SB, (E) showing SB modified with nano-ZnO and fluorescein nanoleakage, and (F) displaying SB modified with ZnCl2 without fluorescein nanoleakage. Abbreviations on the images include a for adhesive, rt for resin tags, t for dentinal tubules, FL for reflective filler, and HL for hybrid layer.

4.6. Conclusion

The integration of nanotechnology into dentistry holds the promise of enhancing the quality of current treatment procedures and patient care. It can introduce innovative methods for synthesizing dental materials, improving efficacy, accuracy, and treatment speed while simultaneously reducing costs. Nanotechnology research has the potential to contribute to the development of new techniques for the early diagnosis and treatment of oral malignant diseases. Additionally, advancements in nanotechnology and antimicrobial materials could significantly enhance therapeutic approaches in dentistry.

The progress of research in creating highly advanced, restorative nanomaterials is crucial for their successful implementation in dentistry. Before introducing new materials into clinical practice, it is imperative to have sufficient clinical data to ensure safety and efficacy. This review article highlights the potentials and capabilities of nanotechnology in the dental field. Looking ahead, nanotechnology may become a cornerstone in both dental and medical sciences. Rigorous and accurate steps in implementing this technology could lead to favorable social, economic, and improved oral health outcomes for people in the near future.

4.7. Quiz 4.

1. What are some properties of Silver Nanoparticles (AgNPs) in dental materials?
a). High antibacterial efficacy
b). Enhanced mechanical properties
c). Promotion of bone formation
d). Reduction of polymerization shrinkage
e). Increased lactic acid formation

2. Which nanoparticles are utilized for remineralization in dental composites?
a). Zinc Oxide Nanoparticles (ZnO NPs)
b). Titanium Dioxide-Based Nanoparticles (TiO2NPs)
c). Aluminium Oxide Nanoparticles (Al2O3 NP)
d). Silicon Dioxide Nanoparticles (SiO2 NPs)
e). Graphene Oxide Nanoplatelets

3. What is the function of Carbon Nanotubes (CNTs) in dental composites?
a). Antibacterial properties
b). Increased abrasion resistance
c). Enhance mechanical properties
d). Stimulate osteogenic differentiation
e). Act as drug delivery carriers

4. How do Quaternary Ammonium Methacrylate (QAM) Nanoparticles contribute to dental materials?
a). Inhibit biofilm formation
b). Promote secondary caries
c). Increase solubility
d). Enhance cytotoxicity
e). Improve biocompatibility

5. What are the potential applications of Graphene Oxide Nanoplatelets in dentistry?
a). Targeted drug delivery
b). Blocking dentinal tubules
c). Enhanced mechanical properties
d). Prevention of oral biofilm formation
e). Reduction of tooth resistance

6.Which of the following requirements must dental restorative materials meet?
a). Lack of toxicity
b). Inhibition of bacterial growth
c). Effective separation from the oral environment
d). Mechanical properties similar to dental structures
e). Capability for restoring tooth shape

7.What are some classifications of dental restorative materials based on filler particles?
a). Macrofill
b). Microfill
c). Hybrid
d). Minifill
e). Nanofill

8.Which mechanical properties can nanofillers improve in composite materials?
a). Shrinkage profile
b). Flexural strength
c). Tensile strength
d). Wear resistance
e). Color stability

9.What are some potential applications of nanofillers in dental adhesives?
a). Enhancing bond stability
b). Inhibiting bacterial growth
c). Facilitating remineralization
d). Improving color stability
e). Increasing wear resistance

10. Which components are typically found in dental adhesive systems?
a). Etchants
b). Primers
c). Adhesives
d). Nanoparticles
e). Fillers

References

[1]. Mount, G. J. Minimal intervention dentistry: Rationale of cavity design. *Operative Dentistry*, Vol. 28, No. 1, 2003, pp. 92–99.
[2]. Hua, Y., L. Gu, and H. Watanabe. Micromechanical analysis of nanoparticle-reinforced dental composites. International Journal of Engineering Science, Vol. 69, 2013, pp. 69–76.
[3]. Hojati, S. T., H. Alaghemand, F. Hamze, F. A. Babaki, R. Rajab-Nia, M. B. Rezvani, et al. Antibacterial, physical and mechanical properties of flowable resin composites containing zinc oxide nanoparticles. Dental Materials, Vol. 29, No. 5, 2013, pp. 495–505.
[4]. Turssi, C. P., J. L. Ferracane, and L. L. Ferracane. Wear and fatigue behavior of nano-structured dental resin composites. Journal of Biomedical Materials Research Part B: Applied Biomaterials, Vol. 78, No. 1, 2006, pp. 196–203.
[5]. Moshaverinia, A., S. Ansari, Z. Movasaghi, R. W. Billington, J. A. Darr, and I. U. Rehman. Modification of conventional glass-ionomer cements with N-vinylpyrrolidone containing polyacids, nano-hydroxy and fluoroapatite to improve mechanical properties. Dental Materials, Vol. 24, No. 10, 2008, pp. 1381–1390.
[6]. Uysal, T., A. Yagci, B. Uysal, and G. Akdogan. Are nano-composites and nano-ionomers suitable for orthodontic bracket bonding?The European Journal of Orthodontics, Vol. 32, No. 1, 2010, pp. 78–82.
[7]. Samuel, U. and J. P. Guggenbichler. Prevention of catheter-related infections: The potential of a new nano-silver impregnated catheter. International Journal of Antimicrobial agents, Vol. 23, 2004, pp. 75–78.
[8]. Yoshida, K., M. Tanagawa, S. Matsumoto, T. Yamada, and M. Atsuta. Antibacterial activity of resin composites with silver-containing materials. European Journal of Oral Sciences, Vol. 107, No. 4, 1999, pp. 290–296.
[9]. Bürgers, R., A. Eidt, R. Frankenberger, M. Rosentritt, H. Schweikl, G. Handel, et al. the anti-adherence activity and bactericidal effect of microparticulate silver additives in composite resin materials. Archives of Oral Biology, Vol. 54, No. 6, 2009, pp. 595–601.
[10]. Yoshida, K., M. Tanagawa, and M. Atsuta. Characterization and inhibitory effect of antibacterial dental resin composites incorporating silver-supported materials. Journal of Biomedical Materials Research A, Vol. 47, No. 4, 1999, pp. 516–522.
[11]. Cheng, L., M. D. Weir, H. H. Xu, J. M. Antonucci, N. J. Lin, S. Lin-Gibson, et al. Effect of amorphous calcium phosphate and silver nanocomposites on dental plaque microcosm biofilms. Journal of Biomedical Materials Research Part B: Applied Biomaterials, Vol. 100, No. 5, 2012, pp. 1378–1386.
[12]. Punia, S. K., P. Nadig, and V. Punia. An in vitro assessment of apical microleakage in root canals obturated with gutta-flow, resilon, thermafil and lateral condensation: A stereomicroscopic study. Journal of Conservative Dentistry: JCD, Vol. 14, No. 2, 2011, pp. 173–177.
[13]. Weir, M. D., L. C. Chow, and H. H. Xu. Remineralization of demineralized enamel via calcium phosphate nanocomposite. Journal of Dental Research, Vol. 91, No. 10, 2012, pp. 979–984.
[14]. Wu, D., W. Fan, A. Kishen, J. L. Gutmann, and B. Fan. Evaluation of the antibacterial eflcacy of silver nanoparticles against enterococcus faecalis biofilm. Journal of Endodontics, Vol. 40, No. 2, 2014, pp. 285–290.
[15]. Pourjavadi, A., M. Bagherifard, and M. Doroudian. Synthesis of micelles based on chitosan functionalized with gold nanorods as a light sensitive drug delivery vehicle. International Journal of Biological Macromolecules, Vol. 149, 2020, pp. 809–818.
[16]. Alkilany, A. M., L. B. Thompson, S. P. Boulos, P. N. Sisco, and C. J. Murphy. Gold nanorods: Their potential for photothermal therapeutics and drug delivery, tempered by the complexity of their biological interactions. Advanced Drug Delivery Reviews, Vol. 64, No. 2, 2012, pp. 190–199.
[17]. Heo, D. N., W.-K. Ko, H. R. Lee, S. J. Lee, D. Lee, S. H. Um, et al. Titanium dental implants surface-immobilized with gold nanoparticles as osteoinductive agents for rapid osseointegration. Journal of Colloid and Interface Science, Vol. 469, 2016, pp. 129–137.
[18]. Ruparelia, J. P., A. K. Chatterjee, S. P. Duttagupta, and S. Mukherji. Strain specificity in antimicrobial activity of silver and copper nanoparticles. Acta Biomaterialia, Vol. 4, No. 3, 2008, pp. 707–716.
[19]. Kishen, A., Z. Shi, A. Shrestha, and K. G. Neoh. An investigation on the antibacterial and antibiofilm eflcacy of cationic nanoparticulates for root canal disinfection. Journal of Endodontics, Vol. 34, No. 12, 2008, pp. 1515–1520.
[20]. Gutiérrez, M. F., P. Malaquias, V. Hass, T. P. Matos, L. Lourenço, A. Reis, et al. The role of copper nanoparticles in an etch-and-rinse adhesive on antimicrobial activity, mechanical properties and the durability of resin-dentine interfaces. Journal of Dentistry, Vol. 61, 2017, pp. 12–20.
[21]. Aydin Sevinç, B., and L. Hanley. Antibacterial activity of dental composites Containing zinc oxide nanoparticles. Journal of Biomedical Materials Research Part B: Applied Biomaterials, Vol. 94, No. 1, 2010, pp. 22–31.
[22]. Srakaew, V., P. Ruangsri, K. Suthin, P. Thunyakitpisal, and W. Tachaboonyakiat. Sodium-phosphorylated chitosan/zinc oxide complexes and evaluation of their cytocompatibility: An approach for periodontal dressing. Journal of Biomaterials Applications, Vol. 27, No. 4, 2012, pp. 403–412.
[23]. Yuan, J.-H., Y. Chen, H.-X. Zha, L.-J. Song, C. et al. Determination, characterization and cytotoxicity on HELF cells of ZnO nanoparticles. Colloids and Surfaces B: Biointerfaces, Vol. 76, No. 1, 2010, pp. 145–150.
[24]. Wang, Y., L. Yuan, C. Yao, L. Ding, C. Li, J. Fang, et al. A combined toxicity study of zinc oxide nanoparticles and vitamin C in food additives. Nanoscale, Vol. 6, No. 24, 2014, pp. 15333–15342.

[25]. Kasraei, S., L. Sami, S. Hendi, M.-Y. AliKhani, L. Rezaei-Soufi, and Z. Khamverdi. Antibacterial properties of composite resins incorporating silver and zinc oxide nanoparticles on streptococcus mutans and lactobacillus. Restorative Dentistry & Endodontics, Vol. 39, No. 2, 2014, p. 109.
[26]. Wang, Y., H. Hua, W. Li, R. Wang, X. Jiang, and M. Zhu. Strong antibacterial dental resin composites containing cellulose nanocrystal/zinc oxide nanohybrids. Journal of Dentistry, Vol. 80, 2019, pp. 23–29.
[27]. Özcan, M. and C. Hämmerle. Titanium as a reconstruction and implant material in dentistry: Advantages and pitfalls. Materials, Vol. 5, No. 9, 2012, pp. 1528–1545.
[28]. Chaturvedi, T. P. An overview of the corrosion aspect of dental implants (titanium and its alloys). Indian Journal of Dental Research, Vol. 20, No. 1, 2009, pp. 91–98.
[29].Gogniat, G. and S. Dukan. TiO2 photocatalysis causes DNA damage via fenton reaction-generated hydroxyl radicals during the recovery period. Applied and Environmental Microbiology, Vol. 73, No. 23, 2007, pp. 7740–7743.
[30]. Garcia-Contreras, R., M. Sugimoto, N. Umemura, M. Kaneko, et al. Alteration of metabolomic profiles by titanium dioxide nanoparticles in human gingivitis model. Biomaterials, Vol. 57, 2015, pp. 33–40.
[31]. Padovani, G. C., V. P. Feitosa, S. Sauro, et al. Advances in dental materials through nanotechnology: Facts, perspectives and toxicological aspects. Trends in biotechnology, Vol. 33, No. 11, 2015, pp. 621–636.
[32]. Sodagar, A., M. S. A. Akhoundi, A. Bahador, Y. F. Jalali, Z. Behzadi, F. Elhaminejad, et al. Effect of TiO2 nanoparticles incorporation on antibacterial properties and shear bond strength of dental composite used in orthodontics. Dental press journal of orthodontics, Vol. 22, No. 5, 2017, pp. 67–74.
[33]. Meng, W., Y. Zhou, Y. Zhang, Q. Cai, L. Yang, and B. Wang. Effects of hierarchical micro/nano-textured titanium surface features on osteoblast-specific gene expression. Implant dentistry, Vol. 22, No. 6, 2013, pp. 656–661.
[34]. Dorkhan, M., T. Yücel-Lindberg, J. Hall, G. Svensäter, and J. R. Davies. Adherence of human oral keratinocytes and gingival fibroblasts to nano-structured titanium surfaces. BMC Oral Health, Vol. 14, No. 1, 2014, pp. 1–9.
[35]. Lohbauer, U., A. Wagner, R. Belli, C. Stoetzel, A. Hilpert, H. D. Kurland, et al. Zirconia nanoparticles prepared by laser vaporization as fillers for dental adhesives. Acta Biomaterialia, Vol. 6, No. 12, 2010, pp. 4539–4546.
[36]. Enomoto, K., Y. Ichijo, M. Nakano, M. Kikuchi, et al. Unique hydrophobization and hybridization via direct phase transfer of ZrO2 nanoparticles from water to toluene producing highly transparent polystyrene and poly(methyl methacrylate) hybrid bulk materials. Macromolecules, Vol. 50, No. 24, 2017, pp. 9713–9725.
[37]. Wang, J., and R. Stevens. Zirconia-toughened alumina (ZTA) ceramics. Journal of Materials Science, Vol. 24, No. 10, 1989, pp. 3421–3440.
[38]. Chan, K. S., D. P. Nicolella, B. R. Furman, S. T. Wellinghoff, H. R. Rawls, and S. E. Pratsinis. Fracture toughness of zirconia nanoparticle-filled dental composites. Journal of Materials Science, Vol. 44, No. 22, 2009, pp. 6117–6124.
[39]. Souza, J. C., J. B. Silva, A. Aladim, O. Carvalho, R. M. Nascimento, F. S. Silva, et al. Effect of zirconia and alumina fillers on the microstructure and mechanical strength of dental glass ionomer cements. Open Dentistry Journal, Vol. 10, No. 1, 2016, pp. 58–68.
[40]. Gad, M. M., A. Rahoma, A. M. Al-Thobity, and A. S. ArRejaie. Influence of incorporation Of ZrO2 nanoparticles on the repair strength of polymethyl methacrylate denture bases. International Journal of Nanomedicine, Vol. 11, 2016, pp. 5633–5643.
[41]. Jasim, B. S. and I. J. Ismail. The effect of silanized alumina nanofillers addition on some physical and mechanical properties of heat cured polymethyl methacrylate denture base material. Journal of Baghdad College of Dentistry, Vol. 26, No. 2, 2014, pp. 18–23.
[42]. Safarabadi, M., N. Khansari, and A. Rezaei. An experimental investigation of HA/AL2O3 nanoparticles on mechanical properties of restoration materials. Engineering Solid Mechanics, Vol. 2, No. 3, 2014, pp. 173–182.
[43]. Llorente, A., B. Serrano, J. Baselga, G. Gedler, and R. Ozisik. Nanoindentation and wear behavior of thermally stable biocompatible polysulfone–alumina nanocomposites. RSC Advances, Vol. 102, No. 102, 2016, pp. 100239–100247.
[44]. Hamouda, I. M. Current perspectives of nanoparticles in Medical and dental biomaterials. Journal of Biomedical Materials Research, Vol. 26, 2012, pp. 143–151.
[45]. Yu, J., H. Yang, K. Li, J. Lei, L. Zhou, and C. Huang. A novel application of nanohydroxyapatite/mesoporous silica biocomposite on treating dentin hypersensitivity: An in vitro study. Journal of Dentistry, Vol. 50, 2016, pp. 21–29.
[46]. Besinis, A., R. van Noort, and N. Martin. Infiltration of demineralized dentin with silica and hydroxyapatite nanoparticles. Dental Materials, Vol. 28, No. 9, 2012, pp. 1012–1023.
[47]. Chu, Y. Q., Y. Tong, T. L. Zhang, F. L. Huang, and X. Z. Wang. Synthesis of nanodiamond reinforced dental composite resins and their mechanical properties. Fullerenes, Nanotubes and Carbon Nanostructures, Vol. 20, No. 4–7, 2012, pp. 628–632.
[48]. Lee, D. K., S. V. Kim, A. N. Limansubroto, A. Yen, A. Soundia, C. Y. Wang, et al. Nanodiamond-Gutta percha composite biomaterials for root canal therapy. ACS Nano, Vol. 9, No. 11, 2015, pp. 11490–11501.
[49]. Protopapa, P., E. Kontonasaki, D. Bikiaris, K. M. Paraskevopoulos, and P. Koidis. Reinforcement of a PMMA resin for fixed interim prostheses with nanodiamonds. Dental Materials Journal, Vol. 30, No. 2, 2011, pp. 222–231.
[50]. Ge, J., Q. Jia, W. Liu, M. Lan, B. Zhou, L. Guo, et al. Carbon dots with intrinsic theranostic properties for bioimaging, red-light-triggered photodynamic/photothermal simultaneous Therapy in vitro and in vivo. Advanced Healthcare Materials, Vol. 5, No. 6, 2016, pp. 665–675.

[51]. Yaghini, E., A. M. Seifalian, and A. J. MacRobert. Quantum dots and their potential biomedical applications in photosensitization for photodynamic therapy. Future Nanomedicine, Vol. 4, No. 3, 2009, pp 353–363.
[52]. Wang, Y. and L. Chen. Quantum dots, lighting up the research and development of nanomedicine. Nanomedicine: Nanotechnology, Biology and Medicine, Vol. 7, No. 4, 2011, pp. 385–402.
[53]. Kanaparthy, R. and A. Kanaparthy. The changing face of dentistry: Nanotechnology. International Journal of Nanomedicine, Vol. 6, 2011, pp. 2799–2804.
[54]. Loo, C., A. Lowery, N. Halas, J. West, and R. Drezek. Immuno-targeted nanoshells for integrated cancer imaging and therapy. Nano Letters, Vol. 5, No. 4, 2005, pp. 709–711.
[55]. El-Sayed, I. H., X. Huang, and M. A. El-Sayed. Selective laser photo-thermal therapy of epithelial carcinoma using anti-EGFR antibody conjugated gold nanoparticles. Cancer Letters, Vol. 239, No. 1, 2006, pp. 129–135.
[56]. Mercado, N., P. Bhatt, V. Sutariya, F. L. E. Florez, and Y. V. Pathak. Application of nanoparticles in treating periodontitis: Preclinical and clinical overview. In: Surface Modification of Nanoparticles for Targeted Drug Delivery, Y. V. Pathak, Ed. Springer International Publishing, Cham, pp. 467–480.
[57]. Li, F., M. D. Weir, J. Chen, and H. H. K. Xu. Effect of charge density of bonding agent containing a new quaternary ammonium methacrylate on antibacterial and bonding properties. Dental Materials, Vol. 30, No. 4, 2014, pp. 433–441.
[58]. Hoque, J., P. Akkapeddi, C. Ghosh, D. S. S. M. Uppu, and J. Haldar. A biodegradable polycationic paint that kills bacteria in vitro and in vivo. ACS Applied Materials & Interfaces, Vol. 8, No. 43, 2016, pp. 29298–29309.
[59]. Cheng, L., M. D. Weir, K. Zhang, D. D. Arola, X. Zhou, and H. H. K. Xu. Dental primer and adhesive containing a new antibacterial quaternary ammonium monomer dimethylaminododecyl methacrylate. Journal of Dentistry, Vol. 41, No. 4, 2013, pp. 345–355.
[60]. Abramovitz, I., N. Beyth, G. Weinberg, A. Borenstein, D. Polak, D. Kesler-Shvero, et al. In vitro biocompatibility of endodontic sealers incorporating antibacterial nanoparticles. Journal of Nano-materials, Vol. 2012, 2012.
[61]. Beyth, N., Y. Houri-Haddad, L. Baraness-Hadar, I. Yudovin-Farber, A. J. Domb, and E. I. Weiss. Surface antimicrobial activity and biocompatibility of incorporated polyethylenimine nanoparticles. Biomaterials, Vol. 29, No. 31, 2008, pp. 4157–4163.
[62]. Selwitz, R. H., A. I. Ismail, and N. B. Pitts. Dental caries. The Lancet, Vol. 369, No. 9555, 2007, pp. 51–59.
[63]. White, J. M. and W. S. Eakle. Rationale and treatment approach in minimally invasive dentistry. Journal of the American Dental Association (1939), Vol. 131 Supplement 1, 2000, pp. 13S–19S.
[64]. Ericson, D., E. Kidd, D. McComb, I. Mjör, and M. Noack. Minimally invasive dentistry - concepts and techniques in cariology. Oral Health & Preventive Dentistry, Vol. 1, 2003, pp. 59–72
[65]. Xu, H. H. K., J. L. Moreau, L. Sun, and L. C. Chow. Nanocomposite containing amorphous calcium phosphate nanoparticles for caries inhibition. Dental Materials, Vol. 27, No. 8, 2011, pp. 762–769.
[66]. Li, X., W. Liu, L. Sun, K. E. Aifantis, B. Yu, Y. Fan, et al. Resin composites reinforced by nanoscaled fibers or tubes for dental regeneration. BioMed Research International, Vol. 2014, 2014,
[67]. Wang, S.-F., L. Shen, W.-D. Zhang, and Y.-J. Tong. Preparation and mechanical properties of chitosan/carbon nanotubes composites. Biomacromolecules, Vol. 6, No. 6, 2005, pp. 3067–3072.
[68]. Ajayan, P. M. Nanotubes from carbon. Chemical Reviews, Vol. 99, No. 7, 1999, pp. 1787–1800.
[69]. Wang, W., F. Watari, M. Omori, S. Liao, Y. Zhu, A. Yokoyama, et al. Mechanical properties and biological behavior of carbon nanotube/polycarbosilane composites for implant materials. Journal of Biomedical Materials Research Part B: Applied Biomaterials, Vol. 82B, No. 1, 2007, pp. 223–230.
[70]. Park, J. E., I.-S. Park, M. P. Neupane, T.-S. Bae, and M.-H. Lee. Effects of a carbon nanotube-collagen coating on a titanium surface on osteoblast growth. Applied Surface Science, Vol. 292, 2014, pp. 828–836.
[71]. Bhirde, A. A., V. Patel, J. Gavard, G. Zhang, A. A. Sousa, A. Masedunskas, et al. targeted killing of cancer cells in vivo and in vitro with EGF-directed carbon nanotube-based drug delivery. ACS Nano, Vol. 3, No. 2, 2009, pp. 307–316.
[72]. Lv, L., X. Han, L. Zong, M. Li, J. You, X. Wu, and C. Li. Biomimetic hybridization of kevlar into silk fibroin: Nanofibrous strategy for improved mechanic properties of flexible composites and filtration membranes. ACS Nano, Vol. 11, No. 8, 2017, pp. 8178–8184.
[73]. Cooper, C. A., D. Ravich, D. Lips, J. Mayer, and H. D. Wagner. Distribution and alignment of carbon nanotubes and nanofibrils in a polymer matrix. Composites Science and Technology, Vol. 62, No. 7, 2002, pp. 1105–1112.
[74]. An, J.-W., D.-H. You, and D.-S. Lim. Tribological properties of hot-pressed alumina–CNT composites. Wear, Vol. 255, No. 1, 2003, pp. 677–681.
[75]. Chen, Q., Y. Zhao, W. Wu, T. Xu, and H. Fong. Fabrication and evaluation of bis-GMA/TEGDMA dental resins/composites containing halloysite nanotubes. Dental Materials, Vol. 28, No. 10, 2012, pp. 1071–1079.
[76]. Lvov, Y. and E. Abdullayev. Functional polymer–clay nanotube composites with sustained release of chemical agents. Progress in Polymer Science, Vol. 38, No. 10, 2013, pp. 1690–1719.
[77]. Avani, F., S. Damoogh, F. Mottaghitalab, A. Karkhaneh, and M. Farokhi. Vancomycin loaded halloysite nanotubes embedded in silk fibroin hydrogel applicable for bone tissue engineering. International Journal of Polymeric Materials and Polymeric Biomaterials, Vol. 69, No. 1, 2020, pp. 32–43.
[78]. Pan, Y., H. Zhang, D. Shi, J. Sun, S. Du, F. Liu, et al. Highly ordered, millimeter-scale, continuous, single-crystalline graphene monolayer formed on Ru (0001). Advanced Materials, Vol. 21, No. 27, 2009, pp. 2777–2780.
[79]. Sava, S., A. Tonea, B. Stanca, C. Alb, C. Sarosi, and D. Dudea. The study of new composites with graphene used in dentistry. Studia Universitatis Babes-Bolyai, Chemia, Vol. 60, 2015.

[80]. Sarosi, C., A. R. Biris, A. Antoniac, S. Boboia, C. Alb, I. Antoniac, et al. The nanofiller effect on properties of experimental graphene dental nanocomposites. Journal of Adhesion Science and Technology, Vol. 30, No. 16, 2016, pp. 1779–1794.
[81]. Hu, W., C. Peng, W. Luo, M. Lv, X. Li, D. Li, et al. Graphene-based antibacterial paper. ACS Nano, Vol. 4, No. 7, 2010, pp. 4317–4323.
[82]. Ji, H., H. Sun, and X. Qu. Antibacterial applications of graphene-based nanomaterials: Recent achievements and challenges. Advanced drug Delivery Reviews, Vol. 105, 2016, pp. 176–189.
[83]. Das, M. R., R. K. Sarma, R. Saikia, V. S. Kale, M. V. Shelke, and P. Sengupta. Synthesis of silver nanoparticles in an aqueous suspension of graphene oxide sheets and its antimicrobial activity. Colloids and Surfaces B: Biointerfaces, Vol. 83, No. 1, 2011, pp. 16–22.
[84]. Rago, I., A. Bregnocchi, E. Zanni, A. G. D'Aloia, F. D. Angelis, M. Bossu, et al. antimicrobial activity of graphene nanoplatelets against Streptococcus Mutans. Presented the 2015 IEEE 15th International Conference on Nanotechnology (IEEE-NANO), 2015.
[85]. Rodríguez-Lozano, F. J., D. García-Bernal, S. Aznar-Cervantes, et al. Effects of composite films of silk fibroin and graphene oxide on the proliferation, cell viability and mesenchymal phenotype of periodontal ligament stem cells. Journal of Materials Science: Materials in Medicine, Vol. 25, No. 12, 2014, pp. 2731–2741.
[86]. Park, K. O., J. H. Lee, J. H. Park, Y. C. Shin, J. B. Huh, J.-H. Bae, et al. Graphene oxide-coated guided bone regeneration membranes with enhanced osteogenesis: spectroscopic analysis and animal study. Applied Spectroscopy Reviews, Vol. 51, No. 7–9, 2016, pp. 540–551.
[87]. Rosa, V., H. Xie, N. Dubey, T. T. Madanagopal, S. S. Rajan, J. L. P. Morin, et al. Graphene oxide-based substrate: Physical and surface characterization, cytocompatibility and differentiation potential of dental pulp stem cells. Dental Materials, Vol. 32, No. 8, 2016, pp. 1019–1025.
[88]. Jadhav, K., R. Hr, S. Deshpande, S. Jagwani, D. Dhamecha, S. Jalalpure, K. Subburayan, et al. Phytosynthesis of gold nanoparticles: Characterization, biocompatibility, and evaluation of its osteoinductive potential for application in implant dentistry. Materials Science and Engineering: C, Vol. 93, 2018, pp. 664–670.
[89]. Niska, K., N. Knap, A. Kędzia, M. Jaskiewicz, W. Kamysz, and I. Inkielewicz-Stepniak. Capping agent-dependent toxicity and antimicrobial activity of silver nanoparticles: An in vitro study. Concerns about potential application in dental practice. International Journal of Medical Sciences, Vol. 13, No. 10, 2016, pp. 772–782.
[90]. Barot, T., D. Rawtani, and P. Kulkarni. Physicochemical and biological assessment of silver nanoparticles immobilized halloysite nanotubes-based resin composite for dental applications. Heliyon, Vol. 6, No. 3, 2020.
[91]. Acosta-Torres, L. S., L. M. López-Marín, R. E. Núñez-Anita, G. Hernández-Padrón, and V. M. Castaño. Biocompatible metal-oxide nanoparticles: Nanotechnology improvement of conventional prosthetic acrylic resins. Journal of Nanomaterials, Vol. 2011, 2010.
[92]. Del Carpio-Perochena, A., A. Kishen, A. Shrestha, and C. M. Bramante. Antibacterial properties associated with chitosan nanoparticle treatment on root dentin and 2 types of endodontic sealers. Journal of Endodontics, Vol. 41, No. 8, 2015, pp. 1353–1358.
[93]. Burrow, M.F. Composite Adhesive Restorative Materials for Dental Applications. In Non-Metallic Biomaterials for Tooth Repair and Replacement; Elsevier: Amsterdam, The Netherlands, 2013; pp. 235–269.
[94]. Ferracane, J.L. Resin Composite—State of the Art. Dent. Mater. 2011, 27, 29–38.
[95]. Coutinho, E.; Cardoso, M.V.; De Munck, J.; Neves, A.A.; Van Landuyt, K.L.; Poitevin, A.; Peumans, M.; Lambrechts, P.; Van Meerbeek, B. Bonding Effectiveness and Interfacial Characterization of a Nano-Filled Resin-Modified Glass-Ionomer. Dent. Mater. 2009, 25, 1347–1357.
[96]. Falsafi, A.; Mitra, S.B.; Oxman, J.D.; Ton, T.T.; Bui, H.T. Mechanisms of Setting Reactions and Interfacial Behavior of a Nano-Filled Resin-Modified Glass Ionomer. Dent. Mater. 2014, 30, 632–643.
[97]. Xu, H.H.K.; Moreau, J.L.; Sun, L.; Chow, L.C. Nanocomposite Containing Amorphous Calcium Phosphate Nanoparticles for Caries Inhibition. Dent. Mater. 2011, 27, 762–769
[98]. Taheri, M.M.; Abdul Kadir, M.R.; Shokuhfar, T.; Hamlekhan, A.; Shirdar, M.R.; Naghizadeh, F. Fluoridated Hydroxyapatite Nanorods as Novel Fillers for Improving Mechanical Properties of Dental Composite: Synthesis and Application. Mater. Des. 2015, 82, 119–125
[99]. Eick, J.D.; Kotha, S.P.; Chappelow, C.C.; Kilway, K.V.; Giese, G.J.; Glaros, A.G.; Pinzino, C.S. Properties of Silorane-Based Dental Resins and Composites Containing a Stress-Reducing Monomer. Dent. Mater. 2007, 23, 1011–1017.
[100]. Xu, H.H.K.; Eichmiller, F.C.; Antonucci, J.M.; Schumacher, G.E.; Ives, L.K. Dental Resin Composites Containing Ceramic Whiskers and Precured Glass Ionomer Particles. Dent. Mater. 2000, 16, 356–363.
[101]. Xu, H.H.; Quinn, J.B.; Smith, D.T.; Giuseppetti, A.A.; Eichmiller, F.C. Effects of Different Whiskers on the Reinforcement of Dental Resin Composites. Dent. Mater. 2003, 19, 359–367.
[102]. Miao, X.; Zhu, M.; Li, Y.; Zhang, Q.; Wang, H. Synthesis of Dental Resins Using Diatomite and Nano-Sized SiO2 and TiO2. Prog. Nat. Sci. Mater. Int. 2012, 22, 94–99.
[103]. Van Landuyt, K.L.; Yoshihara, K.; Geebelen, B.; Peumans, M.; Godderis, L.; Hoet, P.; Van Meerbeek, B. Should We Be Concerned about Composite (Nano-)Dust? Dent. Mater. 2012, 28, 1162–1170.

5. Nanotechnology in Prosthodontics

Prosthodontics, a branch of dentistry also known as prosthetic dentistry, focuses on restoring missing teeth in dental arches through the use of various techniques and materials, including implants, single-tooth restorations, and removable prostheses such as dentures. Wear resistance is a critical factor in assessing the quality of dentures, and nanotechnology has been applied to address wear-related challenges in prosthodontics [1].

In a study conducted by Ghazal et al., the wear susceptibility of various denture materials was explored. Denture teeth composed of feldspathic ceramic (FC), nanofilled composite resin (NCR) containing SiO2 nanoparticles (12 nm in size, 36–42 wt.%), and acrylic resin were evaluated using a chewing simulator. The findings indicated that ceramic dentures demonstrated the highest resistance to wear, surpassing even natural teeth. Remarkably, nanofilled denture resin caused considerably less damage to natural teeth, rendering it a viable material choice for partial dentures [2].

Dentures constructed from nanocomposites comprising poly(methyl methacrylate) (PMMA) as the composite matrix and montmorillonite nanosheets (MMT) as a modifier underwent biocompatibility assessments. Zheng et al. conducted various tests, including cytotoxicity evaluations, acute systemic toxicity assessments, oral mucous membrane irritation examinations, guinea pig maximization tests, and mouse bone marrow micronucleus tests. The findings indicated that the composite demonstrated favorable biocompatibility as a denture base material. Subsequent studies by Wang et al. focused on thermal stability, demonstrating high thermal stability and considering the material promising for denture construction [3].

The issue of polymerization shrinkage during the manufacturing of dentures based on acrylic resin was addressed by introducing carbon nanotubes into the resin. The results indicated a reduction in shrinkage, with no visible shrinkage observed at a nanotube concentration of 0.5% (wt.%). This approach shows potential for mitigating polymerization shrinkage in denture fabrication.

These studies highlight the application of nanotechnology in prosthodontics to enhance wear resistance, biocompatibility, and other key properties of denture materials, contributing to the development of more advanced and effective dental prosthetics [4].

Prosthetic restorations, particularly complete dentures made of polymethyl methacrylate (PMMA) resin or acrylic particle implants, play a crucial role in tooth recovery and oral rehabilitation. Nanoparticles, such as silver (Ag), zirconia (ZrO2), and titanium dioxide (TiO2), have found successful applications in PMMA to address issues like stomatitis caused by Candida colonization.

In prosthodontics, the incorporation of nanoparticles into PMMA has been explored for various benefits. For example:

1. ***Antimicrobial Properties***: The use of nanoparticles, such as TiO_2, has been employed to enhance the antimicrobial properties of PMMA denture mixtures. This is particularly important in preventing conditions like stomatitis caused by Candida colonization.
2. ***Structural and Chemical Improvements***: The combination of TiO_2 nanoparticles with three-dimensional PMMA denture mixtures has been shown to not only provide antimicrobial benefits but also improve the structural and chemical features of the prosthetic restorations. This can contribute to the overall performance and longevity of the prosthetic devices.

These advancements demonstrate how the integration of nanoparticles into PMMA in prosthodontics can offer multifaceted benefits, ranging from enhanced antimicrobial properties to improvements in structural and chemical characteristics. This ongoing research and development aim to improve the quality and functionality of prosthetic restorations for better oral health outcomes.

In prosthodontics, the occurrence of denture stomatitis is a significant concern, with Candida species, particularly C. albicans, being prominently involved in the initiation and progression of these lesions [5, 6, 7]. To combat fungal infections, researchers have explored the integration of antifungal agents, such as silver nanoparticles, into denture materials.

Wady et al. developed a denture composed of acrylic resin modified with silver nanoparticles to target C. albicans. However, experiments revealed that while unloaded nanoparticles displayed robust antifungal activity against Candida, silver nanoparticles bound within a resin matrix exhibited

no activity. The limited release of silver ions from the hydrophobic acrylic resin was proposed as an explanation for this lack of efficacy [8].

Nam et al. investigated the antifungal efficacy of silver nanoparticles embedded in polymerized acrylic discs. Various concentrations of silver nanoparticles were tested, and discs containing 20 and 30 wt.% of nanoparticles demonstrated latent antifungal properties. Elution tests revealed a maximal concentration of Ag+ at 0.356 mg/L, while the minimal inhibitory concentration (MIC) for silver ions was determined to be 3.0 mg/mL. The antifungal activity was attributed to the direct interaction of fungi with the denture surface, as the MIC was not attained solely through nanosilver release. Thermal analysis indicated enhanced thermal stability with the inclusion of nanofillers, although color assessment suggested a need for improvement to minimize color loss [9].

These studies highlight the potential of silver nanoparticles as antifungal agents in denture materials, with considerations for release kinetics, direct interaction with fungi, and additional material properties such as thermal stability and color retention [10].

5.1. 3D-Printed Nanocomposite Denture-Base Resins

The research aims to investigate the impact of incorporating zirconium dioxide nanoparticles (ZrO_2NPs) into 3D-printed denture-base resins on various mechanical and physical properties compared to conventional heat-polymerized acrylic resin. The study seeks to evaluate flexure strength, elastic modulus, impact strength, hardness, and surface roughness, with the null hypothesis assuming no effect on these properties with the addition of ZrO_2NPs.

The background provides context for the study, emphasizing the prevalence of complete edentulism in the geriatric population and the common use of polymethyl methacrylate (PMMA) for denture fabrication. PMMA, while cost-effective and aesthetically pleasing, has certain drawbacks, including low strength, polymerization shrinkage, susceptibility to microbial colonization, and low wear resistance. To address these issues, researchers have explored the reinforcement of PMMA, and nanoparticles, particularly ZrO_2NPs, have shown promise in improving its properties.

The research also discusses the advent of 3D printing in dentistry, specifically in the fabrication of complete denture bases. While 3D printing offers advantages such as reduced time, improved tissue adaptation, and accuracy in comparison to conventional methods, there are still concerns about its mechanical and physical properties. The study aims to address these concerns by examining the impact of ZrO_2NPs on 3D-printed denture-base resins.

The hypotheses and objectives of the study are clearly outlined. The null hypothesis posits that the addition of ZrO_2NPs would have no effect on flexure strength, impact strength, surface hardness, and surface roughness of 3D-printed material. The researchers aim to test this hypothesis by conducting a comprehensive evaluation of the specified mechanical and physical properties.

The background provides a comprehensive overview of the research landscape, highlighting the significance of the study in improving denture materials for the geriatric population. The incorporation of nanoparticles into 3D-printed denture-base resins is a novel approach, and the research aims to contribute valuable insights into the potential benefits of this reinforcement method.

5.1.1. Effect of ZrO_2 Nanoparticles on the Mechanical and Surface Properties In Vitro

The researchers determined the sample size for their in vitro study using a power analysis. They employed the World Health Organization formulae for sample size calculation. The key parameters considered for this calculation were:

- Study Power: 80%
- Level of Significance (α): 5%
- Marginal Error: 5%

These parameters are common in statistical analyses and help ensure that the study has a high probability (80%) of detecting a true effect if it exists, with a 5% chance of making a Type I error (rejecting incorrectly a null hypothesis that is actually true). The 5% marginal error represents the precision or allowable error in the estimates.

The sample size calculation is a critical step in the planning of experiments, as it ensures that the study is adequately powered to detect meaningful effects. In this context, the researchers want to ensure that the number of samples they collect is sufficient to achieve the desired statistical power while maintaining an acceptable level of significance and marginal error.

5.1.1.1. Nanocomposites Mixture Preparation

In the study, three types of denture base materials were used:

Heat-polymerized PMMA (Polymethyl Methacrylate): This is a conventional denture base material that is polymerized using heat.

Denture 3D+ (Next Dent, Soesterberg, The Netherlands): A 3D-printed resin designed for denture fabrication.

DentaBase (ASIGA, Sydney, Australia): Another 3D-printed resin used for denture base fabrication.

For the 3D-printed resins (Denture 3D+ and DentaBase), different concentrations of Zirconium Dioxide Nanoparticles (ZrO2NPs) were added: 0.5wt%; 1wt% ; 3wt% and 5wt%.

One additional group for each resin remained without the addition of ZrO_2NPs, serving as the unmodified (control) group.

The ZrO_2NPs used in the study had a high purity of 99.9%, and their average granularity was reported to be 40 nm with a surface area of 9 m²/g. The nanoparticles were treated with a silane-coupling agent (TMSPM) before being added to the 3D-printing resins. This treatment is commonly used to enhance the interaction between nanoparticles and polymer matrices [11].

The study aimed to evaluate the influence of incorporating ZrO2 nanoparticles (ZrO2NPs) into 3D-printed denture base resins at different concentrations on a range of mechanical and physical properties. These properties included flexural strength, impact strength, surface roughness, and hardness. The incorporation of nanoparticles into dental materials is a common strategy to enhance their mechanical and antimicrobial properties [12].

5.1.1.2. Specimen's Preparation

The study followed the ISO 20795-1:2013 standard for preparing specimens and conducting tests. Here are the key details regarding the specimens and their preparation:

Flexure-Properties Test:

Specimen Dimensions: Rectangular bar with dimensions of (64 × 10 × 3.3 ± 0.2 mm).

Purpose: Used for the flexure-properties test.

Impact Strength Test:

Specimen Dimensions: (50 × 6 × 4 mm) with a 1.2 mm edgewise V-notch, leaving a residual depth of 4.8 mm under the notch.

Purpose: Used for measuring impact strength.

Surface Roughness and Hardness Tests:

Specimen Dimensions: (15 × 2 mm).

Purpose: Used for surface roughness and hardness tests.

Material Used for Control Group (Heat-polymerized PMMA):

Material: Major.Base.20 MAJOR (Prodotti Dentari S.p.A., Italy).

Fabrication: Wax pattern was created with the required dimensions, invested in stone inside the flask, and heat-polymerized at 73 °C for 90 min and then at 100 °C for an additional 30 min.

Material Used for 3D-Printed Specimens:

3D Printing Machines: NextDent 5100 (NextDent, Netherlands) and ASIGA MAXTM (ASIGA, Australia).

Design: Specimens were designed using an open-source CAD system (123D design, Autodesk) and saved as STL files.

Mixing and Printing: Pure resin was mixed using an LC 3D Mixer, and nanoparticles were added. The resin was then distributed into bottles with different concentrations, shaken, and 3D printed with a layer thickness of 50 µm and 90-degree orientation.

Post-curing: Specimens were exposed to UV light (405 nm) for polymerization. Post-curing duration was 20 min for ASIGA specimens and 10 min for NextDent specimens.

Cleaning: Specimens were cleaned using isopropyl alcohol (99.9%) and immersed in a bowl containing glycerol.

Finishing and Polishing: Excess resin was trimmed, and specimens were finished and polished using silicon carbide grinding paper and polishing tools.

Thermo-Cycling: All specimens underwent 5000 cycles in a thermocycling machine to simulate temperature changes occurring intraorally over half a year.

The study aimed to evaluate the mechanical and physical properties of the specimens, including flexural strength, impact strength, surface roughness, and hardness. The specimens were subjected to standardized procedures to ensure consistency in testing conditions.

The flexure strength and elastic modulus, impact strength, hardness, and surface roughness (μm) were measured using the three-point bending test, Charpy's impact test, Vickers hardness test, and a profilometer, respectively. The data were analyzed by ANOVA and Tukey's post hoc test ($\alpha = 0.05$).

5.1.1.3. Results

The FTIR (Fourier Transform Infrared) results for ASIGA and NextDent, with varying ZrO2 concentrations (0 wt%, 0.5wt%, 1wt%, 3wt%, and 5wt%), along with pure PMMA, have been analyzed. Here are the key observations:

1. Differences Between 3D-Printed Resins and Pure PMMA:
   - The spectra for 3D-printed resins (ASIGA and NextDent) differ from those of pure PMMA.
   - Noticeable differences are observed in the 1600 and 400 cm^{-1} range of the spectra.
2. Characteristic Bands for ASIGA and NextDent:
   - For the ASIGA group, the strongest and widest bands are observed at ~1026 and ~465 cm^{-1}.
   - For the NextDent resins, the most intense bands appear at ~1060 and ~457 cm^{-1}.
3. Common Bands with Pure PMMA:
   - Despite the differences, common characteristic features are identified between 3D-printed resins (ASIGA and NextDent) and pure PMMA resin.
   - Common bands are attributed to CH3 and CH2 stretching vibrations (2920 cm^{-1}) and carbonyl groups (1705 cm^{-1}) in the PMMA chain.
4. Similarity Between ASIGA and NextDent:
   - The comparison between ASIGA and NextDent reveals almost identical features and bands.
   - This similarity confirms the homogeneous dispersion of ZrO2 NPs into both ASIGA and NextDent 3D-printed resins.
5. Confirmation of Chemical Structure Differences:
   - The FTIR spectra indicate that the chemical structure is different to some extent for ASIGA and NextDent groups compared to pure PMMA base denture.
   - Despite differences, the comparison shows consistent features and bands between the two 3D-printed resin groups.

In summary, the FTIR analysis suggests that while there are differences in the chemical structure between 3D-printed resins and pure PMMA, the dispersion of ZrO2 NPs is homogeneous in both ASIGA and NextDent resins. Additionally, the similarity between ASIGA and NextDent spectra indicates consistent features in the chemical composition of the two 3D-printed resin groups (Figure 5.1.).

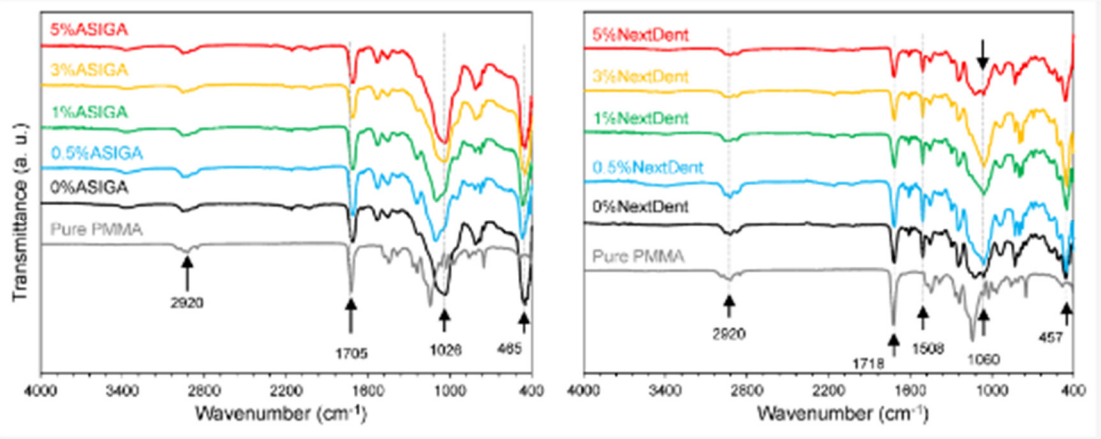


Figure 5.1. FTIR spectra of ASIGA and NextDent groups at different ZrO_2 concentrations (0, 0.5, 1, 3, and 5 wt.%). The FTIR spectrum of pure PMMA specimen is also shown [12].

The SEM (Scanning Electron Microscopy) analysis (Figure 5.2 and Figure 5.3) revealed characteristic changes between the control (unmodified) and ZrO2NP-modified 3D-printed denture-base resins (ASIGA and NextDent groups). Here are the key observations:

Homogeneous Distribution at Low Concentrations:

At low concentrations of ZrO2NPs, both ASIGA and NextDent groups exhibited a unitary and well-distributed arrangement of nanoparticles within the resin matrix (Figure 5.2. C,D and Figure 5.3. C,D).

Cluster Formation at High Concentrations:

At high concentrations of ZrO2NPs, some clusters of nanoparticles were observed on the fractured surfaces of both ASIGA and NextDent groups (Figure 5.2. F and Figure 5.3. E,F).

Control Specimens (Unmodified):

Control specimens (unmodified) displayed random faint lamellae, indicating a brittle type of fracture (Figure 5.2. A and Figure 5.3. A).

Features of Unmodified Specimens:

Unmodified NextDent and ASIGA specimens exhibited features with small lamellae and a smooth background (Figure 5.2. B and Figure 5.3. B).

Surface Changes in Modified Specimens:

Modified specimens, especially at higher concentrations of ZrO2NPs, showed a gradual change from a smooth to a rough surface with the appearance of nanoparticles (Figure 5.2. C–F and Figure 5.3. C–F).

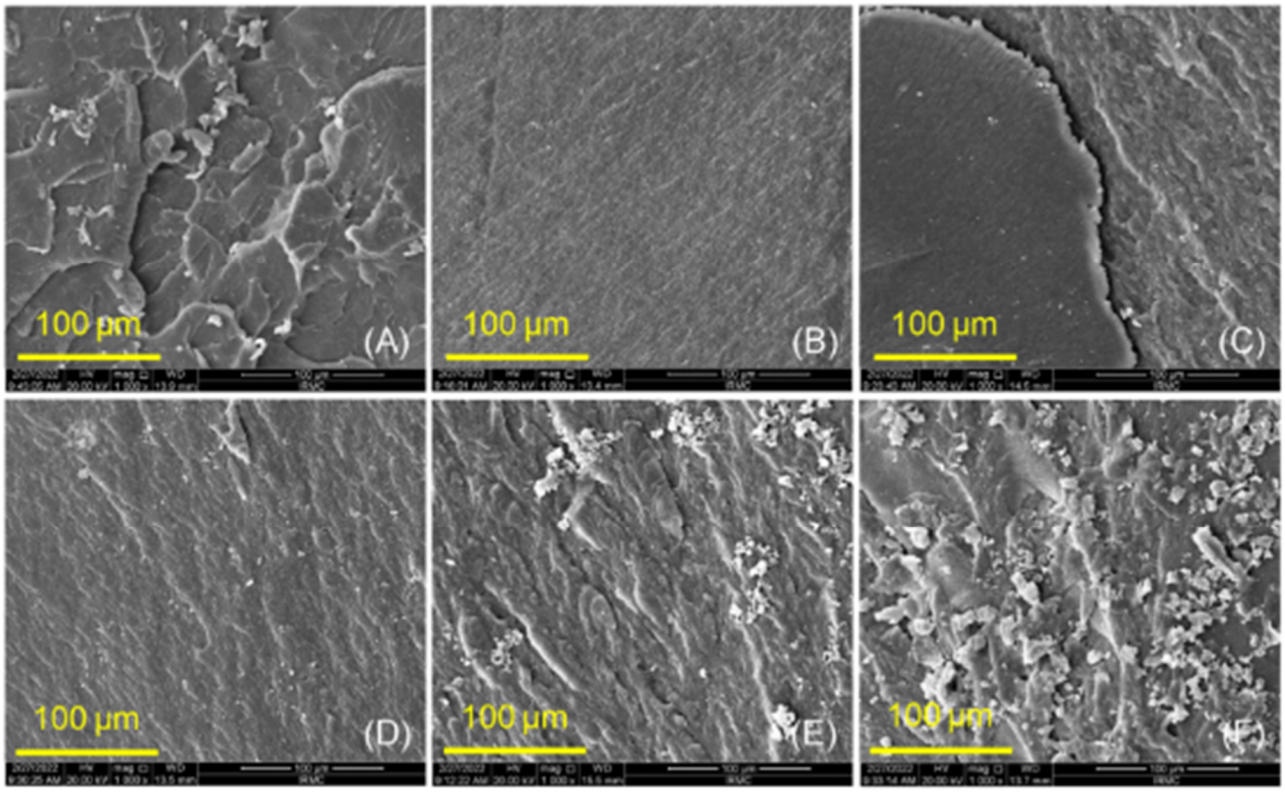


Figure 5.2. SEM images of ASIGA group at different concentrations of ZrO_2NPs (0, 0.5, 1, 3, and 5 wt.%). (A) pure PMMA, (B) 0 wt.% ASIGA, (C) 0.5 wt.% ASIGA, (D) 1 wt.% ASIGA, (E) 3 wt.% ASIGA and (F) 5 wt.% ASIGA. The scale bars are 100 µm [12].

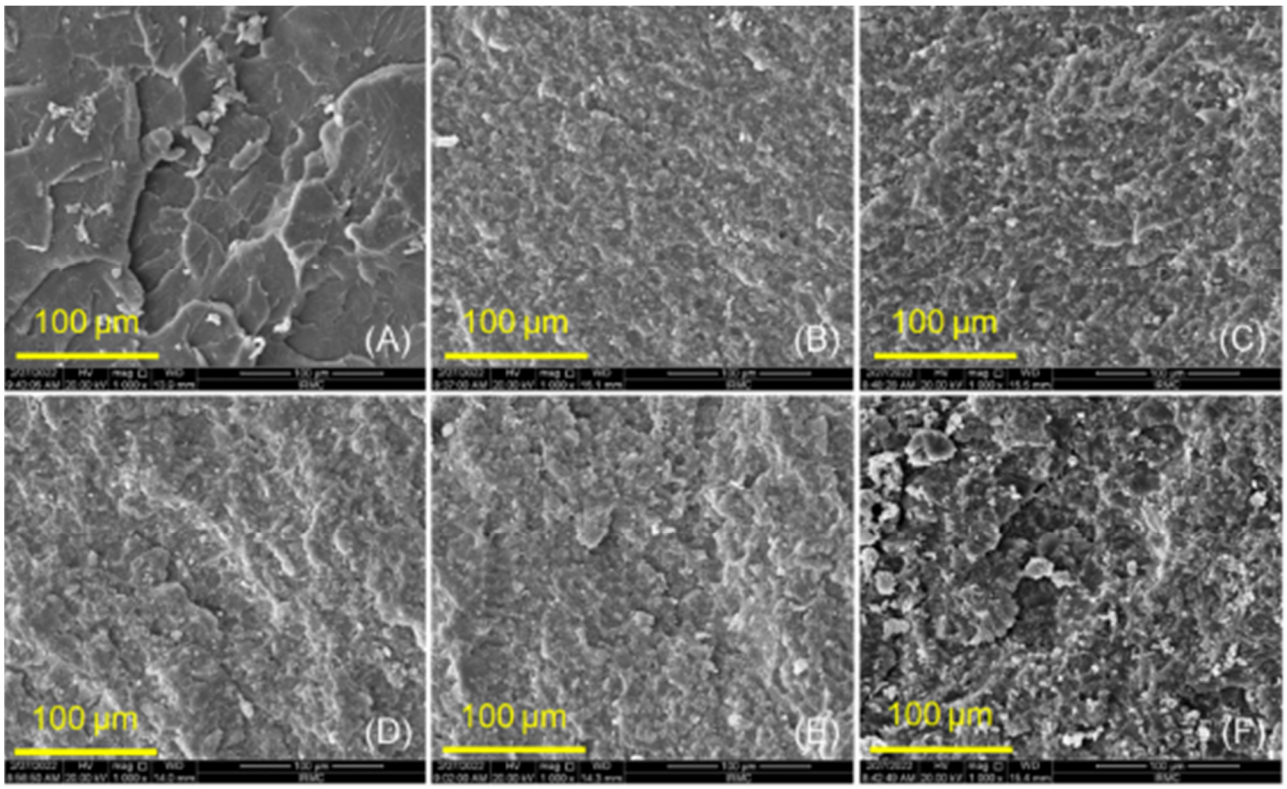


Figure 5.3. SEM images of NextDent group at different concentrations of ZrO_2NPs (0, 0.5, 1, 3, and 5 wt.%). (A) pure PMMA, (B) 0 wt.% NextDent, (C) 0.5 wt.% NextDent, (D) 1 wt.% NextDent, (E) 3 wt.% NextDent and (F) 5 wt.% NextDent. The scale bars are 100 µm [12].

In summary, SEM analysis highlighted that the addition of ZrO_2NPs led to changes in the surface characteristics of the 3D-printed denture-base resins. The distribution of nanoparticles was

homogenous at low concentrations, but clusters were observed at higher concentrations. The control specimens displayed a brittle fracture pattern, while the unmodified specimens showed small lamellae with a smooth background. The introduction of ZrO_2NPs resulted in surface changes, including a transition from smooth to rough surfaces, especially at higher nanoparticle concentrations.

5.1.1.4. Discussions

This detailed in vitro study focused on the effects of incorporating ZrO2 nanoparticles (ZrO2NPs) into 3D-printed denture-base resins, comparing them with both conventional heat-polymerized PMMA and unmodified 3D-printed resins. Here are the key findings and observations:

General Observations:

1. **Increased Geriatric Population and Complete Edentulism:**
   - The study acknowledged the rise in the geriatric population and the prevalence of complete edentulism, making complete dentures a common treatment choice.
2. **Challenges of 3D Printing in Denture Production:**
   - Despite the advantages of 3D printing in dentistry, including ease of fabrication and accuracy, there were acknowledged challenges such as inferior mechanical and physical properties compared to traditional methods.
3. **Introduction of ZrO2 Nanoparticles:**
   - ZrO2NPs were introduced to address the limitations of 3D-printed denture-base resins. Zirconium dioxide (ZrO2) was chosen for its biocompatibility, strength, and antibacterial/antifungal effects.

Experimental Setup:

4. **Materials Used:**
   - Heat-polymerized PMMA and two 3D-printed resins (NextDent and ASIGA) were used in the study. ZrO2NPs were added to 3D-printed resins in various concentrations (0.5%, 1%, 3%, 5%).
5. **Specimen Fabrication:**
   - Specimens for testing (flexural strength, impact strength, hardness, and surface roughness) were fabricated using both conventional and 3D printing methods. ZrO2NPs were silanized before incorporation into 3D-printed resins.
6. **Thermal Cycling Simulation:**
   - To simulate oral conditions, specimens underwent 5000 thermal cycles, representing half a year of clinical use.

Experimental Results:

7. **Flexural Strength:**
   - Unmodified 3D-printed resins showed lower flexural strength compared to heat-polymerized PMMA.
   - The addition of ZrO2NPs led to a concentration-dependent increase in flexural strength, particularly in ASIGA resin.
8. **Elastic Modulus:**
   - All 3D-printed resins exhibited lower elastic moduli compared to heat-polymerized PMMA.
   - Addition of ZrO2NPs significantly increased elastic modulus in NextDent, while ASIGA showed no significance.
9. **Impact Strength:**

- Unmodified 3D-printed resins had lower impact strength than heat-polymerized PMMA.
- Addition of ZrO2NPs resulted in a significant increase in impact strength, except for ASIGA where improvement was not observed.

10. **Surface Hardness:**
    - 3D-printed resins showed lower hardness compared to heat-polymerized PMMA.
    - Addition of ZrO2NPs led to an insignificant decrease in hardness values.
11. **Surface Roughness:**
    - 3D-printed resins had higher surface roughness compared to heat-polymerized PMMA.
    - Addition of ZrO2NPs did not result in significant changes in surface roughness.

Conclusions and Recommendations:

12. **Clinical Implications:**
    - Despite lower mechanical properties, 3D-printed resins, especially when modified with ZrO2NPs, show promise for clinical applications in denture fabrication.
13. **Suggestions for Further Research:**
    - The study suggests further investigations into the biocompatibility of nanocomposite 3D-printed resins.
    - It recommends exploring different 3D-printed materials, denture configurations, and dynamic loading conditions.

Limitations:

The study acknowledges limitations, including the use of only one type of nanoparticle, one printing orientation, and the need for more comprehensive simulations of intraoral conditions.

5.1.1.5. Conclusions

This study provides valuable insights into the mechanical behavior and surface properties of 3D-printed resins, specifically comparing them with heat-polymerized acrylic resin and assessing the impact of incorporating ZrO2 nanoparticles (ZrO2NPs). Here are some key observations and conclusions from the study:

1. Comparison with Heat-Polymerized Acrylic Resin:
    - The 3D-printed resins demonstrated inferior mechanical behavior and surface properties when compared with heat-polymerized acrylic resin. This aligns with the acknowledged challenges of 3D printing in dentistry, as discussed in the introduction.
2. Effect of ZrO2NPs Addition:
    - The addition of ZrO2NPs was found to improve the properties of 3D-printed resins in comparison to heat-polymerized acrylic resins. This suggests that nanocomposite formulations could enhance the performance of 3D-printed dental materials.
3. Flexural Strength (FS):
    - The flexural strength in the ASIGA group showed a concentration-dependent relationship with ZrO2NPs. Higher concentrations led to increased flexural strength. However, this relationship was not observed in the NextDent group. This indicates that the impact of ZrO2NPs on flexural strength may vary depending on the specific 3D-printed resin composition.
4. Impact Strength:
    - Unlike flexural strength, the impact strength in the ASIGA group did not show a concentration-dependent relationship with ZrO2NPs. Additionally, the impact strength in

both ASIGA and NextDent groups remained inferior to that of heat-polymerized acrylic resin. This implies that while ZrO2NPs may enhance some mechanical properties, further improvements are needed in impact strength.

5. Elastic Modulus and Hardness:
   - The addition of ZrO2NPs did not result in an increase in elastic modulus or hardness in either the ASIGA or NextDent groups. This suggests that the impact of ZrO2NPs on these properties may be limited, and other factors or modifications may be required to enhance elastic modulus and hardness.
6. Surface Roughness:
   - Both ASIGA and NextDent groups showed a rise in the roughness of the surface with the addition of ZrO2NPs. While nanocomposite formulations may offer improvements in certain mechanical properties, there seems to be a trade-off with an increase in surface roughness. This emphasizes the importance of balancing different material characteristics for optimal clinical performance.
7. Clinical Suitability:
   - The study concludes that nanocomposite 3D-printed resins, especially those modified with ZrO2NPs, are suitable for clinical use. The observed improvements indicate progress in overcoming the limitations associated with 3D-printed dental materials.
8. Recommendations for Future Research:
   - The study suggests that further investigations are needed to understand the relationship between nanoparticle concentrations and various mechanical properties. Additionally, addressing the limitations and optimizing the formulation could lead to even better clinical outcomes.

5.1.2. The effect of incorporating TiO_2 nanoparticles on the growth of Candida albicans

The study aims to evaluate the antifungal properties of the composite material against Candida albicans and assess its biocompatibility. The passage also mentions the advantages of 3D printing in dentistry, particularly in the fabrication of removable dentures. The incorporation of TiO2 NPs is highlighted for its potential antifungal properties, and previous studies supporting this approach are referenced.

The objectives of the study are outlined, with the first null hypothesis suggesting no difference in biological effects between the nanocomposite material and a control, and the second null hypothesis proposing that the composite material would not exhibit antifungal properties.

5.1.2.1. Resin Material and TiO_2 NPs

The material used for the denture base manufacturing in the study and the characterization of the titanium dioxide nanoparticles (TiO2 NPs) used in the research implies:

1. Denture Base Material:
   - The denture base material used is NextDent Denture 3D+ light-cured resin, a commercial product from 3D Systems in Soesterberg, Netherlands.
   - The composition of the resin is provided in weight percentage (w/w%):
     - Ethoxylated bisphenol A dimethacrylate (75%)
     - 7,7,9-trimethyl-4,13,14,dioxo-3,14,diazahexadecane-1,16-diyl bismethacrylate (10%–20%)
     - 2-hydroxyethyl methacrylate (5%–10%)
     - Silicon dioxide (5%–10%)
     - Diphenyl (2,4,6-trimethylbenzoyl) phosphine oxide (1%–5%)
     - Titanium dioxide (<0.1%)
2. Titanium Dioxide Nanoparticles (TiO2 NPs):
   - Silane-coated titanium dioxide NPs from Skyspring Nanomaterials, Texas, USA, were used.
   - The TiO2 NPs have a size of 10–30 nm and are in the rutile form (99.5%).

- Silane coupling agents were used to coat the TiO2 NPs, facilitating the bonding of organic materials to the inorganic surfaces and ensuring homogeneous distribution of the nanoparticles.

3. FTIR Analysis:
   - Fourier-transform infrared (FTIR) analysis was conducted to determine the functional groups within the TiO2 powder.
   - The FTIR spectra were measured in the wavelength range of 4000–400 cm−1 with a resolution of 4 cm−1.
   - Spectra were obtained using a Spotlight 200i FT-IR Microscope System from Perkin-Elmer, Ohio, USA, with an average of 32 scans at room temperature.

This information provides insight into the specific composition of the denture base material and the characteristics of the TiO2 NPs, including their size, form, and surface treatment. The FTIR analysis indicates the functional groups present in the TiO2 powder, which is crucial for understanding its chemical properties and potential interactions with the 3D-printed resin.

5.1.2.2. Cells Cultures Preparations

This section outlines the procedures for cell culture, cell viability assessment, cytotoxicity evaluation, and antifungal testing as part of the experimental setup. Additionally, it provides details on the statistical analysis used for data interpretation.

1. Cell Culture:
   - Primary human gingival fibroblast (HGF) cells were cultured according to ISO 10993-5 guidelines.
   - HGF cells were maintained in growth medium provided by the manufacturer, and the medium contained various components at specific concentrations.
   - Cells were initially cultured in a T75 flask and maintained in an incubator under controlled conditions (37°C, 5% CO2, 95% air).
   - Subsequently, cell passaging was carried out using 0.25% trypsin, following which the cells were seeded into a 24-well culture plate at a predetermined density for subsequent experiments.
2. Cell Viability Assessment:
   - AlamarBlue™ cell viability reagent was used for colorimetric experiments at four time points (1, 3, 5, and 10 days).
   - Three biological replicates were used for each test.
   - Viability was measured using a microplate reader, and images were captured with a light microscope.
   - Cell viability was calculated using a specific equation (Equation 1).
3. Cytotoxicity Evaluation:
   - A Pierce™ Lactate dehydrogenase (LDH) cytotoxicity assay kit was used to assess cytotoxicity at four time points (1, 3, 5, and 10 days).
   - LDH release from cells was measured using a microplate reader.
   - Cytotoxicity was determined using a specific equation (Equation 2).
4. Antifungal Test:
   - Antifungal activity against Candida albicans was evaluated using composite material discs.
   - Candida albicans suspension was prepared and adjusted for microbial cell concentration.
   - Composite material discs were incubated with Candida albicans, washed, and sonicated to detach fungal cells.
   - Colonies were counted and reported as colonies forming unit per milliliter (CFU/mL).
5. Statistical Analysis:
   - Data analysis was performed using SPSS software (version 25).

- Shapiro–Wilk and Levene's tests were employed to assess normal distribution and homogeneity of variance.
- Two-way ANOVA was used to analyze the effects of materials and time, followed by Tukey's multiple comparison test.
- One-way ANOVA and Tukey's tests were performed for comparing different CFUs/mL groups.

This comprehensive methodology covers the steps involved in cell culture, viability assessment, cytotoxicity evaluation, antifungal testing, and the statistical analysis plan for data interpretation.

5.1.2.3. Results

The cell viability results demonstrated that all nanocomposite groups (A, C, E) exhibited a high proliferation rate of human gingival fibroblast (HGF) cells at day 1, ranging from 70% to 95.9%. Group C showed the highest proliferation rate at day 1, but no significant differences were reported between the groups. Subsequently, there was a slight drop in proliferation percentages at day 3, which is considered a normal reaction of cells to a new object in their environment. However, the proliferation rates increased at day 5 and continued to rise at day 10 for all groups.

The proliferation rate at day 5 and day 10 was highest for group C, followed by groups A and E. Two-way ANOVA analysis indicated no significant difference between any of the TiO2 concentration groups at any time point. This suggests that the addition of TiO2 nanoparticles at different concentrations did not significantly impact the cell viability of HGF cells over the tested duration.

The homogeneity of the distribution and normal distribution of the data, as indicated by statistical tests, strengthens the reliability of the results. The consistent and high cell viability observed in all nanocomposite groups suggests the biocompatibility of the TiO2 nanoparticle-incorporated resin composite material, making it suitable for potential applications in dental prosthetics.

It's important to note that the study focused on three representative groups with different TiO_2 nanoparticle concentrations (minimal and highest concentrations), and the results indicate a favorable response of HGF cells to the nanocomposite materials.

The cytotoxicity results showed that, at day 1, there were no significant differences in cytotoxicity between different groups, and the overall cytotoxicity was low. Group C exhibited the highest cytotoxicity at day 1, but the differences between groups were not statistically significant.

As the testing period progressed, cytotoxicity increased for all groups at day 3, day 5, and day 10. The order of cytotoxicity from lowest to highest changed over time, with Group C consistently exhibiting the highest cytotoxicity, followed by Groups E and A.

Two-way ANOVA indicated a statistical difference at day 1 for 0 wt.% TiO_2, showing an increase in cytotoxicity at day 5 and day 10. However, no significant differences were observed between different time points for the other TiO_2 concentration groups.

The increase in cytotoxicity over time could be attributed to factors such as the accumulation of degradation products or changes in the material's surface properties affecting cell-material interactions. The results suggest that the cytotoxicity of the TiO_2 nanoparticle-incorporated resin composite material may vary over time, emphasizing the importance of long-term assessments in understanding the biocompatibility of dental materials.

It's worth noting that the observed cytotoxicity values, even at their highest, are relatively low, suggesting that the TiO_2 nanoparticle-incorporated resin composite material has acceptable cytocompatibility for potential dental prosthetic applications. However, further studies, including in vivo assessments, are recommended to validate these findings and understand the material's behavior in a more complex biological environment.

The antifungal activity results demonstrated a significant difference in the number of fungal colonies grown on the surfaces of 3D-printed nanocomposite specimens with different TiO2 concentrations compared to control discs without added TiO_2 NPs. The colonies count decreased as

the TiO_2 NPs increased in groups B, C, and D, with the lowest count observed in these groups. Group E, on the other hand, exhibited a significant increase in colonies count compared to the other groups.

This suggests that the incorporation of TiO_2 NPs into the resin composite material has an impact on the antifungal activity, and there appears to be a concentration-dependent effect. Groups with higher TiO_2 concentrations (B, C, and D) showed a significant decrease in fungal colonies count compared to groups with lower concentrations (A and E). The increase in colonies count in group E could be attributed to various factors, including the interaction between TiO_2 NPs and the resin matrix, which may influence the release of antifungal agents.

The results support the hypothesis that TiO_2 NPs, known for their antifungal properties, contribute to the inhibition of Candida albicans growth on the 3D-printed nanocomposite specimens. The concentration-dependent effect emphasizes the importance of optimizing the TiO_2 concentration to achieve the desired antifungal activity.

While these findings are promising, it's essential to consider other factors that may influence antifungal activity, such as exposure time, environmental conditions, and the specific mechanisms involved in the interaction between TiO_2 NPs and fungal cells. Further investigations and in vivo studies are necessary to validate and understand the practical implications of these results in a clinical context.

This comprehensive study investigated the addition of titanium dioxide nanoparticles (TiO2 NPs) to 3D-printed denture base resin, aiming to enhance mechanical properties and introduce antifungal capabilities. The research explored the impact on human cell viability, cytotoxicity, and the ability to inhibit Candida albicans growth. Here are the key findings and implications:

1. Denture Base Material and 3D Printing:

Acrylic-based resins have long been used for denture base manufacturing.

3D printing in prosthetic manufacturing has streamlined the process, improving quality and reducing the need for multiple patient visits.

However, 3D-printed photo-cured resin is not as strong as conventionally heat-cured PMMA.

2. Addition of TiO_2 NPs:

TiO_2 NPs were incorporated into the denture base resin to address strength issues.

Previous studies suggested TiO_2 NPs' potential as antifungal agents.

The study aimed to assess TiO_2 NPs' effects on human cell viability, cytotoxicity, and antifungal properties.

3. Biocompatibility Assessment:

Human gingival fibroblast (HGF) cells were chosen for in vitro biocompatibility assessment.

Cell viability and cytotoxicity assays were performed with different TiO2 NP concentrations.

Results indicated no cytotoxic effects, and all tested groups showed high cell viability, confirming biocompatibility.

4. Antifungal Properties:

The study focused on Candida albicans, a common cause of denture stomatitis.

TiO_2 NPs exhibited antifungal properties, with a concentration-dependent effect.

Higher TiO_2 concentrations led to a significant reduction in fungal colonies.

5. Concentration Optimization:

TiO_2 concentrations were optimized to balance antifungal efficacy and mechanical properties.

Agglomeration of particles occurred at higher concentrations, affecting mechanical properties negatively.

6. Implications for Clinical Use:

The study demonstrated the feasibility of 3D-printing TiO_2-reinforced denture base composite material with antifungal activity.

TiO_2 NPs contributed to self-cleaning characteristics, potentially reducing the risk of denture-related oral stomatitis.

The material showed promise for edentulous patients in maintaining prosthesis cleanliness.

7. Recommendations for Future Research:

Further studies are recommended to assess long-term antifungal properties.

Extensive clinical trials are necessary to validate the material's suitability for clinical use over an extended period.

The clinical relevance of the antifungal properties should be investigated in real-world scenarios.

5.1.2.4. Conclusions

The results of the study indicate that 3D-printed denture base resin with titanium dioxide nanoparticles (TiO2 NPs) incorporated at concentrations up to 0.50 wt.% exhibited statistically significant antifungal properties against Candida albicans. This means that the addition of TiO2 NPs at these concentrations effectively inhibited the growth of fungal colonies on the denture base resin surface.

Moreover, the study found that the modified denture base resin did not show any cytotoxic effects against human gingival fibroblast (HGF) cells. This is a crucial aspect of biocompatibility, suggesting that the modified material is safe for contact with oral tissues, which is particularly important for dental prosthetics.

However, when the TiO2 NP concentration was increased to 0.75 wt.%, there was a slight reduction in the antifungal action against fungal colonies. Although this reduction was statistically insignificant, it suggests that there might be an optimal concentration range for TiO2 NPs where antifungal properties are maximized without compromising other aspects of material performance.

The study concludes that the optimal concentration of TiO2 NPs for the denture base resin is determined as 0.25 wt.%. This concentration likely represents a balance between achieving effective antifungal properties and maintaining other desirable material characteristics, such as mechanical strength and 3D printability.

These findings have implications for the development of 3D-printed denture base materials with enhanced antifungal capabilities, potentially contributing to improved oral health outcomes for individuals using dentures. The study underscores the importance of carefully optimizing nanoparticle concentrations to achieve desired functional properties in dental materials.

5.1.3 Unconventional Nanoparticles in Dentistry Assessment of the mechanical properties of PMMA/Silica/Zirconia. Nanocomposite as a denture base material

The development of composite materials for denture bases, specifically focusing on the incorporation of nano silica (SiO2) and zirconia (ZrO2) particles to improve mechanical properties implies:

Reinforcement Strategies:

Previous studies have explored various combinations of reinforcing materials, such as particles, fibers, and whiskers, to enhance material properties.

Multiple reinforcements are often more effective than a single type, as each reinforcement type can improve different material properties.

Organic-Inorganic Hybrid Nanocomposites:

Hybrid nanocomposite materials, combining organic polymers with inorganic nano-fillers, have been studied extensively.

Nanofillers exhibit superior enhancements in properties compared to macro or micro-fillers.

Nanocomposites inherit both the increased rigidity and durability of inorganic fillers and the processability and flexibility of organic polymers.

Preparation of Hybrid Materials:

To create homogeneous hybrid materials, researchers often enhance the affinity between organic polymers and inorganic fillers.

Coupling agents, such as 3-(methacryloxy)propyl-trimethoxysilane (MPTS), are used to improve chemical bonding between the polymer base and nanoparticles.

Nanoparticles Used:

Silica nanoparticles are commonly used due to their promising properties, including rigidity and antimicrobial features.

TiO_2/SiO_2 nanoparticles in PMMA resin showed strong antimicrobial activity against cariogenic bacteria.

Zirconia nanoparticles (ZrO2) are known for high mechanical strength, toughness, stiffness, wear resistance, and thermal stability.

Novel Nanocomposite ($PMMA/SiO_2/ZrO_2$):

The study introduces a novel nanocomposite material, $PMMA/SiO_2/ZrO_2$, for denture bases.

The hypothesis is that adding a mixture of nano silica and zirconia will improve the mechanical properties, including impact strength, transverse strength, roughness, and hardness of PMMA.

Lack of Prior Studies on $PMMA/SiO_2/ZrO_2$ Nanocomposites:

The text mentions that there is no existing report studying the mechanical properties of $PMMA/SiO_2/ZrO_2$ nanocomposites specifically as a denture base material.

Study Objectives:

The primary goal of the study is to investigate whether the addition of nano silica/zirconia mixture improves the mechanical properties of PMMA, focusing on impact strength, transverse strength, roughness, and hardness.

5.1.3.1. Materials and Methods

The materials used in this study focusing on the development of nanocomposite denture base materials were:

1. Denture Base Material:
   - Heat curing poly methyl methacrylate powder (SUPERACRYLP®P PLUS, Czech Republic) and methyl methacrylate liquid monomer (SUPERACRYLP®P PLUS, Czech Republic) were utilized as the denture base material.
2. Inorganic Fillers:
   - Silicon dioxide (SiO_2) nanoparticles with a size of 20 nm (Sigma-Aldrich, Germany) were chosen as one of the inorganic fillers.
   - Zirconium oxide (ZrO_2) nanoparticles with a size less than 100 nm (Sigma-Aldrich, Germany) were selected as another inorganic filler.
3. Solvent and Coupling Agent:
   - Toluene (GCC, UK) was used as a solvent in the preparation of the nanocomposite.
   - 3-(methacryloxy)propyl-trimethoxysilane (Sigma-Aldrich, Germany) served as a coupling agent. Its role is to enhance the bonding between the organic base (poly methyl methacrylate) and the inorganic fillers (SiO2 and ZrO2 nanoparticles).
4. Pilot Study for Optimum Nano SiO_2/ZrO_2 Weight Percentages:
   - A pilot study was conducted to determine the optimal weight percentages of nano SiO_2 and nano ZrO_2.
5. Group Division:
   - Specimens were divided into ten groups based on varying concentrations of nano SiO_2 and nano ZrO_2.

The study is focused on finding the right combination and concentrations of SiO_2 and ZrO_2 nanoparticles in the denture base material. The use of a coupling agent suggests an emphasis on achieving a strong bond between the organic and inorganic components of the nanocomposite for improved properties.

Group	Percentage of nano SiO2 by weight	Percentage of nano ZrO2 by weight	Weight of PMMA powder	Weight of PMMA liquid
Control	0%	0%	44 g	20 ml
A	3%	3%	43.12 g	20 ml
B	5%	3%	42.9 g	20 ml
C	7%	3%	42.68 g	20 ml
D	3%	5%	42.9 g	20 ml
E	5%	5%	42.68 g	20 ml
F	7%	5%	42.46 g	20 ml
G	3%	7%	42.68 g	20 ml
H	5%	7%	42.46 g	20 ml
J	7%	7%	42.24 g	20 ml

Figure 5.4. Pilot study specimen grouping

5.1.3.2. Results

This study that investigated the impact of adding a nano silica/zirconia mixture on the mechanical properties of PMMA denture base material. Here's a summary of the findings:

1. AFM Topographic Image:
   - The AFM topographic image of PMMA/SiO2/ZrO2 nanocomposites revealed a standardized dispersion of nanoparticles throughout the polymer matrix. The use of an ultrasonic probe for dispersion and surface modification contributed to this uniform distribution.
   - Nanoparticle size in the nanocomposite was observed to be about 70–140 nm.
2. Impact Strength Test:
   - Impact strength values of the experimental group (with added nano silica/zirconia) were higher than the control group.
   - The improved impact strength is attributed to high interfacial strength between the nano filler and the matrix, preventing crack spread. The nanoparticles may also dissipate energy, improving impact strength.
   - Previous studies with different nano fillers (ZrO2-Al2O3) added to PMMA also showed improved impact strength.
3. Transverse Strength Test:
   - The nanocomposite demonstrated higher transverse strength compared to the control group.
   - The good distribution of nano fillers within the polymer, limiting segmental motions of macromolecular chains, contributed to improved transverse strength.
   - Transformation toughening, where nano silica and zirconia deplete energy of crack propagation, also played a role in increasing transverse strength.
4. Surface Hardness:
   - The hardness of the nanocomposite increased with the amount of filler loading and the dispersion homogeneity of nano zirconia and nano silica within the material.
   - Increased hardness was linked to the higher cross-linking density, making the polymer more rigid and resistant to penetration.
5. Surface Roughness:
   - Surface roughness of modified PMMA was insignificantly increased compared to the control group.
   - The slight increase in roughness was attributed to differences in particle size and the relatively high filler loading amount, which could lead to the formation of some filler aggregates on the surface.

In summary, the addition of the nano silica/zirconia mixture improved impact strength, transverse strength, and hardness of PMMA denture base material without significantly affecting surface

roughness. These enhancements are attributed to factors like good nanoparticle dispersion, transformation toughening, and increased cross-linking density.

5.1.3.3. Conclusions

The study concludes that the incorporation of a mixture of nano silica and nano zirconia into PMMA denture base material has the potential to increase certain mechanical properties, including impact strength, transverse strength, and hardness. The study found that an insignificant effect on surface roughness was observed. The optimal ratio of nano fillers for obtaining these improvements was determined to be 5% by weight nano silica and 5% by weight nano zirconia.

5.2. Characterization of dental prosthesis based on nano-fluorapatite glass-ceramic fabricated by shell sintering technology

5.2.1. Introduction

In recent years, the integration of additive manufacturing (AM) technologies has significantly transformed various industries, optimizing capabilities and expanding the scope of manufacturing processes [13]. Simultaneously, advancements in manufacturing technology for dental prostheses have been marked by the adoption of CAD/CAM techniques, three-dimensional (3D) scanning, and advanced medical image processing, representing the forefront of dental prosthesis fabrication [2,3].

Figure 5.5. underscores the prevalent techniques employed in the production of dental crowns, a key component in orthodontics. Notably, CAD/CAM has emerged as the predominant technique in prosthodontics across several regions, including Brazil and Europe [4]. Despite this dominance, AM continues to find utility in specific applications, such as the fabrication of medical/dental models and temporary dentures. Challenges hindering wider adoption of AM in prosthodontics include its comparatively lower mechanical strength, limitations in available ceramic and biocompatible materials, and a scarcity of comprehensive clinical data [14, 15, 16].

MATERIAL	TECHNIQUE	LEUCITE	CADCAM	INFILTRATION AND COLORING	GLAZING	SINTERING	POLISHING	CEREC / INLAB	DYONICS POWER	CEREC CONNECT	PROCERA	3M ESPE	LAVA COS	SIRONA CONNECT	KAVO	DEGUDENT	CEREC MCXL	CERECAC	ZIRKONZAHN	CELAY (MIKRONA)
GLASS-CERAMIC	79	31	11	4	3	2	0	1	0	0	0	0	0	0	0	0	0	0	0	0
ZIRCONIA	45	1	0	3	1	4	3	1	0	1	0	0	0	0	0	0	0	0	0	0
POLYMER-CERAMIC COMPOSITE	22	0	1	0	0	0	0	0	0	0	0	0	0	0	0	0	0	0	0	0
YTTRIA STABILIZED ZIRCONIA	22	0	0	0	0	0	0	0	0	0	0	0	0	0	0	0	0	0	0	0
METALLIC	7	0	0	0	0	0	0	0	0	0	0	0	0	0	0	0	0	0	0	0
POLYMERIC MATERIAL	6	0	0	0	0	0	0	0	0	0	0	0	0	0	0	0	0	0	0	0
ALL-CERAMIC	4	0	0	0	0	0	0	0	0	0	0	0	0	0	0	0	0	0	0	0
ALUMINA	4	3	1	2	0	0	0	0	0	0	0	0	0	0	0	0	0	0	0	0
METAL-CERAMIC COMPOSITE	2	0	0	0	0	0	0	0	0	0	0	0	0	0	0	0	0	0	0	0
IN-CERAM SPINELL	2	0	0	0	0	0	0	0	0	0	0	0	0	0	0	0	0	0	0	0

Figure 5.5. The modern prosthodontic technology, with numerous articles highlighting the most notable dental crown materials and methods.

Despite their market dominance, CAD/CAM techniques in dental prosthesis manufacturing come with certain drawbacks. These include the requirement for highly trained professionals to operate complex 5-axis computer numerical control (CNC), high costs associated with raw materials, significant waste generation, elevated operating and maintenance costs, and short tooling lifetimes, sometimes producing only one unit for certain raw materials.

In contrast, additive manufacturing (AM) holds the potential to revolutionize dental prosthesis manufacturing by offering advantages such as improved automation, scalability, flexibility in raw material options, design freedom, cost-effectiveness, and rapid fabrication. While AM has found

success in various industries such as aerospace, automotive, electronics, medical applications, and tissue engineering, its application in dentistry is still evolving and currently faces challenges that limit its competitiveness [17, 18, 19, 20, 21, 22, 23, 24, 25].

Figure 5.5. indicates that the CAD/CAM milling process is the most common technique for manufacturing dental prostheses, primarily using glass-ceramic raw materials like leucite and fluorapatite additions. Zirconia and yttria-stabilized zirconia are gaining popularity due to their excellent mechanical properties and market acceptance.

Processes like hot press and injection molding show a preference for glass-ceramic materials, as other materials are less easily processed using these techniques. Manual processes, despite being commercially widespread, pose challenges in terms of reproducibility from a scientific standpoint and are limited to a narrow range of materials. Additive manufacturing processes, specifically selective laser sintering (SLS) and selective laser melting (SLM), are extensively used for metallic prostheses due to their suitability for consolidating metallic materials.

Other AM techniques like stereolithography (SLA) slurry, multijet, fused deposition modeling (FDM), and SLA casting still exhibit limited use in dental prostheses. This presents a significant opportunity for further exploration and research in scientific publications and practical applications.

Considering both the positive and negative aspects of these procedures, it is evident that AM technologies currently face challenges such as low mechanical strength, bio-reactivity, high costs, and limited availability of ceramic raw materials and biocompatible materials. Consequently, AM is predominantly employed for temporary applications, casting patterns, and models, particularly in polymer applications.

Faced with the challenge of meeting the quality and sustainability goals outlined by the United Nations, innovative approaches become imperative. One such groundbreaking solution is the development of Shell Sintering Technology (SST) to produce high-strength ceramic crowns from fully biocompatible commercial dental materials. It's crucial to note that SST, distinct from additive manufacturing (AM), achieves the final part by sintering ceramic or metallic powder within the shell mold.

This study aims to explore the potential application of SST in crafting dental prostheses using Nano-Fluorapatite-Glass-Ceramic, with a focus on characterizing and optimizing the fabrication process.

The procedure, illustrated in Figure 5.6. commences with dental Computer-Aided Design (CAD) technology to generate a 3D model, which is then processed in a Computer-Aided Manufacturing (CAM) system. Subsequently, a shell mold and Numerical Code (NC) are produced in the CAM process. The layer-by-layer construction of the shell mold is accomplished using a gas-assisted Shell Maker equipment based on ceramic materials.

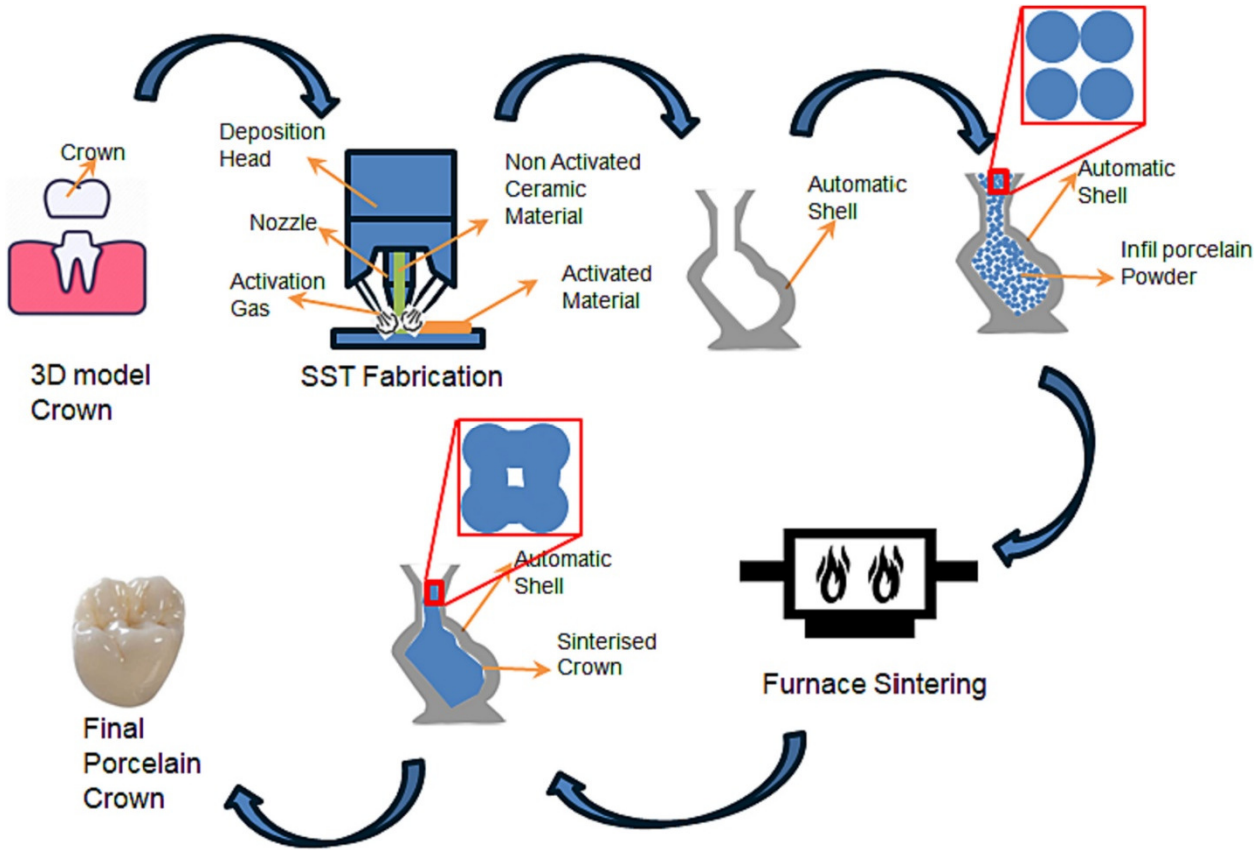


Figure 5.6. Diagram showing how ceramic dental prostheses are made using indirect AM.

The composite material undergoes chemical activation facilitated by assisted gas, which simultaneously seals the mold and creates minute pores for enhanced material retention and grain density. Once the shell mold reaches completion, it is filled with Nano-Fluorapatite-Glass-Ceramic powder, shaping the dental prosthesis.

The filled mold undergoes thermal processing in an electronically controlled furnace, where powder particles sinter and fuse together. Following the cooling process, the mold disintegrates, unveiling the finalized dental prosthesis.

Despite the impressive resolution of AM techniques like SLA and multijet printing, they require dimensions and geometrical accuracy comparable to FDM techniques. Research indicates that high resolution primarily impacts roughness rather than dimensional accuracy [26, 27, 28]. Photopolymer resins and slurry-based processes, despite their capabilities, often lead to significant anisotropic geometrical distortion, making them suitable for casting patterns, lost wax (resin) casting, and investment casting [29, 30].

Shell Sintering Technology, besides its cost-effectiveness, represents a novel approach capable of producing products with a high percentage of ceramic and metallic content [31, 32, 33].

Fluorapatite glass-ceramic-based materials, along with lithium disilicate and leucite, are widely used in dental applications, available in various forms such as powder, pressable ingots, and CAD/CAM Milling blocks [34].

This study employs a multivariable approach to investigate the significant impact of control factors on responses, aiming to characterize the viability of the novel technique for dental prosthesis production in nano-fluorapatite-glass-ceramic material. Shrinkage and procedure viability serve as study responses, with holding temperature, holding time, and heating rate identified as control factors. Material formulation, testing specimen shape, and fabrication parameters remain constant throughout the study.

5.2.2. Materials and Methods

The study employed a multivariable methodology using a 3 × 4 factorial design, with holding temperature (T_h), holding time (t_h), and heating rate (H_r) as control factors to assess the viability of the proposed method and determine the main effects of these factors on responses. Shrinkage and process feasibility served as response factors, while sintering equipment, debinding parameters, additive manufacturing equipment, fabrication parameters, and material formulation were held constant.

Figure 5.7. outlines the levels and values assigned to each control factor. The holding temperature values ranged from 700 °C to the glazing temperature of nano-fluorapatite-glass-ceramic (745 °C). Conversely, the range for holding time and heating rate was determined based on sintering parameters such as nucleation, grain growth, and diffusion. The debinding temperature spanned from 200 to 400 °C, with a defined heating rate of 2 °C/min.

Control factors	Level			
	-2	-2	0	1
Holding time (t_{hold})[min]		15	30	45
Holding temperature (T_{hold})[°C]	700	715	730	745

Figure 5.7. Experiment design, Where:
T_{hold} is the Holding Temperature – period where the temperature is kept constant (min.)
t_{hold} is the holding time or plato time – temperature which is kept constant during a period (°C).
H_{rate} is the heating rate of sintering furnace, fixed in 2 °C/min.

In this study, the IPS e.max Ceram® Power Dentin A2, manufactured by Ivoclar Vivadent, served as the raw material.

To fill the shell mould with ceramic material, the Zirclab Ceramiclab Feeder and Compactor were utilized. This equipment ensured complete filling of the ceramic powder inside the shell and compacted the powder in a 1:2 ratio.

The debinding and sintering process was carried out using a Kota 1600 W electrical Furnace with PID controller, featuring 4 ramp curves and an insulation muffle. The main control parameters and schematic sintering temperature curves, following the CRH (constant rate heating) technique, are depicted in Figure 5.8.

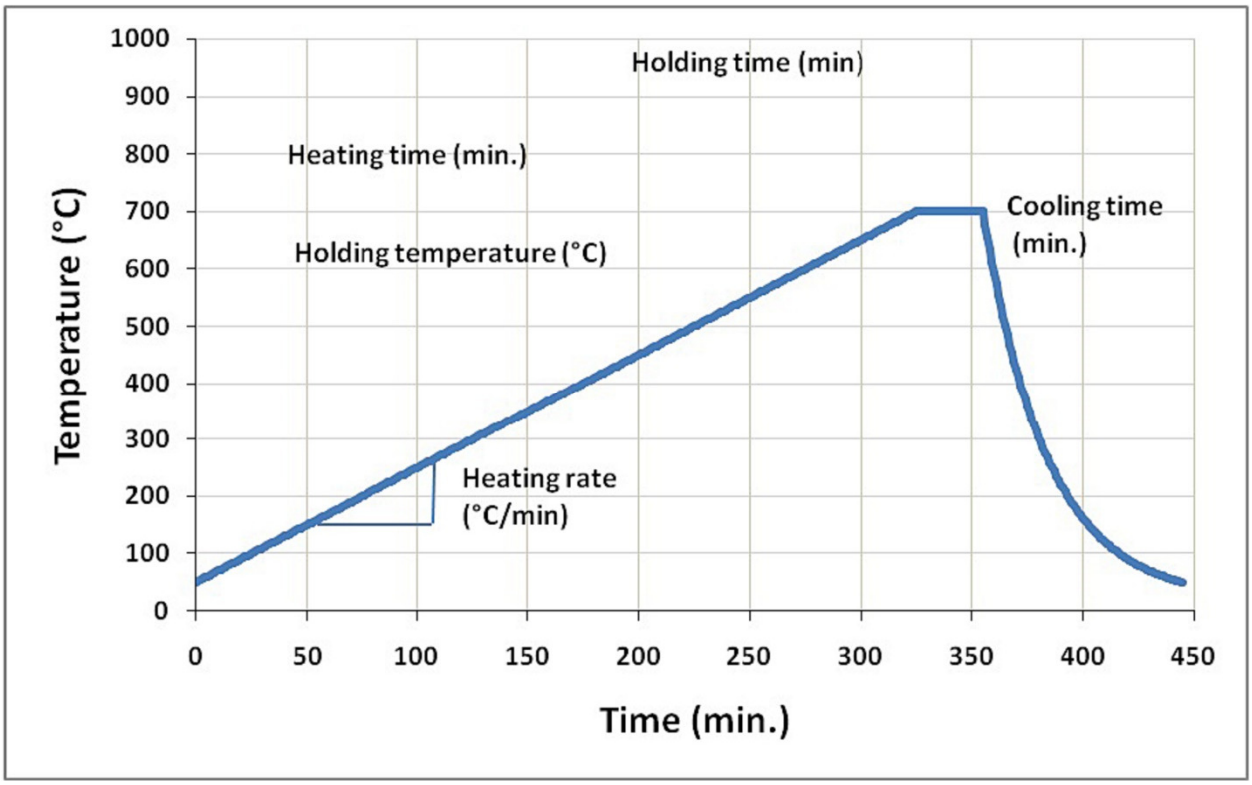


Figure 5.8. Illustration of sintering temperature curves and control factors: Holding Temperature (T_{hold}), holding time (t_{hold}).

Flexural testing and measurement of flexural strength were conducted using an EMIC DL10000 universal testing machine, adhering to ISO 6872 standards. SST-manufactured test specimens were employed, with 20 trials conducted for each test type under the same conditions.

For image processing, MATLAB software was employed, and digital images were captured using a Digital Microscope Electronic Magnifier with up to 1600× magnification. Specimen measurements were taken using a 0.05 mm caliper, and computational image processing was utilized to identify dimensional distortions. Subsequent to measurement, MATLAB was used for statistical analysis and demonstrating the geometrical variation of the external profile of the object.

Volume, density, and mass measurements were obtained following ISO 17060 guidelines.

A feasibility response scale ranging from -1 to +1 was established, where -1 indicated a partially sintered crown, -0.5 denoted sintering with porosity, -0.25 represented a granular piece, 0 indicated good feasibility, +0.25 signified viability with slight cracks, +0.5 suggested major cracks or substantial melting, and +1 indicated extensive melting, forming a spherical shape resembling a ball.

It is crucial to note that the feasibility criteria in this study are derived from prior research characterizing sinterization and the final application of dental prostheses [201].

The filling channels were positioned on the top part of the crown, with an orientation of 55°, as illustrated in Figure 5.9.

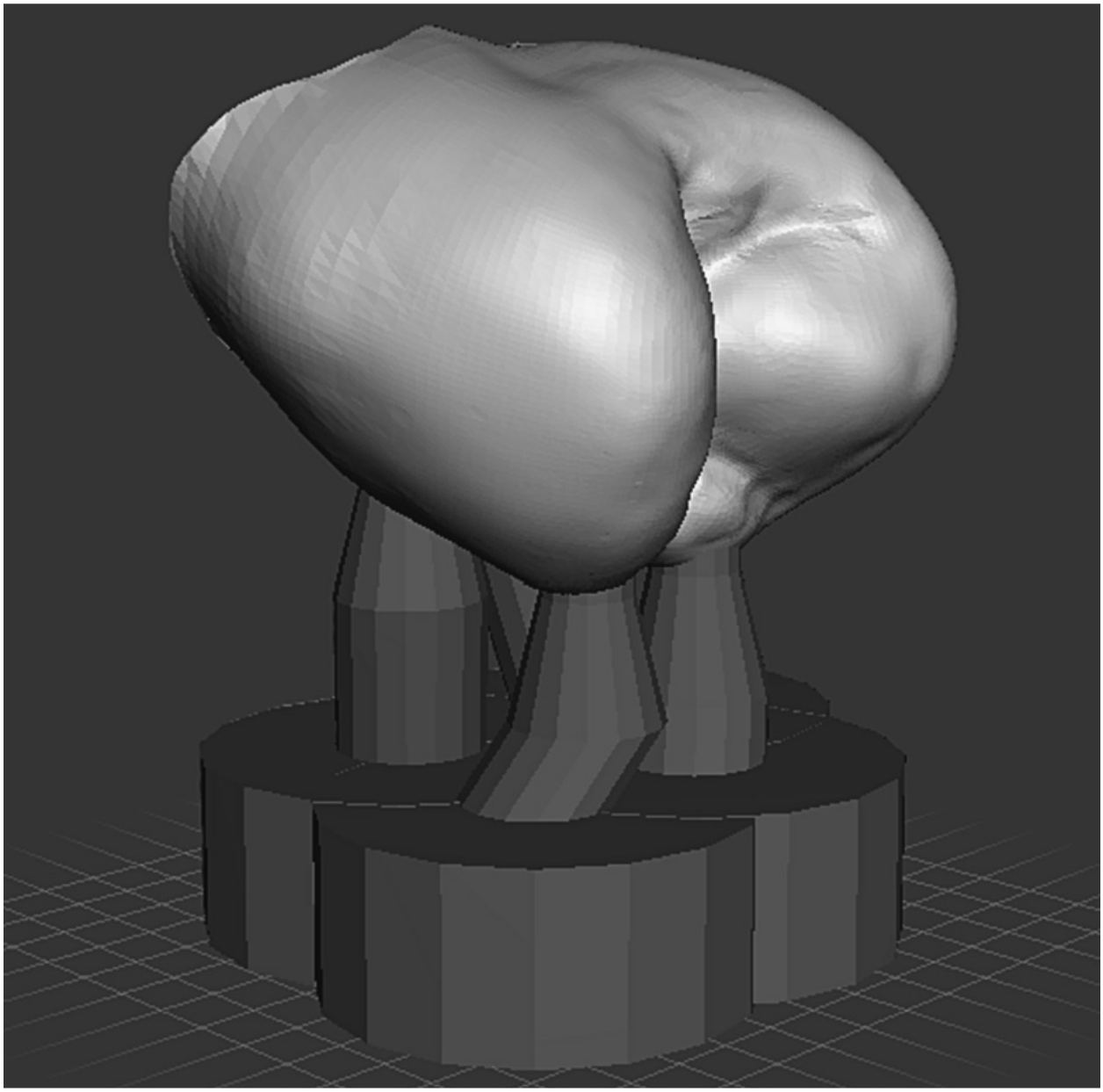


Figure 5.9. Schematic of filling channel and crown orientation.

A Shell Sintering Technology machine, with an average ZrSiO4 composition of 80%, was employed to fabricate the specimens. The material temperature, chamber temperature, extrusion temperature, layer thickness, gap between fabrication lines, tool diameter, and aided gas flow were set at 30°C, 75°C, 210°C, 0.2 mm, 0.2 mm, 0.6 mm, and 0.1 m/s, respectively. The manufacturing environment was maintained at an ambient temperature of 25°C and a relative humidity of 30%.

Before initiating the study, the repeatability and error of the AM-generated shell mould were determined. Ten samples of the shell mould were produced, and their external and internal geometry were measured. Internal geometry evaluation involved transversal cuts to ensure that the deviation between CAD and AM-generated moulds was within 0.15 mm, with an error of 2% in the small dimension of the mould. Image profilometry and 3D scanning from Shine 3D DS-Ex were used for this measurement.

To verify the microstructure of the sintered material, a ceramographic test was conducted following ASTM E112 [35] and ASTM E1382 [36] standards. Systematic and controlled sample preparation was performed, embedding the sample in crystalline polyester resin for subsequent microscopy procedures. Manual abrasion with sandpaper of varying grit sizes (150, 320, 600, and 1500) was carried out, with each sandpaper used for approximately 5 minutes. The direction of abrasion changed by 45° between sandpaper changes to ensure uniform surface roughness.

After the grinding stage, polishing was conducted using a rubber bur and alumina paste until the surface achieved complete reflectivity. Subsequently, concentrated phosphoric acid was applied for a 2-hour chemical attack. Finally, the surface was lightly colored with a red dye to aid in the identification and quantification of particles present on the sample's surface.

5.2.3. Results and Discussions

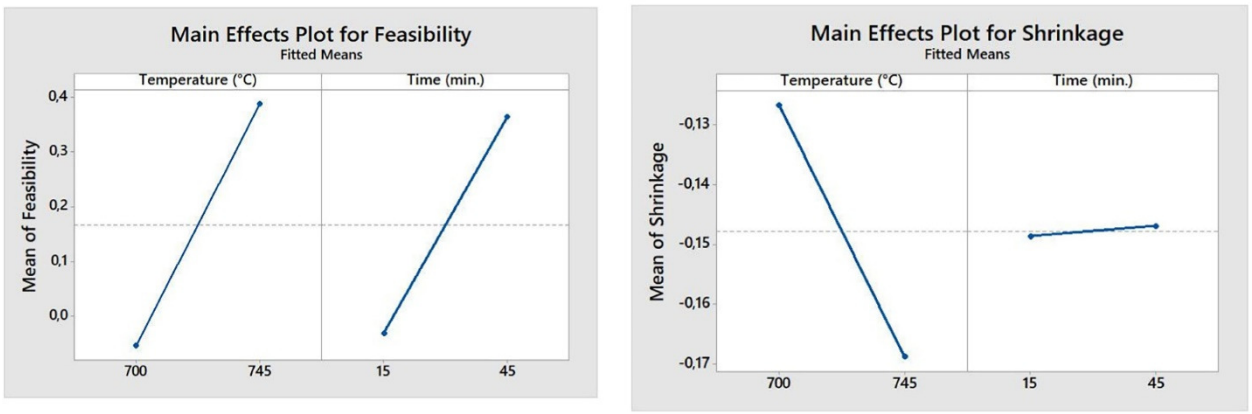
The overall feasibility assessment of the concept was favorable, and a suitable process window was established. The crown was manufactured at low sintering temperatures to prevent excessive melting that could alter the geometry. As depicted in Figure 5.10., the main effects for feasibility are positive, indicating that an increase in temperature and time within the range of 700 to 745 °C for T_{hold} and 15 to 45 minutes for t_{hold} leads to an increase in feasibility. There were no secondary interactions observed for this response.

On the contrary, there are negative main effects for shrinkage, which is expected as higher sintering temperatures lead to more significant shrinkage, with secondary effects for this control factor. Additionally, there is a small effect of holding time (t_{hold}) on shrinkage, providing valuable information.

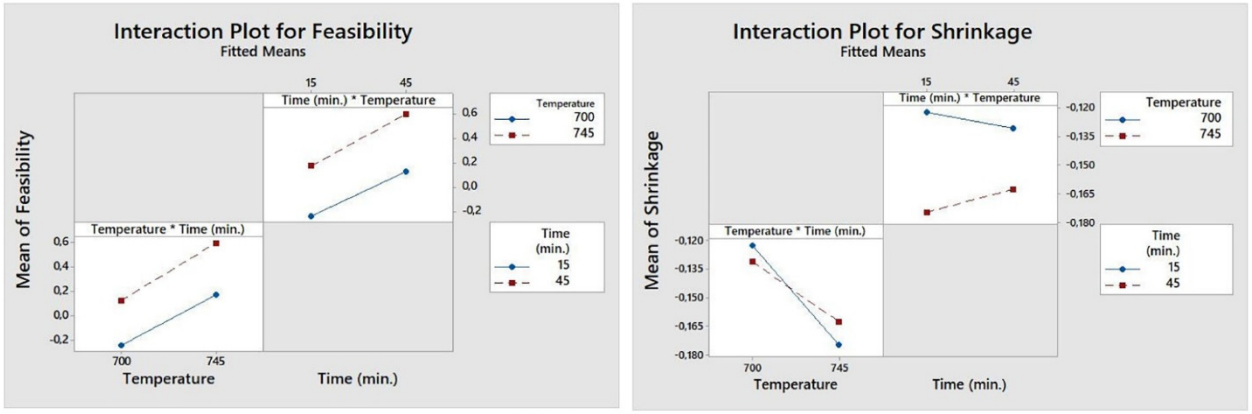
In summary, holding temperature (Th) had the most significant impact on both variables when assessing the main effects of control variables on feasibility and shrinkage (Fig. 5.11.). Conversely, holding time ($_{thold}$) has a substantial effect on feasibility but a minor impact on shrinkage within the studied interval.

A comparison diagram illustrating the geometrical concept for feasibility as a function of holding temperature and holding time is also depicted in Figure 5.12. In this diagram, a feasibility line delineates the outcomes that were deemed possible and impracticable from a geometrical perspective.

The study unveiled the process window of SST for fabricating Nano-Fluorapatite Glass-Ceramic prostheses. This window can be defined by the relationship between time and temperature, indicating the absorbed energy utilized in the sintering process. Conversely, parameters leading to infeasibility are characterized by high densification and excessive deformation due to a decrease in viscosity.



(a) Main effects plots



(b) Interactions plots

Figure 5.10. Main effect and interactions plot for the feasibility and shrinkage responses according to the 3 × 4 DOE.

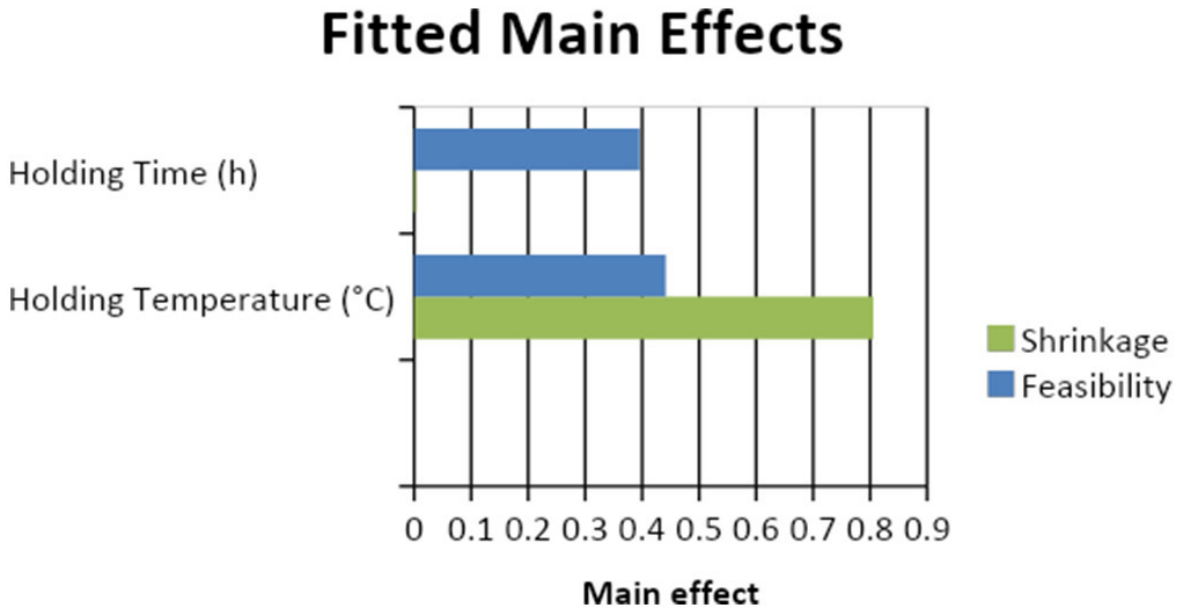


Figure 5.11. Control parameter's main effect on feasibility and shrinkage.

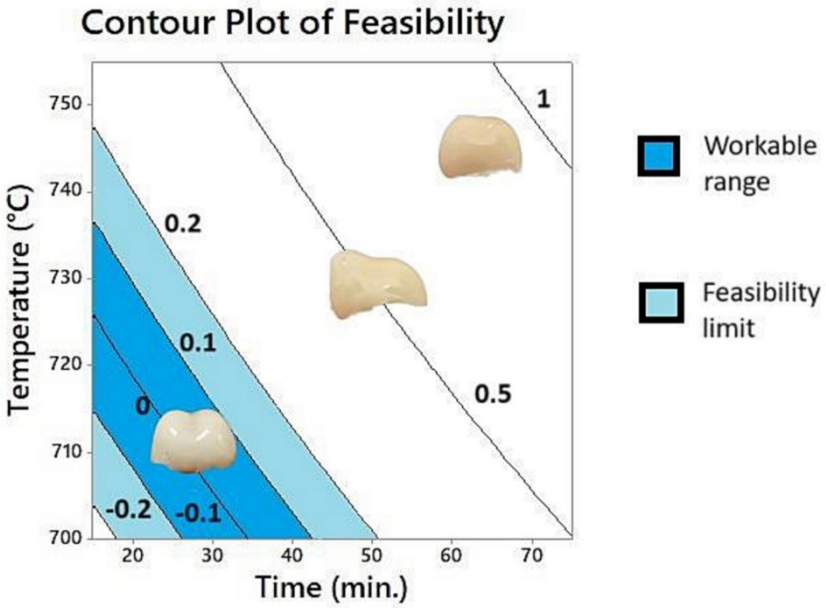


Figure 5.12. Contour diagram of holding temperature and holding time on process feasibility.

The sintered material produced under the optimal conditions (T_{hold} = 700 °C and t_{hold} = 30 min) exhibited a vitreous phase with 3.8% crystal precipitations in ceramography, featuring an average grain size of 11 µm, as depicted in Figure 5.13. Approximately 50% of grains are distributed in the vicinity of this average, as shown in Figure 5.14.

Figure 5.15. illustrates contour diagrams of feasibility and shrinkage, along with an overlapping diagram indicating the process window. This visualization helps comprehend the behavior of material properties in relation to holding temperature and holding time, facilitating the identification of optimal values for the best outcomes.

Figure 5.15. (a) indicates that values of feasibility near zero (indicative of very good feasibility) can be achieved in the blue areas, signifying workable conditions for the SST technique.

In Figure 5.15. (b), the green zones represent areas with minimum values of shrinkage. When both diagrams are overlapped in Figure 5.15 (c), it reveals the best conditions for obtaining crowns with excellent feasibility and minimal shrinkage, observed in the white area of the overlapping diagram.

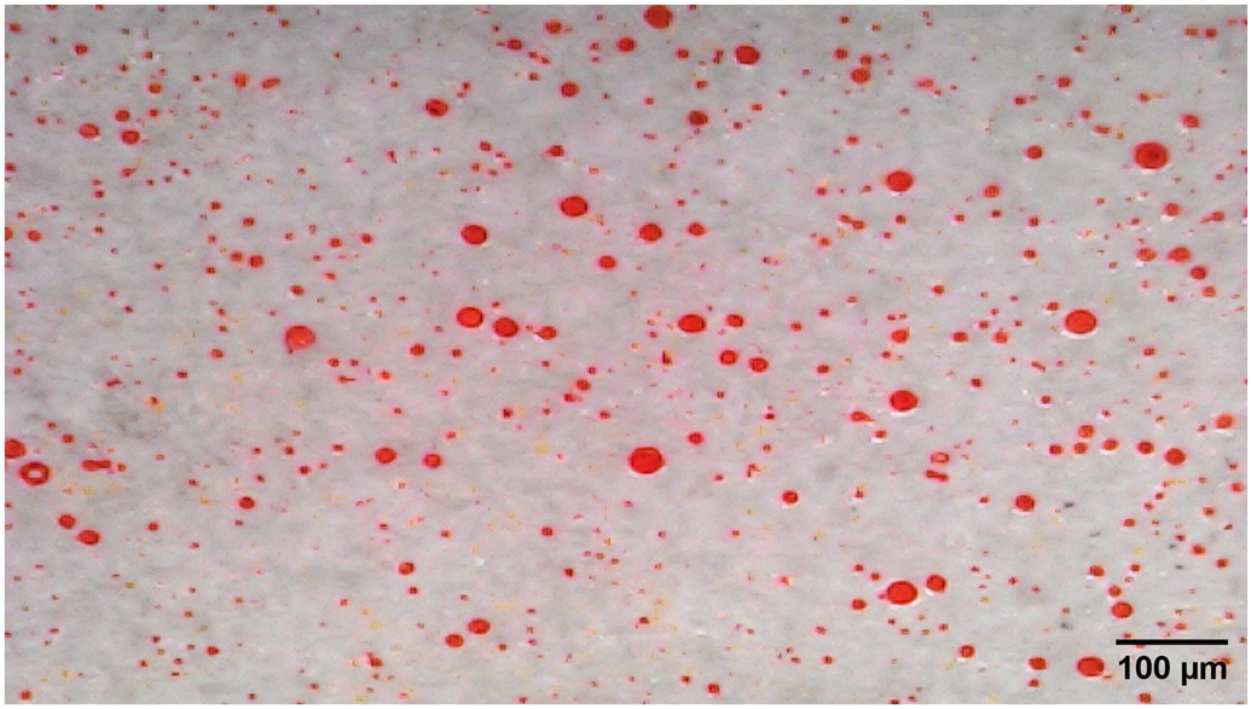


Figure 5.13. Ceramography of sintered nano-fluorapatite glass-ceramic material.

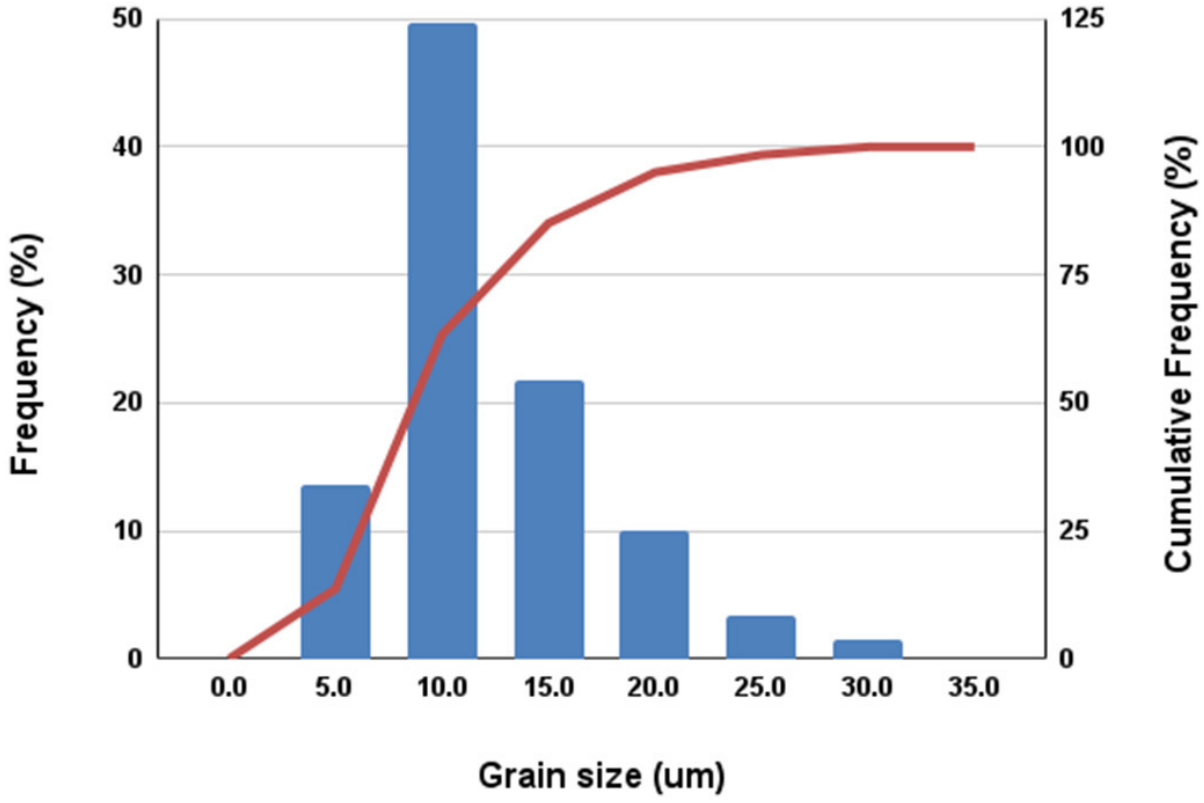


Figure 5.14. Grain size distribution of sintered nano-fluorapatite glass-ceramic in the study optimal point.

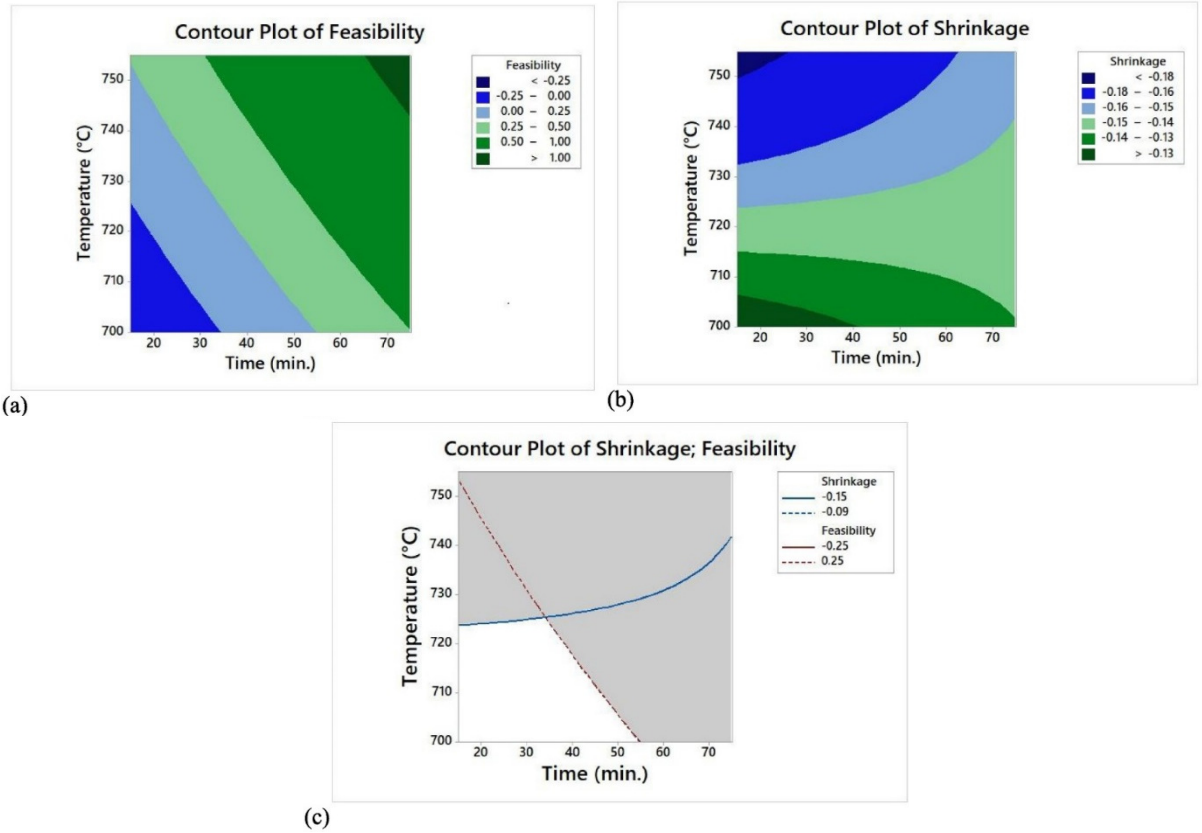


Figure 5.15. Contour diagrams of feasibility, shrinkage and the overlapping diagram, showing the best conditions for crown manufacturing using SST.

Figure 5.16. presents a comparison of flexural strength between the proposed method and material (NFGC) and other typical methods and materials used for fabricating dental prostheses. It's crucial to note that the current findings show values equivalent to those observed in normal dental applications. Further research might enhance flexural strength to approach slip-casting strength

levels. Additionally, the volumetric shrinkage for typical CAD/CAM milling dental applications ranges from 5 to 30%. The values found in this work (10 to 14%) are within this range, indicating potential application in the field.

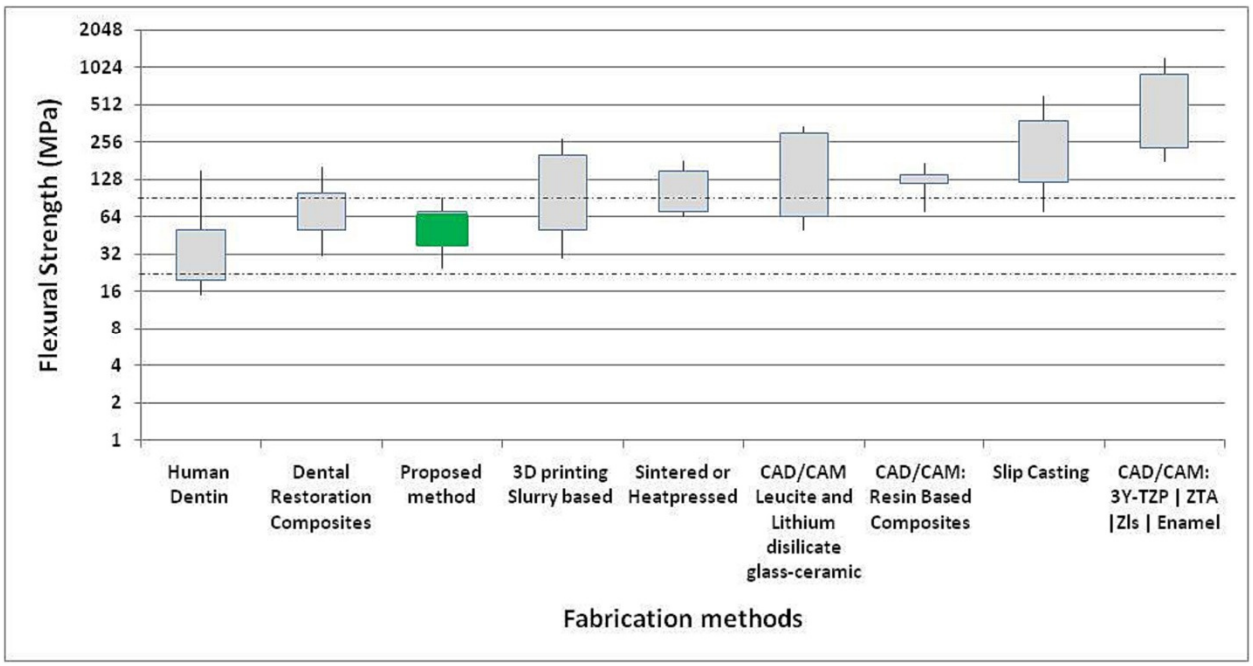


Figure 5.16. Flexural strength of the proposed method (SST) and typical dental prosthesis

The fabrication of dental prostheses typically involves multiple stages, including finishing and making-up, to enhance the aesthetic appearance of the prosthesis and achieve a resemblance to the original human dent. In such applications, key factors to consider are the geometrical features, mechanical properties, and biocompatibility of the dental prosthesis.

Figure 5.17. illustrates the successful implementation of this idea, showcasing a new approach to manufacture Nano-Fluorapatite Glass-Ceramic dental prostheses using Shell Sintering Technology.

The illustration features a dental crown designed for cementing, and it is important to note that this prosthetic has not undergone finishing or make-up, highlighting the technology's potential.

While preliminary results suggest the feasibility of the proposed approach, further research is needed to enhance mechanical strength, explore a broader range of glass-ceramic materials, and assess biocompatibility.

Various approaches can be considered to improve properties, including thermal treatment, the introduction of nanoparticles, and the use of reinforcement materials.

Additional studies can contribute to refining the process and expanding the application of Shell Sintering Technology in dental prosthesis manufacturing.

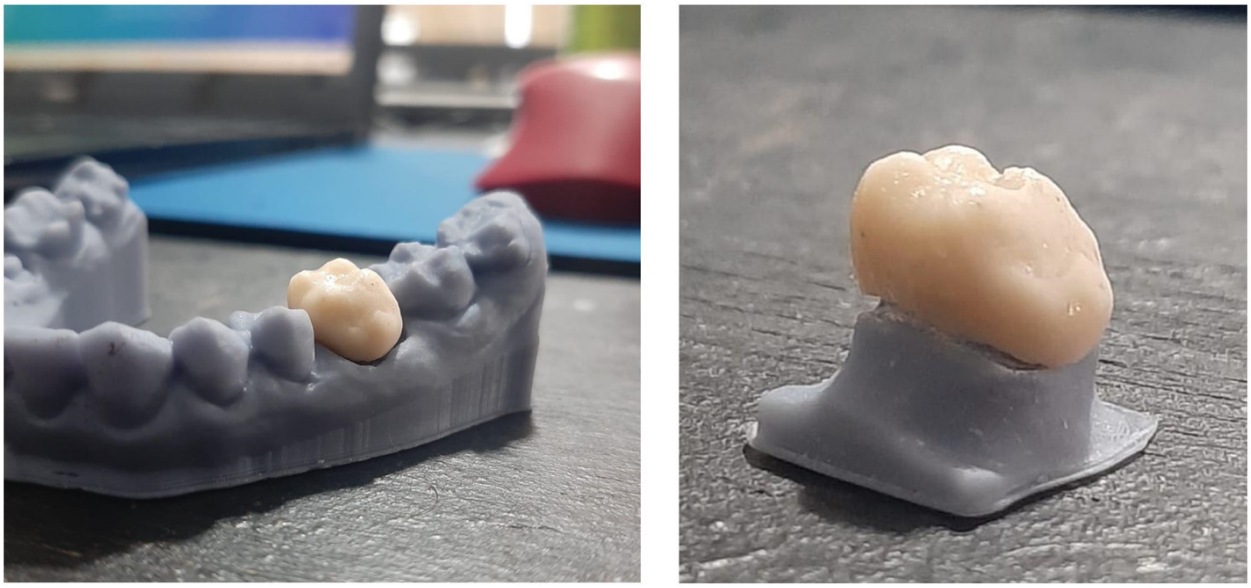


Figure 5.17. Dental crown based on Nano-Fluorapatite Glass-Ceramic fabricated by Shell Sintering Technology (SST) with no makeup nor finishing.

5.2.4. Conclusions

This study explored the potential of Shell Sintering Technology (SST) for producing Nano-Fluorapatite Glass-Ceramic prostheses, offering new perspectives for additive manufacturing (AM) in dentistry and medical applications. SST, capable of withstanding high fabrication temperatures, was employed, showcasing its versatility.

The research highlighted the significant influence of holding temperature on feasibility and shrinkage, with holding time also playing a crucial role in feasibility. The Design of Experiments (DOE) model identified optimal conditions for achieving crowns with excellent feasibility and minimal shrinkage in the SST technique.

In the optimal scenario, the flexural strength ranged between 55 and 65 MPa, accompanied by an average grain size of 11 μm in crystal precipitations within the vitreous phase, as revealed by ceramography. Further investigations are warranted to delve into the impact of heating treatments on enhancing mechanical and geometrical characteristics. Additionally, the incorporation of new materials and exploration of diverse applications should be considered in future research.

5.3. Reduced wear of enamel with novel fine and nano-scale leucite glass-ceramics

This study aims to explore whether leucite glass-ceramics with fine and nano-scale structures, featuring minimal matrix microcracking, exhibit a reduction in in vitro tooth wear. This research is likely motivated by the desire to enhance the durability and wear resistance of all-ceramic restorations, addressing issues such as brittle fracture and wear on opposing teeth often associated with leucite glass-ceramics.

5.3.1. Introduction

The study addresses the common issues of brittle restoration fracture and wear on opposing teeth associated with the use of glass-ceramic and high-strength ceramic core materials in aesthetic restorations. The researchers aim to explore wear interactions between enamel and ceramic materials, considering abrasive, adhesive, fatigue, and corrosive mechanisms that lead to material loss. The focus is on developing less abrasive ceramic materials to minimize enamel wear, particularly for patients prone to bruxism.

Prior research suggested a critical crystal size for microcracking in leucite glass-ceramics, emphasizing the importance of matrix microcracking and crystal-matrix decoupling in determining

strength. The study aims to refine crystal sizes to submicron and nanometer ranges in leucite glass-ceramics and investigate their effects on wear mechanisms against enamel. The researchers have produced optimized fine and nano-scale leucite glass-ceramics with high flexural strength and minimal matrix microcracking.

The hypotheses to be tested include whether fine and nano-scale leucite glass-ceramics, which are characterized by minimal matrix microcracking, are linked to a decrease in in vitro tooth wear. The study aims to enhance understanding of wear characteristics in these innovative materials and their potential influence on human enamel wear.

5.3.2. Materials and Methods

Freshly extracted human adult molar teeth were obtained and subjected to storage and disinfection using a 30% water and 70% ethanol solution. The teeth were stored in a tissue bank at the Department of Oral and Maxillofacial Surgery, Institute of Dentistry, Bart's and The London School of Dentistry, with ethical approval obtained (Med. Ethics REC:06/Q0603/98). Teeth with pointed configurations, demineralizations, or surface defects were excluded through visual screening conducted by a single operator using a stereoscopic microscope (Wild-M3B, Heerbrug, Switzerland).

Individual wet-sectioned cylinder cusps were obtained using a 2.75 mm inner diameter core drill from UKAM Industrial Superhard Tools, CA, USA. These cusps were further screened for defects and then embedded in photo-curing resin (Palatray, Heraeus-Kulzer, UK) in the form of cylinders with dimensions of 6 mm in diameter and 14.5 mm in height. Curing was performed for 1 minute from three different sides using a 3M-ESPE Elipar™ Freelight™ from Germany.

Twelve Ceramco-3 disc specimens (Batch-No: 02111576, Dentsply, Ceramco, NJ, USA) were prepared by mixing 0.96 g of dentine powder with 0.3 mL of modeling liquid (C.H.B24066, Vita-Zahnfabrik, Germany). The mixture was condensed using a steel mold and plunger under a force of 1 kg × 10^3 for 1 minute. The specimens were sintered (Multimat-MCII, Dentsply, Weybridge, UK) following the manufacturer's instructions, with one dentine and one simulated overglaze firing cycle. The sintered disc dimensions were 14 mm in diameter and 2 mm in thickness.

Glass-ceramics were synthesized with either fine-scale (FS) or nano-scale (NS) leucite crystallites. In each case, 1.6 g of glass-ceramic powder samples were dry compacted into powder ingots and sintered under vacuum in a porcelain furnace (Multimatt-MCII, Dentsply, Konstanz, Germany) from 538 °C at a rate of 38 °C/min to 1040 °C with a 2-minute hold. For each group, twelve specimens were prepared by sprueing Perspex discs (14 mm × 2 mm) onto muffle bases, investing (IPS-Empress Esthetic speed investment, Ivoclar-Vivadent, Schaan, Liechtenstein), pre-heating (850 °C, 45 min), and heat-extruding the ingots using dental heat-pressing machines (FS: Cerampress, Jeneric-Pentron, USA; NS: EP3000, Ivoclar-Vivadent). The heat pressing cycles included a ramp from 700 to 1040 °C at 40 °C/min, a 15-minute hold, and a 10-minute pressing time. The discs were divested using 50 μm glass beads (SG4017, Bracon Ltd., Etchingham, UK) at 0.5 × 10^5 Pa pressure, and sprues were removed using a diamond disc (006, Bracon Ltd.). Both NS and FS groups received one simulated stain and one simulated overglaze firing according to Chen et al. Simulated stain and simulated overglaze firings were conducted on all groups to simulate firings required for dental restorations and to account for any increases in leucite volume fraction that could have affected the experimental outcomes.

All disc specimens were wet-lapped with P600 SiC paper to achieve flatness and standardize the test surface. Subsequently, specimens were cleaned in an ultrasonic bath with an aqueous detergent solution for 10 minutes and then rinsed with water.

All glass-ceramic disc and tooth specimens underwent a 24-hour storage period in deionized water prior to testing. These specimens were organized in groups of three pairs, with one pair fixed in specially designed holders on the upper member and the other pair on the lower member of a servo-hydraulic test frame (Bionix-858, MTS, MN, USA). The opposing glass-ceramic disc and tooth specimens underwent 300,000 simulated masticatory cycles at a rate of 2 Hz, with a continuous flow of deionized water at 37 °C. Each specimen was loaded with 13.5 N, followed by a lateral excursion

movement achieved by rotating the axial shaft under displacement control by 1.5°. A controlled cuspal contact time of 0.25 seconds was employed to complete a cycle.

A validated wear quantification protocol, previously described and established for repeatability and reproducibility, was employed for the study.19 White-light profilometry (Proscan-2000, Scantron, Taunton, UK) along with dedicated software (Proform ver. 1.41, Proscan-2000 ver. 2.1.8.8+ software, Scantron, UK) were utilized to determine volume and mean-height loss by superimposing digitized surfaces of specimens from before and after wear testing. An S16/3.5 Chromatic sensor (Stil S.A., Aix-en-Provence, France) was used for all scans, operating at 30 Hz with step sizes of 20 μm for teeth and 30 μm for glass-ceramic discs. The wear data were subjected to analysis using the Kruskal–Wallis One-Way ANOVA on ranks (Sigma-stat, ver. 2.03, SPSS Inc.) and a multiple comparison test (Student–Newman–Keuls).

Polished and etched glass-ceramic specimens were subjected to gold coating and examined using scanning electron microscopy (FEI Inspect F, Oxford Instruments, Oxfordshire, UK). The micrographs obtained were utilized for quantifying leucite crystal size, number, and area fraction through quantitative image analysis software (Sigma-Scan Pro 5.0, Systat Software, Inc., IL, USA).

Surface topography images were captured following wear testing from a glass-ceramic disc/tooth pair per test group, post-cleaning with ethanol. Two sets of images were obtained—one of the entire wear pattern (2.5 × 2.5 mm, step-size: 5 μm [x, y]) and another focusing inside the same wear patterns (0.5 × 0.5 mm, step-size: 1 μm [x, y]). Raw data from the 1 μm step-size acquired profilometric images (501 x and y lines) were analyzed for surface roughness (Ra) using Proscan-2000 ver. 2.1.8.8+ software (Scantron). Additionally, after gold coating, secondary electron imaging (SEI) images of the same areas that were scanned using profilometry were acquired.

5.3.3. Results

The worn surfaces of the Ceramco-3 glass-ceramic disc/tooth group exhibit increased waviness and damage compared to the FS and NS glass-ceramic disc/tooth groups (Figure 5.18., Figure 5.19.). All recorded surface roughness values (Ra, Table 2) for the FS and NS glass-ceramic disc/tooth groups were lower than those for the Ceramco-3 group. The NS group had slightly increased values of tooth Ra compared to the FS group. The Ceramco-3 glass-ceramic group had lower mean y than x values, and an orientation of the wear grooves parallel to the y-axis of scanning was observed for the Ceramco-3 glass-ceramic group (Figure 5.18.a and a′). The Ra values for the FS group for both tooth/glass-ceramic specimens are the same in x and y directions, indicating a non-oriented wear pattern for the FS (Figure 5.18., Figure 5.19.) and NS (Figure 5.18., Figure 5.19.) glass-ceramic disc/tooth groups.

5.3.4. Discussions

The ability to produce uniform leucite glass-ceramic microstructures with fine spherical crystals in glasses with minimal microcracking may have implications for the wear properties of the NS and FS groups. Sliding wear in ceramics has been described as a mechanism consisting of mild wear (dislocation plasticity controlled) transitioning to severe fracture/flaw-controlled wear with cone/radial or lateral cracking. The Ceramco-3 group produced larger wear marks than the experimental groups, and the onset of a more abrasive wear process was evident for all specimens tested. Larger depth and area of wear marks were thought to be microcrack (lateral and cone) induced wear, dependent on material microstructure and high friction, whereas ploughing was a process of plastic deformation.

The experimental groups (NS and FS) were less destructive to enamel structure, allowing for glass-ceramic removal while leaving smoother tooth/glass-ceramic surface profiles. This may be due to the roundness and diminishing size effect of the leucite particles in the experimental groups, causing wear via more plastic processes. The fine and nano-scale leucite glass-ceramics exhibited significantly lower tooth mean-height loss compared to the coarser-grained Ceramco-3 group. The wear in the experimental groups was associated with a reduction in enamel wear, and the nano-scale leucite glass-ceramic group (NS) exhibited the lowest tooth mean-height loss.

The smooth and even wear of the NS and FS materials, along with their less abrasive microstructures, allow for easy intraoral adjustment and produce polished and less plaque-retentive surfaces. The materials exhibited less surface damage and susceptibility to fracture during wear, making them suitable for strong, durable, and low-wear restorations. The study confirms that reduced enamel wear is indeed associated with fine and nano-scale leucite glass-ceramics characterized by minimal matrix microcracking. The findings suggest clinical importance as ceramic restoration wear rates should approximate those of enamel to reduce cuspal structure loss and facial height loss. In vivo testing is necessary to confirm these in vitro results.

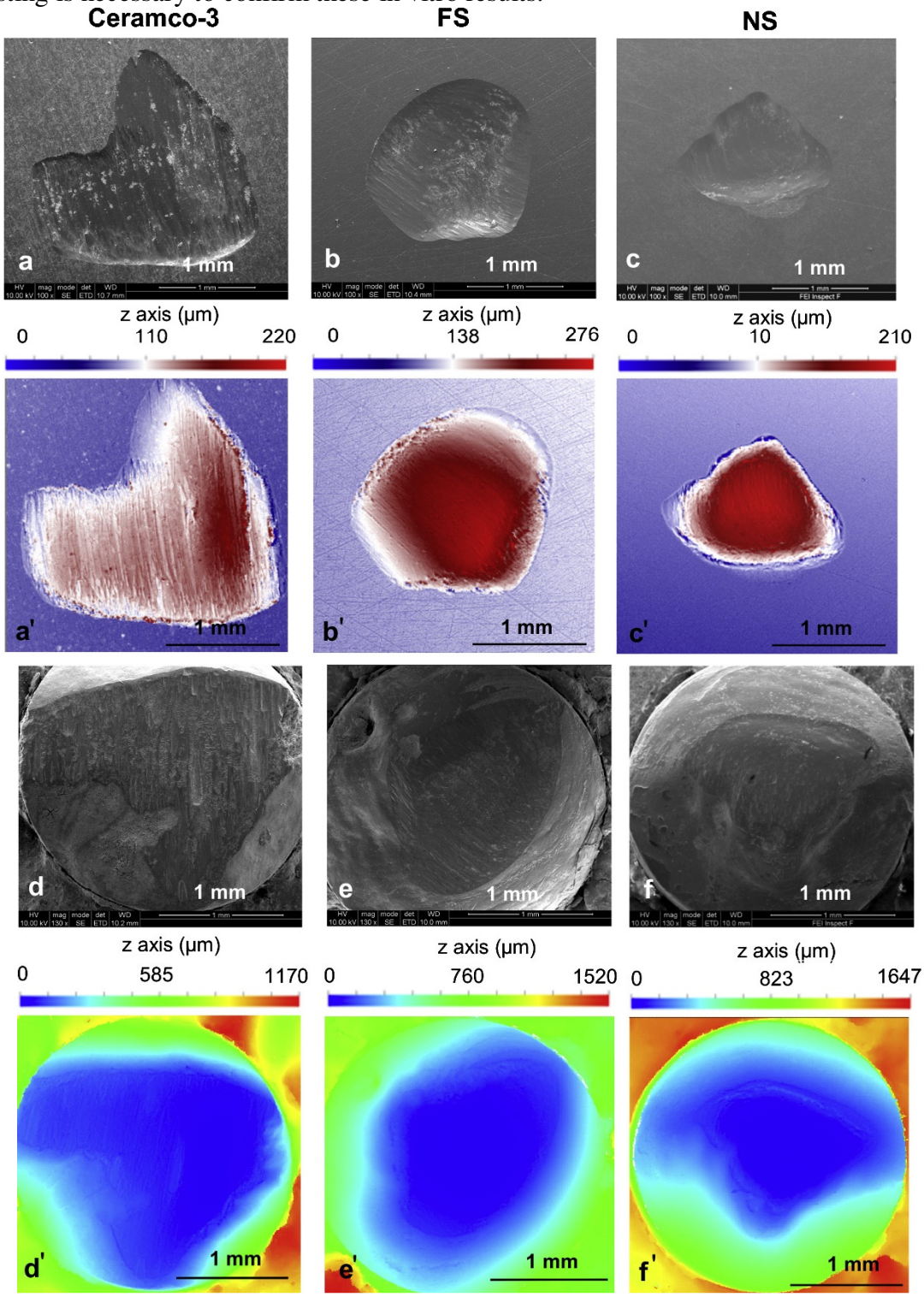


Figure 5.18. SEI and profilometry images of the surface topography of the worn areas of: (a, a') Ceramco-3 glass-ceramic disc and (d, d') the tooth antagonist; (b, b') FS glass-ceramic disc and (e, e') the tooth antagonist; (c, c') NS glass-ceramic disc and (f, f') the tooth antagonist. The colour gradient (profilometry images) illustrates height gradient.

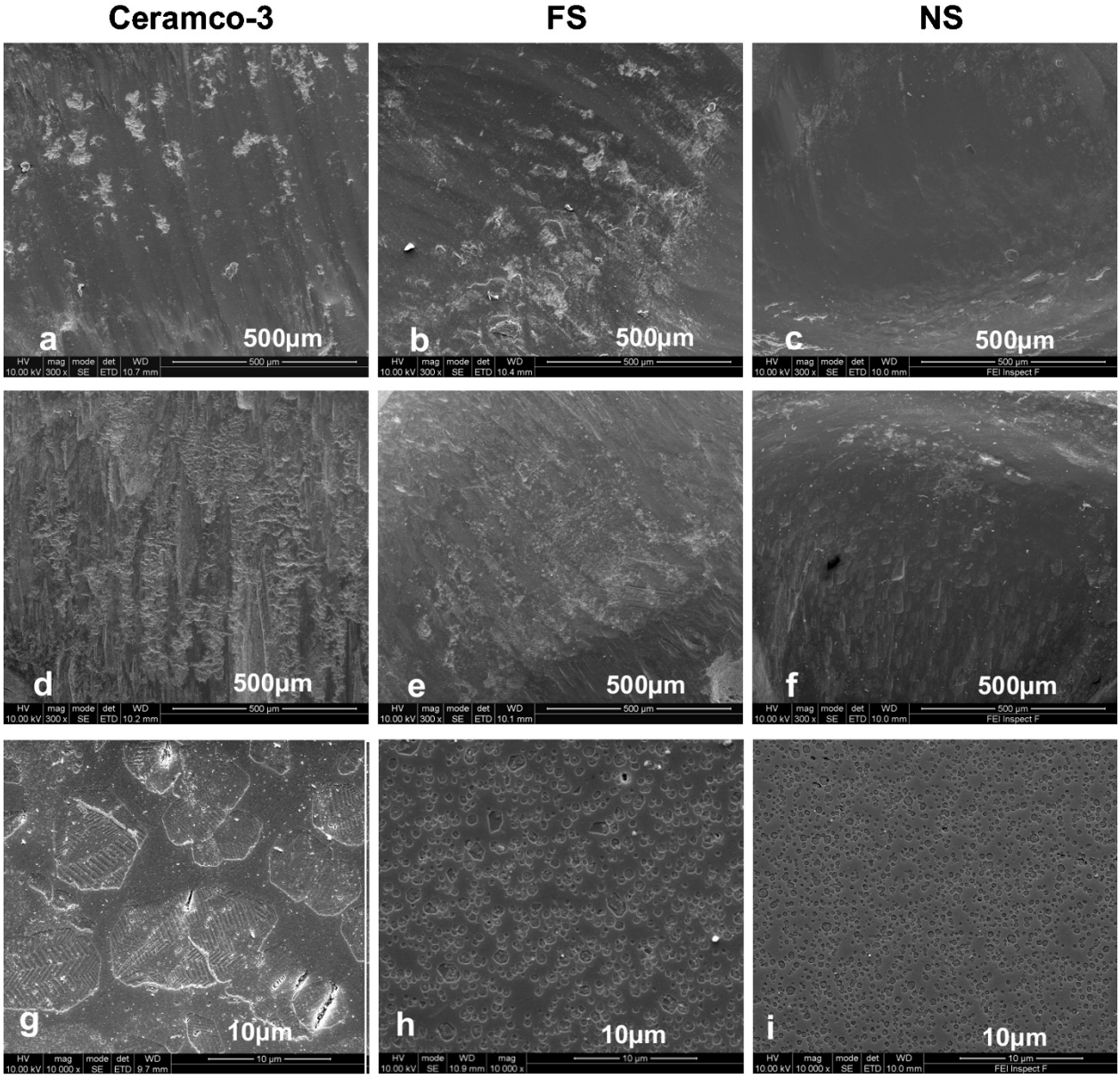


Figure 5.19. SEI images of the surface topography within the worn areas of (a) Ceramco-3 glass-ceramic disc and (d) the tooth antagonist; (b) FS glass-ceramic disc and (e) the tooth antagonist; (c) NS glass-ceramic disc and (f) the tooth antagonist. SEI images of the glass-ceramics' microstructure: (g) Ceramco, (h) FS and (i) NS.

If confirmed, these materials could provide processable options for strong, durable, and low-wear restorations that are easily adhesively bonded, addressing issues associated with tooth enamel wear and restoration failure.

5.3.5. Conclusions

The study's findings suggest that the use of fine and nano-sized leucite glass-ceramics could result in a reduction in in vitro tooth wear. These materials, characterized by high strength and low wear, may offer solutions to the challenges associated with tooth enamel wear and restoration failure. The positive outcomes indicate the potential clinical importance of these glass-ceramics for creating durable and low-wear dental restorations. However, further research and in vivo testing would be essential to validate and translate these findings into clinical applications.

5.4. Evaluation of shear bond strength of a novel nano-zirconia and veneering ceramics

The research aims to assess the bond strength of slip-cast experimental nano-zirconia with various commercially available veneering ceramics through a shear bond test and to observe the mode of bonding failure. The investigation is motivated by the need to address technical complications, such as veneering porcelain chipping, associated with zirconia-ceramic dental restorations. Traditional zirconia frameworks are layered with veneering feldspathic porcelain, and despite the excellent mechanical properties of zirconia, issues such as chipping are still reported.

The study focuses on a novel nano-zirconia material developed through controlled colloidal processing and slip-cast technique. This material is claimed to offer advantages such as denser and more homogeneous slurry with minimal porosity. The mechanical properties of this nano-zirconia fabricated by slip cast are compared with those produced by commercial dry-press techniques.

The investigation aims to contribute to the understanding of the core–veneer bond strength of the novel nano-zirconia material and its potential as an alternative for dental restorations. The bond strength will be assessed through shear bond testing, and the study will also examine the failure modes of the bonding interface.

Overall, the research addresses a critical aspect of dental restorations, seeking to enhance the bond strength between zirconia cores and veneering ceramics to reduce complications such as chipping in clinical applications. The findings may have implications for the development of more reliable and durable dental restorations.

5.4.1. Experimental procedure

The study employed three core systems: Metal, Cercon, and Experimental zirconia. Additionally, two veneering materials, InLine and Ceramkiss, were used, resulting in six core–veneer combinations. For each combination group, 10 samples were fabricated. The samples underwent a rigorous selection process, excluding any with macroscopic cutting defects after the sintering process. The desired geometry of 11 mm diameter and 3 mm thickness was achieved for the included samples. Any deformed or fractured samples during manufacturing or the sintering process, as well as those with poor attachment to the lateral arms of the testing machine, were excluded from the study.

For each core–veneer combination, a total of 10 samples were fabricated following the mentioned procedures.

The veneering process involved layering each core material with its respective veneering material.

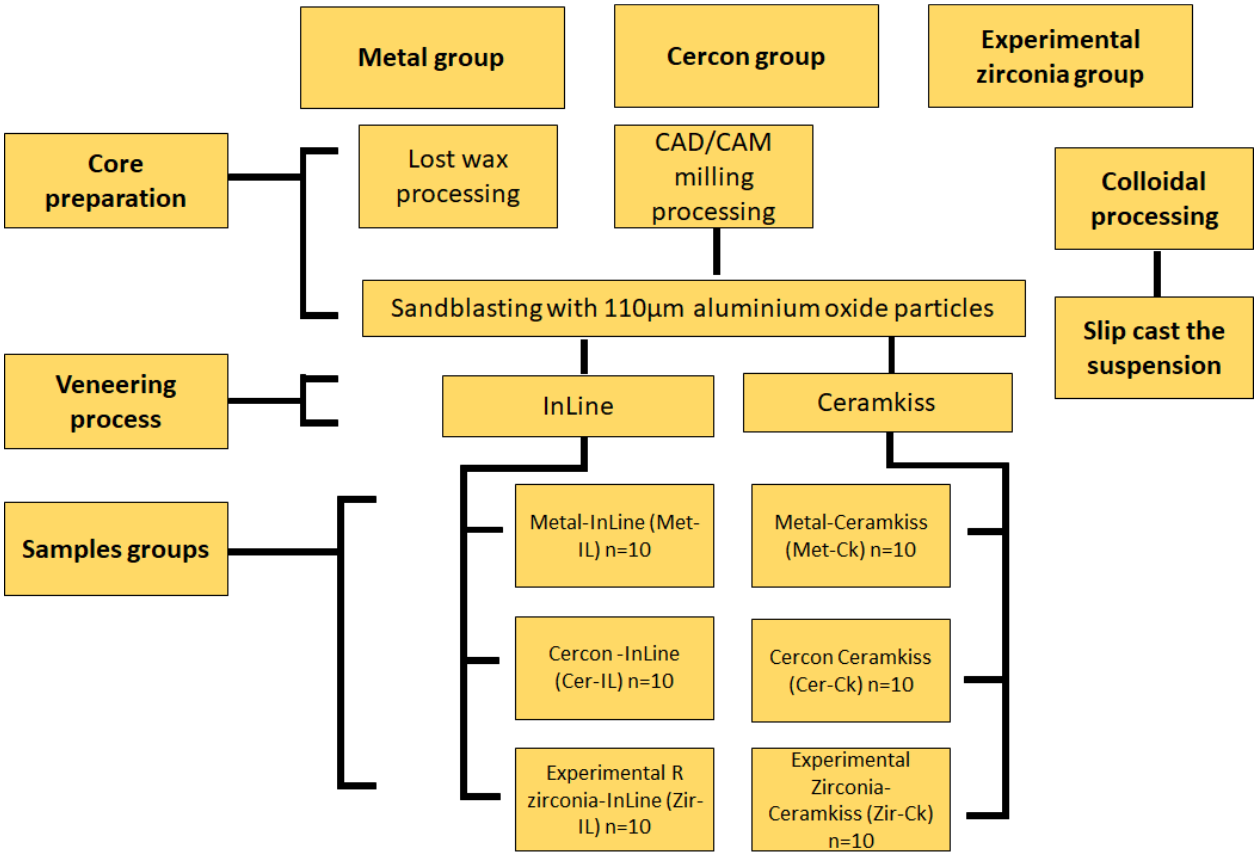


Figure 5. 20. Flow chart of sample preparations.

InLine veneering material (VITA InLine, Vita Zahnfabrik) was used for the metal core, while Ceramkiss veneering material (Ceramkiss, BEGO) was used for both Cercon and Experimental zirconia cores. The veneering materials were applied in layers and fired according to the manufacturer's instructions for each material. This process was performed for each of the 10 samples in every core–veneer combination group.

After the veneering process, the samples were visually inspected for any defects or irregularities. Only samples without macroscopic cutting defects were included in the study. The shear bond test was conducted using a universal testing machine to evaluate the bond strength between the core and veneer materials.

The shear bond test was conducted using a universal testing machine (Instron 3366, Instron Corporation) with a crosshead speed of 0.5 mm/min until failure was observed. The samples were firmly secured in the testing machine, and a shear force was applied at the interface between the core and veneer until debonding occurred. The peak load at the point of failure was recorded in Newtons (N), and the shear bond strength was calculated by dividing the peak load by the bonded surface area. The mode of failure was examined visually and categorized into three types:

1. Adhesive failure: Complete separation at the core-veneer interface.
2. Cohesive failure: Fracture within either the core or veneer material.
3. Mixed failure: Combination of adhesive and cohesive failures.

The data obtained from the shear bond test were analyzed statistically to compare the bond strength among the different core-veneer combinations. Additionally, the distribution of failure modes was reported for each combination.

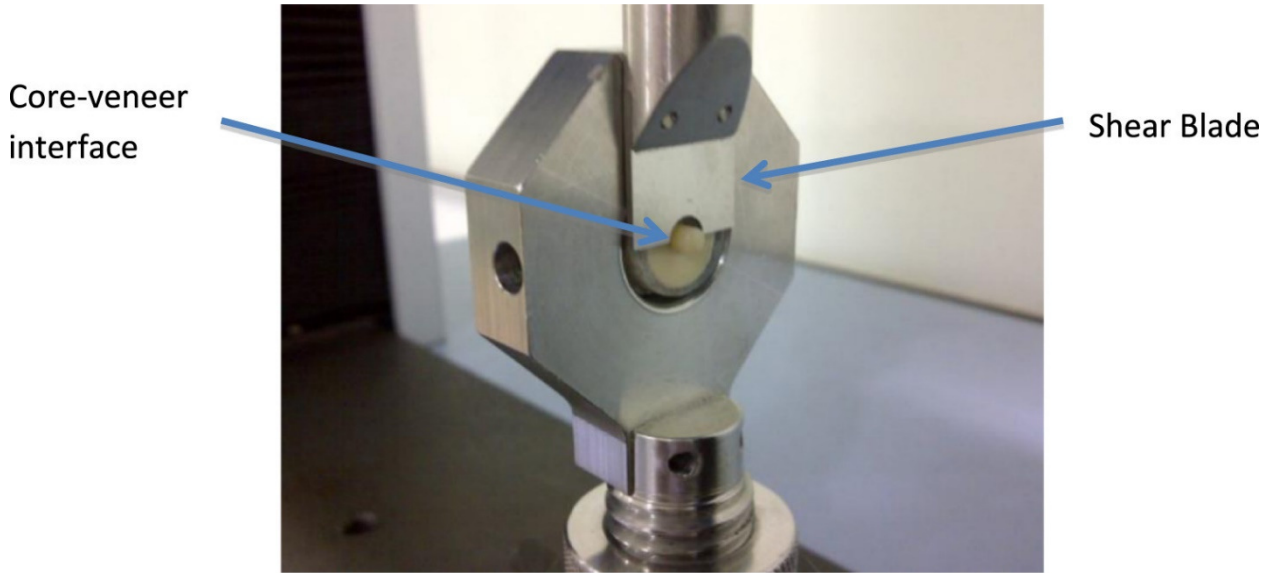


Figure 5.21. Mounted shear blade and sample on Universal Testing Machine (Shimadzu®).

The sample size for this study was determined based on a statistical power of 90%, as observed in preliminary tests with a sample size of 10 per core–veneer assembly. Independent t-tests were employed to analyze the comparison within core groups, and one-way ANOVA with Tukey's post-hoc test was used to compare within the veneering porcelain groups. Two-way ANOVA analysis was conducted to assess the interaction effects between cores, veneers, and core–veneer combinations. The predetermined level of significance for all statistical testing was set at a p-value of 0.05 or less.

5.4.2. Conclusions

In this study's confines, experimental zirconia exhibited comparable outcomes to a commercially available zirconia (Cercon®) when both were veneered with the same veneering porcelain. The SBS results lead to the conclusion that zirconia produced through slip casting or compaction techniques demonstrates similar bonding capabilities with veneering porcelain. The strength of the bond between the core and veneer appears to depend on the material used. When utilizing veneering porcelain specifically designed for the core material, no significant differences in SBS were observed among the experimental zirconia, Cercon®, and metal. The study's findings underscore the crucial role of Coefficient of Thermal Expansion (CTE) in both core and veneer materials. Clinically, these results emphasize the importance of selecting veneering porcelain tailored to the core material and vice versa, as this significantly influences the core–veneer bond strength. Combinations of core and veneer with superior SBS exhibited cohesive failures in the veneering porcelain, while inferior SBS assemblies demonstrated mixed cohesive and adhesive failures.

5.5. Quiz 5.

1. The incorporation of nanoparticles into PMMA has various benefits:
a.) Antimicrobial properties
b.) Structural improvements
c.) Chemical improvements
d.) Mechanical improvements
e.) Microbial properties

2. Which of the following affirmations about 3D-Printed Nanocomposites Denture-Base Resins are true?
a.) The research aims to investigate the impact of incorporating lithium disilicate nanoparticles
b.) The research aims to investigate the impact of incorporating zirconium dioxide nanoparticles
c.) The study seeks to evaluate flexure strength
d.) The study seeks to evaluate only elastic modulus
e.) The study seeks to evaluate hardness with the null hypothesis assuming effects on these properties

3. What drawback does PMMA have?
a.) cost-effective
b.) aesthetically pleasing
c.) low strength
d.) polymerization shrinkage
e.) low wear resistance

4.) 3D printing has the following properties:
a.) reduced time
b.) excellent mechanical properties
c.) improved tissue adaptation
d.) accuracy
e.) excellent physical properties

5. Which materials were used in the following study: The effect of incorporating TiO2 nanoparticles on the growth of Candida albicans?
a.) Cobalt chrome nanoparticles
b.) Titanium dioxide nanoparticles
c.) FTIR analysis
d.) Denture base materials
e.) Stainless steel

6. Which of the following affirmations about cell viability assessment are false?
a.) Two biological replicates were used for each test
b.) Cell viability was calculated using a random equation
c.) AlamarBlue™ cell viability reagent was used for colorimetric experiments at four time points
d.) Viability was measured using a microplate reader
e.) Images were captured with a stereo microscope

7. Antifungal test:
a.) Antifungal activity against Candida albicans was evaluated using litihium disilicate discs
b.) Lithium disilicate discs were incubated with Candida albicans
c.) Colonies were counted and reported as colonies forming unit per milliliter (CFU/mL)
d.) Candida albicans suspension was prepared and adjusted for microbial cell concentration
e.) Composite material discs were incubated with Candida albicans

8. Which of the following sentences about the transverse strength test used in Unconventional Nanoparticles in Dentistry Assessment of some mechanical properties of PMMA/Silica/Zirconia Nanocomposite as a denture base material are true?
a.) The nanocomposite demonstrated higher transverse strength compared to the control group
b.) The good distribution of nano fillers within the polymer contributed to improved transverse strength
c.) Transformation toughening also played a role in increasing transverse strength
d.) Transformation toughening did not play a role in increasing transverse strength
e.) Zirconia demonstrated higher transverse strength compared to the control group

9*. The shell sintering technology machine used to fabricate dental prosthesis was set to:
a.) 100°C
b.) 75°C
c.) 45°C
d.) 35°C
e.) 85°C

10. The following materials were used in the study Reduced wear of enamel with novel fine and nano-scale leucite glass-ceramics:
a.) Plastic teeth
b.) Freshly extracted human adult premolars
c.) Freshly extracted human adult molars
d.) The teeth were disinfected using a 30% water and 70% ethanol solution
e.) The teeth were stored in a plastic container

References

[1]. Saeed, F.; Muhammad, N.; Khan, A.S.; Sharif, F.; Rahim, A.; Ahmad, P.; Irfan, M. Prosthodontics Dental Materials: From Conventional to Unconventional. Mater. Sci. Eng. C 2020, 106, 110167.
[2]. Ghazal, M.; Hedderich, J.; Kern, M. Wear of Feldspathic Ceramic, Nano-Filled Composite Resin and Acrylic Resin Artificial Teeth When Opposed to Different Antagonists. Eur. J. Oral Sci. 2008, 116, 585–592.
[3]. Zheng, J.; Su, Q.; Wang, C.; Cheng, G.; Zhu, R.; Shi, J.; Yao, K. Synthesis and Biological Evaluation of PMMA/MMT Nanocomposite as Denture Base Material. J. Mater. Sci. Mater. Med. 2011, 22, 1063–1071.
[4]. Wang, X.; Su, Q.; Hu, Y.; Wang, C.; Zheng, J. Structure and Thermal Stability of PMMA/MMT Nanocomposites as Denture Base Material. J. Therm. Anal. Calorim. 2014, 115, 1143–1151.
[5]. Dağistan, S.; Aktas, A.E.; Caglayan, F.; Ayyildiz, A.; Bilge, M. Differential Diagnosis of Denture-Induced Stomatitis, Candida, and Their Variations in Patients Using Complete Denture: A Clinical and Mycological Study. Mycoses 2009, 52, 266–271.
[6]. Chandra, J.; Mukherjee, P.K.; Leidich, S.D.; Faddoul, F.F.; Hoyer, L.L.; Douglas, L.J.; Ghannoum, M.A. Antifungal Resistance of Candidal Biofilms Formed on Denture Acrylic in Vitro. J. Dent. Res. 2001, 80, 903–908.
[7]. He, X.Y.; Meurman, J.H.; Kari, K.; Rautemaa, R.; Samaranayake, L.P. In Vitro Adhesion of Candida Species to Denture Base Materials. Mycoses 2006, 49, 80–84.
[8]. Panáček, A.; Kolář, M.; Večeřová, R.; Prucek, R.; Soukupová, J.; Kryštof, V.; Hamal, P.; Zbořil, R.; Kvítek, L. Antifungal Activity of Silver Nanoparticles against Candida spp. Biomaterials 2009, 30, 6333–6340.
[9]. Wady, A.F.; Machado, A.L.; Zucolotto, V.; Zamperini, C.A.; Berni, E.; Vergani, C.E. Evaluation of Candida albicans Adhesion and Biofilm Formation on a Denture Base Acrylic Resin Containing Silver Nanoparticles: Antifungal Activity of Silver Nanoparticles. J. Appl. Microbiol. 2012, 112, 1163–1172.
[10]. Nam, K.-Y.; Lee, C.-H.; Lee, C.-J. Antifungal and Physical Characteristics of Modified Denture Base Acrylic Incorporated with Silver Nanoparticles: Antifungal Denture Base with Silver. Gerodontology 2012, 29, e413–e419.
[11]. Rahman, H.A. The effect of addition nano particle ZrO2 on some properties of autoclave processed heat cure acrylic denture base material. J. Bagh. Coll. Dent. 2015, 27, 32–39.
[12]. Ayad, N.M.; Badawi, M.F.; Fatah, A.A. Effect of reinforcement of high-impact acrylic resin with zirconia on some physical and mechanical properties. Arch. Oral Res. 2008, 24, 245–250.
[13]. M.W.M. Cunico, J. de Carvalho, Development of novel additive manufacturing technology: an investigation of a selective composite formation process, Rapid Prototyp J, 22 (2016), pp. 51-66.
[14]. T.A. Sulaiman, Materials in digital dentistry—a review, J Esthet Restor Dent, 32 (2020), pp. 171-181.
[15]. R. Li, T. Chow, J. Matinlinna, Ceramic dental biomaterials and CAD/CAM technology: state of the art, J Prosthodont Res, 58 (2014), 10.1016/j.jpor.2014.07.003.
[16]. S. Gali, S. Sirsi, 3D printing: the future technology in prosthodontics, J Dent Health Oral Res, 11 (2015), pp. 37-40.
[17]. Najmon JC, Raeisi S, Tovar A. Review of additive manufacturing technologies and applications in the aerospace industry. In: Additive manufacturing for the aerospace industry. Elsevier; 2019. p. 7–31.
[18]. Espera AH, Dizon JRC, Chen Q, Advincula RC. 3D-printing and advanced manufacturing for electronics. Prog Addit Manuf 2019:1–23.
[19]. Saengchairat N, Tran T, Chua C-K. A review: additive manufacturing for active electronic components. Virtual Phys Prototyp 2017;12:31–46.
[20]. Ng WL, Chua CK, Shen Y-F. Print me an organ! Why we are not there yet. Prog Polym Sci 2019;97:101145.
[21]. Lee JM, Ng WL, Yeong WY. Resolution and shape in bioprinting: strategizing towards complex tissue and organ printing. Appl Phys Rev 2019;6:011307.
[22]. Prinz FB, Atwood CL, Aubin RF, Beaman JJ, Brown RL, Fussell PS, et al. Rapid prototyping in Europe and Japan. Center for Advanced Technology; 1997. p. 102.
[23]. Vandenbroucke B, Kruth J-P. Selective laser melting of biocompatible metals for rapid manufacturing of medical parts. Rapid Prototyp J 2007;13:196–203.
[24]. Wong J. Biocompatible tantalum fiber scaffolding for bone and soft tissue prosthesis. in, Google Patents, 2010.
[25]. Mueller B. Additive manufacturing technologies–rapid prototyping to direct digital manufacturing. Assem Autom 2012:32.
[26]. Ishida Y, Miyasaka T. Dimensional accuracy of dental casting patterns created by 3D printers. Dent Mater J 2016;35:250–6.
[27]. Shujaat S, Shaheen E, Novillo F, Politis C, Jacobs R. Accuracy of cone beam computed tomography–derived casts: a comparative study. J Prosthet Dent 2020; 125:95–102.
[28]. Dikova T, Dzhendov D, Ivanov D, Bliznakova K. Dimensional accuracy and surface roughness of polymeric dental bridges produced by different 3D printing processes. Arch Mater Sci Eng 2018;94:65–75.
[29]. Denry I, Kelly J. Emerging ceramic-based materials for dentistry. J Dent Res 2014; 93:1235–42.
[30]. Torabi K, Farjood E, Hamedani S. Rapid prototyping technologies and their applications in prosthodontics, a review of literature. J Dent 2015;16:1.
[31]. Thompson Y, Gonzalez-Gutierrez J, Kukla C, Felfer P. Fused filament fabrication, debinding and sintering as a low cost additive manufacturing method of 316L stainless steel. Addit Manuf 2019;30:100861. https://doi.org/10.1016/j.addma.2019.100861.

[32]. Sa'ude N, Ibrahim M, Ibrahim MHI. Mechanical properties of highly filled ironABS composites in injection molding for FDM wire filament. Materials Science Forum, Trans Tech Publ; 2014. p. 448–53.
[33]. Abdullah AM, Rahim TNAT, Mohamad D, Akil HM, Rajion ZA. Mechanical and physical properties of highly ZrO2/β-TCP filled polyamide 12 prepared via fused deposition modelling (FDM) 3D printer for potential craniofacial reconstruction application. Mater Lett 2017;189:307–9.
[34]. El-Meliegy E, Van Noort R. Glasses and glass ceramics for medical applications. Springer science & business media; 2011.
[35]. Materials ASfTa.. Standard test methods for determining average grain size. Subcommittee E0408 on Grain Size 2021. https://doi.org/10.1520/E0112- 13R21.
[36]. Materials ASfTa.. Standard test methods for determining average grain size using semiautomatic and automatic image analysis. Subcommittee E04.14 on quantitative. Metallography 2023. https://doi.org/10.1520/E1382-97R23

6. Nanotechnology in Tissular Engineering

Dental hard tissues such as enamel, cement, and bone are formed through the organized accumulation of hydroxyapatite (HA) crystals under the influence of carbon dioxide. However, enamel possesses distinctive characteristics compared to other hard tissues. Unlike them, enamel lacks collagen, which renders it unable to undergo remodeling. In enamel mineralization, the spontaneous self-assembly of the amelogenin protein into nanospheres plays a pivotal role in controlling the growth of apatite crystals, facilitated by carbon dioxide. This unique process holds potential for application in the production of other mineralized tissues, such as bone and cementum, where nanostructures are similarly involved [1].

6.1. Nanohydroxyapatite in dentistry: A comprehensive review

Hydroxyapatite (HA) has received significant attention as a biomaterial in both medical and dental fields owing to its biocompatibility and its essential role as the primary component of the body's hard tissues, notably bone and teeth. Serving as a plentiful source of calcium and phosphate, HA is valuable in remineralizing demineralized enamel regions, particularly in the context of incipient carious lesions [2].

Despite its significance, HA's porous structure is associated with poor mechanical properties. Nano-hydroxyapatite (nHA), however, presents notable advantages over normal HA. It boasts superior solubility, increased surface energy, and enhanced biocompatibility. The smaller size of nHA results in a larger reaction surface, contributing to its excellent bioactivity compared to larger crystals. nHA has emerged as a promising element in caries prevention by facilitating the remineralization of affected enamel and dentin following bacterial acid attacks in early carious lesions.

Incorporating nHA into dentifrices enables it to penetrate tooth porosities, forming a protective coating on the tooth surface and effectively remineralizing the organic scaffold affected by carious attacks. Beyond dental applications, nHA exhibits potential as a scaffolding material for bone regeneration, mimicking the chemical and crystal structure of bone. Notably, Gel-nHA scaffolds have demonstrated odontogenic activity conducive to endodontic regeneration.

Despite the promising applications of nanotechnology, concerns about cytotoxicity and safety persist. Some studies suggest that nano-hydroxyapatite may infiltrate systemic regions through oral epithelium, potentially leading to cytotoxic effects. Given the diverse applications in dentistry, it is crucial to prioritize the use of low or non-toxic agents for oral applications, ensuring the safety of both patients and dental professionals. Rigorous screening tests for potential toxicity should precede the clinical application of these materials [3].

The synthesis of nanohydroxyapatite (nHA) can be achieved through various methods, including co-precipitation, wet precipitation, hydrothermal, mechanochemical, hydrolysis, solid-state, and sol-gel techniques. Among these, the wet chemical precipitation method stands out as the most commonly employed due to its high reproducibility, simplicity, and cost-effectiveness. A notable advantage of this synthesis approach is that water is the sole byproduct. nHA obtained through wet precipitation is non-stoichiometric, whereas the solid-state method yields stoichiometric nHA.

For large-scale and rapid synthesis of nHA powder, the microwave hydrothermal method with ultrasonic atomization precipitation can be employed. This process results in nano-powder with a homogeneous size distribution and excellent dispersibility (Cai et al., 2019). Additionally, the electrospinning technique is utilized to create nanofibrous scaffolds coated with nHA, presenting a promising material for applications in bone tissue engineering, wound dressing, and healing bone defects. The electrospinning method involves coating nHA on various polymers such as cellulose, poly(L-lactide), collagen, and chitosan, enhancing the bioactivity of polymeric nanofibers.

6.1.1. Applications of Nanohydroxyapatite in dentistry

Nanohydroxyapatite (nHA) emerges as a revolutionary material with numerous applications in the field of dentistry. Its versatility is demonstrated in various dental procedures, including

implantology, management of dentin hypersensitivity, bleaching procedures, and the prevention and restoration of dental caries, as further detailed in the following section (Figure 6.1).

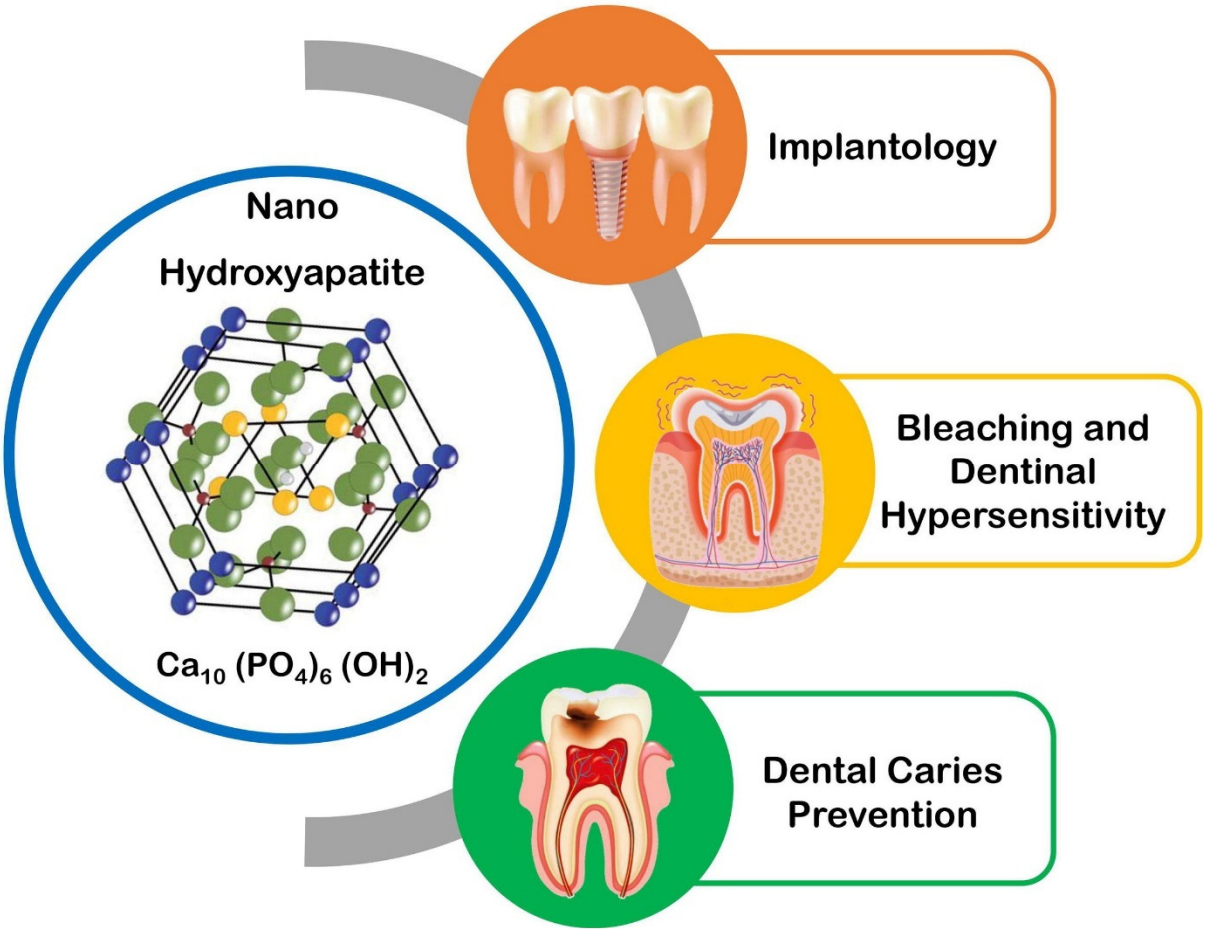


Figure 6.1. Various Dental Applications of Nanohydroxyapatite [4].

6.1.1.1. Implantology

Nanohydroxyapatite (nHA) is extensively utilized to enhance the performance of dental implants, particularly when coating stainless steel and titanium implants. This coating aims to improve bone bonding and stimulate new bone formation, resulting in enhanced bone-to-implant contact. In vivo studies have shown that the deposition of nHA crystals onto dental implants induces a biological effect, with a notable presence of osteoblasts, osteoclasts, and proinflammatory markers.

Research by Oliveira et al. investigated the impact of nHA-coated implants on gene expression, revealing its potential benefits in promoting bone formation, especially in diabetic rats. Furthermore, the use of nanohydroxyapatite-silicate based cement has shown promise in enhancing the primary stability of dental implants, particularly in cases of circumferential bony defects around implants.

Combining nHA with Zinc Oxide nanoparticles (nZnO) has exhibited antibacterial properties on titanium discs, offering a potential approach to address bacterial concerns related to dental implants [4]. Memarzadeh et al. studied the antibacterial efficiency of nZnO as a coating material, as well as a composite coating comprising 75% nZnO and 25% nHA, revealing strong antibacterial action against Staphylococcus aureus.

Studies by Jimbo et al. compared nanoscale HA-coated implants with uncoated counterparts, finding similar bone-to-implant contact but significantly improved tissue quality around the hydroxyapatite-coated implants, as demonstrated through nano-indentation [4]. The mechanical and biological properties of Ti-6Al-4V dental implants were enhanced through coating with nHA using a modified mechanical coating technique [4].

In vitro investigations have also explored the use of a composite solution comprising collagen, bone morphogenic protein-2, and nHA coated onto dental implants. This composite solution exhibited strong expression of osteonectin, a marker of osteoblastic differentiation, and induced mesenchymal stem cell differentiation and osteoblastic differentiation. When placed on rabbit tibias, these coated dental implants demonstrated greater bone formation after 4 weeks.

6.1.1.2. Bleaching and dentinal hypersensitivity

Desensitizing gels incorporating remineralizing agents such as fluoride, casein phosphopeptide amorphous calcium phosphate (CPP-ACP), and nanohydroxyapatite (nHA) are employed to alleviate hypersensitivity following bleaching, a condition affecting 70% of bleached patients [4]. Due to its surface remineralization properties, which create an apatite coating on the tooth's surface, nHA is preferred over traditional desensitizing agents in hypersensitivity treatment. NHA exhibits a high affinity for demineralized surfaces, binding to them and forming microclusters that create an even layer of apatite, fully covering prismatic and interprismatic enamel. Consequently, nHA restores altered enamel morphology while preserving enamel crystallinity.

A study by Browning et al. [4] evaluated the efficacy of an nHA paste in reducing bleaching-related tooth sensitivity. The study found that the nHA paste significantly reduced tooth sensitivity compared to a non-nano hydroxyapatite (zero-HA) placebo paste, with only 29% reporting sensitivity in the nHA group compared to 51% in the non-nano hydroxyapatite group [4]. Another study by Shetty et al. [4] demonstrated that desensitization was significantly enhanced by hydroxyapatite at 25% concentration in a liquid slurry and 100% concentration in a dry sol form.

NHA paste has been shown to heal minute enamel flaws, preventing sensory reactions associated with bleaching-related tooth sensitivity. Ferraz et al. reported that varying concentrations of nHA in 35% hydrogen peroxide had no adverse effects on enamel and deep dentin bleaching or enamel bond strength post-bleaching [4]. Additionally, studies found that nHA derived from chicken eggshell increased enamel microhardness after bleaching, and bleaching agents containing hydrogen peroxide loaded with nHA preserved the interprismatic enamel structure without altering enamel morphology and composition [4]. Monterubbianesi et al. demonstrated that a 6% hydrogen peroxide bleaching gel enriched with nHA served as a safe and effective at-home bleaching system, maintaining enamel microstructure without changing color [4].

Comparative studies have indicated that 2.5% arginine and nHA are equally effective for managing post-bleaching dentin sensitivity [4]. Clinical studies further report enhanced performance and relief from dentine hypersensitivity with nHA-containing agents [4]. Toothpaste formulations containing 10% or 15% nHA, either alone or supplemented with potassium nitrate, were found to be as effective as calcium sodium phosphosilicate for relieving dentine hypersensitivity symptoms when applied at least twice daily. Moreover, toothpaste with 15% nHA was more effective than 10% nHA at reducing dentin sensitivity. A 20% nHA cream was shown to be equally effective as a 20% pure silica-containing dental cream in relieving dentine hypersensitivity symptoms (Amaechi et al., 2018). Dentifrices containing nHA have demonstrated complete closure of dentine tubules and intertubular dentine coverage with significant mineral deposition on the dentin surface [4].

6.1.1.3. Nano-hydroxyapatite in dental caries prevention

Nano-hydroxyapatite (nHA) has been incorporated into toothpaste formulations for caries prevention since the 1980s, particularly in Japan, where it received approval as an anti-caries agent in 1993 [4]. The primary mechanism of nHA in preventing dental caries lies in its strong binding affinity with proteins, plaque, and bacteria fragments, creating an increased surface area for proteins to bind. Acting as a filler, nHA repairs enamel surface depressions due to its small size, promoting remineralization by depositing apatite nanoparticles in enamel defects.

NHA serves as a calcium phosphate reservoir, maintaining a state of super-saturation with enamel minerals, thus enhancing remineralization and inhibiting demineralization [4]. It can reprecipitate minerals on carious lesion surfaces through its surface bioactivity and chemical

resemblance to tooth enamel, inducing constant enamel caries remineralization by forming a homogeneous apatite layer on demineralized enamel surfaces (Figure 6.2).

Research by Huang et al. [4] demonstrated that a 10% nHA suspension is the most optimal concentration for remineralizing incipient carious lesions, with a notable increase in remineralization effect at this concentration compared to 5%. Higher concentrations did not significantly enhance remineralization, potentially due to the blockage of enamel surface porosities by deposited nHA. The calcium concentration in nHA solutions was significantly higher than in micro hydroxyapatite solutions, promoting the saturation of oral fluids with hydroxyapatite and facilitating apatite mineral deposition in carious regions.

NHA rinses have been shown to increase tooth microhardness, and there is evidence suggesting a synergistic role in remineralization when combined with fluoride. NHA in a 0.05% sodium fluoride mouth rinse has been found to be helpful in remineralizing early carious lesions [4]. Studies have explored novel formulations, such as zinc carbonate nHA, demonstrating comparable remineralizing capacity to fluoride on enamel and dentin [4]. Combining nHA with ozone therapy has shown increased effectiveness in remineralizing initial carious lesions compared to individual applications [4].

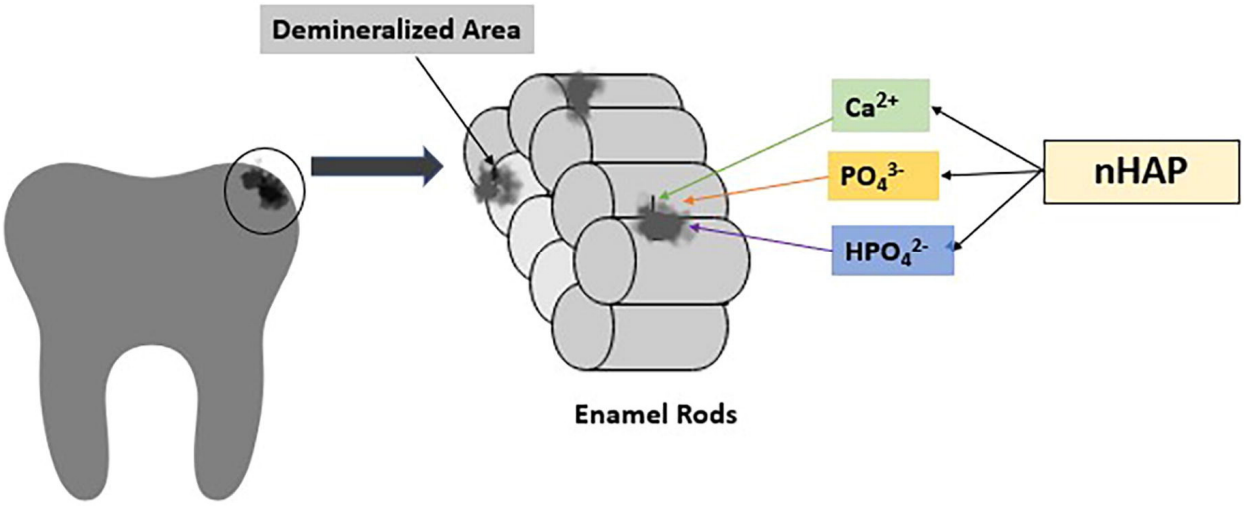


Figure 6.2. Mechanism of Action of Nanohydroxyapatite (nHAP) on Initial Enamel Caries [4].

Comparative studies have evaluated the remineralization potential of nHA dentifrices against fluoride-containing and other formulations, revealing positive effects. The use of 10% nHA dentifrice on demineralized enamel surfaces after orthodontic debonding showed enhanced remineralization (Verma et al., 2021). In primary teeth, nHA toothpaste demonstrated a remineralizing effect similar to 1000 ppm fluoridated toothpaste [4].

A 20% nHA cream demonstrated equal effectiveness to a 20% pure silica-containing dental cream in alleviating dentine hypersensitivity symptoms [4]. Clinical studies have corroborated the remineralizing effects of nHA-containing agents, including dental lotions and toothpastes, in patients undergoing orthodontic treatment [4]. Research comparing various dentifrices, such as bioactive glass Novamin, nHA, functionalized tricalcium phosphate, and grape seed extract, revealed differences in surface microhardness recovery, with bioactive glass Novamin exhibiting the highest efficacy [4].

In summary, the research indicates that nHA has significant potential in preventing dental caries and remineralizing early carious lesions. However, further clinical evidence is needed to fully validate its efficacy in reducing dental caries formation. Additionally, nHA exhibits antibacterial properties, inhibiting the colonization of Streptococcus mutans, and can influence gene expression related to glucosyltransferases responsible for glucans production. Substituted nHA-based toothpaste formulations have also been investigated for their effects on early colonization and biofilm formation, demonstrating varying outcomes based on the type of metal ion substitution.

6.1.1.4. Nanohydroxyapatite in Glass Ionomer Cement (GIC)

Incorporating hydroxyapatite (HA), the most stable derivative of calcium phosphate salts, into Glass Ionomer Cement (GIC) has been pursued to enhance several of its properties. Studies have indicated that the addition of nano-hydroxyapatite (nHA) to GIC leads to improvements in compressive strength, flexural strength, microhardness, reduction in cytotoxicity, increased fluoride ion release, and enhanced antibacterial properties.

Research by Barandehfard et al. (2016) demonstrated that the incorporation of nHA into cement increased its compressive strength, reaching values between 107 and 113.6 MPa due to the increased crystallinity of hydroxyapatite [4]. Moheet et al. (2018) reported a 53.34% increase in flexural strength with the addition of 10% nHA to GIC, attributed to the porosity of hydroxyapatite particles. The larger surface area of nHA particles also contributed to enhanced acid-base reactivity, leading to increased fluoride ion release [4].

Kheur et al. (2020) studied the effects of integrating nHA into glass ionomer luting agents, comparing them with conventional GICs, resin-modified GIC, and adhesive resin. While adhesive resin exhibited maximum flexural strength and the highest shear bond strengths, the experimental nHA-modified glass ionomer cement demonstrated improved bonding of polyacid's carboxyl groups with the calcium present in natural teeth to synthetic hydroxyapatite [4].

Alatawi et al. (2019) investigated the incorporation of various concentrations of nHA into GIC, observing increased fluoride ion release and significant bacterial inhibition against Streptococcus mutans, particularly with an 8% concentration of nHA. Noorani et al. (2017) compared the cytotoxicity of nHA-silica incorporated into GIC with conventional GIC and resin-modified GIC on human Dental Pulp Stem Cells (DPSCs). The experimental nHA-silica-GIC showed comparable cytotoxicity to conventional GIC but superior performance compared to resin-modified GIC [4].

Pagano et al. explored a complex hybrid product containing GIC, nHA, mucosal defensive agent, and antibiotic emulsion, evaluating its mechanical, thermal, and biological properties. The study revealed improved mechanical properties in the oral cavity due to the wet environment and the presence of the powder-formulated antibiotic. The addition of nHA, with its antibiotic and mucosal defensive properties, significantly decreased the overall toxicity of the cement [4].

6.1.1.5. Nanohydroxyapatite in dental composite

Meena et al. conducted a study investigating the addition of 5–20 wt% nano-hydroxyapatite (nHA) and Mineral Trioxide Aggregate (MTA) to dental composite. The research revealed that the inclusion of nHA as a filler improved the thermal stability of the dental composite compared to MTA filler (Meena et al., 2017). Another study examined the effects of micro/nHA rod additions to composite resins on strength and remineralization. Hybrid nano-rods and micro-rods of hydroxyapatite-filled composites demonstrated promising applications for teeth restoration (Wu et al., 2019) [4].

Lung et al. found that reinforcing the composite resin matrix with 30 wt% silanized-nHA improved the physical and mechanical properties of a Bis-GMA-based composite resin (Lung et al., 2016). Yadav et al. aimed to assess the efficacy of 3-methacryloxypropyl trimethoxy silane and 3-aminopropyl triethoxysilane-treated nHA filler in developing high-strength, thermally-stable photocurable dental composite with enhanced thermo-mechanical properties. This functionalized nHA-based dental composite material was considered as a substitute for restorative dentistry (Yadav and Gangwar, 2021) [4].

In a study evaluating the thermo-mechanical and thermogravimetric properties of dental composite restorative materials, alumina nHA and titanium oxide nHA hybrid forms were assessed. The results indicated that the alumina nHA-filled dental composite exhibited more significant properties than the titanium oxide dental composite material.

6.1.1.6. Application of Nanohydroxyapatite in orthodontics

The application of nano-hydroxyapatite (nHA) beneath orthodontic bands was found to decrease microleakage, although it did not have an impact on tooth color changes after orthodontic

debonding (Malekpour et al., 2022; Enan and Hammad, 2013). In the context of active orthodontic treatment, the use of a biomimetic nHA solution demonstrated a reduction in hard tissue demineralization. However, this remineralizing treatment led to reduced bond strength values for both brackets and attachments. Interestingly, composite attachments exhibited higher adhesion values compared to brackets. Furthermore, when compared to demineralized enamel, remineralized enamel with biomimetic nHA displayed higher microhardness values [4].

6.1.1.7. Nanohydroxyapatite in Periodontal Tissue Regeneration

Nanohydroxyapatite (nHA) is increasingly seen as a promising alternative to autogenous bone grafts for periodontal and alveolar tissue regeneration due to its biocompatibility, minimal morbidity, and lack of toxicity. When combined with other active particles or biologic mediators, nHA can enhance periodontal tissue regeneration further, making it beneficial for supporting alveolar bone regeneration in cases of periodontitis.

Studies have demonstrated that nHA-based hydrogels can enhance the regeneration of extraction sockets in animals with periodontitis, suggesting their potential for post-extraction socket preservation and future dental implant placement. Additionally, nHA grafts have shown promising results in periodontal regeneration, particularly in treating intrabony defects.

Composite scaffold materials incorporating nHA, such as Nano-Hydroxyapatite-Modified Collagen (nHAC) and Fibroblast Growth Factor (bFGF) composites, have been developed to regenerate and repair periodontal tissue. These scaffolds provide a conducive environment for cell growth and attachment and have shown positive outcomes in periodontal tissue regeneration.

Moreover, nHA-incorporated scaffolds, like 1% nHA/chitosan scaffolds, have demonstrated enhanced cytocompatibility and encouraged the growth of Human Periodontal Ligament Cells (HPLCs) compared to pure chitosan scaffolds. These scaffolds have also shown potential in periodontal tissue regeneration in diabetic patients, aiding in the regeneration of periodontal bone tissues.

Beyond periodontal applications, nHA holds promise in repairing bone abnormalities resulting from trauma or surgery and can be utilized in tissue engineering and regeneration in various oral surgical procedures, including repairing cleft lip and palate and periodontal therapies.

However, it's crucial to consider the cytotoxicity of nHA. Some studies have reported potential cytotoxic effects of nHA particles on human oral epithelial cells. Nonetheless, the safety of nanomaterials, including nanohydroxyapatite, remains a subject of ongoing debate and research.

6.2. Scaffold design and stem cells for tooth regeneration

The tooth is a vital organ that develops through complex interactions between epithelium and mesenchyme tissues. Researchers in the field of tissue engineering are working towards building mineralized dentin, enamel, and cementum using different dental cells. The ultimate goal is to reconstruct a tooth crown with its root.

In the human tooth, the crown is responsible for functions such as chewing, while the root attaches to the central alveolar bone within the periodontal ligament. The tooth roots are protected by cementum, a mineralized bone tissue generated by dental mesenchyme-derived cementoblasts. The roots are attached to the adjacent alveolar bone through the periodontal ligament, which allows for tooth movement and transfers mechanical stimuli during activities like chewing and orthodontic treatments.

Tooth damage or loss can occur due to various factors such as periodontal disease, dental caries, trauma, or genetic disorders. According to data from the National Institute of Dental and Craniofacial Research in the USA, a significant percentage of adults, particularly those over 70 years old, experience moderate to severe periodontal disease, and about 25% have lost their teeth. Globally, around five billion people have suffered or are currently experiencing dental diseases.

This clinical challenge poses a significant burden on healthcare systems, with estimated expenditures on dental care comprising about 5-10% of healthcare budgets in industrialized countries.

Restoring lost tooth tissue is a complex and costly task, and addressing this challenge will continue to be a significant concern for years to come. Tissue engineering techniques hold promise in providing solutions for tooth regeneration and restoration, aiming to alleviate the impact of tooth loss due to various oral health issues.

6.2.1. Introduction

The regeneration of adult teeth, which do not naturally regenerate, poses challenges that current dental therapies, such as artificial dentition, tooth transplantation, and dental implants, aim to address. Tooth development during formative stages involves intricate interactions between mesenchymal cells and epithelial cells, leading to the secretion and buildup of mineralized dentin, enamel, and cementum, ultimately resulting in the generation of the tooth crown and its root(s). Due to the complex forces experienced during mastication and the diverse tissue types associated with teeth, tissue regeneration of the entire tooth is challenging.

Recent efforts in teeth tissue regeneration focus on applying biological knowledge to design therapies promoting teeth tissue regeneration. Researchers aim to repair one or more tooth tissues or even re-grow an intact tooth for complete substitution. Complete tooth regeneration is complicated by the need to regenerate a tooth at a site where one no longer exists.

Tooth engineering and regeneration present an attractive proposition due to the accessibility and non-life-threatening nature of dental tissues. The main objective is to regenerate the entire tooth or its root, which can be integrated into the jaw bone, providing a functional substitute for missing teeth and potentially replacing artificial dental implants. This approach offers advantages such as alleviating patient suffering, minimizing infection risks, reducing recovery time, and preventing or delaying complete tooth loss.

Various approaches, including scaffold-based tooth regeneration, induction of a third dentition, assembly of different bioengineered component parts, cell pellet engineering, chimeric tooth engineering, and gene-manipulated tooth regeneration, have been explored. Among these, synthetic scaffold-based tooth regeneration is currently a widely accepted technique, involving pre-designed and optimized scaffolds.

The scaffold's role in providing an environment for guiding the generation of the natural extracellular matrix (ECM) is crucial. Scaffold design and optimization should ensure mechanical integrity, functionality, and proper surface morphology for cell adhesion and differentiation. The selection of biomaterials that mimic the ECM of the tissue to be replaced is critical, and scaffolds should be biocompatible, conductive, and possess suitable mechanical properties Figure 6.3).

Scaffold sterilization is essential to prevent infection and rejection, and interconnected porosity is required for cell and growth factor placement and vascular growth. The choice of scaffolding material, its form (gel, foam, or fiber), and surface topology play pivotal roles in dental structure morphogenesis, with surface morphology needing to closely resemble the natural ECM. Osteoblasts cultured on different ceramic materials have been shown to express different types of collagen and alkaline phosphatase mRNA.

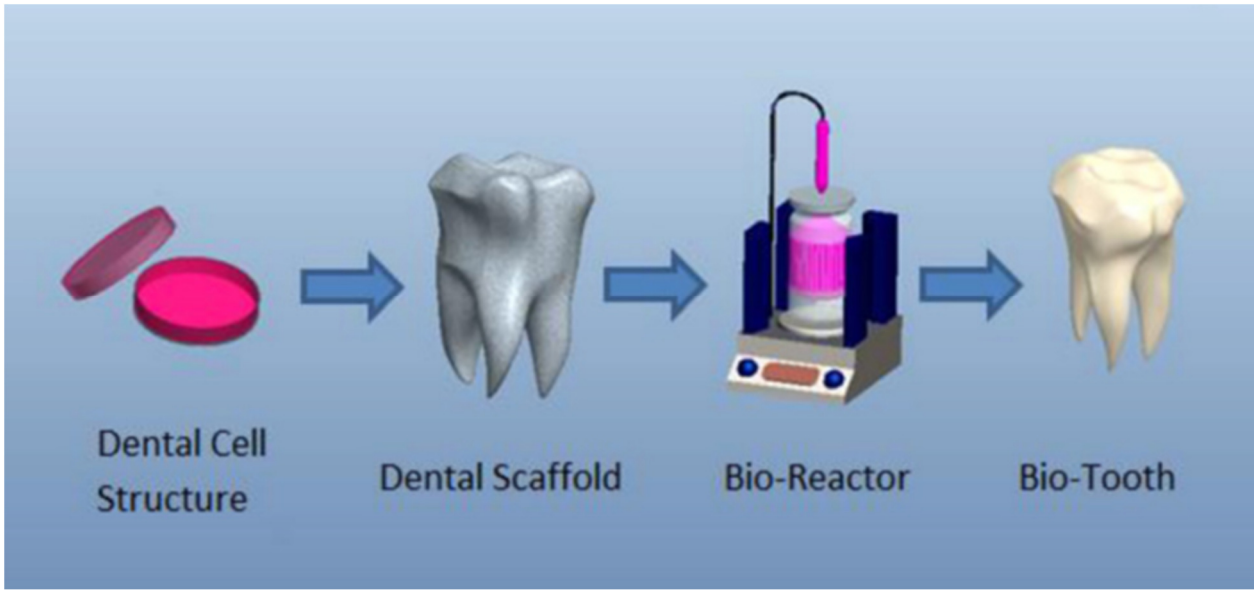


Figure 6.3. Schematic illustration of tissue engineering of tooth [5].

Constructing the correct scaffold with the right mechanical and physical characteristics is a complex and challenging task. This paper highlights significant developments in teeth tissue engineering and outlines future challenges in the field.

6.2.2. Scaffolds for teeth tissue engineering: Biological polymer scaffolds

These diverse scaffold materials fulfill various requirements in teeth tissue engineering, offering a range of mechanical properties, degradation rates, and compatibility with surrounding tissues. Researchers continue to explore and optimize these scaffolds for enhanced performance in promoting tooth regeneration and integration.

Types of Biomaterial Scaffolds for Teeth Tissue Engineering:

Hydroxyapatite Ceramics:

Description: Long-lasting porous hydroxyapatite ceramics are used for teeth tissue engineering.

Properties: Provide chemical stability and physical properties matching surrounding tissues, mimicking the mineral component of natural teeth.

Applications: Used for their resemblance to natural teeth and ability to support engineered tissues.

Collagen and Chitosan:

Description: Scaffolds of intermediate type, including collagen and chitosan, are employed in teeth tissue engineering.

Properties: Possess inherently transpiring molecules, supporting cell attachment.

Applications: Used for forming new engineered tissues due to their biocompatibility.

Polyglycolic Acid (PGA):

Description: Moderately short-lasting polymer used as a scaffold.

Properties: Exhibits controlled degradation.

Applications: Employed in teeth tissue engineering for biocompatibility and degradability.

Polylactic Acid (PLA):

Description: Polymer used as a scaffold for teeth tissue engineering.

Properties: Offers controlled degradation and suitable mechanical strength.

Applications: Chosen for biocompatibility and ability to support cell proliferation.

Polyglycolic Acid-Poly-L-lactic Acid (PGA-PLLA) and Polylactic Polyglycolic Acid (PLGA):

Description: Combinations of polyglycolic acid and poly-L-lactic acid (PGA-PLLA) and polylactic polyglycolic acid (PLGA) are scaffold materials.

Properties: Provide a balance of controlled degradation and mechanical strength.
Applications: Employed in teeth tissue engineering for their tunable properties.

6.2.2.1. Collagen

1. Collagen, a protein present in sinew, cartilage, bone, and skin, is widely employed in tissue regeneration due to its excellent biocompatibility, resemblance to the extracellular matrix, low immunogenicity, and ability to form diverse shapes.

- Properties:
  - Excellent biocompatibility.
  - Structural similarity to the extracellular matrix.
  - Low immunogenicity and cytotoxicity.
  - Formability into various shapes.
- Applications: In tooth regeneration, collagen scaffolds retain cells, support proliferation and differentiation, and facilitate the formation of calcified tissues, showcasing potential for structured matrix formation akin to pulpal tissue.

2. Protein:
   - Overview: Various proteins serve as scaffold materials for teeth tissue engineering.
   - Properties: Biocompatible and conducive to promoting cell growth and differentiation.
   - Applications: Utilized in combination with other materials for tooth regeneration.
3. Chitosan:
   - Overview: Derived from chitin, chitosan functions as a natural polymer scaffold material.
   - Properties: Biocompatible and supportive of cell growth and differentiation.
   - Applications: Employed in tooth tissue engineering for its biocompatibility and regenerative stimulation.
4. Silk:
   - Overview: The natural fiber silk is explored as a scaffold material.
   - Properties: Biocompatible and provides a suitable environment for cell growth.
   - Applications: Investigated for potential contributions to tooth regeneration.
5. Alginate:
   - Overview: Derived from seaweed, alginate serves as a scaffold material.
   - Properties: Biocompatible and easily moldable into desired shapes.
   - Applications: Explored in tooth tissue engineering, offering support for cell proliferation and differentiation.
6. Hyaluronic Acid:
   - Overview: Hyaluronic acid, a component of connective tissue, is explored for its scaffold potential.
   - Properties: Biocompatible and contributes to tissue hydration and regeneration.
   - Applications: Investigated for its role in tooth regeneration.

Derivatives of Natural Polymers:

- Various derivatives of natural polymers are harnessed as scaffold materials, providing enhanced properties for specific applications in tooth tissue engineering.

These natural polymers and their derivatives hold promise as scaffold materials in teeth tissue engineering, fostering a biocompatible environment conducive to cell growth, proliferation, and differentiation. Ongoing research aims to optimize their utilization for improved outcomes in tooth regeneration.

In a groundbreaking study by Honda et al. [48], a pioneering technique was introduced to sequentially seed epithelial cells and mesenchymal cells on collagen scaffolds. The innovative approach involved directly combining the two cell types, and the resultant cell-scaffold constructs were then implanted into immunocompromised rats. The outcomes of this study, as depicted in Figure 6.4. revealed that the in vivo-developed tooth morphology closely resembled that of a natural tooth. Notably, each scaffold yielded only one tooth structure, underscoring the effectiveness of the

proposed cell-seeding technique. This novel method demonstrates promising potential for controlling the morphology of regenerated teeth, marking a significant advancement in the field of tooth regeneration [5].

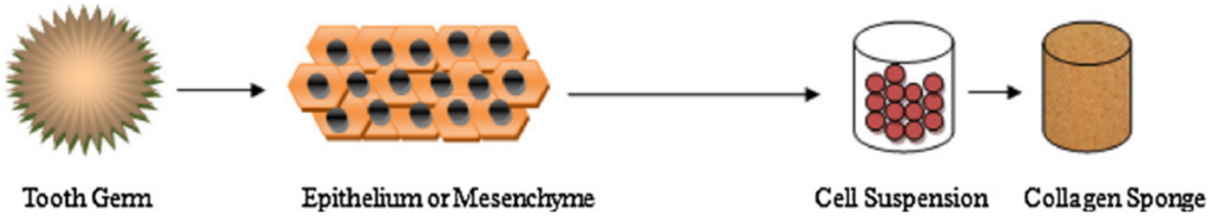


Figure 6.4. Schematic illustration of epithelial and mesenchymal cell suspension from tooth germ [5].

6.2.2.2. Chitosan

Chitosan, derived from the deacetylation of chitin, undergoes a solubilization process when its deacetylation reaches around 50%, transforming into a water-soluble substance in acidic environments. This transformation occurs through the protonation of the –NH2 function on the C-2 position of the D-glucosamine recurrence unit, resulting in a polyelectrolyte in acidic media. Known for its biocompatibility and biodegradability, chitosan is extensively used in various tissue engineering applications in conjunction with other polymers [5].

A noteworthy development involves the creation of a three-dimensional multilayered co-culture system utilizing blends of type I collagen and chitosan. This system, seeded with mesenchymal-derived dental pulp stem cells (DPSCs) and HAT-7 dental epithelial cells, facilitates epithelial—mesenchymal interactions. The HAT-7 cell line, originating from the cervical loop of the murine incisor, serves as an epithelial stem cell line. The outcome of this co-culture technique, after 24 days, demonstrates the observation of calcium deposits. Notably, the scaffold's layered macroscale bio-mimetic structure, characterized by tunable mechanical properties, supports the movement of both cell types in all directions [5].

Chitosan also proves to be an effective DNA carrier. Zhang et al. [5] combined a plasmid encoding the platelet-derived growth factor B (PDGFB) gene with chitosan and coral to construct a porous chitosan/coral scaffold. Human periodontal ligament cells (HPLCs) were then seeded onto the scaffold, which was implanted into athymic mice, creating a gene-activated scaffold. The in vivo results demonstrated superior proliferation characteristics of HPLCs on the seeded scaffold compared to the pure coral scaffold. This suggests that the seeded scaffold outperformed the non-seeded one. Further experiments involved porous chitosan/collagen scaffolds loaded with TGF-b1, revealing not only the proliferation of HPLCs but also the recruitment of cells from adjacent tissues into the scaffold. This indicates that chitosan/collagen scaffold linked with TGF-b1 holds great potential as an excellent substrate contestant in periodontal tissue regeneration [5].

6.2.2.3. Silk protein

Silk proteins, known for their biodegradability, biocompatibility, and non-immunogenic properties, offer a promising avenue for tissue engineering. Approved by the Food and Drug Administration (FDA), silk proteins can be chemically linked to peptides, such as arginine-glycine-aspartic acid (RGD), using carbodiimide chemistry. The application of silk-based scaffolds has proven successful in bone tissue engineering [5].

The efficacy of silk properties in hard tissue engineering is evident in a study where four scaffolds, with or without RGD peptide, were crafted from biomaterial silk protein. These scaffolds featured varying pore diameters, ranging from 250 to 550 mm.

Tooth bud cells were seeded onto these scaffolds, which were then implemented in 4-day postnatal rat tooth models. Following a 20-week implantation in rat mandibles, harvested scaffolds displayed regeneration of mineralized tissue in all instances.

Analyses of the implants revealed the formation of bioengineered mineralized tissue, with the most robust outcomes observed in 550 mm pore RGD-containing scaffolds and comparatively less robust results in 250 mm pore-sized scaffolds without RGD [5].

This underscores the potential of silk protein scaffolds in promoting mineralized tissue regeneration, presenting a biocompatible solution for tooth engineering applications.

6.2.2.4. Alginate

Alginate, a natural polysaccharide sourced from brown seaweed, possesses several appealing physical properties, making it an ideal candidate for various applications. These properties include biocompatibility, gentle gelation conditions, and low immunogenicity. Purified alginate has found extensive use in the food and pharmaceutical industries, as well as in biomedical, biomaterial, and therapeutic applications (Figure 6.5).

Materials	Features	Applications
Collagen	• Acts as a connective tissue. • Main protein of sinew, cartilage, bone and skin. • Low immunogenicity and cytotoxicity.	• Tissue engineering • Occular Surgery • Drug delivery system Reconstructive surgery, orthopedics and dentistry. • Teeth tissue engineering.
Silk protein	• Strength blood vessel • Biodegradable, biocompatible and non-immuogenic. • Approved by Food and Drug Administration (FDA). • Can be coupled via carbodimide chemistry to peptides.	• Useful for bone tissue engineering.
Alginate	• Natural polysaccharide, obtained from seaweed. • Biocompatible, mildness of gelation condition and low immunogenecity. • Can degrade by enzymolysis in vivo with no cytotoxicity • Alginate beads are usually made by calcium ion cross-linking	• Used in food and pharmaceutical industries. • Also in biomedical, biomaterial and therapeutic application. • Wound dressing • Drug delivery system • Cell culture media • Neural tissue engineering
Hyaluronic acid (HA)	• Can be chemically and structurally modified for different applications. • HA sponge has an appropriate structure, biocompatibility and biodegradation as a scaffold for dental pulp regeneration. • Important constituent of Extracellular Matrix (ECM)	• Tissue engineering. • Viscoelastic properties are useful for medical applications.
Chitosan	• Most abundant polymer after cellulose • Biocompatible and biodegradable.	• Tissue engineering. • Chitin could serve as replacements for bone, cartilage, arteries, veins, and musculo-fascial replacement
Peptide	• Good DNA carrier. • Useful for electrospinning • When the degree of deactylation of chitin reaches 50%, it becomes soluble and is called chitosan • Chitosan is the only pseudo natural cationic polymer • Peptides and proteins are replacing polymers as biomaterials. • Can be integrated with other organic and inorganic components to form nano-composites. • Plays a key role in activating cellular interactions and tissue regeneration.	• Tissue engineering. • Bone, cartilage and dentin

Figure 6.5. Main physical characteristics of various biomaterials [5].

In a notable study, an alginate scaffold seeded with rat dental-pulp-derived cells and human dental pulp cells was implanted in the backs of nude mice. The results demonstrated that the seeded cells underwent differentiation into odontoblast-like cells, actively promoting calcification in the tooth [5].

Furthermore, an innovative approach involved the creation of an injectable self-gelling alginate gel with macro-pores (pores in the micrometer range). This was achieved by blending alginate microspheres of calcium with soluble alginate solutions. The resulting soft macro-porous gels proved effective in encouraging cellular penetration and facilitating access to microspheres that dispersed therapeutic factors within the matrix during in vivo immunotherapy [5]. This highlights the versatility of alginate in contributing to tooth regeneration efforts, showcasing its potential in creating biocompatible scaffolds for dental tissue engineering.

6.2.2.5. Hyaluronic acid and its derivatives

The term "hyaluronic acid" was coined from "hyalos," signifying glassy or vitreous, and "uronic acid." It represents an unbranched polysaccharide comprising repeating disaccharides, specifically D-glucuronic acid and N-acetyl-D-glucosamine [5]. Hyaluronic acid and its derivatives boast remarkable potential in the field of tissue engineering due to their ability to undergo chemical and structural modifications tailored for diverse applications.

In the context of dental pulp regeneration, hyaluronic acid sponge emerges as a promising component. To achieve an effective restorative treatment for dental pulp accompanied by sound dentin development, combinations of growth factors with hyaluronic acid sponge are deemed necessary. Beyond its role in promoting dental pulp regeneration, hyaluronic acid sponge exhibits favorable attributes such as appropriate physical structure, biocompatibility, and biodegradability, positioning it as a viable implant for advancing dental tissue regeneration endeavors [5].

6.2.2.6. Peptide

In the realm of hard tissue engineering, which encompasses bone, cartilage, and dentin, there is a growing affinity for utilizing protein or peptide constructs, particularly those based on polyether ester amide (protein). The increasing popularity of these constructs can be attributed to the unique characteristics of peptides, which are predominantly nano-scale biological materials. Their seamless integration into organic or inorganic components facilitates the creation of diverse nano-composites. These syntheses exhibit exceptional biocompatibility and possess advantageous physico-chemical traits, fostering cellular interactions and promoting the production of tissue matrices.

A notable category within this domain is self-assembling peptides or peptide amphiphiles, rooted in the principles of protein-protein interactions and folding. Recent studies have explored the combination of two dental stem cell lines with peptide-amphiphile hydrogel scaffolds. This research has revealed differences in morphology, proliferation, and differentiation behaviors, underscoring the potential of combining cells with scaffolds to streamline the tissue engineering process. This approach is recommended for applications spanning both soft and mineralized matrices in the context of dental tissue regeneration [5]. The evolving landscape of these materials suggests promising features and applications, as outlined below.

6.2.3. Scaffolds for teeth tissue engineering: Ceramic Scaffolds

Dentin, a complex composite material, comprises a mineral phase of hydroxyapatite and a hydrogel reinforcing phase primarily composed of type I collagen. The chemical resemblance of calcium phosphate salts to the mineral component of natural dentin, coupled with their biocompatibility and ability to form mineralized tissues, positions them as advantageous elements in endodontic therapy.

The utilization of hydroxyapatite (HA) scaffolds has shown effectiveness in dentin or dentin-pulp complex regeneration. Strategies involving nano- or micro-structured scaffolds, mimicking the three-dimensional configurations of natural bone or teeth, have garnered considerable interest. A

novel approach involves the self-assembly of one-dimensional hydroxyapatite nanorods, strategically placed to simulate bone or enamel-like structures. Porous cylindrical HA implants, featuring a hollow center, have been employed for tooth regeneration, with promising results indicating enhanced osteogenesis within the composite scaffold.

Synthetic HA scaffolds, such as ENGIpore#, seeded with human dental follicle stem cells, exhibited notable cell attachment and colonization. Over time, a three-dimensional organization of cells and the presence of dense material around cell clusters were observed, demonstrating the scaffold's potential for morphological structure and extracellular matrix production analysis. Further experiments with porcine dental papilla cells on beta-tricalcium phosphate (b-TCP) scaffolds and human dental pulp stem cells on electrospun Poly(L-lactic acid)/multi-walled carbon nanotubes/hydroxyapatite nanofibrous scaffolds showcased successful construction of dentin-pulp complex-like structures.

Notably, b-TCP/chitosan porous scaffolds encouraged dental pulp stem cells to multiply, promoted vascular tissue ingrowth, and supported cell differentiation towards osteoblasts and cementoblasts. Constructs like HA-chitosan with fibroblast growth factor (bFGF) also demonstrated favorable 3D environments for cellular structure, differentiation, proliferation, and mineralization.

While studies on Electrospun Poly(L-lactic acid)/multi-walled carbon nanotubes/hydroxyapatite nanofibrous scaffolds show promise, the long-term effects of materials like multi-walled carbon nanotubes in tissue engineering remain under exploration, emphasizing the need for further research in this dynamic field [5].

6.3. New technology in scaffold processing

Traditional methods for crafting open porous scaffolds involve techniques such as solvent casting/salt leaching, phase separation, gel casting, precipitation, and emulsion freeze-drying. While these methods theoretically offer good pore interconnectivity and surface morphology control, scaffolds produced are limited to a single polymer and may lack accurate and controllable porous structures. Additionally, these techniques often involve time-consuming organic solvent purification phases, posing challenges for immediate implementation.

CO2 gas foaming methods, despite their speed and ability to create micro-cellular configurations, still face limitations in achieving optimal pore interconnectivity essential for cell in-growth. A proposed solution involves a salt-leaching and gas foaming technique, aiming to address this challenge; however, the efficient removal of salt from the construct remains a subject for further exploration.

Current research endeavors are extensively focused on exploring innovative techniques to tailor scaffolds precisely for teeth tissue engineering. This pursuit aims to overcome existing limitations and revolutionize scaffold fabrication processes, ensuring enhanced control over porous morphology and facilitating immediate implementation without sacrificing accuracy.

6.3.1. Electrospinning technique

The electrospinning technique has become a versatile and user-friendly method for customizing scaffold characteristics to meet the diverse requirements of various tissue engineering applications. It offers exceptional control over pore interconnectivity, as well as internal and external scaffold geometry.

The fundamental principle of electrospinning involves the pumping of a polymer in a liquid phase through a thin needle with a specific diameter toward a conductive object. When the necessary high voltage is applied, the electric power overcomes the surface tension forces of the polymer solution. This results in the formation of a jet of polymer fibers. As the polymer jet is drawn toward an electrically grounded collecting plate or tube, it undergoes a thinning process due to solvent evaporation, ultimately yielding finely crafted fibers. (Figure 6.6.)

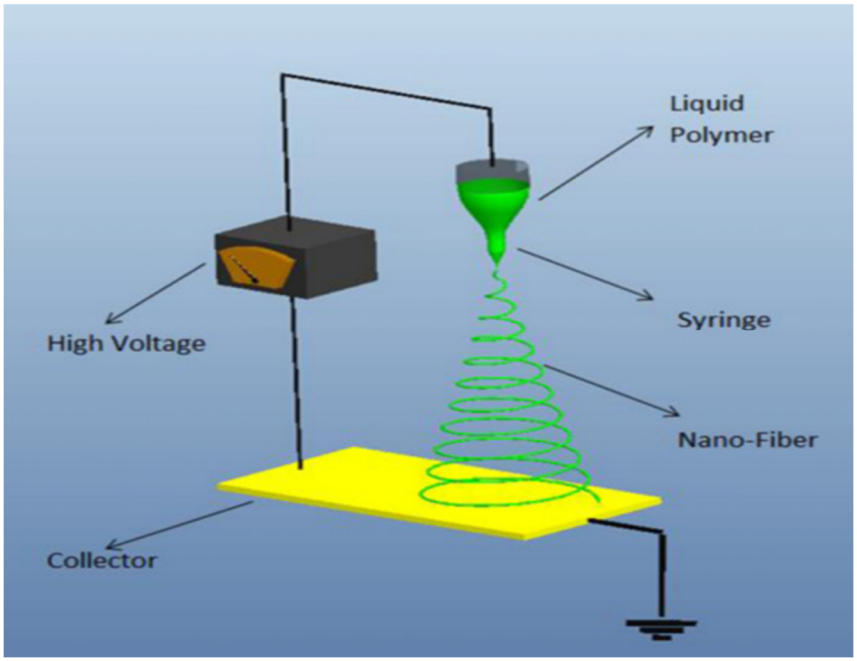


Figure 6.6. Electro-spinning procedure [5].

The electrospinning technique has revolutionized the production of scaffolds using a broad range of biodegradable and biocompatible polymers, resulting in flat sheets with specific fiber arrangements [5]. These fibrous scaffolds typically have sizes ranging from 5 nm to a maximum of 1000 nm [5]. One of the main advantages of this technology lies in its ability to produce scaffolds that closely mimic the extracellular matrix (ECM), featuring small pore sizes, high density, and a large surface area—essential attributes for an effective scaffold [5].

In a study conducted by Yang et al. [5], dental pulp stem cells (DPSCs) were seeded on electrospun poly (ε-caprolactone) (PCL)/gelatin scaffolds, both with and without the addition of nano-hydroxyapatite (nHA). Although there were no signs of tissue ingrowth within the cell syntheses and construct, clear in vivo hard tissue regeneration was observed. The addition of nHA in the constructs, however, upregulated the expression of specific odontogenic genes.

Collagen and/or elastin meshes were successfully arranged through electrospinning from aqueous solutions, utilizing crosslinking with N-(3-dimethylaminopropyl)-N0-ethylcarbodiimide (EDC) and N-hydroxysuccinimide (NHS) to create scaffolds with the necessary porosity and surface area. The electrospinning manufacturing method has been employed to form multilayered scaffold constructs with desired characteristics in terms of surface morphology and mechanical integrity [5]. Additionally, electrospinning of ethylene vinyl alcohol (EVOH) nanofibers has supported the culture of smooth muscle cells (SMCs) and fibroblasts [5]. Electrospun PCL scaffolds have shown promise in encouraging mineralized tissue formation, positioning them as strong candidates for hard tissue-engineering applications.

6.3.2. Rapid prototyping technology

Rapid prototyping (RP) technologies, also known as solid freeform fabrication, have gained widespread application in biomedical and tissue engineering. In this cutting-edge technique, precise 3D scaffold models, based on computer-aided design (CAD) or computed tomography (CT) scan files, are meticulously constructed layer by layer through the cyclic deposition and dispensation of material. These 3D models serve various purposes, including the creation of physical models for tissues, personalized implants, surgical aids, and CT scan-based tissue engineering scaffolds. Currently, several RP technologies are available in the market, such as three-dimensional printing (3DP), fused deposition modeling (FDM), stereolithography apparatus (SLA), and selective laser sintering (SLS).

One prominent illustration of RP technology is 3D printing (3DP), as depicted in Figure 6.7. The work of Kim et al. [5] explored the potential use of 3DP technology in conjunction with the salt leaching technique for polymeric scaffold fabrication. Through salt leaching, the authors successfully obtained cylindrical porous scaffolds with excellent interconnectivity featuring 800 mm porous channels and 45–150 micro-porosities. Additionally, computer-aided design/manufacturing tools, specifically CAD/CAM for RP (3D) printing, were employed to identify hydroxyapatite (HA) scaffolds [5].

Another RP technique, fused deposition modeling (FDM), is showcased in Figure 6.8. This method constructs 3D models from CT scans or CAD solid models. The FDM technique utilizes a thermoplastic filament material pushed by two rollers inside a specially designed electrically heated dispensable head/extruder. The semi-molten polymer is then deposited layer by layer in the X and Y directions on a platform that is progressively lowered in the Z direction after each completed layer, gradually building up the desired 3D model.

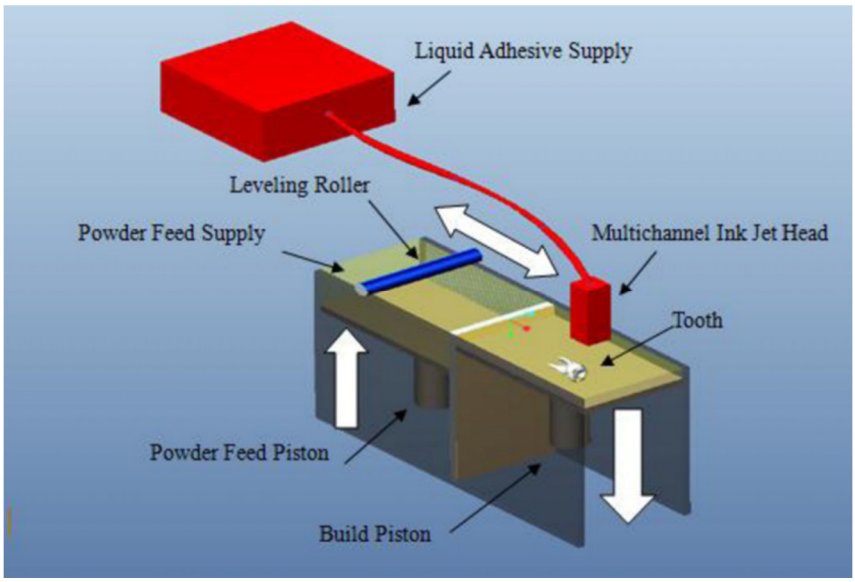


Figure 6.7. Schematic illustration of 3D-printing [5].

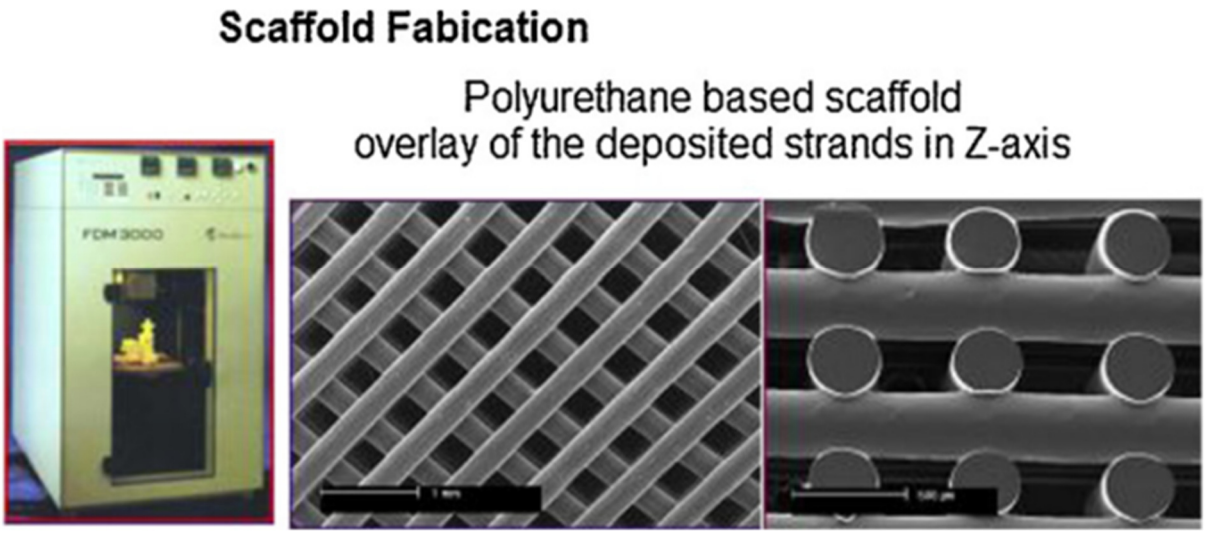


Figure 6.8. Scaffold Fabrication using FDM carried out at Swinburne University, Australia [5].

Rapid prototyping (RP) technologies have revolutionized tissue engineering, providing unprecedented control and precision in scaffold design and fabrication. These technologies, including three-dimensional printing (3DP), fused deposition modeling (FDM), stereolithography apparatus

(SLA), and selective laser sintering (SLS), offer versatile solutions tailored to various biomedical applications.

In FDM, a computer control system optimizes parameters based on the thermoplastic material and design requirements. Woodfield et al. [5] utilized FDM-like processes to create polyethylene glycolterephthalate—polybutylene terephthalate (PEGT/PBT) scaffolds, achieving a broad range of mechanical properties suitable for articular cartilage applications.

SLA employs photopolymerization, where liquid polymer material is dispensed in a bath and solidified by a UV laser. This process proceeds layer by layer, tracing the laser beam along model boundaries until a 3D structure is formed. This method allows for precise control and fine detailing, resulting in high-quality constructs. Liquid low-molecular-weight copolymers, initiated by ring-opening polymerization and end-functionalized with coumarin or methacrylate groups, have demonstrated efficacy in SLA for tissue engineering applications [5].

SLS employs a CO2 laser beam to sinter layers of powdered polymeric materials, constructing a solid model. The high porosity and surface area of SLS-fabricated constructs, combined with mechanical integrity, make this method advantageous. Williams's group successfully created poly(ε-caprolactone) (PCL) scaffolds using SLS [5], showcasing the potential for hybrid scaffold fabrication by combining different materials [5].

In a groundbreaking approach, Park et al. [5] employed a multi-scale computational design method for the construction of composite polycaprolactone (PCL)-poly (glycolic acid) (PGA) scaffolds. These scaffolds, targeting cell replacement for the creation of human tooth dentin—ligament—bone complexes, exhibited interfacial formation of fibers that advanced and integrated within the scaffold, resulting in tooth cementum-like tissue, ligament, and bone formations [5].

6.3.3. Supercritical fluid-gassing process

Maspero et al. [5] have introduced a pioneering method for the rapid creation of net-shaped porous scaffolds, demonstrating a remarkable advancement in scaffold fabrication. This groundbreaking technique involves the swift consolidation of Poly (lactic-co-glycolic acid) (PLGA) particles in a mold utilizing sub-critical carbon dioxide (CO2), enabling the rapid generation of an accurate porous replica of a tooth root without the use of organic solvents.



Figure 6.9. Schematic illustration of tooth root replicausing Pro-engineer software [5].

The process begins with the construction of a mold using sterile polyvinylsiloxane, meticulously capturing the precise geometry of the tooth. The tooth root is placed into the polymer, creating an impression. After setting, the root is removed, and the mold is filled with sterile PLGA particles of varying sizes, typically in the range of 700 to 1400 micrometers. This results in the formation of an intricately porous tooth root replica.

Utilizing this innovative molding technique, open porous scaffolds with the desired shape are effortlessly fabricated, as illustrated in Figure 6.9. Gravimetric analysis revealed a total scaffold porosity of 69 ± 4%, indicating the accessible volume for specific fluids within the scaffold. This rapid, solvent-free approach holds tremendous promise for efficient scaffold production in tissue engineering applications [5].

6.3.4. Self-assembling technology

The utilization of hydrogel scaffolds combined with dental stem cell lines and peptide-amphiphiles represents a significant advancement in tissue engineering for dental tissue regeneration. By incorporating specific cell adhesion sequences like RGD and enzyme-cleavable sites into the scaffold, cell-matrix interactions are enhanced, thereby promoting the differentiation and proliferation of stem cells. This innovative approach holds promise for regenerating dental tissues by initiating novel regenerative processes that go beyond the limitations of traditional inert biomaterials.

Two types of stem cells, human exfoliated deciduous teeth (SHED) and dental pulp stem cells (DPSCs), along with different osteogenic enhancements, were cultured in PA hydrogels for four weeks. The study revealed effective differentiation and proliferation of both cell types within the hydrogel scaffolds. SHED cells exhibited a spindle-shaped morphology, high proliferation rates, and collagen regeneration, contributing to soft tissue formation. DPSCs, on the other hand, displayed a decreased proliferation rate, adopting an osteoblast-like phenotype with expression of osteoblast marker genes and mineral deposits.

The technique enabled the creation of three-dimensional (3D) PA self-assembly configurations of nanofibers and tissues. Due to the favorable physical properties of hydrogels, they can be injected into small and irregular defects, making the approach suitable for engineering both soft and hard mineralized matrices in dental tissue engineering [5].

In another innovative technique, Yang et al. [5] introduced a three-dimensional pellet cultivation method for periodontal ligament stem cells (PDLSCs), aiming to mimic the biological microenvironment conducive to regeneration. Culturing human PDLSCs with ascorbic acid in a medium derived from growing apical tooth germ cells resulted in the assembly of cells into attaching cell pieces and the generation of single-cell pellets with a substantial extracellular matrix. Implanting PDLSC pellets into immunocompromised mice revealed the establishment of a regularly aligned cementum/PDL-like composite.

These advancements showcase the potential of combining stem cells, hydrogels, and biomimetic environments to enhance the regeneration of dental tissues, opening avenues for future clinical applications in repairing periodontal defects.

6.3.5. Artificial polymer scaffolds

Synthetic polymers have gained prominence in tooth tissue engineering due to their superior mechanical integrity and machinability compared to biological materials. The use of progressively extending biodegradable polymers has been explored extensively in dental repair.

In one of the earliest examples, Young et al. dissociated cells from tooth tissues and seeded them onto biodegradable polyglycolate/poly-L-lactate (PGA/PLLA). This pioneering work provided molecular evidence that the bioengineering of tooth crowns using PGA fleece mimics the natural growth of teeth. PGA fleece emerged as a promising construct for human gingival fibroblasts, and its structural factors were found to significantly influence cell proliferation.

Stem cells from human exfoliated deciduous teeth were seeded into a synthetic open-cell construct made from D, D-L, L-polylactic acid, resulting in the regeneration of pulp tissue scaffolds. In vivo testing in human teeth with a cleaned and shaped root canal showed clear indications of cell

adherence within all investigated pulp constructs, suggesting the viability of implanting tissue-engineered pulp constructs into teeth after cleaning and shaping.

Another study explored the use of a multi-scale computational design to fabricate a scaffold consisting of polycaprolactone (PCL)-poly (glycolic acid) (PGA) for specific cell implementation of genetically modified human cells, generating a human tooth dentin—ligament—bone complex in vivo. The results demonstrated the interfacial production of parallel- and obliquely-oriented fibers, leading to the creation of tooth cementum-like tissue, ligament, and bone assemblies.

A novel technique involved constructing polylactic acid-co-polyglycolic acid (PLGA) scaffolds using CO2 as a solvent, resulting in net-shaped porous scaffolds with high porosity and interconnectivity essential for teeth regeneration. Electrospun composite scaffolds made of PCL/gelatin/nHA supported the proliferation and odontogenic differentiation of dental pulp stem cells (DPSCs). However, the pore size of the electrospun scaffolds was identified as a factor influencing tissue ingrowth.

To accelerate the repair of mandibular defects in the Yucatan mini-pig, tooth-bone hybrid simulation was achieved by combining tooth bud cell-seeded scaffolds with autologous iliac crest bone marrow stem cell-seeded scaffold. The regenerated structures included dentin, enamel, pulp, cementum, periodontal ligament, and alveolar bone, demonstrating the feasibility of regenerating teeth and associated alveolar bone in a single process.

Scaffolds constructed of poly (Et methacrylate-co-hydroxyethyl acrylate) [P(EMA-co-HEA)] with SiO2 and aligned tubular pores resembled natural dentin in structure and properties. These constructs induced apatite precipitation on their surfaces in vitro and were anticipated to facilitate integration into host mineralized tissue, encourage cell growth, and perform well in in vivo dentin rejuvenation.

These advancements highlight the potential of synthetic polymers in driving innovations in tooth tissue engineering for regenerative dentistry [5].

6.4. Challenges in optimizing 3D scaffold for dentin-pulp complex regeneration

Tissue engineering is an interdisciplinary field that involves the integration of cell biology, biotechnology, biomaterials, and biochemical components to create artificial organs and tissues or restore damaged tissues. The ultimate goal is to replicate the dynamic processes of natural tissues, allowing for the repair or replacement of injured or diseased organs. The term "tissue engineering" emerged in the late 1980s, signifying the inception of this innovative approach to regenerative medicine.

The key components of tissue engineering involve seeding cells onto a scaffold, cultivating the structure in vitro until maturity, and subsequently transplanting it into the body. This process leverages the natural tissue regeneration mechanisms, with blood vessels infiltrating the structure during angiogenesis. The scaffold, often made from synthetic biodegradable materials, eventually degrades, leaving behind newly regenerated tissue at the implantation site.

Understanding and replicating the dynamic processes of tissues are crucial for successful tissue engineering. Synthetic biodegradable materials, referred to as scaffolds, play a pivotal role by providing a three-dimensional environment for cell growth. These scaffolds can be designed to mimic the in vivo environment, promoting cell differentiation into the desired tissue types. The integration of growth factors and biopolymers further enhances the functionality of tissue engineering constructs.

In the past two decades, tissue engineering has witnessed significant advancements. These include the development of biodegradable scaffolds, the incorporation of cells and biopolymers to create complex tissue constructs, the use of bioreactors to provide developmentally relevant signals to cultured tissues, and the characterization and isolation of adult and embryonic stem cells. Clinically, notable progress has been made in the replacement of skin and cartilage, which are relatively simpler tissues to engineer.

Despite these successes, challenges persist in the field of tissue engineering. Ongoing research aims to overcome obstacles and further refine techniques, leading to broader applications in regenerative medicine. Continued advancements are anticipated to expand the scope of tissue

engineering, offering innovative solutions for the repair and replacement of diverse tissues and organs [6].

6.4.1. Introduction

The text discusses the importance of maintaining the integrity of dental enamel and dentin for both functional and aesthetic reasons. Damage to these structures exposes the dentin-pulp complex to various injuries caused by microbial, traumatic, and iatrogenic factors. Specific endodontic therapy is required in cases of intense pulp damage, involving the removal of pulp tissue and the filling of the root canal to promote physiological apexification.

The traditional endodontic procedure interrupts physiological apexification, raising the need for tissue regeneration strategies as promising alternatives. The text explores cell-free therapy, which involves using biomaterials with signaling agents for guided tissue regeneration. This approach is particularly relevant for compromised teeth with incomplete root formation, as the healthy apical papilla contains stem cells.

The focus then shifts to the development of scaffolds with nanofiber topography using the electrospinning technique. These nanofiber scaffolds mimic the structural and functional nanomorphology of the extracellular matrix, enhancing cell adhesion and tissue synthesis. The text emphasizes the significance of nanofiber arrangement, such as random or aligned disposition, in influencing cell migration and metabolism.

The association of biomaterials with chemotactic agents, particularly fibronectin (FN), is highlighted for guided pulp tissue regeneration. The study aims to develop FN-loaded nanofiber scaffolds with variable morphology and assess their bioactive and chemotactic potential on human apical papilla cells (hAPCs) using a specific in vitro model.

In summary, the text underscores the importance of tissue regeneration strategies in endodontics, focusing on cell-free therapy, nanofiber scaffolds, and the use of chemotactic agents like fibronectin to enhance the regenerative potential of dental tissues [7].

6.4.2. Materials and Methods

This study involved obtaining apical papilla cells (hAPCs) from four third molars with incomplete root formation, sourced from donors aged 16–18 years, of both sexes. The primary culture of hAPCs was established using the enzymatic digestion technique. Ethical approval was obtained, and informed consent was provided by the patients and their guardians.

A pool of hAPCs was created by combining cells from all apical papillae after passage 1. This pool was then expanded until passage 3 in culture, utilizing complete alpha minimum essential medium (α-MEM) supplemented with fetal bovine serum and antibiotic/antifungal agents. The cells were characterized for the presence of a subpopulation of stem cells from apical papilla (SCAPs) by evaluating the expression of multipotent stem cell markers (Nanog, Oct-3/4, CD-146, STRO-1, and CD-44) through immunofluorescence analysis. The cells at passage 3–6 were utilized for all subsequent laboratory experiments.

Experimental nanofiber scaffolds were synthesized using solutions of 10%, 12.5%, and 15% polycaprolactone (PCL) prepared in chloroform/dimethylformamide through the electrospinning technique. The solutions were injected through needles in an electric field, with positive and negative poles fixed to the needle tip and aluminum metal collector, respectively. The resulting nanofiber scaffolds were categorized as random (NR) or aligned (NA) based on the type of collector used.

The established groups were NR-10%PCL, NA-10%PCL, NR-12.5%PCL, NA-12.5%PCL, NR-15%PCL, and NA-15%PCL. Morphological characterization was performed using scanning electron microscopy to assess nanofiber diameters and interfibrillar spaces. For biological evaluation, the scaffolds were placed in wells, sterilized, and subjected to a disinfection/washing protocol. Human apical papilla cells (hAPCs) were seeded on the scaffolds, and viability, proliferation, adhesion, and spreading were analyzed at 1, 3, and 7 days of incubation. Control groups with cells seeded on round glass coverslips were included for comparison. The experiments were conducted with specific sample sizes (n) for each analysis.

In this part of the study, the groups NR-10% PCL and NA-10% PCL were selected for association with different concentrations of fibronectin (FN). The following groups were formed:

1. SC-NR
2. SC-NA
3. SC-NR + 5FN
4. SC-NA + 5FN
5. SC-NR + 10FN
6. SC-NA + 10FN

To confirm the adsorption of FN into the nanofiber scaffolds, an immunofluorescence assay was performed after incubating the scaffolds for 7 days at 37°C. The bioactive potential of the FN-loaded scaffolds was then evaluated, including cell migration analysis, viability, proliferation, adhesion, spreading, total collagen synthesis, type I collagen synthesis, and gene expression analysis of specific genes.

The experimental design involved specific procedures, such as centrifugation, washing, fixation, immunofluorescence staining, seeding of human apical papilla cells (hAPCs), and various assays for evaluating cellular and molecular responses. The experiments were conducted with specific sample sizes (n) for each analysis.

In this phase of the study, nanofiber scaffolds (NR-10% PCL and NA-10% PCL) were associated with different concentrations of fibronectin (FN), forming six groups (SC-NR, SC-NA, SC-NR + 5FN, SC-NA + 5FN, SC-NR + 10FN, SC-NA + 10FN). The adsorption of FN into the scaffolds was confirmed through an immunofluorescence assay conducted after a 7-day incubation period at 37°C.

The bioactive potential of the FN-loaded scaffolds was then systematically assessed, encompassing multiple aspects:

1. Cell Migration Analysis: The capacity of cells to migrate towards the scaffolds was qualitatively and quantitatively analyzed.
2. Viability, Proliferation, Adhesion, and Spreading: Various assays were conducted at different time intervals (1, 3, and 7 days) to assess the viability, proliferation, adhesion, and spreading of human apical papilla cells (hAPCs) on the scaffolds.
3. Total Collagen Synthesis and Type I Collagen Synthesis: The synthesis of total collagen and type I collagen was evaluated, providing insights into the extracellular matrix production.
4. Gene Expression Analysis: The gene expression of specific genes (GAPDH, ITGA5, ITGAV, COL1A1, COL3A1) was determined through real-time polymerase chain reaction (PCR) assays, shedding light on molecular responses.

The experimental design included meticulous procedures such as centrifugation, washing, fixation, immunofluorescence staining, and seeding of hAPCs. The study employed specific sample sizes (n) for each analysis, ensuring robustness and reliability in the obtained results. The multifaceted evaluation aimed to comprehensively understand the biological responses to FN-loaded nanofiber scaffolds (Figure 6.10.).

After washing the specimens with PBS, they were transferred to new glass slides for analysis under a fluorescence microscope (Leica DM 5500B). For quantitative analysis, four images were chosen from each group for measuring the distance (μm) covered by cells inside the SC-TB (scaffold-cell transwell insert).

The methodology involved the following steps:

1. Image Selection: Four images were selected from each experimental group.
2. Measurement of Cell Migration: Three standardized fields were chosen within each image for analysis. A specific tool in the ImageJ software was employed to measure the migration distance of human apical papilla cells (hAPCs).
3. Quantitative Assessment: The values obtained from the migration analysis were considered as an experimental unit. The sample size for this analysis was 12 per group.

This systematic approach aimed to quantitatively evaluate the migration of hAPCs inside the scaffold-cell transwell insert, providing insights into the chemotactic potential and effectiveness of the nanofiber scaffolds associated with fibronectin.

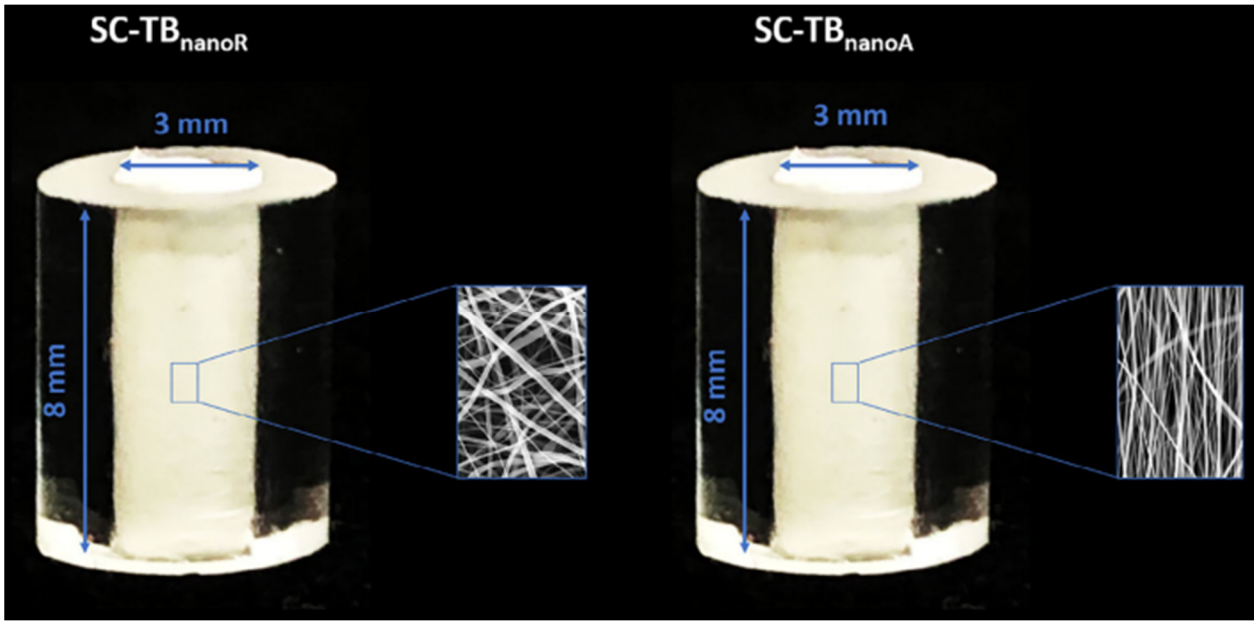


Figure 6.10. Representative images of SC-TB$_{nanoR}$ and SC-TB$_{nanoA}$ inserted in cylindrical device that simulated in vitro regenerative therapy of teeth with incomplete root formation [7].

6.4.3. Results

The preliminary immunofluorescence analysis conducted in this study revealed positive staining for several multipotent stem cell markers in primary cells obtained from the apical papilla. The markers included Nanog, Oct-3/4, CD-146, STRO-1, and CD-44 (Figure 6.11.). Green fluorescence (FITC) indicated positive staining for these markers, while blue fluorescence represented the cell nucleus (Hoescht). The cells incubated only with IgG-FITC served as a negative control for this analysis.

The positive staining for these multipotent stem cell markers suggests the presence of a subpopulation of stem cells from the apical papilla (SCAPs) in the primary culture used for subsequent experiments. This characterization provides a basis for understanding the cellular composition and potential regenerative capacity of the primary cell culture.

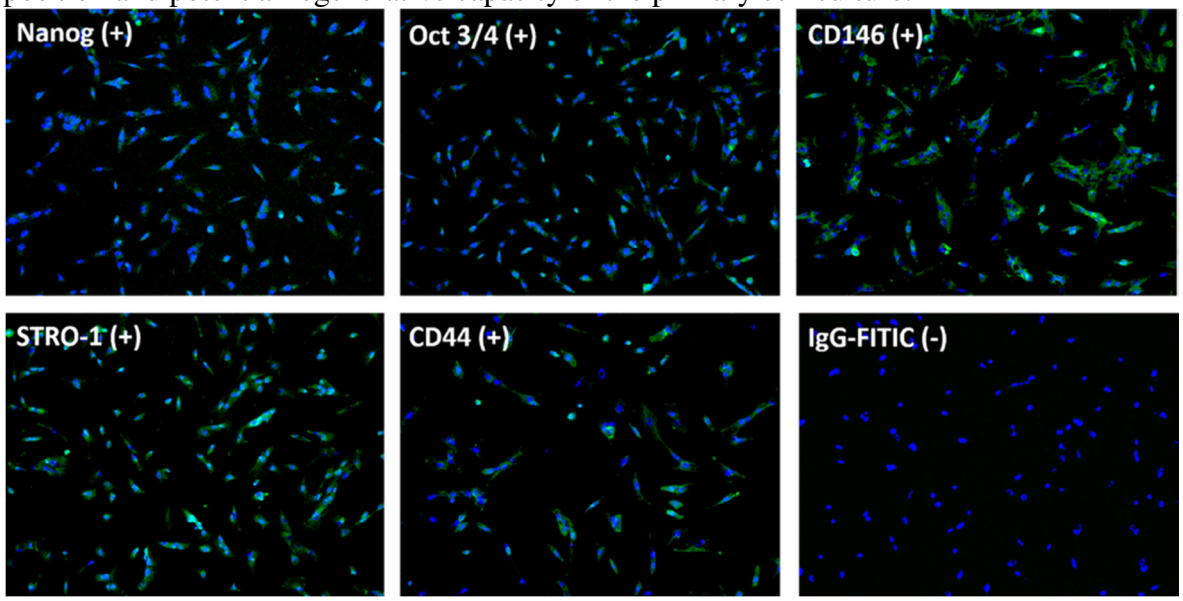


Figure 6.11. Immunofluorescence staining for multipotent stem cells markers (10× magnification). Green fluorescence (FITC) indicated positive staining for Nanog, Oct-3/4, CD-146, STRO-1, and CD-44. Blue fluorescence indicated cell nucleus (Hoescht). Cells incubated only with IgG-FITC represented negative control of this analysis [7].

The fabrication of nanofiber scaffolds was achieved using a flat static collector for random nanofibers (Groups NR-10%PCL, NR-12.5%PCL, NR-15%PCL) and a cylindrical rotary collector for aligned nanofibers (Groups NA-10%PCL, NA-12.5%PCL, NA-15%PCL). The concentration of PCL influenced the scaffold morphology, with higher concentrations resulting in thicker nanofibers and smaller interfibrillar spaces (Figure 6.12).

- Morphological Characteristics:
  - Random nanofiber scaffolds (NR) had thicker nanofibers and smaller interfibrillar spaces.
  - Aligned nanofiber scaffolds (NA) exhibited a more organized structure.
- Cellular Response:
  - Live/Dead assay images demonstrated cytocompatibility for all nanofiber scaffold formulations.
  - Enhanced cell viability was observed in NR-10%PCL and NA-10%PCL groups at 3 and 7-day periods.
  - Cell proliferation increased for all groups over time.
  - NR-10%PCL, NA-10%PCL, and NA-12.5%PCL maintained higher cell viability at 7 days.
  - Cells on random or aligned 10% PCL nanofiber scaffolds showed increased adhesion and spreading.
  - Architecture of nanofibers influenced cell morphology, with more elongated cells on aligned scaffolds and polygonal cells on random scaffolds.

These findings indicate that the nanofiber scaffold formulations, especially NR-10%PCL and NA-10%PCL, exhibit favorable characteristics for cellular responses such as viability, proliferation, adhesion, and spreading. The influence of scaffold morphology on cell behavior underscores the importance of design considerations in tissue engineering applications (Figure 6.13 and 6.14).

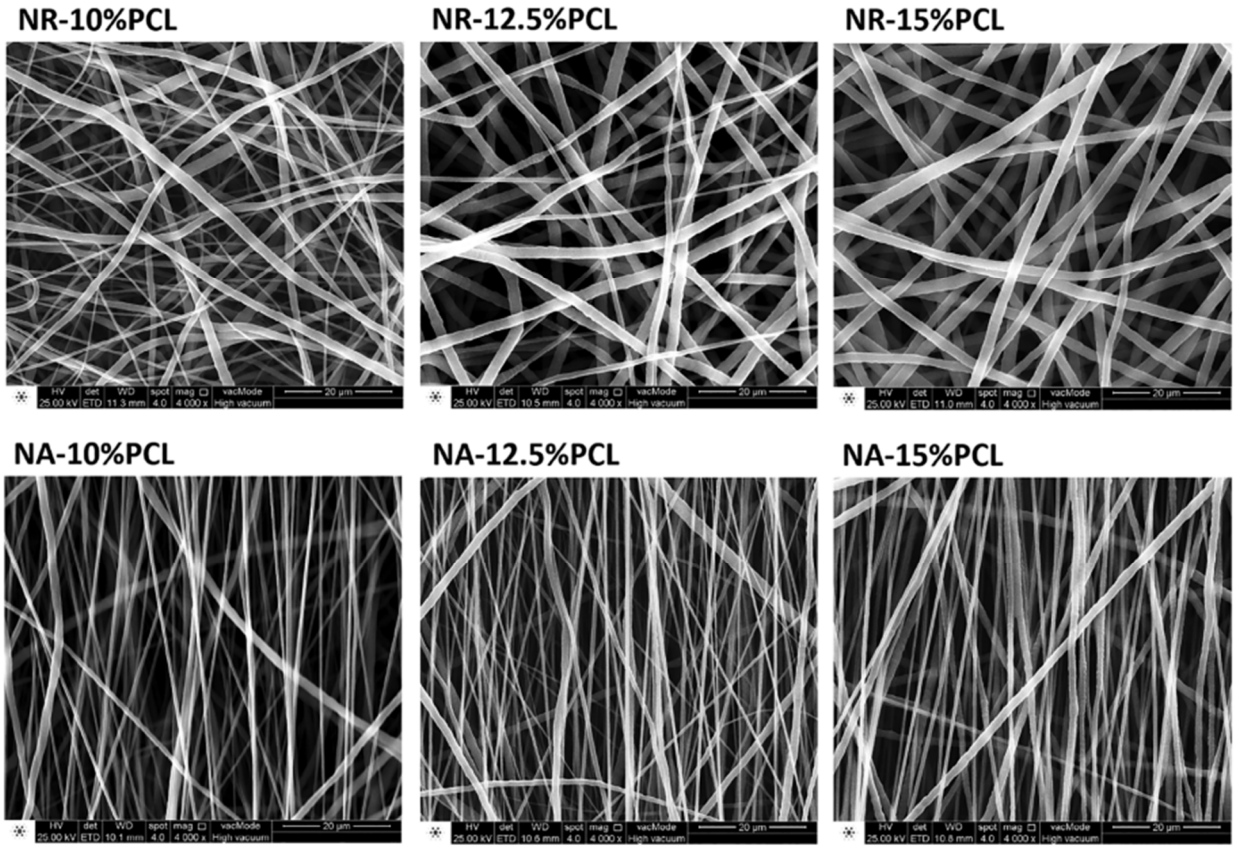


Figure 6.12. Scanning electron microscopy images of nanofiber scaffolds according to parameters tested (4000× magnification) [7].

The immunofluorescence images in Figure 7 indicate that the adsorption of FN onto nanofibers is concentration-dependent. This adsorption pattern influences the bioactive potential of the nanofiber scaffolds, with the highest chemotactic potential observed in groups SC-NR + 10FN and SC-NA + 10FN ($p < 0.05$; Figure 6.15.a). The Transwell assay images (Figure 6.15.b) confirm that cells seeded on the upper surface migrated to the lower surface, reaching the FN-loaded scaffolds below (Figure 6.16).

- Chemotactic Potential:
  - FN adsorption on nanofibers is concentration-dependent.
  - Highest chemotactic potential observed in SC-NR + 10FN and SC-NA + 10FN groups.
- Transwell Assay:
  - Cells migrated from the upper surface of the insert to the lower surface, reaching FN-loaded scaffolds.

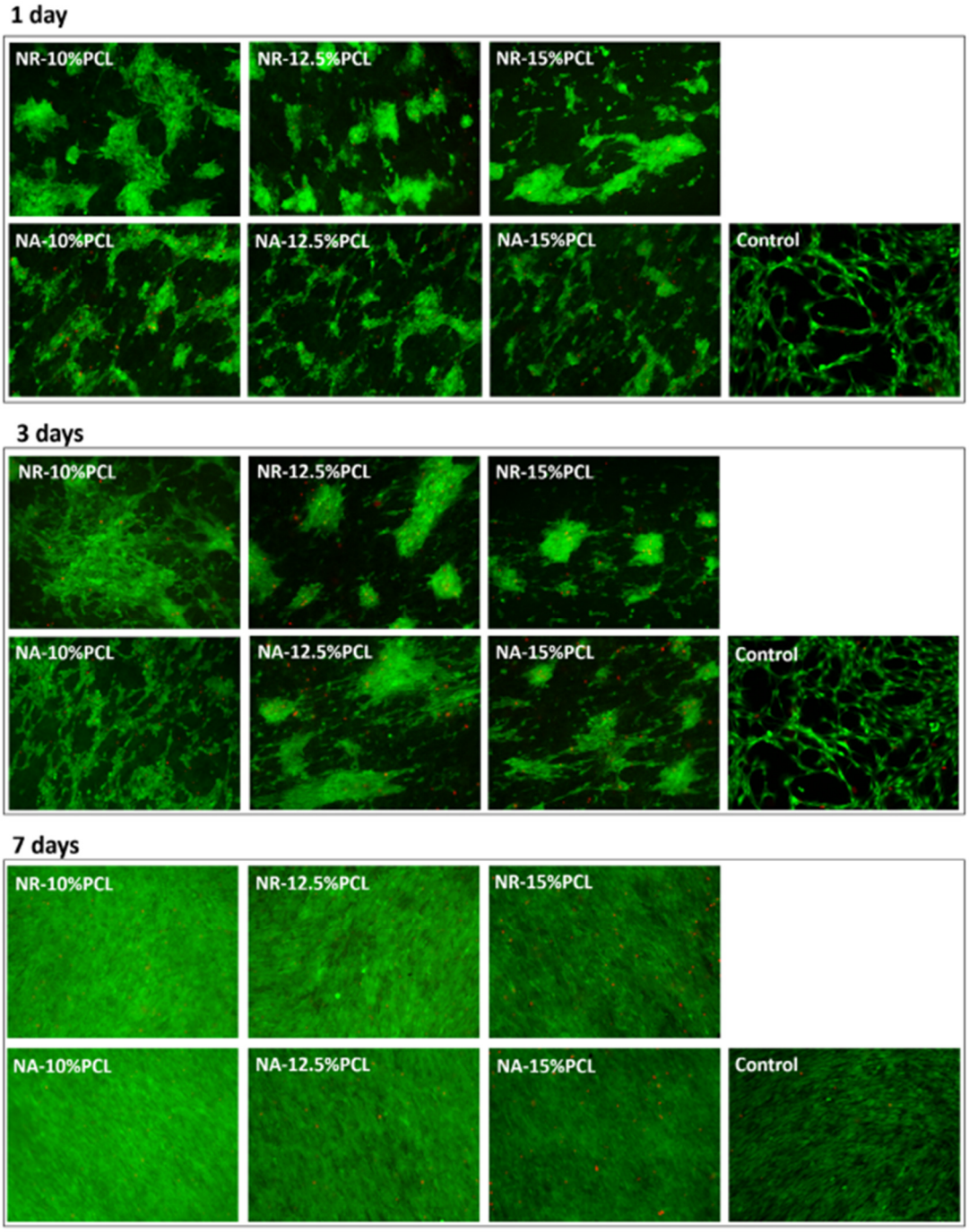


Figure 6.13. Cell viability on different formulations of nanofiber scaffolds (10× magnification). Green fluorescence indicated live cells. Red fluorescence indicated dead cells [7].

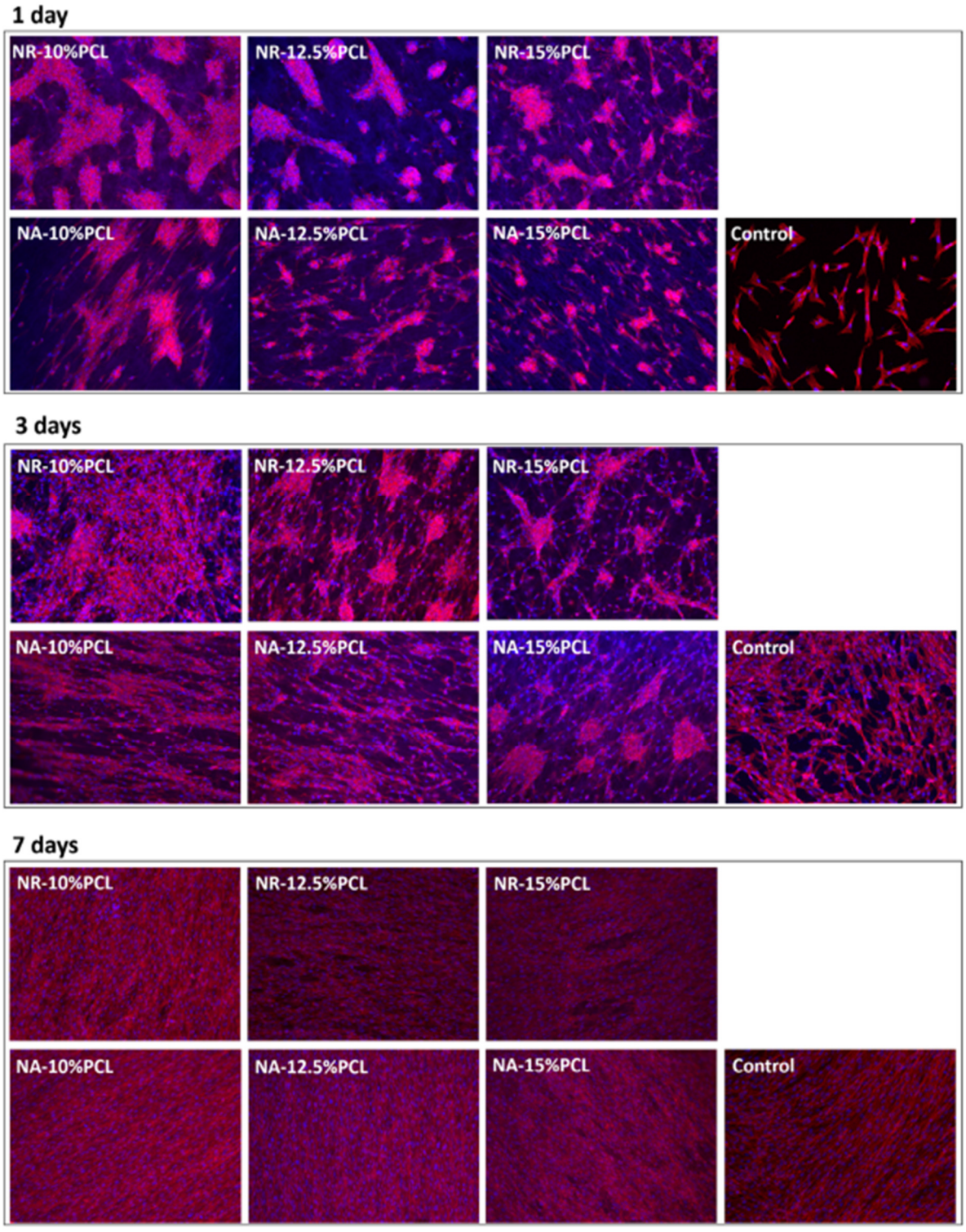


Figure 6.14. Cell adhesion and spreading on different formulations of nanofiber scaffolds (10× magnification). Red and blue fluorescence indicated actin filaments and cell nucleus, respectively [7].

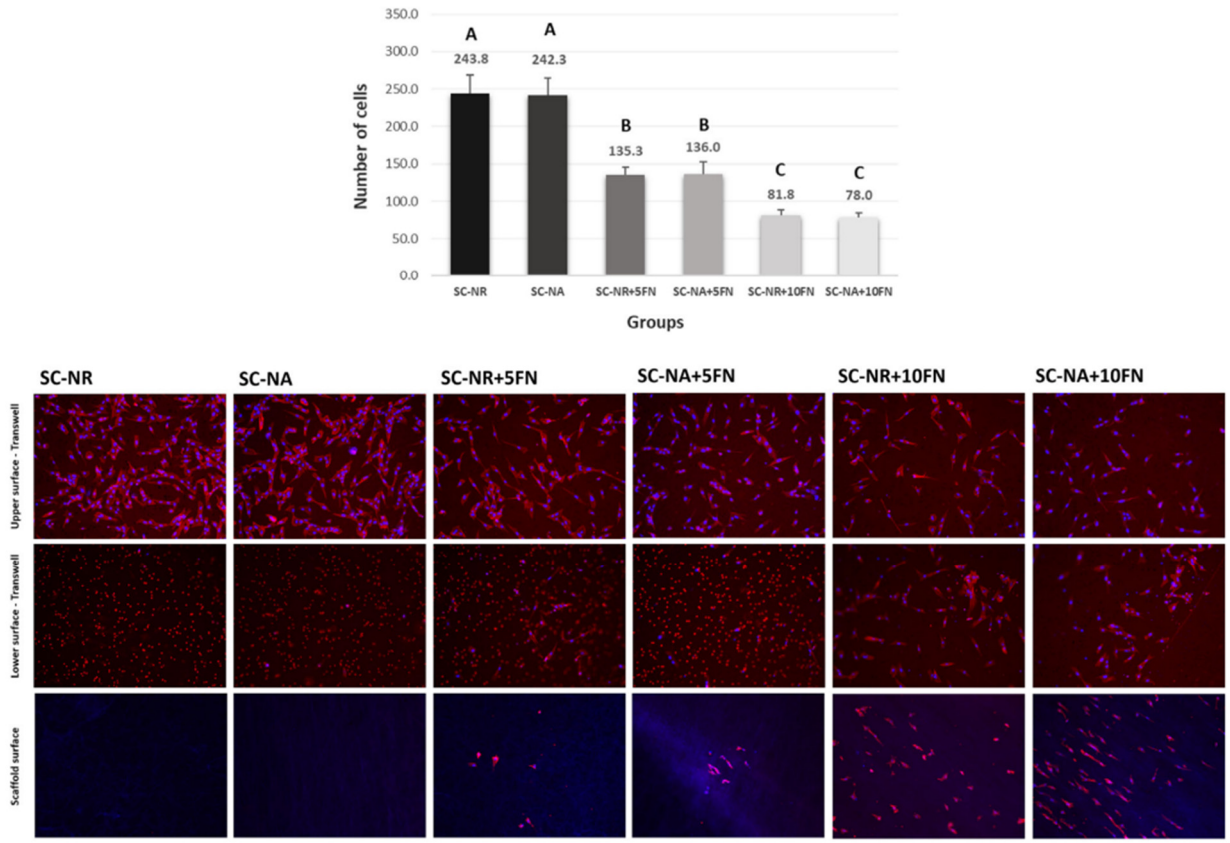


Figure 6.15. Active cell migration assay. (a) Mean and SD of number of cells on upper surface of transwell inserts according to group (n = 4; one-way ANOVA/Tukey tests; α = 0.05). Different capital letters demonstrated significant difference between groups. (b) Images of upper and lower surface of transwell inserts and scaffold surface of each group (10× magnification). Red fluorescence indicated cytoskeleton of cells. Blue fluorescence indicated cell nucleus [7].

- Cellular Responses:
  - Increased FN incorporation improved cell viability, proliferation, adhesion, spreading, total collagen, and type I collagen synthesis.
  - Nanofiber topography influenced only the morphological pattern of hAPCs.
- Gene Expression:
  - Higher expression of ITGA5, ITGAV, COL1A1, and COL3A1 observed in SC-NR + 10FN and SC-NA + 10FN groups compared to control.

These findings demonstrate that FN adsorption onto nanofiber scaffolds enhances their bioactive potential, promoting cellular responses such as chemotaxis, viability, proliferation, adhesion, spreading, and collagen synthesis. The topography of nanofibers influences the morphological pattern of cells, while FN concentration plays a crucial role in achieving optimal bioactivity. Additionally, increased gene expression in specific markers suggests a positive impact on cellular functions.

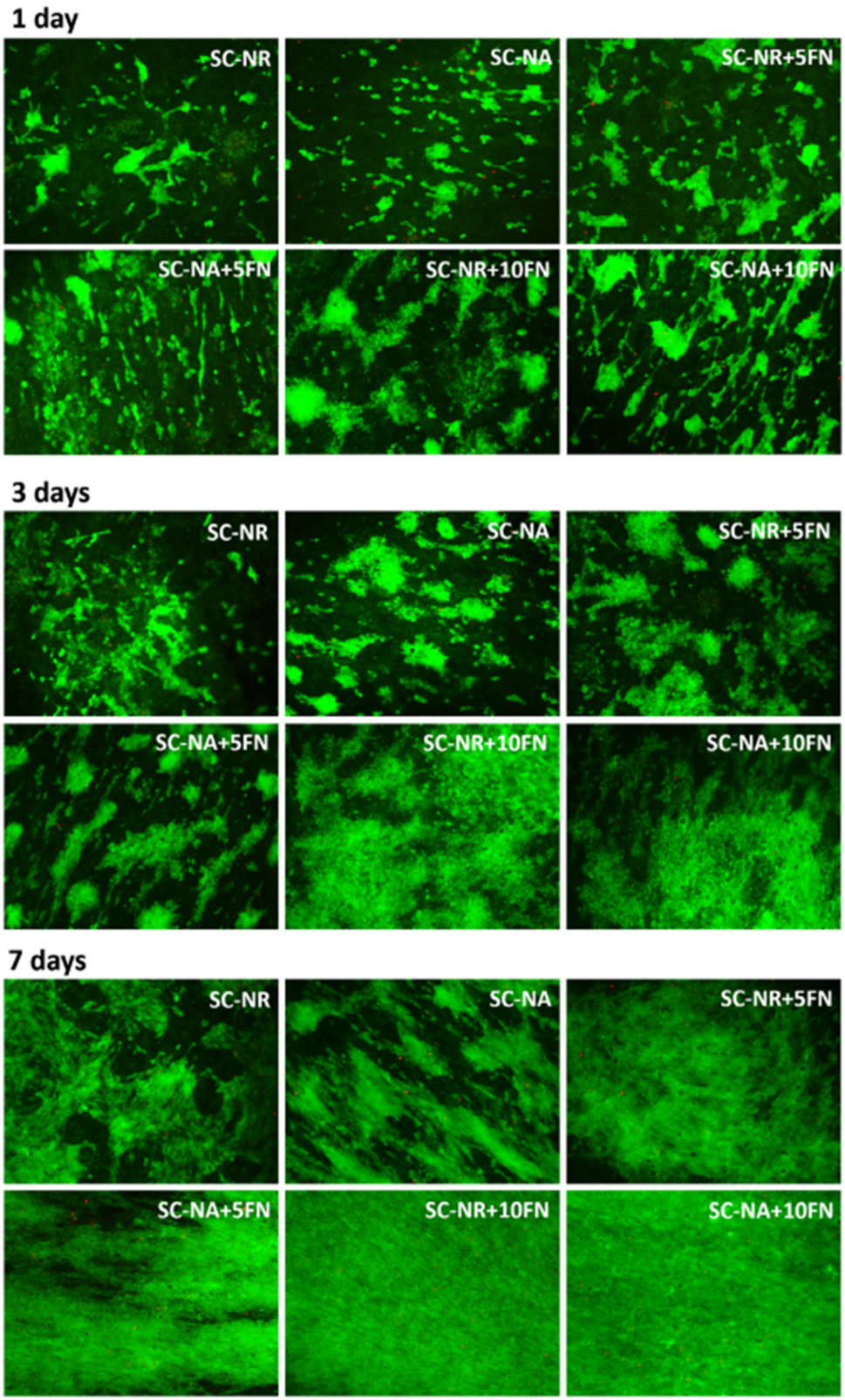


Figure 6.16. Cell viability on nanofiber scaffolds either associated with fibronectin, or not (10× magnification). Green and red fluorescence indicated live and dead cells [7].

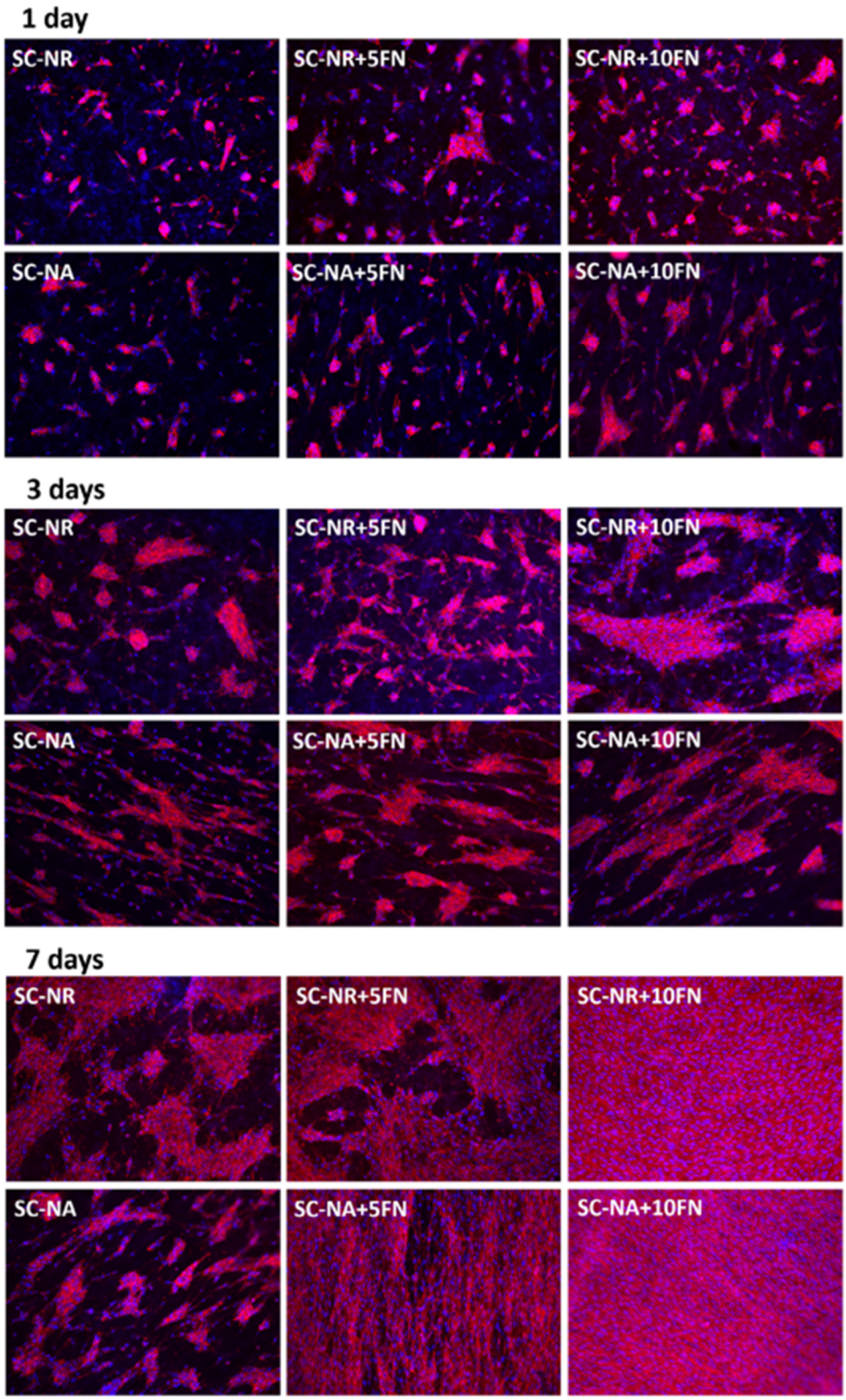


Figure 6.17. Cell adhesion and spreading on nanofiber scaffolds either associated with fibronectin, or not (10× magnification). Red and blue fluorescence indicated Actin filaments and cell nucleus, respectively [7].

6.4.4. Discussions

The study's key findings are as follows:

- Cellular Responses:
  - Increased fibronectin (FN) incorporation positively impacted:
    - Cell viability
    - Proliferation

- Adhesion
- Spreading
- Total collagen synthesis
- Type I collagen synthesis

- Nanofiber topography influenced only the morphological pattern of human apical papilla cells (hAPCs).

- Gene Expression:
  - Higher expression of specific genes (ITGA5, ITGAV, COL1A1, and COL3A1) was observed in groups with FN (SC-NR + 10FN and SC-NA + 10FN) compared to the control group.

This study demonstrates that incorporating FN onto nanofiber scaffolds enhances their bioactive potential, leading to favorable cellular responses, including improved cell behavior, increased collagen synthesis, and specific gene upregulation. The study emphasizes the significance of FN concentration in achieving optimal bioactivity. The topography of nanofibers primarily influences the morphological patterns of cells. These findings contribute to our understanding of the potential applications of FN-loaded nanofiber scaffolds in tissue engineering and regenerative medicine.

The study investigated the impact of fibronectin (FN)-loaded nanofiber scaffolds on human apical papilla cells (hAPCs) in the context of dental pulp regeneration. Key findings and discussions include:

1. Cellular Responses:
   - FN incorporation influenced cell behavior, enhancing:
     - Viability
     - Proliferation
     - Adhesion
     - Spreading
     - Total collagen and type I collagen synthesis
2. Gene Expression:
   - Higher expression of ITGA5 and ITGAV (α5 and αV integrins) was observed in FN-loaded groups (SC-NR + 10FN and SC-NA + 10FN).
   - Increased expression of COL1A1 and COL3A1 (type I and type III collagen) suggested FN's role in promoting collagen synthesis.
3. Mechanisms of Action:
   - FN likely influences cell cycle progression, positively regulating cyclin-dependent kinases.
   - FN was associated with increased cell proliferation, possibly through integrin-mediated pathways.
   - FN-loaded scaffolds promoted the synthesis of a new matrix, evidenced by increased COL1A1 and COL3A1 expression.
4. Topography Influence:
   - Different topographies (random vs. aligned nanofibers) did not significantly impact gene expression in hAPCs.
   - The plasticity of hAPCs might explain the maintenance of phenotypic expression across diverse topographies.
5. In Vitro Model:
   - The study developed an in vitro model mimicking pulp regeneration in teeth with incomplete root formation.
   - Aligned nanofibers in FN-loaded scaffolds enhanced cell migration, resembling a crucial mechanism for cell proliferation in three-dimensional structures.

The study suggests that FN-loaded nanofiber scaffolds hold promise for promoting dental pulp tissue regeneration, emphasizing the need for further in vivo assessments. The role of FN, coupled with nanofiber topography, demonstrates potential applications in tissue engineering for dental applications (Figure 6.18) [7].

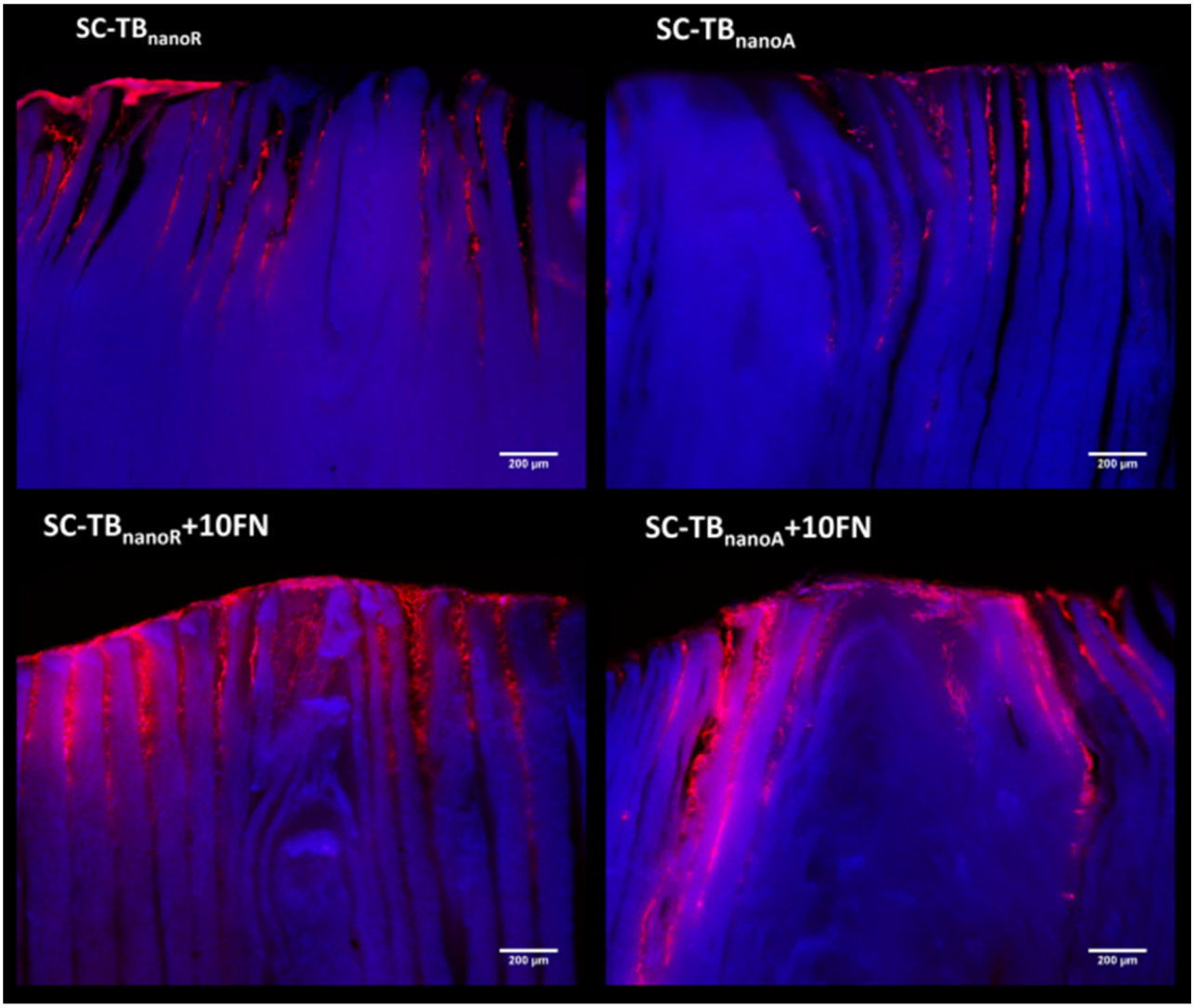


Figure 6.18. Cell migration assay on tubular nanofiber scaffolds. (a) Mean and SD of distance (µm) covered by the cells inside the scaffolds (n = 12; one-way ANOVA/Tukey tests; α = 0.05). Different capital letters demonstrate significant difference among groups. (b) Representative images of the hAPCs migration (5× magnification). Actin filaments of the cells are shown in red fluorescence

6.5. New Challenges and Prospective Applications of Three-Dimensional Bioactive Polymeric Hydrogels in Oral and Craniofacial Tissue Engineering

The scarcity of tissues and organs for transplantation is a pressing global health challenge, with many individuals in need not receiving necessary transplants. Regenerative medicine, often synonymous with tissue engineering, holds promise for repairing and restoring injured organs and tissues, offering potential solutions to address this shortage. This interdisciplinary field encompasses stem cell technologies, tissue engineering, and material science, providing innovative approaches to rejuvenate tissue functionality.

Traditional reliance on donated tissues and organs raises concerns about donor limitations and immunological resistance. Additionally, issues like transplant tourism exacerbate inequalities in healthcare access, highlighting the need to address economic disparities and improve healthcare systems worldwide.

Efforts to enhance techniques and technologies for expanding tissue and organ supplies are crucial. Campaigns promoting organ donation and improving organ utilization aim to increase accessibility to transplants and advance scientific research. Regenerative dentistry and medicine are key components of these efforts, with hydrogels and scaffolds playing vital roles in tissue regeneration.

Hydrogels, with their unique properties and ability to integrate well with surrounding structures, hold promise for enhancing therapeutic approaches to bone tissue creation. Injectable polymeric scaffolds, particularly suited for complex dentofacial tissues, offer advantages such as painless application and adaptability to irregular deformities.

Overall, regenerative dentistry and medicine offer hope for addressing the growing prevalence of debilitating diseases and disorders by providing innovative solutions for tissue regeneration and organ transplantation.

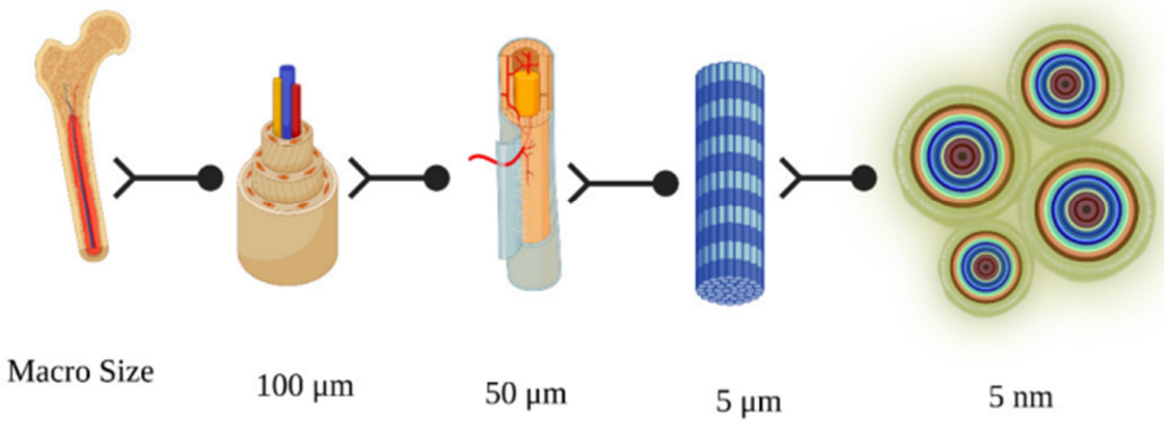


Figure 6.19. Bone macroscopic and microscopic structure.

6.5.1. Bio Scaffolds for Dental and Osseous Tissue Engineering

The biomaterial-dependent tissue engineering approach, which gained prominence in the early 1990s, aims to overcome the limitations of conventional cell implantation therapies. One of the main challenges faced in such therapies is poor retention of implanted cells at the site of injury, leading to limited therapeutic effectiveness. To address this issue, tissue engineers focus on creating grafts that serve as bio-active replacements to promote tissue regeneration, preservation, or enhancement of cellular activity.

However, traditional approaches to tissue engineering have encountered several drawbacks, including inadequate tissue regeneration, insufficient nutrient delivery to cells, and suboptimal elimination of metabolic waste. These challenges highlight the importance of creating an optimal environment to support cell viability and functionality.

In this regard, 3D-designed biomaterials, such as scaffolds, play a crucial role. Scaffolds provide a structural framework that mimics the natural extracellular matrix, offering support for cell adhesion, proliferation, and differentiation. By precisely engineering the properties of scaffolds, such as porosity, surface chemistry, and mechanical strength, tissue engineers can create an environment conducive to cell growth and tissue regeneration.

Overall, the biomaterial-dependent tissue engineering approach represents a promising strategy for developing advanced therapies that can effectively promote tissue regeneration and repair. By harnessing the capabilities of 3D-designed biomaterials, tissue engineers can overcome many of the challenges associated with conventional cell-based therapies and pave the way for innovative treatments in regenerative medicine.

Natural polymers	Polysaccharides; e.g., chitosan, alginate, hyaluronic acid etc. Proteins; e.g., collagen, gelatin, albumin, etc.
Synthetic polymers	Polyglycolic acid, polycaprolactone, etc.
Ceramics	Hydroxyapatite, bio glass, ?-tricalcium phosphates, etc.
Hybrid	Natural polymers with synthetic poly- mers; e.g., chitosan and PLGA(poly(D,L-lactide-co-glycolide)). Natural polymers with ceramics e.g., chitosan and hydroxyapatite Two or more artificial scaffolds e.g., PEG (polyethylene glycol) and PLGA Synthetic polymers with bio ceramic e.g., PLGA with hydroxyapatite
Metals	Gold, silver, titanium, etc.

Figure 6.20. Classification of biomaterials implemented in tissue engineering [8].

Although bone autografts have long been considered the standard approach for bone regeneration, their clinical application is limited due to both scarcity and complications arising from donor sites. Allografts, while more readily available and manageable, may trigger hypersensitivity reactions. Consequently, there is a growing demand for innovative synthetic bone graft materials that can effectively substitute and enhance bone tissue.

Numerous biomaterials, including bioceramics, metals, and polymers, have been investigated for their potential in tissue regeneration strategies, as illustrated in Figure 6.20.

Of particular interest are hydrogels, which offer several advantages in tissue repair. These polymeric structures are composed of cross-linked hydrophilic domains, providing mechanical stability and creating a favorable environment for the natural development of cells.

6.5.2. Pre-Requisites of Hydrogels for Dental and Osseous Regeneration

Hydrogels have garnered widespread popularity in medical applications due to their biocompatibility, biodegradability, resemblance to the extracellular matrix (ECM) architecture, and practical ease of use. With the continuous progress of personalized medicine, there is an increasing need to develop hydrogels for transporting biological substances, eliminating the requirement for open surgery and facilitating a shift towards minimally invasive techniques for biomaterial and cell application. A crucial consideration in this context is the economic feasibility of scaffolds to enable their extensive clinical application. Figure 6.21. illustrates the essential requirements for a tissue engineering scaffold.

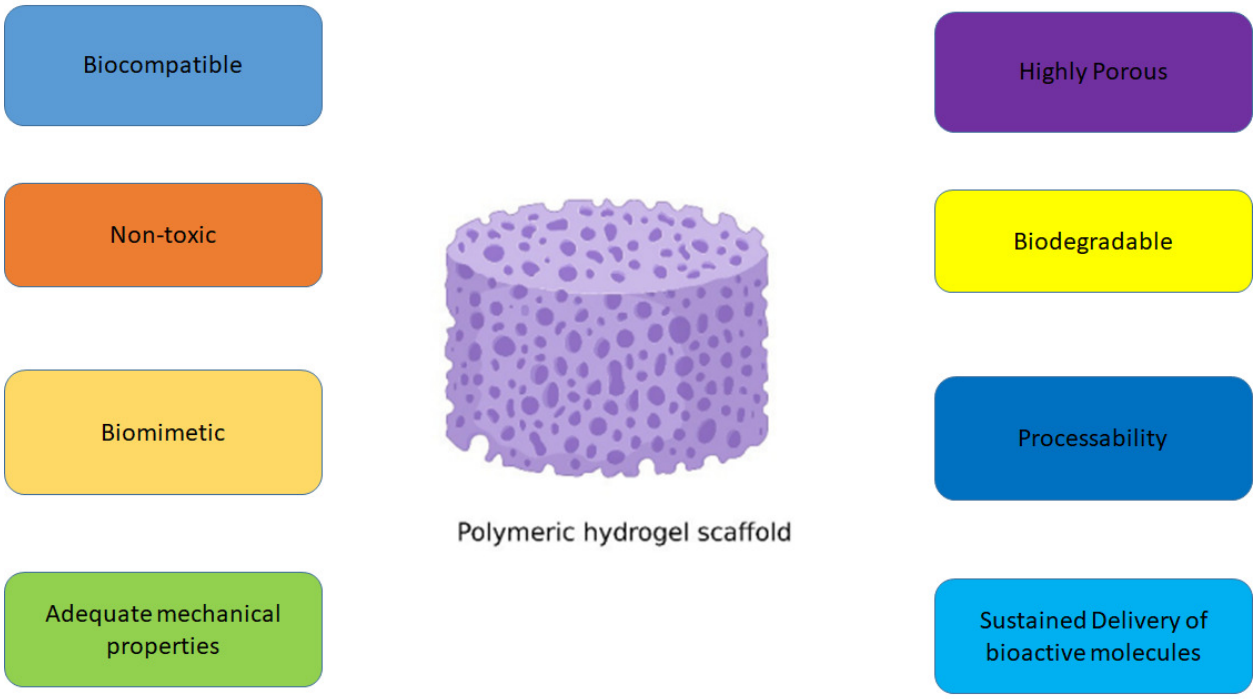


Figure 6.21. Requirement of tissue engineering scaffold [8].

6.5.2.1. Cytotoxicity

Injectable hydrogels must prioritize non-toxicity and gentle solidification conditions both before, during, and after injection. For scaffolds used to encapsulate cells, gelation should occur without harming the cells, and injectable materials should be free from initiators, cross-linkers, or other compounds that could harm cell health. The polymeric process should avoid raising temperatures to levels that could induce thermal damage at the defect site, and scaffolds should not trigger immunological responses.

Naturally derived hydrogels are generally considered safe, although the cross-linking chemicals used may pose some risk. However, cytotoxicity remains a significant concern for synthetic hydrogels [8]. Currently, the Food and Drug Administration (FDA) has only approved PLA (polylactic acid—a biopolymer), PEG, and PLGA for clinical use. Other components involved in the gelation process, such as promoters, chemical agents, stabilizers, and moisturizing ingredients, may exhibit cytotoxicity if not properly removed or if they penetrate tissues or trapped cells.

6.5.2.2. Biological Responses

The host's reaction to a scaffold is crucial, requiring that the biomaterial does not trigger a persistent inflammatory response or display severe cytotoxicity. A biocompatible substance should support cell growth and proliferation without causing toxicity or immune reactions. The level of cell attachment to biomaterials is a key indicator of biocompatibility, as it is necessary for cell adhesion and the regulation of various downstream cellular processes.

Natural polymer hydrogels are widely regarded as biocompatible materials due to their structural similarity to the physiological extracellular matrix (ECM) and the retention of cell-adhesion domains during manufacturing. However, caution is warranted when using natural hydrogels sourced from animals in tissue engineering to minimize the risk of cross-infections and inflammatory reactions.

On the other hand, synthetic hydrogels often lack inherent cell attachment sites, necessitating modifications to enhance host response. Incorporating RGD (Arg-Gly-Asp) peptides is beneficial for artificial biomaterials, and additional modifications such as introducing fibronectin sequences like

CD44 and CD168 may be necessary. Furthermore, copolymer hydrogels made from a combination of natural and synthetic polymers have demonstrated improved biocompatibility.

6.5.2.3. Mechanical Characteristics

An essential aspect of biomaterials used as frameworks in tissue engineering is achieving optimal structural integrity. Following processing, hydrogels need to possess appropriate mechanical strength. In-situ gelation becomes crucial to withstand biomechanical loads and offer transient support for cells [32]. The structural integrity of the biomaterial is primarily influenced by the initial stiffness of the polymer subunits, the types of cross-linkers, the density of crosslinking, and shrinkage resulting from the hydrophilic/hydrophobic equilibrium [8]. Injectable hydrogels, owing to their thermodynamic compatibility with water, exhibit durability compared to other scaffolds.

Hydrogels must support cells and withstand mechanical stress, necessitating suitable mechanical properties [8]. Apart from crosslinking density, permeability, and hydrogel composition, hydrogel structure, quantity, and manufacturing process also significantly affect mechanical properties [8]. Increasing material porosity and crosslinking density can enhance mechanical properties, but this might compromise cellular response and degradability [8]. Hence, achieving a balance between the mechanical properties of hydrogels and their degradation capacity is crucial [8].

Incorporating microspheres or bioceramics into the polymer improves the mechanical properties of injectable scaffolds [8]. Rigidity and hardness are two critical mechanical properties of injectable hydrogels. The hydrogel should be sufficiently rigid to form a stable framework for cells and robust enough to protect the framework from premature degradation. Increasing crosslinking intensity enhances hydrogel stiffness and durability, albeit prolonging the degradation period of the scaffold. Therefore, maintaining a delicate balance between structural integrity and degradation is vital for the effective use of hydrogels.

6.5.2.4. Degradation

The materials utilized in constructing hydrogels must undergo gradual degradation to accommodate the formation of newly generated tissues. Ideally, the degradation rate should align with the pace of new tissue synthesis. Hydrogels can degrade through one of three methods: simple dissolution, hydrolysis, or enzymatic cleavage. Hydrogels formed via physical cross-linking lose their structure and dissolve in a solution when environmental factors, such as temperature and pH, fluctuate. Ionic cross-linked hydrogels respond to changes in ion strength in the solution, dissolving as ions leach out of the structure. Simple dissolution doesn't lead to degradation since the hydrogel components remain intact.

The most common mechanism for hydrogel breakdown involves the degradation of labile ester bonds in the matrix core, such as lactide or glycolide fragments in PLGA [8]. The rate of hydrolysis is affected by factors like cross-linker concentration, molecular mass, shape, porosity, and the amount of remaining monomer. Increasing the crosslinking capacity, molecular mass, or hydrophobicity of the polymer tends to decrease the hydrogel's degradation rate. Local cellular activity may also contribute to further breakdown of the polymeric matrix [8]. While various degradation methods exist, it's crucial that the breakdown products of the hydrogel are biocompatible and do not provoke an immune response. Ideally, the degradation of the hydrogel yields naturally biocompatible compounds within the body.

6.5.3. Classification of Hydrogels

Hydrogels represent the most extensively researched scaffolds, and their classification is based on origin, crosslinking methods, polymeric composition, and form. Figure 6.22. illustrates the categorization of hydrogels [8].

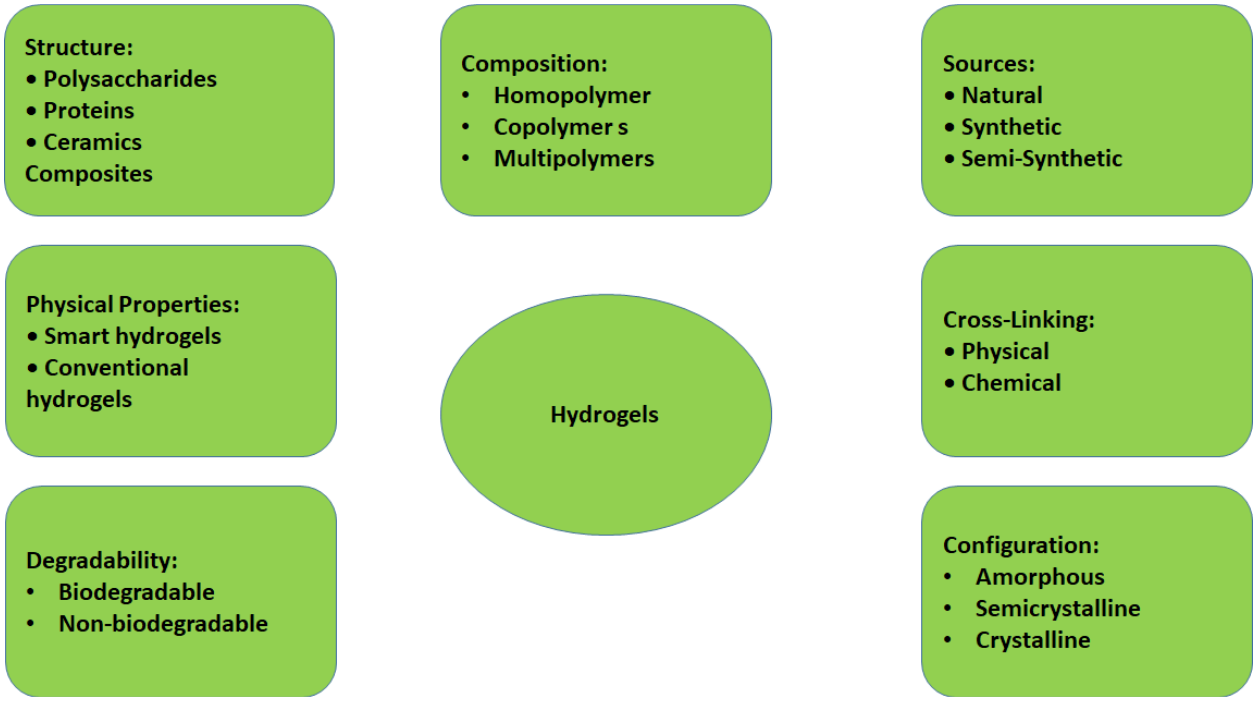


Figure 6.23. Classification of hydrogels [8].

Polymers undergo self-assembly to form physically cross-linked hydrogels when exposed to changes in environmental factors such as temperature and ionic concentration [8]. Unlike chemically cross-linked hydrogels that generate heat during formation at the gelation site, physically cross-linked hydrogels cannot develop under extreme conditions such as radiation, chemical agents, or crosslinking agents. However, it is important to note that physically cross-linked hydrogels are generally less stable than their chemically cross-linked counterparts, as depicted in Figure 6.24.A.

Application	Advantages
Drug delivery	• Improved medication protection and stability • Long-term drug retention and controlled drug release • Responsive medication release in responding to environmental cues such as pH
Detoxification	• Detoxification agent restriction to disease site • Extended accumulation and continuous release of degradable materials
Immune modulation	• unintended consequences • Elimination • Therapeutic and medication doses were regulated; and cargo was released in response to internal and environmental cues.
Tissue engineering	• Excellent physical and mechanical qualities • Localized and regulated medication distribution • Increased bioavailability

Figure 6.24.A. Advantages of polymeric hydrogel for dental and osseous regeneration [8].

6.5.4. Chemical Structure of Polymeric Hydrogels

6.5.4.1. Natural Polymers

The chemical structures of natural polymers are detailed in Figure 6.24.B.

Polysaccharides	Proteins
Alginate	Collagen
Starch	Gelatin
Cellulose	Silk
Chitosan	Fibrin
Cyclodextrin	Albumin
Dextran	
Gum polysaccharides	
Pectin	
Pullulan	
Heparin	
Chondroitin sulfate	

Figure 6.24.B. Classification of natural polymers according to their structure [8].

Polysaccharides

Polysaccharides, as indicated in Figure 6.25., have been considered less influential in controlling cellular and tissue functions compared to peptides and even lipids [8].

Plants	Mucilage, Pectin, Hemicellulose, Gums Cellulose, Glucomannan, Starch
Algae	carrageenans, alginates
Animals	cellulose, glycosaminoglycans, hyaluronic acid, chitosan, Chitin
Bacteria	cellulose, Dextran
Fungal	yeast glucans, chitosan, chitin, pollulan, Elsinan

Figure 6.25. Classification of polysaccharides according to their origin [8].

Chitosan

Chitosan, derived from chitin through deacetylation, stands out as one of the most extensively used polysaccharides in tissue regeneration. Its popularity is attributed to its remarkable bioactivity, processability, biocompatibility, and controlled degradation by enzymes. Chitosan exhibits solubility exclusively in acidic solutions, undergoing a sol-gel transition as the pH shifts from acidic to neutral. Notably, it possesses bioadhesive properties, establishing a temporary strong connection between epithelial cells [8]. Additionally, chitosan demonstrates potent antimicrobial activity against various pathogens.

In a study by Xu et al. [8], an injectable and thermo-responsive hydrogel comprising chitosan/β-sodium glycerophosphate (β-GP)/gelatin was developed. This hydrogel showcased anti-inflammatory properties, bone regenerative capacity, and promoted periodontal regeneration. Another study by Yan et al. [8] suggested the creation and testing of an enzymatically hardened chitosan hydrogel for repairing intrabony periodontal abnormalities. These hydrogels exhibited robust biodegradability and biocompatibility.

Alginate

Alginate, derived from brown algae, consists of repeated components dispersed widely in the cell walls. Its content, sequencing, and molecular mass can vary depending on the source. Alginate's ability to form hydrogels through ionic crosslinking makes it biocompatible and non-immunogenic. However, it comes with drawbacks such as low cell attachment, poor mechanical strength, and a slow degradation rate. Therefore, modifications are often necessary to achieve desired characteristics. For instance, the incorporation of RGD or laminin into alginate has been shown to enhance cell adherence, viability, and multiplication [8].

In a study by Diniz et al. [8], injectable oxidized alginate microbeads were developed, encapsulating periodontal ligament and gingival mesenchymal stem cells. For endodontics regeneration, Devillard et al. [8] created collagen/alginate-based stem cell composite frameworks. Addressing peri-implantitis, a significant concern in dental implantology, RGD-alginate hydrogel

incorporating stem cells demonstrated effective antibacterial capabilities against Aggregatibacter actinomycetemcomitans [8].

Dobie et al. [8] explored the use of alginate hydrogels to deliver TGF-β1 to the dentin pulp complex, aiming to promote reparative procedures. Alginate hydrogels treated human tissue cultures, initiating the upregulation of dentin matrix secretion. On cut pulpal surfaces, the hydrogels induced odontoblast-like cell development. Alginate hydrogels thus serve as suitable templates to facilitate dental regeneration and distribute growth factors to enhance the dental pulp's intrinsic regenerative capacity.

Hyaluronic acid

Hyaluronic acid, a naturally occurring polysaccharide in the body, is known for its high apparent viscosity, allowing it to be administered via injections and form a gel within the body [8]. The enzyme hyaluronidase can degrade hyaluronic acid into smaller molecular weight molecules. In the context of dental pulp stem cell (DPSC) growth, 2-aminoethyl methacrylate (AEMA)-modified hyaluronic acid (HA) (AEMA-HA) hydrogels replicate the in vivo 3D environment. Consequently, with further optimization in the future, these hydrogels hold significant promise for clinical use in regenerative medicine and various therapeutic applications [8].

Cellulose

Cellulose, typically a linear polysaccharide molecule, is notable for its low cost and renewable nature, being the most abundant natural polysaccharide. It is regarded as one of the least harmful materials on Earth, offering advantages such as bioactivity, degradability, recyclability, dimensional stability, and non-toxicity [8]. While cellulose is an excellent starting material, its utility is limited due to challenges in dissolving. Nevertheless, its intriguing biological activities make cellulose and its derivatives commonly employed in biological applications [8].

In a study by B. Li et al., simvastatin was incorporated into TiO2 nanotubes, and a thermo-responsive chitosan-glycerin-hydroxypropyl methylcellulose hydrogel (CGHH) was overlaid on these nanotubes. These constructs exhibited enhanced osteogenesis capability at normal body temperature and demonstrated antimicrobial characteristics in the presence of infection, making them promising materials for practical implementation.

Starch

Starch, a natural and recyclable polysaccharide, possesses a range of characteristics such as safety, nontoxicity, widespread abundance, low cost, cytocompatibility, degradability, and biosafety [8]. Native starch consists of varying proportions of amylose and amylopectin (15–30% and 70–85%, respectively), depending on species, growth conditions, and harvesting processes. The biochemical nature and physical arrangement of starch components significantly influence its diverse applications [8]. Introducing additional subunits to its networks allows starch to acquire new functionalities, expanding its utility [8]. Over the past few decades, modified starches, due to their altered architecture, have been utilized to transport various nanoparticles for therapeutic treatments against diseases [8].

Nonionic starch derivatives, particularly those from hydroxyalkyl starch, exhibit excellent application performance owing to their strong hydrophilicity and viscosity stability. A 3D-printed hydroxyapatite—Zn2+ functionalized starch composite demonstrates enhanced mechanical and biological features, making it suitable as a bone filler in low load-bearing defects, such as craniomaxillofacial bone.

Xyloglucan

Xyloglucan, esteemed for its bioadhesive properties and ability for local gelation, has emerged as a compelling and advantageous biopolymer in drug delivery research [8]. Widely employed in the pharmaceutical industry, xyloglucan has found applications in drug delivery systems, as evidenced by recent publications on xyloglucan-based drug carriers for biomedical purposes, including thermo-

sensitive hydrogel and thermos-reversible hydrogel in situ [8]. This polysaccharide holds significant potential and warrants further investigation in academic research.

Injectable xyloglucan hydrogels have demonstrated effective utility in bone and cartilage regeneration [8]. A mucoadhesive hydrogel composed of methylcellulose/xyloglucan exhibits suitable syringeability for ease of administration at 25 °C. In comparison with a commercial preparation, this hydrogel displays a more sustained release of Metronidazole (MTZ). As a result, the in-situ distribution of MTZ for the treatment of periodontitis can be achieved using the methylcellulose/xyloglucan hydrogel.

Cyclodextrin

Cyclodextrins (CDs), cyclic oligosaccharides discovered in 1903 by Franz Scharfing using a bacterial decomposition of starch [8], have been utilized in dental tissue regeneration due to their excellent biocompatibility and lack of bio toxicity.

Dextran

Dextran, a polysaccharide synthesized by bacterial strains and readily accessible, has seen extensive application in medicine and pharmacy owing to its degradability, biocompatibility, lack of immunogenicity, and absence of antigenic properties [8]. Scaffolds comprising glycidyl methacrylated dextran (Dex-GMA) and gelatin, with microspheres loaded with bone morphogenetic proteins, displayed remarkable alkaline phosphatase (ALP) expression, osteocalcin content, and calcium deposition. Histological examination in dogs further demonstrated neo-osteogenesis and periodontal ligament regeneration. Thus, this scaffold holds promise for utilization in periodontal regeneration.

Carrageenan

Carrageenans, sulfated polysaccharides with a large molecular mass isolated from red seaweeds, bear similarities to extracellular matrix-derived glycosaminoglycans. Carrageenan has been shown to exhibit exceptionally low cytotoxicity and no mutagenicity in various investigations [8]. However, concerns about safety have arisen when synthesized in nano complexes. A study found that carrageenan/chitosan nanoparticles at concentrations ranging from 0.1 to 3 mg/mL had no impact on in vitro L929 fibroblasts [8].

The three-dimensional structure of carrageenan promotes osteoblast growth and adherence [8]. When combined with nano hydroxyapatite, it enhances osteoblast activity [8]. Adding carrageenan to scaffolds increases the compressive strength of the hydroxyapatite-collagen hybrid hydrogel [8]. Hybrid carrageenan hydrogels with varying nano hydroxyapatite proportions showed minimal cytotoxicity against human osteoblast cells and potent antimicrobial activity against Pseudomonas aeruginosa. Additionally, treating cells with carrageenan nano gel and whitlockite nanoparticles up-regulated Runt-related transcription factor-2 and osteopontin protein expression [8].

For the treatment of periodontitis, κ-carrageenan oligosaccharide composite hydrogels have been effectively developed, exhibiting antibacterial and anti-inflammatory effects. Consequently, κ-carrageenan emerges as a promising candidate for periodontitis treatment.

Gum

Natural gum polysaccharides exhibit exceptional biological properties, which have led to their extensive use across various applications. They are recognized for their superior effectiveness compared to synthetic and semi-synthetic materials [8]. Research indicates a substantial rise in the utilization of gums in the pharmaceutical industry and tissue engineering. Their popularity as scaffolding material stems from their optimal bioactivity, degradability, and water solubility [8].

Natural Polysaccharide	Delivery System	Outcome
Carrageenan	Nano-HA/gum Arabic/k-carrageenan composite	Without cytotoxicity, osteoblast-like cells exhibit substantial osteogenic signals.
Carrageenan	Ag/carrageenan/gelatin nanocomposite	The unique Ag/carrageenan-gelatin hydrogel's antimicro- bial, drug carriers, and anti- tumor capabilities
54646Ncarboxy-ethyl-chitosanhyaluronic-acid-aldehyde	N-carboxyethyl chitosan/hyaluronic acid-alde-hyde loaded with nano hydroxyapatite	preserving alveolar ridge in-tegrity and facilitating soft tissue healing process
regenerated cellulose (rCL) nanofibers/chitosan (CS)		The rCL/CS scaffold aided bio mineralization and in- creased the survival, adher- ence, and multiplication of preosteoblast cells (MC3T3- E1).
Chitosan/hyaluronic acid	Chitosan nanohydrogel/poly-e-caprolactone (PCL) loaded with nanotriclosan and flurbiprofen	RUNX2, OCN, and OPN gene expression increases. The best results were achieved with 10 wt% and 25 wt% nano pearl.
chitosan	Chitosan nanohydrogel/poly-e-caprolactone (PCL) loaded with nanotriclosan and flurbiprofen	The combination of antimicrobial and antiinflammation properties resulted in a remarkable treatment outcome
Gelatin/Alginate	Gelatin-alginate-graphene oxide nano framework	Amplification of the tran-scription of osteoblast enhancing factors and ALP.
Carrageenan	Carrageenan/whitlockite nano composite hydrogel	Improved osteogenic development and ALP expression
Carrageenan	Carrageenan/nanohydroxyapatite composite scaffold	Enhancement of osteogenic differentiation without the use of pharmacological drugs
Chitosan	Chitosan gold nanoparticles mixed with peroxisome proliferator-activated ligand	Optimizing the outcome of implant placement in diabetic patients (bone development and mineralization)
Alginate/chitosan	Alginate/chitosan loaded with nanohydroxylapatite	Increased hydroxyapatite levels stimulate MC3T3 cell development and calcification.
Alginate	Alginate hydrogel mixed with bovine dental pulp extracellular matrix (PECM)	Accelerated differentiation in the mineralizing environment lead to mineralization at the hydrogel's perimeter. HA hydrogels integrating PL enhanced cell functions and hDPSC mineralized matrix formation.

Hyaluronic acid hydrogel	Photo crosslinking of methacrylated HA incorporated with PL	Accelerated differentiation in the mineralizing environment lead to time-dependent mineral deposition at the hydrogel's perimeter. HA hydrogels integrating PL enhanced cell functions and hDPSC mineralized matrix formation.
Chitosan	Ag-blended bioactive glass micro particles mixed with chitosan (Ag-BG/CS).	Ag-BG/CS enhanced the odontogenic differentiation capability of lipopolysaccharide-increased inflammatory reactivity in dental pulp cells and shown antimicrobial and anti-inflammatory activities.

Figure 6.26. Natural polysaccharides as scaffolds for Dental and craniofacial tissues regeneration [8].

The remarkable properties of natural gums make them well-suited for applications in nanocomposites, including nanoparticles (NPs) and synthetic polymers, to facilitate cellular proliferation [8]. For example, gellan gum hydrogels cross-linked with carbodiimide induce in vitro vacuolation of human tooth-derived stem cells [8]. The utilization of natural polysaccharides as scaffolds for dental and craniofacial tissue regeneration is further depicted in Figure 6.26.

PROTEINS:

Albumin

Albumin, an endogenous, non-glycosylated protein primarily synthesized in the liver, constitutes a significant portion of plasma. It has garnered considerable attention in bioengineering research, with numerous studies delving into its structure and therapeutic properties [8].
Extensive investigations are underway regarding albumin's antimicrobial effects, revealing its role as an anti-attachment peptide that inhibits biofilm formation by enhancing the net negative charge and hydrophilicity of various surfaces [8]. Despite lacking a recognized cell-binding domain, albumin-coated bone-related scaffolds have been shown to facilitate cellular adhesion and proliferation, thus proving to be a valuable addition to scaffolds for enhanced bone regeneration [8].

Due to its flexibility, affordability, and bioactivity, albumin emerges as an attractive biomaterial for biomedical research and treatments. Much of the therapeutic research on albumin has focused on its utility as a carrier protein or nanoparticle to improve drug bioavailability and target site delivery [8]. For instance, chitosan coating on bovine serum albumin (BSA) microparticles loaded with NELL-like molecule 1 (NELL-1) stabilizes the BSA microsphere, enabling controlled release of NELL-1 while maintaining biocompatibility, making it an excellent candidate for osseous tissue regeneration [8].

Recombinant human serum albumin (rHSA) has been engineered to transport sodium benzoate, salicylic acid, and warfarin. The hydrogel formed from rHSA exhibited sustained release of medications with albumin affinities, highlighting its potential as a carrier for prolonged drug delivery [8]. Furthermore, freeze-drying an albumin gel crosslinked with transglutaminase resulted in a scaffold with physical and mechanical properties resembling collagen scaffolds. Successful differentiation of human mesenchymal stem cells (MSCs) into osteoblasts within these scaffolds demonstrated their potential for bone tissue engineering and regenerative therapies [8].

Collagen

Collagen stands out as one of the most commonly used bioactive scaffolds, serving as the primary organic component in various connective tissues, including bone and the periodontal ligament (PDL). Collagen contains motifs, such as Arg-Gly-Asp, recognized by plasma membrane receptors, facilitating cell attachment and subsequent biological responsiveness, rendering it highly biocompatible [8]. Additionally, within the extracellular matrix (ECM), collagen can serve as a reservoir for growth factors. Although self-assembled collagen hydrogels exhibit low biomechanical toughness, crosslinking, often with agents like glutaraldehyde, is employed to enhance their mechanical properties. However, the use of non-biodegradable crosslinkers may affect the hydrogel's degradation behavior and biological control. To address this issue, incorporating degradable elements provides a more favorable approach to adjusting its degradability. Initially utilized as a dermal substitute, collagen gels have become widely adopted in tissue regeneration [8]. A collagen membrane with biphasic calcium phosphate (BCP) showcased superior outcomes, including the inhibition of soft tissue invasion into periodontal defects and remarkable bone regeneration, compared to a hydroxypropylmethyl cellulose (HPMC) membrane with BCP in a canine model after 12 weeks [8]. Choi et al. found that a proanthocyanidins (PAC)-treated collagen gel exhibited increased surface roughness and enhanced periodontal ligament (PDL) cell adhesion [8]. In a canine model addressing class II furcation deficiencies, a collagen hydrogel scaffold injected with fibroblast growth factor-2 (FGF-2) demonstrated the production of cementum-like tissue and PDL-like Sharpey's fibers without ankyloses and root resorption.

Gelatin

Gelatin, a partially hydrolyzed protein derived from collagen, undergoes transformation influenced by factors such as pH, temperature, and duration of harvesting. As a denatured biopolymer, gelatin serves as a scaffolding material, addressing concerns related to immunological and microbial transmission often associated with collagen. It exhibits biocompatibility and biodegradability both in vitro and in vivo. The intrinsic cell-binding characteristics of gelatin, inherited from collagen, play a crucial role in effective biodegradation and cell attachment. Its sol-gel transition at approximately 37 °C, close to physiological conditions, necessitates the use of chemical cross-linkers for stability during in vivo implantation as an injectable biomaterial. Recent research has explored enhancements through chemical modifications, with GelMA (methacrylamide-functionalized gelatin) being one such option, preserving regions crucial for cellular interactions. Studies, such as the one by Zuo et al., have fabricated multi-compartment osteon-like structures with interconnected channels using GelMA hydrogels to mimic the haversian canal in natural bone tissues. In vitro experiments involving human osteosarcoma cells (MG63) and HUVEC cells in various compartments demonstrated the expression of osteogenic and vasculogenic genes [8]. GelMA, particularly in hybrid hydrogels, has been investigated for cartilage tissue engineering. For instance, Klein's team explored cartilage tissue healing using GelMA-hyaluronic acid (HA) scaffolds [8]. Strategies such as incorporating IL-4 into TG gels for enhanced M2 polarization of macrophages (Mφs) and utilizing SDF-1α for cell homing in high-stiffness hydrogels have been explored by Heo et al. to facilitate significant periodontal tissue regeneration.

Fibrinogen

Fibrin gel, formed through the interaction between commercially purified allogenic fibrinogen and thrombin, key proteins in blood clotting, has emerged as a valuable material for a range of applications in tissue engineering. Flanagan et al. discovered that fibrin used as a cell transport material leads to the development of autologous and mechanically robust constructs with significant tissue growth in vivo [8]. Fibrin holds promise for applications as an autologous scaffolding biomaterial in dental engineering or dentistry, enabling the creation of implantable structures. Kretlow et al. conducted research to identify biomaterials conducive to the regeneration of complex tissues, highlighting the suitability of injectable biomaterials, particularly those from aqueous solutions, as optimal carriers for cells and bioactive ingredients in dental tissue engineering [8].

Studies by Rajangam et al. underscored the utility of fibrin (Fbn) and fibrinogen (Fbg) as scaffolds due to their capacity to achieve uniform cell distribution, high cell seeding efficiency, and consistent cell migration, proliferation, and differentiation into specific organs and tissues through the release of extracellular matrix (ECM) [8]. Fibrin emerges as an ideal platform for dental tissue engineering purposes, and its unique nano and micro features have been leveraged to fabricate various scaffolds, including hydrogels, nanofibers, nanoparticles, microfibers, microtubes, and microspheres. These diverse scaffolds find applications in various tissue engineering endeavors, particularly within the field of dental tissue engineering.

Silk Fibroin

Silk fibroin (SF) is an insoluble peptide containing large hydrophobic motifs, derived from silkworms, arachnids, and other insects. It can be easily isolated and utilized to create silk-derived scaffolds free of sericin [8]. SF stands out due to its highly versatile material properties, exceptional biocompatibility, and minimal foreign body reaction in vivo, making it an outstanding framework material. SF has attracted significant attention in biological and pharmacological research owing to its remarkable mechanical properties, superior biocompatibility, predictable biodegradability, and low antigenicity. Bombyx mori silk fibroin (BSF) has been extensively investigated as a tissue-engineered scaffold, particularly for bone formation [8]. For instance, Wang et al. demonstrated the encapsulation of human mesenchymal stem cells (HMSC) in sonication-triggered SF hydrogels, revealing cell proliferation and survival in stable cultures after a week of in vitro development [8] (Figure 6.27).

6.5.4.2. Synthetic Polymers

Polyethylene glycol (PEG)

Polyethylene glycol (PEG) is a versatile biomaterial widely utilized in various biological and pharmaceutical applications, owing to its exceptional properties such as excellent bioactivity, biocompatibility, anti-fouling characteristics, water solubility, and compatibility with chemical reagents [8]. Due to its high hydrophilicity, PEG can be easily transformed into a hydrogel through crosslinking. Chemically cross-linked PEG hydrogels exhibit a more integrated structure and superior mechanical strength. However, the anti-fouling property of PEG, also known as the "stealth characteristic," hinders cell-PEG interaction, leading to reduced cell adhesion on the PEG hydrogel surface. To address this limitation, bioactive substances are often incorporated into PEG to enhance its cellular attraction. Grafting PEG with natural biomolecules like collagen can significantly improve its bioactivity [8]. Additionally, copolymerizing PEG with poly(e-caprolactone) (PCL) introduces thermo-responsive functionality and enhanced bioactivity to the resulting scaffold, making it well-suited for local tissue engineering applications [139]. In clinical applications, PEG hydrogel membranes have demonstrated efficacy in treating bone dehiscence defects around dental implants, proving equally effective as traditional collagen membranes with simpler clinical management [8]. PEG-fibrinogen (PF) hydrogels have been employed to support dental pulp stem cells (DPSCs), showing potential benefits for use in regenerative endodontics.

Natural Protein	Delivery System	Experiment Design	Outcome
Collagen	Collagen hydrogel loaded with Rat pulpcells marked with indium-111-oxine	Implantation in the rat emptied pulp chamber.	Functioning fibroblasts, neovasculature, and nerve fibers were seen in the collagen hydrogel one month after inser- tion.
Collagen	Blends with nano keratin, and hydroxyapatite	Histomorphometry on critical size defects in rat calvaria	bio-compatibility, biodegradability, and increased density of newly formed bone
Gelatin	Cross-linked gelatin hydrogel micro particles were encapsulated with fi- broblast growth factor 2 (FGF-2) and mixed with collagen sponge pieces	Detection of expression of DSPP (Dentin Sialophosphoprotein)	Regulated FGF2 release from gelatin hydrogels resulted in the production of dentin-like particulates with dentin defects above exposed pulp.
Fibrin	Incorporation of clindamycin loaded Poly (D, L) Lactic Acid nanoparticles (CLINloaded PLA NPs).	Cell viability and anti-microbial assay	Fibrin hydrogels incorporating CLIN-loaded PLA NPs reduced bac- terial colonization and had an antimicrobial property towards E. faecalis. In cellularized hydro- gels, DPSC survival and type I collagen production were comparable to the unmodified groups
Silk Fibroin	Silk Fibroin/Cellulose Hydrogel	Cell viability	The hydrogels promote MC3T3 cell development into osteoblasts and are predicted to be a promising matrix for osteogenesis

Figure 6.27. Natural protein in sonication-triggered SF hydrogels [8].

Poly (a-Hydroxy Esters)

Poly(alpha-hydroxy esters), such as poly(glycolic acid) (PGA), poly(lactic acid) (PLA), and their copolymers like PLGA and PCL, are widely used artificial scaffolds in tissue engineering. These materials are well-defined and FDA-approved for specific therapeutic applications. PGA, with a high degree of crystallization, exhibits optimal mechanical properties and is insoluble in most chemical reagents. PLA, composed of D-lactide and L-lactide isomers, has a semi-crystalline structure, resulting in poor solubility and high physical strength. The copolymer PLGA, derived from PGA and PLA, exhibits varying hydrophilicity and degradation rates based on the GA/LA ratio.

In the realm of dental pulp stem cells, the gelatin/PLGA-PEG-PLGA composite hydrogel demonstrated biocompatibility, and these hydrogels exhibited properties akin to articular cartilage with favorable biocompatibility for chondrocytes [8]. Amoxicillin-loaded PLGA layers on titanium implants displayed effective antibacterial properties [8].

PCL is biocompatible and soluble in various organic media. In bone tissue engineering, 3D-printed PCL/GelMA hybrid scaffolds exhibited high cell survival, osteogenic differentiation, and mineralization, making them promising for bone tissue engineering applications [8]. However, PCL has a slower biodegradation rate compared to PGA, PLA, and PLGA.

Poly(alpha-hydroxy esters) typically do not dissolve in water, and creating hydrogels from them involves modification with additional hydrophilic components. For example, a PEG-PLGA-PEG triblock blend can form a gel at body temperature, providing an injectable hydrogel [8]. These materials can also be shaped into injectable microspheres for use as cell carriers and drug delivery vehicles in tissue regeneration.

Poly (N-Isopropyl Acrylamide)

Poly(N-isopropyl acrylamide) (PNIPAM) is a thermos-sensitive polymer widely utilized in biomedical engineering. A thermo-sensitive injectable hydrogel, comprising a copolymer based on poly(N-isopropylacrylamide) (PNIPAAm) and graphene oxide (GO), was developed in a study by P. Ghandforoushan et al. This hydrogel demonstrated the ability to promote alkaline phosphatase (ALP) activity and increase the expression of Runt-related transcription factor 2 and osteocalcin in human dental pulp stem cells (hDPSCs). The findings suggest that this hydrogel could be applied in bone tissue engineering due to its osteogenic capability [8].

Pluronic Block Copolymers

Pluronics are triblock copolymers comprised of poly(ethylene oxide) (PEO) and poly(propylene oxide) (PPO). In an aqueous solution, Pluronics display a distinctive thermo-sensitive sol-gel transition. Due to the high concentration of PEO, the system dissolves at low temperatures. The sol-gel transition is influenced by various factors, including the PEO/PPO ratio, molecular weight, block size, and block sequencing. The resulting PEO-PPO-PEO hydrogel possesses structural integrity and ease of manipulation. However, Pluronic block copolymers encounter limitations as injectable biomaterials, including non-processability and rapid disintegration. Enhancing their biodegradability and bioactivity can be achieved by combining them with natural materials through copolymerization [8] (see Figure 6.28 for details).

Hydrogel	Delivery Vehicle	Experiment Design	Outcome
Polylactic polyglycolic acid-polyethylene glycol (PLGA-PEG)		Clinical Trial	A biological strat- egy may create a conditions favora- ble to therapeutic regeneration of dental and pa- radental tissues.
PLGA	Lactoferrin and substance P in a chitin/PLGA-$CaSO_4$ hydrogel	Clavarial rat defect	In mice, clavarial bone regeneration was enhanced compared to con- trols.
PEG	PEG-maleate-citrate (PEGMC) (45% w/v), acrylic acid (AA) cross linker (5% w/v), 2.20-Azobis (2-methylpropionamidine) dihydrochloride (AAPH) photo-initiator (0.1% w/v),	Cell viability	
PEG	A Tetra-PEG Hydrogel Based Aspirin Sustained Release System	In vitro and in vivo analyses	When periodontal ligament stem cells (PDLSCs) were co-incubated with hydrogel materials, in vitro tests revealed that cell growth was somewhat aided and osteogenic development was significantly enhanced. Furthermore, an in vivo investigation revealed that the aspirin controlled release approach greatly aided PDLSCs-mediated bone defect healing.
Poly-Nisopropylacrylamide (NIPAAm)	NIPAAm cross-linked by PEG-DMA	DSPP in the outer cell layer	DPSCs in the construct's outermost surface developed into odontoblast-like cells, whilst DPSCs in the inner layer remained stem cells. In vivo, blood vessel-rich pulp-like tissues were created.

Figure 6.28. Hydrogel in synthetic materials [8].

6.5.4.3. Hybrid Polymeric Hydrogels

Recent research has focused on addressing the limited structural rigidity of single-component hydrogels by exploring composite or hybrid hydrogel matrices to enhance hydrogel stiffness [8]. Biocompatible physically cross-linked polymers like polyurethanes and polyesters, as well as chemically cross-linked polymers like poly(glycerol sebacate) (PGS) and poly(citrate diol) (PCD), have been investigated. These degradable composites offer adjustable degradation, mild

biocompatibility, and excellent mechanical performance [154]. Despite their weak biocompatibility or limited structural rigidity, they have shown promising applications in tissue regeneration [8].

The design of hybrid polymers for biodegradable elastomers with tailored optimal qualities for specific tissue-specific needs has emerged as an attractive alternative for various biomedical applications. PGS-PCL hybrid elastomers, fabricated through solvent electrospinning, exhibited enhanced nano-fibrous structure formation, with mechanical properties comparable to human aortic valve tissues [8]. Incorporating gelatin into PGS elastomers significantly improved their mechanical characteristics and bioactivity [8]. In another study, Osaheni et al. [8] developed poly([2-(methacryloyloxy)ethyl] dimethyl-(3-sulfopropyl) ammonium hydroxide) with varied quantities of biocompatible zwitterionic polymers, achieving up to 80% reduction in friction. This scaffold holds potential applications in dentistry to minimize friction and wear on dental materials [8]. Figure 6.29 provides an overview of different applications of hydrogel materials.

Material		**Application**	**Outcomes**
Alginate-Matrigel hy- drogel encapsulated with bioactive glass micro particles		In vitro (human dental pulp MSCs)	Despite a decrease in elasticity due to the in- corporation of bioactive glass microparticles, the incorporation of Mat- rigel in the hydrogel combination promotes MSC osteogenic differ- entiation.
3D-printed heparin-collagen network en- closing MSCs, rein- forced with -TCP na- noscale framework, and complexed with human bone morpho- genetic protein type 2 (rhBMP-2)		In vitro (human dental pulp MSCs); In vivo (rat dorsum defects)	In vitro: the capability of heparin-conjugated col- lagen matrix to retain rhBMP-2 bioactivity and improve MSC survival and osteogenic growth. MSCs' osteogenic differ- entiation capacity and the formation of ectopic osteogenesis in vivo
Bacterial cellulose en- capsulated with bone morphogenetic protein type 2 (BMP-2)		In vivo (frontal sinus lift rabbit model)	Bacterial cellulose has demonstrated great bio- compatibility. Bacterial cellulose, when combined with BMP-2, aided bone repair while also acting as a barrier membrane and a drug release prolonger, as in- dicated by histological and immunohistochemi- cal tests.

Chitosan-Gelatin hydrogel incorporating nanodimensional bio- active glass particles		Human dental pulp MSCs in vitro; rat femoral deformities in vivo	Biocompatibility and ability to generate bone- like apatite crystalliza- tion in vitro In vivo, the chitosan- gelatin hydrogel con- taining 5% bioactive glass nanostructures generated the highest bone regeneration out-comes.
Composite bisphosphonate-linked hyalu- ronic acid-calcium phosphate hydrogel		In vivo (sinus lift rabbit model)	In a histomorphometric analysis, the synthetic granular calcium phos- phate material and deproteinized cow mineral xenograft stimu- lated more bone repair
3D-bioprinted biphasic osteon-like framework comprising human mesenchymal stem cells (hMSCs) and hu- man umbilical vein en- dothelial cells (HU- VECs) enclosed in a fi- brin-polycaprolactone hydrogel		In vitro (commercial hMSCs and HUVECs) In vivo (rat cranial bone defects)	in vitro; Significant in- crease in transcription of angiogenic biomarkers In vivo: histological analysis of explanted bi- omaterials demonstrated a boost in the quantity of blood ves- sels per square meter (the capacity to stimu- late angiogenesis) in the three-dimensional bi- oprinting osteon-like framework.
Gelatin-coated ?-trical- cium phosphate (BTCP) scaffolds with rhBMP- 2-loaded chitosan nanoparticles delivery system		In vitro (human buccal fat pad MSCs)	Gelatin-coated TCP scaf- folding with rhBMP-2- loaded chitosan nano-particles promoted cell survival and adhesion while progressively re- leasing rhBMP-2 at a therapeutic dosage that allowed MSCs to de- velop into osteoblasts.
Alginate-gelatin meth- acrylate (GelMA) hydrogel		In vitro (human gingival MSCs and human bone marrow MSCs)	Because of the hydro- gel's reduced flexibility, the addition of GelMA to alginate impairs the hydrogel osteogenic de- velopment beginning of encapsulated MSCs. The biological character- istics of alginateGelMA, as well as the existence of inductive cues, gov- ern MSC differentiation into osteoblasts.

Crosslinked PNIPAM-co-DMAc hydrogel loaded with hydroxyapatite nanoparticles		In vitro (commercial human MSCs); In vivo (rat femur defects)	Commercial human MSCs' capacity to drive osteogenic development in vitro; in vivo: biocom- patibility, capacity to combine with surround- ing structures, and en- hanced accumulation of early indicators of bone regeneration.
Sodium alginate/hydroxyethylcellulose/ hydroxyapatite compo- site	Semi-synthetic	In vitro (commercial human MSCs); In vivo (rat femur defects)	The capacity of the hy- drogel composite scaf- folds to support hMSC cell survival and prolif- eration in vitro. Histological studies demonstrated neo-oste- ogenesis to heal the damaged sites 6 weeks following scaffold place- ment.
3D polyvinyl alcohol-tetraethylorthosilica-tealginate-calcium ox- ide biocomposite cryogels	Semi-synthetic	In vivo (rat cranial bone defects)	The bone defect is al- lowed to repair during a 4-week period while its components are recircu- lated from the defect area. Osteoblastic function at the injured area, with a 2 to 4 week surge in de- velopment towards the osteoblastic lineage and osteoblast maturation.
Triblock poly(ethylene glycol)-poly (e-caprolactone)-poly(ethylene glycol) copolymer, collagen and nanohydroxyap- atite	Semi-synthetic, injecta- ble	In vivo (rabbit calvarial bone defects)	After 4, 12, and 20 weeks, bone regenera- tion was evaluated. The creation of new bone tissue from the border of defects and the surface of native bone towards the center was established by radi- ological and pathologi- cal investigations. Non-loading defects have a great potentiality for correction via mini- mally invasive surgical procedures.

Figure 6.29. Hydrogel materials applications [8].

6.6. Application of dental stem cells in three-dimensional tissue regeneration

Stem cells possess inherent regenerative potential, particularly due to their multipotent properties, making them invaluable for tissue repair. In dentistry, five distinct types of dental stem cells—dental pulp stem cells (DPSCs), stem cells from human exfoliated deciduous teeth (SHEDs), periodontal ligament stem cells (PDLSCs), stem cells from apical papilla (SCAP), and dental follicle progenitor cells (DFPCs)—play pivotal roles in various stages of tooth development (Figure 1). Apart from their significance in dental tissue repair, these cells exhibit versatility by contributing to the regeneration of neural, adipose, bone, and cartilage tissues [9].

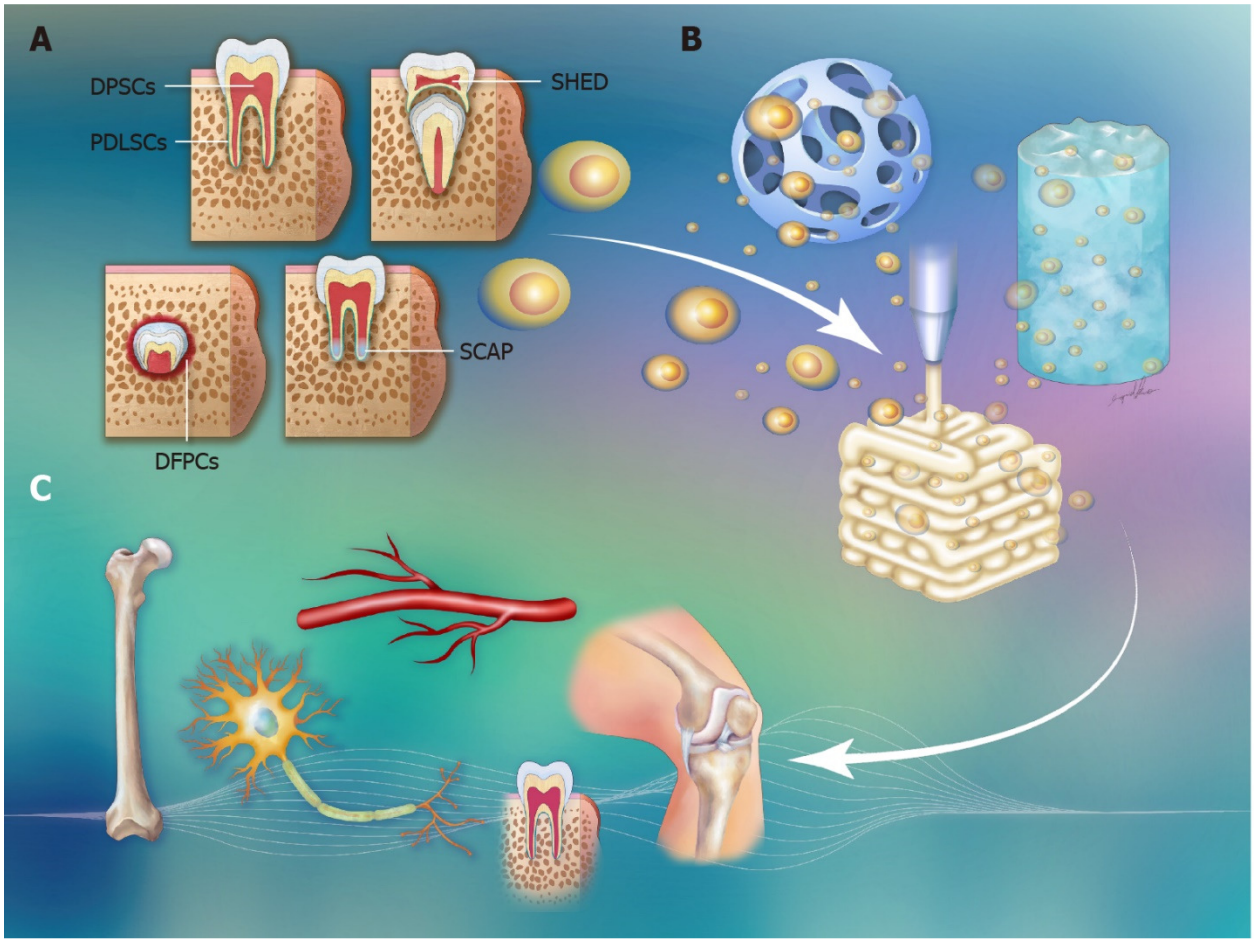


Figure 6.30. Schematic illustration depicting the process of three-dimensional tissue regeneration using dental stem cells: A: Harvesting of five different types of dental stem cells during distinct tooth developmental stages. B: Incorporation of dental stem cells with various forms of three-dimensional (3D) biomaterials, including microspheres, hydrogels, or 3D printed scaffolds, to generate 3D engineered tissue. C: Induction of dental stem cells to differentiate into diverse tissue types, such as teeth, neurons, bone, blood vessels, and cartilage [9].

The field of therapeutic medicine has embraced three-dimensional (3D) tissue engineering, wherein cells are introduced into engineered scaffolds to emulate the microenvironment of human tissues during the differentiation process. Notably, cells cultured in 3D conditions exhibit morphologies and gene expressions more closely aligned with those observed in native tissues [9]. An exciting prospect in dentistry involves the utilization of customized 3D tooth implants with dental stem cells seeded in appropriate scaffolds as replacements for lost teeth. The concept extends beyond tooth repair, garnering increasing interest in the broader context of 3D tissue regeneration facilitated by dental stem cells.

In exploring the literature on the utilization of dental stem cells in three-dimensional (3D) tissue regeneration, a database search was conducted using custom scripts with the "easyPubMed" and "PubMed.mineR" packages in R for the PubMed database [9]. Queries were customized with keywords such as "pulp stem cells," "exfoliated deciduous teeth stem cell," "periodontal ligament stem cell," "apical papilla," "dental follicle cells," "3D," "tissue," "regeneration," and "engineering." The results, formatted in the "abstract" style using the "easyPubMed" package, underwent analysis through the "PubMed.mineR" package. Out of the 88 papers identified based on the criteria, only one-third presented original research on dental stem cells in 3D tissue regeneration. This review aims to provide a comprehensive perspective on each type of dental stem cell and its combination with 3D tissue scaffolds, including microspheres, hydrogels, or 3D printed scaffolds, for the regeneration of teeth, neurons, bone, blood vessels, and cartilage (Figure 6.30 and Figure 6.31.).

Dental stem cells	Biomaterials	Addition of materials/growth factors/cells	Type of tissue regeneration
DPSCs			
DPSCs	Cap porous granules, NF-gelatin/MgP	No	Odontogenic differentiation
	SS-PLLA-b-PLYS, PNIPAAm, NF-PLLA	No	Pulp-dentin regeneration
	Coll/HA/PLCL, ABM/ABM-P-15, PVA/PU	No	Bone tissue
	OMMT/PVA	No	Neuro-like cells
	Matrigel	No	Endotheliocytes and pericytes
	Collagen gel	SDF1, bFGF	Dental pulp tissue
		BMP7	
DPSCs with growth factors	Ti6Al4V	Poly-L-lys coating	Osteoblastic differentiation
	Porous silk fibroin	bFGF	Dental pulp tissue
	PCL	VEGF, BMP2	Vascularized bone tissue
	HP hydrogel	bFGF	Spinal cord
DPSCs with other cells	Matrigel and collagen gel	Human normal oral epithelial cells	Epithelium invagination-like structure
	PCL/PLDLA	Endothelial cells	Vascularized bone tissue
	PLLA/PLGA	Human neonatal dermal fibroblasts	Spinal cord
DPSCs in 3D printed scaffolds	HA/TCP	Apical papilla (SCAP)	Pulp-dentin regeneration
	PCL	Platelet-rich plasma	Calvaria bone
	Alg-Gel		Bone
	PLAS		Neural differentiation
	AMP/ECM		Craniomaxillofacial bone

SHED			
SHED with growth factors	No	EGF, FGF	Spinal cord
	No	SHED-conditioned medium	Sciatic nerve
SHED in 3D formed scaffolds	Polylactoglycolide, hemisphere	SHED aggregated	Bone tissue
PDLSCs			
PDLSCs	Hydroxyapatite/?-tricalcium phosphate (HA/ B-TCP)		Periodontal tissue
	GelMA/PEG		PDLSC proliferation
PDLSCs with growth factors	PLGA	CTGF, BMP-7, BMP-2	Periodontal tissue
	Platelet-rich fibrin	Aspirin	Periodontal tissue
PDLSCs with other cells	Collagen/Chitosan	Somatic MSCs and DPSCS	Odontogenic differentiation
	No	HUVECs	Periodontal tissue
	PLGA-PEG-PLGA thermal hydrogel	PDLSCs overexpressing PDGF-BB	Alveolar bone tissue
SCAP			
SCAP with growth factors	PLLA nanofibrous microspheres (NF-MS)	BMP-2	Pulp-dentin regeneration
	No	BMP-2, SDF-1α	Odontoblast differentiation
	Alg-Dent hydrogel	Dentin ECM	Pulp-dentin regeneration
DFPCs			
DFPCs	Coll-nano-HA/OPS		Bone tissue

Figure 6.31. List of dental stem cells used for three-dimensional tissue regeneration [9].

DFPCs: Dental follicle progenitor cells; SCAP: Stem cells from apical papilla; PDLSCs: Periodontal ligament stem cells; SHED: Human exfoliated deciduous teeth; DPSCs: Dental pulp stem cells; SDF1: Stromal-derived factor-1α; bFGF: Basic fibroblast growth factor; BMP-7: Bone morphogenetic protein-7; Ti6Al4V: Titanium-6-aluminum-4-vanadium; Poly-L-lys: Poly-L-lysine; CaP: Calcium phosphate; OECs: Human normal oral epithelial cells; PLCL: Collagen (Coll)/hydroxyapatite (HA)/poly(l-lactide-coε-caprolactone); NF-gelatin/MgP: Gelatin/magnesium phosphate; VEGF: Vascular endothelial growth factor; BMP-2: Morphogenetic protein-2; EGF: Epidermal growth factor; FGF: Fibroblast growth factor; PCL: Polycaprolactone; NF-SMS: Nanofibrous spongy microspheres; SS-PLLA-b-PLYS: Star-shaped poly(l-lactic acid)-block-poly(l-lysine); PLDLA: Poly-L/D-lactide; ECs: Endothelial cells; HA/TCP: Hydroxyapatite/tricalcium phosphate; OMMT/PVA: Chitosan-intercalated montmorillonite/poly(vinyl alcohol); PRP: Platelet-rich plasma; pNIPAAm: Poly-N-isopropylacrylamide gel; HP: Heparin-poloxamer hydrogel; NF-PLLA: Nanofibrous poly(l-lactic acid) scaffolds; Alg-Gel: Alginate/gelatin hydrogel; 3DP-PLASs: Polylactic acid scaffolds; ABM: Bone mineral; ABM-P-15: Biomimetic collagen peptide; PVA: Polyvinyl alcohol; PU: Polyurethane; AMPs: Amorphous magnesium phosphates; ECM: Extracellular matrix; PLLA: Polylactoglycolide scaffolds; NF-MS: Nanofibrous microspheres; SDF-1α: Normal cell-derived factor-1α; GelMA: Gelatin methacrylate; PEG: Poly(ethylene glycol); dimethacrylate; PLGA: Poly(lactic-co-glycolic acids); CTGF: Connective tissue growth factor; HUVECs: Human umbilical vein endothelial cells; Coll-nano-HA/OPS: Collagen-nanohydroxyapatite/phosphoserine.

6.6.1. DPSCs (dental pulp stem cells)

DPSCs, first identified within the soft connective tissue of the dental crown in 2000, exhibit characteristics resembling those of mesenchymal stem cells (MSCs), including a high proliferation rate, multilineage potential, and immunomodulatory properties (Figure 6.30) [9]. Unlike BMSCs, DPSCs are notable for causing minimal morbidity at the donor site, displaying a higher proliferation rate, and demonstrating multipotency, rendering them preferable as sources of stem cells for tissue regeneration [9]. Co-culturing DPSCs with apical bud cells (ABCs) has shown more active odontogenic differentiation compared to BMSCs co-cultured with ABCs [9]. DPSCs have also exhibited enhanced neural differentiation of IMR-32 cells in contrast to BMSCs, underscoring their superiority in fostering neural differentiation [9]. Notably, DPSCs, particularly focused on dental pulp and bone tissue regeneration, have demonstrated a higher proliferation rate and superior osteogenic capacity in bone mineral-coated (ABM) scaffolds with a biomimetic collagen peptide (ABM-P-15), even generating a more organized collagenous matrix after in vivo implantation [9]. Distinct gene expression patterns in DPSCs, compared to bone marrow stem cells, further underscore their unique gene expression profiles [9].

In the domain of 3D tissue regeneration, DPSCs have been explored using various biomaterials and techniques. A bioink incorporating human DPSCs and fibrinogen with polycaprolactone (PCL) was engineered for dentin pulp complex structures [9]. DPSCs seeded on nanofibrous spongy microspheres composed of star-shaped poly(l-lactic acid)-block-poly(l-lysine) (SS-PLLA-b-PLYS) contributed to dental pulp tissue regeneration [9]. Poly-N-isopropyl acrylamide (pNIPAAm) gel containing DPSCs, designed in a rod shape, filled root canals for pulp tissue regeneration [9]. DPSCs combined with simvastatin and nanofibrous poly(l-lactic acid) (NF-PLLA) scaffolds, as well as a mixture of polyvinyl alcohol (PVA) and polyurethane (PU), demonstrated potential for tissue regeneration [9]. Utilizing self-assembling peptides with structures akin to the extracellular matrix (ECM), a 3D scaffold composed of collagen (Coll), hydroxyapatite (HA), and poly(L-lactide-co"-caprolactone) (PLCL) enhanced DPSC adhesion, viability, and bone regeneration [9]. DPSCs grown in a peptide-based scaffold, featuring RGD- and vascular endothelial growth factor (VEGF)-mimetic peptide epitopes, exhibited improved survival and angiogenic and odontogenic differentiation [9].

Growth factors have been integrated into studies related to DPSCs and tissue regeneration, such as stromal-derived factor-1α, basic fibroblast growth factor (bFGF), and bone morphogenetic protein-7 (BMP-7) for dental pulp regeneration [9]. Seeding DPSCs on 3D calcium phosphate (CaP) porous granules promoted odontogenic differentiation [9]. Porous silk fibroin scaffolds incorporating bFGF were employed for root canal space filling [9]. DPSCs, in conjunction with platelet-rich plasma (PRP), were applied to 3D printed PCL mesh for bone regeneration in a rat calvaria defect model [9]. Metal ions, like magnesium (Mg), incorporated into nanofibrous gelatin biomaterials, enhanced odontogenic proliferation and differentiation when seeded with DPSCs [9].

3D printing techniques have played a pivotal role in advancing DPSC-related research, showing improved cell proliferation, odontoblastic differentiation, and bone mineralization in DPSC-loaded 3D printed scaffolds compared to traditional 2D cultures [9]. Combining DPSCs with vascular endothelial growth factor (VEGF) and bone morphogenetic protein-2 (BMP-2) in 3D-printed constructs resulted in vascularized bone structures [9]. Additionally, DPSCs and stem cells from apical papilla (SCAP) mixed with collagen gel were loaded into a cone-shaped 3D printed hydroxyapatite/tricalcium phosphate (HA/TCP) scaffold for dental pulp regeneration [9]. Furthermore, DPSC-loaded bioink containing amorphous Mg phosphates and ECM contributed to increased bone density during craniomaxillofacial bone regeneration [9]. The precise control offered by 3D printing allows the exploration of microenvironmental effects on cell proliferation and differentiation, as seen in studies with polylactic acid scaffolds (PLASs) printed in different gap sizes [9].

Beyond their osteogenic and odontoblastic potential, DPSCs have been investigated for their chondrogenic potential, differentiating into fibrous cartilage rather than hyaline cartilage [9]. DPSCs derived from cranial neurons have demonstrated the ability to differentiate into neuron-like cells for

axon regeneration [9]. When seeded within chitosan-intercalated montmorillonite/poly(vinyl alcohol) (OMMT/PVA) nanofibrous mesh, DPSCs differentiated into neuron-like cells [9]. Additionally, DPSCs in a thermosensitive heparin-poloxamer hydrogel, along with bFGF, enhanced motor and sensory functional recovery after spinal cord injury repair [9]. The co-seeding of DPSCs and human adipose microvascular endothelial cells in a prevascularized scaffold promoted revascularization, axon regeneration, myelin deposition, and sensory recovery in a rat complete spinal cord transection model [9]. DPSCs seeded in Matrigel were found to differentiate into endotheliocytes and pericytes in serum-free culture media, secreting VEGF [9].

6.6.2. SHED (stem cells from human exfoliated deciduous teeth) cells

SHED (stem cells from human exfoliated deciduous teeth) cells, discovered in 2003, exhibit positive expression of embryonic stem cell markers such as OCT4 and NANOG, as well as stage-specific embryonic antigens (SSEA-3 and SSEA-4), and mesenchymal stem cell markers (STRO-1 and CD146) [9]. Compared to DPSCs, SHEDs demonstrate higher levels of osteocalcin expression and alkaline phosphatase activity [9]. Characterized as more immature than DPSCs, SHEDs display characteristics of both "osteoblast-like" and "odontoblast-like" cells, expressing markers like osteocalcin and RUNX-2 [53]. Remarkably, when cultured in a medium containing dexamethasone, SHEDs differentiate into adipocytes, and after two weeks of in vitro osteogenic medium culture, they begin to secrete extracellular mineralized matrix, showcasing their multilineage potential as alternative dental stem cell sources [9].

In the field of 3D tissue regeneration, SHEDs demonstrate remarkable capabilities. Cultured in vitro for seven days, SHEDs aggregate and form a 3D ossification hemisphere, eventually leading to the formation of a self-formed 3D woven bone tissue, as confirmed by alizarin red staining [9]. Utilizing a 3D polylactoglycolide scaffold fabricated through surface-selective laser sintering, SHEDs demonstrate elevated expression of osteocalcin, highlighting their potential as cell sources for scaffolds in tissue bone engineering [9]. Beyond bone regeneration, SHEDs also show promise as a source of neurons. Incubation in neurodifferentiation medium supplemented with epidermal growth factor (EGF) and fibroblast growth factor (FGF) results in increased expression of neuron markers, including βIII-tubulin, microtubule-associated protein 2, tyrosine hydroxylase, and Nestin [9]. This underscores the neurogenic potential of SHEDs. In scenarios such as spinal cord injury, SHEDs have been demonstrated to rescue hindlimb locomotor function, and SHED-conditioned medium contributes to peripheral nerve regeneration in rat sciatic nerve defects, increasing Schwann cells, axon density, and the number of regenerated myelinated fibers [9].

Moreover, the injection of SHEDs into the brain at the site of perinatal hypoxia-ischemia (HI) injury improves the survival rate of HI-injured mice by inhibiting the expression of proinflammatory cytokines [9]. Despite the multidifferentiation potency and fewer ethical concerns associated with SHEDs in clinical applications, only a limited number of studies have explored their application in 3D-printed scaffolds for tissue regeneration. This might be attributed to the lack of standardized or popularized methods for the collection, treatment, and storage of harvested SHEDs.

6.6.3. PDLSCs (periodontal ligament stem cells)

Periodontitis, a widespread oral ailment, results in the deterioration of periodontal tissue and, in severe cases, tooth loss [9]. Various treatments for periodontal regeneration strive to repair the impaired periodontium. PDLSCs (periodontal ligament stem cells), extracted from mature periodontal ligaments, express stem cell markers such as CD105, CD90, and CD73 [9]. Seo et al. [9] effectively isolated PDLSCs from human third molars, showcasing the expression of STRO-1 and CD146/MUC18 stem cell markers. In addition to marker expression, PDLSCs demonstrate osteogenic and adipogenic potential, positioning them as alternative cell sources for tissue regeneration [9]. The regenerative process of periodontal tissue, illustrated by PDLSCs incorporated with hydroxyapatite/β-tricalcium phosphate (HA/β-TCP) carriers, involves heightened PDLSC proliferation, formation of collagen matrix, assembly of collagen fibers leading to cemental-like tissue, mineralization, and maturation of the cemental-like tissue [9].

In the domain of 3D tissue regeneration, a precisely controlled 3D collagen scaffold, influencing pore size, pore wall alignment, and percolation diameter, demonstrated that larger percolation diameters increased PDLSC cell elongation and directionality, while pore size influenced cell invasion and distribution [9]. The addition of growth factors further enhanced tissue regeneration capacity. Connective tissue growth factor (CTGF) promoted the differentiation of periodontal ligament fibroblasts during cemental tissue formation [9]. BMP-7 induced cementogenic differentiation by acting as a progenitor for cementoblasts, while BMP-2, involved in cementogenic differentiation, increased the expression of cementum attachment protein (CAP) [9]. Comparison of the effects of CTGF, BMP-7, and BMP-2, incorporated into 3D printed PLGA microspheres, revealed that BMP-7 triggered thicker cementum-like layers, better integration with the dentin surface, and higher expression of cementum protein 1 [9].

Alongside growth factors, inhibiting inflammatory reactions has been shown to improve tissue formation. Reductions in tumor necrosis factor-alpha and interferon-gamma levels by introducing BMMSCs enhanced bone regeneration [9]. Aspirin promoted BMMSC-based calvarial bone regeneration, and platelet-rich fibrin-containing PDLSCs treated with aspirin increased periodontal bone formation [9]. A novel approach involves coculturing human umbilical vein endothelial cells (HUVECs) with PDLSCs to form 3D cell sheet constructs, resulting in thicker periodontal ligament-like arrangements, suggesting that HUVECs contribute to regulating the thickness of the periodontal compartment [9]. Genetically modified PDLSCs, overexpressing platelet-derived growth factor BB (PDGF-BB), introduced via a lentiviral construct, incorporated into PLGA-PEG-PLGA thermal hydrogel, promoted bone formation in alveolar bone defects [9].

Exploring the incorporation of somatic MSCs in tissue regeneration, a mixture of PDLSCs, somatic MSCs, and DPSCs cocultured within 3D collagen/chitosan scaffolds demonstrated significant promotion of growth factors, transcription factors, and signaling molecules related to odontogenic differentiation [9]. Applying 3D PDLSC-loaded constructs to study the effect of the growth microenvironment on PDLSC differentiation revealed that the composition of the ECM, as influenced by the gradient of gelatin methacrylate (GelMA) and poly(ethylene glycol) (PEG) dimethacrylate, influenced PDLSC behavior in terms of proliferation and cell spreading [9].

6.6.4. SCAP (stem cells from apical papilla)

SCAP (stem cells from apical papilla) are exclusively located at the tip of the developing tooth root before the tooth erupts. While sharing some similarities with DPSCs, SCAP differs in function and characteristics. Unlike DPSCs, which act as sources of replacement odontoblasts, SCAP are the primary source of odontoblasts involved in the formation of root dentin [9]. SCAP, similar to DPSCs, express stem cell markers (STRO-1, CD146, and CD34) along with other MSC markers (CD73, CD90, and CD105), but uniquely express CD24, a marker not found in DPSCs [9]. SCAP are relatively easy to isolate from the tips of developing roots, involving digestion with collagenase to obtain single-cell suspensions, followed by growth under routine cell culture conditions [9].

In the realm of 3D tissue regeneration, SCAP with osteogenic potential derived from dental roots have been utilized for dentin regeneration. Injectable PLLA nanofibrous microspheres (NF-MS) encapsulating controlled BMP-2 release were combined with SCAP, resulting in enhanced mineralization and osteodentin formation, showcasing potential for dental tissue repair [9]. Additionally, SCAP cotreated with stromal cell-derived factor-1α, promoting odontoblast differentiation of dental pulp cells, demonstrated odontogenic differentiation-related gene and protein expression [9]. PDGF-BB, known for promoting angiogenesis, when added to SCAP, facilitated proliferation, new bone formation, and mineralization in a rat calvaria defect model [9]. SCAP's secretion of TGBβ3, a growth factor involved in tissue regeneration, was elevated when grown in a 3D microenvironment, prompting the incorporation of SCAP into 3D scaffolds for tissue regeneration [9].

Capitalizing on the secretion properties of SCAP, a 3D scaffold-free stem-cell sheet-derived pellet (CSDP) was developed, forming a cell sheet rich in secreted ECM. CSDP exhibited odontogenic/osteogenic potential, forming dental pulp-like and dentin-like tissue after implantation

into the subcutaneous layer in immunodeficient mice [9]. Dental ECM, known to enhance cell proliferation and mineralization, was applied to a printable alginate to create a novel SCAP-loaded bioink termed dentin-derived bioink. This bioink, enriched with soluble dentin molecules, significantly enhanced odontogenic differentiation [9].

6.6.5. Dental Follicle Progenitor Cells (DFPCs)

The dental follicle, a connective tissue surrounding the enamel organ and dental papilla, forms a vascular fibrous sac. In 2005, Morsczeck et al. [9] successfully isolated dental follicle progenitor cells (DFPCs) from the dental follicle of human third molar teeth, expressing stem cell markers such as Notch and Nestin. These DFPCs demonstrated potential for osteogenic, adipogenic, chondrogenic, and neural differentiation, laying the groundwork for their application in tissue regeneration, including salivary glands, dental roots, and bone tissue [9].

In the domain of 3D tissue regeneration, limited studies have explored the integration of DFPCs. Cultivating DFPCs in a 3D rotatory culture system revealed the expression of various follicle markers, including CD44, CD90, CD146, CD31, CD34, and CD45Ag. Additionally, their differentiation potential was enhanced when cultured in a 3D dynamic culture system. For the creation of 3D tissue constructs, DFPCs were seeded into 3D porous scaffolds made of collagen-nanohydroxyapatite/phosphoserine (collagen-nano-HA/OPS) biocomposite cryogels and implanted into the subcutaneous layer of nu mice. These 3D DFPC-loaded collagen-nano-HA/OPS constructs exhibited superior osteogenic differentiation, evidenced by higher levels of osteopontin secretion [9].

6.6.6. CLINICAL APPLICATIONS OF DENTAL STEM CELLS

The clinical utilization of dental stem cells in autologous or allogeneic transplantation has been introduced, with strict regulation for biological safety being imperative, including examinations for viruses, pathogenic microorganisms, and potential sources with animal origins [9]. The recommendation for the same-species origin in the stem cell culture system aims to minimize immune responses in cell therapy [9]. Despite fewer than 10 reported cases of dental stem cell use in clinical applications, indicating a gap between basic research and clinical practice, their regenerative potential has been supported by clinical results, particularly in bone regeneration, periodontitis, and dental pulp regeneration based on DPSCs [9].

However, challenges such as harvest contamination, limited cell availability, and invasive harvesting methods hinder dental stem cells from being the most suitable choice for tissue regeneration. Ethical concerns, cell sources, and varying results in the long-term survival of grafted dental stem cells also contribute to the obstacles faced in their clinical application. For instance, the survival of autologous PDLSCs was detected after 8 weeks in an ovine periodontal defect model, while donor PDLSCs were untraceable two weeks after implantation into recipient mice [9]. The impact of autologous or allogeneic stem cell sources on the survival rate of transplanted cells remains a subject for further investigation.

Dental-derived stem cells, possessing mesenchymal stem cell properties, hold promise as cell sources for tissue regeneration. DPSCs, SHEDs, and PDLSCs exhibit higher growth potential than BMSCs, and each dental stem cell type presents unique differentiation potentials in the corresponding tissue type. While dental stem cells have potential in adipogenesis, chondrogenesis, and neurogenesis, their primary clinical utility lies in regenerative dentistry. Emphasizing the trend of 3D tissue engineering, the review underscores the feasibility of applying dental stem cells in translational medicine and their role as valuable resources for 3D tissue regeneration.

6.7. Resorbable Membranes for Guided Bone Regeneration: Critical Features, Potentials, and Limitations

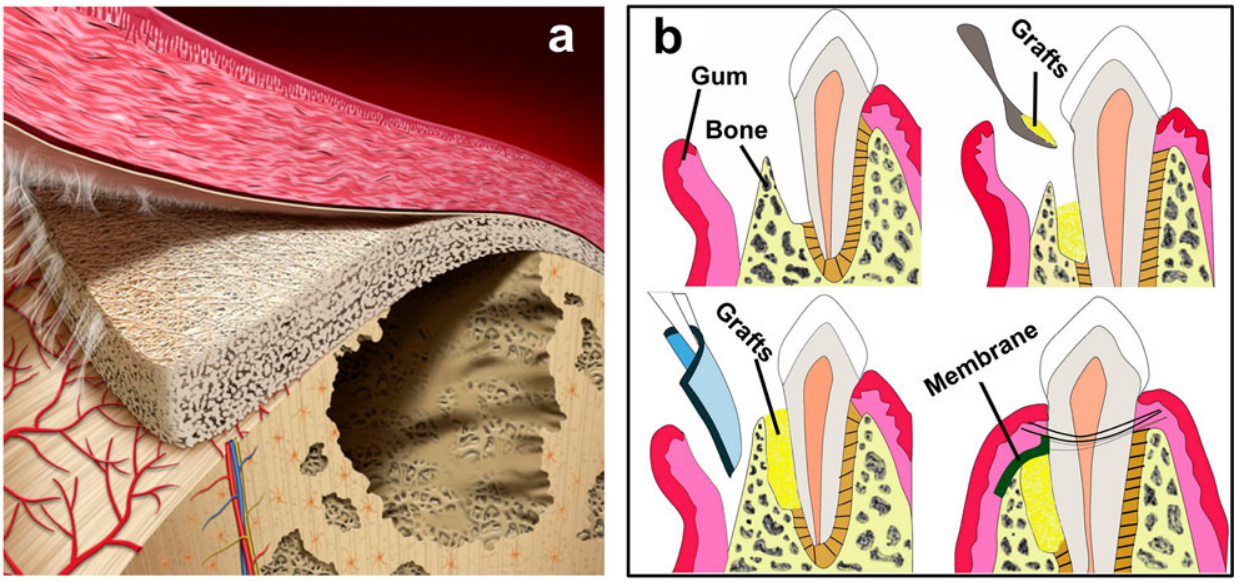
To mitigate bone loss and disorders in the maxillofacial region caused by aging, congenital diseases, cancer, trauma, tooth loss, and periodontal disease, augmentation procedures are often necessary before implant treatment. Clinicians employ various methods such as guided bone

regeneration (GBR), distraction osteogenesis, and split-crest surgery to achieve effective bone tissue repair. GBR, in particular, is widely embraced and utilized in about 40% of patients with bone defects. It entails the use of a barrier membrane during surgery to foster the growth of new bone tissue in areas where bone loss has occurred due to injury or disease (Figure 6.32.a).

The barrier membrane acts as a physical barrier, preventing the infiltration of soft tissue such as fibroblasts, while facilitating the migration of bone cells into the area for new bone formation. Its primary objective is to hinder and exclude the rapid migration of epithelial cells and fibroblasts to the defect site by placing a membrane between hard and soft tissues. Typically applied in dental implant surgery, GBR aims to augment the available bone to support the implant and repair bone defects resulting from periodontal disease or traumatic injury. The procedure involves making a small incision in the soft tissue, creating space for the barrier membrane and bone graft material, and suturing the tissue closed (Figure 6.32.b). Recovery time varies depending on the extent of bone loss and the specific procedure used.

To ensure the success of guided bone regeneration (GBR), four key biological principles must be achieved:

1. Primary Wound Closure: Establishing uninterrupted wound healing is crucial for GBR success.
2. Exclusion of Epithelium and Connective Tissue: The objective is to exclude epithelial and connective tissues while promoting angiogenesis to ensure an adequate blood supply to the region.
3. Space Maintenance: Providing adequate space for bone regeneration is essential to facilitate the migration of osteogenic cells to the defect region.



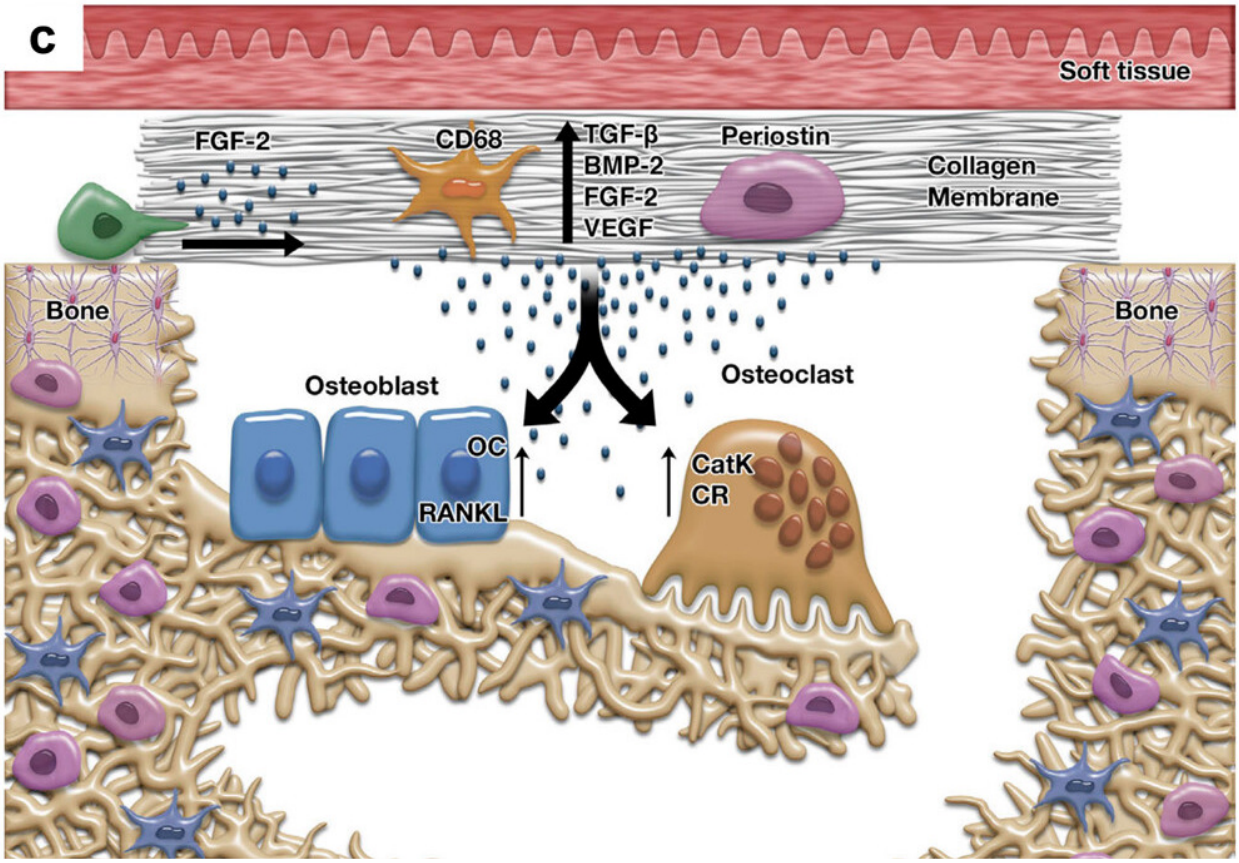


Figure 6.32. (a) Schematic illustrations of the principle of guided bone regeneration (GBR) and (b) the combination of guided tissue regeneration (GTR) and bone graft techniques for periodontal defects management. (c) Illustration of the cellular and molecular cascades occurring during the GBR process [10].

Stability: Maintaining stability in the fibrin clot and implanted material is crucial to prevent disturbances in the healing process.

Osseous regeneration, the process of growing new bone tissue to fill areas of bone loss, relies on the migration of osteogenic cells to the defect region (Figure 1c). This can be achieved through various techniques and materials, including the use of growth factors. Growth factors are substances that promote the growth and differentiation of cells, such as bone cells, and can be derived from various sources.

The GBR procedure aims to create an environment conducive to bone regeneration by isolating the bone defect from surrounding soft tissue and providing necessary growth factors and bone graft materials. Once the new bone tissue forms, it integrates with the surrounding natural bone, providing a stable foundation for dental implants and other restorations.

After GBR surgery, a sequence of events leads to bone regeneration:

1. Inflammatory Response: Immediately after surgery, the body's immune system initiates an inflammatory response, necessary for debris and bacteria removal and recruiting cells essential for healing.
2. Blood Clot Formation: In the first 24 hours, the grafted space fills with blood clots enriched by growth factors and chemoactive agents like cytokines.
3. Cell Migration: Osteoblasts and osteoclasts migrate to the bone defect site. Mesenchymal stem cells (MSCs) with osteogenic differentiation capability are transported to the area via newly formed vessels, contributing to the formation of osteoid structures (Figure 6.32.c).
4. Osteoblasts and Osteoclasts: These cells play pivotal roles in bone formation and resorption, proliferating and forming a clot that serves as a scaffold for new bone formation upon injury.

6.7.1. Barrier Membranes

Barrier membranes play a critical role in guided bone regeneration (GBR) procedures. They are utilized to segregate the bone defect from surrounding soft tissue, acting as physical barriers to prevent the infiltration of undesired cells, such as gingival tissue (Figure 6.33.a). Moreover, these membranes serve as scaffolds for the migration of osteogenic cells responsible for generating new bone.

Recent research has indicated that barrier membranes may actively contribute to bone regeneration in areas with defects. To outline the characteristics of an ideal barrier membrane for GBR, five main criteria have been identified:

1. Biocompatibility: The membrane should be compatible with the biological environment, minimizing adverse reactions.
2. Space Maintenance: It should offer adequate space for bone regeneration, facilitating the migration of osteogenic cells.
3. Occlusive Functionality: The membrane should effectively prevent the infiltration of undesired soft tissue.
4. Easy Handling: Clinicians should find the membrane easy to manipulate during surgery.
5. Bioactivity: The membrane may possess bioactive properties that aid in the regeneration process (Figure 6.33.b).

Several generations of barrier membranes have been developed for GBR procedures. First-generation membranes are constructed from highly purified, synthetic materials like polytetrafluoroethylene (PTFE). These membranes exhibit resistance to displacement, excellent mechanical stability, and long-term durability. However, they are nonresorbable, necessitating a second surgery for removal, which increases cost and patient burden. The excessive rigidity of these materials can also lead to complications, such as membrane exposure.

Advancements in membrane development aim to address these limitations by providing membranes with improved biocompatibility, resorbability, and handling characteristics. These enhancements contribute to the overall success and effectiveness of GBR procedures in bone regeneration.

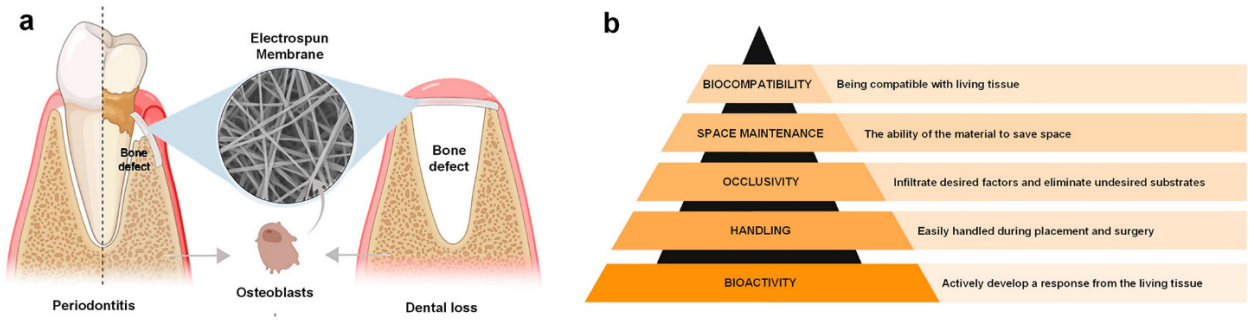


Figure 6.33. (a) Schematic illustration of the placement of an electrospun barrier membrane for GBR in scenarios involving periodontitis and dental loss. (b) Five main criteria to define practical barrier membranes for GBR [10].

The evolution of barrier membranes in guided bone regeneration (GBR) has led to the development of different generations, each addressing specific challenges and improving the overall effectiveness of the procedure.

First Generation:

Composition: Highly purified, synthetic materials such as polytetrafluoroethylene (PTFE).

Characteristics: Nonresorbable, providing stability and resistance to displacement.

Drawbacks: Require a second surgery for removal, leading to increased cost and potential complications.

Second Generation:

Types:

Naturally sourced: Made from biodegradable biomaterials like chitosan, collagen, gelatin, silk.

Synthetic absorbable: Tailored for specific mechanical and degradation properties.

Advantages: Overcome the limitations of nonabsorbable membranes.

Challenges: Naturally sourced membranes may have poor mechanical stability, and synthetic absorbable membranes may have limited barrier functionality due to the resorption process.

Third Generation:

Tissue Engineering Approach:

Multifunctional membranes: Act as barriers and enable controlled release of specific agents.

Incorporate bioactive agents: Antibiotics, growth factors, adhesion factors.

Advancements: Move beyond fundamental GBR principles.

Benefits: Enhance cell migration, proliferation, differentiation, and extracellular matrix deposition for faster and more efficient tissue regeneration.

Controlled Release: Allows for a controlled release of growth factors, reducing the required dose and minimizing side effects.

Application: Suitable for more effective wound healing.

Cost Consideration: These membranes are relatively more expensive than other types.

The third generation represents a significant advancement by incorporating the principles of tissue engineering, providing multifunctional membranes that actively contribute to the wound healing process. While these membranes may have a higher cost, their enhanced capabilities make them a valuable option in certain clinical scenarios where efficient tissue regeneration is crucial.

6.7.2. Natural Resorbable Membranes

Natural Resorbable Barrier Membranes in GBR:

1. Composition:
   - Derived from natural materials like collagen, gelatin (derived from collagen), chitosan, silk, etc.
   - These materials are designed to resorb or break down over time in the body.
2. Applications:
   - Wound Healing: Used in various medical procedures to aid in wound healing.
   - Tissue Engineering: Applied in tissue engineering for regenerative purposes.
   - GBR Procedures: Act as barriers in guided bone regeneration (GBR) procedures.
3. Function in GBR:
   - Separation: Used to separate the bone defect from surrounding soft tissue.
   - Bone Formation: Promotes bone formation in the isolated area.
4. Mechanism:
   - Gradual resorption over time, allowing the natural healing process to take place.
   - Eliminates the need for a second surgery to remove the membrane.
5. Biocompatibility:
   - Biocompatible with the body's tissues.
   - Integration into the natural healing process.
6. Limitations:
   - Mechanical Stability: May have poorer mechanical stability compared to synthetic materials.
   - Resorption Time: Resorption process may limit barrier functionality over time.
7. Advantages:
   - Avoids Second Surgery: Eliminates the need for a second surgical procedure to remove the membrane.
   - Natural Integration: Integrates with the natural healing process of the body.
8. Considerations:
   - Selection based on the specific requirements of the patient, the procedure, and the desired outcome.
   - Balancing the advantages of natural resorption with the need for mechanical stability.

Natural resorbable barrier membranes offer a biocompatible and integration-friendly option in GBR procedures, promoting bone formation without the necessity for a second surgery. However,

careful consideration of mechanical stability and resorption time is crucial in selecting the most suitable material for specific clinical scenarios.

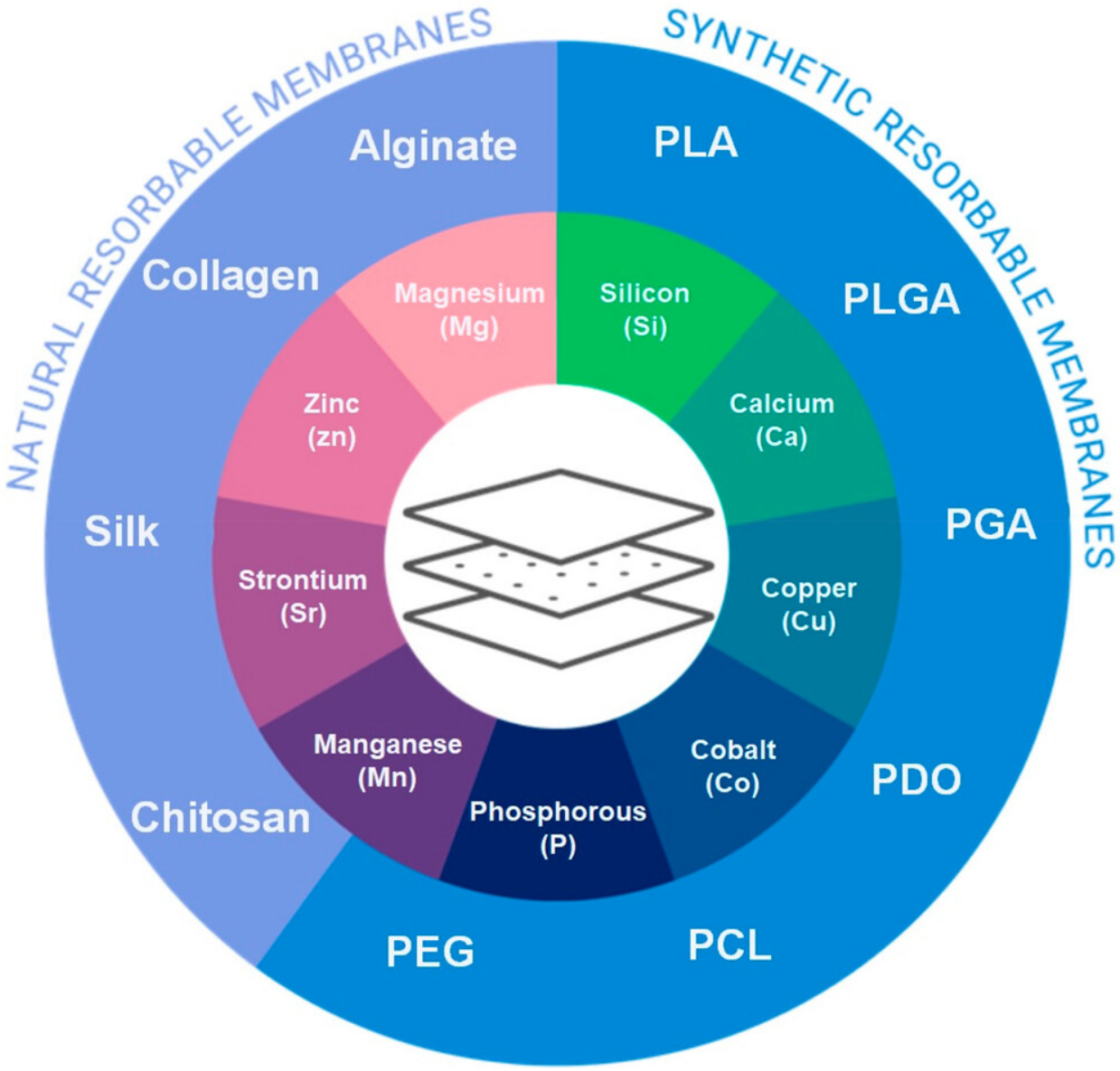


Figure 6.34. Classification of resorbable membranes based on their natural or synthetic origins in the outer layer. The inner layer displays the current substances used for bioactivity enhancement [10].

6.7.2.1. Collagen

Collagen in Bone Regeneration:

1. Abundance and Importance:

- Structural Proteins: Collagens constitute the most abundant structural proteins in mammals, making up 30% of the total protein mass.
- Extracellular Matrix (ECM): The ECM comprises 28 types and at least 46 polypeptide chains, constituting one-third of total human protein and 75% of the dry weight of the skin.

2. Discovery and History:

- Discovered in the 1890s by Mall and Young, who produced gelatin from reticular tissue.
- Siegfried identified reticulin as a type of fiber in connective tissue artifact from collagen in 1904.

3. Structure:

- Triple Helix Structure: Collagen consists of three parallel left-handed polyproline type II polypeptide strands (α chains) forming a right-handed triple helix structure.

- ECM Varieties: Collagen exists in various forms such as fibrils, beaded filaments, anchoring fibrils, and networks.

4. Collagen Types:

- Heterotypic Fibrils: Most collagen fibrils are heterotypic, comprising at least two different fibrillar collagen types.
- Tissue-Specific Composition: Different tissues contain specific collagen compositions; for instance, cartilage fibrils consist mainly of collagen type II cross-linked with types XI, IX, and III, while skin and cornea contain types I and III (skin) and types I and IV (cornea).

5. Sources:

- Collagen is extracted from various animal tissues like skin, tendon, and cartilage (from calves, mice, fish, chickens, birds).
- Commercial Availability: Collagen-based membranes are commercially available, biocompatible, and biodegradable.

6. Challenges and Limitations:

- Mechanical Stability: Collagen faces rapid loss of mechanical stability, especially in liquid or high humidity environments.
- Cost and Supply: It is relatively expensive with limited supply sources, posing challenges in bone regeneration applications.
- Degradation Variability: Degradation rates vary based on collagen origin (porcine, bovine) and tissue source (skin, tendon, pericardium).

7. Enhancement Strategies:

- Bioactivity Enhancement: Studies focus on enhancing bioactivity by loading collagen membranes with active organic and inorganic compounds.
- Organic Compounds: Growth factors, cytokines, anti-inflammatory agents.
- Inorganic Compounds: Calcium phosphate substrates, bioceramics.

Collagen, despite its abundance in the body, encounters challenges in bone regeneration applications, particularly regarding mechanical stability and cost. Ongoing research aims to overcome these limitations by enhancing the bioactivity of collagen-based membranes.

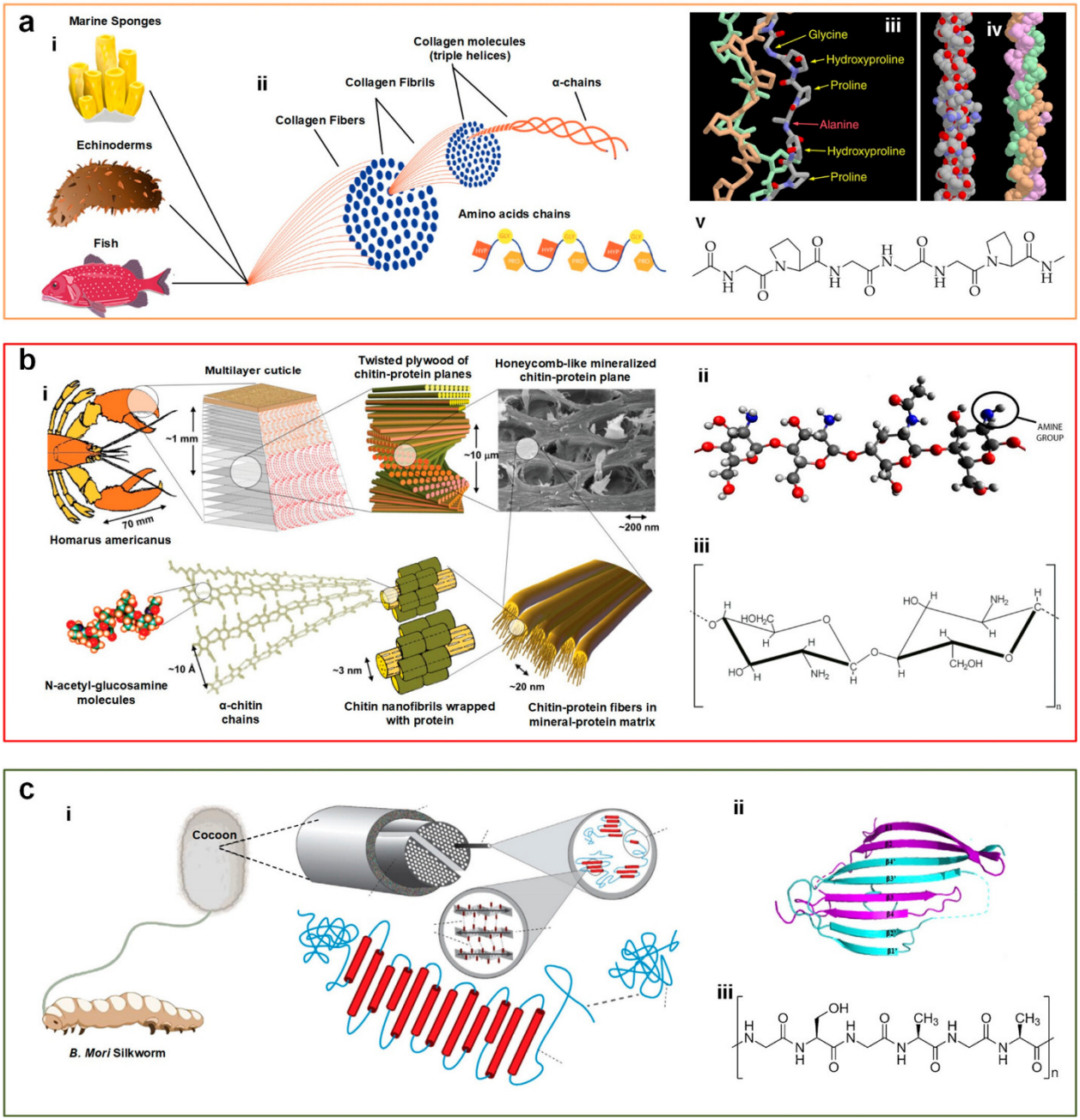


Figure 6.35. (a) Collagen, (b) chitosan, and (c) silk fibroin. (a-i) Some sea creatures are exemplary sources for collagen. (a-ii) Hierarchical microstructure of the collagen fiber. (a-iii) In the chemical composition of type I bovine collagen, the triple helix formation is composed of three frequently recurring amino acid sequences: (GlyPro/Hyp-Ala). (a-iv) 3D models of the type I bovine collagen: model at the left is highlighted by nitrogen atoms in blue and oxygen atoms in red, while the model at the right is color-coded to emphasize the three chains. (a-v) Chemical structure of collagen. (b-i) Hierarchical structure of the lobster cuticle. (b-ii) 3D structure of chitosan. (b-iii) Chitosan chemical structure. (c-i) Structure of Bombyx mori silk from the cocoon spun by B. mori silkworm. Silk fibroin displays two different structures, silk I and silk II, with distinct configurations. Silk I is characterized by an α helix formation, while silk II has an antiparallel β-sheet nanocrystal conformation. The 3D modeling (c-ii) and chemical structure (c-iii) of silk fibroin [10].

Collagen's Role in Guided Bone Regeneration (GBR):

1. Biological Significance:
   - Integral ECM Component: Collagen plays a vital role in the extracellular matrix (ECM).
   - Structural Support: Functions as a structural scaffold, facilitating cell attachment, proliferation, and tissue regeneration.

2. Benefits in GBR:
   - Cell Adhesion and Proliferation: Supports cell adhesion and proliferation, crucial for effective tissue regeneration.
   - Augmented Bone Formation: Contributes to heightened bone formation when incorporated in GBR procedures.
3. Bioactive Molecule Carrier:
   - Growth Factor Transport: Acts as a carrier for bioactive molecules, especially growth factors.
   - Regeneration Enhancement: Enables controlled growth factor release, further amplifying bone regeneration.
4. Material Attributes:
   - High Biocompatibility: Demonstrates excellent biocompatibility, minimizing the risk of adverse reactions.
   - Natural Biodegradability: Naturally degrades over time, aligning with the body's healing and regeneration processes.
   - Low Immunogenicity: Minimizes immune responses, ensuring safety for medical applications.
5. Versatile Material Forms:
   - Flexibility in Applications: Collagen can be processed into diverse forms, providing versatility in GBR applications.
   - Membranes, Sponges, Gels: Available in membrane, sponge, and gel forms, catering to a range of clinical requirements.

Collagen emerges as a promising material in GBR, not only due to its biological significance in facilitating cell functions and tissue regeneration but also because of its advantageous material properties. Its versatility and ability to act as a carrier for bioactive molecules make it a valuable component in the realm of regenerative dentistry and bone reconstruction.

6.7.2.2. Chitosan

Chitosan in Guided Bone Regeneration (GBR):

1. Origin and Characteristics:
   - Derived from Chitin: Chitosan, depicted in Figure 4b, is derived from chitin through the deacetylation process.
   - Biocompatible and Biodegradable: Exhibits biocompatibility, biodegradability, non-toxicity, antioxidant, anticancer, anti-inflammatory, and hemocompatible properties.
   - Unique Functionalities: Features amino groups and a hydroxyl group, attracting both negatively and positively charged molecules, enhancing mechanical and biological properties.
2. Biomedical Applications:
   - Widespread Attention: Gains extensive attention for biomedical applications, particularly in tissue regeneration.
   - Modifiability and Versatility: Can be modified with bioactive molecules and processed into diverse forms like membranes, hydrogels, sponges, and fibers.
3. Production Techniques:
   - Various Methods: Produced using techniques such as solvent casting, compression molding, freeze-drying, electrospinning, dense gas foaming, and microwave-assisted methods.
4. GBR Potential:
   - Cell Adhesion and Proliferation: Demonstrates the ability to promote cell adhesion and proliferation, essential for tissue regeneration.
   - Bone Stimulation: Stimulates bone formation and regeneration, showcasing potential for GBR applications.
   - Antibacterial Properties: Possesses antibacterial properties, contributing to infection prevention during bone healing.

5. Material Attributes and Challenges:
   - Biocompatible and Biodegradable: Exhibits low immunogenicity, biocompatibility, and biodegradability.
   - Processing Versatility: Can be processed into films, sponges, and microspheres, allowing for diverse applications.
   - Challenges: Faces challenges like poor mechanical properties and limited control over degradation rates.
6. Active Research Area:
   - Ongoing Exploration: Despite challenges, chitosan-based materials show potential in bone regeneration, prompting active research.
   - GBR Applications: While not yet a common natural resorbable membrane for GBR, ongoing research aims to evaluate its efficacy and safety.

Chitosan stands out as a promising candidate in GBR, leveraging its unique characteristics and ongoing research efforts to address challenges, emphasizing its potential impact in bone regeneration applications.

6.7.2.3. Silk Fibroin

Silk Fibroin in Guided Bone Regeneration (GBR):

1. Natural Polymer Source:
   - Derived from Silkworms: Silk fibroin, represented in Figure 4c, is a natural polymer obtained from Bombyx mori silkworm.
   - Bioinspired Material: Recognized as an excellent bioinspired material for tissue engineering and bone regeneration applications.
2. Biological Characteristics:
   - Biocompatibility and Biodegradability: Exhibits outstanding biocompatibility, biodegradability, and oxygen-water vapor permeability.
   - Mechanical Properties: Boasts favorable mechanical and physical properties, comparable to collagen.
   - Osteogenic Induction: Serves as a biodegradable scaffold inducing osteogenesis, mineral resorption, and bone regeneration in vivo.
3. Degradation and Resorption:
   - Nontoxic Degradation Products: Upon degradation, produces nontoxic amino acids easily absorbed in vivo.
   - Tunable Degradation Time: Allows tunable degradation time, ranging from a few days to several months.
4. Challenges and Strategies:
   - Brittleness Issue: Dries out and becomes brittle, impacting handling, mechanical strength, and durability.
   - Strategies: Strategies include adding plasticizers, controlling water content, and optimizing the manufacturing process to eliminate rigid β-sheet structures.
   - Sensitivity to pH and Temperature: Can be sensitive to changes in pH and temperature, affecting mechanical properties.
5. Forms and Shapes:
   - Versatile Fabrication: Fabricated in various forms – hydrogels, mats, films, and sponges – due to ease of processing.
   - Biomedical and Dental Applications: Excellent material for GBR in biomedical and pharmaceutical applications, particularly in dentistry.
6. Active Sites and Bonding Potential:
   - Bioactive Molecule Bonding: Active sites on silk surface facilitate bonding with bioactive molecules like growth factors and stem cells.
   - Facilitating Bone Regeneration: Contributes to bone regeneration and osteodifferentiation.

7. Manufacturing Techniques:
   - Diverse Techniques: Fabrication techniques include electrospinning, spin-coating, freeze-drying, micropatterning, and bioprinting.
   - Composite Materials: Silk-based composites incorporating polymers, hydroxyapatite, magnesium oxide, graphene, and antibacterial agents.
8. Enhancing Osteogenic Characteristics:
   - Functional Graded Membranes (FGMs): FGMs with silk fibroin and poly(ethylene oxide) (PEO) nanofibers for enhanced osteogenic cell growth and bone regeneration.
   - Stability and Degradability: Demonstrates excellent stability and degradability in artificial saliva solution.

Silk fibroin emerges as a versatile and promising material for GBR, leveraging its inherent biological properties and overcoming challenges through strategic modifications and innovative manufacturing techniques. Ongoing research focuses on enhancing its osteogenic characteristics for optimized GBR applications.

6.7.3. Synthetic Resorbable Membranes

Synthetic Resorbable Membranes in Guided Bone Regeneration (GBR):

1. Biocompatible and Degradable Design:
   - Objective: Engineered to be biocompatible and degrade over time, facilitating absorption by the body.
   - Promotes Regeneration: Aims to promote the regeneration of new bone tissue during the degradation process.
2. Examples of Synthetic Resorbable Membranes:
   - Polylactic Acid (PLA): PLA is one of the examples utilized for GBR. (101–103)
   - Polyglycolide (PGA): PGA is another synthetic membrane employed for GBR. (3,104)
   - Poly(lactic-co-glycolic) Acid (PLGA): PLGA, a copolymer of lactic and glycolic acids, is utilized in GBR. (103,105)
   - Polydioxanone (PDO): PDO is recognized as a synthetic resorbable membrane for GBR. (106,107)
   - Polycaprolactone (PCL): PCL serves as a resorbable membrane in GBR applications. (108–110)
   - Polyethylene Glycol (PEG): PEG membranes are employed in GBR procedures. (111,112)
3. Challenges of Synthetic Bioresorbable Membranes:
   - Resorption Rate Control: Synthetic membranes face challenges in controlling resorption rates, influenced by factors such as local pH.
   - Inertness Issues: Lack of inertness due to unfavorable reactions during degradation.
4. Resorption Rate and pH Dependency:
   - Uncontrolled Resorption: Synthetic membranes may lack precise control over their resorption, leading to variability in outcomes.
   - pH-Dependent Changes: Local pH variations can impact the resorption behavior of synthetic bioresorbable membranes.

Synthetic resorbable membranes offer a promising avenue for GBR, leveraging materials like PLA, PGA, PLGA, PDO, PCL, and PEG. However, addressing challenges related to resorption rate control and maintaining inertness during degradation remains crucial for optimizing their effectiveness in bone regeneration.

6.7.3.1. PLA

Poly(lactic acid) (PLA) in Guided Bone Regeneration (GBR):

1. Biodegradable Polymer for GBR:

- Composition: PLA is a biodegradable polymer composed of repeating lactic acid units (Figure 6.36.).
- Polyester Family: It belongs to the polyester family of synthetic polymers.

2. Biomedical Application in GBR:
   - Barrier Membranes: PLA is utilized to synthesize barrier membranes for biomedical applications, especially in GBR.
   - Cell Migration Control: PLA membranes act as barriers, preventing cell migration from soft tissue into bone defects while facilitating ingrowth of new bone cells.
3. Versatility in Forms and Combinations:
   - Forms: PLA can be fashioned into various forms like films, fibers, and meshes.
   - Combinations: Combining PLA with materials like chitosan, hydroxyapatite, or growth factors enhances its properties.
4. Adjustable Properties:
   - Molecular Weight and Crystallinity: PLA's physical and mechanical properties are adjustable by altering molecular weight and degree of crystallinity.
   - Enhancements: Adjustments improve handling, stability, and barrier characteristics of PLA membranes.
5. Challenges and Disadvantages:
   - Slow Degradation Rate: PLA's drawback includes a slow degradation rate, potentially leading to prolonged inflammation.
   - Acidic Degradation Products: Degradation results in acidic byproducts, increasing the risk of foreign body reactions.
6. Overcoming Limitations:
   - Modification Studies: Research focuses on modifying PLA, exploring copolymers and composite materials.
   - Enhanced Properties: Aimed at improving degradation rates and biocompatibility for more effective GBR applications.

Poly (lactic acid) serves as a versatile and promising material in GBR, with ongoing studies directed towards overcoming its limitations and enhancing its effectiveness in promoting bone regeneration.

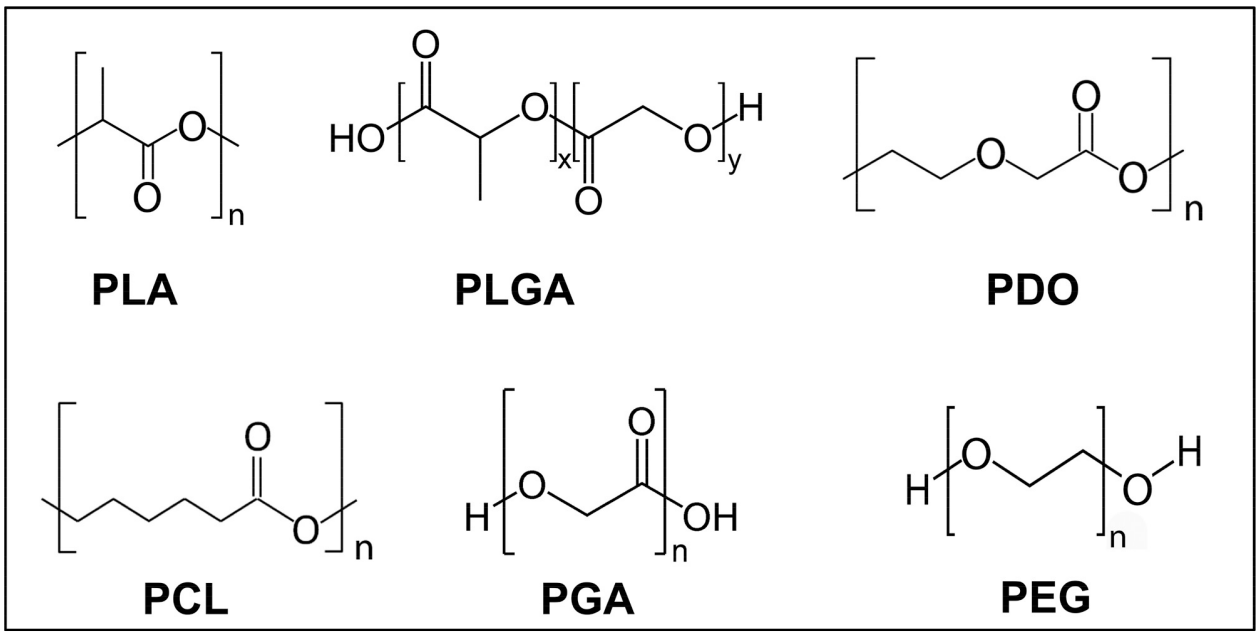


Figure 6.36. Chemical formulas of the classical synthesized polymers used as barrier membranes.

6.7.3.2. PGA

Polyglycolide (PGA) in Guided Bone Regeneration (GBR):

1. Biodegradable Polymer for GBR:
   - Composition: PGA is a biodegradable synthetic polymer composed of repeating glycolic acid units (Figure 5).
   - Polyester Family: A member of the polyester family, PGA has gained significant attention for GBR applications.
2. Degrades and Absorbs:
   - Degradation Time: PGA initiates degradation within weeks after implantation and is entirely absorbed within a few months.
   - No Removal Needed: Complete absorption negates the requirement for implant removal, minimizing infection and complications linked to nondegradable materials.
3. Versatile Medical Applications:
   - High Tensile Strength: PGA's high tensile strength makes it suitable for various medical applications like sutures, surgical mesh, tissue engineering scaffolds, and GBR barrier membranes.
   - Mechanical Improvements: When combined with materials like collagen or calcium phosphate, PGA's mechanical properties and degradation rate can be enhanced.
4. Biocompatibility and Bone Formation:
   - Promoting Bone Growth: Studies indicate PGA-based membranes promote new bone formation in GBR procedures.
   - Biocompatible Degradation Products: Degradation byproducts are biocompatible and nontoxic.
5. Thermal Stability and Sterilization:
   - High Thermal Stability: PGA exhibits high thermal stability and a high melting point, facilitating sterilization processes.
6. Inflammatory Response Mitigation:
   - Acidic Degradation Concerns: PGA may cause an inflammatory response due to acidic degradation products.
   - Modification Strategies: Modifications such as blending with other polymers or surface-modifying with hydroxyapatite aim to overcome inflammatory concerns.

Polyglycolide emerges as a promising candidate for GBR, with its biodegradability, versatile applications, and ongoing modifications to address potential inflammatory responses.

6.7.3.3. PLGA

PLGA in Biomedical Applications and GBR:

1. Biodegradable Copolymer:
   - Composition: PLGA (Poly(lactic-co-glycolic acid)) is a biodegradable and biocompatible copolymer composed of repeating units of lactic acid and glycolic acid (Figure 5).
   - Hydrolytic Degradation: PLGA undergoes hydrolysis in the body over time, allowing for controlled biodegradation.
2. Adjustable Degradation Rate:
   - Lactic Acid to Glycolic Acid Ratio: The degradation rate of PLGA can be finely tuned by adjusting the ratio of lactic acid to glycolic acid in the copolymer.
3. Desirable Properties for Biomedical Use:
   - Biocompatibility: PLGA exhibits good biocompatibility, making it suitable for various medical applications.
   - Controlled Degradation: The copolymer offers controlled degradation, ensuring it breaks down in a controlled manner.
   - Tunable Mechanical Properties: PLGA's mechanical properties can be adjusted, providing flexibility for different applications.

4. Versatile Applications:
   - Drug Delivery: PLGA microspheres are utilized for sustained drug delivery in the medical field.
   - Tissue Engineering: PLGA scaffolds find applications in tissue engineering, providing temporary support for new tissue growth.
5. Thermoplastic Nature:
   - Moldable and Shapable: PLGA is a thermoplastic polymer, allowing it to be melted and molded into various shapes, enhancing its versatility.
6. GBR Applications:
   - Scaffold Material: In GBR, PLGA is employed as a scaffold material, offering temporary support for new bone tissue growth.
   - Cell Attachment and Proliferation: PLGA scaffolds facilitate cell attachment and proliferation, promoting the formation of new bone tissue.
7. Tailored Mechanical Properties and Degradation Rate:
   - Optimized Conditions: PLGA scaffolds can be designed with specific mechanical properties and pore sizes, optimizing conditions for bone growth.
   - Matched Degradation Rate: The degradation rate of PLGA scaffolds can be adjusted to align with the rate of new bone growth.

PLGA's versatility, controllable properties, and compatibility make it a valuable asset in various biomedical applications, particularly in GBR, where it plays a crucial role in supporting and promoting new bone tissue formation.

6.7.3.4. PDO

Polydioxanone (PDO) in GBR and Surgical Applications:

1. Biocompatible and Absorbable Material:
   - Polymer Composition: PDO (Polydioxanone) is a biocompatible and absorbable polymer composed of repeating units of p-dioxanone (Figure 5).
   - Polyester Family: It belongs to the polyester family of polymers.
2. Versatile Surgical Applications:
   - Suture Material: PDO is commonly used as a suture material in various surgical procedures.
   - Flexibility and Handling: PDO sutures are flexible, easy to handle, and find applications in general surgery, orthopedics, and ophthalmology.
3. Degradation Characteristics:
   - Gradual Loss of Strength: PDO sutures start losing strength within the initial days after surgery.
   - Complete Absorption: Complete absorption by the body occurs within 4–6 months, providing a gradual breakdown.
4. Minimal Tissue Reaction:
   - Good Handling Properties: PDO is known for its good handling properties during surgical procedures.
   - Minimal Tissue Reaction: It exhibits minimal tissue reaction, contributing to reduced infection and wound healing complications.
5. Nonantigenic Nature:
   - Nonimmunogenic: PDO sutures are nonantigenic, reducing the likelihood of causing an immune response.
   - Low Tissue Reaction: Minimal tissue reaction further diminishes the risk of infection and complications in wound healing.
6. Balanced Mechanical and Degradation Properties:
   - Strength and Degradation Rate: PDO maintains a balance of mechanical strength and suitable degradation rate.

- Promising for GBR: These characteristics make PDO a promising option for GBR applications.

7. Challenges and Considerations:
   - High Cost: Despite its advantages, PDO is associated with high costs.
   - Tissue Inflammation: PDO may cause some tissue inflammation, requiring careful consideration in clinical use.

Polydioxanone's biocompatibility, absorbability, and balanced properties position it as a valuable material in surgical settings, particularly in GBR, where its characteristics contribute to effective wound closure and reduced complications.

6.7.3.5. PCL

Polycaprolactone (PCL) in Biomedical Applications:

1. Versatile Biodegradable Polymer:
   - Polyester Structure: PCL is a biodegradable thermoplastic polymer with an aliphatic polyester structure.
   - Six-Carbon Ester Units: Its repeating units consist of caprolactone, forming a six-carbon ester in the chemical formula [−(C6H10O2)n−] (Figure 5).
2. Diverse Applications:
   - Biomedical Material: PCL is widely used in biomedical applications, including controlled drug delivery, bioresorbable sutures, and as a component in 3D printing filaments.
   - Alternative to Petroleum-Based Plastics: PCL's flexible and amorphous structure provides distinctive mechanical properties, offering an alternative to petroleum-based plastics.
3. Material Properties:
   - Mechanical Characteristics: PCL exhibits good toughness, flexibility, and a low melting temperature due to its unique structure.
   - Resistance to Deformation: It maintains strength and shape even when subjected to bending or twisting.
4. Biocompatibility and Slow Degradation:
   - Ease of Processing: PCL is easy to process and biocompatible, making it suitable for various applications.
   - Controlled Degradation: Degradation rate can be controlled by modifying molecular weight and blending with other polymers.
5. Biological Perspective:
   - Carrier for Bioactive Agents: PCL serves as a carrier for bioactive agents like growth factors, antibiotics, and stem cells.
   - Enhancing Bone Regeneration: In osteogenesis, PCL can be crafted into porous scaffolds, creating an optimal environment for cell growth and promoting new bone tissue formation.
6. Water and Chemical Resistance:
   - High Water and Chemical Resistance: PCL is highly resistant to water and most organic materials, enhancing its suitability for biomedical, tissue engineering, and wound healing applications.
7. Applications in Drug Delivery and 3D Printing:
   - Controlled Drug Delivery: PCL microspheres and nanoparticles are employed in controlled drug delivery systems.
   - 3D Printing Filaments: Its compatibility with 3D printing makes PCL a valuable component in the fabrication of medical implants and structures.

Polycaprolactone's diverse applications, coupled with its biocompatibility, slow degradation, and resistance to deformation, position it as a versatile material in the realm of biomedical sciences and tissue engineering.

6.7.3.6. PEG

Polyethylene Glycol (PEG) in GBR and Tissue Engineering:

1. Bioresorbable Polymer:
   - Biocompatible and Low Toxicity: PEG is a bioresorbable polymer known for its excellent biocompatibility, low toxicity, and ease of processing (Figure 5).
   - Composite Applications: PEG is efficiently utilized in composite membranes and can be blended with other polymers, offering diverse options for GBR membrane design.
2. Barrier Membrane for GBR:
   - Hydrogel Effectiveness: Studies, particularly in animal models like rabbits, have explored PEG hydrogel as a promising barrier membrane for GBR.
   - Bone Regeneration Promotion: PEG-hydroxyapatite hybrid hydrogel has demonstrated the ability to support bone cell growth and promote bone regeneration both in vitro and in vivo, showcasing its potential in bone tissue engineering.
3. Enhancing Material Properties:
   - Plasticizer Role: PEG has been utilized as a plasticizer to enhance the material properties of other polymers, including Polycaprolactone (PCL).
   - Hardness Reduction: Its role in PCL formulations helps decrease hardness, lower the glass transition temperature, and reduce solvent requirements in manufacturing processes.
4. Clinical Outcomes in GBR:
   - Multicentered Clinical Trial: A multicentered randomized clinical trial by Jung et al. compared clinical outcomes of PEG with native collagen membranes in bony dehiscence-type defects around bone-level dental titanium implants.
   - Comparable Vertical Bone Fill: Results indicated that both PEG and collagen groups exhibited comparable vertical bone fill (59% and 64%) and a change in defect height.
   - Marginal Bone Level and Soft Tissue Conditions: Secondary parameters like marginal bone level (MBL) and soft tissue conditions were also recorded after 18 months of loading, with no statistical difference observed between the two groups.

In conclusion, PEG emerges as a promising material in GBR and bone tissue engineering applications, leveraging its biocompatibility, versatility in composite formulations, and positive outcomes in clinical trials.

6.7.4. Bioactive Composite Membranes

Bioactive composite membranes are innovative materials designed for various medical applications, including tissue engineering, drug delivery, and wound healing. By combining biocompatible and biodegradable polymers with bioactive molecules, these membranes aim to enhance biological activity and interaction with cells and tissues.

1. Tissue Engineering Advancements:
   - Collagen and Elastin-Like Polypeptide Hydrogel: Pal et al. developed a hydrogel with an interpenetrating network of collagen and elastin-like polypeptide, encapsulating BMP-2, doxycycline, and 45S5 Bioglass.
   - Enhanced Stem Cell Response: This composite hydrogel showed improved human adipose-derived stem cell attachment, proliferation, and differentiation toward the osteogenic lineage.
   - In Vivo Application: Implantation in a rat cranial defect model resulted in the development of mature mineralized tissue, showcasing potential for enhanced bone healing post-cranioplasty.
2. Drug Delivery Applications:
   - Sustained and Localized Delivery: Bioactive composite membranes serve as effective platforms for drug delivery.
   - Tailored Release of Therapeutic Agents: Bioactive molecules within these membranes can be engineered to release drugs or therapeutic agents over time, ensuring sustained and localized delivery to specific tissues.

3. Key Requirements for GBR Application:
   - Biocompatibility and Biodegradability: The success of bioactive composite membranes in GBR relies on their ability to be biocompatible and biodegradable.
   - Interaction with Cells and Tissues: Incorporation of bioactive molecules such as growth factors, peptides, and proteins facilitates interaction with cells, promoting cell proliferation, differentiation, and migration.
   - Enhanced Bone Healing: Application in GBR involves fostering the development of mature mineralized tissue, crucial for improved bone healing.
4. Future Research Directions:
   - Continued Exploration: Ongoing research aims to further enhance the efficacy of bioactive composite membranes in GBR and other medical applications.
   - Innovations in Bioactive Molecules: Advances in understanding the interactions between bioactive molecules and cells will drive innovations in membrane design.

In summary, bioactive composite membranes represent a cutting-edge approach in the medical field, with significant potential in tissue engineering, drug delivery, and GBR applications. Ongoing research will likely unveil further breakthroughs in material design and bioactive molecule incorporation, contributing to advancements in regenerative medicine.

6.7.4.1. Biocompatibility

The integration of collagen materials in surgical sites can elicit a foreign body reaction (FBR), an immune response triggered by the presence of foreign materials in the body. FBR involves complex processes mediated by immune cells and inflammatory mediators, leading to acute inflammation followed by resolution and remodeling. Monocytes and macrophages, crucial in this response, can adopt proinflammatory (M1) or proregenerative (M2) phenotypes, with a successful switch from M1 to M2 being pivotal for effective healing and regeneration.

FBR Minimization Strategies: To minimize FBR in Guided Bone Regeneration (GBR), biocompatible materials and techniques are employed. Chu et al. demonstrated the potential of epigallocatechin-3-gallate (EGCG)-modified collagen membrane (E-Col membrane) as an excellent barrier membrane for minimizing FBR and enhancing bone regeneration in vivo.

EGCG and Its Benefits: EGCG, the primary catechin in green tea, exhibits anticancer, anti-inflammatory, antifibrosis, and pro-osteogenesis characteristics. It has been suggested to modulate macrophage polarization in biomaterials. The study revealed that EGCG modification prevented keratinocyte migration, creating an environment conducive to osteoblast function without adverse effects on viability and adhesion.

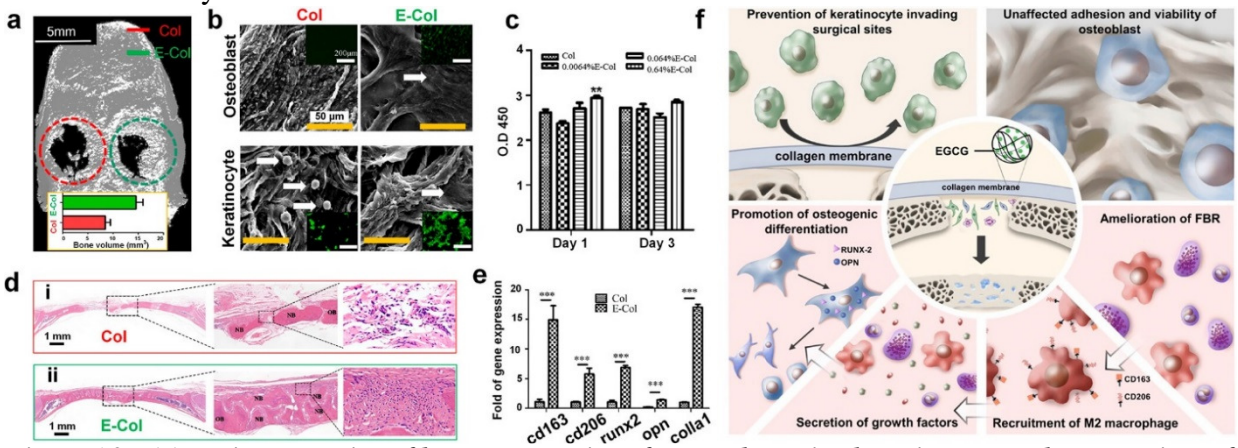


Figure 6.37. (a) In vivo promotion of bone regeneration after membrane implantation. Inset: the comparison of defect size with the bone volume using Micro-CT 4 weeks post membrane implantation of Col and E-Col. (b) SEM images of keratinocytes and osteoblast seeded on EGCG-modified collagen membranes with insets to show their corresponding live/dead staining. (c) Cell viability and (d) H&E staining of membrane sites 8 weeks post membrane implantation of Col (red rectangle circled) and E-Col (green rectangle circled), NB represents new regenerated bone. (e) Results of qPCR, which demonstrated that expression of CD206, CD163, RUNX2, OPN, and colla1 was significantly upregulated in E-Col compared to that of Col. (f) Schematic diagrams on the function of EGCG-modified collagen membrane [10].

In Vivo Bone Regeneration: The modified membrane with EGCG exhibited significantly higher cell viability compared to unmodified ones. Quantitative polymerase chain reaction (qPCR) analysis demonstrated increased expression of markers associated with proregenerative macrophages (CD206, CD163), osteogenesis (RUNX2, OPN), and collagen production (colla1) in E-Col membranes compared to pure collagen membranes.

Enhanced Bone Healing: Observations of bone healing indicated that EGCG-modified collagen membranes facilitated a switch from M1 to M2 phenotype, creating a favorable environment for bone regeneration. Thicker and more organized bone formation was noted, while the pure collagen membrane showed increased fibrous tissue, an undesirable outcome.

Conclusion: The study highlights the favorable attributes of EGCG-modified collagen membranes in mitigating FBR, creating an environment conducive to proregenerative macrophage polarization, and promoting in vivo bone regeneration in the context of guided bone regeneration practices. These findings underscore the potential of innovative biomaterial modifications in optimizing outcomes in regenerative medicine.

Recent progress in osteogenesis regulation involves the incorporation of nutrient elements that significantly enhance osteogenic differentiation. This innovative approach goes beyond creating a mere physical barrier, evolving toward bioactive barriers capable of osteo-immunomodulation, thereby presenting an effective strategy to improve bone regeneration.

Calcium Ions and Calcium-Sensing Receptor (CaSR): Calcium ions play a crucial role in triggering the calcium-sensing receptor (CaSR), a member of the G protein-coupled receptor superfamily. CaSR is a key player in maintaining calcium homeostasis. Activation of CaSR has been linked to a reduction in Wnt5A protein, leading to the suppression of inflammation. This insight into the role of calcium ions suggests their potential in creating an environment conducive to osteogenic differentiation.

Zinc Ions and Immune Cell Functionality: Zinc ions contribute to the normal function and development of immune cells. Deficiency in zinc can impair the production and signaling processes of inflammatory cytokines. By ensuring an adequate supply of zinc ions, the membrane supports immune cell functionality, potentially influencing the immune response during bone regeneration.

Silicon Ions and Wnt3 Pathway Activation: Silicon ions, when released from the membrane, are speculated to activate the Wnt3 pathway. This pathway is a signaling molecule crucial in the regulation of bone formation and remodeling. The incorporation of silicon ions presents an intriguing avenue for influencing specific signaling pathways that contribute to enhanced osteogenesis.

Paradigm Shift: The reported findings underscore the need for a paradigm shift in the design of the next generation of membranes. Moving beyond the conventional role of a physical barrier, the emphasis is on transforming membranes into bioactive barriers. Osteo-immunomodulation emerges as a focal point, aligning with the understanding that immune responses intricately intertwine with osteogenic processes. The integration of nutrient elements, such as calcium, zinc, and silicon ions, into membranes reflects a progressive approach to bone regeneration. By influencing specific cellular pathways and immune responses, bioactive barriers hold promise in ushering in a new era of effective osteogenesis regulation.

6.7.4.2. Mechanical Stability

Mechanical stability stands as a pivotal factor in the efficacy of Guided Bone Regeneration (GBR) barrier membranes, as their collapse into defect spaces can impede bone regeneration. Overcoming the limitations of mechanical instability in aqueous environments is crucial for expanding the applications of barrier membranes in biomedicine and pharmaceuticals (Figure 6.38).

Cross-Linking for Stability: Cross-linking is a common strategy to enhance membrane stability, making them less susceptible to rapid enzymatic degradation. Cross-linked membranes exhibit superior mechanical stability compared to their non-cross-linked counterparts. However, the use of many cross-linkers is hindered by their toxicity or immunogenicity, limiting their in vivo applications.

UV Radiation as a Non-Toxic Cross-Linking Technique: Addressing the challenge of toxic cross-linkers, Acevedo et al. proposed the use of UV radiation as a non-toxic cross-linking technique to bolster the mechanical properties of a biodegradable gelatin-chitosan membrane. Gelatin and chitosan, combined in a polyelectrolyte complex, form a biopolymer with enhanced physical and mechanical properties. Gelatin, derived from incomplete denaturation of collagen, offers cost-effectiveness and reduced antigenicity.

Membrane Composition: The gelatin-chitosan membrane comprised 56% gelatin, 42% chitosan, and a homogeneous distribution of 1% titania (TiO2) and 1% hydroxyapatite (HAp) nanoparticles. Gelatin's favorable properties, such as cell adhesion and proliferation, coupled with chitosan's contributions, create a versatile copolymer capable of embedding biological molecules like growth factors.

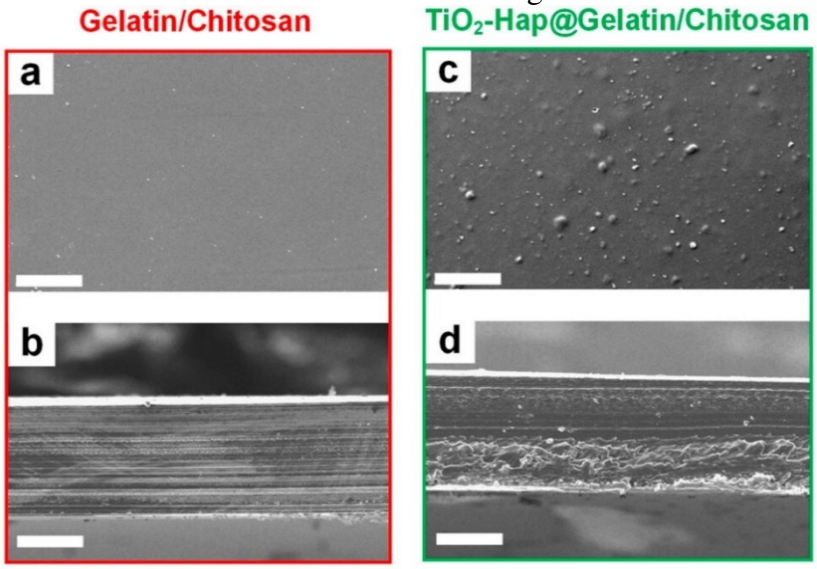
UV Cross-Linking Optimization: UV radiation doses were systematically varied, demonstrating a significant enhancement in membrane stiffness with increasing UV doses, indicative of efficient cross-linking. The optimal mechanical properties were achieved at an optimum UV dosage of 20 J·cm–2, signifying the maximum cross-linking state.

Biocompatibility and Concerns: The UV-treated membranes exhibited improved cell adhesion, spreading, and growth velocity, affirming their acceptable biocompatibility. However, as the UV treatment increased, the degradation percentage decreased to zero, raising concerns, especially regarding non-resorbable titania nanoparticles, classified as a possible human carcinogen by the World Health Organization's International Agency for Research on Cancer (IARC).

Conclusion: The study presents UV radiation as a promising non-toxic cross-linking technique, effectively enhancing the mechanical stability of gelatin-chitosan membranes. Balancing biocompatibility and potential concerns associated with nanoparticles remains a critical consideration for future applications in GBR.

Efforts to enhance barrier membranes for Guided Bone Regeneration (GBR) applications have led to innovative combinations of materials. Ansarizadeh et al. have developed a novel membrane by synergizing collagen-chitosan with lyophilized advanced platelet-rich fibrin (A-PRF). This composite membrane showcases remarkable mechanical stability, cell viability, degradability, and osteogenic differentiation (Figure 6.39.).

Mechanical Enhancement through Synergy: Systematic adjustments in the Chit/Col weight ratio and A-PRF concentration unveiled a substantial boost in Young's modulus, peaking at 8 MPa for a Chit/Col ratio of 4 and A-PRF concentration of 0.58 mg·mL–1.



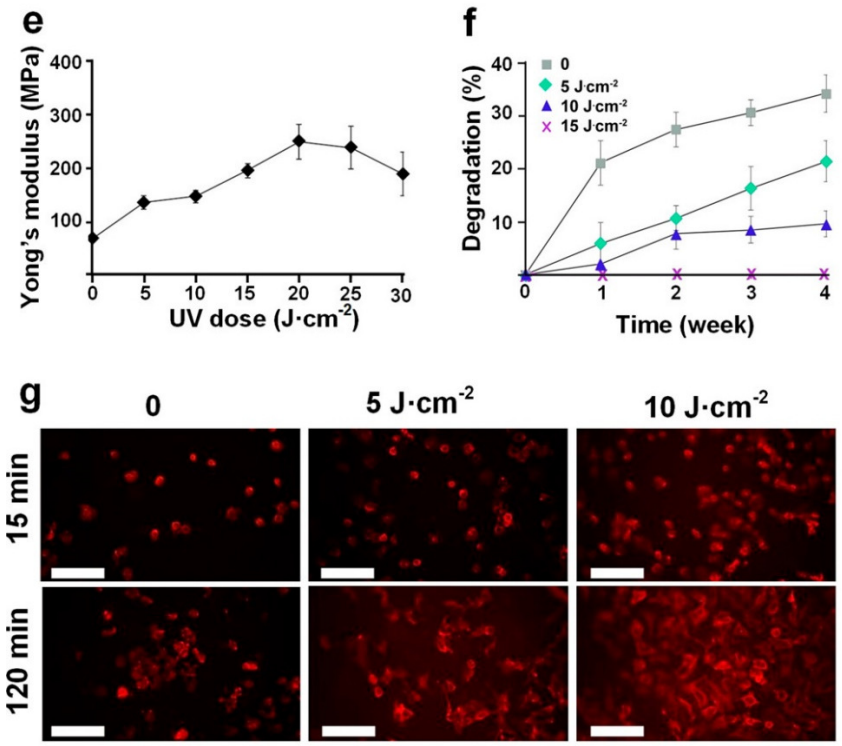
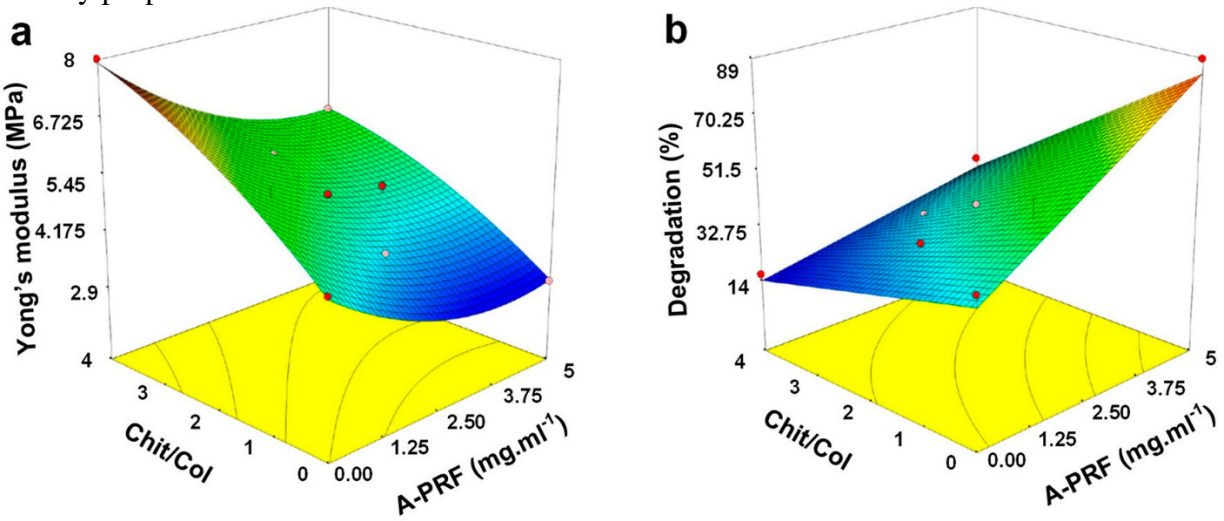


Figure 6.38. SEM images of the nanocomposed gelatin-chitosan membrane: (a) top view and (b) transversal section of the membrane without nanoparticles (red rectangle circled) and corresponding (c) top and (d) side views of membrane incorporated with nanoparticles (green rectangle circled). (e) Mechanical and (f) degradation behavior of the UV-irradiated nanocomposed gelatin-chitosan membranes. (g) Cell spreading on UV-irradiated nanocomposed gelatin-chitosan membranes at different time intervals. Scale bars are 100 µm. MEF cells in suspension (2,5 × 10^5 cells/film) were allowed to attach and spread onto UV-irradiated membranes (0, 5, and 10 J·cm^{-2}) for 15 and 120 min [10].

This improvement can be attributed to heightened cross-linking between collagen and chitosan chains due to free amine groups in chitosan, leading to morphological changes, reduced pore size, and increased interconnectivity within collagen-based membranes.

Pore Size, Cell Infiltration, and Nutrient Diffusion: Smaller pore sizes have previously been associated with enhanced mechanical properties, cell infiltration, nutrient diffusion, and improved cell survival rates. The observed reduction in pore size in the developed membranes contributes to these positive attributes, supporting the potential effectiveness of the membrane in GBR applications.

Cell Viability and Adhesion: An increase in Chit/Col weight ratio and A-PRF concentration positively influenced cell viability, ascribed to a higher number of amine groups facilitating improved cell adhesion. The synergy between the two components results in a membrane with superior cell-friendly properties.



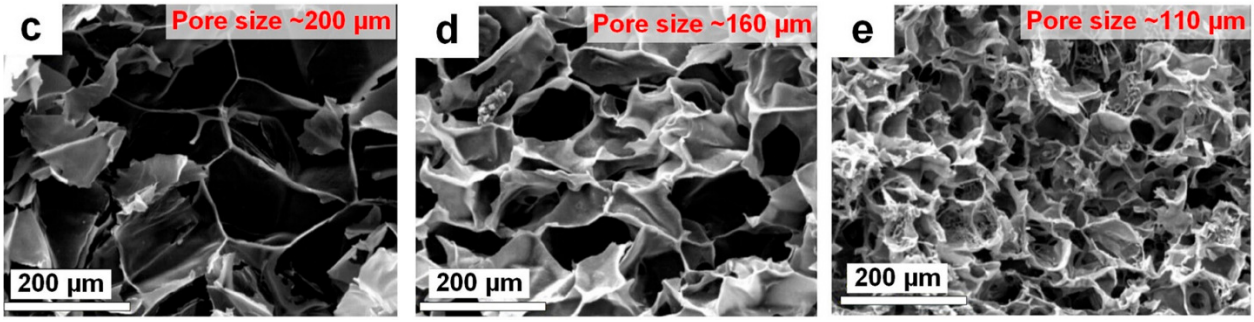


Figure 6.39. (a) Effect of Chit/Col weight ratio and A-PRF concentration on Young's modulus of the membrane. (b) Effect of Chit/Col weight ratio and A-PRF concentration on degradation rate of membrane. The cross-sectional SEM images of membranes made of (c) collagen, (d) collagen-chitosan (Chit/Col weight ratio = 1), and (e) collagen/chitosan (Chit/Col weight ratio = 4) [10].

Degradation Rate and Growth Factors: Increased A-PRF concentration correlates with a heightened degradation rate in the fabricated membranes. This is attributed to the higher degradability of fibrins, leading to an elevated release rate of growth factors compared to collagen and chitosan. This dynamic feature could play a crucial role in promoting tissue regeneration.

Optimization through Mathematical Modeling: Utilizing a response surface methodology, a polynomial model was constructed to explore the correlation between the independent variables (Col/Chit/A-PRF ratios) and predict the optimum ratios. This mathematical approach aids in fine-tuning the membrane composition for optimal performance in GBR applications.

Conclusion: The study demonstrates a synergistic approach in membrane development for GBR, combining collagen-chitosan with lyophilized A-PRF. The optimized membrane composition showcases enhanced mechanical stability, cell viability, and degradability, laying the groundwork for further advancements in GBR technologies.

Chen et al. introduced a novel composite scaffold by combining elastin-like polypeptide (ELP) and silk fibroin (SF) through a simple and environmentally friendly dehydrothermal treatment. This scaffold exhibited unique mechanical properties and demonstrated support for the adhesion, proliferation, and differentiation of bone mesenchymal stem cells and chondrocytes in vitro. Furthermore, it showed promising results in enhancing cartilage and subchondral bone repair in vivo. The versatility of this composite makes it a potential biomaterial for tissue repair and osteochondral applications.

Influence of Resorbable Collagen Membrane Type on GBR Healing: Omar et al. conducted a comparative study on the efficacy of two resorbable collagen membranes for Guided Bone Regeneration (GBR) in rat femurs. The elastin-collagen membrane exhibited a higher percentage of new bone formation in the central defect area compared to pure collagen. Molecular analysis revealed variations in BMP2 expression, suggesting that the choice of resorbable collagen membrane can impact the healing process in GBR procedures. These findings underscore the importance of membrane selection in optimizing GBR outcomes.

Reinforcement with Elastin-Like Polypeptide (ELP) for Improved Mechanical Properties: Gurumurthy et al. reinforced collagen with Elastin-Like Polypeptide (ELP) and optimized the composite composition using response surface methodology. The optimized collagen-ELP composite displayed enhanced tensile strength, elastic modulus, and toughness. ELP contributed to reduced residual water content and interacted with collagen, resulting in a dense microstructure. These reinforced composites hold promise for constructing rigid, porous structures suitable for tissue engineering applications.

Enhancing Mechanical Properties with Poly(ε-caprolactone) (PCL): PCL, a biodegradable and biocompatible polymer, has been employed to enhance the mechanical stability of barrier membranes. Previous studies reported the development of natural-synthetic polymers, incorporating PCL, with improved mechanical properties and modulated degradation rates. To address PCL's slow degradation, Joo et al. designed a dual-layered membrane embedding PCL and gelatin into an alginate sheet. An activation stage involved embedding beta-tricalcium phosphate (β-TCP) molecules into the

membrane, leveraging its biocompatibility for potential applications in bone tissue engineering and dental implants.

These advancements in composite scaffolds and reinforced membranes underscore the dynamic progress in tailoring biomaterials for optimal GBR outcomes, encompassing mechanical strength, biocompatibility, and tissue regenerative potential.

Alginate-based materials have been employed in Guided Bone Regeneration (GBR) to protect bone defects and act as a source of growth factors, promoting bone formation and remodeling. These materials, besides enhancing bone repair and regeneration, also reduce the risk of complications like bacterial infection. Alginate exhibits pH-dependent strength properties, becoming firm in the acidic environment of the wound area. Studies combining PCL, gelatin, and β-TCP have shown improved cell attachment, osteogenic differentiation, and cell proliferation. (Figure 6.40.).

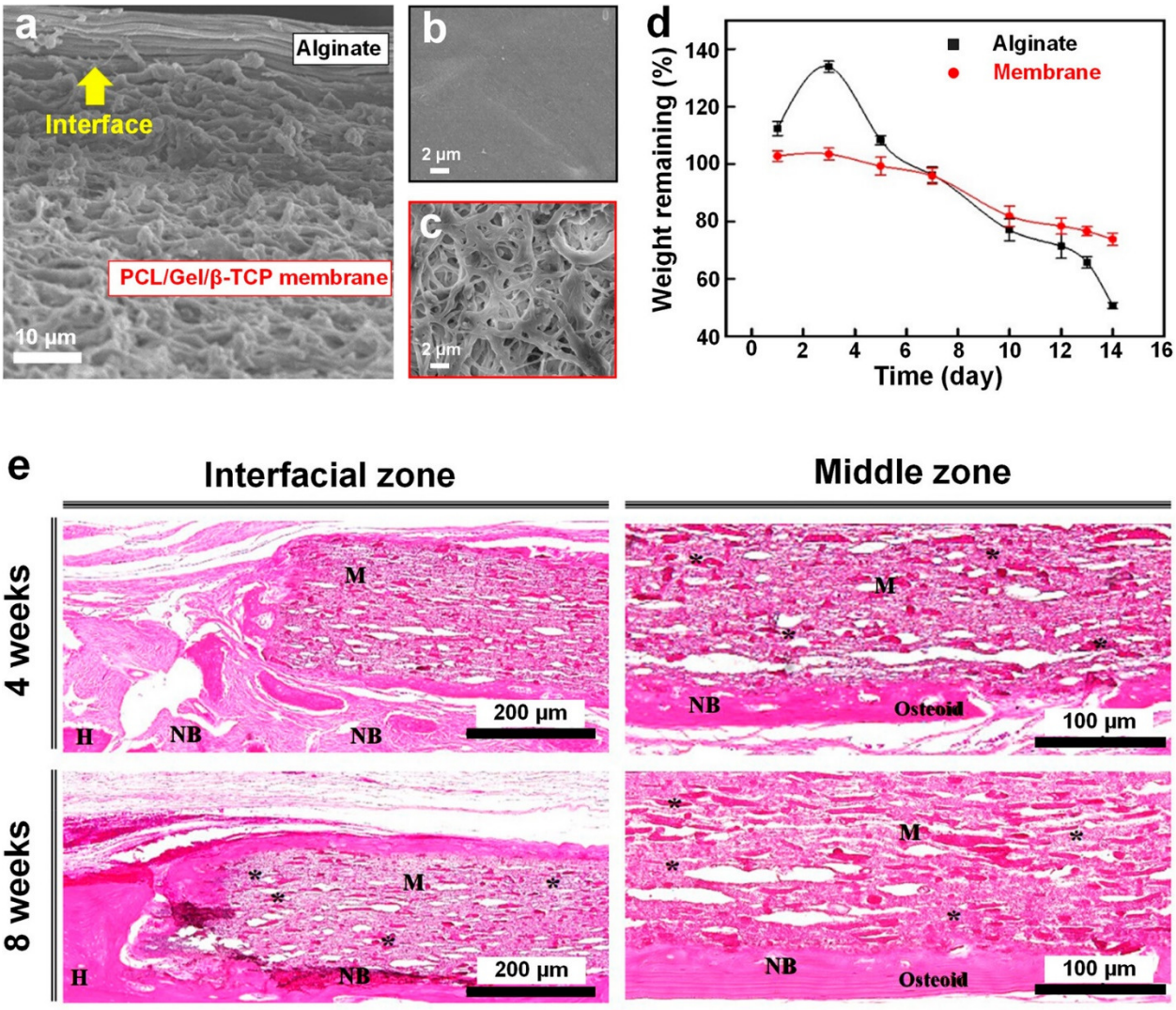


Figure 6.40. SEM images of (a) a dual-layered membrane made of (b) an alginate sheet and (c) the electrospun cross-linked PCL/Gel/β-TCP membrane. The yellow arrow indicates the alginate-membrane interface. (d) Quantitative study of in vitro post degradation weight loss of electrospun membrane and casted alginate sheet. (e) H&E stained images of electrospun membrane after 4 and 8 weeks of implantation. M: membrane, H: host, NB: new bone formation. Asterisk (*) denotes the bone ingrowth via pores of the membrane [10].

In vivo histologic analysis demonstrated good space maintenance, impressive new bone formation, and integration into surrounding tissues without inflammation.

Addressing Poor Cell Adhesion of PCL with β-TCP Inclusion: PCL, a biodegradable and biocompatible polymer, is known for its poor cell adhesion and inadequate wettability properties due to low surface energy and hydrophobicity.

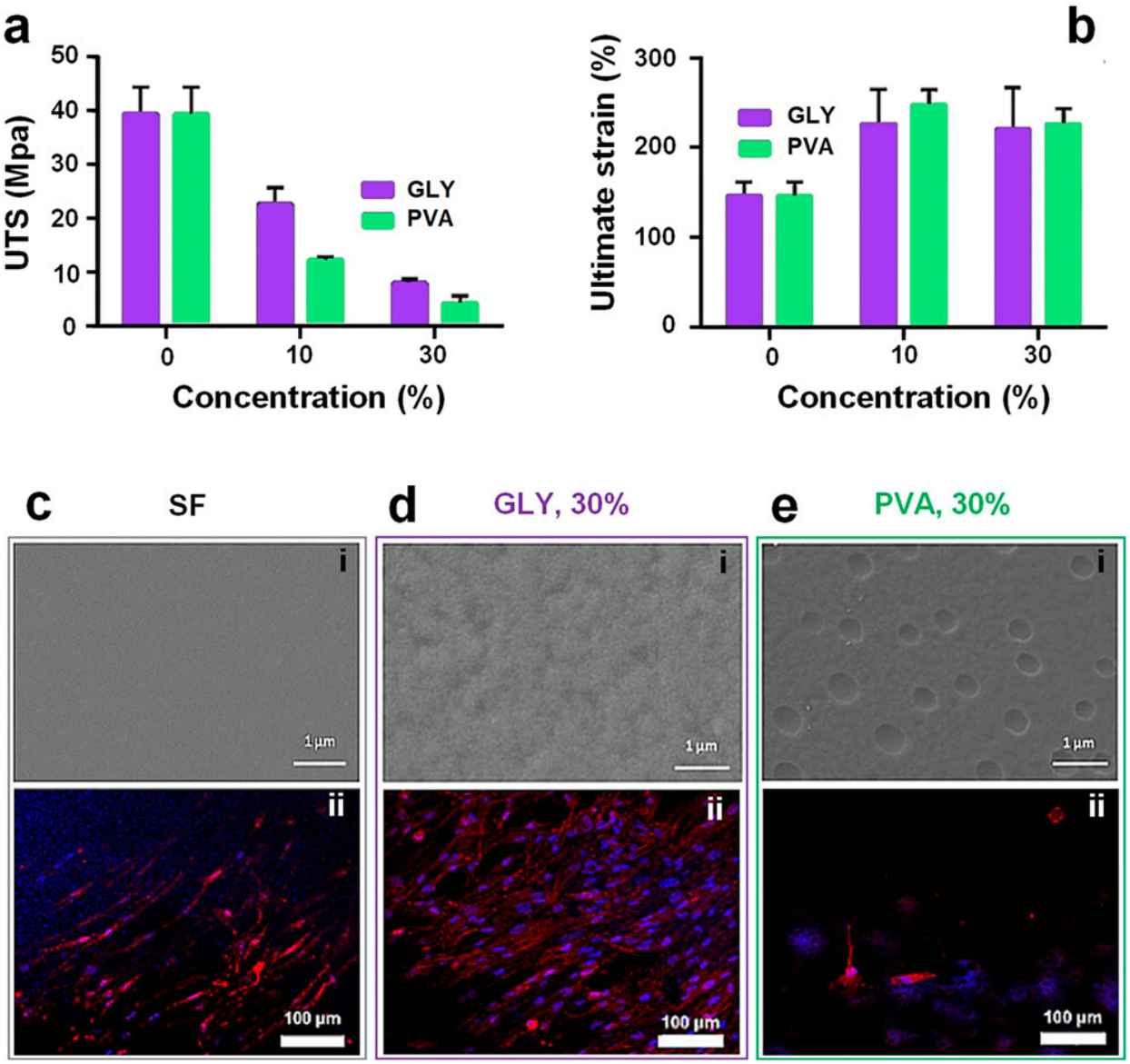


Figure 6.41. Representative (a) ultimate tensile stress (UTS) and (b) ultimate strain of membranes with different GLY and PVA content. (i) SEM micrographs and (ii) confocal images of the produced SF-based membranes: (c) pure SF, (d) 70SF:30GLY, and (e) 70SF:30PVA dried for 12 h [10].

To address this, studies have incorporated β-TCP into PCL-gelatin membranes. β-TCP not only enhances cell adhesion but also acts as a precursor for Ca2+ and PO43– ions, encouraging bone regeneration in osteogenesis. Electrospun nanofibers with β-TCP showed improved mechanical stability, wettability, and roughness, along with enhanced cell affinity and proliferation. The inclusion of β-TCP resulted in optimal mechanical properties, higher hydrophilicity, and increased gene expression of osteogenic markers.

Flexible Silk Fibroin Membrane with Plasticizers (GLY and PVA): Silk fibroin, while possessing high tensile strength, becomes brittle upon drying, limiting its elongation. To overcome this, Geão et al. designed a flexible silk fibroin membrane by incorporating glycerol (GLY) and polyvinyl alcohol (PVA) as plasticizers. GLY and PVA increased membrane elongation significantly while reducing ultimate tensile strength. The addition of 10% plasticizer improved surface roughness with an acceptable degree of transparency. In vitro studies demonstrated enhanced human periodontal ligament cell adhesion, viability, and proliferation with GLY, attributing it to the higher hydrophilicity caused by hydroxy (–OH) groups (Figure 6.41.).

These developments highlight the versatility of biomaterials, including alginate, PCL, and silk fibroin, in tailoring membranes for GBR applications, addressing challenges such as poor cell

adhesion, brittleness, and mechanical instability. Incorporation of specific additives and techniques enhances their properties, paving the way for improved outcomes in bone regeneration [10].

6.7.5. Antibacterial Activity

Bacterial infection in Guided Bone Regeneration (GBR) membranes poses a significant challenge, potentially leading to complications and procedure failure. Common bacterial species causing infection include Streptococcus spp, Staphylococcus spp, and Porphyromonas gingivalis.

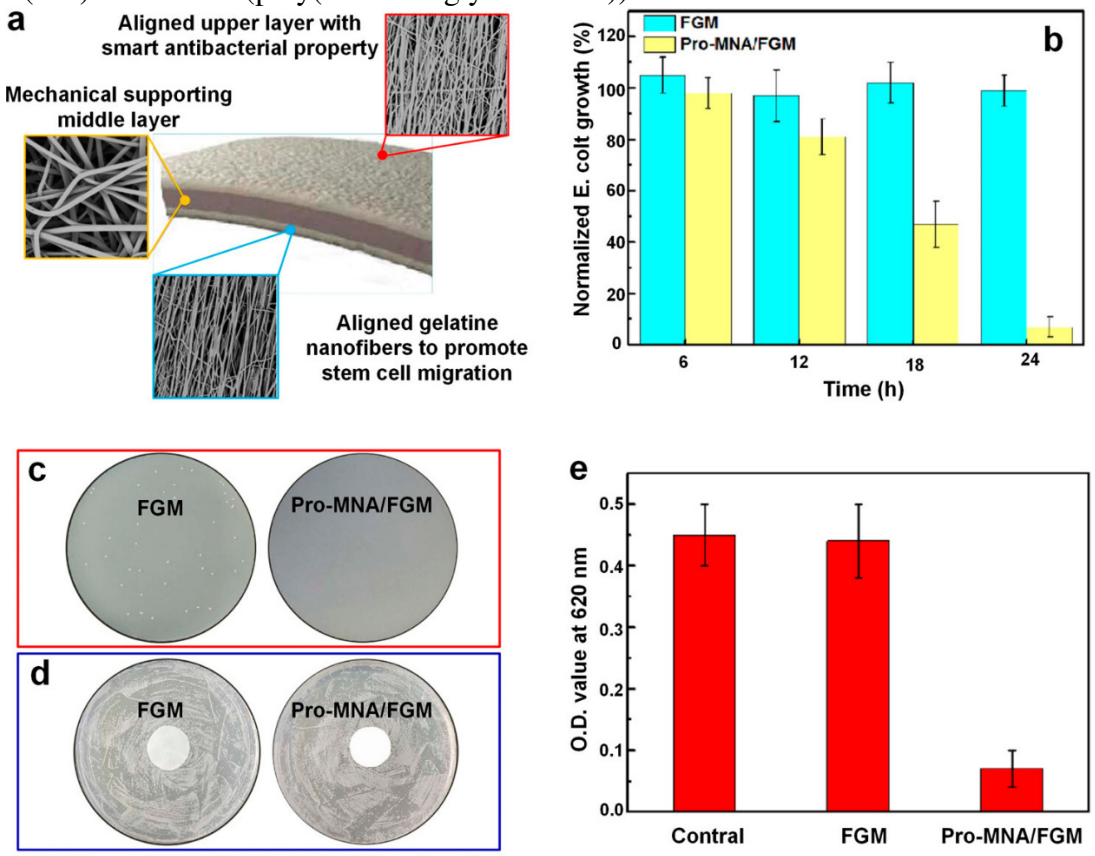
Directly doping membranes with antibiotics is a reported solution, but uncontrollable continuous release hinders real-world applications. He et al. designed a two-layered Functionally Graded Membrane (FGM) with gelatin as the surface layer for biocompatibility and PCL as the core material.

This membrane exhibited enhanced mechanical properties compared to gelatin alone. The interfacing space was loaded with pro-metronidazole (Pro-MNA), a hydrophobic and water-insoluble prodrug form of metronidazole, to create a self-defensive membrane with controllable antibiotic release. Pro-MNA/FGM significantly restrained bacterial growth, demonstrating infection-responsive release triggered by esterase accumulation and decreased pH value.

Pro-MNA/FGM inhibited bacterial growth, prevented bacterial adhesion on cells, and exhibited inherent self-defensive antibacterial properties.

Epithelial cell adhesion and proliferation were enhanced, attributed to the synergistic effect of chemical composition and fiber alignment. These developments offer a promising approach to combating bacterial infection in GBR membranes, potentially improving overall procedure outcomes (Figure 6.42.).

Abe et al. discovered that the PLCL (poly(L-lactic acid-co-caprolactone)) bilayer membrane exhibited reduced bacterial adhesion and effectively blocked bacterial penetration compared to collagen (Col) and PLGA (poly(lactic-co-glycolic acid)) membranes.



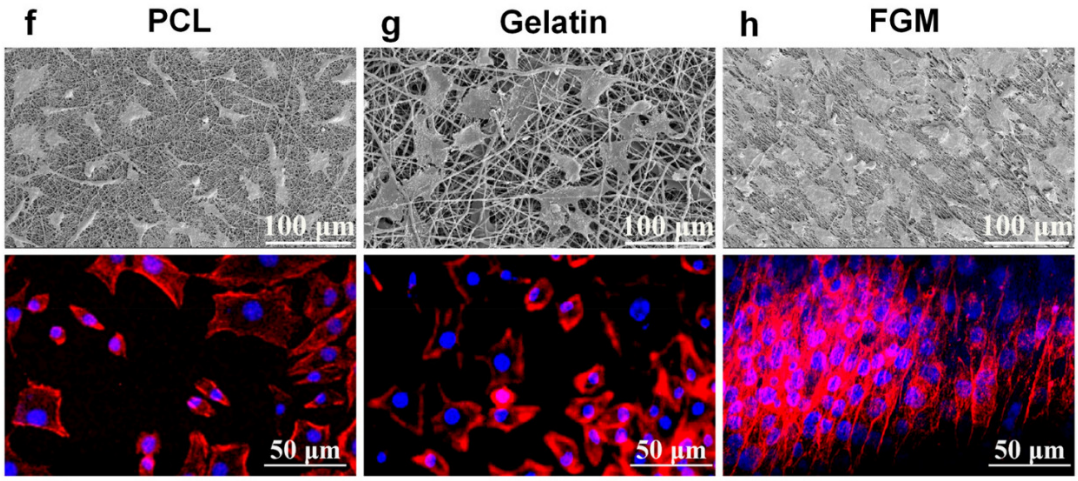
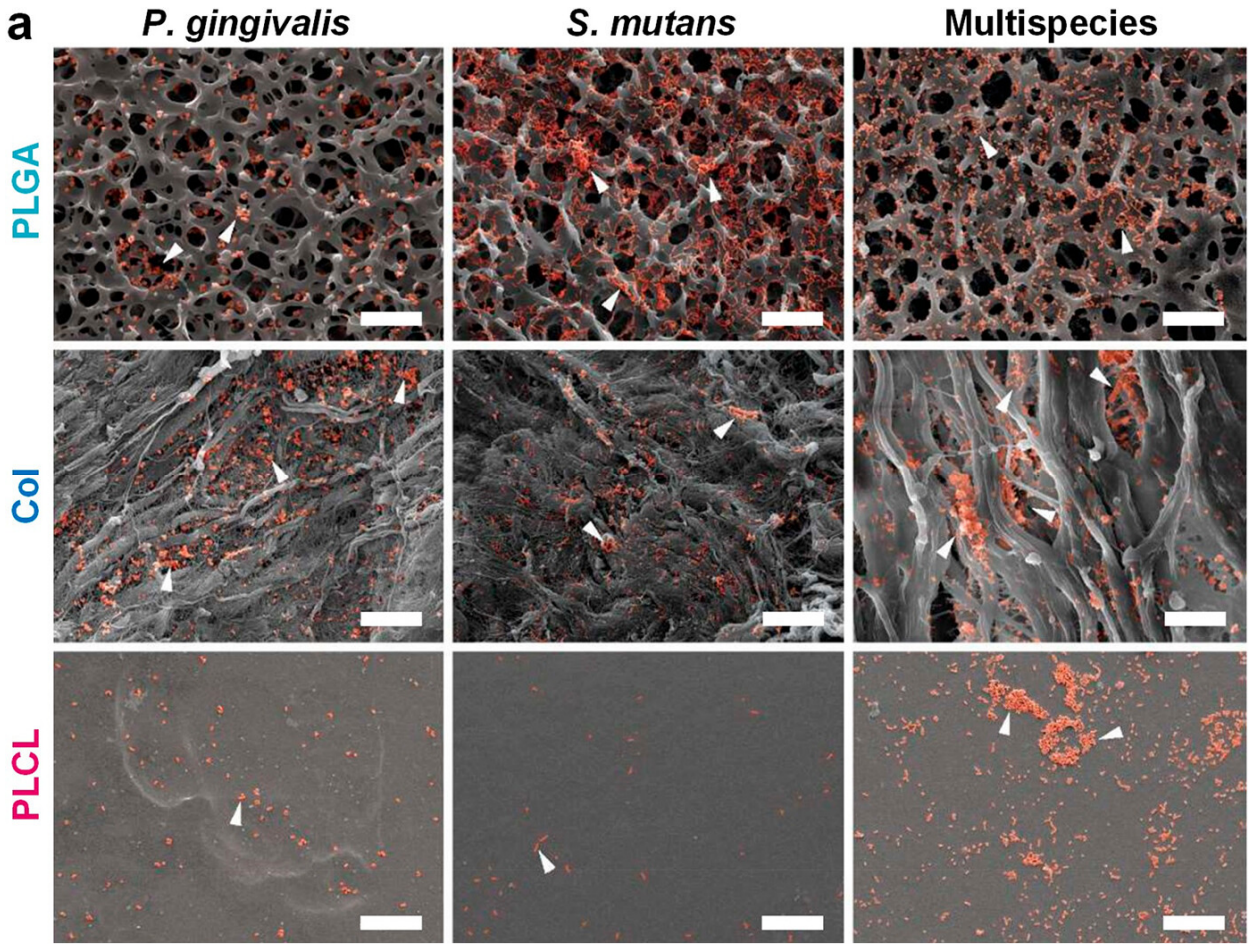


Figure 6.42. (a) Sandwich structured multifunctionalized graded membrane. (b) Normalized growth of E. coli incubated with the membranes for different durations. (c, left) Plate samples showing colonies of S. aureus and inhibition zone of the membrane: the sample incubated with FGM (without Pro-MNA loading) shows some bacterial colonies were formed. (c, right) No bacterial colonies formed for the sample incubated with Pro-MNA/FGM. (d) Nonetheless, both the control sample and Pro-MNA/FGM did not exhibit a consistently stable inhibition zone, which suggests that no MNA diffused from the membrane. (e) Quantitative study of the OD. values in the bacteria-cell infection model to investigate the bacterial growth. (f-h) SEM micrographs (up) and confocal fluorescent images (bottom) of cells proliferated on R-PCL, R-gelatin, and FGM membranes for 7 days [10].

The study involved assessing the adherence of P. gingivalis and Streptococcus mutans to the membranes.



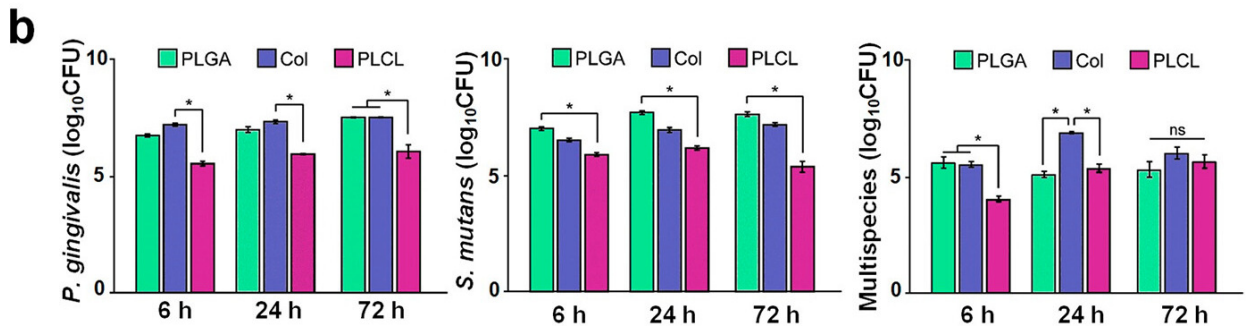


Figure 6.43. (a) SEM images of the P. gingivalis, S. mutans, and multiple bacteria obtained from human saliva cultured on PLGA, Col, and PLCL membranes after 24 h. White arrows indicate the bacterial cells (colored in orange for a clear vision). All scale bars are10 µm. (b) CFU counts of cultured P. gingivalis, S. mutans, and multiple bacteria obtained from human saliva on the three membranes at different time intervals.

Key findings include:

1. P. gingivalis Adherence:
   - The PLCL membrane showed fewer adherent P. gingivalis cells compared to PLGA and Col membranes.
   - Significantly lower numbers of adherent P. gingivalis were observed on the PLCL membrane compared to the Col membrane.
   - No statistical difference between PLCL and PLGA membranes until after 72 hours of incubation with P. gingivalis.
2. S. mutans Adherence:
   - The PLCL membrane exhibited significantly fewer adherent S. mutans cells than the PLGA membrane after 6, 24, and 72 hours of incubation.
   - The PLCL membrane had a lower number of adherent cells compared to the Col membrane, although statistical significance was not found.
3. Human Saliva Bacterial Counts:
   - CFU counts from membranes incubated with bacteria from human saliva indicated that the PLCL compact layer had significantly fewer CFUs than PLGA and Col at 6 hours.
   - After 72 hours of incubation, no statistical differences in CFU counts were observed between any of the groups.

The favorable properties of the PLCL membrane, including reduced bacterial adhesion and penetration, suggest potential benefits for regenerative treatments. The membrane's efficient barrier function may be particularly advantageous in managing complications in guided tissue and bone regeneration, making it a promising candidate for enhancing regenerative outcomes in clinical settings (Figure 6.43.).

6.7.6. Cell Proliferation Enhancement

Growth factors play a pivotal role in stimulating and regulating bone growth and healing, particularly in procedures like Guided Bone Regeneration (GBR) and Guided Tissue Regeneration (GTR). These procedures involve the delivery of growth factors to the defect site through carrier materials. Some commonly used growth factors in oral surgery include Platelet-derived growth factor (PDGF), Growth/differentiation factor 5 (GDF-5), Fibroblast growth factor-2 (FGF-2), and recombinant human bone morphogenetic proteins (rhBMP-2 and rhBMP-9).

Challenges in Growth Factor Application:

- Determining the optimal dose for GTR and GBR procedures is challenging.
- Lack of consensus and standardization in growth factor production and preparation.
- Increased costs associated with growth factor usage.

Hydrogel-Based Biomaterials for Tissue Engineering:

- Shirzaei Sani et al. introduced a methacrylated hyaluronic acid (MeHA) and elastin-like polypeptide (ELP) hydrogel.

- This hydrogel is elastic, antimicrobial, and adhesive, addressing limitations of traditional hydrogels.
- Incorporation of zinc oxide nanoparticles enhances antimicrobial properties.
- In vivo implantation demonstrates biodegradability and promotion of autologous tissue integration.

Bioactive Collagen Membranes with Growth Factors:

- Yamano et al. investigated collagen membranes loaded with PDGF and GDF-5 for bone regeneration.
- GDF-5 showed accelerated, dose-dependent bone regeneration compared to PDGF.
- GDF-5-loaded membranes exhibited higher ALP, cell proliferation, and osteogenic gene expression.
- Thoma et al. compared rhPDGF-BB and rhBMP-2 for bone regeneration around dental implants in dogs.

FGF-2 in Alveolar Ridge Preservation:

- Wang et al. explored the use of Fibroblast Growth Factor-2 (FGF-2) in alveolar ridge preservation.
- Acellular dermal matrix (ADM) membranes loaded with FGF-2 significantly inhibited alveolar bone width reduction.
- FGF-2-loaded membranes showed an inhibitory effect on alveolar bone width reduction compared to control groups.

These studies highlight the diverse approaches in utilizing growth factors and biomaterials to enhance tissue regeneration in GBR and GTR procedures, addressing challenges and improving clinical outcomes (Figure 6.44).

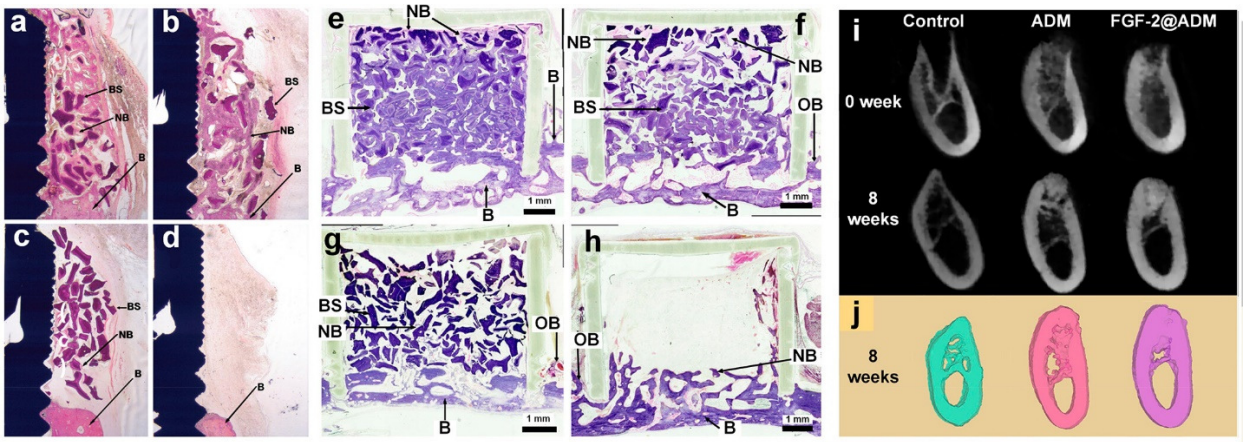


Figure 6.44. Bone growth at 8 weeks on varying membrane groups: (a) DBBM/BMP-2, (b) DBBM/PDGF, (c) DBBM, and (d) control. H&E stained images of the histologic slide of different group cylinders after 8 weeks of healing: (e) DBBM/BMP-2, (f) DBBM/PDGF, (g) DBBM, and (h) empty control. (i) CBCT observation of extraction socket healing between control, ADM, and FGF-2@ADM immediately and 8 weeks after surgery. (j) 3D reconstruction images of the middle region of extraction socket matching to the three groups mentioned above 8 weeks post-surgery.

BMP-9 Overview:

- BMP-9 belongs to the BMP family of growth factors, playing a crucial role in bone formation regulation.
- It exhibits a potent osteogenic effect in various animal models.

Carrier Systems for BMP-9:

- Study by Kobayashi et al. evaluated the effectiveness of two carrier systems, porcine-derived CM (Collagen Membrane) and DBBM (Deproteinized Bovine Bone Mineral), for BMP-9 delivery in a rabbit calvarial defect model.
- CM treated with rhBMP-9 led to complete resolution of horizontal bone deficiency with no signs of multinucleated giant cells (MNGC).

- New bone height and area significantly increased in CM-rhBMP9 and DBBM-rhBMP9 groups compared to control, CM, and DBM groups.
- DBM-rhBMP-9 resulted in a significantly greater amount of mineralized tissue compared to DBM alone.
- CM, when combined with rhBMP-9, may offer a more consistent stimulation of bone growth and complete coverage of affected areas.

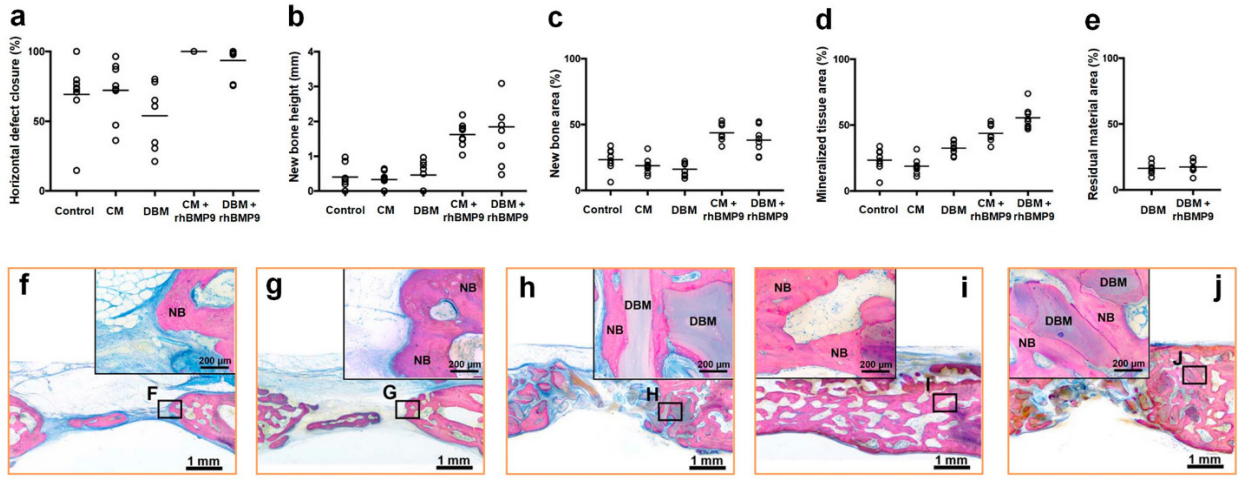


Figure 6.45. Histomorphometrical measurements of linear parameters: (a) percentage of horizontal defect closure in each group; (b) length of maximum new bone height in the middle area of defect; (c) percentage of new bone area, (d) mineralized tissue area, and (e) residual material area in DBM and DBM1rhBMP9 groups. Dot plots show the data for all specimens and the bars indicate the average of the values in each group. Pictures of the toluidine blue and fuchsin staining in bone defects at 8 weeks in (f) control, (g) CM, (h) DBM, (i) CM+rhBMP9, and (j) DBM+rhBMP9 groups. Insets correspond to the rectangles accordingly. NB shows new bone, and DBM refers to residual materials [10].

Comparison of Carrier Systems:

- Another study compared bone regeneration performance of rhBMP-9 loaded on DBBM and CM in a rabbit model.
- CM/rhBMP-9 samples achieved nearly complete closure of horizontal bone defects with new bone layers in CM-implanted areas and bone growth surrounding DBBM materials.
- Both DBBM/rhBMP-9 and CM/rhBMP-9 significantly enhanced new bone formation, demonstrated by increased mineralized tissue volume and new bone height and area.
- CM/rhBMP-9 showed higher effectiveness in promoting wound closure compared to DBBM-rhBMP-9, possibly due to the higher absorption tendency of BMP-9 by CM over other bone grafts and barrier membranes.

Conclusion:

- BMP-9, when combined with appropriate carrier systems, shows promise in promoting bone growth and regeneration.
- Further research is needed, including large animal studies with various bone grafts and barrier membranes, to validate and explore these results comprehensively (Figure 6.45. and 6.46.).

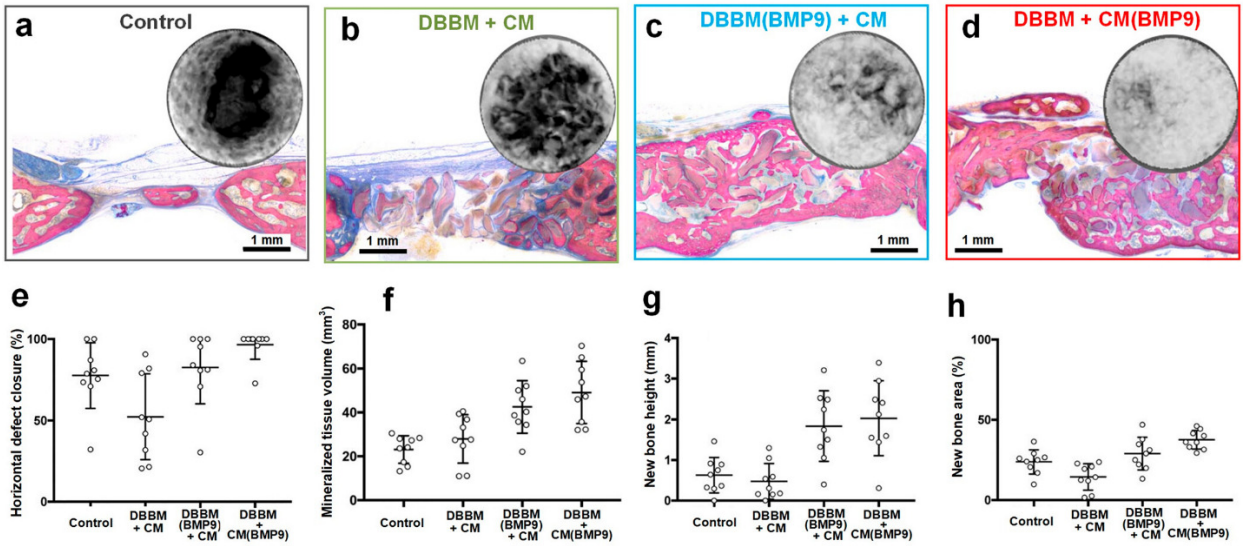


Figure 6.46. Toluidine blue and fuchsin staining on the middle sections in the bone defects at 8 weeks in (a) control, (b) DBBM/CM alone, (c) DBBM(BMP9)+CM, and (d) DBBM+CM(BMP9) groups. Insets: μCT images in bone defects from the top view at 8 weeks. (e) Statistical study of the horizontal bone defect closure. (f) Mineralized tissue volume measured by μCT, (g) length of new bone height in the middle area of the defect, and (h) new bone area. Dot plots present data for all specimens, and bars indicate the average and SD of the values in each group [10].

6.8. Quiz 6.

1. Which of the following properties are characteristic of collagen scaffolds used in tooth tissue engineering?
a). Excellent biocompatibility
b). Controlled degradation
c). Mimicking the mineral component of natural teeth
d). Ability to support cell growth and differentiation
e). Chemical stability

2. What are the characteristics of nanofiber scaffolds fabricated using the electrospinning technique?
a). Thicker nanofibers and larger interfibrillar spaces in random nanofiber scaffolds
b). Thicker nanofibers and smaller interfibrillar spaces in aligned nanofiber scaffolds
c). More organized structure in random nanofiber scaffolds
d). Enhanced cell viability observed in all nanofiber scaffold formulations
e). Cells on random or aligned 10% PCL nanofiber scaffolds showed decreased adhesion and spreading

3*. What was observed in terms of cellular response to the fabricated nanofiber scaffolds using the electrospinning technique?
a). Live/Dead assay images demonstrated cytotoxicity for all nanofiber scaffold formulations
b). Enhanced cell viability was observed only in NR-15%PCL group at 3 and 7-day periods
c). Cell proliferation decreased for all groups over time
d). NR-10%PCL, NA-10%PCL, and NA-12,5%PCL maintained higher cell viability at 7 days
e). Cells on random or aligned 15% PCL nanofiber scaffolds showed increased adhesion and spreading

4. Which characteristics make hydrogels suitable for tissue engineering applications?
a). Biocompatibility
b). Biodegradability
c). Ability to mimic extracellular matrix architecture
d). Mechanical rigidity
e). Resistance to enzymatic cleavage

5. What are essential for the degradation of hydrogels in tissue engineering?
a). Gradual breakdown to accommodate new tissue formation
b). Simple dissolution in solution
c). Hydrolysis of ester bonds
d). Rapid degradation to prevent immune reactions
e). Enhanced mechanical strength

6. Which of the following are methods employed in three-dimensional (3D) tissue engineering for dental stem cell regeneration?
A) Introducing cells into engineered scaffolds to mimic the microenvironment of human tissues.
B) Administering dental stem cells directly into the bloodstream for tissue repair.
C) Utilizing customized 3D tooth implants with dental stem cells seeded in appropriate scaffolds.
D) Implanting dental stem cells into native tissues without any scaffolds.
E) Culturing dental stem cells in isolation without any engineered structures.

7. Which of the following characteristics are attributed to dental pulp stem cells (DPSCs) based on the provided passage?
A) DPSCs possess a higher proliferation rate compared to bone marrow stem cells (BMSCs).
B) DPSCs have been primarily explored for their application in liver tissue regeneration.
C) Co-culturing DPSCs with apical bud cells (ABCs) has shown enhanced odontogenic differentiation compared to co-culturing with BMSCs.
D) DPSCs lack multipotency and can only differentiate into one type of tissue.
E) DPSCs have not shown any potential for neural differentiation in comparison to other types of stem cells.

8. Which of the following statements accurately describe dental follicle progenitor cells (DFPCs) and their role in tissue regeneration, as per the provided passage?
A) DFPCs are primarily isolated from the enamel organ of human third molar teeth.
B) DFPCs express stem cell markers such as Notch and Nestin and possess potential for osteogenic, adipogenic, chondrogenic, and neural differentiation.
C) Studies have extensively explored the integration of DFPCs in 3D tissue regeneration, revealing their enhanced differentiation potential in various culture systems.
D) DFPCs have shown limited differentiation potential and are only useful for bone tissue regeneration.
E) DFPC-loaded collagen-nano-HA/OPS constructs have demonstrated inferior osteogenic differentiation compared to other scaffolds in in vivo experiments.

9. Which of the following statements accurately describe natural resorbable barrier membranes in guided bone regeneration (GBR) procedures?
A) These membranes are primarily composed of synthetic materials like polyethylene.
B) Their main function in GBR procedures is to remain permanently in the body without undergoing any resorption.
C) They facilitate bone formation by separating the bone defect from surrounding soft tissue and promoting bone growth in the isolated area.
D) Natural resorbable barrier membranes necessitate a second surgery to remove them once bone regeneration is complete.
E) These membranes are biocompatible with the body's tissues and integrate into the natural healing process, gradually resorbing over time.

10. Which of the following statements accurately describe bioactive composite membranes and their applications in guided bone regeneration (GBR) and other medical fields?
A) Bioactive composite membranes combine non-biodegradable polymers with bioactive molecules to enhance biological activity.
B) They have shown potential for enhanced bone healing by fostering the development of mature mineralized tissue, as demonstrated in a rat cranial defect model.
C) Bioactive composite membranes are primarily used for wound healing applications and have limited efficacy in tissue engineering.
D) In drug delivery applications, these membranes are incapable of sustaining the localized release of therapeutic agents over time.
E) Key requirements for successful GBR application of bioactive composite membranes include biocompatibility, biodegrability, and the incorporation of bioactive molecules to promote cell proliferation and differentiation.

References

[1]. Kong, L.X., Peng, Z., Li, S.D., Bartold, M., 2006. Nanotechnology and its role in the management of periodontal diseases. Periodontology 2000 40, 184-196.

[2]. Pepla E, Besharat LK, Palaia G, Tenore G, Migliau G. Nano-hydroxyapatite and its applications in preventive, restorative and regenerative dentistry: a review of literature. Ann Stomatol (Roma). 2014 Nov 20;5(3):108-14. PMID: 25506416; PMCID: PMC4252862.

[3]. Shahriar Shahi, Fatemeh Dehghani, Elaheh Dalir Abdolahinia, Simin Sharifi, Elham Ahmadian, Márió Gajdács, Krisztina Kárpáti, Solmaz Maleki Dizaj, Aziz Eftekhari, Taras Kavetskyy, Effect of gelatinous spongy scaffold containing nano-hydroxyapatite on the induction of odontogenic activity of dental pulp stem cells, Journal of King Saud University - Science, Volume 34, Issue 8, 2022, 102340, ISSN 1018-3647, https://doi.org/10.1016/j.jksus.2022.102340.

[4]. C. Pushpalatha, V.S. Gayathri, S.V. Sowmya, Dominic Augustine, Ahmed Alamoudi, Bassam Zidane, Nassreen Hassan Mohammad Albar, Shilpa Bhandi, Nanohydroxyapatite in dentistry: A comprehensive review, The Saudi Dental Journal, Volume 35, Issue 6, 2023, Pages 741-752, ISSN 1013-9052, https://doi.org/10.1016/j.sdentj.2023.05.018.

[5]. Li, Zhang & Morsi, Yosry (Yos) & Wang, Yanying & Li, Yubao. (2013). Review scaffold design and stem cells for tooth regeneration. Japanese Dental Science Review. 49. 14–26. 10.1016/j.jdsr.2012.09.001.

[6]. Zahedah, Rola & Dinç, Bircan. (2023). Challenges in Optimizing 3D Scaffold for Dentin- Pulp Complex Regeneration. Bulletin of Biotechnology. 4. 68-73. 10.51539/biotech.1242537.

[7]. Leite, Maria Luisa & Soares, Diana & Anovazzi, Giovana & Soares, Igor & Hebling, Josimeri & Costa, Carlos. (2020). Development of fibronectin□loaded nanofiber scaffolds for guided pulp tissue regeneration. Journal of Biomedical Materials Research Part B: Applied Biomaterials. 109. 10.1002/jbm.b.34785.

[8]. Atia, G.A.N.; Shalaby, H.K.; Ali, N.G.; Morsy, S.M.; Ghobashy, M.M.; Attia H.A.N.; Barai, P.; Nady, N.; Kodous, A.S.; Barai, H.R. Three Dimensional Bioactive Polymeric Hydrogels for Oral, and Craniofacial Tissue Engineering: New Challenges and Prospective Applications: A Narrative Review. Pharmaceuticals 2023, 16, 702.

[9]. Hsiao HY, Nien CY, Hong HH, Cheng MH, Yen TH. Application of dental stem cells in three-dimensional tissue regeneration. World J Stem Cells 2021; 13(11): 1610-1624.

[10]. Sara Abtahi, Xiaohu Chen, Sima Shahabi, and Noushin Nasiri, Resorbable Membranes for Guided Bone Regeneration: Critical Features, Potentials, and Limitations, ACS Materials Au **2023**, 3 (5), 394-417, DOI: 10.1021/acsmaterialsau.3c00013

7. Nanotechnology in Orthodontics

Nanotechnology offers promising avenues for innovation in various aspects of orthodontic treatment. Ongoing research aims to leverage nanomaterials to improve the performance, comfort, and outcomes of orthodontic interventions. Further studies are needed to fully explore the potential of nanotechnology in orthodontics and to translate these advancements into clinical practice effectively [1].

Application of Nanotechnology in Orthodontics:

1. Orthodontic Elastomeric Ligatures:
   - Nanomaterials are being explored for the development of elastomeric ligatures used in orthodontic treatment.
   - These materials aim to improve the properties of traditional elastomers, such as elasticity, durability, and biocompatibility.
2. Orthodontic Power Chains:
   - Nanotechnology is applied to enhance the performance of orthodontic power chains, which are used for tooth movement.
   - Nanomaterials may improve the flexibility, strength, and frictional properties of power chains, leading to more efficient and comfortable orthodontic treatment.
3. Orthodontic Miniscrews:
   - Nanomaterials are investigated for the fabrication of orthodontic miniscrews used as temporary anchorage devices.
   - These materials aim to improve the stability, biocompatibility, and osseointegration of miniscrews, enhancing their effectiveness in orthodontic treatment.
4. Friction Force Reduction:
   - Nanotechnology offers strategies to reduce friction between orthodontic brackets and archwires, which can influence the efficiency and comfort of treatment.
   - Surface modifications using nanomaterials aim to minimize frictional resistance, allowing smoother tooth movement during orthodontic therapy.
5. Nanorobots and Tissue Engineering:
   - Emerging research explores the potential of nanorobots and tissue engineering in orthodontics.
   - Nanorobots may enable precise and targeted delivery of therapeutic agents, while tissue engineering approaches aim to regenerate oral tissues for orthodontic purposes.
6. Stem Cells for Bone Augmentation and Cartilage Regeneration:
   - Nanotechnology plays a role in harnessing stem cells for bone augmentation and cartilage regeneration in orthodontic procedures.
   - Nanomaterials may provide scaffolds and growth factors to support the proliferation and differentiation of stem cells for tissue regeneration.

7.1. Orthodontic Elastomeric Ligatures

The use of orthodontic elastomeric ligatures (OEM) in orthodontic treatment provides numerous benefits such as quick application and patient comfort at a low cost. However, these ligatures are prone to microbiological colonization during treatment, leading to increased accumulation of bacterial plaque, enamel decalcification, and worsened oral health indicators such as bleeding rates. The irregular surfaces of orthodontic auxiliaries contribute to the difficulty in maintaining proper oral hygiene and self-cleansing, exacerbating bacterial growth.

Efforts to mitigate the effects of microbiological biofilms on oral health have led to investigations into the chemical characteristics of elastic ligatures and modifications to inhibit bacterial colonization. Some studies have explored ligatures that release fluoride, but results regarding their effectiveness against decalcification and long-term antimicrobial properties have been inconsistent.

An emerging approach involves incorporating nanoparticles into elastomeric ligatures to confer anticariogenic or anti-inflammatory properties, or to deliver antibiotic drugs such as benzocaine. Medicated wax applied to orthodontic brackets has also been explored for its ability to release benzocaine, reducing mucosal irritation associated with brackets.

Recent studies have investigated the use of silver nanoparticles in orthodontic ligatures due to their strong antibacterial properties. Silver nanoparticles have been shown to counter dental biofilms and reduce enamel demineralization without compromising the mechanical characteristics of the material or the effectiveness of orthodontic therapy. Silver nanoparticles can be obtained using minimally invasive methods from natural sources such as flowers and mushrooms. Silver exhibits superior antibacterial efficacy compared to other metals and has good compatibility with human cells. However, further research is needed to ascertain their biocompatibility in orthodontic applications [1].

7.2. Orthodontic Power Chains

Orthodontic power chains, commonly used in orthodontic practices, are typically composed of polymeric materials such as polyesters or polyethers formed through polymerization. They offer several clinical advantages, including affordability, user-friendliness, and the ability to provide light and continuous forces for tooth movement. Additionally, power chains are highly flexible and aid in space closure, particularly in cases involving tooth extraction.

However, power chains also have limitations. Their mechanical effectiveness diminishes over time, necessitating periodic replacement. Both intrinsic and external factors contribute to the degradation of power chains, leading to permanent deformation. Intrinsic factors include material composition, production methods, and external morphology, while external factors encompass oral cavity temperature, pH, and moisture absorption. Additionally, power chains are hydrophilic and prone to discoloration over time due to fluid absorption from the oral cavity, which can compromise oral health maintenance.

To address these challenges, researchers have explored surface treatments such as nanoimprinting to enhance the physical properties of power chains. Nanoimprinting involves creating nanostructures, known as nanopillars, on the surface of the chains. Studies, such as the one conducted by Cheng et al. in Taiwan, have shown promising results with nanoimprinting. This treatment transforms the material from hydrophilic to hydrophobic, mitigating the shortcomings associated with conventional power chains and potentially improving their performance and longevity in orthodontic treatment [1].

7.3. Orthodontic Bands

Fixed orthodontic treatment often involves the placement of dental bands, which are crucial for various orthodontic movements.

However, these auxiliaries can lead to the accumulation of bacterial plaque, especially in hard-to-reach posterior dental areas, posing challenges for oral hygiene maintenance.

Prolonged plaque retention around orthodontic brackets and bands can result in a rapid shift in the oral bacterial flora, favoring acidogenic bacteria like Streptococcus mutans and Lactobacilli. This, in turn, increases the risk of enamel demineralization, white spot lesions, and cavities.

To address these issues, various methods have been studied to prevent cariogenic events, with fluoride-containing products being a commonly explored option. However, the efficacy of such products heavily depends on patient compliance and the accuracy of domiciliary hygiene procedures.

Advancements in technology have enabled the addition of antimicrobial agents to dental resins and cements, aiming to reduce the incidence of white spot lesions and cavities while maintaining adhesion properties.

These agents may include zinc oxide, chlorhexidine, and fluorides, which help in reducing the acidic oral environment and bacterial metabolism.

Furthermore, the incorporation of antibacterial release materials, such as silver nanoparticles, into band cements has been investigated to improve oral hygiene during orthodontic treatment.

These resins demonstrate mechanical properties comparable to conventional materials and are generally considered biocompatible. However, further studies are required to validate their efficiency in the oral environment over the duration of an entire orthodontic treatment [1].

7.4. Orthodontic Miniscrews

Managing anchorage during orthodontic treatment is crucial for achieving successful outcomes.

Temporary anchorage devices (TADs), such as miniscrews, miniplates, and implants, have been integrated into orthodontic practice to assist in controlling anchorage and creating the desired force system while minimizing undesired tooth movements.

TADs are inserted into the bone to provide direct or indirect orthodontic anchorage. Direct anchorage occurs when TADs function independently, while indirect anchorage involves supporting and reinforcing anchoring teeth.

These devices typically achieve stability through mechanical means, such as cortical or bicortical stabilization, without requiring biomechanical osseointegration (figure 7.1.).

Among TADs, miniscrews have become preferred by clinicians due to their versatility, simplicity of insertion and removal, affordability, and ease of use by orthodontists without the need for surgical intervention.

Miniscrews can be inserted at various sites in the maxilla and mandible, including the vestibular bone, interradicular space, zygomatic buttress, symphysis, and hard palate.

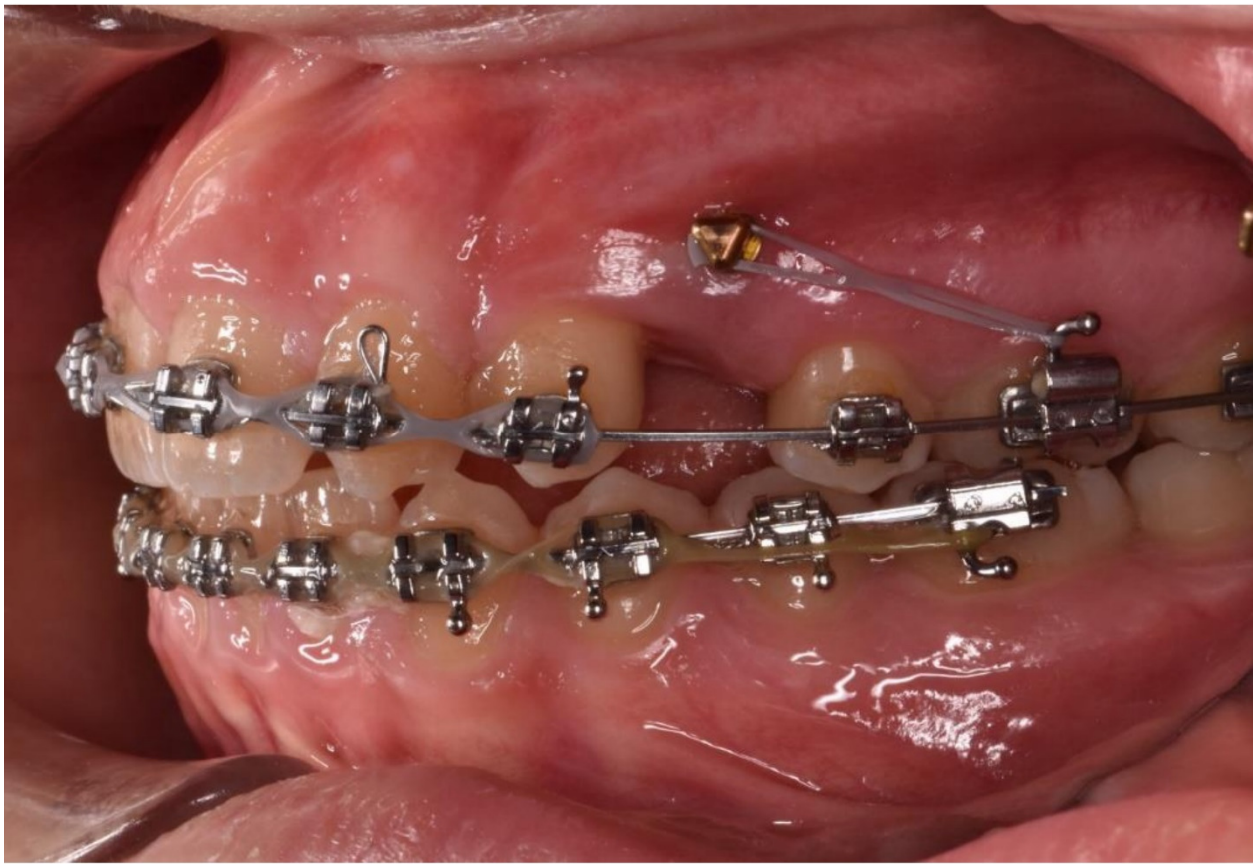


Figure 7.1. Vestibular miniscrew to enhance molar mesialization [1].

Close intimacy between the bone and miniscrew surface is crucial for achieving stability and resistance to orthodontic forces. Inflammatory processes can compromise primary stability and lead to premature miniscrew loss.

Surface modification of miniscrews using nanotechnology, such as TiO2 nanotube arrays, has been studied to enhance stability and osseointegration.

These modified miniscrews can also be loaded with drugs like recombinant human bone morphogenetic protein-2 (RhBMP-2) and ibuprofen to promote tissue health and decrease inflammation at the insertion site, thereby reducing patient discomfort.

Moreover, these modified miniscrews can be designed to deliver various drugs, including antibiotics, aspirin, and Vitamin C, further enhancing their therapeutic potential.

Additionally, surface modification improves the surface roughness of the miniscrews and enhances wettability compared to conventional products, contributing to better overall performance [1].

7.5. Prevention of Dental Caries and Control of Oral Biofilm

One of the primary objectives of modern dentistry is to enhance prevention measures and reduce the necessity for invasive treatments. Nanotechnology presents promising avenues for addressing these goals, particularly in controlling bacterial biofilms and promoting remineralization following tooth decay. This advancement could facilitate better oral hygiene maintenance, especially for young patients who are at a high risk of dental decay (Figure 7.2.).

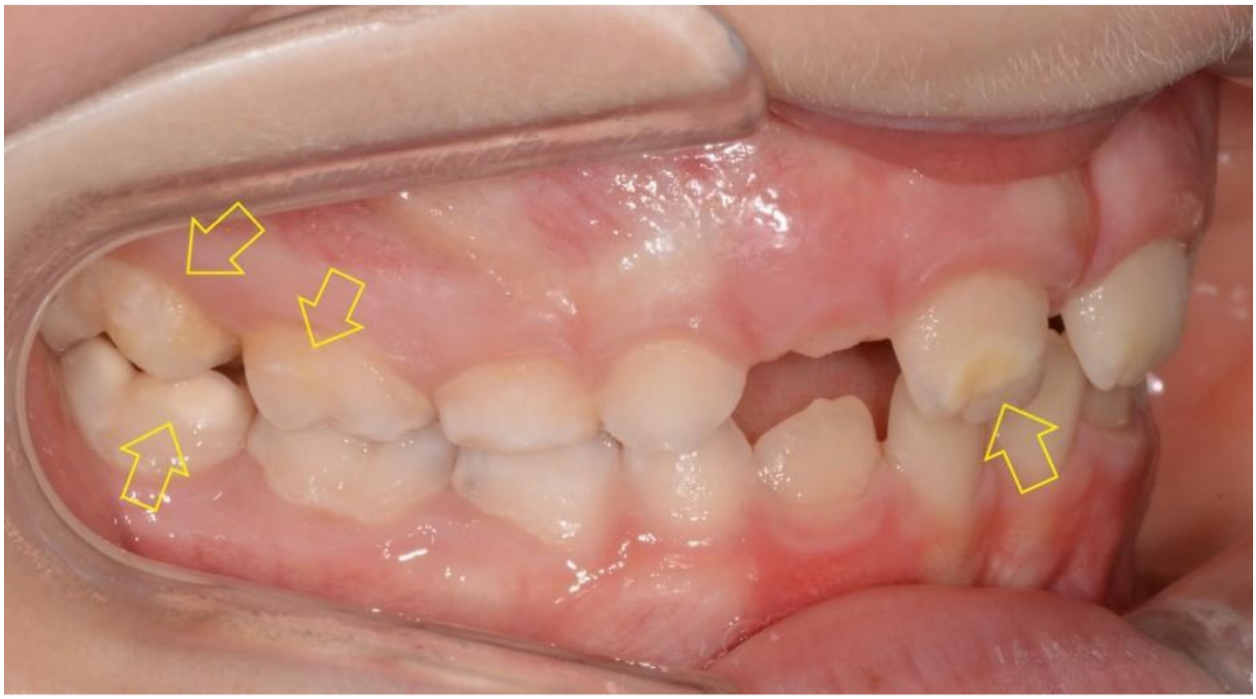


Figure 7.2. Molar incisor hypomineralization. Orthodontic treatment can affect dental tissue and lead to cavities [1].

White spot lesions or enamel demineralization, often resulting from acid biofilms, are common occurrences, particularly during orthodontic treatments due to increased plaque presence and retention around orthodontic brackets. To combat caries development around these brackets, antibacterial adhesives incorporating nanoparticles such as TiO2, SiO2, or silver nanoparticles (SNPs) have been investigated. TiO2 nanoparticle incorporation has demonstrated prolonged antibacterial effects without compromising adhesive properties, while SNP adhesives have shown effective antibacterial properties. However, the use of SNP adhesives in orthodontics may be limited due to potential enamel discoloration.

Another approach to reducing caries-related failures involves modifying archwires or brackets with coatings containing nanoparticles like TiO2 doped with nitrogen or Ag-Zr nanocomposites. These modifications aim to inhibit bacterial biofilm formation and subsequent enamel demineralization.

Early enamel lesions can be remineralized using dentifrices containing nanosized calcium carbonate or other inorganic materials such as hydroxyapatite (HA) with zinc, fluoride, or carbonate. These materials can be incorporated into toothpaste or mouthwashes to promote remineralization and prevent further enamel degradation.

While some studies have demonstrated the efficacy of nanomaterial-based products in preventive dentistry, the literature remains controversial regarding their superiority over conventional methods. New studies are exploring the potential of dental robots (dentifrobots), nanorobots incorporated into oral hygiene products to clean gingival margins and prevent calculus formation. These dentifrobots metabolize trapped organic matter into harmless vapors and are safely inactivated upon ingestion.

These strategies may offer alternatives to fluoride materials, especially for individuals at higher risk of fluorosis. However, further research is needed to assess the degradation and safety profiles of these new particles, ensuring they pose no additional risks to oral health.

7.6. Coated Orthodontic Archwires

Reducing frictional forces in orthodontic treatment is crucial for enhancing treatment efficiency, minimizing treatment time, and reducing the risk of root resorption. Friction occurs between the bracket and archwire surfaces, opposing the intended tooth movement, and can result in the loss of a significant portion of the applied orthodontic force.

Various strategies have been explored over the years to mitigate friction in orthodontic systems, including bracket design modifications and the use of different archwire alloys and surface treatments. Recently, nanotechnology has emerged as a promising approach to reducing frictional forces by coating orthodontic archwires with films containing nanoparticles, particularly MoS2 (molybdenum disulfide) and W2 (tungsten disulfide). These nanoparticles, such as inorganic fullerene-like tungsten disulfide (IF-WS2), form layered structures that provide excellent lubricity due to weak van der Waals forces between the layers.

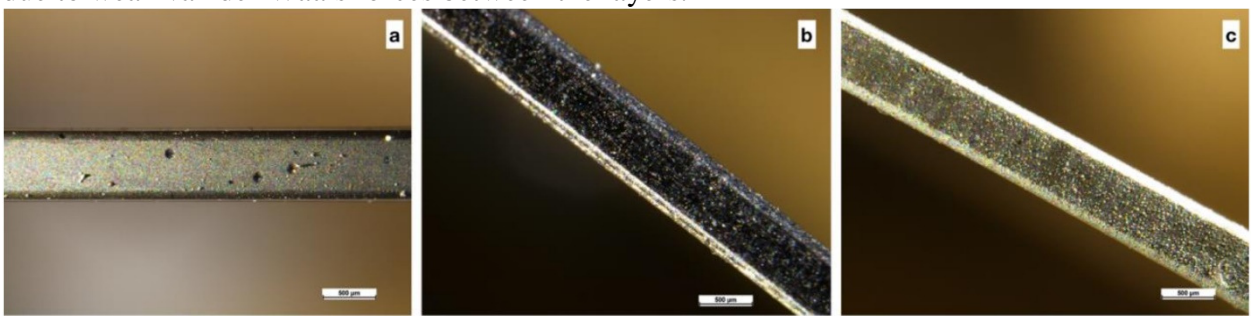


Figure 7.3. Stainless steel archwires, 0.19 × 0.25, coated with MoS_2 (molybdenum disulfide) and W2 (tungsten disulfide) [1].

The unique physical and chemical properties of these nanoparticles, including their ability to maintain intimate contact with metal surfaces, dissipate less energy under force load, and exhibit low reactivity, make them ideal candidates for reducing friction in orthodontic systems. Additionally, they have shown no toxic effects in animal studies, but further research is needed to ensure their safety in humans throughout the duration of orthodontic treatment.

In summary, incorporating nanoparticles such as MoS2 and W2 into orthodontic archwire coatings holds promise for significantly reducing frictional forces, thereby improving treatment outcomes and patient comfort. However, continued research is essential to validate their efficacy and safety for clinical use in orthodontics [1].

7.7. Nanomaterials Application in Orthodontics

Nanotechnology has revolutionized various fields of dentistry, including orthodontics, by introducing nanomaterials with enhanced properties such as antimicrobial activity, durability, and strength. Nanomaterials, characterized by their particle size of less than 100 nm, offer a higher

surface-to-mass ratio, resulting in increased reactivity and absorption in the body. However, concerns regarding potential cytotoxicity necessitate further research.

In orthodontics, the prolonged wearing of braces can lead to increased plaque accumulation and a higher risk of caries, often manifesting as white spot lesions (WSLs). Research confirms accelerated WSL accumulation during orthodontic treatment, posing esthetic and clinical challenges. Traditional materials like resin composites, commonly used in orthodontics, lack bacteriostatic properties and can promote plaque accumulation and secondary caries.

Nanotechnology holds promise in preventing adverse effects associated with orthodontic treatment. Nanoparticles incorporated into restorative materials, adhesives, and oral care products exhibit remineralizing and antibacterial properties, addressing WSLs and plaque accumulation. Moreover, nanotechnology aids in diagnosing dental diseases and enhancing implant surfaces and impression materials.

Orthodontic applications of nanotechnology extend to coating wires, ligatures, and brackets, as well as shaping memory polymers and bonding materials. By controlling biofilm formation, reducing bacterial activity, and promoting anticariogenic effects, nanomaterials contribute to shorter treatment times and improved patient outcomes.

While nanotechnology offers numerous benefits in medicine and dentistry, concerns persist regarding its safety for humans and the environment. Nanoparticles' ability to penetrate tissues raises questions about potential biological impacts, necessitating comprehensive research on environmental and toxicological properties for sustainable nanomaterial application.

In conclusion, the current use of nanoparticles in orthodontics demonstrates significant potential in enhancing treatment outcomes and patient care. However, ongoing research is essential to address safety concerns and ensure responsible application of nanotechnology in dentistry [2].

7.7.1. Nano-Coatings in Orthodontic Archwires

Minimizing frictional forces between orthodontic wires and brackets can enhance tooth movement and reduce treatment time. Nanoparticles, such as inorganic fullerene-like tungsten sulfide (IF-WS2), have been utilized in dry lubricants to achieve this goal. These nanoparticles act as solid-phase materials, reducing friction without requiring a liquid medium. In studies, IF-WS2 nanoparticles have been incorporated into coatings for orthodontic stainless-steel wires, demonstrating reduced friction through friction tests conducted on Instron machines. Scanning electron microscopy (SEM) and energy dispersive X-ray spectroscopy (EDS) analysis confirmed the impregnation of IF-WS2 nanoparticles in the Ni-P matrix of the coated wires.

Furthermore, atomic force microscopy (AFM) has been employed to assess the surface roughness of different orthodontic wires, including stainless steel (SS), beta-titanium (β-Ti), and nickel-titanium (NiTi). Surface roughness measurements obtained via AFM contribute to understanding the effectiveness of sliding mechanics, corrosion behavior, and aesthetics of orthodontic arches. Additionally, the influence of decontamination and clinical exposure on the modulus of elasticity, hardness, and surface roughness of SS and NiTi archwires has been evaluated using AFM coupled with a nanoindenter. Results from these assessments indicated that while decontamination and clinical exposure had no statistically significant effect on NiTi wires, they did have a significant effect on SS wires.

However, it's important to note that the clinical implications of these findings regarding orthodontic movement remain uncertain. Further diagnostic studies are needed to determine the practical significance of statistical analyses and testing of orthodontic archwires on treatment outcomes [2].

7.7.1.1. Nano Coatings Reducing Friction on Orthodontic Archwires

Orthodontic arches play a crucial role in generating biomechanical forces to move teeth and correct malocclusions. The materials commonly used for orthodontic arches include stainless steel (SS), nickel-titanium (NiTi), and beta-titanium (β-Ti) alloys. In orthodontic treatments employing sliding mechanics, friction between the archwire and brackets significantly influences tooth

movement. Friction arises when moving objects come into contact, causing resistance to movement proportional to the force applied and dependent on surface characteristics such as smoothness, chemical reactivity, and lubrication.

To minimize frictional forces and expedite tooth movement, researchers have explored various methods, including coating NiTi substrates with cobalt and inorganic fullerene-like tungsten sulfide (IF-WS2) nanoparticles via electrodeposition. Studies have demonstrated that such coatings can reduce friction by up to 66% compared to uncoated substrates, presenting promising applications in orthodontic treatments. However, it's essential to consider potential drawbacks, such as allergic reactions in patients with nickel sensitivity due to the introduction of nickel in the coating. Therefore, further research is warranted to assess the biocompatibility of these coatings on stainless steel and NiTi wires through animal models and human trials [2].

7.7.1.2. Delivering Nanoparticles from an Elastomeric Ligature

Elastomeric ligatures in orthodontics serve not only as tools for mechanical support but also as potential carriers for nanoparticles with various therapeutic properties. These nanoparticles may possess anti-cariogenic or anti-inflammatory properties and can even contain embedded antibiotic drug molecules.

Previous studies have demonstrated the ability of elastomeric ligatures to release fluoride, which is known for its anti-cariogenic effects. The release of fluoride from these ligatures follows a pattern characterized by an initial burst of fluoride in the first few days, followed by a gradual decrease over time. This sustained release of fluoride can effectively combat enamel demineralization, particularly around orthodontic brackets during treatment.

Overall, incorporating therapeutic nanoparticles into elastomeric ligatures represents a promising approach to enhance the preventive and therapeutic aspects of orthodontic treatment, particularly in mitigating the risk of dental caries and inflammation associated with orthodontic appliances [2].

7.7.1.3. Shape Memory Polymers (SMP) in Orthodontics

In recent years, there has been a significant interest in developing aesthetic orthodontic wires that complement the color of teeth, thereby enhancing the overall appearance of orthodontic appliances. Shape memory polymers (SMPs) have emerged as promising materials for this purpose.

SMPs possess the unique ability to remember and temporarily fix equilibrium shapes under specific temperature and stress conditions. They can later revert to their original shape when subjected to appropriate stimuli, such as changes in temperature or light activation. This property makes SMPs particularly suitable for orthodontic applications, as they can provide controlled and consistent forces for tooth movement.

When placed in the oral cavity, SMP orthodontic wires can be activated by body temperature or light-activated photoactive nanoparticles, facilitating tooth movement. Compared to traditional orthodontic materials, SMP wires offer several advantages. They provide lighter and more consistent forces, resulting in reduced discomfort for patients. Additionally, SMP materials are transparent, stainable, and stain-resistant, offering a more aesthetically pleasing option for patients undergoing orthodontic treatment.

Moreover, the high percent elongation of SMP apparatus allows for the application of continuous forces over a wide range of tooth movement, potentially reducing the frequency of patient visits. Looking ahead, the development of shape-memory nanocomposite polymers holds promise for further advancements in the field of orthodontic biomaterials, particularly in the production of aesthetic orthodontic wires [2].

7.7.1.4. Control of Oral Biofilms during Orthodontic Treatment

The application of nanoparticles in dentistry offers a promising avenue for enhancing antimicrobial properties of dental materials, particularly due to the increased surface area to volume

ratio that nanoparticles possess. This trait significantly boosts their biocidal effects, especially in the case of metal nanoparticles like silver, which are renowned for their microbial inhibitory capabilities.

Enhanced Antimicrobial Activity: Metal nanoparticles, with their size typically ranging from 1 to 10 nm, display potent biocidal properties against bacteria. Silver nanoparticles are especially notable within this group for their broad-spectrum antimicrobial effects. These properties make them ideal candidates for incorporation into dental products to enhance their efficacy against oral pathogens.

Integration into Dental Materials: Researchers have explored various methods to harness the antimicrobial potential of nanoparticles in dentistry. One effective strategy has been embedding nanoparticles into dental materials. For instance, resin composites that include silver ion-releasing fillers have been shown to exert antibacterial effects specifically against oral streptococci, which are common culprits behind dental caries and other oral infections.

Case Study - Experimental Composite Adhesive: A notable study by Ahn et al. explored the application of nanoparticles in dental adhesives. The study compared an experimental composite adhesive (ECA) that incorporated silica nanofillers and silver nanoparticles with conventional composite adhesives and a resin-modified glass ionomer (RMGI). The findings revealed several key points:

- **Surface Characteristics:** The ECA displayed a rougher surface compared to traditional adhesives, a feature attributed to the incorporation of silver nanoparticles.
- **Antimicrobial Activity:** The ECA demonstrated a significantly lower rate of bacterial adhesion compared to conventional adhesives. Notably, this reduction in bacterial adhesion was maintained even in the presence of saliva, indicating the robustness of the antimicrobial effect.
- **Growth Inhibition:** Bacterial cultures containing ECA exhibited slower growth rates, further underscoring the antimicrobial efficacy of the nanoparticle-enhanced adhesive.
- **Mechanical Properties:** Importantly, the study also confirmed that the inclusion of nanoparticles did not adversely affect the shear bond strength or the fracture strength of the bond compared to conventional adhesives.

Implications for Dental Practices: This research highlights the potential benefits of incorporating nanoparticles, particularly silver nanoparticles, into dental materials. By doing so, it is possible to create dental adhesives and other materials that not only meet the mechanical demands required for dental repairs but also offer added antimicrobial properties to reduce the risk of infection and improve overall oral health outcomes.

The integration of nanoparticle technology in dental materials represents a forward-thinking approach to combating microbial challenges in dentistry. As research progresses, such innovations could lead to more widespread use of nanoparticle-enhanced materials in clinical settings, potentially setting new standards for preventive and restorative dental care.

7.7.2. Bracket Materials

The development of orthodontic materials and products has significantly improved the outcomes for patients in terms of functionality, health, and aesthetics, while also enhancing the technical performance for orthodontists. Brackets, being a fundamental component of orthodontic treatment, need to meet various criteria to function effectively. These include good biocompatibility, appropriate hardness and strength, smooth archwire slots to minimize friction, smooth surfaces to reduce plaque accumulation, precise customization for each tooth, high corrosion resistance, and the potential for ionic release.

Orthodontic braces are typically manufactured using three main methods: casting, injection molding, and milling, with materials ranging from metals, plastics, ceramics, and combinations thereof. Among metallic compositions, stainless steel is commonly used due to its affordability, high modulus of elasticity, and favorable biomechanical properties. Stainless steel alloys like austenitic, martensitic, ferritic, duplex, and precipitation-hardening varieties offer different advantages, with conventional type 316 L being a common choice.

However, concerns regarding corrosion have led to the development of alternatives like the 17-4 PH alloy, which demonstrates improved corrosion resistance, frictional behavior, and cytotoxicity compared to austenitic stainless steels. While nickel content in brackets can be allergenic, cytotoxic, and mutagenic, the introduction of non-nickel or low-nickel content stainless steel alloys has addressed these concerns, offering improved corrosion resistance without nickel release.

Titanium, known for its lack of allergenicity and increased corrosion resistance, has also gained popularity in bracket construction. Commercially pure titanium grade 4 and Ti-6Al-4V alloy are commonly used types, offering superior corrosion resistance due to the stable titanium oxide layer.

Gold-coated brackets, plated with 24 karat gold, provide a brighter appearance and better mechanical properties compared to conventional stainless-steel alloys. They are also preferred by patients allergic to nickel. Moreover, nano-sized gold particles can be incorporated into orthodontic appliances, such as aligners, to enhance antibacterial activity and prevent biofilm formation, demonstrating positive biocompatibility both in vitro and in vivo.

Overall, advancements in orthodontic materials, including the use of different metals and nanotechnology, contribute to improved treatment outcomes, patient comfort, and oral health (Figure 7.4.).

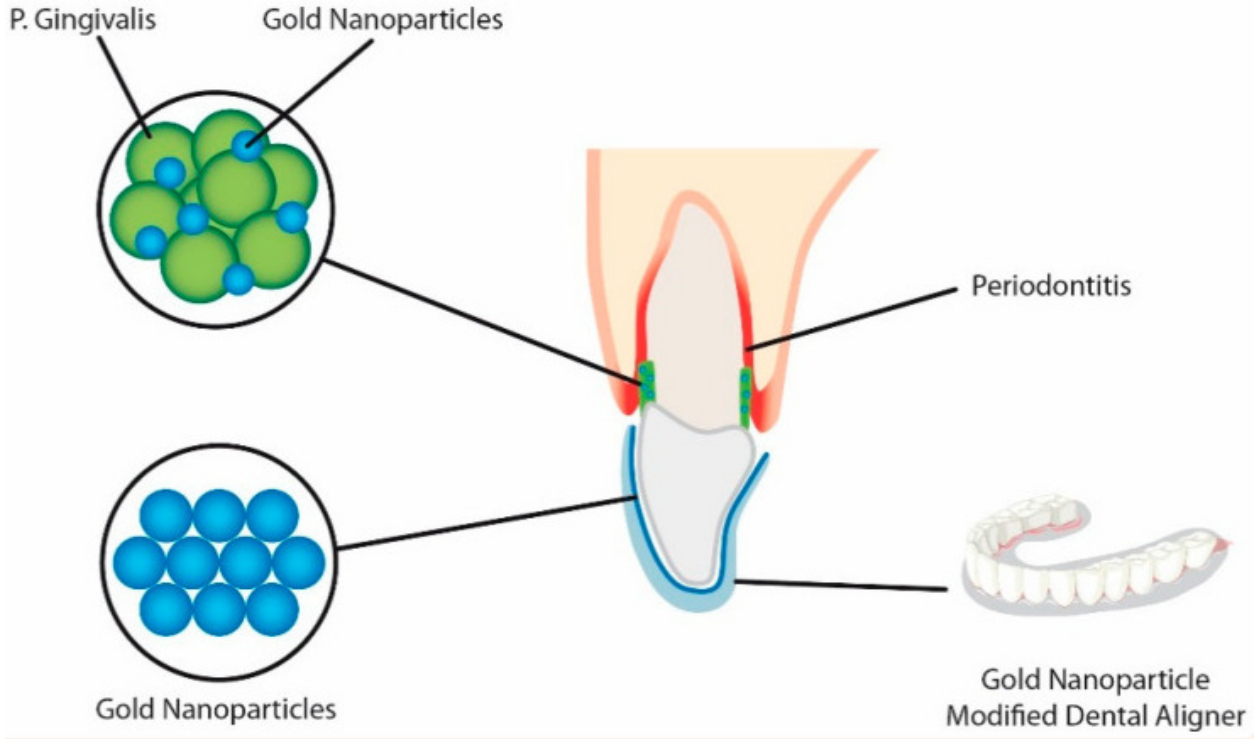


Figure 7.4. Visual representation of the effectiveness of aligners coated with modified gold nanoparticles in combating the bacterium Porphyromonas gingivalis, a key pathogen implicated in periodontal disease. This innovative approach to dental aligner design aims to enhance antibacterial activity and prevent biofilm formation, a common challenge in orthodontic treatments.

Platinum-coated and cobalt-chromium brackets represent two advanced alternatives in orthodontic bracket technology, each bringing unique properties to enhance orthodontic treatment. Here's a detailed comparison and analysis of these materials in relation to traditional stainless steel and titanium brackets:

Platinum-Coated Brackets

Advantages:

- **Biocompatibility:** Platinum coatings are highly biocompatible, reducing the risk of allergic reactions for patients sensitive to other metals.
- **Corrosion Resistance:** The platinum layer offers superior resistance to corrosion, which is crucial for maintaining the bracket's integrity and appearance throughout the treatment duration.

- **Reduced Friction:** Due to the hardness of the platinum surface, these brackets exhibit less friction against orthodontic wires. This can facilitate smoother wire movement, potentially speeding up treatment time and improving patient comfort.
- **Allergenicity Prevention:** The platinum layer acts as a barrier that prevents the diffusion of potentially allergenic metals such as nickel, cobalt, and chromium from the bracket into the oral environment. This is particularly beneficial for patients with known sensitivities.

Unique Features:

- A special implantation process enhances the durability and effectiveness of the platinum coating, ensuring the barrier against metal diffusion remains intact.

Cobalt-Chromium Brackets

Advantages:

- **Corrosion Resistance:** Cobalt-chromium brackets display excellent corrosion resistance, comparable to that of platinum-coated brackets. This feature is essential for long-term durability and oral health.
- **Friction Resistance:** These brackets show comparable friction resistance to stainless steel brackets and are slightly superior when used with stainless steel wires, though they may exhibit more friction compared to titanium brackets.

Comparative Drawbacks:

- **Friction with Different Wires:** While cobalt-chromium brackets work well with stainless steel wires, they may not perform as effectively with beta-titanium wires, which could affect the choice of materials based on specific treatment needs or wire preferences.

General Considerations

- **Material Selection:** The choice between platinum-coated, cobalt-chromium, stainless steel, and titanium brackets often depends on a combination of factors including patient allergies, treatment requirements, and cost considerations.
- **Cost and Accessibility:** Platinum-coated brackets might be more expensive due to the precious metal used, whereas cobalt-chromium brackets could offer a cost-effective alternative with many of the same benefits.

In addressing the aesthetic concerns associated with metal brackets, ceramic and plastic brackets have been widely utilized in orthodontic practice. Plastic brackets, initially made of acrylic and later polycarbonate, faced issues such as water sorption, color changes, and increased adhesion of pathogens. Reinforcement with other materials like ceramic or fiberglass fillers, chemical modification of polymers, and the use of alternative polymers have been explored to improve their properties. Plastic brackets may be suitable for clinical use when reinforced with a metal slot.

The biocompatibility of plastic materials, particularly regarding cytotoxic effects, remains an important consideration. Research has investigated the effects of particle- and fiber-reinforced polycarbonate brackets on cell viability. Polyoxymethylene brackets offer improved hardness and smoothness but may release formaldehyde over time.

Efforts are ongoing to identify an ideal polymer that combines optical transparency with mechanical stiffness, resistance to water absorption, and degradation, without releasing toxic compounds like Bis-GMA and TEGDMA. Ceramic brackets, typically composed of aluminum oxides, offer advantages in terms of rigidity, abrasion resistance, biocompatibility, and resistance to discoloration.

There are different types of ceramic brackets, including polycrystalline and monocrystalline forms, with polycrystalline zirconia brackets being the toughest but opaque, and monocrystalline alumina brackets being clearer but with lower fracture toughness. Ceramic brackets may pose challenges related to iatrogenic enamel damage, bonding and debonding, and frictional resistance, including bracket breakage and fracture resistance during ligature or archwire forces. These considerations guide orthodontists in selecting the most appropriate bracket materials for their patients.

7.7.3. Nanomaterials in Orthodontics

Nanomaterials offer versatile solutions to address various challenges encountered during orthodontic treatment, particularly in managing friction and reducing biofilm formation.

Friction is a significant factor during orthodontic treatment, especially during tooth retraction or alignment. Traditional methods to overcome high friction, such as applying higher forces, can lead to undesirable anchorage loss. Alternatively, altering bracket design or wire shape and size can help reduce friction. Another promising approach involves coating orthodontic brackets or wires with nanoparticles, effectively reducing friction without compromising anchorage.

In addition to addressing friction, nanoparticles offer antibacterial properties that can help reduce biofilm formation during orthodontic treatment. One strategy involves coating orthodontic brackets or wires with nanoparticles, creating a hostile environment for bacterial growth. Another approach is to incorporate nanoparticles into orthodontic adhesives or acrylic materials, enhancing their antibacterial properties. Nanocomposite materials offer several advantages, including excellent optical properties, easy handling, and polishability. Furthermore, nanofillers can reduce the surface roughness of orthodontic adhesives, which is crucial in preventing bacterial adhesion.

Overall, the versatility of nanomaterials makes them valuable tools in orthodontic clinical treatment, offering solutions to improve treatment outcomes and patient comfort.

Nanomaterial	Method of Use	Application
Silver NPs (AgNPs)	Applied as a coating agent on titanium	Implants
Zinc oxide NPs (ZnONPs)	Incorporated into dental resins	Resin composite adhesives
Chitosan NPs	Conjugated with silver nanoparticles	Resin composites adhesives.
Copper (1) oxide NPs (Cu2ONPs)	Antimicrobial effect în resin adhesives	Resin composites adhesives
Titanium (IV) oxide NPs (TIO2NPs)	Nanotubes on titanium surfaces and Incorporated with ZnONPs	Implants
Gold NPs (AuNPs)	Modified gold nanoparticles (AuDAPT) coated onto orthodontic aligners	Antimicrobial coated aligner
Carbonate hydroxyapatite nanocrystal	Antibacterial and antidemineralizing properties	Toothpastes, mouthwashes and composite resins.
Amorphous Calcium Phosphate (ACP)	Antibacterial and antidemineralizing properties	Antibacterial and antidemineralizing properties
Novel Poly(1-lactic acid) (PLLA)/Multi-walled carbon nanotubes [MWNTs)/hydroxyapatite (HA) nanofibrous scaffolds	Polymer solution FOR entire-tooth regeneration	Dental Surface applications
Bioactive peptide-Amphiphile nanofibers	Branched peptide Amphiphile molecules containing the peptide motif Arg Gly Asp, or "RGD"	Dental surface applications

Figure 7.5. Nanomaterials application in dentistry [2].

Nanomaterials offer remarkable versatility and applicability in various aspects of orthodontic clinical treatment. These materials, characterized by their nanoscale dimensions, possess unique properties that make them valuable in addressing numerous challenges encountered in orthodontics. Some key areas where nanomaterials demonstrate versatility in orthodontic treatment include:

Friction Reduction: Nanoparticles can be incorporated into orthodontic wires, brackets, and ligatures to minimize friction between the components. This reduction in friction facilitates smoother tooth movement, enhances treatment efficiency, and reduces patient discomfort (Figure 7.5.).

Biofilm Control: Nanoparticles with antimicrobial properties can be integrated into orthodontic materials to inhibit bacterial growth and biofilm formation. This helps prevent oral infections, decay, and other complications associated with prolonged orthodontic treatment.

Enhanced Mechanical Properties: Nanomaterials can improve the mechanical strength, durability, and flexibility of orthodontic appliances, leading to more reliable and long-lasting treatment outcomes.

Aesthetic Solutions: Nanoparticles can be used to develop aesthetically pleasing orthodontic materials, such as tooth-colored brackets and wires, to enhance patient satisfaction and compliance with treatment.

Biocompatibility: Nanomaterials can be engineered to exhibit excellent biocompatibility, reducing the risk of adverse reactions and promoting tissue integration, which is essential for patient safety and comfort.

Drug Delivery: Nanoparticles serve as effective carriers for delivering therapeutic agents, such as antimicrobials or growth factors, directly to the target site within the oral cavity, optimizing treatment outcomes and minimizing systemic side effects.

Surface Modification: Nanoparticles can be used to modify the surface properties of orthodontic appliances, such as roughness and wettability, to improve adhesion, reduce plaque accumulation, and enhance overall oral hygiene.

Overall, the versatility of nanomaterials holds immense promise for advancing orthodontic clinical treatment, offering innovative solutions to enhance efficiency, effectiveness, and patient satisfaction in orthodontic care (Figure 7.6.).

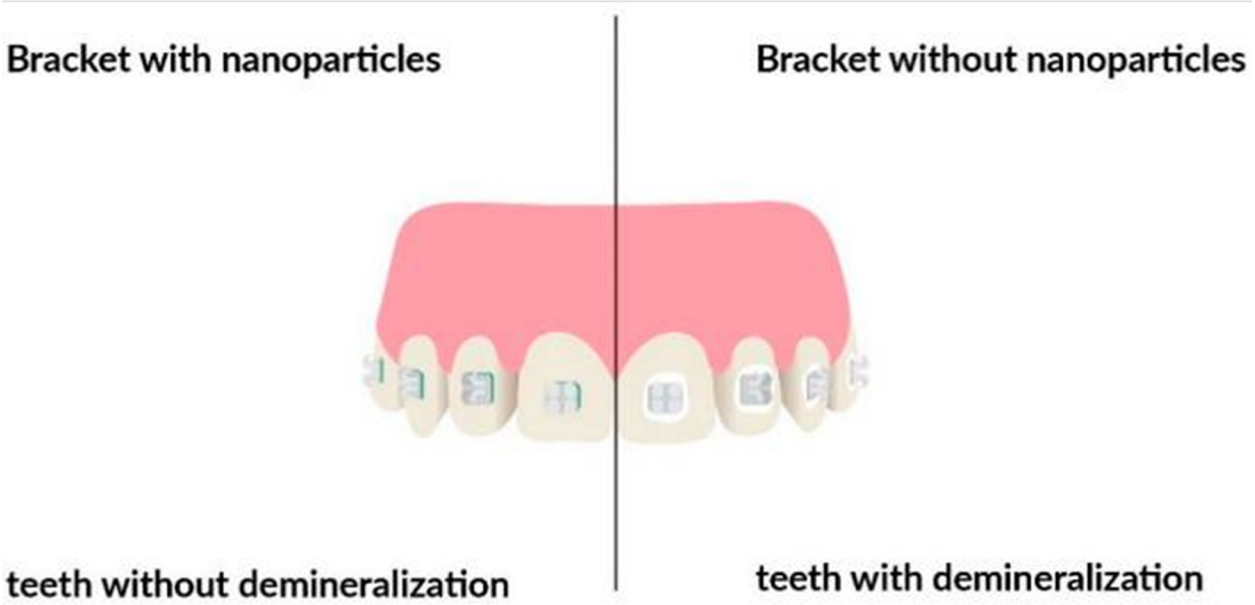


Figure 7.6. Comparison of teeth demineralization development with and without nanoparticles' covered brackets [2].

7.7.3.1. Silver Nanoparticles (AgNPs) Coating

Silver nanoparticles (AgNPs) have emerged as promising antimicrobial agents with broad-spectrum activity against various microorganisms, including Streptococcus mutans, a key bacteria implicated in dental caries. In the orthodontic field, incorporating AgNPs into different orthodontic

appliances has shown potential in combating dental biofilm and reducing enamel demineralization during and after orthodontic treatments.

Studies have demonstrated that AgNPs can effectively inhibit bacterial adherence of S. mutans on the surfaces of orthodontic brackets and wires. Smaller AgNP samples have been found to exhibit the most significant antiadherence activities for orthodontic appliances compared to nickel–titanium (NiTi) and stainless steel (SS) wires. Moreover, coverage of AgNPs on human dentin has been shown to prevent biofilm formation and inhibit bacterial growth.

For AgNPs to be effective, they should form stable suspensions with appropriate zeta potential values to limit agglomeration. Smaller AgNPs have been found to release more silver ions, which enhances their antimicrobial effect. The antimicrobial mechanism of AgNPs involves inhibiting microbial metabolism and impairing the production of extracellular polysaccharides, leading to bacterial dysfunction.

AgNP-coated orthodontic brackets have demonstrated the potential to decrease the appearance of white spot lesions during orthodontic treatment. They may also be beneficial for patients with compromised immune systems, diabetes, or elevated risk of endocarditis.

In addition to silver, other nanoparticles such as chitosan, copper, zinc, hydroxyapatite, and silicon dioxide can also be incorporated into composites to reduce bacterial activity and growth. These nanoparticles offer alternative approaches to enhance the antimicrobial properties of orthodontic materials, contributing to improved oral health outcomes for patients undergoing orthodontic treatment [2].

7.7.3.2. Chitosan

Chitosan, derived from the deacetylation of chitin, is a naturally occurring polysaccharide known for its non-toxic, biodegradable, biocompatible, and antibacterial properties. Studies have shown its effectiveness against various bacteria such as Aggregatibacter actinomycetemcomitans, Porphyromonas Gingivalis, and Streptococcus mutans, as well as fungi.

While chitosan's reduced solubility in water limits its application as a mouthwash, its properties make it highly desirable for use in dental materials. Its insolubility allows it to be maintained within materials in the oral cavity over an extended period. Histologically, chitosan inhibits bacterial activity through mechanisms such as enzyme inactivation, lipopolysaccharide substitution, metal ion chelation, and formation of acidic polymers like teichoic acid.

Unlike chlorhexidine (CHX), which is released and dissipates quickly in the oral cavity, chitosan's low solubility and melting temperature enable it to remain effective for a longer duration. This characteristic makes chitosan a promising candidate for incorporation into dental materials aimed at combating bacterial growth and promoting oral health [2].

7.7.3.3. Copper Oxide

Studies, such as the one conducted by Yassaei et al. [2], have demonstrated that copper oxide (CuO) nanoparticles exhibit comparable antibacterial properties to silver nanoparticles. While both materials are effective against Streptococcus mutans bacteria, it was observed that the curing time increased with the use of copper compared to silver. However, copper nanoparticles offer the advantage of being more cost-effective and both physically and chemically stable.

Research has shown that copper and copper-zinc nanoparticles have a significant inhibitory effect on various microbes, including Streptococcus mutans. Additionally, CuO nanoparticles have been found to reduce biofilm formation by up to 70-80%. When incorporated into adhesive materials, CuO particles have demonstrated similar effectiveness in reducing biofilm formation. Furthermore, CuO nanoparticles can act as nano-fillers, enhancing the shear bond strength of adhesives.

Overall, the antibacterial properties and stability of CuO nanoparticles make them promising candidates for use in orthodontic materials, potentially contributing to improved oral health outcomes during orthodontic treatment [2].

7.7.3.4. Nitrogen-Doped Titanium Dioxide (N-Doped TiO2) Brackets

The activation of nitrogen-doped titanium dioxide (TiO2) nanoparticles results in the production of reactive oxygen species (ROS) such as hydroxyl radicals (OH•), superoxide ions (O2•–), hydrogen peroxide (H2O2), and peroxyl radicals (HO2•). These ROS exhibit antimicrobial activity by interacting with lipids, enzymes, and proteins in microbial cells.

Studies, such as the one conducted by Poosti et al. [2], have shown that TiO2 nanoparticles, particularly those doped with nitrogen, have significant antibacterial effects. For example, TiO2 nanoparticles with an average size of 21 ± 5 nm, when blended into light-cured orthodontic composite paste at concentrations of 1%, 2%, and 3%, demonstrated similar antibacterial effects. Similarly, Salehi et al. [74] demonstrated that nitrogen-doped TiO2 brackets exhibited superior antimicrobial activity compared to uncoated stainless-steel brackets. Incorporating TiO2 nanoparticles into adhesives has been shown to enhance their antibacterial activity without compromising their mechanical properties [2]. Nitrogen-doped TiO2 brackets have also been reported to exhibit antibacterial activity against various oral pathogenic bacteria.

Overall, the use of nitrogen-doped TiO2 nanoparticles in orthodontic materials holds promise for reducing microbial colonization and improving oral health outcomes during orthodontic treatment.

7.7.3.5. Zinc Oxide (ZnO)

Studies have shown that increasing the concentration of zinc oxide (ZnO) nanoparticles leads to enhanced antimicrobial activity against microorganisms such as Streptococcus mutans. However, it has also been observed that higher concentrations of ZnO nanoparticles can lead to a reduction in shear bond strength. Interestingly, the combination of ZnO and copper oxide (CuO) coatings on brackets has been found to exhibit better antimicrobial properties against Streptococcus mutans compared to brackets coated with CuO nanoparticles alone.

Several studies, including those by Kachoei et al. [2], Behroozian et al. [2], and Goto et al. [2], have demonstrated that the coating of brackets with ZnO nanoparticles leads to a significant decrease in frictional forces between archwires and brackets. This reduction in friction offers new possibilities for overcoming unwanted friction forces, improving anchorage control, and reducing the risk of root resorption during orthodontic treatment.

Overall, the incorporation of ZnO nanoparticles into orthodontic materials presents a promising approach to enhance antimicrobial properties and reduce friction, thereby potentially improving treatment outcomes and patient comfort.

7.7.4. Relationship between the Orthodontic Arch and Bracket Materials

In orthodontic treatment, various materials are used for brackets and arches. The most common materials for brackets include stainless steel, titanium, ceramics, and plastic. Similarly, arches are typically made of stainless steel, nickel-titanium alloy, chrome-cobalt steel, and titanium-molybdenum alloy.

Friction between the archwire and the orthodontic bracket is a significant factor in orthodontics. This frictional force acts against the traction force (TF) applied to move the teeth. Excessive friction can impede the movement of the brackets along the archwire, making it more challenging to achieve desired tooth positions and treatment outcomes.

Efforts to minimize friction in orthodontic treatment involve various strategies, including the use of different materials for brackets and archwires, modifying the design of brackets and archwires, and applying coatings or additives to reduce frictional resistance. By reducing friction, orthodontists can optimize treatment mechanics, enhance patient comfort, and improve treatment efficiency.

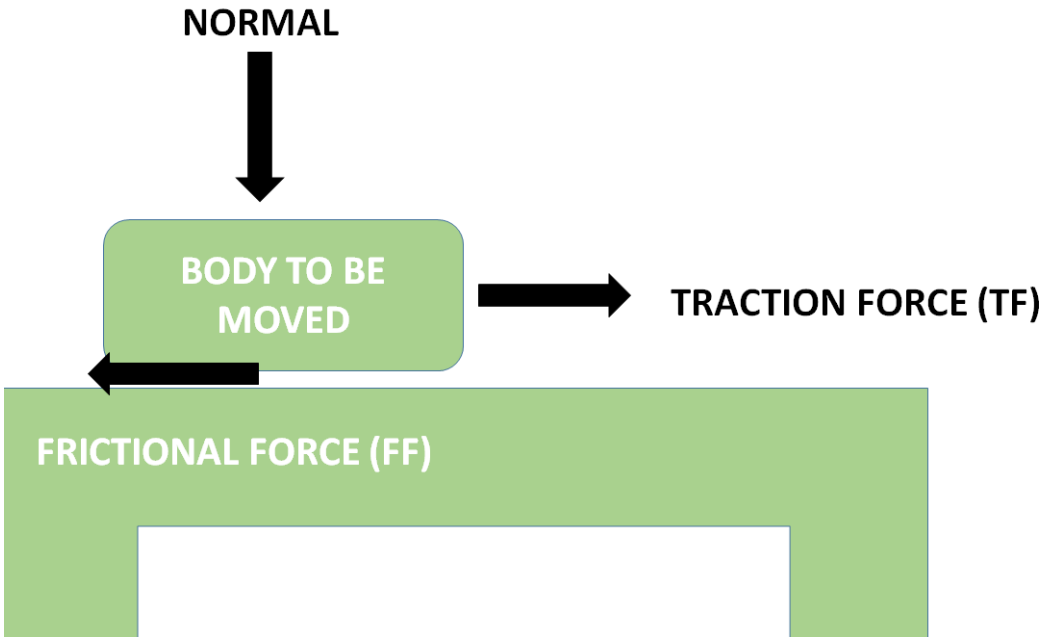


Figure 7.7. Different forces acting over a body under traction on top of a surface. Body to be moved, traction force (TF), friction force (FF), contact surface (CS) [2].

The friction observed in orthodontic sliding mechanics poses a significant clinical challenge for orthodontists, as high levels of friction can hinder the effectiveness of treatment mechanics, reduce the efficiency of tooth movement, and complicate anchorage control. Orthodontic manufacturing companies are continuously seeking new products that can generate less friction during sliding mechanics, and nanoparticles have emerged as a potential solution.

Mechanical factors, such as the material of the archwire and bracket, play a significant role in influencing friction during orthodontic treatment. Stainless steel brackets and archwires are considered the gold standard for sliding mechanics. The shape and size of the archwire also affect friction, with larger diameter archwires generally exhibiting greater friction. Rectangular wires typically cause more friction than round wires. Additionally, the material of the archwire impacts friction, with stainless steel wires generally producing less friction than NiTi or titanium-molybdenum alloy wires. The type of bracket, such as stainless steel or titanium, also influences friction, with titanium brackets showing greater friction. Ceramic brackets tend to produce more friction than stainless steel brackets, while self-ligating brackets may offer reduced friction, although further research is needed to confirm this.

Biological factors, such as the presence of saliva and debris on the surface of orthodontic arches, also influence friction. Saliva can act as a lubricant or adhesive, affecting friction accordingly. Proper composition and amount of saliva are crucial for maintaining optimal treatment conditions. Biofilm and debris accumulation on orthodontic arches can increase friction, highlighting the importance of plaque control during orthodontic treatment.

Nanomaterials with proven bacteriostatic effects can help reduce bacterial load and plaque accumulation on orthodontic elements, thereby indirectly reducing frictional forces. Incorporating nanoparticles into orthodontic treatment protocols can improve both mechanical and biological factors by reducing the friction coefficient at the arch-lock interface and creating less favorable conditions for plaque accumulation. Overall, the use of nanoparticles in orthodontic treatment shows promise for improving treatment outcomes and reducing friction-related challenges.

7.7.5. Microbial Colonization Associated with Different Kinds of FOAs.

Fixed orthodontic appliances indeed pose challenges to oral hygiene and can create retentive areas for plaque and debris accumulation, particularly around the bracket adhesive-enamel junction.

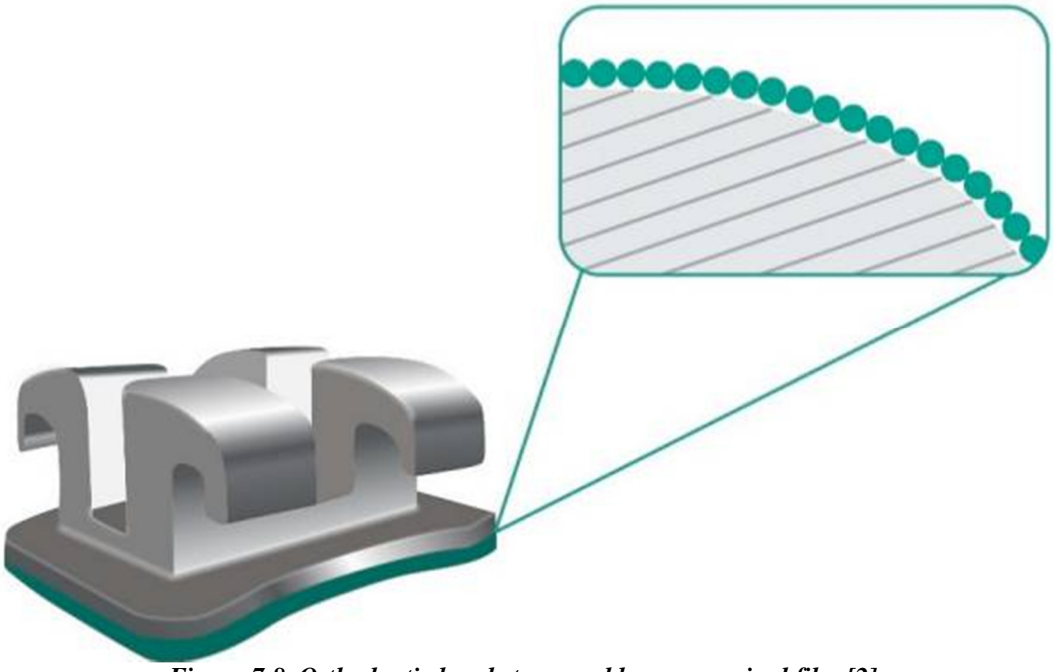


Figure 7.8. Orthodontic bracket covered by a nano-sized film [2].

This accumulation of plaque can lead to enamel decalcification, white spot formation, and dental caries adjacent to the brackets. The difficulty in cleaning these areas with daily brushing exacerbates the problem (Figure 7.8.).

The material and design of orthodontic brackets, as well as the method of ligation, significantly contribute to microbial adhesion and biofilm formation. Factors such as surface roughness and surface-free energy also influence the quantity and quality of plaque accumulation. Electrostatic attractions and van der Waals forces further enhance the adhesion of microorganisms to surfaces, making it challenging to remove microbial growth around orthodontic appliances.

Despite these challenges, bonded brackets offer several advantages over bands, including better aesthetics, ease of placement and removal, and improved accessibility for oral hygiene maintenance. However, effective oral hygiene practices, including regular brushing and flossing, along with professional dental cleanings, are essential to mitigate the risks associated with plaque accumulation and reduce the incidence of dental problems during orthodontic treatment. Additionally, the integration of antimicrobial materials or coatings, such as nanoparticles, into orthodontic appliances may offer further benefits in reducing plaque accumulation and promoting oral health.

7.7.6. Introduction of Nanofillers or NP (Silver, TiO2) to Orthodontic Adhesives

The use of orthodontic adhesives, particularly those containing nanofillers such as silver nanoparticles (AgNPs), has shown promise in reducing bacterial adhesion and biofilm formation around orthodontic appliances. While orthodontic adhesives have been found to retain cariogenic streptococci to some extent, the incorporation of nanofillers has been shown to reduce surface roughness and potentially inhibit bacterial adhesion without compromising shear bond strength.

Silver nanoparticles have been widely studied for their antimicrobial properties against various bacteria, fungi, and viruses, including cariogenic Streptococcus mutans. Resin composites containing silver ions have demonstrated antibacterial effects against oral streptococci, and the addition of silver nanoparticles to orthodontic adhesives has been shown to reduce the adhesion of cariogenic streptococci without affecting shear bond strength. Furthermore, silver nanoparticles can be incorporated into acrylic orthodontic materials to prevent biofilm formation and Candida proliferation, which is particularly important in reducing the risk of orthodontic stomatitis.

In addition to silver nanoparticles, other nanofillers such as titanium dioxide (TiO2) and silicon dioxide (SiO2) have been investigated for their antimicrobial properties when added to acrylic orthodontic materials. However, the inclusion of nanoparticles in acrylic resin may affect the

mechanical properties of the final product, with some studies reporting a decrease in flexural strength with higher nanoparticle concentrations.

Studies evaluating the adhesion of bacteria and fungi to different types of orthodontic materials have shown varying results. While some studies found no significant difference in bacterial adhesion between stainless steel, plastic, and ceramic brackets, others reported differences in adhesion levels depending on the bracket material. Titanium brackets were found to have the greatest number of CFUs (colony-forming units) when Candida albicans was evaluated alone, attributed to the rough surface of titanium brackets. In contrast, gold brackets showed the least number of CFUs, likely due to the inert properties of gold. Plastic and ceramic brackets exhibited greater adherence to Candida albicans compared to stainless steel brackets, possibly due to their surface characteristics.

Overall, while nanofillers such as silver nanoparticles show promise in reducing bacterial adhesion and biofilm formation around orthodontic appliances, further research is needed to optimize their incorporation into orthodontic materials and evaluate their long-term effectiveness in clinical settings. Additionally, understanding the influence of bracket material and surface characteristics on microbial adhesion is essential for developing strategies to improve oral hygiene and reduce the risk of complications during orthodontic treatment.

7.7.7. Nanomaterials in Orthodontics and Their Use in the Nearest Future

The incorporation of nanoparticles into various dental materials, including those used in orthodontics, presents a promising avenue for improving the efficacy and outcomes of orthodontic treatment.

Nanoparticles are increasingly being utilized in dentistry for various purposes, ranging from conservative dentistry to prosthetics, due to their unique properties and versatility.

In orthodontics, the use of nanomaterials holds potential for enhancing the mechanical properties of orthodontic appliances, such as brackets and archwires, as well as for modulating the bacterial flora in the oral cavity. By incorporating nanoparticles into orthodontic materials, such as alloys used for brackets and archwires, it may be possible to improve their biomechanical performance and durability. This can lead to more effective tooth movement, better control of anchorage, and ultimately, more predictable treatment outcomes.

Moreover, nanoparticles have demonstrated antimicrobial properties, which can help mitigate the risk of bacterial adhesion and biofilm formation around orthodontic appliances. This may contribute to reducing the incidence of complications such as enamel demineralization and white spot lesions during orthodontic treatment.

The future integration of nanoparticles into orthodontic appliances has the potential to enhance treatment quality, reduce treatment-related complications, and improve patient satisfaction.

By allowing for better control of tooth movement and anchorage, orthodontists can more accurately achieve treatment goals set during diagnosis, resulting in improved patient outcomes and quality of life post-treatment.

However, it is important to address concerns regarding the compatibility and safety of nanoparticles in orthodontic applications.

Further research is needed to ensure the safety and efficacy of nanoparticle-containing orthodontic materials, as well as to optimize their proportions and formulations.

Overcoming these challenges will enable the widespread adoption of nanoparticle technology in orthodontics, leading to more efficient and effective orthodontic treatment for patients.

7.7.8. Materials in Orthodontics and Their Use in the Nearest Future

The future applications of nanotechnology in orthodontics hold immense potential for advancing treatment modalities and improving patient outcomes. Some of these innovative applications include:

Shape-memory polymers: These polymers have the ability to change shape in response to external stimuli such as heat or light. In orthodontics, low stiffness transparent polymer arches can be used that transform into arches with specific elasticity when exposed to heat or light. This technology can enhance treatment effectiveness and aesthetics.

Self-healing materials: Similar to biological systems, self-healing materials have been developed that can repair themselves when damaged. Micro-ducts containing therapeutic agents can be incorporated into orthodontic locks and archwires. When a breach occurs, nanobubbles burst, releasing the therapeutic agents to fill the gap and promote healing.

Biometric adhesives: These adhesives utilize localized van der Waals forces to form strong, reversible bonds between materials without the need for chemical substances. This enamel-friendly bonding mechanism, sometimes referred to as "geckel," ensures adequate bond strength without the need for enamel conditioning, improving patient comfort and reducing treatment time.

Self-cleaning materials: Inspired by aircraft coatings, self-cleaning materials utilize titanium oxide nanocoatings to prevent contamination and maintain cleanliness. Photocatalytic activity resulting from the interaction of titanium oxide with light can be harnessed in orthodontic materials to create surfaces that resist microbial adhesion and promote oral hygiene.

Nano-changes on temporary anchorage devices (TADs): By modifying the surface properties of TADs at the nanoscale, their retention can be enhanced while still allowing for easy removal when no longer needed. This can improve the stability and effectiveness of orthodontic anchorage, facilitating more precise and efficient treatment outcomes.

These advancements in nanotechnology have the potential to revolutionize orthodontic treatment by offering more personalized, efficient, and patient-friendly solutions. However, further research and development are needed to fully explore the capabilities and safety of these emerging technologies in orthodontic practice [2].

7.7.9. Conclusions

The integration of nanotechnology into the field of dentistry, particularly orthodontics, holds immense promise for advancing treatment outcomes and patient care. Recent research has highlighted the potential benefits of nanoparticles in various aspects of orthodontic therapy, including bonding materials, bracket and wire coatings, and antimicrobial properties.

Nanoparticles have demonstrated efficacy in enhancing the mechanical and antibacterial characteristics of orthodontic materials. They can be incorporated into acrylic resins, cements, and adhesives to prevent enamel demineralization and reduce friction between wires and brackets, thereby improving treatment efficiency. Additionally, nanoparticles have been shown to increase the shear bond strength of adhesives, contributing to better treatment outcomes.

Moving forward, there are several key areas for further exploration and development in the use of nanomaterials in orthodontics:

Optimizing friction reduction: Continued research is needed to identify novel approaches for minimizing unwanted friction forces during orthodontic treatment. This includes investigating new materials and surface modifications that can enhance anchorage control and reduce the risk of resorption.

Monitoring patient treatment: Given the dynamic nature of the oral cavity environment, it is essential to closely monitor patients undergoing orthodontic treatment with nanomaterials. Biocompatibility and cytotoxicity considerations are paramount, and ongoing evaluation of adverse effects is necessary to ensure patient safety.

Evidence-based practice: As the use of nanomaterials in orthodontics expands, it is critical to base treatment decisions on sound evidence and rigorous research. Continued studies generating stronger evidence will help guide clinical practice and optimize patient outcomes.

Interdisciplinary collaboration: The future of orthodontics will benefit from interdisciplinary collaboration between dental professionals and experts in nanomaterial science. This collaborative approach will facilitate the development of innovative solutions and ensure the safe and effective integration of nanotechnology into orthodontic practice.

Overall, the application of nanotechnology in orthodontics is poised for continued growth and innovation. By harnessing the potential of nanomaterials, orthodontists can enhance treatment outcomes, improve patient care, and usher in a new era of precision orthodontics.

7.8. Quiz 7.

1. Which of the following statements accurately describe the application of nanotechnology in orthodontics, based on the provided passage?

A) Nanomaterials are primarily used to develop orthodontic brackets with improved aesthetics but do not affect treatment outcomes.

B) Orthodontic elastomeric ligatures aim to enhance properties such as elasticity, durability, and biocompatibility through the incorporation of nanomaterials.

C) Nanotechnology is solely applied to orthodontic power chains to increase their strength without considering improvements in flexibility or frictional properties.

D) Surface modifications using nanomaterials are employed to increase friction between orthodontic brackets and archwires, thus facilitating smoother tooth movement.

E) Emerging research in orthodontics explores the use of nanorobots for targeted delivery of therapeutic agents and tissue engineering approaches for regeneration of oral tissues.

2. Which approach has been explored to mitigate microbiological colonization in orthodontic treatment?

A) Smooth surfaces of orthodontic elastomeric ligatures (OEM).

B) Fluoride-releasing ligatures with consistent effectiveness.

C) Incorporation of nanoparticles for anticariogenic or anti-inflammatory properties.

D) Medicated wax for fluoride release reducing mucosal irritation.

E) Silver nanoparticles obtained from natural sources for antibacterial efficacy.

3*. What methods have been studied to prevent cariogenic events associated with fixed orthodontic treatment, as described in the passage?

A) Increasing the frequency of orthodontic adjustments.

B) Using dental resins and cements with added antimicrobial agents such as zinc oxide, chlorhexidine, and fluorides.

C) Encouraging patients to avoid dental hygiene practices during orthodontic treatment.

D) Implementing dietary restrictions to minimize acidogenic bacteria growth.

E) Applying orthodontic bands with smooth surfaces to reduce plaque accumulation.

4. Which of the following methods have been explored to enhance stability and osseointegration of miniscrews in orthodontic practice, as described in the passage? Select all that apply.

A) Surface modification using nanotechnology, such as TiO2 nanotube arrays.

B) Embedding of miniscrews within the tooth structure.

C) Application of high-frequency vibrations during miniscrew insertion.

D) Use of chemical adhesives to attach miniscrews to the bone surface.

E) Coating miniscrews with traditional metallic alloys.

5. Which strategies have been explored to mitigate friction in orthodontic treatment, as described in the passage? Select all that apply.

A) Bracket design modifications.

B) Using archwire alloys with increased friction.

C) Applying surface treatments to archwires.

D) Coating orthodontic archwires with films containing nanoparticles.

E) Utilizing organic lubricants for reducing friction.

6. Which benefits of nanotechnology in orthodontics are highlighted in the passage? Select all that apply.

A) Increased plaque accumulation reduction

B) Enhanced treatment outcomes.

C) Remineralizing properties.
D) Safety concerns.
E) Traditional material superiority.

7. Which techniques have been used to assess the effectiveness of reducing frictional forces between orthodontic wires and brackets using nanoparticles, as described in the passage?
A) Scanning electron microscopy (SEM) and energy dispersive X-ray spectroscopy (EDS) analysis.
B) Atomic force microscopy (AFM) to evaluate surface roughness of orthodontic wires.
C) Conducting friction tests on Instron machines.
D) Nanoindenter coupled with AFM to assess the influence of decontamination and clinical exposure on wire properties.
E) Statistical analyses of clinical outcomes related to orthodontic movement.

8. Which advantages do shape memory polymers (SMPs) offer as orthodontic wires, as described in the passage? Select all that apply.
A) Ability to remember and temporarily fix equilibrium shapes.
B) Controlled and consistent forces for tooth movement.
C) Activation by changes in temperature or light.
D) Enhanced stain resistance compared to traditional materials.
E) Reduced frequency of patient visits due to high percent elongation.

9. What benefits do silver nanoparticles (AgNPs) offer in orthodontics, as described in the passage?
A) Broad-spectrum activity against various microorganisms.
B) Reduction of enamel demineralization during and after orthodontic treatments.
C) Promotion of biofilm formation and bacterial growth on human dentin.
D) Inhibition of bacterial adherence on orthodontic appliances.
E) Enhanced antiadherence activities for larger AgNP samples.

10. How can the incorporation of nanoparticles into orthodontic materials potentially improve orthodontic treatment?
A) Enhancing mechanical properties of orthodontic appliances.
B) Modulating bacterial flora in the oral cavity.
C) Increasing the risk of bacterial adhesion and biofilm formation.
D) Reducing the effectiveness of tooth movement.
E) Decreasing treatment-related complications such as enamel demineralization.

References

[1]. De Stefani, A.; Bruno, G.; Preo, G.; Gracco, A. Application of Nanotechnology in Orthodontic Materials: A State-of-the-Art Review. Dent. J.2020, 8, 126. https://doi.org/10.3390/dj8040126.

[2]. Zakrzewski W, Dobrzynski M, Dobrzynski W, Zawadzka-Knefel A, Janecki M, Kurek K, Lubojanski A, Szymonowicz M, Rybak Z, Wiglusz RJ. Nanomaterials Application in Orthodontics. Nanomaterials (Basel). 2021 Jan 28;11(2):337. doi: 10.3390/nano11020337. PMID: 33525572; PMCID: PMC7912679.

8. Nanoparticles for Oral Cancer Diagnosis and Therapy

Oral cancer represents a significant global health challenge, with limited survival rates and debilitating consequences for patients. Traditional diagnostic and treatment methods often fall short in terms of accuracy and effectiveness, highlighting the need for innovative approaches. Biomaterials with unique properties have emerged as promising tools in mediating cell behaviors and treating diseases, including oral cancer.

In recent years, nanomaterials have garnered considerable attention in the field of biomedical diagnostics and therapeutics. Their ability to exploit the unique characteristics of tumor microenvironments, such as angiogenesis and hypoxia, has opened new avenues for more targeted and effective interventions. Nanoparticles (NPs) can passively target tumors through the enhanced permeability and retention (EPR) effect, which allows them to accumulate in tumor tissues while minimizing systemic toxicity (Figure 8.1.).

Moreover, active targeting strategies involving the conjugation of NPs with specific ligands or antibodies have shown promise in further enhancing tumor targeting and reducing off-target effects. NPs can serve as carriers for contrast agents in imaging, as well as deliver active drugs for chemotherapy, photosensitizers for photodynamic therapy (PDT), and gene therapy agents. Additionally, certain NPs possess unique optical, magnetic, and electrical properties that can be harnessed for both diagnosis and therapy.



Figure 8.1. Nanoparticles for oral cancer diagnosis and therapy.

Various types of NPs, including organic and inorganic ones, offer distinct advantages in terms of size, reactivity, and functional modification. Examples include liposomes, dendrimers, polymeric NPs, gold NPs, magnetic NPs, quantum dots, and carbon nanotubes. The versatility of these NPs allows for tailored approaches to oral cancer diagnosis and treatment, offering the potential for improved outcomes and reduced side effects. However, several challenges remain in the widespread implementation of NPs in oral cancer management. These include optimizing NP design for enhanced targeting and delivery, ensuring biocompatibility and safety, and addressing issues related to scalability and cost-effectiveness. Despite these challenges, the ongoing advancements in nanotechnology hold great promise for revolutionizing the diagnosis and treatment of oral cancer. In summary, the application of NPs in oral cancer diagnosis and therapy represents a rapidly evolving

field with significant potential for improving patient outcomes. Continued research and innovation in NP design and application are essential for overcoming existing limitations and realizing the full potential of nanotechnology in oral cancer management [1].

8.1. Liposomes for Oral Cancer Diagnosis and Therapy

Liposomes are versatile nanocarriers composed of amphiphilic phospholipid bilayers, forming closed spherical particles with a hydrophilic core. (Figure 8.2. (a)).

` These nanovesicles can encapsulate hydrophilic payloads within their aqueous core or hydrophobic payloads within the lipid bilayer, offering flexibility in drug delivery. In the context of tumor targeting, liposomes can exploit the enhanced permeability and retention (EPR) effect to passively accumulate within tumor tissues.

Additionally, active targeting strategies involve the attachment of specific ligands to the liposome surface, enabling selective binding to tumor-specific receptors.

For example, folate-bound liposomes can target folate receptors overexpressed on tumor cells, enhancing their specificity and efficacy (Figure 8.2. (b)).

The stability characteristics and encapsulation efficiency of liposomal formulations can vary significantly depending on their composition and structure.

These differences can be leveraged to tailor liposomal formulations to meet specific diagnostic and therapeutic needs, allowing for precise control over drug delivery and release kinetics (Figure 8.2. (c)).

Overall, liposomes represent promising nanocarriers for targeted drug delivery in cancer therapy, offering the potential for enhanced efficacy and reduced off-target effects.

Their ability to encapsulate a wide range of payloads and be modified with targeting ligands makes them valuable tools in the development of advanced diagnostic and therapeutic strategies for cancer treatment. [1].

8.1.1. Liposomes for Oral Cancer Diagnosis

Liposomes have emerged as valuable tools in cancer diagnosis, with applications ranging from imaging to targeted therapy. One notable application involves labeling liposomes with radionuclides, such as 64Cu, to enable imaging of tumors. This labeling is typically achieved by conjugating the radionuclide to an anchor molecule that is either present within the hydrophilic core of the liposome or encapsulated within the phospholipid bilayer.

Studies, such as the one conducted by Mahakian et al., have demonstrated the potential of 64Cu-labeled liposomes for detecting early-stage tumors. In comparison to traditional imaging techniques like 18F-FDG positron emission tomography (PET), 64Cu-labeled liposomes offer advantages in terms of sensitivity and specificity, allowing for the early detection of tumors.

By leveraging the unique properties of liposomes, including their ability to encapsulate imaging agents and target specific receptors on tumor cells, researchers can develop innovative strategies for cancer diagnosis and monitoring. The use of radionuclide-labeled liposomes holds promise for improving the accuracy and efficiency of tumor detection, ultimately leading to better patient outcomes.

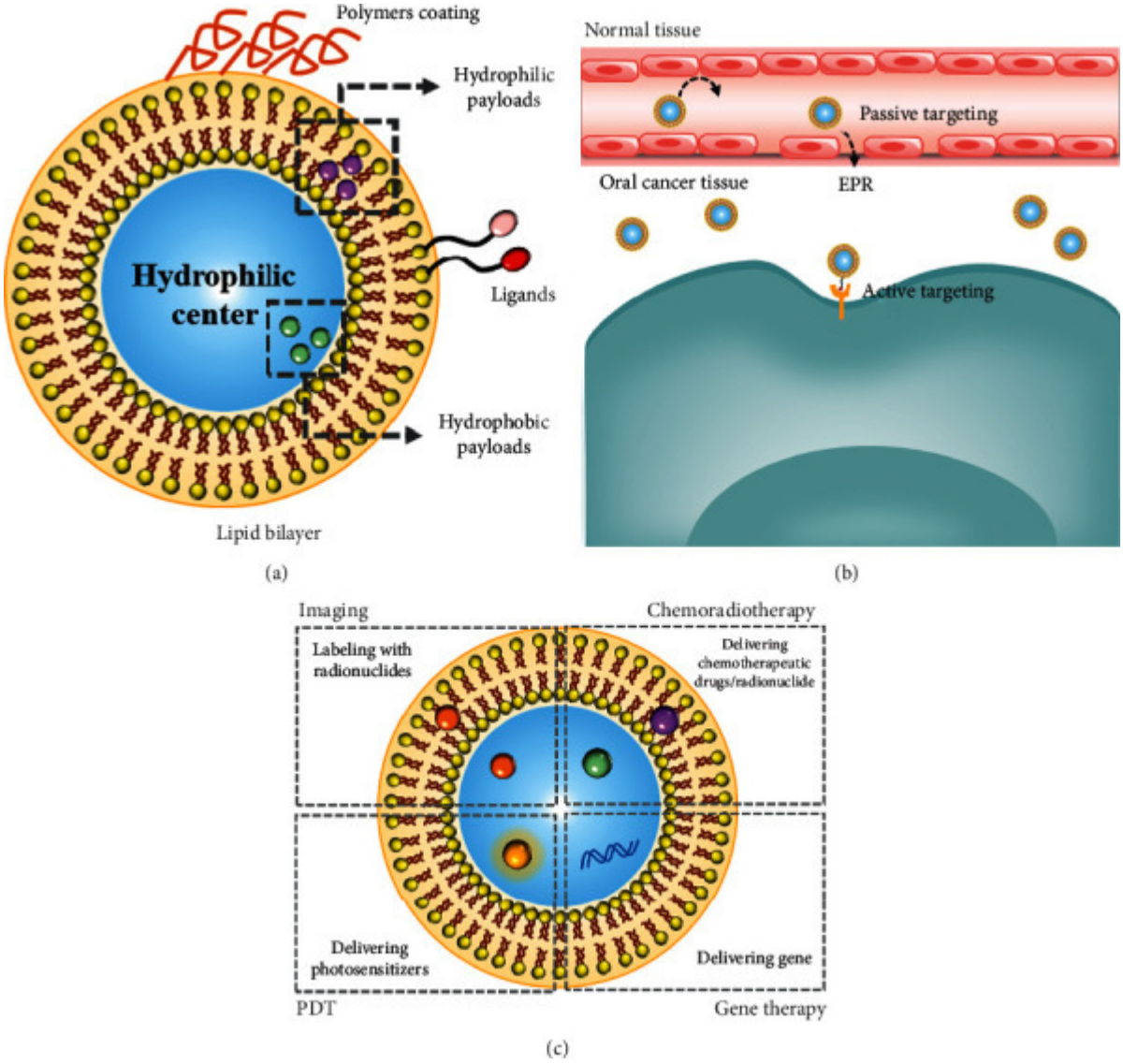


Figure 8.2. (a) The structure of liposomes. (b) The methods of liposome entering cancer tissue. (c) Diagnosis and therapy of liposomes.

8.1.2. Liposomes for Oral Cancer Therapy

Liposomes have emerged as versatile delivery systems for anticancer agents, aiming to enhance drug efficacy while minimizing adverse effects. However, their clearance by the reticuloendothelial system (RES) poses a challenge. To address this, biocompatible polymers like polyethylene glycol (PEG) are often used to coat liposome surfaces, prolonging circulation time and enhancing drug delivery to tumors.

Numerous studies have investigated liposomal formulations loaded with various anticancer drugs, such as doxorubicin, curcumin, paclitaxel, carboplatin, and cisplatin. These formulations have demonstrated increased apoptotic effects on cancer cells compared to free drugs. Combination therapies involving two or more anticancer drugs, along with supplements, have shown improved efficacy in inducing cancer cell apoptosis.

Liposomes have also shown promise in gene therapy for oral cancer treatment, serving as non-viral vectors to deliver therapeutic genes into target cells. Additionally, liposomes have been explored as carriers for radionuclides in tumor radiotherapy, including boron neutron capture therapy (BNCT) and photodynamic therapy (PDT). In BNCT, boron-rich liposomes selectively deliver 10B agents to tumor tissue, enhancing the effectiveness of neutron irradiation in inhibiting tumor cell growth. In PDT, liposomal formulations loaded with photosensitizers (PS) generate reactive oxygen species (ROS) upon light activation, inducing cancer cell death. Moreover, liposomal formulations have been

utilized to enhance the cytotoxicity of anticancer drugs in combination with PDT or chemotherapy, demonstrating potential synergistic effects.

Overall, liposomes offer a promising platform for the delivery of various therapeutic agents in oral cancer treatment, with the potential to improve efficacy and reduce adverse effects. Further research and clinical studies are warranted to optimize liposomal formulations and advance their application in oral cancer therapy [1].

8.2. Dendrimers for Oral Cancer Diagnosis and Therapy

Dendrimers are highly organized, branched macromolecules that hold great potential for advancing both the diagnosis and treatment of oral cancer. Their unique structural attributes and versatile functionality allow for numerous applications in medical science, particularly in oncology.

Structure of Dendrimers

Dendrimers are characterized by their multi-branched, tree-like structures, which consist of three key components:

1. **Central Core:** This core acts as the foundation from which branches proliferate.
2. **Repeated Branches:** These branches radiate out from the core in a controlled, symmetrical pattern, allowing for precise molecular engineering.
3. **Terminal Functional Groups:** The surface of the dendrimer, which can be customized with various functional groups to achieve specific interactions and functionalities.

Synthesis Methods

Dendrimers are synthesized through two primary methods, each influencing the final structure and properties of the molecules:

- **Divergent Method:** This method begins at the central core and builds outward, layer by layer. It allows for high levels of control over the structure but can lead to defects as the dendrimer grows.
- **Convergent Method:** Starting from the outer branches and moving inward towards the core, this approach often results in dendrimers with fewer structural defects and better-defined molecular weights but can be challenging for creating large structures.

Applications in Oral Cancer

Diagnosis

Dendrimers can be engineered to serve as platforms for diagnostic agents in oral cancer. Their ability to be functionalized with imaging agents, such as fluorescent markers or magnetic particles, makes them useful in advanced imaging techniques. For example, dendrimers can enhance the contrast in MRI scans or carry fluorescent tags for use in confocal microscopy, aiding in the early detection and localization of cancerous cells.

Therapy

In the realm of treatment, dendrimers offer significant advantages for drug delivery and gene therapy:

- **Targeted Drug Delivery:** Dendrimers can encapsulate anti-cancer drugs, protecting them from degradation before reaching their target. Their surface functional groups can be modified to recognize and bind specifically to cancer cells, enhancing the efficacy of the drug while minimizing side effects on healthy cells.
- **Gene Transfection:** Dendrimers are also used in gene therapy for cancer, where they can deliver genetic material into cells. By carrying genes that can induce apoptosis (cell death) in cancer cells or correct mutations, dendrimers play a crucial role in gene-based cancer therapies.

Dendrimers represent a frontier in nanotechnology with significant potential to impact the field of oral cancer diagnosis and therapy. Their customizable nature and precise architecture make them ideal candidates for carrying therapeutic agents directly to cancer cells, thus improving the specificity and effectiveness of treatment. Continued research and development in this area are expected to lead to more innovative solutions for managing oral cancer, ultimately improving patient outcomes.

8.2.1. Dendrimers for Oral Cancer Diagnosis

Dendrimers are increasingly being utilized as sophisticated tools for the early diagnosis of oral cancers due to their unique properties and structural versatility. The development of DNA-dendrimer and polypyrrole (DDPpy) sensors by Wei et al. is a significant advancement in this area, focusing on the sensitive detection of key biomarkers associated with oral cancer.

Structure and Functionality of DDPpy Sensors

The DDPpy sensors combine the benefits of dendrimers with the conductive properties of polypyrrole, a polymer known for its electrical conductivity and stability. This hybrid structure enhances the sensor's functionality in several ways:

- **High Specificity:** The dendrimer component provides a high density of active sites for biomarker binding, which can be precisely tailored to target specific molecules like interleukin-8 RNA and proteins, as well as interleukin-1β protein.
- **Improved Bioaffinity:** Dendrimers in the sensor structure improve the overall bioaffinity for the target biomarkers. This means the sensors can more effectively bind to these molecules, leading to more accurate and reliable detection.
- **Conductive Properties:** Integrating polypyrrole grants the sensors enhanced electrical properties, which are crucial for the transduction of the biological interaction into a measurable electrical signal. This feature is particularly useful in creating biosensors that provide quick and quantifiable results.

Application in Oral Cancer Diagnosis

The ability to detect specific biomarkers related to oral cancer, such as interleukin-8 and interleukin-1β, is vital for early diagnosis and effective management of the disease. These biomarkers are indicative of inflammation and cellular changes that could signify the early stages of cancer development. By utilizing DDPpy sensors:

- **Early Detection:** The enhanced sensitivity and specificity of the sensors allow for the early detection of oral cancer biomarkers, potentially before the disease progresses to a more advanced stage.
- **Non-invasive Testing:** Deploying dendrimer-based sensors could lead to non-invasive testing methods, such as saliva tests, that are less discomforting to patients compared to traditional biopsy methods.
- **Personalized Medicine:** The precise detection and quantification of biomarkers can also aid in tailoring individual treatment plans, aligning with the principles of personalized medicine.

Future Prospects

The promising results obtained by Wei et al. pave the way for further research and development in dendrimer-based sensors for cancer diagnostics. Continued advancements could lead to:

- **Enhanced Sensor Accuracy:** Ongoing improvements in dendrimer chemistry and sensor technology could yield even more precise and efficient diagnostic tools.
- **Broader Applications:** While currently focused on oral cancer, similar sensor designs could be adapted for other cancers or diseases with known biomarkers.
- **Integration into Clinical Practice:** As these sensors are refined and validated through clinical trials, they could become routine tools in dental and medical diagnostics, greatly enhancing early detection capabilities.

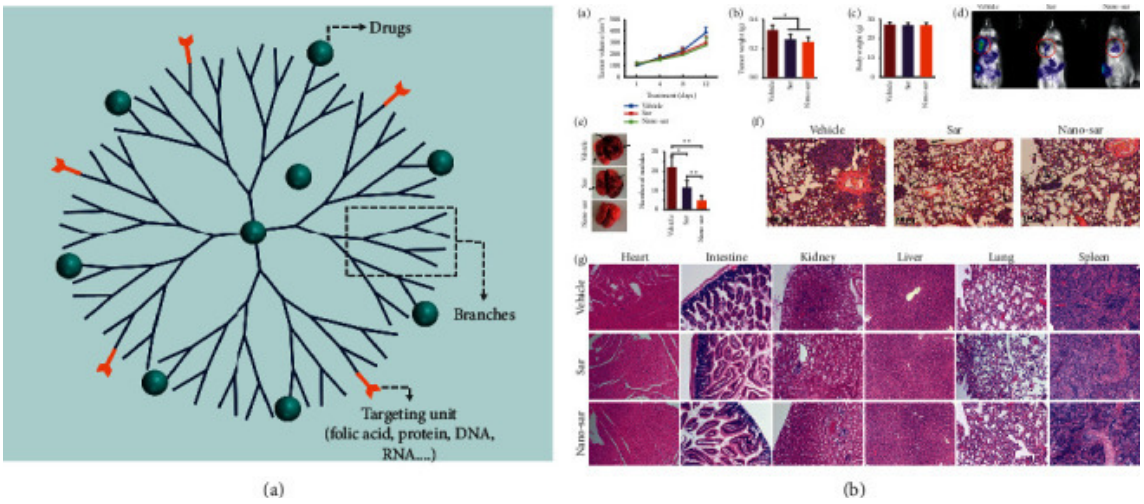


Figure 8.3. Representation of two key components showcasing the innovative use of dendritic nanostructures in the treatment and diagnosis of head and neck squamous cell carcinoma (HNSCC), emphasizing their multifunctional capabilities and therapeutic advantages: (a): Multifunctional Dendritic Carrier; (b): Nano-Sar in Cancer Treatment [1].

8.2.2. Dendrimers for Oral Cancer Therapy

Dendrimers serve as effective drug delivery systems by encapsulating drugs within their interior cavity or by covalently conjugating drugs to their terminal functional groups. This versatility has led to their widespread use in drug delivery applications. For instance, Ward et al. coencapsulated methotrexate (an anticancer drug) and folic acid (FA, a targeting agent) in acetylated generation 5 dendrimers, resulting in better tumor control compared to free drug when tested on xenograft tumor growth models. Furthermore, dendrimers have shown potential in gene transfection. Liu et al. demonstrated that polyamidoamine (PAMAM) dendrimers could effectively deliver shRNAs to silence human telomerase reverse transcriptase (hTERT) in oral squamous cell carcinoma (OSCC) cells and xenograft mouse models, leading to cell apoptosis and inhibition of tumor growth. Moreover, FA-decorated PAMAM dendrimers of generation 4 showed improved gene transfection efficiency. Additionally, dendritic nanoparticles loaded with saracatinib (Nano-sar) effectively inhibited invasion and metastasis of head and neck squamous cell carcinoma by blocking Src kinase activity (Figure 8.3.).

8.3. Orthodontic Miniscrews Gold Nanoparticles for Oral Cancer Diagnosis and Therapy

Gold nanoparticles (NPs) have become increasingly important in biomedical applications, particularly in cancer diagnostics and therapy, due to their unique properties and functional capabilities. Here's an elaboration on their features, mechanisms of tumor targeting, and the effectiveness of conjugation strategies for enhanced targeting:

Properties of Gold Nanoparticles

- **Biocompatibility**: Gold NPs are well-tolerated by human tissues, making them suitable for medical applications.
- **Bioconjugation**: They can be easily attached to various biomolecules, allowing for targeted therapeutic or diagnostic applications.
- **Size and Stability**: Their size can be precisely controlled during synthesis, ranging from a few nanometers to tens of nanometers, which along with their high colloidal stability, makes them ideal for biological applications.
- **Optical Properties**: Gold NPs have unique and tunable optical properties, including strong plasmon resonance, which can be leveraged for imaging and therapeutic heat generation.

Tumor Targeting via Gold Nanoparticles

- **Enhanced Permeability and Retention (EPR) Effect**: This phenomenon is utilized for the passive targeting of tumors. Due to leaky vasculature in tumor tissues, gold NPs can accumulate more readily within tumor sites than in normal tissues.
- **Cellular Uptake**: Once accumulated at the tumor site, gold NPs can enter cells predominantly through endocytosis, facilitated by their nanoscale size. However, the extent of uptake through passive targeting alone is limited.

Enhancement of Targeting through Bioconjugation

- **Active Targeting**: To overcome the limitations of passive targeting, gold NPs are often conjugated with specific antibodies or ligands. For example, conjugation with anti-EGFR antibodies enhances their ability to specifically bind to cancer cells that overexpress the EGFR protein.
- **El-Sayed et al.'s Findings**: This study highlighted that anti-EGFR-antibody-conjugated gold NPs could achieve a more uniform and specific distribution on cancer cells compared to noncancerous cells. The specificity stems from the ability of the conjugated antibodies to recognize and bind to EGFR, a common biomarker overexpressed in many types of cancer cells.

Figure 8.4: Illustration of Passive vs. Active Targeting

- This figure likely demonstrates the differences in distribution patterns between non-conjugated (passively targeted) and antibody-conjugated (actively targeted) gold NPs. Such illustrations are critical for understanding how conjugation can significantly improve the specificity and efficacy of gold NPs in targeting tumor tissues.

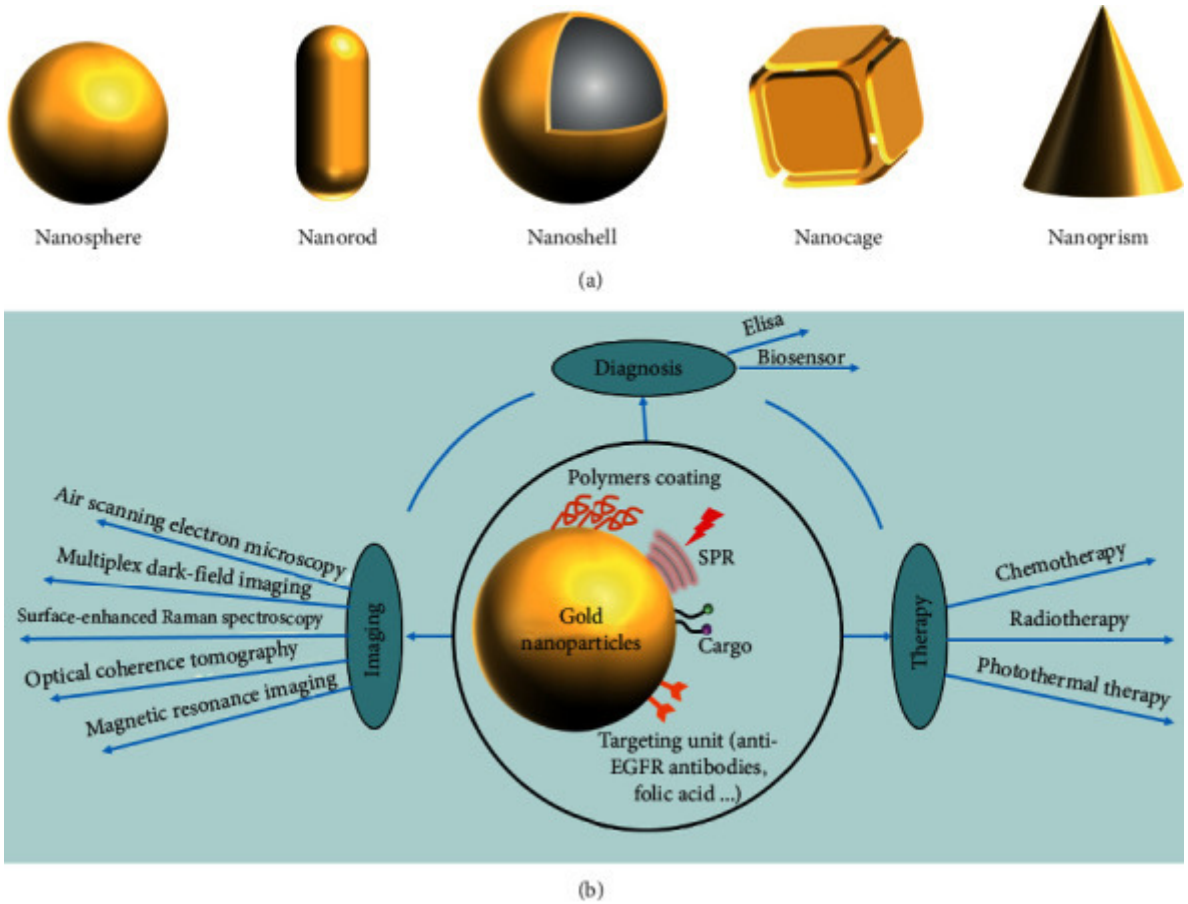


Figure 8.4. (a) The geometries of gold NPs. (b) Diagnosis and therapy of gold NPs. [1].

8.3.1. Gold Nanoparticles for Oral Cancer Diagnosis

Gold nanoparticles (NPs) have transformed the landscape of cellular imaging and diagnosis of oral cancer, leveraging their unique optical properties and versatility in conjugation with other

diagnostic molecules. Here's a detailed overview of how gold nanoparticles are being used to advance the diagnosis of oral cancer:

Optical Properties and Imaging Techniques

- **Surface Plasmon Resonance (SPR)**: Gold NPs exhibit strong light scattering abilities due to the SPR phenomenon when irradiated with near-infrared (NIR) and visible light. This property makes them exceptionally useful in dark-field microscopy, where they provide brighter signals than traditional chemical fluorophores, enhancing the visibility of cellular and anatomical details crucial for early cancer diagnosis.

Multifunctional Nanoplatforms

- **Conjugation with Antibodies**: Gold nanorods, for example, can be conjugated with anti-EGFR monoclonal antibodies. This specific binding ability allows them to differentiate between benign, premalignant, and malignant oral lesions effectively, offering a targeted approach to diagnosing oral cancer.
- **Enhancement in Electron Microscopy**: In air scanning electron microscopy, gold NPs improve the delineation of tumor margins, a crucial factor in surgical oncology for ensuring complete tumor removal.

Dynamic Imaging and Diagnostic Tools

- **Matrix Metalloproteinase 2 Sensing**: Upconversion nanoparticles conjugated with gold NPs enable the dynamic imaging of cancer cells, providing real-time insights into cellular behaviors and cancer progression.
- **Multiple Dark-Field Imaging**: Non-plasma-scattering probes based on gold NPs allow for repeated imaging of live cancer cells, aiding in continuous monitoring without damaging the cells.

Advanced Diagnostic Techniques

- **Optical Coherence Tomography (OCT)**: Acid-transforming gold nanoclusters are used in OCT to detect early-stage cancers, enhancing the resolution and depth of imaging.
- **Surface-Enhanced Raman Spectroscopy (SERS)**: Gold NPs significantly boost the spectral intensities in SERS, a non-invasive technique that provides detailed molecular insights, which is particularly useful for diagnosing oral squamous cell carcinoma (OSCC).
- **Immunosensing Platforms**: Gold-NP-reduced graphene-oxide-based bioelectrodes serve as potent immunosensing platforms, enhancing the electrochemical detection of biomarkers associated with oral cancer.
- **Enhanced ELISA Protocols**: Gold nanoparticles also improve the sensitivity and limit of detection in conventional ELISA protocols, such as those used for detecting osteopontin, a marker associated with oral cancer progression.

The integration of gold nanoparticles into various diagnostic modalities for oral cancer represents a significant advancement in oncology. By enhancing imaging contrast, enabling targeted detection, and improving the sensitivity of biochemical assays, gold NPs provide a comprehensive approach to the early detection and management of oral cancer. These innovations not only facilitate more accurate diagnostics but also open new avenues for personalized medicine, where treatments can be tailored based on precise imaging and molecular characterization of tumors.

8.3.2. Gold Nanoparticles for Oral Cancer Therapy

Gold nanoparticles (NPs) are extensively utilized as drug carriers in oral cancer therapy, offering various benefits in terms of drug delivery and treatment efficacy. Folic acid-gold-bilirubin (FGB) NPs have been shown to induce cell apoptosis in oral cancer cells through active targeting mediated by folic acid and the delivery of bilirubin, resulting in the generation of reactive oxygen species (ROS), DNA damage, and alteration of mitochondrial membrane potential.

Gold NPs can also enhance the efficacy of chemotherapeutic drugs such as 5-fluorouracil by sensitizing oral cancer cells to chemotherapy. Moreover, they can improve the sensitivity of oral cancer cells to radiation therapy, enhancing the effects of X-ray irradiation against oral cancer cells in vitro by inducing apoptosis.

In addition to their role in drug delivery, gold NPs are efficient converters of photon-thermal energy and can be utilized for photothermal therapy (PTT). Gold NPs can absorb near-infrared (NIR) light and convert it into heat energy, leading to hyperthermia in tumor cells, which are more sensitive to heat than normal cells. This property makes them effective agents for PTT in oral cancer treatment.

Combining chemotherapy with photothermal therapy, a nanoplatform consisting of podoplanin antibody-conjugated gold NPs loaded with doxorubicin (DOX) has been investigated for enhanced antitumor efficacy. This system facilitates targeted drug delivery to tumor sites and enhances drug release under the acidic conditions of tumor cells' endolysosomal compartments.

Furthermore, multifunctional gold nanoshells coated with superparamagnetic iron oxide have been explored for thermal tumor destruction while minimizing thermal damage to surrounding normal tissues under MRI-visible guidance.

The cytotoxicity induced by gold NPs in oral cancer cells is associated with autophagy-mediated mechanisms. Additionally, the use of upconversion NPs conjugated with gold nanorods has been shown to enhance plasmon-mediated photodynamic therapy (PDT), providing a promising approach for oral cancer treatment.

8.4. Magnetic Nanoparticles for Oral Cancer Diagnosis and Therapy

Magnetic nanoparticles (MNPs) come in various shapes and can be modified to exhibit high magnetic properties, stability, biocompatibility, and biodegradability. These properties make them suitable for a wide range of applications in the medical field, including magnetic resonance imaging (MRI), drug delivery systems, and hyperthermic treatment of cancers, including oral cancer.

Synthesizing MNPs involves several methods, such as coprecipitation, thermal decomposition, microemulsion, hydrothermal, sol-gel, combustion, and polyol syntheses. Each method offers unique advantages and can be tailored to produce MNPs with specific properties suitable for different applications (Figure 8.5).

However, one challenge in the application of MNPs is their potential uptake by the reticuloendothelial system (RES) and tendency to agglomerate, which limits their effectiveness. To address this challenge, polymeric coatings can be applied to MNPs to provide a barrier against RES uptake and prevent nanoparticle agglomeration. These coatings improve the stability and biocompatibility of MNPs, enhancing their suitability for various biomedical applications, including targeted drug delivery and cancer treatment.

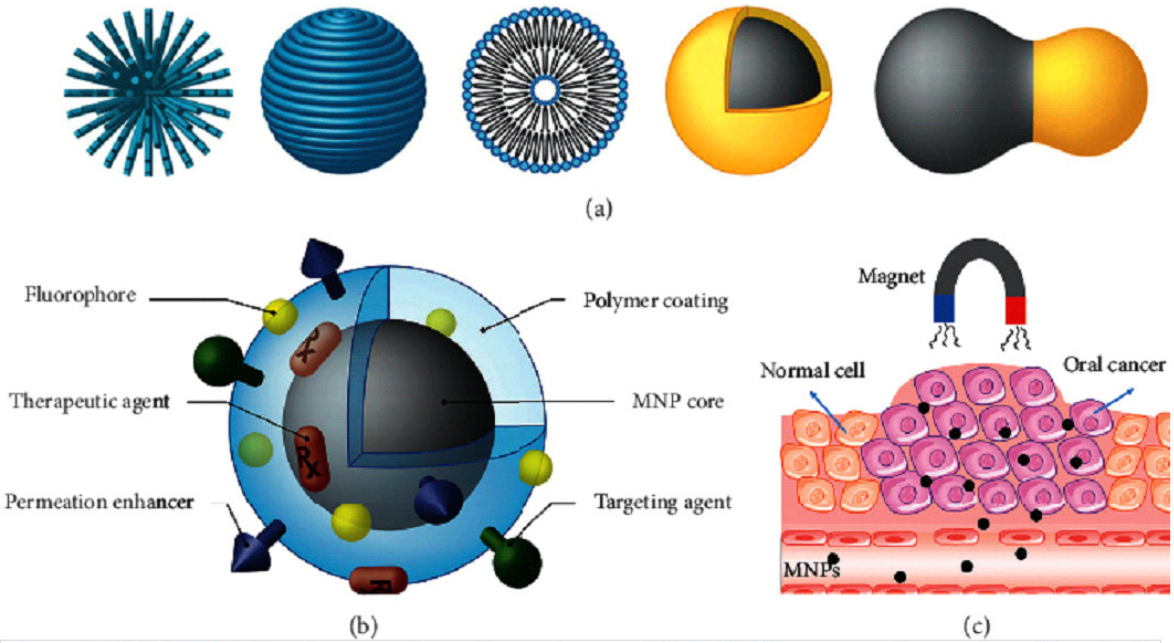


Figure 8.5. (a) MNP structures and coating schemes [1]. (b) MNP possessing various ligands to enable multifunctionality [1]. (c) The therapeutic effect of magnetic NPs under the control of an external magnetic field. [1].

8.4.1. Magnetic Nanoparticles for Oral Cancer Diagnosis

Indeed, magnetic nanoparticles (MNPs) are promising candidates for enhancing magnetic resonance imaging (MRI) as contrast agents. MRI is a powerful noninvasive imaging modality used widely in clinical medicine for diagnosing various conditions. MNPs can serve as contrast agents by influencing proton relaxation, thereby improving the visualization of tissues and organs in MRI scans.

One advantage of MNPs in MRI is their ability to be selectively injected into tumor sites, allowing for precise imaging of tumors without affecting surrounding healthy tissues. This targeted delivery minimizes potential side effects and enhances the accuracy of tumor detection and localization.

As research progresses, the development of active targeting MNPs holds promise for further improving tumor detection and localization in MRI. By utilizing the unique molecular signatures of diseases, such as specific biomarkers expressed by tumors, active targeting MNPs can enhance the specificity and sensitivity of MRI for detecting and characterizing tumors. This advancement could significantly impact medical and biological diagnostics, offering clinicians better tools for early detection and accurate diagnosis of various diseases, including cancer.

8.4.2. Magnetic Nanoparticles for Oral Cancer Therapy

Magnetic nanoparticles (MNPs) offer a promising avenue for targeted drug delivery systems, allowing drugs to be specifically delivered to tumor sites under the influence of an external magnetic field. However, the nonporous surface of MNPs can be a limitation in drug carrier applications. To address this challenge, researchers have developed strategies to modify the surface of MNPs to increase drug loading capacity and enhance drug release at the tumor site.

For example, Zhang et al. synthesized MNPs modified with polyacrylic acid (PAA) to increase the loading capacity of bleomycin (BLM), a chemotherapeutic drug. These BLM-MNPs were effectively targeted to tumor tissue under the influence of a magnetic field, releasing BLM locally and steadily to inhibit tumor growth.

In recent years, NP-based gene therapy has emerged as a promising approach for cancer treatment, leveraging RNA interference (RNAi) mechanisms to silence specific genes involved in cancer progression. MNPs can be designed to target these genes, facilitating the delivery of small interfering RNA (siRNA) or microRNA (miRNA) to cancer cells. For instance, Jin et al. developed an siRNA delivery system using MNPs coated with polyethyleneimine (PEI), enabling efficient gene silencing of B-cell lymphoma-2 (BCL2) and Baculoviral IAP repeat-containing 5 (BIRC5) genes, which promote cancer cell survival.

Moreover, MNPs have shown potential in hyperthermia-based cancer therapies, such as photothermal therapy (PTT) and magnetic fluid hyperthermia. PTT utilizes gold nanoparticles to selectively heat and kill cancer cells upon exposure to near-infrared light, while magnetic fluid hyperthermia induces cellular damage and apoptosis by generating heat under an alternating magnetic field (AMF). MNPs conjugated with antibodies targeting specific biomarkers, such as CD44 and integrin $\alpha v\beta 6$, have demonstrated efficacy in inhibiting tumor growth through hyperthermia without damaging surrounding normal tissues.

Combining hyperthermia with chemotherapy, known as thermochemotherapy, has emerged as a promising strategy to enhance anticancer treatment effectiveness while reducing the effective dosage of chemotherapeutic agents. For instance, Sato et al. demonstrated the synergistic effects of magnetic hyperthermia combined with cisplatin chemotherapy, suggesting that thermochemotherapy could offer improved outcomes compared to either treatment alone.

Overall, MNPs hold great promise in advancing targeted drug delivery and cancer therapy, offering versatile platforms for precision medicine approaches in the treatment of oral cancer and other malignancies [1].

8.5. Quantum Dots for Oral Cancer Diagnosis and Therapy

Quantum dots (QDs) represent a class of semiconductor nanocrystals with unique optical properties, making them valuable tools in various biomedical applications. These nanocrystals typically range in size from 1 to 10 nanometers in diameter and are composed of elements from groups II-IV, IV-VI, or III-V of the periodic table.

One of the key advantages of QDs is their high fluorescence intensity, coupled with a narrow emission spectrum and broad absorption spectrum. This means that they can absorb a wide range of wavelengths, from ultraviolet to near-infrared (NIR) light, and emit light at a specific wavelength, making them useful for various imaging and sensing applications.

In cancer therapy, QDs have shown promise as probes for imaging and carriers for drug delivery. Their fluorescence properties allow for precise imaging of cancer cells or tissues, aiding in diagnosis and monitoring of treatment responses. Additionally, QDs can be functionalized with targeting ligands to specifically deliver therapeutic agents to cancer cells, potentially enhancing treatment efficacy while minimizing side effects on healthy tissues.

Moreover, QDs can be engineered to generate reactive oxygen intermediates/species (ROIs/ROS) or produce heat when exposed to light, particularly in the NIR range. This property can be exploited for photodynamic therapy (PDT) or photothermal therapy (PTT) of cancer. In PDT, QDs can produce cytotoxic ROS upon light activation, leading to selective destruction of cancer cells. In PTT, QDs can absorb NIR light and convert it into heat, which can induce hyperthermia and cause localized tumor cell death.

Overall, the unique optical properties of quantum dots make them versatile tools in cancer therapy, with potential applications ranging from imaging and drug delivery to phototherapy. Continued research into QD-based theranostic platforms holds promise for improving the diagnosis and treatment of cancer.

8.5.1. Quantum Dots for Oral Cancer Diagnosis

Quantum dots (QDs) offer superior optical characteristics compared to traditional organic fluorescence materials, thanks to their unique quantum size and surface effects. Researchers have demonstrated the advantages of QDs in various applications, including cell labeling and cancer diagnosis.

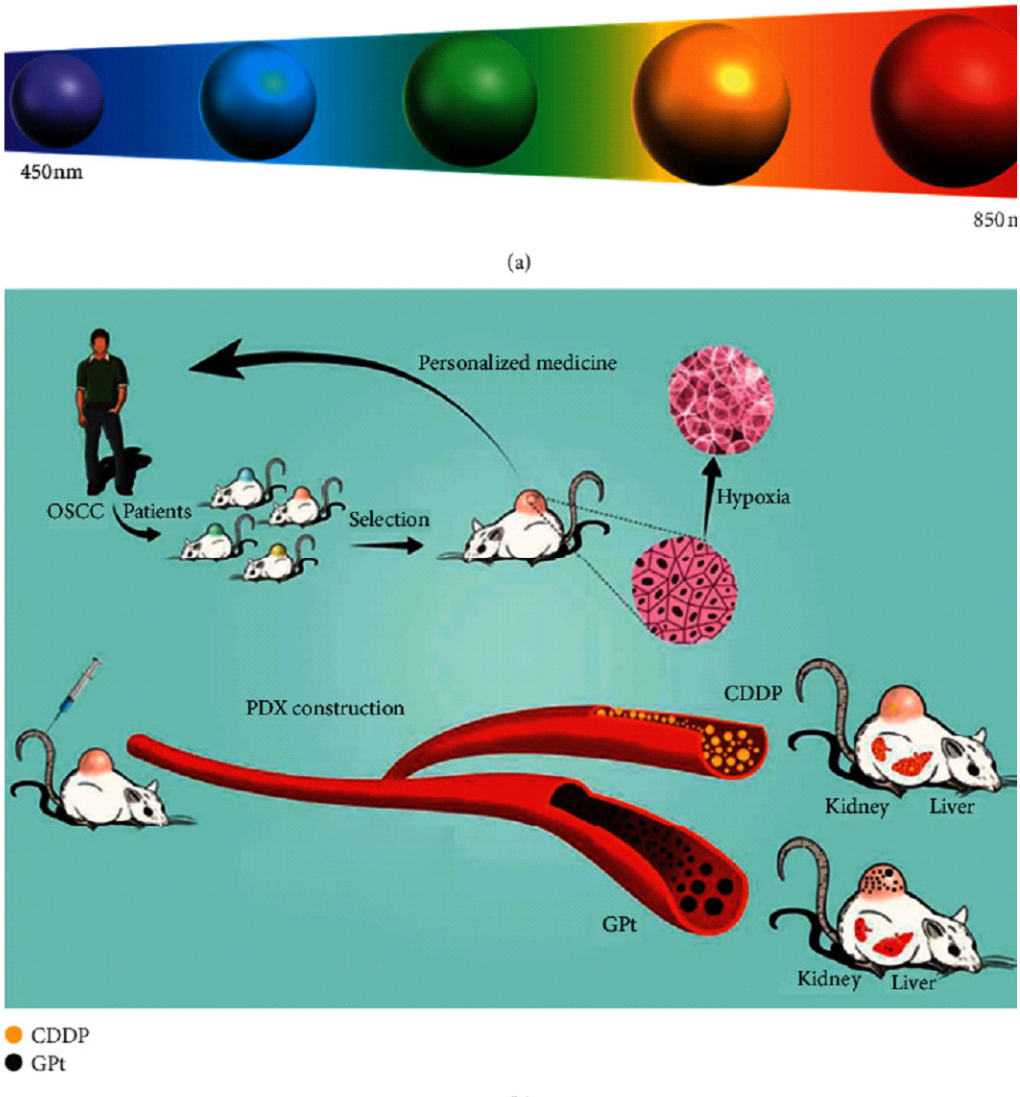


Figure 8.6. (a) The fluorescence emission properties of QDs can be modulated by changing their size. (b) Schematic illustration of a multifunctional anticancer platform against hypoxia-induced chemoresistance of OSCC [1].

For instance, Zhao et al. utilized QDs labeled Tca8113 cells alongside the FITC labeling technique. They observed that QDs exhibited significantly higher fluorescence intensity and photostability compared to FITC. This makes QDs more suitable for long-term dynamic observation of cell physiological changes, offering researchers a powerful tool for studying cellular processes.

Furthermore, the excellent optical properties of QDs have been harnessed for cancer diagnosis. Yang and Chen, for example, developed EGFR-antibody-conjugated QD800 for targeted and in vivo imaging of human buccal squamous cell carcinoma cell line (BcaCD885) in an oral squamous cell carcinoma (OSCC) animal model. QD800, with its maximal emission wavelength of 800 nm, demonstrated strong tissue penetration, making it suitable for visible fluorescence imaging of cancer cells.

These studies highlight the potential of QDs as versatile tools in biomedical research and cancer diagnostics, offering enhanced fluorescence intensity, photostability, and tissue penetration compared to traditional organic fluorophores. As research in this field continues, QDs may play an increasingly important role in advancing our understanding of cellular processes and improving cancer detection and diagnosis.

The utilization of quantum dots (QDs) in multifunctional nanoparticle probes has enabled the detection of molecular biomarkers in oral cancer cells with high sensitivity and specificity.

In a study by Xue et al., semiconductor QDs were employed in immunofluorescence histochemistry (QDs-IHC) to investigate the role of Caveolin-1 (Cav-1) in the carcinogenesis and development of tongue squamous cell carcinoma. The findings suggested that Cav-1 protein functions as an oncogene in the progression of tongue squamous cell carcinoma, highlighting the potential of QDs in elucidating molecular mechanisms underlying cancer development.

Moreover, detecting biomarkers at extremely low levels of nucleic acids and proteins poses a significant challenge. To address this, Xue et al. utilized QDs in situ hybridization (QDISH) to examine the connection between oral squamous cell carcinoma (OSCC) and human papillomavirus (HPV). The results indicated that QDISH offers higher sensitivity compared to conventional methods like ISH, demonstrating the utility of QDs in enhancing detection sensitivity for biomarkers associated with oral cancer.

Additionally, the development of biosensors based on QDs represents a significant advancement in biomarker detection. Xu et al. introduced a novel electrochemical method for detecting interleukin-8 (IL-8) using DNA-templated CdTe/CdS QDs (DNA-QDs). In this approach, IL-8 is treated with tris (2-carboxyethyl) phosphine (TCEP) to obtain active thiols (SH), which are then recognized and separated by magnetic beads (MBs). Subsequently, anti-IL-8@MBs are easily coupled with DNA-QDs via the Michael addition reaction, providing a simple and effective means of detecting IL-8 by monitoring the electrochemical responses of DNA-QDs.

These studies demonstrate the versatility and potential of QDs in various aspects of oral cancer research, including molecular characterization, biomarker detection, and diagnostic applications, offering valuable insights into disease pathology and providing innovative strategies for early detection and treatment monitoring.

8.5.2. Quantum Dots for Oral Cancer Therapy

The study aimed to develop a method using quantum dots (QDs) conjugated with specific antibodies (goat anti-mouse QD525nm-IgG and goat anti-mouse QD655nm-IgG) for the dynamic observation of physiological changes in heat shock protein 70 (HSP70) and heat shock factor 1 (HSF-1) in SCC-25 cells induced by heat shock. This approach allowed for long-term monitoring of cellular responses to heat shock and provided insights into strategies to modulate the activation of HSF-1 and accumulation of HSP70 in oral cancer.

Carbon quantum dots (CQDs) represent a novel class of fluorescent nanoparticles derived from carbon, offering exceptional biocompatibility and stable fluorescence properties. Das et al. developed an N-doped mesoporous hollow CQD (NCQD) with efficient thermal conversion capabilities and superior fluorescence imaging characteristics. This NCQD formulation was utilized to track the therapeutic response of photothermal therapy (PTT), offering potential applications in cancer treatment.

Graphene quantum dots (GQDs), another type of carbon quantum dots, have garnered attention for their unique properties. Wei et al. synthesized a polyethylene-glycol-GQDs-Pt (GPt) nanocomposite designed for the targeted delivery of platinum (Pt) to oral squamous cell carcinoma (OSCC) cells. This nanocomposite demonstrated enhanced chemotherapeutic efficacy against OSCC under both normoxic and hypoxic conditions, suggesting its potential as a promising treatment strategy for oral cancer.

These studies highlight the versatility of quantum dots in biomedical applications, ranging from dynamic cellular imaging to targeted drug delivery systems. By harnessing the unique properties of quantum dots, researchers are advancing the development of innovative approaches for cancer diagnosis, monitoring, and treatment [1].

8.6. Polymeric Nanoparticles for Oral Cancer Diagnosis and Therapy

Polymeric nanoparticles (NPs) represent a versatile platform for drug delivery in cancer therapy, utilizing both natural and synthetic polymers. These nanoparticles can be categorized into

two primary types: nanocapsules and nanospheres, each offering distinct encapsulation strategies and drug delivery mechanisms.

Nanocapsules feature a vesicular structure with an internal cavity where active pharmaceutical ingredients (APIs) are encapsulated. The drugs may reside within this cavity, protected by a polymeric shell, allowing for controlled release and targeted delivery to cancerous tissues.

On the other hand, nanospheres consist of drugs either trapped within the core of the particle or adsorbed onto the surface of the polymer matrix. This design enables efficient loading and release of drugs, offering flexibility in therapeutic applications.

Polymeric nanoparticles offer several advantages for cancer therapy. They are relatively simple to fabricate and customize, allowing for tailored drug delivery systems. Moreover, they exhibit excellent biocompatibility, minimizing adverse effects on healthy tissues. The diverse range of available polymers enables the design of nanoparticles with specific properties suited to different therapeutic needs. Additionally, polymeric nanoparticles can mimic biological structures, enhancing their interaction with biological systems and improving drug delivery efficiency.

Overall, polymeric nanoparticles hold promise as effective drug delivery vehicles for cancer therapy, leveraging their favorable characteristics to improve treatment outcomes while minimizing side effects. Continued research and development in this field are essential for advancing the use of polymeric nanoparticles in clinical settings (Figure 8.7.) [1].

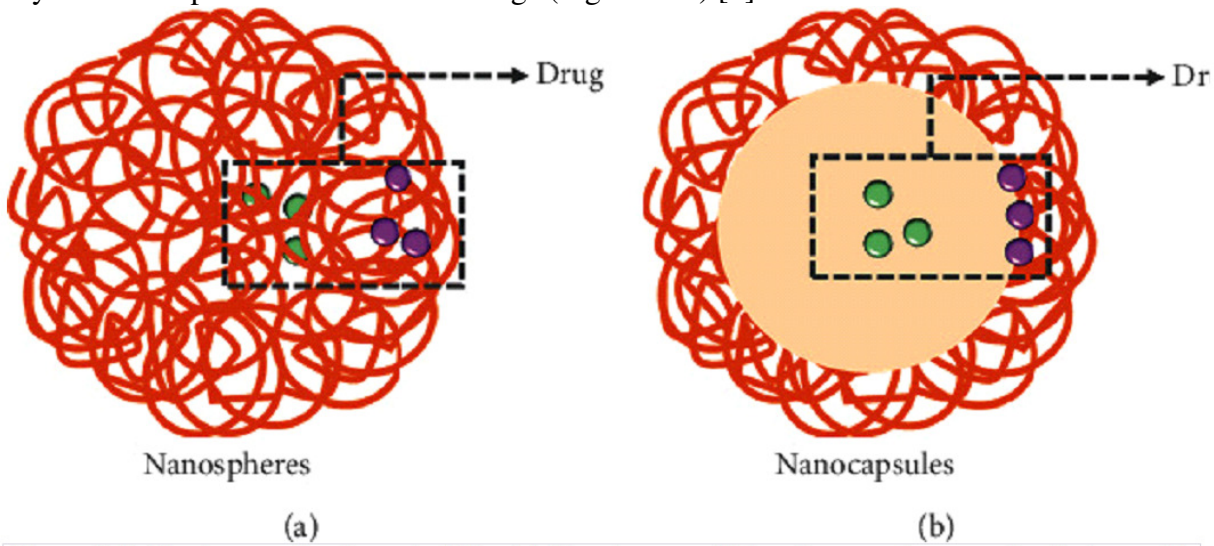


Figure 8.7. The types of polymeric NPs. (a) The drug could be dispersed or covalently bound to the polymer matrix in nanospheres. (b) The drug could be encapsulated in the interior of the vesicular cavity or enclosed by the solidified polymeric shell in nanocapsules [1].

8.6.1. Polymeric Nanoparticles for Oral Cancer Diagnosis

Polymeric nanoparticles (NPs) have become increasingly significant in the field of medical imaging and targeted therapy, particularly for cancers like oral cancer. Their ability to be functionalized with various targeting ligands and drugs makes them a versatile tool for enhancing diagnosis and treatment strategies. Here's a detailed discussion on the use of polymeric NPs, focusing on their role in photoacoustic imaging and endoscopic detection:

Targeted Photoacoustic Imaging

Polymeric nanoparticles can serve as effective contrast agents in photoacoustic imaging by absorbing light at specific wavelengths and converting it into sound waves. This property allows for deep tissue penetration and high-resolution imaging of cancerous tissues. The enhancement of photoacoustic imaging using polymeric NPs can provide more accurate localization and characterization of tumor tissues, facilitating early detection and precise monitoring of treatment responses.

High-Performance Nanoparticle for Fluorescent Endoscopic Detection

- **Yang et al.'s Research**: This study highlights the development of a high-performance nanoparticle designed specifically for the fluorescent endoscopic detection of oral cancer. These nanoparticles likely incorporate fluorescent markers that emit light upon excitation, making them suitable for use in endoscopy, a technique that allows for direct visualization of the mucosal surface and the immediate detection of malignant lesions.
- **Folic-Acid-Conjugated Chitosan NPs**: These nanoparticles are particularly noteworthy because they are conjugated with folic acid, targeting folate receptors that are often overexpressed on the surface of oral cancer cells. The presence of folic acid on the nanoparticles enhances their ability to specifically bind to cancer cells and be internalized via endocytosis, improving the efficacy of diagnostic imaging.

Enhanced Drug Delivery

- **N-Succinyl Chitosan (SCHI) Polymer**: This variant of chitosan has been modified to carry a negative charge, which can be used to enhance the delivery of drugs like 5-aminolevulinic acid (5-ALA). 5-ALA is used as a precursor in the synthesis of photoactive porphyrins, which are compounds that accumulate preferentially in cancer cells and can be visualized under specific lighting conditions.
- **Mechanism of Enhanced Release**: The negative charge on N-succinyl chitosan reduces the interaction intensity between the chitosan polymer and 5-ALA, facilitating a more efficient release of the drug into oral cancer cells. This mechanism not only allows for targeted drug delivery but also enhances the effectiveness of photodynamic therapy, where the released 5-ALA leads to the production of singlet oxygen species that can kill cancer cells upon activation by light.

Implications and Future Prospects

The use of polymeric nanoparticles in the detection and treatment of oral cancer holds significant promise. By combining the specific targeting capabilities of ligand-conjugated nanoparticles with the advanced imaging and therapeutic properties of the polymers, researchers can create more effective, less invasive diagnostic and treatment options. Future research could focus on optimizing these nanoparticles for better stability, targeting efficiency, and controlled drug release, as well as testing their efficacy and safety in clinical trials.

Overall, the developments in polymeric nanoparticles for oral cancer represent a crucial advancement in oncology, aiming to improve patient outcomes through early detection and targeted therapy.

8.6.2. Polymeric Nanoparticles for Oral Cancer Therapy

Polymeric nanoparticles (NPs) have emerged as effective drug delivery systems, offering solutions to challenges such as poor cell permeability and drug degradation. Chitosan NPs, for example, have shown promise in encapsulating various anticancer agents like ellagic acid, glycyrrhetic acid, cisplatin, and curcumin. These NPs can be topically or locally applied to oral tumors, protecting the drugs from biological deactivation and enhancing their bioavailability. Additionally, cationic chitosan NPs exhibit mucoadhesive properties, prolonging their residence time at the delivery site.

Other polymer NPs, such as poly(lactic-co-glycolic acid) (PLGA) NPs and cisplatin-bounded N-vinylpyrrolidone/acrylic acid NPs, have demonstrated increased antiproliferative efficiency when loaded with anticancer drugs and administered locally to tumor sites. Ligand-decorated NPs show specificity in binding to receptor-overexpressed oral squamous cell carcinoma (OSCC) cells, facilitating efficient internalization.

Polyelectrolyte-assembling multilayer NPs (MLNPs) offer a platform for the encapsulation of multiple drugs, leading to superior therapeutic effects compared to single-drug-loaded NPs. Furthermore, ROS-sensitive delivery systems, such as those utilizing thioketal linkers or cupreous complexes embedded into chitosan NPs, enable controlled drug release, enhancing the efficacy of photodynamic therapy (PDT).

To address challenges like tumor recurrence and epithelial to mesenchymal transition (EMT) activation, innovative strategies like polyethylene-glycol-polyethyleneimine-chlorin e6 NPs for Wnt-1 siRNA delivery have been developed. These NPs inhibit the Wnt/β-catenin signaling pathway crucial for EMT under PDT conditions. Additionally, hyperbranched polymers offer a new avenue for drug delivery, enabling the loading of drugs like TH287 and sodium arsenite into hyperbranched poly(amine-ester) (HPAE) NPs. These systems exhibit enhanced sensitivity to drugs after inhibiting the MTH1 protein in tumor cells and can be conjugated with photosensitizers for PDT applications.

Overall, polymeric NPs represent a versatile and promising approach for targeted drug delivery in oral cancer therapy, offering solutions to various challenges encountered in conventional treatment modalities. Continued research in this area is essential for advancing the development of effective and safe therapeutic strategies for oral cancer.

8.7. Other Nanoparticles

Upconversion nanoparticles (UCNs) offer a promising approach to overcome the penetration depth limitations of conventional photodynamic therapy (PDT). Lucky et al. developed anti-EGFR-PEG-TiO2-UCNs for targeted treatment of oral cancer cells. These UCNs can be excited by near-infrared (NIR) light, allowing for deeper tissue penetration and inducing cancer cell destruction in deeper tissues.

Carbon nanotubes have emerged as versatile materials for various applications, including biosensing for oral cancer screening. Vertically aligned carbon nanotube arrays arranged in a 2D interdigitated electrode (IDE) footprint were developed as immunosensors for detecting cancerous inhibitor PP2A (CIP2A) in saliva supernatant. This sensor offers higher sensitivity than traditional ELISA test kits and does not require sample preconcentration or prelabeling techniques, thereby reducing total sensing time.

Polyethylenimine-modified silica nanoparticles have been engineered to carry both MDR1-siRNA and DOX, enabling efficient transfection into human OSCC DOX-resistant cell lines in vitro. This system effectively blocks the expression of multidrug resistance protein 1 (MDR1), thereby reducing multidrug resistance and enhancing the efficacy of chemotherapy.

Metal-organic frameworks (MOFs) have been utilized as drug delivery vehicles for cisplatin and taxol, aiming to enhance sustained release and decrease the burst effect. This approach offers the potential for improved therapeutic outcomes by optimizing drug delivery kinetics and minimizing adverse effects associated with conventional drug administration methods.

8.8. Conclusions

The review underscores the significant advancements made in utilizing nanoparticles (NPs) for both the diagnosis and treatment of oral cancer. The unique properties of NPs, such as their small size, reactivity, and customizable functionalization, make them valuable tools for accurate diagnosis and effective treatment strategies in oral cancer.

NPs offer a versatile platform for visualizing oral cancer, delivering therapeutic agents selectively to tumors, and employing various therapeutic techniques for tumor destruction. Furthermore, the integration of NPs into hybrid systems enhances their versatility, enabling multifunctionality and expanding their potential applications in oral cancer management.

Despite the promising therapeutic activities demonstrated in vitro and in preclinical models, challenges remain in translating these findings into clinical practice. The complex pathophysiology of oral cancer and variations in pharmacokinetics and biodistribution underscore the need for cautious interpretation of preclinical results. Additionally, concerns regarding the safety of NPs, including their potential for cellular dysfunction and adverse effects, must be addressed to ensure their clinical applicability.

Moving forward, efforts to bridge the gap between preclinical research and clinical implementation are crucial. Successful completion of clinical trials will pave the way for the widespread adoption of NP-based diagnostic and therapeutic approaches for oral cancer. Overall,

there is significant potential for the continued development and application of NP-based strategies in the diagnosis and treatment of oral cancer in the foreseeable future.

8.9. Nanotechnology in Oral Cavity Carcinoma: Recent Trends and Treatment Opportunities

Surgical resection remains the primary treatment modality, often accompanied by adjuvant chemoradiotherapy or radiotherapy in cases of locally advanced disease or certain pathological features. However, these multimodal therapies can lead to significant morbidity.

In response to these challenges, the review emphasizes the potential of cancer nanotechnology to revolutionize OCC management. Nanotechnology offers promising opportunities to improve survival outcomes and reduce treatment-related toxicity. The focus is on integrating nanotechnology into diagnostic procedures and future treatment strategies for OCC patients.

By exploring the use of nanotechnology in clinical therapeutic applications, the review aims to shed light on innovative approaches that could enhance the diagnosis and treatment of OCC. It underscores the importance of advancing nanotechnology research to address the unmet needs in OCC management and improve patient outcomes. Overall, the review seeks to contribute to the broader understanding of nanotechnology's role in the OCC landscape [2].

8.9.1. Cancer Nanotechnology

The review outlines the interdisciplinary nature of cancer nanotechnology, which draws upon expertise from various fields including medicine, physics, biology, chemistry, and engineering. Nanotechnology, as defined by the National Nanotechnology Initiative, involves the use of man-made nanoparticles ranging in size from 1 to 100 nanometers, with the potential application in treating solid tumors. While detailed physicochemical characterization of nanoparticles is not the primary focus of the review, the main features are briefly described to provide a scientific basis for the development of nanoparticle-based therapeutics.

The primary objective is to alter the biodistribution of chemotherapeutic agents, minimizing their accumulation in healthy tissue while enhancing uptake in malignant cells. Specifically, in the context of oral cavity carcinoma (OCC) treatment, nanotechnology-based approaches encompass a range of engineered vehicles for drug delivery, including nanoparticles, liposomes, hydrogels, and liquid crystals. These carriers have the potential to penetrate cellular structures and achieve better selective accumulation of therapeutic agents in tumor tissues [3].

Figure 8.8. in the review provides a summary of the main structures, advantages, and limitations of nanocarriers for OCC treatment, offering readers a comprehensive overview of the various nanoparticle-based platforms being investigated for therapeutic purposes.

Nanomaterial	Structure	Advantages	Limitations
Nanoparticle	polysaccharides, proteins and biocompatible/biodegradable polymers	biocompatibility, biodegradability	toxicity?
Liposome	membrane-like lipid layers, often phospholipids and cholesterol	permeability, charge density, steric hindrance	Less stable than nanoparticles
Hydrogel	hydrophilic polymeric chains dispersed in water	hydrophilicity, flexibility, versatility, high water absorptivity, biocompatibility; it interacts with saliva glycoproteins, causing mucoadhesion	slow response time
Liquid crystal materials in	mesophase state	it can be stored for long periods because thermodynamically stable	toxicity?

Figure 8.8. Nanocarriers for oral cavity carcinoma [2].

The global utilization of nanomaterials is driven by their favorable properties such as biocompatibility, biodegradability, mechanical properties, and low toxicity profiles. Ideally, nanomaterials should possess flexibility in terms of size, morphology, and surface properties to enhance tumor accumulation and facilitate drug internalization into cells. Nanoparticles typically traverse cellular membranes through endocytosis, thereby avoiding drug reflux out of the cell, or via the enhanced permeability and retention (EPR) process, taking advantage of the porous vasculature and leaky endothelium of tumor tissues. However, the toxicity of nanomaterials requires thorough evaluation, especially concerning their short- and long-term interactions with biological tissues. The distribution of nanomaterials in the body depends largely on their surface characteristics, and the risk of cardio-pulmonary toxicity should be assessed for each newly developed nanoparticle. While preliminary studies show promising results, larger and longer-term analyses are necessary to confirm their safety [4, 5, 6].

Cisplatin (CDDP) is commonly used as a systemic drug in combination with radiotherapy (RT) for locally advanced OCC. The standard regimen involves high-dose CDDP every 3 weeks administered concurrently with standard fractionated RT, resulting in a modest survival benefit. However, CDDP has limitations such as poor systemic stability, limited water solubility, and frequent side effects. To address these issues, ligand-decorated cancer-targeted CDDP-loaded nanoparticles have been developed. Preclinical studies have demonstrated their ability to enhance drug accumulation in OCC tissues and facilitate rapid intracellular uptake. Human trials are needed to assess their clinical applicability [7, 8].

Nanoparticles also offer potential for enhancing (chemo)radiation therapy ((C)RT) treatment. Prolonging tumor exposure to drugs can enhance synergistic actions with ionizing radiation, inhibit intra-fraction tumor growth, and promote repopulation of normal tissues. This strategy could improve local control rates while limiting exposure to normal tissues, thereby maximizing the therapeutic ratio [9, 10].

8.9.2. Diagnostic Procedures

Magnetic resonance imaging (MRI) with intravenous contrast and computed tomography (CT) are essential components of the pre-treatment work-up for oral cavity carcinoma (OCC),

providing valuable information for accurate staging. In advanced stages or when staging is uncertain, 18F-labeled fluoro-2-deoxyglucose (18F-FDG) positron emission tomography (PET)-CT can also be considered [11].

Advancements in nanotechnology have led to the investigation of various nanoparticles as specific contrast agents in diagnostic exams, aiming to improve accuracy, sensitivity, and specificity. One promising area of research is the use of lymphotropic nanoparticles for nodal staging in OCC [12].

Lymphotropic nanoparticles, such as ferumoxtran-10, are a relatively new class of MRI contrast agents that hold promise for improving the sensitivity of diagnostic exams. Ferumoxtran-10 is an ultrasmall superparamagnetic iron oxide (USPIO) particle covered with low-molecular-weight dextran. Administered intravenously, it enters the physiological iron metabolic pathway and is cleared by draining lymphatic vessels, allowing it to localize within lymph nodes [13].

Due to its small size, ferumoxtran-10 can easily penetrate the capillary wall and is taken up by macrophages within lymph nodes. This enables robust characterization of lymph nodes, independent of their size. Importantly, metastatic nodes can be differentiated from reactive nodes based on signal intensity changes on MRI images, as malignant nodes do not exhibit the same signal reduction observed in normal nodes [14].

Overall, lymphotropic nanoparticles offer a promising approach to improve the accuracy of nodal staging in OCC, potentially reducing false-negative rates and aiding in treatment decisions regarding neck dissection. Continued research in this area may lead to advancements in diagnostic imaging for OCC patients (Figure 8.9.).

Ferumoxtran-10, a lymphotropic nanoparticle-based contrast agent for MRI, has shown promising results in improving the accuracy of nodal staging in oral cavity carcinoma (OCC) patients. Several studies have demonstrated its efficacy in detecting metastatic nodal disease, particularly in normal-sized lymph nodes, which are often a challenge to diagnose accurately using conventional imaging techniques [15].

In a multicenter study involving 147 patients, ferumoxtran-10 MRI achieved an overall accuracy of 93%, sensitivity of 96%, and specificity of 87% in diagnosing pathologic or negative nodes. Notably, it performed even better in head and neck cancer cases, highlighting its potential role in OCC management [16].

Additional studies have corroborated these findings, reporting high sensitivity and specificity of ferumoxtran-10-enhanced MRI in characterizing lymph nodes in head and neck cancer patients. For instance, a study by Mack et al. demonstrated a correct diagnosis in 96.3% of cases, while Curvo-Semedo et al. reported a sensitivity of 100% and an accuracy of 73% [17].

Importantly, these results are supported by a multi-institutional phase III clinical trial, which found high sensitivity and specificity of ferumoxtran-10-enhanced MRI in detecting metastatic nodal disease, with only a few false-negative cases attributed to the presence of micro-metastases [18].

Despite its promising diagnostic performance, the main limitation of ferumoxtran-10-enhanced MRI is the additional time required to perform the post-contrast imaging, as the maximum iron peak in lymph nodes is typically observed 1-2 days after injection. Nonetheless, the potential to detect minimal metastatic disease, particularly in normal-sized lymph nodes, suggests that ferumoxtran-10 MRI could play a valuable role in improving the accuracy of nodal staging in OCC patients. Further research and clinical trials are warranted to validate these findings and determine the optimal use of ferumoxtran-10-enhanced MRI in routine clinical practice.

Diagnosis	Patterns Post Contrast	Characteristic
Non-pathologic node		Node having an overall dark signal intensity, homogenous architecture
Non-pathologic node		Node having an overall dark signal with subtle granularities, homogenous architecture
Non-pathologic node		Node having an overall dark signal other than a central or hilar area of fat seen on T1 sequence, heterogenous architecture
Possibly pathologic node		Less than 50% of node has high signal intensity, heterogenous architecture
Pathologic node		Partial darkening whereby more than 50% of the node has area of high signal intensity; heterogenous architecture
Pathologic node		Node has central high signal with darkening along the peripheral rim, heterogenous architecture
Pathologic node		No blackening of node or node hyperintense to surrounding tissue; is heterogenous or homogenous architecture

Figure 8.9. Patterns of lymph node enhancement for ferumoxtran 10-enhanced magnetic resonance imaging [2].

8.9.3. Treatment Opportunities

Numerous opportunities are being explored to develop safer and more effective therapeutic approaches for oral cavity carcinoma (OCC). This section is categorized into three areas, each representing alternative cancer therapies under evaluation in humans. The applications of nanotechnology in OCC are summarized in Figure 8.10.

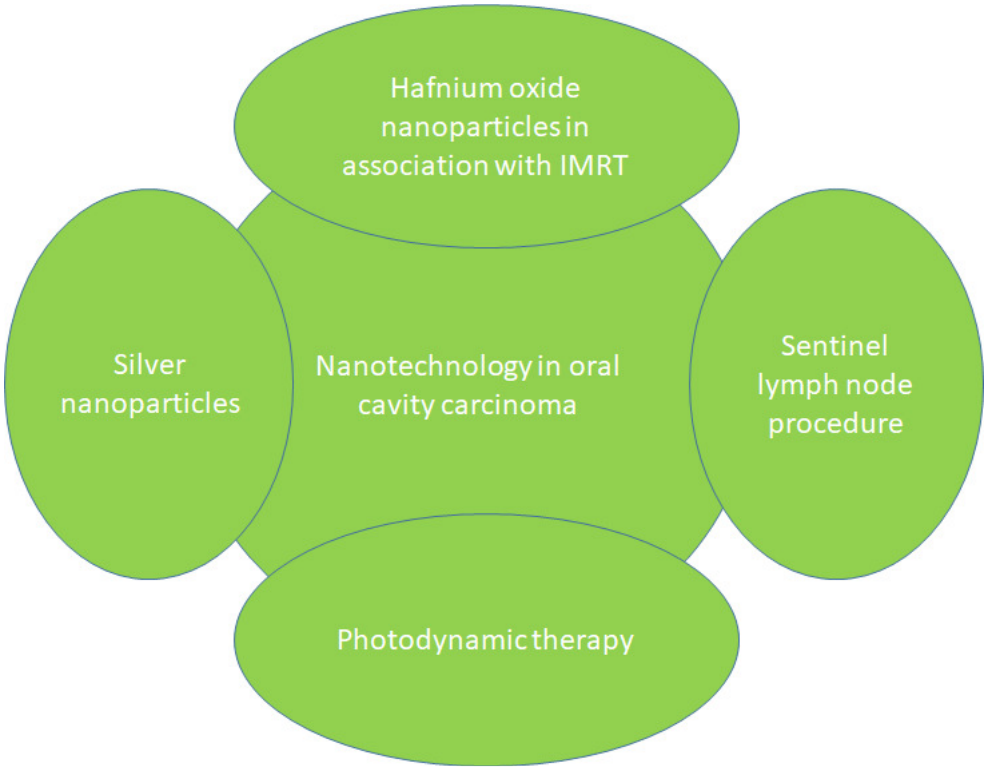


Figure 8.10. Nanotechnology applications in oral cavity carcinoma [2].

8.9.3.1. Ongoing Clinical Trials

There is a significant amount of data demonstrating the efficacy and safety of nanoparticle-based therapies in oral cavity carcinoma (OCC) models, both in vitro and in vivo. However, the translation of these findings into clinical practice has been limited. Only a few current and proposed clinical trials are incorporating nanoparticle formulations into the management of OCC [19, 20].

One such trial is a phase I study (NCT01946867) evaluating the safety and tolerability of NBTXR3, a crystalline solution of hafnium oxide nanoparticles, in combination with intensity-modulated radiation therapy (IMRT) in elderly OCC patients who are unfit for standard chemotherapy. NBTXR3 is designed to enhance cell-localized energy deposition upon exposure to radiation therapy. Patients in this trial receive a single intra-arterial or intra-tumor injection of NBTXR3 followed by IMRT. Preliminary results presented at the 2019 ASCO annual meeting showed that NBTXR3 activated by radiation therapy is safe and well-tolerated, with promising efficacy demonstrated in some patients. The study has progressed to phase II to confirm these findings [21].

Additionally, researchers have explored the potential therapeutic role of silver-based nanoparticles in cancer treatment. Preclinical studies have shown that silver nanoparticles can inhibit the proliferation of various cancer cell lines. The exact mechanism of this anticancer activity is not fully understood but may involve DNA damage, cell cycle arrest, and interference with replication processes. Some studies have also investigated the combination of silver nanoparticles with ionizing radiation, showing promising results in inhibiting tumor growth while preserving non-cancerous cells. Despite the lack of ongoing clinical trials, there are anecdotal reports of silver nanoparticles demonstrating efficacy in highly refractory metastatic head and neck squamous cell carcinoma. Further research is needed to fully evaluate the safety and efficacy of silver nanoparticles in OCC and other cancers, as well as their potential interactions with standard treatment modalities [22, 23].

8.9.3.2. Sentinel Lymph Node Analysis

In the realm of OCC management, there's a growing interest in employing nanotechnology for sentinel lymph node analysis, a procedure commonly utilized in malignancies such as melanoma and breast cancer. Traditionally, this procedure involves injecting a radiotracer around the tumor to

identify the sentinel node—the first lymph node receiving drainage from the primary tumor. If this sentinel node shows no signs of metastasis upon histological examination, the likelihood of metastases in the remaining lymph nodes is significantly reduced, potentially allowing patients to avoid prophylactic lymphadenectomy [24, 25, 26, 27].

However, mastery of this technique requires substantial experience, with the success rate closely linked to the surgeon's expertise. In the context of OCC, where occult lymph node metastasis rates in early stages are notable, sentinel lymph node biopsy offers an alternative to elective neck dissection for identifying occult cervical metastasis in patients with early-stage disease. Nonetheless, the procedure's ability to definitively replace elective neck dissection in such patients remains uncertain [28, 29, 30].

Recent meta-analyses have shown promising results for sentinel lymph node biopsy in early-stage OCC, with high sensitivity and negative predictive values. Immunohistochemistry and early publication were associated with higher sensitivity rates in these studies, supporting the notion that sentinel lymph node biopsy with immunohistochemistry may be a viable alternative to elective neck dissection [31, 32] .

The current standard practice in centers equipped to perform sentinel lymph node analysis involves using lymphoscintigraphy with radio-labelled particles and intraoperative gamma probe localization, often combined with blue dye injection. This approach enables the identification of the sentinel lymph node, guiding subsequent treatment decisions. In regions with limited resources, the use of methylene blue dye alone has been proposed as a cost-effective alternative, showcasing the adaptability of sentinel lymph node analysis in diverse healthcare settings [33, 34, 35].

Importantly, adopting a sentinel lymph node analysis approach may spare patients the surgical complications associated with elective neck dissection, such as shoulder syndrome. Several studies have reported superior functional outcomes following sentinel node biopsy compared to elective neck dissection, highlighting its potential to reduce postoperative morbidity and improve patient quality of life (Figure 8.11.).

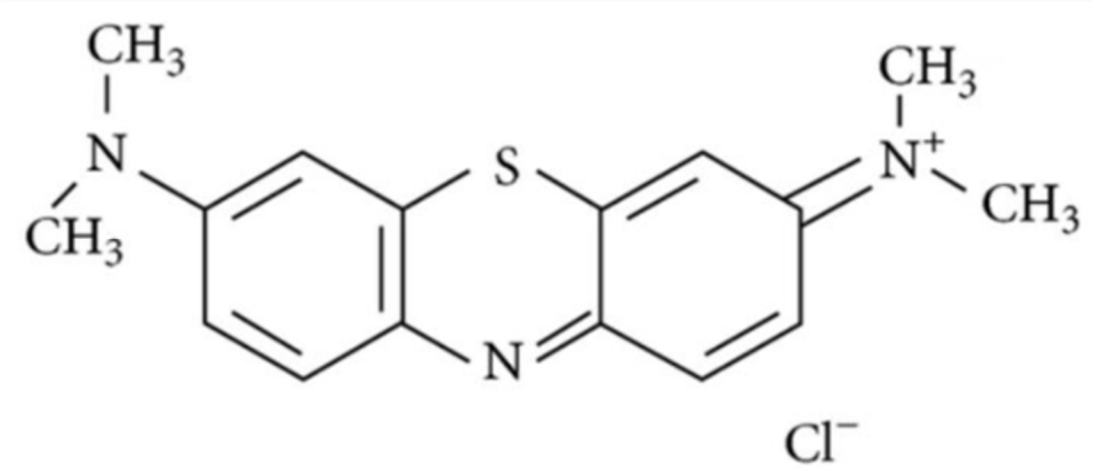


Figure 8.11. Chemical structure of methylene blue dye [2].

The largest study to date on sentinel node biopsy in early OCC involved 94 patients (75 men and 19 women, median age 45 years) with cT1-2 cN0 disease.

Conducted at a major tertiary care cancer center in India, this prospective study utilized peritumoral injection of blue dye (methylene blue 1–2 mL) followed by resection of the blue node, with subsequent selective neck node dissection in all patients.

The primary endpoint was to assess the concordance between the sentinel node and the specimens from elective neck dissection regarding metastatic nodal involvement. Metastatic lymph nodes were predominantly found in level IB (48.6%), followed by IIA (37.1%), III (8.6%), and IA (5.7%).

The study demonstrated good sensitivity (84.6%) and negative predictive value (93.9%) for the procedure, highlighting immunohistochemistry as the preferred technique for detecting micrometastases within lymph nodes [36].

A notable limitation was the occurrence of blue dye spillage in tissue planes, although using a one-millimeter injection appeared to mitigate spillage while still maintaining oncologically adequate results.

However, traditional sentinel lymph node biopsy with blue dye and radioactive tracers involves ionizing radiation, invasiveness, and requires surgical expertise.

In this context, nanotechnology presents an opportunity to perform the sentinel lymph node procedure without the need for radioactive agents, while preserving a clear view of the surgical field [37].

Indocyanine green (ICG, CAS number: 3599-32-4) is an amphiphilic tricarbocyanine dye with a molecular weight of 774.974 g/mol. Its basic chemical structure is depicted in Figure 8.12.

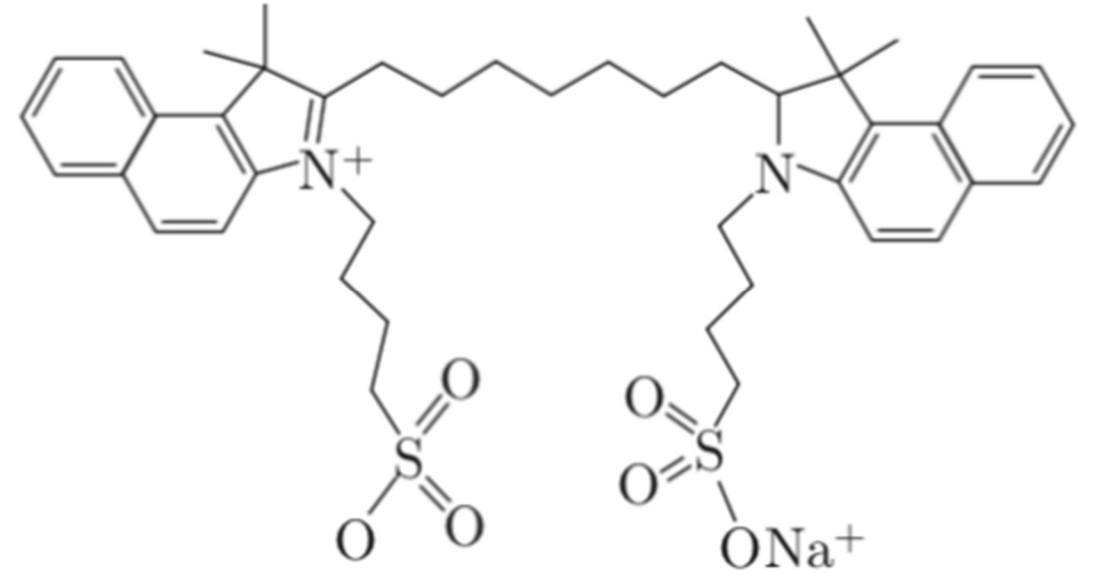


Figure 8.12. Chemical structure of indocyanine green [2].

Indocyanine green (ICG), approved by the FDA in the late 1950s, is routinely utilized in humans for various diagnostic purposes such as determining cardiac output, assessing hepatic function, and studying retinal vessels. Following injection, ICG is rapidly metabolized by the liver and excreted via the bile duct, exhibiting excellent tolerability and safety with rare occurrences of anaphylaxis. Its unique photophysical properties, emitting fluorescent light peaking at around 800 nm, make it well-suited for imaging applications, particularly in fluorescence imaging within the near-infrared (NIR) optic window [38, 39, 40].

To address limitations such as its short half-life, poor hydrolytic stability, aggregation tendencies, lack of target specificity, and poor photo-stability, ICG can be incorporated into various nanoparticle structures, including magnetic, lipid-based, and polymer-based nanoparticles. Near-infrared fluorescence (NIRF) imaging, utilizing ICG-loaded nanoparticles with diameters smaller than 50 nm, has emerged as a promising modality for sentinel lymph node mapping. This approach circumvents issues associated with radioactive agents and blue dye, such as radiation exposure, low spatial resolution, and allergic reactions [41, 42, 43].

Preclinical studies have demonstrated the potential of liposome-encapsulated ICG variants, including glucosylated and mannosylated liposomes, to enhance stability and fluorescence signal compared to free ICG. Clinical studies in various cancers, including melanoma, breast, and gynecological cancers, have shown successful applications of NIRF imaging using ICG-loaded nanoparticles [44, 45, 46].

In the head and neck region, studies have explored the use of ICG for sentinel lymph node mapping in OCC. Researchers have reported successful identification of sentinel lymph nodes using

ICG in OCC patients with clinical N0 status. NIRF imaging with ICG has enabled accurate detection of draining lymph nodes in head and neck cancer patients, with minimal adverse reactions reported. Additionally, efforts have been made to develop hybrid multimodal imaging agents, such as indocyanine green-99mTc-NanoColl, which combine radioactive and fluorescent components for improved localization and visualization of sentinel lymph nodes during surgery.

In conclusion, nanoparticle-based approaches incorporating ICG hold promise for enhancing sentinel lymph node mapping in OCC. Prospective studies are warranted to evaluate their reliability and clinical applicability in improving surgical outcomes for OCC patients.

8.9.3.3. Photodynamic Therapy

Photodynamic therapy (PDT), introduced over a century ago, has found widespread use primarily in dermatologic conditions encompassing inflammatory, infectious, and neoplastic disorders [46, 47, 48. 49]. PDT exerts its cytotoxic effect through the confluence of three essential components: the photosensitizer, light, and oxygen [50, 51, 52] (Figure 8.13.).

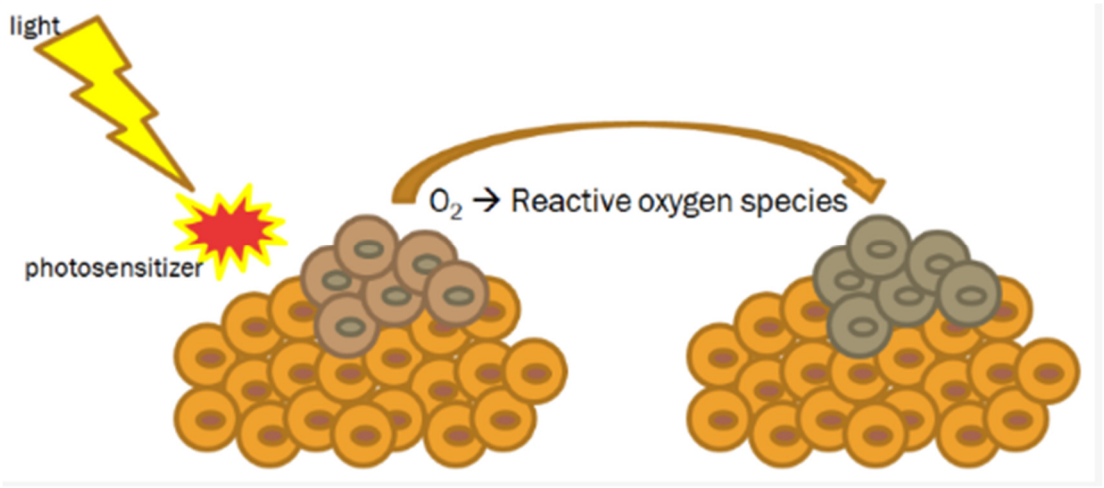


Figure 8.13. Photodynamic therapy: mechanism of action [2].

Traditionally, when oxygen levels drop below 2%, cells become resistant to the effects of PDT. In general, two primary photo-oxidative reactions are described in the literature. Type I reactions yield highly reactive radical cations and neutral radicals that can directly interact with substrate molecules, such as DNA bases. In type II reactions, the formation of photo-excited states activates molecular oxygen through electron or energy transfer reactions. The subsequent production of reactive oxygen species initiates a rapid cascade of chemical changes, leading to cellular and tissue damage [53, 54, 55].

Theoretically, any light source with suitable spectral characteristics can be used in PDT. For example, laser dyes like Rhodamine B (RhB) and sulforhodamine B (Kiton Red S; KRS) are commonly employed, generating up to 7 watts of red light. The efficacy of PDT is influenced by two key parameters: the duration of light delivery and the dose rate of light. Higher dose rates generally result in greater cytotoxicity [56, 57].

An ideal PDT photosensitizer should exhibit selective retention with high tumor-to-tissue ratios (2:1, 3:1, 4:1, 5:1), high quantum yields of singlet oxygen, adequate tissue penetration depth, and photolability to damage tumor tissue while minimizing harm to surrounding normal tissues. The therapeutic index of photosensitizers is primarily related to their lipophilicity and hydrophilicity and can be enhanced by coupling them with nanoparticles. Most photosensitizers have a heterocyclic ring structure similar to that of hemoglobin and can be administered systemically, topically, or via local injection. Porfimer sodium (photofrin II), meta-tetrahydroxyphenylchlorine (m-THPC, Foscan), and 5-aminolaevulinic acid (5-ALA) are among the most commonly used photosensitizers due to their stable and defined mixtures [58, 59].

The potential application of PDT in the treatment of head and neck cancers has been recognized. A recent systematic review examined PDT efficacy in head and neck cancer treatment from 1985 to 2015. Twelve studies involving 465 patients were included, with various photosensitizers and light sources used. PDT was generally well-tolerated, with complete response achieved in most cases (>75% in 9 studies). Skin photosensitivity lasting up to 6 weeks was the most significant side effect, along with other acute complications like local pain, burns, trismus, swelling, erythema, edema, pruritus, nausea, and vomiting [60, 61].

Oral cavity malignant lesions are particularly suitable for PDT due to its non-overlapping toxicities with standard therapies. Several publications have described PDT in the treatment of oral cavity cancers over the years, highlighting its potential benefits. Details of the main clinical experiences are summarized in Figure 8.14.

Author	Year	Study Type	OCC Patients	Photosensitizers	Outcomes
Karakullukcu [70]	2011	Retrospective	105	Temoporfin	OR: 91.4%; CR: 68.6%; 2-y DFS: 74%; 5-yDFS: 61%
Biel [71]	2007	Retrospective	161	Photofrin	CR: 93.2%
Schweitzer [72]	2001	Retrospective	10	Photofrin	CR: 80%
Grant [73]	1993	Retrospective	11	Photofrin	CR: 90.9%
Hopper [74]	2004	Phase IIb	121	Meta-tetrahydroxyphenylchlorin	CR: 85%; 1-y OS: 89%; 2-y OS: 75%

OCC: oral cavity carcinoma; OR: overall response; CR: complete response; 2-y DFS: 2-year disease-free survival; 5-y DFS: 5-year disease-free survival; 1-y OS: 1-year overall survival; 2-y OS: 2-year overall survival.

Figure 8.14. Photodynamic therapy in the treatment of oral cavity carcinoma [2].

Most of the data regarding photodynamic therapy (PDT) for oral cavity cancer (OCC) have been obtained retrospectively. Overall, PDT has shown to be highly effective, with the majority of studies reporting high and long-lasting complete response rates, along with excellent cosmetic and functional outcomes. Interestingly, primary oral tongue lesions have shown better responses compared to other sub-sites within the oral cavity, likely due to tissue homogeneity and ease of illumination. Additionally, success rates appear to be associated with early T stage and superficial lesions (depth of invasion < 5 mm).

One notable study by Hopper et al. investigated the efficacy and safety of mTHPC-mediated PDT in OCC patients, specifically focusing on early stage T1-2 N0 lesions. The study found that complete response was achieved in 85% of patients, with a maintenance rate of 85% at 1 year and 77% at 2 years. Complete response rates were particularly high for lesions in the anterior tongue, floor of mouth, lip, and buccal mucosa. However, mild to moderate pain and skin photosensitivity reactions were reported in a notable percentage of patients [62].

Recent advancements in PDT include the development of the interstitial technique, which involves inserting light fibers directly into deep tumor lesions, allowing for targeted light delivery while sparing adjacent healthy tissues. While interstitial PDT has shown effectiveness in oropharyngeal cancers, there is currently a lack of data regarding its application in OCC.

In summary, although literature evidence supports PDT as a safe treatment option for OCC, there is currently no consensus on its routine clinical indication. Further research, particularly prospective studies, is needed to establish the role of PDT in OCC treatment protocols.

8.9.4. Conclusions

Since the inception of nanotechnology, significant progress has been achieved in various oncological domains, including the management of oral cavity cancer (OCC). With active research in diagnostic techniques and advancements in surgical and radiation technologies, nanotechnology holds promise for enhancing OCC patient care. This narrative review provides an overview of available clinical data and outlines potential considerations for future research.

One area of interest is the use of MRI contrast lymphotropic nanoparticles, which have the potential to sensitively and specifically detect minimal metastatic nodal disease in normal-sized lymph nodes. Additionally, fluorescence imaging with indocyanine green appears to be a safe and straightforward method for guiding surgical procedures. Sentinel node biopsy in OCC patients with clinically staged N0 disease is associated with less morbidity and similar prognosis rates compared to elective neck dissection.

Nanoparticles also show promise as radiosensitizers in conjunction with intensity-modulated radiation therapy (IMRT), as they impact key aspects of radiobiology such as radiosensitivity, repair, reoxygenation, redistribution, and repopulation. Photodynamic therapy is particularly suited for recurrent disease due to its minimal toxicity.

However, it's important to acknowledge the limitations of existing research, including the limited number of clinical studies and methodological issues. Further investigation with robust study designs is necessary to validate these findings.

In summary, nanotechnology offers new diagnostic and therapeutic avenues that have the potential to surpass conventional approaches in improving clinical outcomes and treatment efficacy for OCC. Continued research and development in this field hold great promise for advancing OCC management.

8.9.5. Direction for Future Research

Utilizing nanotechnology in the treatment of oral cavity cancer (OCC) holds significant promise for enhancing clinical outcomes and improving the quality of life for patients. Collaborative interdisciplinary research involving various medical specialists, healthcare professionals, biomedical engineers, and cancer biologists is essential for realizing the full potential of nanotechnology in OCC care and maximizing patient benefit and satisfaction.

Strengths:

Nanotechnology offers targeted delivery of therapeutic agents, minimizing damage to healthy tissues while maximizing efficacy against cancerous cells.

Improved imaging techniques using nanoparticles enable more accurate diagnosis, staging, and monitoring of OCC.

Nanoparticle-based radiosensitizers enhance the effectiveness of radiation therapy, potentially leading to better tumor control and reduced side effects.

Photodynamic therapy with nanoparticles allows for precise tumor targeting and minimal toxicity, particularly in cases of recurrent disease.

Weaknesses:

Limited clinical data and studies on nanotechnology applications in OCC.

Challenges in standardizing nanoparticle formulations and delivery methods.

Potential toxicity and side effects associated with certain nanoparticles.

High costs and technical complexities associated with nanoparticle-based therapies.

Opportunities:

Further research and development can lead to innovative nanoparticle-based therapies tailored to the specific needs of OCC patients.

Collaboration between different disciplines can drive advancements in nanotechnology and its application in OCC treatment.

Clinical trials exploring the safety and efficacy of nanoparticle-based interventions in OCC can provide valuable insights.

Threats:

Regulatory hurdles and ethical considerations may delay the translation of nanotechnology-based treatments from research to clinical practice.

Resistance from traditional treatment modalities and healthcare systems may impede the adoption of nanoparticle-based therapies.

Limited resources and funding for research and development in the field of cancer nanotechnology.

In summary, conducting a SWOT analysis (Strengths, Weaknesses, Opportunities, Threats) of nanotechnology in OCC treatment highlights the potential benefits and challenges associated with its implementation. By addressing these factors and fostering interdisciplinary collaboration, the field of nanotechnology can make significant strides in improving outcomes for OCC patients. Figure 8.15. provides an overview of these aspects based on the existing literature.

The integration of nanotechnology into the management of oral cavity cancer (OCC) presents both opportunities and challenges. To effectively evaluate the role of nanotechnology in OCC treatment, clinicians and researchers must prioritize high-quality, evidence-based research and consider several key factors:

Population Selection: Given the diverse anatomical sub-sites within the oral cavity and the variation in lymphatic drainage patterns, studies should carefully select patients based on primary tumor location to enhance study power and relevance.

Primary Endpoints: Clear definition of primary endpoints is crucial for study design. Selection of appropriate endpoints should consider the specific benefits and challenges associated with nanotechnology in OCC treatment, such as accurate imaging, lymph node evaluation, and management of recurrent disease.

Comparator Selection: With updates in staging criteria, selecting appropriate comparators for clinical trials becomes more complex. Methodologically robust study designs are essential to ensure meaningful comparisons and reliable results.

Challenges and Solutions: Overcoming challenges associated with the integration of nanotechnology into routine clinical practice requires innovative solutions. Nanotechnology offers potential solutions for accurate disease staging, intraoperative lymph node evaluation, and management of recurrent disease.

Prospective Studies: Future research efforts should focus on prospective studies to define optimal treatment strategies and assess the real-world effectiveness of nanotechnology in OCC management.

By addressing these considerations and conducting well-designed prospective studies, clinicians and researchers can better understand the potential benefits of nanotechnology in OCC treatment and pave the way for its successful integration into clinical practice.

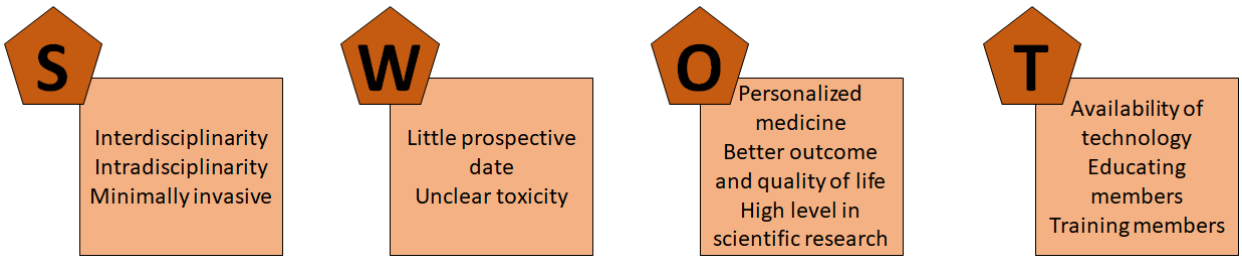


Figure 8.15. Swot analysis of nanotechnology in the treatment of oral cavity carcinoma [2].

8.10. Quiz 8.

1. How do nanoparticles (NPs) contribute to the diagnosis and treatment of oral cancer?
A) By exploiting the enhanced permeability and retention (EPR) effect to passively target tumors.
B) Through active targeting strategies involving the conjugation of NPs with specific ligands or antibodies.
C) By serving as carriers for contrast agents in imaging.
D) By delivering active drugs for chemotherapy, photosensitizers for photodynamic therapy (PDT), and gene therapy agents.
E) By promoting systemic toxicity in tumor tissues.

2*. Which statement best describes the role of liposomes in cancer therapy?
A) Liposomes are inert nanoparticles without any therapeutic potential.
B) Liposomes enhance the growth of tumors by providing them with essential nutrients.
C) Liposomes passively accumulate in tumor tissues through the enhanced permeability and retention effect.
D) Liposomes are exclusively used for targeting healthy tissues in cancer treatment.
E) Liposomes cannot be modified to carry specific drugs for targeted delivery.

3. Which of the following are benefits of using liposomes in drug delivery?
A) Enhanced drug efficacy
B) Reduced adverse effects
C) Prolonged circulation time
D) Increased drug resistance
E) Higher risk of toxicity

4. Which benefits are associated with using polymeric nanoparticles (NPs) in drug delivery for oral cancer therapy?
A) Protection of drugs from biological deactivation
B) Enhanced bioavailability of drugs
C) Prolonged residence time at the delivery site
D) Increased risk of drug degradation
E) Reduced therapeutic effects due to single-drug encapsulation

5. Which of the following statements regarding nanomaterials in oral cancer therapy are accurate?
A) Upconversion nanoparticles (UCNs) are excited by ultraviolet (UV) light.
B) Carbon nanotubes are exclusively utilized for drug delivery in oral cancer treatment.
C) Metal-organic frameworks (MOFs) are employed to decrease sustained release of chemotherapy drugs.
D) Vertically aligned carbon nanotube arrays are developed as immunosensors for detecting cancerous inhibitor PP2A (CIP2A) in saliva supernatant.
E) Polyethylenimine-modified silica nanoparticles have been engineered to carry both MDR1-siRNA and DOX for overcoming drug resistance.

6. What is the primary focus of the review on cancer nanotechnology in oral cavity carcinoma (OCC) management?
A) Exploring traditional treatment modalities
B) Integrating nanotechnology into diagnostic procedures and future treatment strategies C) Investigating alternative surgical techniques
D) Analyzing the psychological impact of OCC on patients
E) Assessing the dietary habits of OCC patients

7. Which fields contribute to the interdisciplinary nature of cancer nanotechnology?
A) Medicine
B) Physics
C) Literature
D) Psychology
E) Astronomy

8*. Which nanoparticle has shown promising results in improving the accuracy of nodal staging in oral cavity carcinoma (OCC) patients?
A) Gold nanoparticles
B) Liposomal nanoparticles
C) Lymphotropic nanoparticles (ferumoxtran-10)
D) Carbon nanotubes
E) Polymeric nanoparticles

9*. Which procedure involves injecting a radiotracer around the tumor to identify the sentinel node in oral cavity carcinoma (OCC) management?
A) Sentinel lymph node biopsy
B) Elective neck dissection
C) Positron emission tomography (PET)-CT
D) Lymphoscintigraphy
E) Immunohistochemistry

10. Which procedures are commonly utilized in the pre-treatment work-up for oral cavity carcinoma (OCC)?
A) Magnetic resonance imaging (MRI) with intravenous contrast
B) Computed tomography (CT)
C) 18F-labeled fluoro-2-deoxyglucose (18F-FDG) positron emission tomography (PET)-CT
D) Lymphoscintigraphy with radio-labelled particles
E) Intraoperative gamma probe localization

References

[1]. Zheng W, Zhou Q, Yuan C. Nanoparticles for Oral Cancer Diagnosis and Therapy. Bioinorg Chem Appl. 2021 Apr 23;2021:9977131. doi: 10.1155/2021/9977131. Retraction in: Bioinorg Chem Appl. 2023 Dec 6;2023:9895049. PMID: 33981334; PMCID: PMC8088384.

[2]. De Felice, F.; Cavallini, C.; Barlattani, A.; Tombolini, M.; Brugnoletti, O.; Tombolini, V.; Polimeni, A. Nanotechnology in Oral Cavity Carcinoma: Recent Trends and Treatment Opportunities. Nanomaterials 2019, 9, 1546. https://doi.org/10.3390/nano9111546.

[3]. Calixto, G.; Bernegossi, J.; Fonseca-Santos, B.; Chorilli, M. Nanotechnology-based drug delivery systems for treatment of oral cancer: A review. Int. J. Nanomed. 2014, 9, 3719–3735.

[4]. Hoet, P.H.; Brüske-Hohlfeld, I.; Salata, O.V. Nanoparticles—Known and unknown health risks. J. Nanobiotechnol. 2004, 2, 12.

[5]. Malam, Y.; Loizidou, M.; Seifalian, A.M. Liposomes and nanoparticles: Nanosized vehicles for drug delivery in cancer. Trends Pharmacol. Sci. 2009, 30, 592–599.

[6]. Pignon, J.P.; le Maître, A.; Maillard, E.; Bourhis, J.; MACH-NC Collaborative Group. Meta-analysis of chemotherapy in head and neck cancer (MACH-NC): An update on 93 randomised trials and 17,346 patients. Radiother. Oncol. 2009, 92, 4–14.

[7]. Puyo, S.; Montaudon, D.; Pourquier, P. From old alkylating agents to new minor groove binders. Crit. Rev. Oncol. Hematol. 2014, 89, 43–61.

[8]. Dasari, S.; Tchounwou, P.B. Cisplatin in cancer therapy: Molecular mechanisms of action. Eur. J. Pharmacol. 2014, 740, 364–378.

[9]. Wang, Z.Q.; Liu, K.; Huo, Z.J.; Li, X.C.; Wang, M.; Liu, P.; Pang, B.; Wang, S.J. A cell-targeted chemotherapeutic nanomedicine strategy for oral squamous cell carcinoma therapy. J Nanobiotechnology 2015, 13, 63.

[10]. Caster, J.M.; Patel, A.N.; Zhang, T.; Wang, A. Investigational nanomedicines in 2016: A review of nanotherapeutics currently undergoing clinical trials. Wiley Interdiscip. Rev. Nanomed. Nanobiotechnol. 2017, 9, e1416.

[11]. Robbins, K.T.; Medina, J.E.; Wolfe, G.T.; Levine, P.A.; Sessions, R.B.; Pruet, C.W. Standardizing neck dissection terminology. Official report of the academy's committee for head and neck surgery and oncology. Arch. Otolaryngol. Head Neck Surg. 1991, 117, 601–605.

[12]. Mack, M.G.; Balzer, J.O.; Straub, R.; Eichler, K.; Vogl, T.J. Superparamagnetic iron oxide-enhanced MR imaging of head and neck lymph nodes. Radiology 2002, 222, 239–244

[13]. Mack, M.G.; Rieger, J.; Baghi, M.; Bisdas, S.; Vogl, T.J. Cervical lymph nodes. Eur. J. Radiol. 2008, 66, 493–500.

[14]. Anzai, Y.; Piccoli, C.W.; Outwater, E.K.; Stanford, W.; Bluemke, D.A.; Nurenberg, P.; Saini, S.; Maravilla, K.R.; Feldman, D.E.; Schmiedl, U.P.; et al. Evaluation of neck and body metastases to nodes with ferumoxtran 10-enhanced MR imaging: Phase III safety and efficacy study. Radiology 2003, 228, 777–788.

[15]. Hudgins, P.A.; Anzai, Y.; Morris, M.R.; Lucas, M.A. Ferumoxtran-10, a superparamagnetic iron oxide as a magnetic resonance enhancement agent for imaging lymph nodes: A phase 2 dose study. AJNR Am. J. Neuroradiol. 2002, 23, 649–656

[16]. Wang, Y.X.; Hussain, S.M.; Krestin, G.P. Superparamagnetic iron oxide contrast agents: Physicochemical characteristics and applications in MR imaging. Eur. Radiol 2001, 11, 2319–2331.

[17]. Hoffman, H.T.; Quets, J.; Toshiaki, T.; Funk, G.F.; McCulloch, T.M.; Graham, S.M.; Robinson, R.A.; Schuster, M.E.; Yuh, W.T. Functional magnetic resonance imaging using iron oxide particles in characterizing head and neck adenopathy. Laryngoscope 2000, 110, 1425–1430.

[18]. Sigal, R.; Vogl, T.; Casselman, J.; Moulin, G.; Veillon, F.; Hermans, R.; Dubrulle, F.; Viala, J.; Bosq, J.; Mack, M.; et al. Lymph node metastases from head and neck squamous cell carcinoma: MR imaging with ultrasmall superparamagnetic iron oxide particles (Sinerem MR)—Results of a phase-III multicenter clinical trial. Eur. Radiol. 2002, 12, 1104–1113.

[19]. Le Tourneau, C.; Moreno, V.; Salas, S.; Mirabel, X.; Calvo, E.; Doger, B.; Florescu, C.; Thariat, J.; Fijuth, J.; Rutkowski, T.; et al. Hafnium oxide nanoparticles NBTXR3 activated by radiotherapy as a new therapeutic option for elderly/frail HNSCC patients. J. Clin. Oncol 2019, 37, 6069.

[20]. Satapathy, S.R.; Mohapatra, P.; Preet, R.; Das, D.; Sarkar, B.; Choudhuri, T.; Wyatt, M.D.; Kundu, C.N. Silver-based nanoparticles induce apoptosis in human colon cancer cells mediated through p53. Nanomedicine (Lond. 2013, 8, 1307–1322.

[21]. Swanner, J.; Mims, J.; Carroll, D.L.; Akman, S.A.; Furdui, C.M.; Torti, S.V.; Singh, R.N. Differential cytotoxic and radiosensitizing effects of silver nanoparticles on triple-negative breast cancer and non-triple-negative breast cells. Int. J. Nanomed 2015, 10, 3937–3953.

[22]. Hsin, Y.H.; Chen, C.F.; Huang, S.; Shih, T.S.; Lai, P.S.; Chueh, P.J. The apoptotic effect of nanosilver is mediated by a ROS- and JNK-dependent mechanism involving the mitochondrial pathway in NIH3T3 cells. Toxicol. Lett. 2008, 179, 130–139.

[23]. Singh, J.; Moore, W.; Fattah, F.; Jiang, X.; Zheng, J.; Kurian, P.; Beg, M.S.; Khan, S.A. Activity and pharmacology of homemade silver nanoparticles in refractory metastatic head and neck squamous cell cancer. Head Neck 2019, 41, E11–E16.

[24]. Alex, J.C.; Krag, D.N. Gamma-probe guided localization of lymph nodes. Surg. Oncol. 1993, 2, 137–143.
[25]. Morton, D.L.; Wen, D.R.; Wong, J.H.; Economou, J.S.; Cagle, L.A.; Storm, F.K.; Foshag, L.J.; Cochran, A.J. Technical details of intraoperative lymphatic mapping for early stage melanoma.Arch. Surg. 1992, 127, 392–399.
[26]. Ross, G.L.; Soutar, D.S.; MacDonald, D.G.; Shoaib, T.; Camilleri, I.G.; Robertson, A.G. Improved staging of cervical metastases in clinically node-negative patients with head and neck squamous cell carcinoma. Ann. Surg. Oncol. 2004, 11, 213–218.
[27]. Liu, M.; Wang, S.J.; Yang, X.; Peng, H. Diagnostic efficacy of sentinel lymph node biopsy in early oral squamous cell carcinoma: A meta-analysis of 66 studies. PLoS ONE 2017, 12, e0170322.
[28]. Hernando, J.; Villarreal, P.; Alvarez-Marcos, F.; Gallego, L.; García-Consuegra, L.; Junquera, L. Comparison of related complications: Sentinel node biopsy versus elective neck dissection. Int. J. Oral Maxillofac. Surg. 2014, 43, 1307–1312.
[29]. Murer, K.; Huber, G.F.; Haile, S.R.; Stoeckli, S.J. Comparison of morbidity between sentinel node biopsy and elective neck dissection for treatment of the n0 neck in patients with oral squamous cell carcinoma. Head Neck 2011, 33, 1260–1264.
[30]. Schiefke, F.; Akdemir, M.; Weber, A.; Akdemir, D.; Singer, S.; Frerich, B. Function, postoperative morbidity, and quality of life after cervical sentinel node biopsy and after selective neck dissection. Head Neck 2009, 31, 503–512.
[31]. Constant, C.R.; Murley, A.H. A clinical method of functional assessment of the shoulder. Clin. Orthop. Relat. Res. 1987, 214, 160–164.
[32]. Mølstrøm, J.; Grønne, M.; Green, A.; Bakholdt, V.; Sørensen, J.A. Topographical distribution of sentinel nodes and metastases from T1-T2 oral squamous cell carcinomas. Eur. J. Cancer 2019, 107, 86–92.
[33]. Chone, C.T.; Aniteli, M.B.; Magalhães, R.S.; Freitas, L.L.; Altemani, A.; Ramos, C.D.; Etchebehere, E.; Crespo, A.N. Impact of immunohistochemistry in sentinel lymph node biopsy in head and neck cancer. Eur. Arch. Otorhinolaryngol. 2013, 270, 313–317.
[34]. Vishnoi, J.R.; Kumar, V.; Gupta, S.; Chaturvedi, A.; Misra, S.; Akhtar, N.; Agarwal, P.; Jamal, N.; Pareek, P. Outcome of sentinel lymph node biopsy in early-stage squamous cell carcinoma of the oral cavity with methylene blue dye alone: A prospective validation study. Br. J. Oral Maxillofac. Surg. 2019, 57, 755–759.
[35]. Ramamurthy, R.; Kottayasamy Seenivasagam, R.; Shanmugam, S.; Palanivelu, K. A prospective study on sentinel lymph node biopsy in early oral cancers using methylene blue dye alone. Indian J. Surg. Oncol. 2014, 5, 178–183.
[36]. Troyan, S.L.; Kianzad, V.; Gibbs-Strauss, S.L.; Gioux, S.; Matsui, A.; Oketokoun, R.; Ngo, L.; Khamene, A.; Azar, F.; Frangioni, J.V. The FLARE intraoperative near-infrared fluorescence imaging system: A first-in-human clinical trial in breast cancer sentinel lymph node mapping. Ann. Surg. Oncol. 2009, 16, 2943–2952
[37]. Sheng, Y.; Wang, Z.; Ngandeu Neubi, G.M.; Cheng, H.; Zhang, C.; Zhang, H.; Wang, R.; Zhou, J.; Ding, Y. Lipoprotein-inspired penetrating nanoparticles for deep tumor-targeted shuttling of indocyanine green and enhanced photo-theranostics. Biomater. Sci. 2019, 7, 3425–3437.
[38]. Wang, H.; Li, X.; Tse, B.W.; Yang, H.; Thorling, C.A.; Liu, Y.; Touraud, M.; Chouane, J.B.; Liu, X.; Roberts, M.S.; et al. Indocyanine green-incorporating nanoparticles for cancer theranostics. Theranostics 2018, 8, 1227–1242
[39]. Hutteman, M.; Mieog, J.S.; van der Vorst, J.R.; Liefers, G.J.; Putter, H.; Löwik, C.W.; Frangioni, J.V.; van de Velde, C.J.; Vahrmeijer, A.L. Randomized, double-blind comparison of indocyanine green with or without albumin premixing for near-infrared fluorescence imaging of sentinel lymph nodes in breast cancer patients. Breast Cancer Res. Treat. 2011, 127, 163–170.
[40]. Hutteman, M.; van der Vorst, J.R.; Gaarenstroom, K.N.; Peters, A.A.; Mieog, J.S.; Schaafsma, B.E.; Löwik, C.W.; Frangioni, J.V.; van de Velde, C.J.; Vahrmeijer, A.L. Optimization of near-infrared fluorescent sentinel lymph node mapping for vulvar cancer. Am. J. Obstet. Gynecol. 2012, 206, 89.e1–89.e5.
[41]. van der Vorst, J.R.; Hutteman, M.; Gaarenstroom, K.N.; Peters, A.A.; Mieog, J.S.; Schaafsma, B.E.; Kuppen, P.J.; Frangioni, J.V.; van de Velde, C.J.; Vahrmeijer, A.L. Optimization of near-infrared fluorescent sentinel lymph node mapping in cervical cancer patients. Int. J. Gynecol. Cancer 2011, 21, 1472–1478.
[42]. Jeong, H.S.; Lee, C.M.; Cheong, S.J.; Kim, E.M.; Hwang, H.; Na, K.S.; Lim, S.T.; Sohn, M.H.; Jeong, H.J. The effect of mannosylation of liposome-encapsulated indocyanine green on imaging of sentinel lymph node. J. Liposome Res. 2013, 23, 291–297.
[43]. Bredell, M.G. Sentinel lymph node mapping by indocyanin green fluorescence imaging in oropharyngeal cancer—Preliminary experience. Head Neck Oncol. 2010, 2, 31.
[44]. van der Vorst, J.R.; Schaafsma, B.E.; Verbeek, F.P.; Keereweer, S.; Jansen, J.C.; van der Velden, L.A.; Langeveld, A.P.; Hutteman, M.; Löwik, C.W.; van de Velde, C.J.; et al. Near-infrared fluorescence sentinel lymph node mapping of the oral cavity in head and neck cancer patients. Oral Oncol. 2013, 49, 15–19.
[45]. Mieog, J.S.; Troyan, S.L.; Hutteman, M.; Donohoe, K.J.; van der Vorst, J.R.; Stockdale, A.; Liefers, G.J.; Choi, H.S.; Gibbs-Strauss, S.L.; Putter, H.; et al. Toward optimization of imaging system and lymphatic tracer for near-infrared fluorescent sentinel lymph node mapping in breast cancer. Ann. Surg. Oncol. 2011, 18, 2483–2491.
[46]. van der Poel, H.G.; Buckle, T.; Brouwer, O.R.; Valdés Olmos, R.A.; van Leeuwen, F.W. Intraoperative laparoscopic fluorescence guidance to the sentinel lymph node in prostate cancer patients: Clinical proof of concept of an integrated functional imaging approach using a multimodal tracer. Eur. Urol. 2011, 60, 826–833.
[47]. Ackroyd, R.; Kelty, C.; Brown, N.; Reed, M. The history of photodetection and photodynamic therapy. Photochem. Photobiol. 2001, 74, 656–669.

[48]. Hopper, C. Photodynamic therapy: A clinical reality in the treatment of cancer. Lancet Oncol. 2000, 1, 212–219
[49]. Jeskdnex, A.; Tappeiner, V.H. Zut behandlung der hautcarcinomit mit fluoresciercnden stoffen. Muench. Med. Wochneshr. 1903, 47, 2042–2044.
[50]. von Tappeiner, H.; Jodlbauer, A. Ueber die Wukung der photodynamischen (fluores- cierenden) Stoffe auf Protozoen und Enzyme. Arch. Klin. Med. 1904, 80, 427–487.
[51]. Pass, H.I. Photodynamic therapy in oncology: Mechanisms and clinical use. J. Natl. Cancer Inst. 1993, 85, 443–456.
[52]. Dougherty, T.J.; Kaufman, J.E.; Goldfarb, A.; Weishaupt, K.R.; Boyle, D.; Mittleman, A. Photoradiation therapy for the treatment of malignant tumors. Cancer Res. 1978, 38, 2628–2635.
[53]. Baptista, M.S.; Cadet, J.; Di Mascio, P.; Ghogare, A.A.; Greer, A.; Hamblin, M.R.; Lorente, C.; Nunez, S.C.; Ribeiro, M.S.; Thomas, A.H.; et al. Type I and type II photosensitized oxidation reactions: Guidelines and mechanistic pathways. *Photochem. Photobiol.* **2017**, *93*, 912–919
[54]. Wondrak, G.T.; Jacobson, M.K.; Jacobson, E.L. Endogenous UVA-photosensitizers: Mediators of skin photodamage and novel targets for skin photoprotection. *Photochem. Photobiol. Sci.* **2006**, *5*, 215–237.
[55]. Gondivkar, S.M.; Gadbail, A.R.; Choudhary, M.G.; Vedpathak, P.R.; Likhitkar, M.S. Photodynamic treatment outcomes of potentially-malignant lesions and malignancies of the head and neck region: A systematic review. *J. Investig. Clin. Dent.* **2018**, *9*.
[56]. Karakullukcu, B.; van Oudenaarde, K.; Copper, M.P.; Klop, W.M.; van Veen, R.; Wildeman, M.; Bing Tan, I. Photodynamic therapy of early stage oral cavity and oropharynx neoplasms: An outcome analysis of 170 patients. *Eur. Arch. Otorhinolaryngol.* **2011**, *268*, 281–288.
[57]. Biel, M.A. Photodynamic therapy treatment of early oral and laryngeal cancers. *Photochem. Photobiol.* **2007**, *83*, 1063–1068.
[58]. Schweitzer, V.G. PHOTOFRIN-mediated photodynamic therapy for treatment of early stage oral cavity and laryngeal malignancies. *Lasers Surg. Med.* **2001**, *29*, 305–313.
[59]. Grant, W.E.; Hopper, C.; Speight, P.M.; Macrobert, A.J.; Bown, S.G. Photodynamic therapy of malignant and premalignant lesions in patients with 'field cancerization' of the oral cavity. *J. Laryngol. Otol.* **1993**, *107*, 1140–1145
[60]. Hopper, C.; Kübler, A.; Lewis, H.; Tan, I.B.; Putnam, G. mTHPC-mediated photodynamic therapy for early oral squamous cell carcinoma. *Int. J. Cancer* **2004**, *111*, 138–146.
[61]. Mimikos, C.; Shafirstein, G.; Arshad, H. Current state and future of photodynamic therapy for the treatment of head and neck squamous cell carcinoma. *World J. Otorhinolaryngol. Head Neck Surg.* **2016**, *2*, 126–129.
[62]. Lydiatt, W.M.; Patel, S.G.; O'Sullivan, B.; Brandwein, M.S.; Ridge, J.A.; Migliacci, J.C.; Loomis, A.M.; Shah, J.P. Head and neck cancers-major changes in the American Joint Committee on cancer eighth edition cancer staging manual. *CA Cancer J. Clin.* **2017**, *67*, 122–137.

9. Nanodiagnostic

The integration of nanotechnology into medicine is poised to revolutionize various aspects of disease diagnosis, treatment, and prevention. Nanoparticles exhibit unique properties that make them invaluable tools in biotechnology, biology, and biomedicine [1]. Some of the key applications and potential impacts of nanotechnology in medicine include:

1. Disease Detection and Diagnosis: Nanoparticles show tremendous potential for detecting disease markers, pre-cancerous cells, viral fragments, specific proteins, antibodies, and other indicators of disease. They enable early disease detection with high sensitivity and specificity, paving the way for more effective diagnosis and treatment planning.
2. Therapy: Nanoparticles play a crucial role in targeted drug delivery, allowing for precise and effective therapy. They can be engineered to deliver therapeutic agents directly to specific cells or tissues, minimizing side effects and maximizing therapeutic efficacy. Nano-based drugs, composed of polymers, metals, or ceramics, offer new treatment options for conditions such as cancer and bacterial infections.
3. Regenerative Medicine: Nanotechnology offers promising solutions for regenerative medicine, providing hope for patients with organ failure or severe injuries. Nano-particle reinforced polymers, artificial joints made from nano-particulate materials, and tissue engineering techniques using nano-materials are just a few examples of how nanotechnology can advance regenerative medicine.
4. Imaging: Nanotechnology enhances medical imaging techniques, allowing for more accurate and detailed visualization of tissues and organs. Nano-based contrast agents improve the sensitivity and specificity of imaging modalities such as magnetic resonance imaging (MRI), enabling early detection of diseases and monitoring of treatment responses.
5. Sensing: Nanotechnology enables the development of highly sensitive and selective biosensors for detecting biomolecules and pathogens. These sensors can be utilized for rapid and accurate diagnosis of various diseases, facilitating timely interventions and improving patient outcomes.
6. Artificial Implants: Nano-engineered materials are used in the development of artificial implants with enhanced biocompatibility and durability. These implants, such as bone replacement materials and micro-cantilevers, offer improved functionality and longevity compared to traditional implants.

Overall, nanotechnology holds immense promise for advancing healthcare and improving patient outcomes. Continued research and innovation in this field are essential to unlock the full potential of nanotechnology in medicine and address unmet medical needs effectively [1].

9.1. Nanotechnology in diagnosis of a number of diseases

The field of nanodiagnostics, which involves the use of nanotechnology for clinical diagnostic purposes, has rapidly evolved to meet the demand for increased sensitivity and earlier detection of diseases. Nanoparticles offer unique advantages as diagnostic probes and therapeutic agents, with applications ranging from in vitro to in vivo diagnosis and treatment.

1. **Targeted Drug/Gene Delivery**: Nanoparticles can be engineered for targeted drug or gene delivery, allowing for precise therapy while minimizing side effects. These nanocarriers can deliver therapeutic agents specifically to cancer cells, enhancing treatment efficacy and reducing systemic toxicity.
2. **Biomolecule-Coated Nanoparticles**: Biomolecule-coated ultra-small superparamagnetic iron oxide particles are used for detecting cancer cells. These particles, when injected into the bloodstream, bind to specific antigens on cancer cells, enabling their detection by magnetic resonance imaging (MRI). This technology enables the early detection of cancer cells and monitoring of therapeutic response.

3. **DNA-Based Nanoparticles**: Multilayer films and capsules synthesized from DNA offer biodegradable and biocompatible platforms for disease diagnosis. These DNA capsules can be tailored to recognize specific biomarkers, making them valuable tools for the diagnosis of various diseases, including cancer.
4. **Optical Tweezers**: Optical tweezers, a nano-manipulation technique, can investigate microscopic forces exerted on cells. By measuring the strength of cells, optical tweezers can aid in the differential diagnosis of tissue growths, cysts, and other abnormalities.
5. **Microfluidic Systems**: Microfluidic or "lab-on-a-chip" systems integrate multiple processes of DNA analysis on a single chip. These systems, composed of microfabricated fluidic channels and detectors, enable the analysis of nanoliter-sized DNA samples with high throughput and precision. Droplet-based microfluidic systems, in particular, offer rapid and controlled mixing of fluids, making them ideal for in vitro diagnostics.
6. **Nanoscale Cantilevers**: Nanoscale cantilevers, resembling microscopic diving boards, can detect single molecules of DNA or protein. These devices, coated with molecules that bind specific substrates, provide rapid and sensitive detection of disease-specific molecules, offering potential applications in disease diagnosis and monitoring (Figure 9.1.).

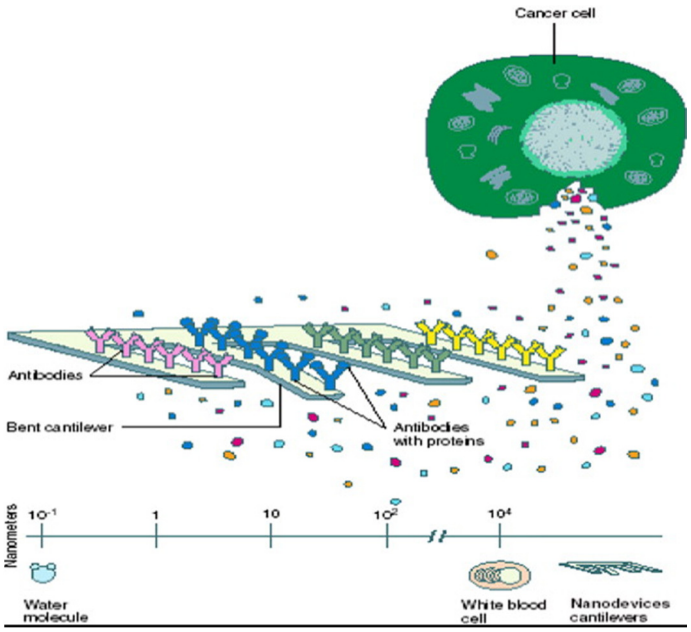


Figure 9.1. Nanoscale cantilevers concept explained by cancer markers [1].

Nanodiagnostics hold great promise for revolutionizing disease diagnosis and treatment by enabling early detection, targeted therapy, and precise monitoring of therapeutic responses. Continued research and innovation in this field are essential for realizing the full potential of nanotechnology in healthcare [1].

The use of DNA-coated gold nanoparticles (NPs) offers a highly sensitive alternative to traditional enzyme-linked immunosorbent assay (ELISA) methods for detecting antigens, particularly in complex protein mixtures such as serum-containing culture medium or crude body fluids. When employed in a sandwich assay, Nano-iPCR and iPCR techniques have demonstrated the ability to detect antigens with 1–3 orders of magnitude higher sensitivity than ELISA.

The principle behind this detection system involves the use of larger magnetic micro particles (MMPs) in combination with gold nanoparticles coated with DNA. In this setup, a monoclonal antibody specific to the target antigen (e.g., prostate-specific antigen, PSA) is immobilized onto the MMPs, serving as a capture agent for free PSA molecules present in the sample. Subsequently, a second antibody specific to PSA, conjugated to the gold nanoparticles, is introduced, forming a "sandwich" complex with the captured PSA molecules.

The presence of the antigen-bound gold nanoparticles can be easily detected and quantified using various methods, such as PCR or imaging techniques. Importantly, the use of MMPs facilitates the efficient separation of the nanoparticle-antigen complexes from the sample matrix, enhancing the sensitivity and specificity of the assay.

This approach leveraging DNA-coated gold nanoparticles and magnetic micro particles enables the detection of extremely low concentrations of serum proteins, down to attomolar levels, offering significant advantages over conventional ELISA methods in terms of sensitivity and specificity. This technology holds great promise for improving diagnostic capabilities in various clinical settings, particularly for the early detection of disease biomarkers (Figure 9.2.).

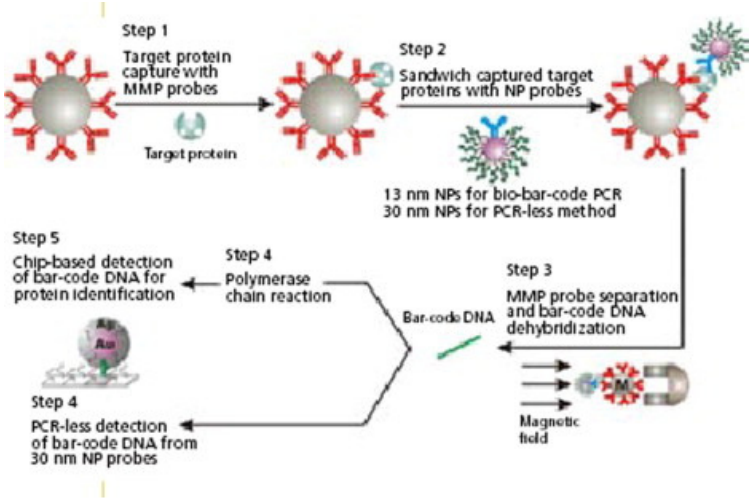


Figure 9.2. DNA labeled nano beads [1].

The utilization of DNA-labeled magnetic nanobeads presents a promising approach for detecting various proteins or nucleic acids with significantly enhanced sensitivity compared to conventional methods. This technology holds the potential to transform even the rarest biomarkers into valuable diagnostic or prognostic indicators, thereby revolutionizing the field of diagnostics.

"Smart" dynamic nanoplatforms represent another innovative approach with the potential to revolutionize disease diagnosis, treatment, and prevention. These nanoclinics could be designed with marker-specific monoclonal antibodies coated with polyethylene glycol (PEG) to evade detection by the immune system. The polymer matrix of such particles could be loaded with contrast agents for enhanced sensitivity in pinpointing abnormal cells, as well as therapeutic agents like reactive oxygen-generating photodynamic sensitizers, which would be activated upon detection of malignant or abnormal cells.

Dendrimers, spherical polymers of uniform molecular weight, offer multifunctional modularity and serve as versatile nanoscale platforms for creating devices capable of detecting multiple proteins simultaneously, thus overcoming the limitations of individual ELISA tests. This approach holds potential for detecting various biomarkers, including those associated with thyroid function, steroid hormones, and inflammatory cytokines.

Circulating peptides and protein fragments shed from cells within the tissue microenvironment offer valuable diagnostic information, with nanosensors capable of detecting alterations associated with diseases such as diabetes, asthma, cardiovascular diseases, and cancer. These nanosensors provide insights into the dynamic changes occurring at the molecular level, aiding in disease diagnosis and management.

Diagnostics based on altered DNA sequence detection leverage single-stranded oligonucleotide-tagged magnetic nanobeads. Target DNA is recognized and volume-amplified to large coils through circularization of linear padlock probes and rolling circle amplification (RCA). The magnetization spectrum of the nanobeads changes upon hybridization with the RCA coils, enabling concentration determination of RCA coils with high sensitivity in the picomolar range. This non-fluorescence-based, cost-efficient diagnostic tool is applicable to genetic disorders, SNP

analysis, and susceptibility to complex diseases, facilitating prevention and management strategies [1].

9.1.1. Detection of disease genes

DNA-based electrochemical sensors represent a powerful tool for detecting mutated genes associated with human disease due to their sensitivity, selectivity, and low cost. These sensors leverage nanoscale interactions between the target in solution, a recognition layer, and a solid electrode surface to achieve high-performance detection.

One innovative approach involves electrochemical amplifications with nanoparticles, which offer enhanced sensitivity and robustness. Clear Read nanoparticle technology, known for its proof of principle, reproducibility, and simplicity, has been utilized with unamplified DNA samples to detect various forms of three genes linked to hypercoagulation disorders. This technology demonstrates the capability to accurately detect genetic mutations associated with disease, offering a rapid and reliable diagnostic tool for identifying individuals at risk.

In summary, DNA-based electrochemical sensors, particularly those incorporating nanoparticle-based amplification techniques, hold great promise for the sensitive and specific detection of mutated genes implicated in human disease. These advancements have the potential to revolutionize diagnostics by providing a cost-effective, rapid, and reliable means of identifying genetic markers associated with various disorders, thereby facilitating early intervention and personalized treatment [1].

9.1.2. Detection of single nucleotide polymorphisms

Nanosphere's Clear Read nanoparticle technology presents a novel method for multiplex single nucleotide polymorphisms (SNP) genotyping directly from total human genomic DNA, bypassing the need for PCR target amplification. This innovative approach to SNP genotyping operates enzyme-free, leveraging the remarkable sensitivity of gold nanoparticle probes.

Within the Clear Read technology, a target DNA SNP segment is enclosed between two oligonucleotide sequences, significantly improving detection sensitivity and specificity. One segment is tailored to detect any DNA mutations, while the other acts as a highly sensitive gold nanoparticle probe, generating a robust signal indicative of the presence of a specific target SNP. This assay design is distinguished by its simplicity, speed, and reliability, rendering it suitable for point-of-care multiplex SNP profiling.

Recent advancements have demonstrated the capability to detect multiple SNPs simultaneously using 20 Nan cantilevers labeled with 20 fluorescence dyes. This represents a significant step forward in SNP genotyping technology, offering enhanced throughput and efficiency in SNP analysis. Overall, Nanosphere's Clear Read nanoparticle technology holds great promise for advancing SNP genotyping capabilities, facilitating rapid and accurate detection of genetic variations for various applications in research and clinical settings [1].

9.1.2.1. Glucose monitoring in vivo by nanosensors

Developing fluorescent micro/nanoscale devices for glucose detection shows promise in enabling non-invasive monitoring of glucose levels. By embedding micro/nanoparticles into the dermis, it becomes feasible to track changes in glucose concentration in the interstitial fluid, offering a less intrusive alternative to conventional blood glucose monitoring methods.

An innovative optical nanosensor, utilizing single-walled carbon nanotubes, demonstrates potential as a glucose sensor. In this method, carbon nanotubes are coated with glucose oxidase, an enzyme facilitating the breakdown of glucose molecules. Additionally, ferricyanide, an electron-hungry molecule, is applied to the surfaces of the nanotubes. In the presence of glucose, it reacts with the glucose oxidase, generating hydrogen peroxide. This hydrogen peroxide then interacts with ferricyanide, diminishing its electron-hungry characteristics. Consequently, the fluorescence of the

nanotubes under infrared light is adjusted, with elevated glucose levels resulting in amplified fluorescence.

This technology offers the advantage of continuous glucose monitoring without the need for multiple sample collections, maximizing patient acceptance and overcoming biocompatibility issues associated with implants. By leveraging the unique properties of carbon nanotubes and enzyme reactions, this approach holds promise for developing highly sensitive and selective glucose sensors for real-time monitoring applications [1].

9.1.2.2. Nanotechnology and Diagnosis of infectious disease

Nanotechnology presents substantial potential for enhancing medical diagnostics, especially in the prompt and precise identification of various diseases, including infectious agents. Operating at the atomic and molecular levels, nanomaterials display distinctive physical, chemical, and biological attributes that can be harnessed for diagnostic purposes.

An exemplary application of bio-nanotechnology involves the utilization of magnetic nanobeads as nanosensors for clinically relevant viruses and bacteria. These nanobeads comprise a supramagnetic iron oxide core enveloped in dextran, with anti-viral antibodies directly attached to the nanobeads. Employing a magnetic field, it is possible to detect as few as five viral particles in a small serum sample. This approach offers heightened sensitivity compared to conventional ELISA-based methods and is both swifter and more economical than PCR-based detection techniques.

Real-time electrical detection of single virus particles can be achieved with high selectivity using nanowire field effect transistors. These nanowires, when modified with antibodies for specific viruses, show discrete conductance changes characteristic of binding and unbinding in the presence of the target virus, demonstrating their specificity.

In the case of pathogenic bacteria, rapid and sensitive detection is crucial for medical diagnosis. Conventional methods often lack ultra-sensitivity or involve delays due to culturing. Nanotechnology-based methods, such as bio-conjugated nanoparticle assays, offer rapid detection of single bacteria within minutes.

Nanotechnology also enables precise localization of antibodies using nanolithography, although nonspecific background binding and detection sensitivity remain challenges. Nevertheless, nanotechnology plays a vital role in identifying and detecting even single viral particles, which is crucial for diseases like AIDS where a small number of viral particles can lead to infection.

Overall, nanotechnology offers innovative solutions for early and sensitive diagnosis of infectious agents, including those with extremely low concentrations. By providing rapid and accurate detection methods, bio-nanotechnology contributes to improved disease management and public health [1].

9.1.2.3. Diagnosis of tuberculosis based on BioMEMS

Nanotechnology holds significant promise for improving tuberculosis (TB) diagnosis and treatment, particularly in countries like India where TB burden is high. Several innovative approaches leveraging nanotechnology have been developed to address this issue.

One such approach involves the use of nanomechanical deflection of microcantilevers for TB diagnosis. In this method, TB-specific antigens adsorb onto the upper surface of the microcantilever, causing deflection, which is measured in terms of piezoresistive changes. This biomicroelectromechanical system (BioMEMS) based microdiagnostic kit offers high specificity, detecting antigens at picogram levels.

NanoLogix's "Identikit" is another promising technology for detecting Mycobacterium avium complex (MAC) infection, which is particularly important for early detection in patients with AIDS. This methodology allows for the detection of MAC pathogens in sputum and stool samples, enabling early treatment before the infection spreads.

In India, the Central Scientific Instruments Organization has developed a nanotechnology-based TB diagnostic kit currently undergoing clinical trials. This kit offers efficiency, portability, and

user-friendliness, making it accessible even in remote areas. Importantly, it does not require skilled technicians for operation and is cost-effective, with tests available for as little as Rs. 30.

Additionally, research groups at institutions like Harvard University, the Postgraduate Institute of Medical Education and Research in India, and the Council for Scientific and Industrial Research in South Africa are investigating the use of polylactide co-glycolide nanoparticles as drug carriers for TB treatment. These nanoparticles hold promise for targeted drug delivery, potentially enhancing treatment efficacy and reducing side effects.

Nanotechnology-based approaches show great potential for improving TB diagnosis and treatment, offering hope for more effective control of this debilitating disease, especially in regions with high disease burden like India [1].

9.1.2.4. Nanotechnology and cardiovascular diseases

The advancement of nanoscience and the utilization of nanotechnology are revolutionizing the landscape of diagnosis, treatment, and prevention of cardiovascular diseases (CVDs). Nano- and microparticles, as central components of nanotechnology, offer a multitude of functions serving as imaging agents, target probes, and therapeutic carriers simultaneously. Although the application of nano- and microparticle-based imaging in cardiovascular interventions is still evolving, it has already demonstrated promising potential in various aspects:

1. **Monitoring of Interventional Procedures**: Nano- and microparticle-based imaging enables real-time monitoring of primary interventional procedures for precise delivery of therapeutics. By incorporating imaging agents into these particles, clinicians can visualize the target sites within the cardiovascular system with enhanced clarity and accuracy.
2. **Enhanced Therapeutic Delivery**: These particles can serve as carriers for therapeutic agents, ensuring their targeted delivery to specific areas affected by cardiovascular diseases. By encapsulating drugs or therapeutic molecules within nano- or microparticles, clinicians can achieve controlled release and prolonged retention at the site of action, thereby maximizing therapeutic efficacy while minimizing systemic side effects.
3. **Assessment of Therapeutic Efficiency**: Post-interventional monitoring of therapeutic efficiency is crucial in evaluating the effectiveness of treatments for cardiovascular diseases. Nano- and microparticle-based imaging techniques provide a means to track the distribution, accumulation, and response of therapeutics within the cardiovascular system over time, allowing clinicians to assess treatment outcomes and make informed decisions regarding patient management.

Nano- and microparticle-based imaging holds significant promise in advancing the field of cardiovascular interventions by facilitating precise delivery of therapeutics, optimizing treatment outcomes, and improving patient care. As research in this area continues to progress, further innovations in nanotechnology are expected to revolutionize the diagnosis, treatment, and prevention of cardiovascular diseases, ultimately leading to improved patient outcomes and enhanced quality of life [1].

9.1.3. Nanotechnology for clinical laboratory diagnostics – salient points

The integration of nanotechnology into diagnostic and therapeutic approaches holds significant promise in transforming healthcare delivery, with several potential benefits:

1. **Tailored Medication**: Utilizing genetic information, medications can be tailored to individual patients, reducing the risk of adverse reactions and improving treatment outcomes.
2. **Enhanced Sensitivity and Speed**: Nanoscale particles used in biological tests increase sensitivity, speed, and flexibility, enabling the detection of minute quantities of substances with higher accuracy.
3. **Reduced Sample Volumes**: Nanotechnology enables testing with smaller sample volumes, minimizing discomfort for patients and reducing the amount of specimen required for analysis.
4. **Improved Disease Detection**: Nanotechnology allows for the detection of microorganisms or molecules that may not be detectable with conventional techniques, leading to earlier diagnosis and intervention for diseases such as cardiovascular diseases, pulmonary hypertension, and cancer.

5. **Faster Test Results**: By reducing the time required for testing, nanotechnology accelerates clinical decision-making, enabling prompt initiation of treatment and potentially reducing healthcare costs associated with prolonged hospital stays or unnecessary procedures.
6. **Targeted Drug Delivery**: Nanoparticles enable targeted drug delivery in cancer therapy, enhancing the efficacy of treatment while minimizing systemic side effects. They can also serve as adjuncts to hyperthermia and photodynamic therapy, further improving treatment outcomes.
7. **Personalized Medicine**: Nanobiotechnology facilitates the development of personalized medicine, allowing for the prescription of therapeutics tailored to individual patients' unique characteristics and disease profiles.

In summary, the integration of nanotechnology into diagnostic and therapeutic approaches offers numerous benefits, including improved sensitivity, speed, and accuracy of tests, enhanced treatment efficacy, and the potential for personalized medicine, ultimately leading to better patient outcomes and more cost-effective healthcare delivery [1].

9.1.4. Insight of nano diagnostics

The development and application of nanotechnology in the medical field indeed raise important considerations regarding public health, safety, environmental protection, and ethical implications. Here are some key points to address these concerns:

1. **Toxicity and Safety**: Nano-particles can exhibit increased reactivity and potentially unknown toxicity compared to larger volumes of the same substance. Comprehensive research into the safety and potential health effects of nanoparticles is crucial before widespread use in medical applications. Regulations and guidelines should be established to ensure the safe development and use of nanotechnology in healthcare.
2. **Environmental Impact**: The release of nanoparticles into the environment raises concerns about their potential ecological impact. Efforts should be made to understand and mitigate any adverse effects on the environment, including potential bioaccumulation in organisms and ecosystems.
3. **Regulatory Oversight**: Regulatory agencies such as the FDA (Food and Drug Administration) play a critical role in ensuring the safety and efficacy of medical devices and technologies, including those based on nanotechnology. Robust regulatory frameworks should be established to evaluate and approve nanodiagnostic devices and other nano-based medical products.
4. **Ethical Considerations**: The use of nanotechnology in diagnostics raises ethical questions regarding patient privacy, consent, and autonomy. Individuals should have the right to control access to their genetic information and be informed about the potential risks and benefits of diagnostic technologies. Transparency and informed consent should be prioritized in the development and implementation of nanodiagnostic tools.
5. **Risk Assessment and Management**: Researchers and developers must conduct thorough risk assessments to identify potential hazards associated with nanodiagnostic devices and implement appropriate risk management strategies. This includes minimizing exposure to nanoparticles and addressing any potential health risks associated with their use.

Overall, while nanotechnology holds great promise for advancing medical diagnostics and treatment, careful consideration of safety, ethical, and environmental concerns is essential to ensure responsible and sustainable implementation in healthcare practices. Collaboration among scientists, healthcare professionals, regulatory agencies, policymakers, and ethicists is crucial to address these complex issues and promote the responsible development and use of nanotechnology in medicine [1].

9.2. Outlook of various diagnostics and nanodiagnostic techniques for COVID-19

The emergence and spread of the novel coronavirus SARS-CoV-2, leading to the COVID-19 pandemic, have highlighted the importance of rapid and accurate diagnostic methods for infectious diseases.

9.2.1. Introduction

Nanotechnology-based approaches have been explored as potential tools for the detection of SARS-CoV-2 due to their sensitivity, specificity, and scalability. Here are some key points regarding the use of nanotechnology in COVID-19 diagnostics:

1. **Nanoparticle-Based Detection**: Nanoparticles can be functionalized with specific antibodies or molecular probes to selectively bind to SARS-CoV-2 antigens or nucleic acids. This approach allows for the sensitive and specific detection of the virus in clinical samples, such as nasopharyngeal swabs or saliva.
2. **Point-of-Care Testing**: Nanotechnology enables the development of portable and rapid diagnostic devices for point-of-care testing. These devices can provide results within minutes, allowing for timely diagnosis and immediate patient management.
3. **Nanobiosensors**: Nanobiosensors, incorporating nanomaterials such as graphene, carbon nanotubes, or gold nanoparticles, can detect SARS-CoV-2 biomarkers with high sensitivity and specificity. These sensors can be integrated into wearable devices or smartphone platforms for remote monitoring and early detection of infection.
4. **Multiplexed Detection**: Nanotechnology-based assays can facilitate the simultaneous detection of multiple targets, enabling the differentiation of SARS-CoV-2 from other respiratory pathogens and the identification of viral variants or mutations.
5. **Enhanced Imaging Techniques**: Nanoparticles can enhance imaging techniques such as microscopy or spectroscopy for the visualization and characterization of SARS-CoV-2 particles or infected cells. This can aid in understanding viral pathogenesis and host-virus interactions.
6. **Nanopore Sequencing**: Nanopore sequencing, a technology that uses nanopores to sequence DNA or RNA molecules, has been utilized for the rapid and real-time detection of SARS-CoV-2 genetic sequences. This approach enables the monitoring of viral evolution and the identification of new variants.
7. **Theranostics**: Nanotechnology can also be applied to theranostic approaches, where diagnostic and therapeutic agents are combined into a single platform. This concept allows for personalized medicine strategies and targeted treatment of COVID-19 (Figure 9.3.) [2].

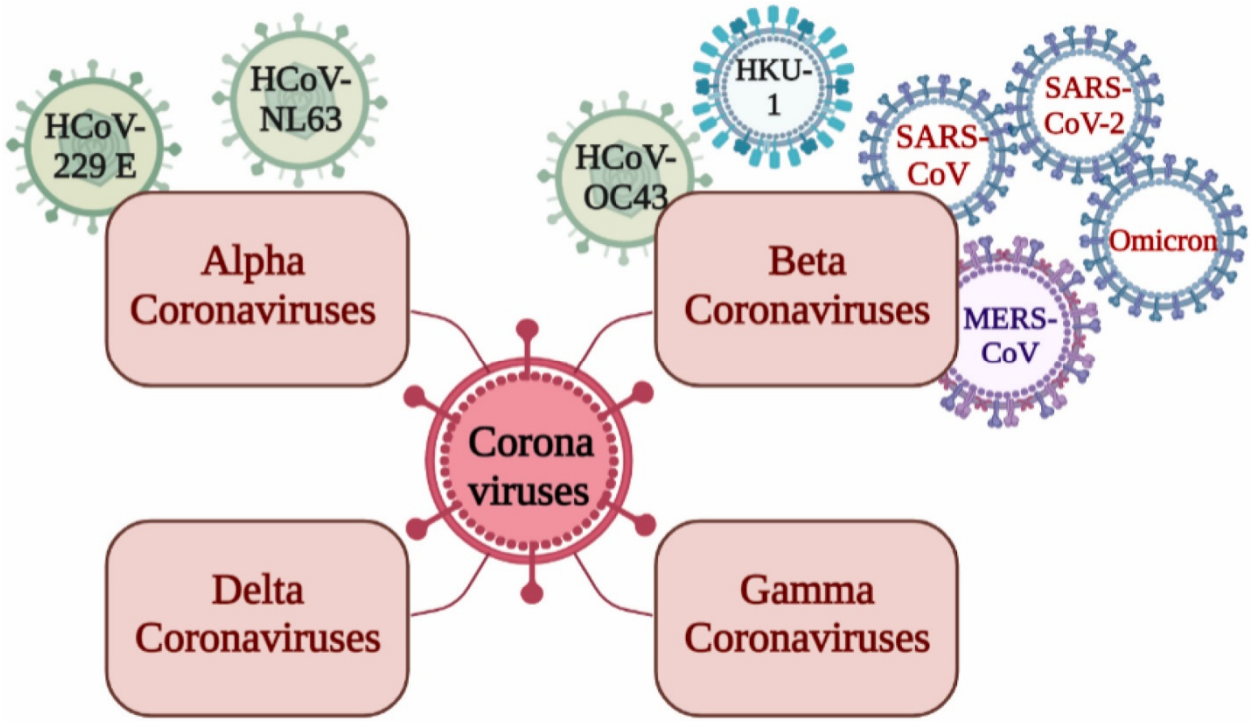


Figure 9.3. Schematic representation of the different types of human coronaviruses [2].

The genetic makeup and mechanisms of SARS-CoV-2, as well as the symptoms and transmission of COVID-19, have prompted the development of various diagnostic techniques to detect the virus and identify infected individuals. Here are some key points regarding COVID-19 diagnostics:

1. Genetic Structure of SARS-CoV-2: SARS-CoV-2 is a positive-sense single-stranded RNA virus belonging to the genus Beta coronavirus and subgenus Sarbecovirus. Its genome codes for polyproteins pp1a and pp1b, which give rise to non-structural and structural proteins, including the spike (S) protein responsible for viral entry into host cells.
2. Mechanism of Infection: The spike protein of SARS-CoV-2 binds to the angiotensin-converting enzyme II (ACE2) receptor on host cells, facilitating viral entry and subsequent replication. This interaction is crucial for the pathogenesis of COVID-19.
3. Symptoms and Implications: COVID-19 symptoms include fever, cough, malaise, dyspnea, and in severe cases, respiratory distress or septic shock. Elderly individuals and those with underlying health conditions are at higher risk of developing severe complications.
4. Transmission: COVID-19 is primarily transmitted through close contact with infected individuals via respiratory droplets, saliva, or airborne particles. Surface-to-human transmission and indirect modes of spread are less common but still possible.
5. Diagnostic Techniques:
    - Reverse Transcription Polymerase Chain Reaction (RT-PCR): Considered the gold standard, RT-PCR detects viral RNA in respiratory samples with high accuracy and sensitivity. It also allows for the differentiation of COVID-19 variants.
    - Smartphone-Based Devices: Utilizing technologies such as CRISPR and CRISPR-associated protein, colorimetric assays, and electrochemical techniques, smartphone-based diagnostic devices offer rapid and portable testing options.
    - Artificial Intelligence (AI)-Based Techniques: AI algorithms have been developed to analyze clinical data, radiological imaging, and other parameters to assist in the identification of COVID-19 cases and disease progression.

These diagnostic methods play crucial roles in controlling the spread of COVID-19 by enabling early detection, contact tracing, and appropriate patient management. Ongoing research and technological advancements continue to enhance the efficiency, accessibility, and reliability of COVID-19 diagnostics.

The classification of COVID-19 variants by the World Health Organization (WHO) into Variants of Concern (VOCs), Variants of Interest (VOIs), and Variants under Monitoring (VUMs) aims to facilitate global monitoring and research efforts. Here are the key points regarding the classification of variants:

1. **Variants of Concern (VOCs)**: These variants exhibit increased transmissibility and/or virulence compared to the original strain of SARS-CoV-2. The Delta and Omicron variants, along with their sublineages (e.g., BA.1, BA.2, BA.3, etc.), are currently classified as VOCs. Previous VOCs include the Alpha, Beta, and Gamma variants.
2. **Variants of Interest (VOIs)**: VOIs are viruses with predicted genetic modifications and significant community transmission, indicating a potential emerging risk to public health. Examples of previously circulating VOIs include Epsilon, Zeta, Eta, Theta, Iota, Kappa, Lambda, and Mu variants.
3. **Variants under Monitoring (VUMs)**: These variants have genetic changes suspected to pose future risks but do not yet meet the criteria to be classified as VOCs or VOIs.

On March 11th, 2022, researchers identified a new recombinant variant called Deltacron, which is a recombination between the Delta and Omicron variants. This variant exhibit characteristic of both parent variants, including mutations in the spike gene similar to the omicron-like spike protein, except for differences in the N-terminal domain (NTD). The NTD and receptor-binding domain (RBD) of the spike protein play crucial roles in virus-host interactions. The convergent mutations in both NTD and RBD of the Deltacron variant increase its kinetic properties for optimized binding to host cells.

Overall, ongoing surveillance and characterization of COVID-19 variants, including Deltacron, are essential for understanding their impact on transmission, disease severity, and vaccine effectiveness [2].

9.2.2. Diagnostic techniques for COVID-19

The diagnostic techniques for detecting COVID-19 encompass a range of approaches, each with its own advantages and limitations:

1. **Nucleic Acid Amplification Tests (NAATs)**: These tests, such as RT-PCR and DNA microarray-based technology like DetectX-Rv, are highly sensitive and specific. However, they involve multi-step sample processing, longer detection times, and a risk of contamination.
2. **Antigen Tests**: These rapid immunoassays are easy to perform and suitable for point-of-care (POC) diagnosis. While less sensitive than NAATs, they are useful for screening, particularly in congregate settings.
3. **Serological Tests**: These tests detect antibodies developed in response to a prior infection but cannot detect current infections. They are commonly used for serosurveillance to determine the prevalence of the disease in a population.
4. **Protein Microarrays**: Lab-on-chip (LOC) devices like the MosaiQ COVID-19 Antibody Microarray detect protein binding interactions or expression levels, providing a high-throughput method for serological testing.
5. **Detection of Immunological Biomarkers**: Some diagnostic approaches focus on detecting changes in immunological biomarkers, such as interleukin-6 (IL-6), which can indicate inflammation and the presence of a cytokine storm.

Each of these diagnostic techniques plays a crucial role in the comprehensive detection and monitoring of COVID-19, offering varying levels of sensitivity, specificity, and suitability for different settings and purposes (Figure 9.4.).

9.2.2.1. Reverse-transcription polymerase chain reaction (RT-PCR)

Nucleic acid amplification by RT-PCR is widely regarded as the most dependable and recommended lab-based diagnostic technique for COVID-19. This method involves reverse transcription of viral RNA into complementary DNA (cDNA), followed by amplification of specific regions of the cDNA. Several target sequences are commonly used, including the RNA-dependent RNA polymerase (RdRp) gene, open reading frame ORF1ab region, envelope protein (E) gene, nucleocapsid protein (N) gene, spike protein (S) gene, and helicase (Hel) gene.

The workflow for RT-PCR diagnosis typically involves a preliminary screening test targeting the E gene, followed by a confirmatory test targeting the RdRp gene. Nasopharyngeal or oropharyngeal swab samples are commonly collected for testing, usually around 5–6 days after symptom onset when viral load is high in the upper respiratory regions. Lower respiratory specimens such as sputum, tracheal aspirates, or bronchoalveolar lavage may also be collected in certain cases.

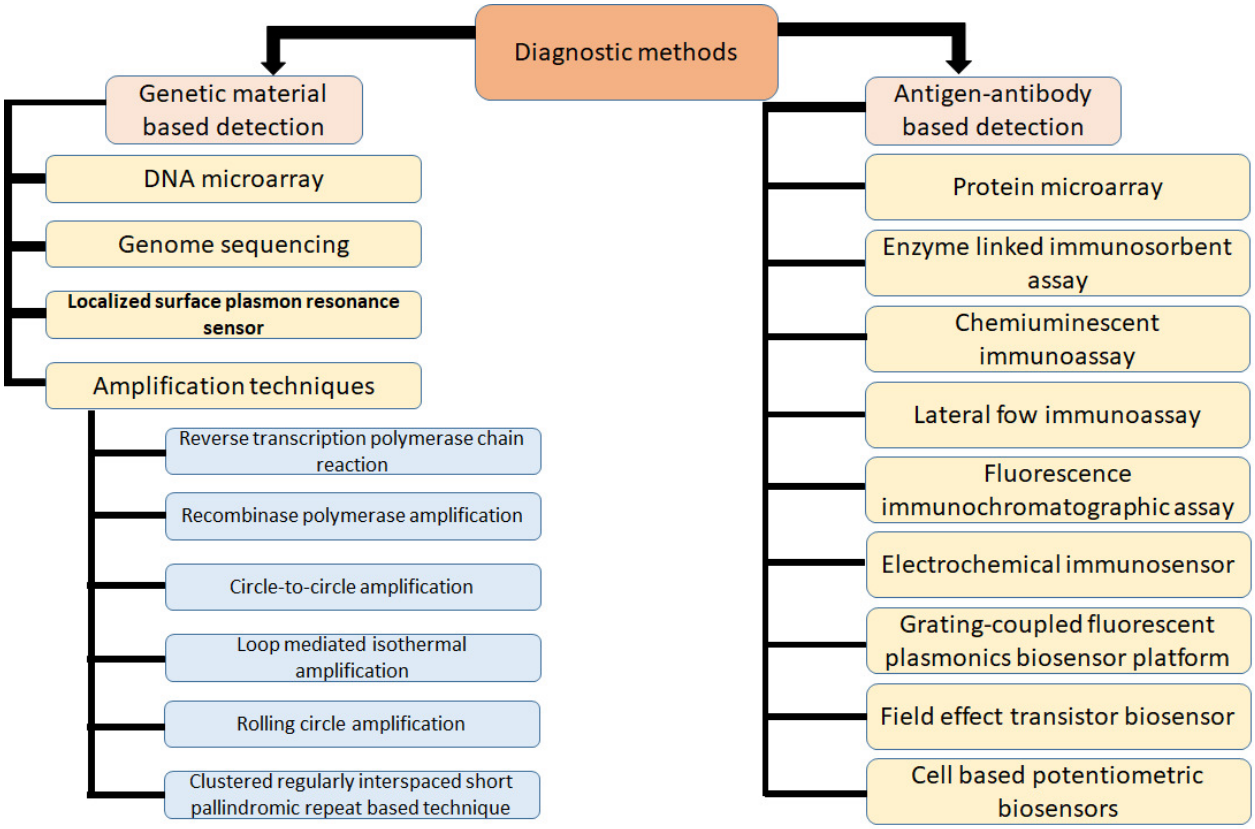


Figure 9.4. Schematic representation of the various diagnostic techniques for COVID-19 [2].

Various RT-PCR assays have been developed targeting different gene regions of the SARS-CoV-2 virus. These assays offer qualitative and quantitative results and can be performed on different sample types, including nasopharyngeal swabs, sputum, and bronchoalveolar lavage. For example, the REAL QUALITY RQ-2019-nCoV assay developed by AB ANALITICA targets the RdRp gene and E gene, providing qualitative results within a short timeframe.

Other RT-PCR assays, such as those developed by Chu et al. and Chan et al., target different gene regions of the virus and offer high sensitivity and specificity. These assays play a crucial role in the accurate and timely diagnosis of COVID-19, facilitating effective patient management and control of the disease spread [2].

9.2.2.2. Chest computerized tomography scan (CT scan)

Chest imaging, particularly computed tomography (CT) scans, holds a pivotal role in clinically assessing and managing patients with lung infections, including those attributed to SARS-CoV-2. Although reverse transcription-polymerase chain reaction (RT-PCR) stands as the primary method for diagnosing COVID-19, CT scans have garnered extensive usage, particularly in situations where RT-PCR testing may be constrained or when there are apprehensions regarding false-negative outcomes.

In the early stages of the COVID-19 pandemic, CT scans were used extensively in China as a diagnostic tool due to the shortage of testing kits and concerns about the sensitivity of RT-PCR. Studies have shown that CT scans have relatively high sensitivity, ranging from 84% to 98%, compared to RT-PCR, making them valuable for identifying pulmonary abnormalities consistent with COVID-19 infection.

However, it's important to note that CT scans may lack specificity, as they cannot reliably differentiate between various respiratory viruses. Additionally, while certain characteristic findings on CT scans, such as ground-glass opacity (GGO), bilateral multifocal GGO, consolidation, peripheral reticulation, and crazy-paving patterns, are associated with COVID-19, they are not exclusive to this infection and can be seen in other respiratory conditions.

Despite these limitations, CT scans remain a valuable tool in the clinical management of COVID-19 patients, providing important information about disease severity, progression, and complications. When used judiciously and in conjunction with clinical and laboratory findings, CT imaging can aid in early detection, risk stratification, and treatment decisions for patients with suspected or confirmed COVID-19 [2].

9.2.2.3. X-ray imaging

Chest X-ray (CXR) is indeed a valuable and widely accessible imaging modality for the initial evaluation of individuals suspected or confirmed to have COVID-19. While it is less sensitive than computed tomography (CT), CXR remains a useful first-line test due to its lower cost, portability, and ease of use.

The sensitivity of CXR for detecting COVID-19-related lung abnormalities is reported to be around 69%, which is lower than that of CT scans. However, CXR findings, such as airspace opacities (consolidations or ground-glass opacities), typically become apparent around 10-12 days after the onset of symptoms, making it a valuable tool for assessing disease progression and severity.

In clinical practice, COVID-19 CXR findings are often classified into categories such as typical, indeterminate, atypical, or negative, based on the pattern and distribution of lung abnormalities observed. This classification helps guide clinical decision-making and further diagnostic workup.

Despite its lower sensitivity compared to CT, CXR remains an important tool in the diagnosis and management of COVID-19, particularly in settings where CT may not be readily available or feasible. When used in conjunction with clinical history, symptoms, and laboratory findings, CXR can provide valuable information to clinicians for timely and appropriate management of COVID-19 patients [2].

9.2.2.4. Magnetic resonance imaging (MRI) scanning

While magnetic resonance imaging (MRI) is a valuable diagnostic tool for various medical conditions, its utility in the context of COVID-19 pneumonia is limited compared to other imaging modalities such as computed tomography (CT) and chest X-ray (CXR). MRI is less commonly used for evaluating lung pathology due to several factors, including its lower anatomical resolution in the lung region, susceptibility to motion artifacts from breathing movements, and relatively longer imaging times.

The main limitation of MRI for assessing lung pathology, including COVID-19-related changes, is its low signal-to-noise ratio in the lung tissue, resulting in poor image quality. This can make it challenging to visualize subtle abnormalities such as ground-glass opacities (GGO) and consolidations, which are characteristic features of COVID-19 pneumonia.

While MRI may provide useful information in certain cases, such as evaluating complications or comorbidities affecting other organs or systems, it is not typically the primary imaging modality used for diagnosing or monitoring COVID-19 pneumonia. Instead, CT scans and CXR are more commonly employed due to their higher sensitivity and specificity for detecting pulmonary abnormalities associated with the disease.

Overall, while MRI may have a role in certain clinical scenarios, its limited utility for imaging lung pathology in COVID-19 patients means it is not routinely used for this purpose. Other imaging modalities, such as CT and CXR, remain the mainstay for evaluating pulmonary manifestations of COVID-19 [2].

9.2.2.5. Genome sequencing

Metagenomic studies of viruses, including SARS-CoV and other infections related to COVID-19 severity, are essential for understanding the genetic diversity and epidemiology of these viruses. One approach commonly used in such studies is amplicon-based sequencing, which involves

amplifying specific regions of viral genomes to identify genetic variations and track viral evolution. This technique is valuable for molecular epidemiology and contact tracing efforts.

Another method used in metagenomic studies is sequence-independent single primer amplification (SISPA), which allows for the detection of viral sequences without prior knowledge of their sequences. SISPA is particularly useful for identifying novel or divergent viral strains that may not be captured by targeted amplicon sequencing approaches.

MinION sequencing, a portable nanopore sequencing platform developed by Oxford Nanopore Technologies, has been increasingly used in viral metagenomic studies. It allows for real-time sequencing of DNA or RNA molecules and has been employed for sequencing SARS-CoV directly from patient samples such as nasopharyngeal swabs. MinION sequencing offers advantages such as rapid turnaround time, portability, and the ability to generate long sequencing reads, which can be beneficial for resolving complex viral genomes and detecting genetic variations.

In summary, metagenomic approaches such as amplicon-based sequencing and SISPA, along with technologies like MinION sequencing, play crucial roles in studying the genetic diversity, transmission dynamics, and evolution of viruses like SARS-CoV, providing valuable insights into the epidemiology and pathogenesis of COVID-19 [2].

9.2.2.6. Microarray technique

Microarray technology is indeed a powerful tool for the rapid and high-throughput detection of various genetic elements, including genes, nucleotide sequences, mutations, and diseases. It has wide-ranging applications in fields such as genomics, proteomics, forensics, and drug screening.

In the context of SARS-CoV detection, microarrays can be employed in two main approaches: aptamer-based microarrays and proteome-based microarrays.

Aptamer-based microarrays: In this approach, viral DNA is first reverse-transcribed into complementary DNA (cDNA), which is then labeled with fluorescent dyes. These labeled cDNA probes are then allowed to hybridize with specific oligonucleotides immobilized on a microarray chip. After washing to remove unbound probes, the signal from the hybridized probes is detected using fluorescence detection methods. This technique enables the detection of specific sequences of SARS-CoV with high sensitivity and specificity.

Proteome-based microarrays: In this approach, peptide sequences derived from viral coat proteins are immobilized on the microarray surface. When the microarray is exposed to a sample containing viral antibodies, these antibodies bind specifically to their corresponding viral epitopes immobilized on the chip. The bound antibodies can then be detected using fluorescence or other detection methods. This method allows for the detection of viral proteins and can be useful for studying antibody responses to SARS-CoV infection.

Microarrays have been utilized to detect different strains of SARS-CoV and to identify mutations, including single nucleotide polymorphisms (SNPs), within viral genes such as the spike (S) gene. With advancements in microarray technology, researchers have achieved high accuracy and sensitivity in detecting and characterizing SARS-CoV variants and genetic variations.

Overall, microarray-based detection methods offer a valuable approach for comprehensive and efficient analysis of viral genomes, allowing for rapid and accurate identification of SARS-CoV and its variants, as well as the study of host immune responses to infection [2].

9.2.2.7. Biosensors

Biosensors play a crucial role in the detection and diagnosis of diseases, including infectious diseases like COVID-19. These devices offer several advantages, including being small, simple, sensitive, portable, and capable of providing rapid results. Biosensors typically consist of a bioreceptor, a transducer, and a signal processor, allowing for the detection and quantification of specific analytes.

In the context of SARS-CoV-2 RNA detection, various biosensor technologies have been developed, each with its own principles and methodologies:

1. Nucleic acid-based biosensors: These biosensors utilize nucleic acid probes that specifically bind to viral RNA sequences. The binding event is then detected using various transduction methods, such as fluorescence or electrochemical signals.
2. CRISPR-Cas9-based paper strips: This innovative approach utilizes the CRISPR-Cas9 system, which is programmed to detect specific RNA sequences of SARS-CoV-2. When the target RNA is present, Cas9 enzyme activity is triggered, resulting in a detectable signal on a paper strip.
3. Antigen-Au/Ag nanoparticles-based biosensors: These biosensors rely on the specific binding of SARS-CoV-2 antigens to antibodies immobilized on gold or silver nanoparticles. The binding event induces a change in the optical or electrochemical properties of the nanoparticles, allowing for the detection of the target antigen.
4. Surface plasmon resonance (SPR) biosensors: SPR biosensors detect molecular interactions based on changes in the refractive index at the surface of a sensor chip. SARS-CoV-2 RNA or antigen binding events can be monitored in real-time by measuring changes in the SPR signal.
5. Optical biosensors: Optical biosensors utilize light-based detection methods to monitor biomolecular interactions. These biosensors may involve fluorescence, luminescence, or absorbance measurements to detect SARS-CoV-2 RNA or antigens.

Each of these biosensor technologies offers unique advantages in terms of sensitivity, specificity, speed, and ease of use. By harnessing the power of biosensors, researchers and healthcare professionals can develop rapid and accurate diagnostic tools for detecting SARS-CoV-2 infection, thereby facilitating timely intervention and control of the COVID-19 pandemic [2].

9.2.2.7.1. Clustered regularly interspaced short palindromic repeats (CRISPR)-based devices

CRISPR-Cas platforms have emerged as powerful tools for point-of-care (POC) diagnostics, offering rapid and accurate detection of viral RNA with high sensitivity and specificity. These platforms leverage the CRISPR system's ability to target specific DNA or RNA sequences and the nuclease activity of Cas proteins to detect the presence of viral RNA.

Two notable methods developed by Sherlock Biosciences and Mammoth Biosciences are the Specific High-sensitivity Enzymatic Reporter UnLOCKing (SHERLOCK) assay and the DNA Endonuclease-Targeted CRISPR Trans Reporter (DETECTOR) assay, respectively. SHERLOCK typically utilizes Cas13 for detection, while DETECTOR employs Cas12. These assays have demonstrated high sensitivity and specificity in detecting viral RNA.

Additionally, isothermal amplification-mediated CRISPR-based biosensing systems, such as SHERLOCK-COVID, have been developed to enable rapid and efficient detection of SARS-CoV-2 RNA.

In India, the Tata Group and CSIR-IGIB have developed the FNCAS 9 Editor Linked Uniform Detection Assay (FELUDA), which utilizes Cas9 protein for SARS-CoV-2 detection with high sensitivity and specificity at a minimal cost.

Efforts are also underway to develop advanced CRISPR-based diagnostic tests that can be paired with smartphone cameras for real-time detection. This technology aims to provide rapid results within 30 minutes, enhancing accessibility and convenience.

Moreover, CRISPR-Cas12-based lateral flow assays (LFAs) have been developed for the detection of SARS-CoV-2 genes, with high sensitivity and specificity. These assays offer a simple and portable solution for POC testing.

Innovative approaches, such as graphene field-effect transistor (GFET)-based electrical biosensing platforms and CRISPR-Chip technology, have also been explored for COVID-19 detection. These platforms demonstrate high sensitivity and rapid detection capabilities, making them promising candidates for POC diagnostics.

9.2.2.7.2. Lateral flow assay/immunoassay (LFA/LFIA)

Lateral flow immunoassays (LFIA) are widely used as rapid and portable point-of-care (POC) devices for the detection of SARS-CoV by analyzing various biomarkers such as antigens, antibodies, nucleic acids, and whole viruses.

Multiplex LFIA allows for the simultaneous detection of multiple targets, such as the RdRp, ORF3a, and N genes, within 30 minutes. This technique has a detection limit of 10 copies per test, making it highly sensitive and suitable for POC applications.

Reverse transcription recombinase polymerase amplification lateral flow assay (RT-RPA-LFA) is a multienzyme field-deployable method used to detect the N gene with an impressive limit of detection (LOD) of 1 ag, demonstrating its high sensitivity for SARS-CoV detection.

Hybrid Capture Fluorescence Immunoassay (HC-FIA) targets viral RNA genes N, E, or ORF1ab and achieves a LOD of 500 copies per mL, providing a sensitive detection method for SARS-CoV.

A dual optical/chemiluminescent LFIA developed by Roda et al. detects salivary and serum IgA using recombinant N protein to capture IgA. This method utilizes gold nanoparticles (AuNP) and horseradish peroxidase (HRP) bioconjugates for detection, offering both optical and chemiluminescent detection options for IgA.

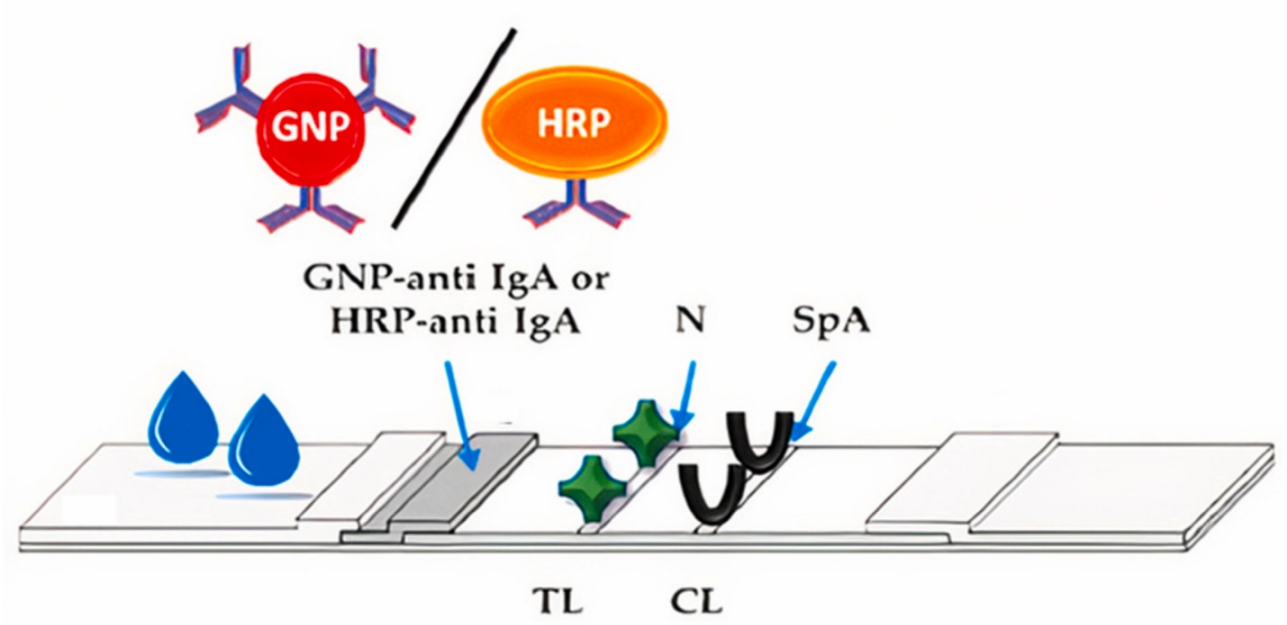
DNA scaffold hybrid chain reaction (DNHCR)-based biosensing assays have also been developed into LFIA, further expanding the capabilities of this technique for SARS-CoV detection.

Overall, LFIA techniques play a crucial role in the rapid and sensitive detection of SARS-CoV, making them valuable tools for POC diagnostics. These techniques leverage nanoparticles for detection, highlighting the importance of nanodiagnostic approaches in advancing diagnostic capabilities (Figure 9.5.).

9.2.2.7.3. Enzyme-linked immunosorbent assay (ELISA)

ELISA (Enzyme-Linked Immunosorbent Assay) is a widely used technique for identifying the presence of antigens or antibodies in a sample. In the context of COVID-19, ELISA has been instrumental in detecting IgG and IgM antibodies against the Rp3 nucleocapsid protein from SARS-CoV. This allows for the serological identification of individuals who have been infected with the virus.

Additionally, ELISA has been used to measure the levels of C-reactive protein and D-dimer in infected patients. Elevated levels of these biomarkers can serve as indicators of infection and disease severity, providing valuable diagnostic information.



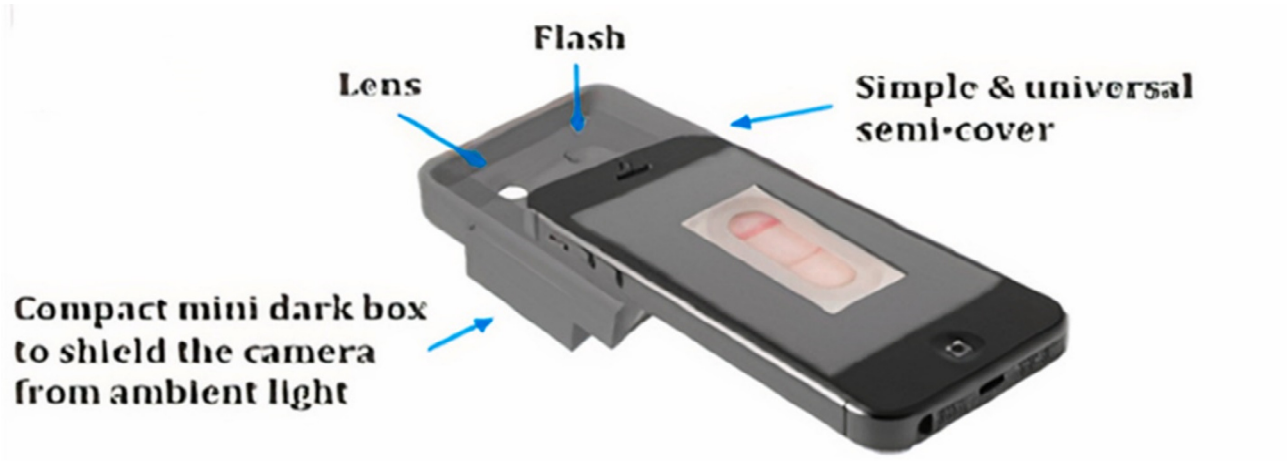


Figure 9.5. Schematic of optical semi-quantitative LFIA using CMOS-based camera [2].

A novel approach to ELISA involves the development of a 96-well wax-printed paper-based immunoassay for SARS-CoV-2 detection in saliva. This device utilizes magnetic beads to immobilize immunological chains, enabling the detection of viral proteins. The results are interpreted colorimetrically using a smartphone application, allowing for rapid and convenient detection of SARS-CoV-2.

Overall, ELISA plays a crucial role in COVID-19 diagnostics by detecting both antigens and antibodies associated with the virus. Its versatility and sensitivity make it a valuable tool in the fight against the pandemic (Figure 9.6.).

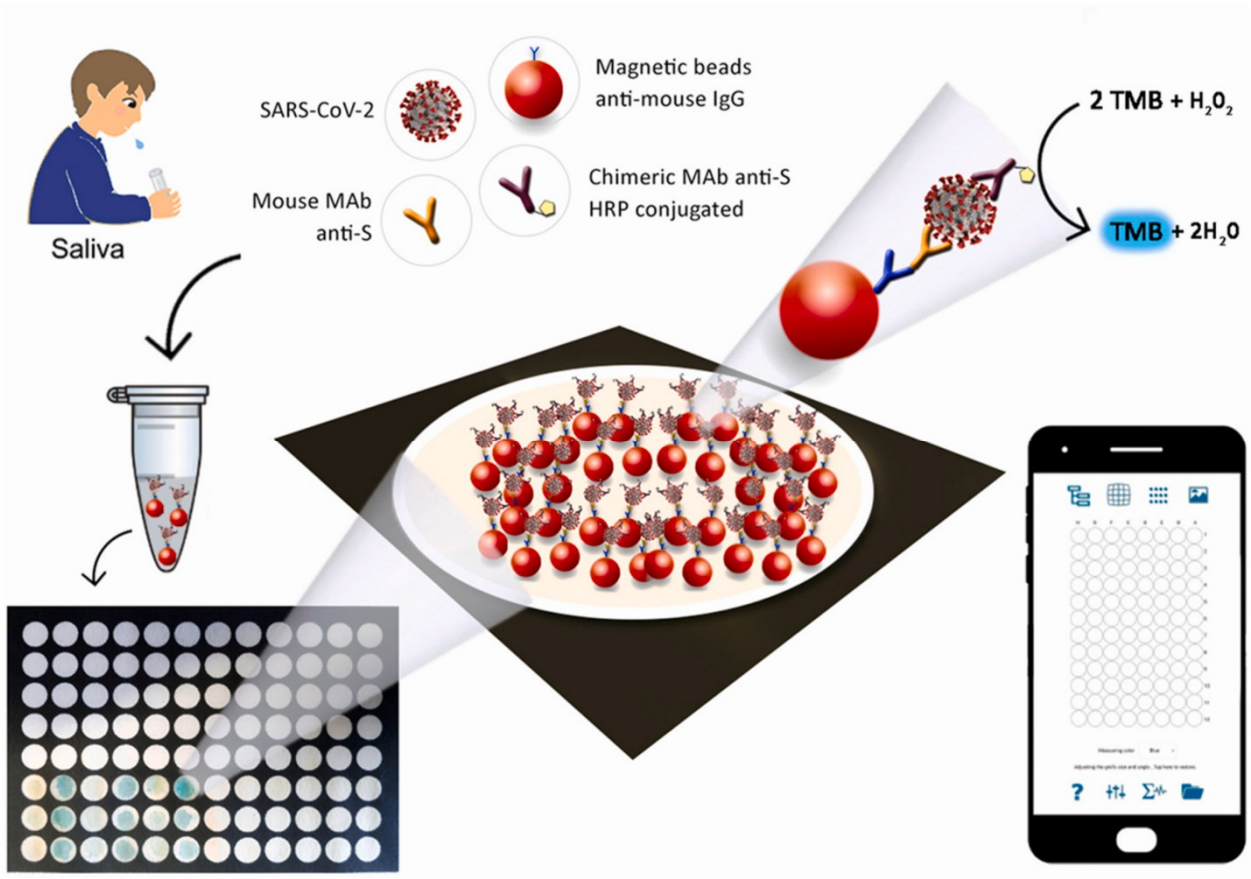


Figure 9.6. Schematic representation of 96-well wax-printed paper-based ELISA immunoassay [2]

9.2.2.7.4. Other biosensors

Several innovative techniques have been developed for the detection of SARS-CoV-2 and associated biomarkers, offering diverse approaches for diagnosis and monitoring of COVID-19.

1. **Covalent Organic Framework (COF) Capsules:** These capsules are fabricated to encapsulate the enzyme Horseradish Peroxidase (HRP), providing an optimal microenvironment for enzyme activity. They enable the detection of SARS-CoV-2 RNA with high sensitivity, ranging from 5 pM to 50 nM, and a low LOD of 0.28 pM.
2. **Label-Free Paper-Based Electrochemical Biosensor:** This biosensor utilizes the SARS-CoV-2 spike protein for antibody detection. It consists of three folding parts: working ePAD, counter ePAD, and closing ePAD. [Fe(CN)6]3-/4- serves as an electrochemical redox indicator, achieving a LOD of 1 ng/mL with high sensitivity and specificity.
3. **Real-Time Electrochemical Biosensor for Reactive Oxygen Species (ROS) Detection:** Elevated ROS levels in the lungs are a crucial biomarker of lung infection. This biosensor detects ROS in sputum samples in real-time, demonstrating a sensitivity and accuracy of 97% for clinical samples.
4. **Piezoelectric Immunosensor:** Developed in 2004 for SARS-CoV-1 detection, this sensor detects analytes from atomized aerosols of sputum samples. It operates within the range of 0.6–4 μg/mL, providing rapid detection within 2 minutes.
5. **Cell-Based Biosensor:** Utilizing a bioelectric recognition assay, this biosensor detects the S1 subunit of the SARS-CoV-2 spike protein. Interaction between a mammalian cell membrane-bound human chimeric antibody and the viral antigen induces a change in membrane structure and potential, generating a strong response for detection.

These diverse biosensing techniques showcase the innovation and versatility in COVID-19 diagnostics, offering various methods for sensitive and rapid detection of the virus and associated biomarkers (Figure 9.7.).

9.2.2.8.1. Loop-mediated isothermal amplification (LAMP)

Isothermal amplification techniques offer valuable alternatives to RT-PCR for nucleic acid detection, providing rapid and easy diagnosis of diseases like COVID-19. Apart from RT-PCR, some prominent isothermal amplification techniques include recombinase polymerase amplification (RPA), rolling circle amplification (RCA), circle-to-circle amplification (C2CA), and loop-mediated isothermal amplification (LAMP).

In LAMP, four primers are utilized, including two forward and two backward primers. Initially, all four primers are employed, but later, only the forward inner primer and the backward inner primer are utilized for cycling.

This technique produces stem-loop DNAs with cauliflower-like structures.

LAMP offers advantages over conventional RT-PCR as nucleic acid amplification occurs at a single temperature of 65 °C, eliminating the need for a thermocycler and enabling rapid diagnosis.

The use of four primers enhances target selectivity and specificity in LAMP.

Reverse transcription-coupled LAMP (RT-LAMP) assays have been developed to directly detect viral RNA with sensitivity comparable to RT-PCR.

For instance, the Lucira COVID-19 All-In-One Test Kit, based on POC-based RT-LAMP technology, has received emergency use authorization for self-testing at home.

Another rapid COVID-19 diagnostic test, the isothermal LAMP-based colorimetric method for COVID-19 (iLACO), has been reported.

This method relies on a color change in the sample, from pink to light yellow, to confirm successful amplification of the ORF1ab gene.

These isothermal amplification techniques offer promising alternatives to traditional RT-PCR, providing rapid, sensitive, and accessible methods for COVID-19 diagnosis, particularly in resource-limited settings or for self-testing at home.

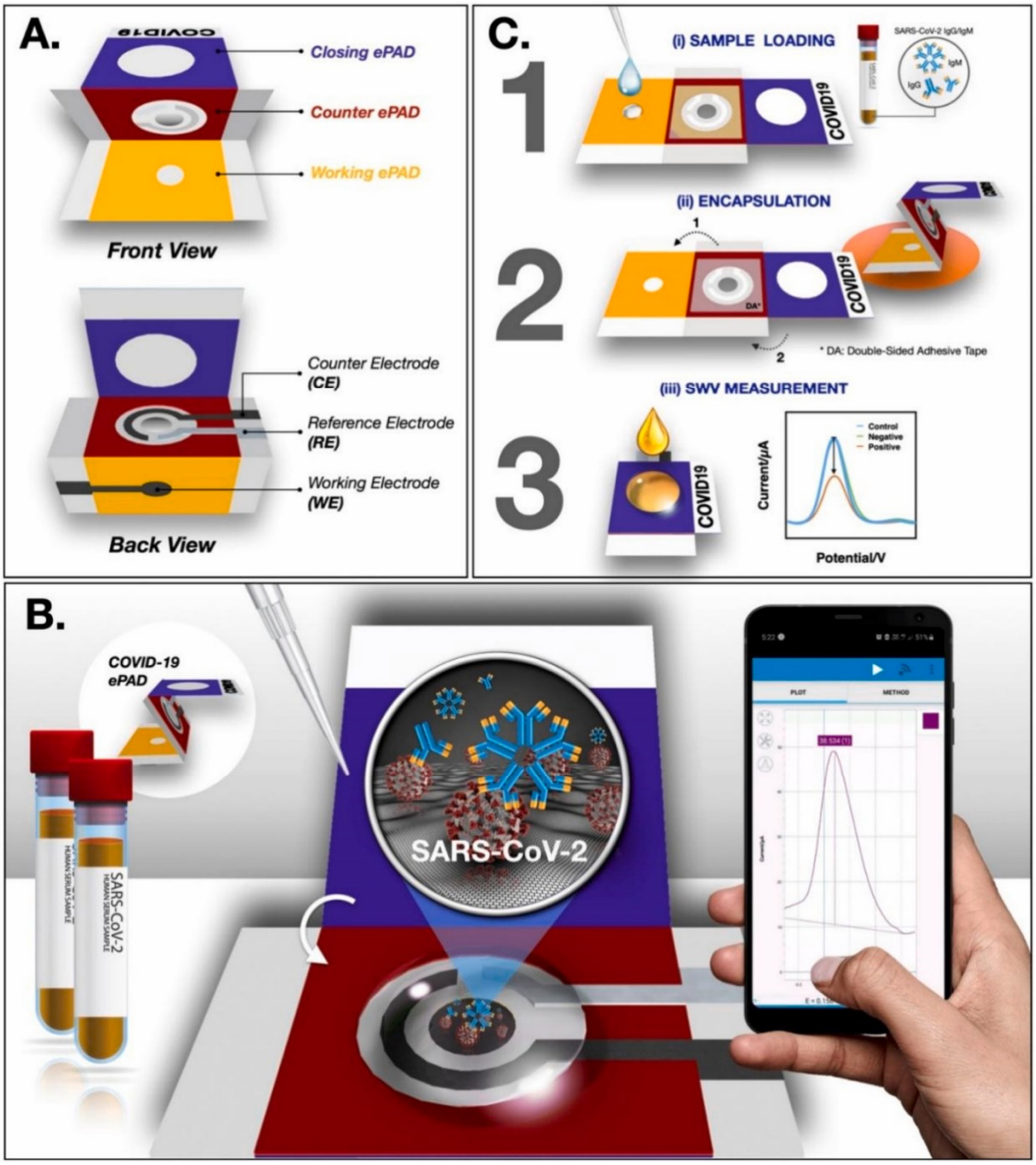


Figure 9.7. Paper-based biosensor, COVID ePAD showing (A) components, (B) principle, and (C) detection method for SARS-CoV-2 antibodies [2].

9.2.2.8.2. Rolling circle amplification (RCA)

Rolling circle amplification (RCA) is an isothermal PCR-based assay that offers rapid, sensitive, and highly efficient detection of SARS-CoV levels. In RCA, circularizable oligonucleotides or padlock probes containing target complementary sequences are hybridized with target DNA or RNA sequences, forming circularized probes. These circularized probes are then amplified using primers and DNA polymerases. Notably, RCA does not require reverse transcriptase for RNA amplification, as in traditional PCR.

RCA can be performed in both liquid and solid phases, with the solid-phase approach involving the use of oligonucleotide-coated magnetic beads. The coronavirus detection capability of RCA is impressive, with amplification up to 10^9 folds within 90 minutes using minimal reagents.

A recent application of RCA is the Padlock Rolling Circle Amplification Nuclease Protection Lateral Flow Assay (PLAN-LFA) platform, which has been utilized to detect SARS-CoV-2 in saliva. In this assay, a padlock probe complementary to the target sequence is designed, hybridized, and ligated to form a circular template. This circular template is then amplified via RCA using polymerases and labeled with nuclease protein probes. When nucleases are added to the linear concatenated RCA product, only double-stranded labeled probes are protected from digestion. The colorimetric lateral flow assay detects the generated fragments, achieving a detection limit of 1.1 pM target DNA (equivalent to 1.3 × 10^6 copies per reaction).

Furthermore, RCA with a nylon mesh medium containing multiple microfluidic pores has been developed for SARS-CoV-2 diagnosis, demonstrating a LOD of 0.7 aM. This approach holds promise for ultrasensitive detection of the virus and could be instrumental in combating the COVID-19 pandemic.

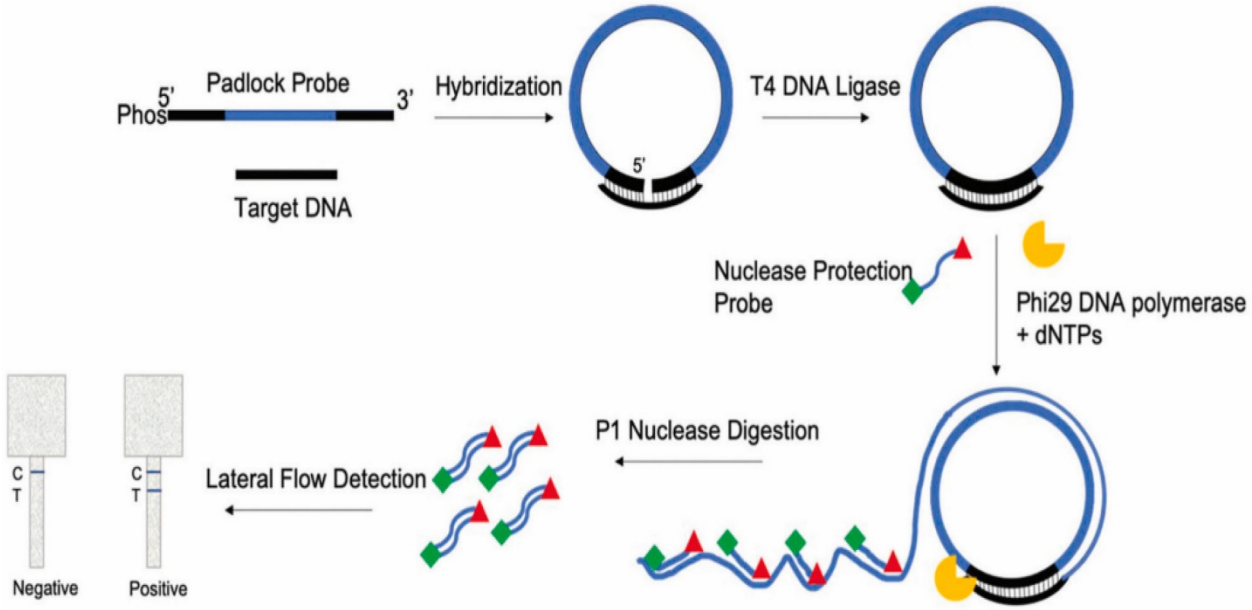


Fig. 9.8. Schematic of PLAN-LFA assay [2].

9.2.2.8.3. Circle-to-circle amplification (C2CA)

Circle-to-circle amplification (C2CA) is a nucleic acid amplification technique that involves multiple rounds of padlock probe ligation and rolling circle amplification (RCA). In the C2CA process, padlock probes are initially hybridized to target DNA or RNA sequences and then ligated to form circularized probes. These circularized probes serve as templates for RCA, producing long concatemeric DNA products.

After the first round of amplification, multiple circles formed by RCA are subjected to endonuclease digestion to break them down into individual units. These units are then ligated again to form new circular templates, which undergo further rounds of amplification in subsequent cycles. This iterative process results in the exponential amplification of the target nucleic acid sequences, generating billions of amplified products.

Homogenous circle-to-circle amplification (HC2CA) is a variant of C2CA that involves a one-pot real-time amplification process with two rounds of RCA. HC2CA simplifies the amplification procedure by performing both the ligation and amplification steps in a single reaction mixture. This approach allows for the real-time monitoring of amplification kinetics and enables rapid detection of target nucleic acids.

In the context of SARS-CoV-2 detection, HC2CA has been utilized in conjunction with optomagnetic biosensors for the identification of the RdRp gene, an essential gene of the virus. The optomagnetic biosensor combines the principles of optics and magnetism to detect the amplified nucleic acid products. This HC2CA-based optomagnetic biosensor has demonstrated a high sensitivity, with a limit of detection (LOD) of 0.4 fM (femtomolar) achieved within 100 minutes. This sensitivity and rapid detection capability make HC2CA-based assays valuable tools for the diagnosis and surveillance of SARS-CoV-2 infections.

9.2.2.9. Intelligence-based techniques

The use of deep learning (DL) and machine learning (ML) techniques for COVID-19 detection has gained significant attention due to their potential to enhance diagnostic accuracy and efficiency, particularly in analyzing medical imaging data such as CT scans, X-rays, and electrocardiogram (ECG) images.

Several DL algorithms have been employed for COVID-19 detection, including convolutional neural networks (CNNs), which are particularly well-suited for image analysis tasks.

Models such as Zeiler and Fergus network (ZFNet) and Dense Convolutional Network-121 (DenseNet121) have also been utilized.

In the evaluation of these DL models, performance metrics such as accuracy, precision, recall, and F1-score are commonly used to assess their efficacy. Customized CNN architectures have been shown to exhibit superior performance in COVID-19 detection tasks, achieving high levels of accuracy and other performance metrics.

Moreover, DL techniques have been applied to analyze ECG images to detect abnormalities in the cardiovascular system of COVID-19 patients.

Deep CNNs, in particular, have demonstrated impressive accuracy, with reported accuracy rates as high as 98.57% in distinguishing between COVID-19 cases and control subjects based on ECG data.

Overall, DL and ML techniques hold promise for improving COVID-19 diagnosis, especially when applied to medical imaging and other diagnostic modalities.

Their ability to efficiently analyze large volumes of data and extract meaningful patterns has the potential to aid healthcare professionals in accurate and timely disease detection and management [2].

9.2.3. Nanodiagnostic techniques for COVID-19 detection

Nanotechnology has made significant contributions to the field of biomedical engineering, particularly in the development of nanodiagnostic tools. These tools integrate nanoscale materials with diagnostic techniques, enabling the creation of advanced diagnostic devices that offer several advantages in healthcare.

Some typical applications of nanotechnology-based diagnostic devices include:

Detection of Biomarkers and Infectious Diseases: Nanotechnology allows for the development of highly sensitive and specific biosensors capable of detecting biomarkers associated with various diseases, including infectious diseases like COVID-19. These biosensors can provide rapid and accurate diagnosis, facilitating timely treatment and containment of outbreaks.

Cancer Therapy: Nanoparticles can be engineered to deliver therapeutic agents directly to cancer cells, minimizing damage to healthy tissues. Additionally, nanotechnology-based diagnostic tools enable early detection of cancer biomarkers, allowing for prompt intervention and personalized treatment strategies.

Targeted Drug Delivery: Nanoparticles can be functionalized to selectively target specific cells or tissues, enhancing the efficacy of drug delivery while minimizing side effects. Nanotechnology-based drug delivery systems enable controlled release of therapeutic agents, improving patient outcomes and treatment compliance.

Food Safety: Nanotechnology-based sensors can detect contaminants and pathogens in food products, ensuring food safety and quality control. These sensors offer rapid and sensitive detection of harmful substances, helping to prevent foodborne illnesses and outbreaks.

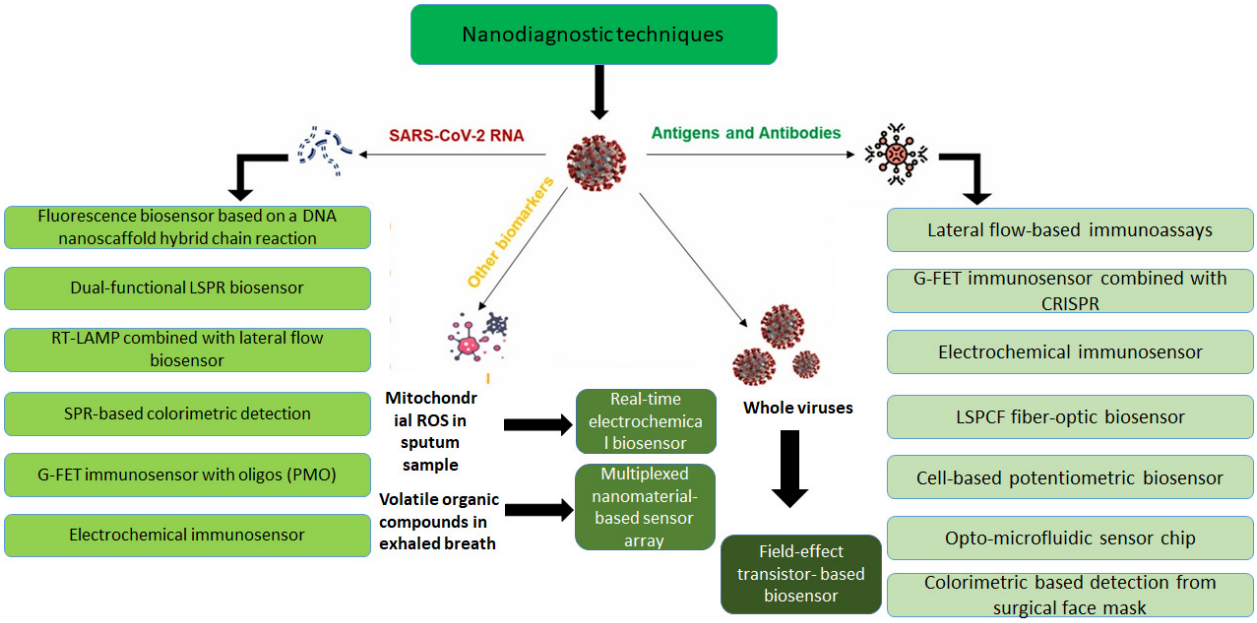


Figure 9.9. Schematic representation of the nanotechnology-based diagnostic devices [2].

Environmental Monitoring: Nanotechnology enables the development of sensors for detecting pollutants and toxins in the environment. These sensors can be deployed in various settings to monitor air and water quality, contributing to environmental sustainability and public health protection.

During the COVID-19 pandemic, nanotechnology-based diagnostic devices have played a crucial role in early detection, continuous monitoring, and surveillance of the virus. These devices offer rapid testing capabilities, allowing for prompt identification of infected individuals and implementation of appropriate containment measures. Additionally, nanodiagnostic tools have facilitated the development of point-of-care devices and lab-on-a-chip technologies, enabling decentralized testing and expanding access to diagnostic services.

Overall, nanotechnology holds great promise for revolutionizing the field of diagnostics, offering innovative solutions for disease detection, treatment, and prevention. Continued research and development in this area are expected to further enhance the capabilities of nanodiagnostic tools and improve healthcare outcomes (Figure 9.9.).

9.2.3.1. Nanosensors

Nanotechnology has enabled the development of advanced biosensing platforms for the detection of COVID-19, leveraging the unique properties of nanomaterials to enhance sensitivity, selectivity, and speed of diagnosis. Nanobiosensors serve as the fundamental component of these diagnostic devices, capable of recognizing analytes and converting them into readable electric signals.

Various nanomaterials are utilized in the fabrication of nanodiagnostic devices to improve their selectivity and performance. These include colloidal gold, gold nanofilms, reduced graphene oxide, activated graphene oxide, cobalt-functionalized TiO2, and poly-aniline, among others. Nanoparticle-based biosensors, such as RT-LAMP-NBS and CovSens, have been developed for the detection of SARS-CoV-2 antigens with high sensitivity and specificity.

Furthermore, dual-functional plasmonic biosensing systems integrating plasmonic photothermal and localized surface plasmon resonance effects have shown increased sensitivity and low limits of detection for viral target sequences. Grating-coupled fluorescent plasmonics and

localized surface plasmon coupled fluorescence biosensors offer multiplexed detection capabilities with high selectivity.

Field-effect transistor (FET)-based biosensors, utilizing graphene sheets functionalized with spike protein-specific antibodies, have demonstrated the ability to detect viral antigens in clinical samples with high sensitivity. Additionally, amplification-free SARS-CoV-2 RNA detection techniques using gold nanoparticle-conjugated graphene field-effect transistors have shown promising results with low limits of detection and differentiation between SARS-CoV-2 and other coronaviruses.

Overall, nanotechnology-based biosensing platforms represent a promising approach for the rapid and accurate diagnosis of COVID-19, offering potential solutions for effective surveillance, containment, and management of the pandemic. Continued research and development in this field are essential for further advancing nanodiagnostic technologies and addressing the ongoing challenges posed by infectious diseases (Figure 9.10.).

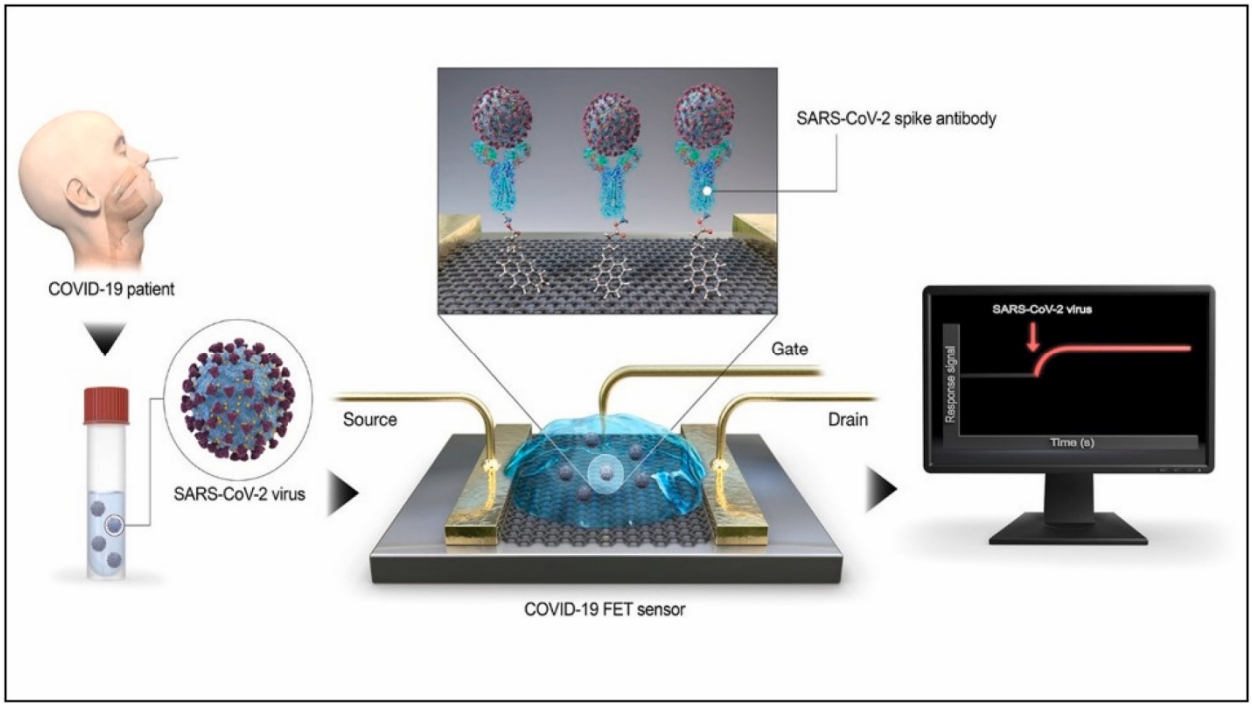


Fig. 9.10. GFET biosensor for detection of SARS-CoV-2 spike protein using spike protein-specific antibodies anchored to the graphene sheet using 1-pyrenebutyric acid N-hydroxysuccinimide ester [2].

The development of various nanotechnology-based biosensors for the detection of coronaviruses, including SARS-CoV-2 and MERS-CoV, has significantly advanced the field of diagnostics, offering rapid, sensitive, and accurate detection methods. These biosensors utilize a diverse range of nanomaterials and sensing principles, demonstrating the versatility and effectiveness of nanotechnology in combating infectious diseases. Here are some key highlights of the biosensors mentioned:

1. **Paper-based Electrochemical Sensor**: Alafeef et al. developed a paper-based electrochemical sensor for SARS-CoV-2 detection using gold nanoparticles conjugated with nucleic acid probes. The sensor achieved high sensitivity and accuracy, with a rapid detection time of 5 minutes.
2. **Electrochemical Immunosensor**: Layqah and Eissa fabricated an electrochemical immunosensor for detecting MERS-CoV spike protein, demonstrating a low limit of detection and quick detection time.
3. **Electrochemiluminescence (ECL) Nanostructured DNA Biosensor**: Gutiérrez-Gálvez et al. constructed an ECL nanostructured DNA biosensor for detecting SARS-CoV-2 DNA sequences. The biosensor exhibited high selectivity, reproducibility, and a low detection limit, enabling the detection of single nucleotide polymorphisms (SNPs).

4. **Fluorescence-based Immunosensor**: Ahmed et al. developed a fluorescence-based immunosensor using zirconium quantum dots for detecting the infectious bronchitis virus (IBV) of coronavirus, showcasing the application of quantum dots in virus detection.
5. **Nanowire Biosensors**: Ishikawa et al. reported the use of indium oxide (In2O3) nanowire biosensors for detecting the nucleocapsid protein of SARS, demonstrating rapid response times even at sub-nanomolar concentrations.
6. **Lanthanide-doped Polystyrene Nanoparticles (LNPs)**: Chen et al. utilized LNPs to develop an immunosensor for detecting SARS-CoV-2 IgG in human serum, addressing the need for accurate anti-SARS-CoV-2 IgG standards in COVID-19 diagnosis.
7. **Microfluidic and Surface-enhanced Raman Spectroscopy (SERS) Techniques**: Jadhav et al. combined microfluidic and SERS techniques for SARS-CoV-2 detection, leveraging the amplification capabilities of silver or gold-fabricated carbon nanotubes in microchannels.
8. **Opto-microfluidic Sensor Chip**: Funari et al. designed an opto-microfluidic sensor chip for detecting antibodies against the spike protein of SARS-CoV-2, based on the localized surface plasmon resonance (LSPR) phenomenon, offering rapid detection from a small volume of plasma.
9. **Cotton Thread-based Microfluidic Immunosensor**: Weng and Neethirajan developed a cotton thread-based microfluidic immunosensor for the rapid detection of IBV and avian coronavirus, demonstrating a portable and cost-effective diagnostic approach.
10. **Exhaled Air Biosensor**: Shan et al. developed a novel biosensor for detecting COVID-19 from exhaled air, utilizing an array of gold nanoparticles to sense volatile organic compounds, offering a non-invasive and multiplexed detection method.
11. **Colorimetric-based Detection Technique**: A non-invasive colorimetric-based detection technique using nanoparticles was developed for detecting SARS-CoV antigens from surgical face masks, providing a simple and rapid diagnostic approach with high sensitivity and specificity.

These diverse biosensing technologies highlight the potential of nanotechnology in addressing the challenges of infectious disease detection and surveillance, offering innovative solutions for global health crises like the COVID-19 pandemic [2].

9.2.3.2. Nanodiagnostic-based LFA devices for COVID-19

Numerous nanodiagnostic devices for detecting COVID-19 are currently in development or have received approval for commercial use. Among these, lateral flow assays (LFAs) are particularly prominent, employing nanobiosensors to detect immune complex reactions in serological tests. LFAs are advantageous for their simplicity and suitability for home use, often requiring minimal expertise to operate. These tests typically employ gold nanoparticles (AuNPs) due to their unique properties, such as high surface-to-volume ratio and biocompatibility.

One example of an LFIA-based device is designed to detect IgG antibodies specific to SARS-CoV-2. In this device, the nucleocapsid protein is immobilized on the strip, while AuNPs are conjugated with anti-human IgG antibodies. This colorimetric assay can achieve sensitivity and specificity rates of 69.1% and 100%, respectively, within 20 minutes (Wen et al., 2020).

Another innovation is the immunochromatographic test (ICT) assay known as Ag Respi-Strip, designed for detecting SARS-CoV-2 in nasopharyngeal samples. Utilizing colloidal gold nanostructures and monoclonal antibodies targeting the nucleoprotein of SARS-CoV-2, this assay demonstrates high specificity (99.5%), albeit with lower sensitivity (57.6%), resulting in an overall accuracy of 82.6% (Mertens et al., 2020).

Furthermore, an ICT-based lateral flow device has been developed to detect SARS-CoV-2 IgM antibodies in serum. This device, incorporating AuNPs, requires a small sample volume and can deliver results within 15 minutes. It boasts impressive sensitivity (100%) and specificity (93.3%) (C Huang et al., 2020).

Despite these advancements, it's important to note that LFIA-based commercial kits for COVID-19 diagnosis are continuously evolving, with several receiving emergency use authorization (EUA) from the United States Food and Drug Administration (FDA).

The remarkable capabilities of nanoparticles in detecting COVID-19-specific markers can be integrated with smartphone-based platforms for convenient monitoring and surveillance. For instance, Abbott's rapid antigen test has been coupled with a built-in mobile application called NAVICA, serving as a digital "boarding pass." This app enables individuals to verify their negative test results effortlessly [2].

9.2.3.3. Advantages and disadvantages of nanodiagnostic devices

The advantages of nanodiagnostic devices stem from the unique properties of the nanomaterials they utilize. Nanobiosensors offer several benefits, including low limits of detection (LOD), ease of use, rapid diagnosis, and potential miniaturization (Borse and Srivastava, 2020; Borse et al., 2020b). These devices enable the development of point-of-care (POC) diagnostic tools, significantly reducing the turnaround time between sample registration and result acquisition compared to traditional molecular diagnostic techniques.

This rapidity facilitates early identification and isolation of infected individuals, crucial for preventing disease spread. Additionally, nanodiagnostic devices alleviate the burden on healthcare workers, particularly during the COVID-19 pandemic, as they are user-friendly, often requiring minimal training. Moreover, these devices are typically simple to operate, often involving just a single-step process, making them suitable for use by volunteers and primary healthcare workers. They are also portable and cost-effective, making them ideal for mass screening in resource-constrained settings. Nanodiagnostic devices extend essential healthcare services to remote populations at an affordable cost, while many offer sensitivity and specificity comparable to conventional methods. Furthermore, integration with smartphones or cloud-based platforms enables efficient surveillance and personalized healthcare.

However, nanodiagnostic devices also have limitations. Most commonly used optical biosensors, such as lateral flow immunoassays (LFIA) based on gold nanoparticles (AuNPs), provide qualitative rather than quantitative results, limiting their utility. Electrochemical biosensors offer quantitative analysis but require specialized equipment for data interpretation, hindering their portability. This limitation also applies to magnetic and plasmonic technologies. Surface plasmon resonance (SPR)-based biosensors may exhibit low specificity and signal-to-noise ratios, while label-based biosensors incur additional costs and may alter binding properties. These challenges can be addressed through techniques such as indirect labeling using the sandwich enzyme-linked immunosorbent assay (ELISA) model, enhancing the sensing of protein analytes while mitigating drawbacks associated with labeling [2].

9.2.4. Future perspectives

The global COVID-19 pandemic has placed immense strain on healthcare systems worldwide, with the relentless surge of variants and fatalities. In response, researchers worldwide have been diligently striving to develop diagnostic devices, therapeutic drugs, and vaccines to combat the crisis.

While numerous devices have been developed, many have not met clinical trial requirements and require further refinement for commercialization. Despite the approval of several vaccine candidates, the emergence of new COVID variants remains a significant concern. With infections continuing to rise, there is an urgent need for simpler and faster diagnostic methods.

Although conventional RT-PCR remains the gold standard for accuracy, point-of-care (POC) techniques such as Loop-mediated Isothermal Amplification (LAMP), CRISPR, and nanodiagnostics offer rapid and more convenient COVID-19 detection. Nanodiagnostic devices, in particular, have garnered attention for their heightened sensitivity, ease of development, and potential for miniaturization.

The advent of lateral flow assays (LFAs) represents a significant advancement in molecular diagnosis facilitated by nanotechnology. Many serological tests authorized for emergency use by regulatory agencies rely on LFA technology, enabling serosurveys to track the spread of the disease.

Additionally, rapid antigen tests like BinaxNOW, when coupled with smartphone apps, offer swift and portable detection at the point of care. These advancements underscore the critical role of nanotechnology in enhancing diagnostic capabilities and combating the COVID-19 pandemic.

Continued research and innovation efforts have led to the development of promising biosensing techniques for diagnosing COVID-19. However, there is an urgent need to scale up automation, enhance sensitivity and specificity, and miniaturize biosensing platforms to enable their deployment in point-of-care (POC) settings. Multiplex assays, lab-on-a-chip (LOC) devices, and smartphone-based technology are emerging as key areas for expansion in nanodiagnostics.

Despite significant progress, detecting and confirming the COVID-19 virus in asymptomatic cases remains a challenge for POC diagnostic techniques.

Improving the sensitivity of current diagnostic devices is crucial in addressing this challenge. Repurposing previously developed biosensors, such as graphene-based field-effect transistor (FET) biosensors, quartz microbalance biosensors, quantum dot (QD)-embedded hydrogel aptasensors, and enzymatic biosensors, holds promise for developing sensitive COVID-19 diagnostic devices.

Moreover, integrating artificial intelligence (AI) and the Internet of Things (IoT) into biosensing devices for intelligent healthcare is gaining traction.

Interdigitated microelectrodes (IDμE) and bio-microelectromechanical systems (BioMEMS)-based biosensing devices are also being explored for their potential in advancing COVID-19 diagnostics.

Figure 9 provides an overview of the proposed areas for future innovation and development in nanodiagnostic techniques for COVID-19 diagnosis.

These advancements aim to address current challenges and enhance the effectiveness of diagnostic tools in combatting the pandemic [2].

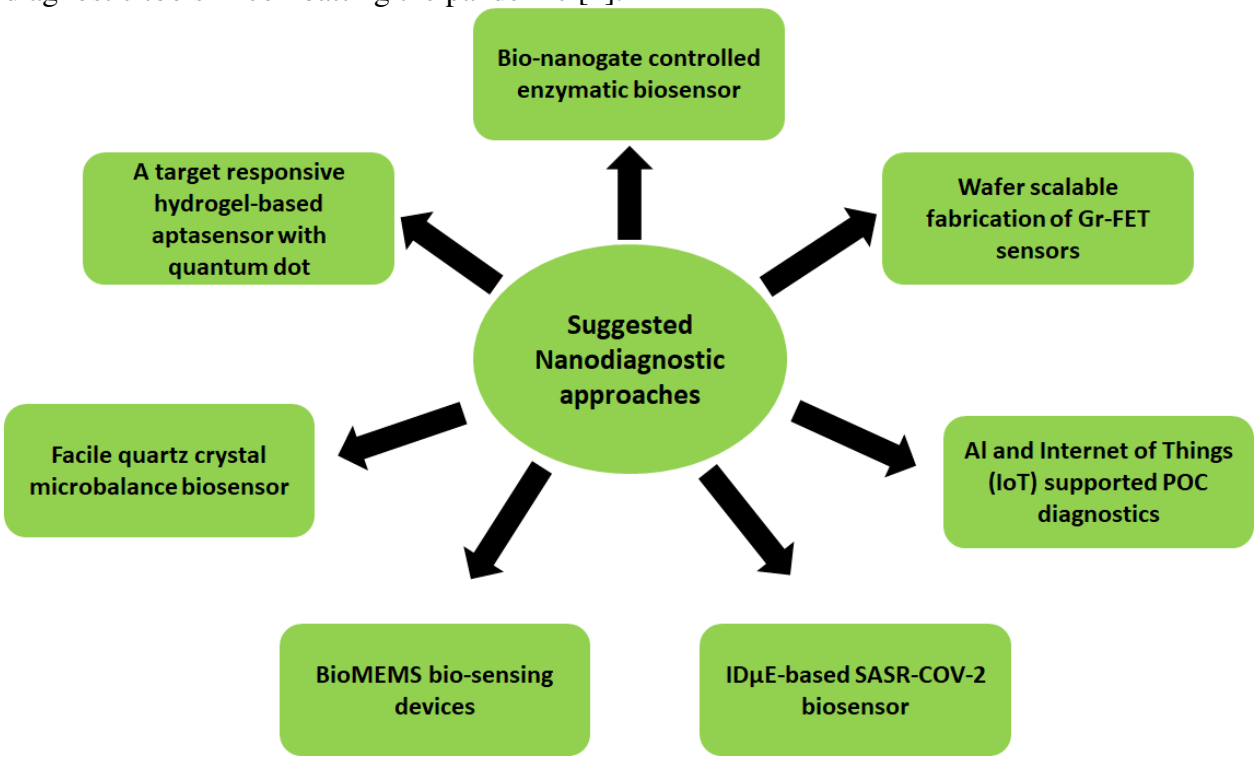


Figure 9.11. Suggested nanodiagnostic approaches for the management of the COVID-19 pandemic [2].

Given the critical nature of disease outbreaks such as COVID-19, technological advancements play a pivotal role in enabling rapid and accurate diagnosis of infectious diseases. The dynamic field of nanotechnology holds significant promise in the creation of cost-effective and user-friendly biomedical devices. These innovations have the potential to revolutionize disease prevention and management, leading to substantial enhancements in healthcare systems worldwide [2].

9.3. Quiz 9.

1. Which of the following statements about nanodiagnostics are correct?
A) Nanoparticles enable targeted drug delivery.
B) Biomolecule-coated particles aid in cancer cell detection.
C) DNA-based nanoparticles offer platforms for disease diagnosis.
D) Optical tweezers diagnose tissue abnormalities.
E) Microfluidic systems analyze DNA samples

2. Which features characterize DNA-based electrochemical sensors for detecting mutated genes associated with human disease?
A) Nanoscale interactions
B) Utilization of Clear Read nanoparticle technology
C) Enhanced sensitivity and robustness with nanoparticle amplification
D) Costliness and time-consuming nature
E) Incompatibility with genetic marker identification

3. Which of the following diagnostic techniques for detecting COVID-19 are known for their high sensitivity and specificity?
A) Nucleic Acid Amplification Tests (NAATs)
B) Antigen Tests
C) Serological Tests
D) Protein Microarrays
E) Detection of Immunological Biomarkers

4. Which of the following statements about CT scans for diagnosing COVID-19 are correct?
A) CT scans are more sensitive than RT-PCR tests.
B) CT scans can reliably differentiate between various respiratory viruses.
C) Ground-glass opacity on CT scans is unique to COVID-19.
D) CT scans are rarely utilized due to their high cost.
E) CT scans are primarily used as the sole diagnostic tool for COVID-19.

5. What is the main limitation of MRI for assessing lung pathology in COVID-19 pneumonia
A) Low signal-to-noise ratio
B) High sensitivity
C) Short imaging times
D) Enhanced anatomical resolution
E) High specificity

6*. Which method is commonly used in metagenomic studies of viruses like SARS-CoV and other infections related to COVID-19 severity?
A) Polymerase chain reaction (PCR)
B) Amplicon-based sequencing
C) Immunohistochemistry (IHC)
D) ELISA (Enzyme-linked immunosorbent assay)
E) Western blotting

7*. Which techniques are commonly used in microarray technology for the detection of genetic elements, including SARS-CoV?
A) Western blotting and ELISA
B) Aptamer-based microarrays and proteome-based microarrays
C) PCR and gel electrophoresis

D) Mass spectrometry and chromatography
E) Immunohistochemistry and flow cytometry

8. Which techniques are commonly used in lateral flow immunoassays (LFIA) for the detection of SARS-CoV?
A) Multiplex LFIA
B) RT-RPA-LFA
C) HC-FIA
D) Dual optical/chemiluminescent LFIA
E) DNA scaffold hybrid chain reaction (DNHCR)

9. Which statements accurately describe rolling circle amplification (RCA) and its applications for SARS-CoV detection?
A) RCA involves the hybridization of circularizable oligonucleotides or padlock probes with target DNA or RNA sequences.
B) RCA requires reverse transcriptase for RNA amplification, similar to traditional PCR. C) RCA can be performed only in liquid phase and not in solid phase.
D) The PLAN-LFA platform utilizes RCA to detect SARS-CoV-2 in saliva.
E) RCA with a nylon mesh medium has a detection limit of 1.1 pM target DNA.

10. Which statements accurately describe the use of deep learning (DL) and machine learning (ML) techniques for COVID-19 detection?
A) DL algorithms such as CNNs are used for image analysis tasks.
B) Performance metrics for evaluating DL models include accuracy, precision, recall, and F1-score.
C) Models like ZFNet and DenseNet121 have been utilized for COVID-19 detection.
D) DL techniques analyze ECG images for detecting abnormalities in COVID-19 patients. E) Deep CNNs have shown high accuracy in distinguishing COVID-19 cases from control subjects based on ECG data.

References

[1]. Khalid Khalaf Alharbi, Yazeed A. Al-sheikh, Role and implications of nanodiagnostics in the changing trends of clinical diagnosis, Saudi Journal of Biological Sciences, Volume 21, Issue 2, 2014, Pages 109-117, ISSN 1319-562X, https://doi.org/10.1016/j.sjbs.2013.11.001.

[2]. Mosam Preethi, Lavanika Roy, Sukanya Lahkar, Vivek Borse, Outlook of various diagnostics and nanodiagnostic techniques for COVID-19, Biosensors and Bioelectronics: X, Volume 12, 2022, 100276, ISSN 2590-1370, https://doi.org/10.1016/j.biosx.2022.100276.

10. Nanoapplications in endodontics

The understanding of endodontic disease highlights the role of biofilm-mediated infection, making the elimination of biofilm bacteria from the root canal system a primary focus in its management. However, the endodontic environment poses challenges for effectively removing surface-adherent biofilm bacteria. Advanced antimicrobial strategies are thus necessary to achieve optimal disinfection of previously infected root canal systems. This step is critical not only for performing conventional root canal treatments reliably but also for developing tissue engineering-based approaches that can facilitate organized repair or regeneration in previously infected teeth.

Nanotechnology represents a rapidly advancing interdisciplinary field, and the utilization of nanomaterials is increasingly common across various healthcare applications. Nanomaterial-based approaches offer distinct advantages over conventional methods. At the nanoscale, materials exhibit markedly different characteristics compared to their macro-scale counterparts. In endodontics, the incorporation of nanotechnology and nanoparticles can provide numerous benefits, including efficient miniaturization techniques and the ability to control molecular assembly. These advancements create promising opportunities for enhancing the prevention, diagnosis, and treatment of endodontic disease [1].

10.1. Nanoparticles for Endodontic Disinfection

The recognition of microbial biofilm as a significant factor in human infection, coupled with the increasing antimicrobial resistance, underscores the need for reliable and effective antimicrobial strategies to combat infectious diseases. Addressing the challenge of bacterial persistence in infected root canals after treatment is crucial. Utilizing various antibacterial nanoparticles holds promise as a potential strategy to enhance the elimination of biofilm bacteria from the root canal system. Nanoparticles have been developed not only to improve root canal disinfection but also to seal the canal space during treatment.

To ensure the therapeutic effectiveness of nanoparticles, it is essential to understand factors such as the efficacy of treatment, the location of infection, and the delivery efficiency of nanoparticles. This chapter aims to address the current limitations in achieving effective root canal disinfection and explores examples of different nanoparticles under development and testing for this purpose.

10.1.1. Introduction

Antimicrobial resistance is an escalating problem, posing a significant challenge in the treatment of numerous infectious diseases. Traditional approaches involving the use of topical or systemic antibiotics have proven ineffective due to various factors. Bacterial biofilms, accounting for approximately 60% of current human infections, contribute significantly to this ineffectiveness, encompassing both implant-related and non-implant-related infections. Moreover, the widespread systemic use of antibiotics has led to multidrug resistance and superinfection by disrupting the balance of commensal microbial flora.

The dwindling search for novel antibiotics has exacerbated the problem, coinciding with the rise in antibiotic-resistant pathogens. This critical situation underscores the urgent need to identify reliable and effective antimicrobial strategies to combat infectious diseases that were once easily treatable. Recognition of microbial biofilm as a key factor in human infection further emphasizes the importance of addressing this challenge and finding alternative solutions [1].

10.1.2. Antibacterial Nanoparticles

Nanoparticles (NPs) are tiny particles with dimensions ranging from 1 to 100 nanometers. Nanotechnology, a field derived from "nano" and "technology," deals with materials at the nanoscale, precisely one billionth of a unit (10^-9). NPs possess unique properties distinct from their bulk

counterparts and find applications in various fields such as drug/gene delivery, imaging, pathogen detection, DNA analysis, tissue engineering, and cancer therapy.

Among the applications of nanoparticles (NPs), those possessing antibacterial properties stand out for their significance. These antibacterial NPs showcase broad-spectrum antimicrobial efficacy and demonstrate reduced tendencies to provoke microbial resistance compared to conventional antibiotics. Metallic nanoparticles such as copper, gold, titanium, and zinc have attracted attention for their antimicrobial attributes, each offering unique physical traits and ranges of activity.

Metallic oxide nanoparticles like magnesium oxide (MgO), calcium oxide (CaO), and zinc oxide (ZnO) have exhibited bactericidal or bacteriostatic effects against both gram-positive and gram-negative bacteria. These NPs produce active oxygen species accountable for their antibacterial prowess, owing to their large surface area and charge density, facilitating robust interactions with bacterial cells.

Heavy metal ions such as copper, zinc, and silver ions impose cytotoxic effects on bacterial cells by inducing oxidative stress, disrupting redox cycling, and impeding bacterial enzymes and DNA replication. Nanoparticles derived from silver (Ag), copper oxide (CuO), and zinc oxide (ZnO) powders are commonly employed for their antimicrobial capabilities. The electrostatic interplay between positively charged NPs and negatively charged bacterial cells, coupled with the accumulation of NPs on the bacterial cell membrane, results in compromised membrane permeability and eventual cell demise.

10.1.3. Bacterial Biofilms as the Therapeutic Target for Antimicrobials

Bacteria play a significant role in approximately 80% of human infectious diseases. In conditions such as dental caries, periodontal disease, and endodontic disease, bacterial growth predominantly occurs in the form of biofilms. Biofilms, structured communities of bacterial cells enclosed in a self-produced polymeric matrix adherent to a surface, pose challenges in clinical management due to their resilience (Figure 10.1.).

Biofilms typically consist of bacterial cells occupying 10–20% of the total volume, with the remainder being the extracellular matrix composed of polysaccharides, proteins, nucleic acids, and salts. This matrix serves to protect bacteria from threats and concentrate nutrients for growth. Water channels within the hydrated matrix facilitate nutrient exchange and communication among bacterial microcolonies within the biofilm.

Microcolonies within biofilms are densely packed aggregates of bacteria adherent to a solid surface. These microcolonies adapt based on environmental conditions and fluid shear forces, with mature biofilms occasionally detaching microcolonies through seeding dispersal, leading to distant infections.

Antimicrobial resistance in biofilms results from various mechanisms, including protection by the EPS matrix, the presence of persister cells with low metabolic activity, and altered microenvironments favoring bacterial survival and growth (Figure 10.2.).

The EPS matrix acts as a physical and chemical barrier, limiting the diffusion of antimicrobials and neutralizing their effects.

Persister cells within biofilms exhibit minimal metabolic activity, allowing them to survive antibiotic treatment.

Altered microenvironments within mature biofilms create gradients of nutrients and redox potential, promoting bacterial growth and reducing susceptibility to antimicrobials.

Additionally, exposure to stress or low antimicrobial levels induces the expression of stress genes, shock proteins, and multidrug efflux pumps in biofilm bacteria, further contributing to antimicrobial resistance [1].

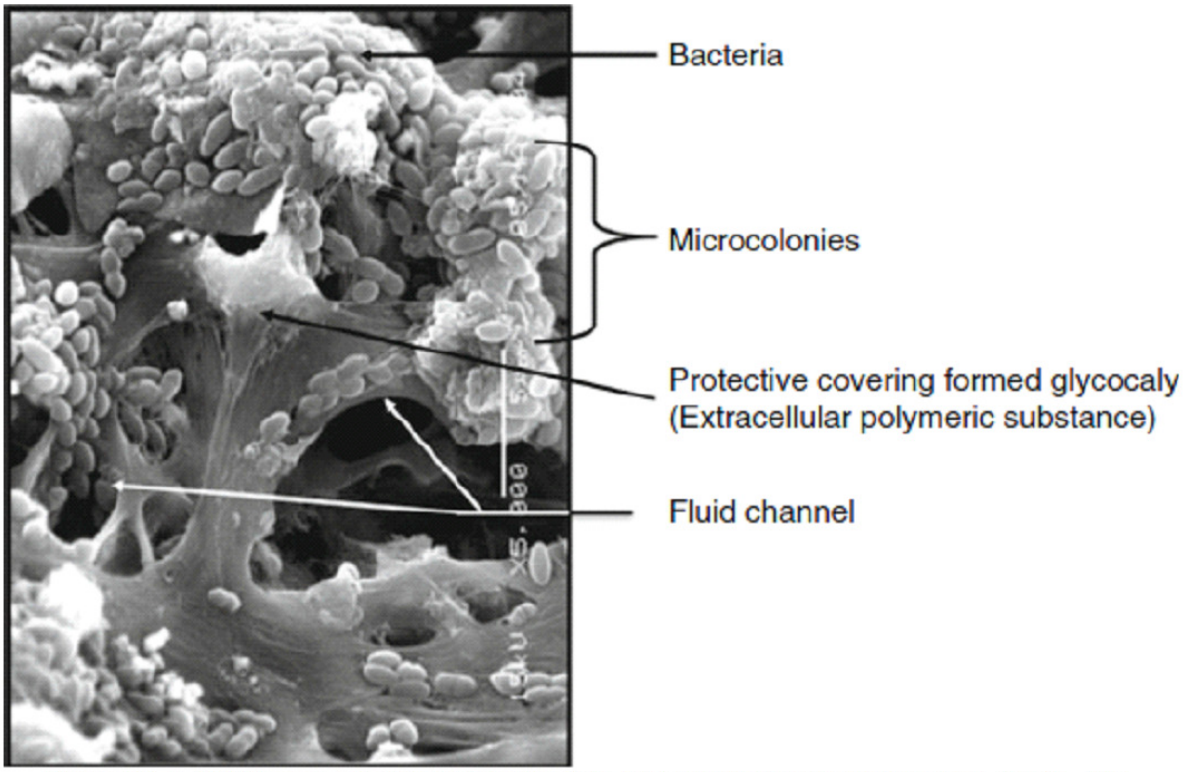


Figure 10.1. ***SEM image showing ultrastructure of bacterial biofilm formed on dentin. The major components of biofilm structures are indicated [1].***

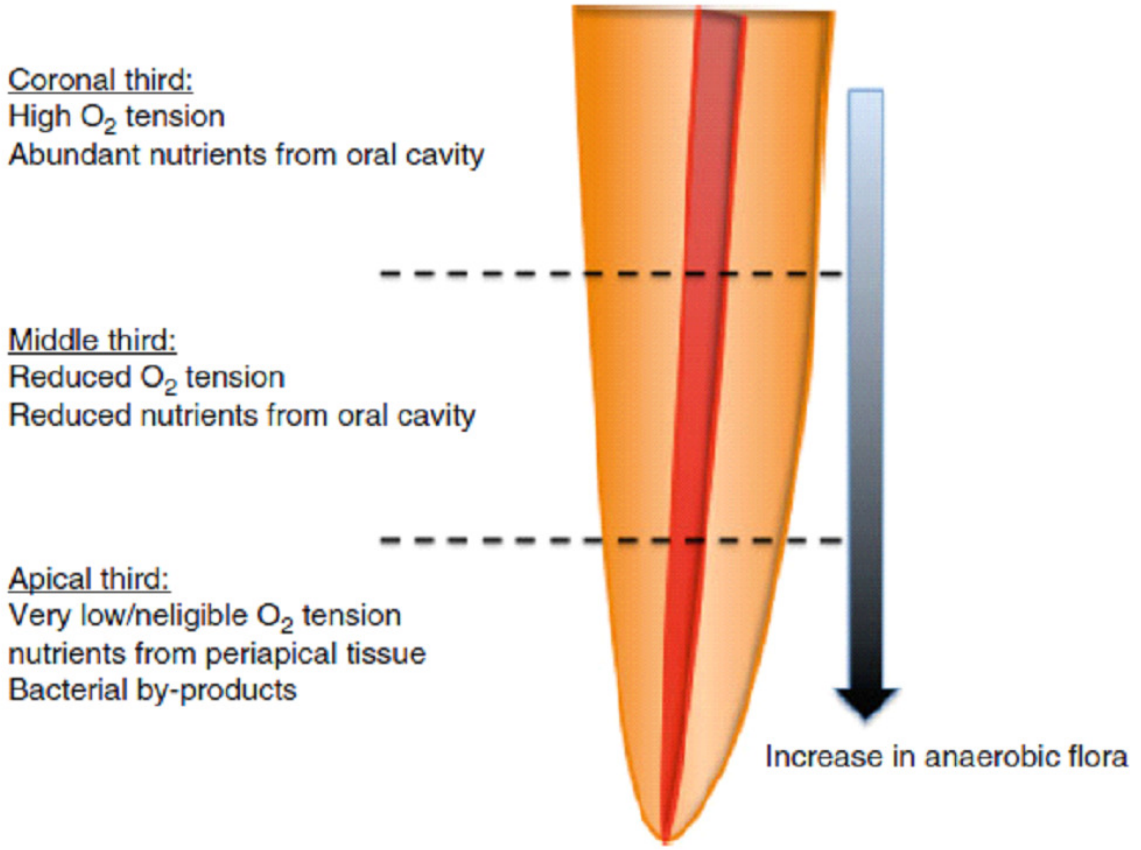


Figure 10.2. The root canal space presents with selective pressures allowing specific bacteria to survive depending on their nutritional and environmental requirements [1].

10.1.3.1. Endodontic Biofilms

Apical periodontitis, also known as endodontic disease, is characterized as a bacterial biofilm-mediated infection. Within the apical region of the root canals, causative bacteria release toxins and irritants that trigger periapical inflammation and the host immune response. Although no specific correlation has been established between bacterial species in the root canal and the clinical presentation of apical periodontitis, studies have shown that bacteria in infected root canals exist as clusters of bacterial aggregates resembling biofilm bacteria.

The root canal environment presents challenging conditions with limited availability of nutrients and oxygen. Consequently, infected root canals harbor a restricted assortment of bacterial species, typically around 5–10, compared to the diverse bacterial species found in the oral cavity. The selection of specific bacterial combinations is influenced by the endodontic milieu, which provides a selective habitat supporting the development of specific proportions of strict and facultative anaerobic flora.

The main treatment goal for endodontic disease is the elimination of microbial biofilms from infected root canals. However, complete eradication of bacterial biofilms from the complex anatomy of root canals remains challenging for clinicians. Previous studies have demonstrated that the presence of viable microbes at the time of filling significantly impacts the success of endodontic treatment, with a higher prevalence of periapical lesions observed in teeth with persistent bacterial presence.

Studies have also reported the prevalence of intraradicular biofilms in treated root canals with apical periodontitis, highlighting the importance of addressing bacterial persistence within treated root canals to prevent treatment failure. Research efforts have therefore focused on understanding the limitations of current root canal irrigation methods and developing newer antibiofilm strategies for endodontic applications [1].

10.1.4. Antimicrobials in Root Canal Therapy

Topical antimicrobials, both as irrigants and medications, are recommended for effectively eliminating bacteria within root canals. However, despite advancements in treatment strategies, the success rates of root canal treatment have not significantly increased over the past few decades. This may be attributed to the limitations of current technologies in addressing the challenges posed by the disease process. The prognosis of endodontic treatment depends on various factors, including the stage of the disease process and whether the treatment is primary or retreatment. Studies have shown that the presence of periapical infection at the time of treatment significantly reduces the healing rate.

Endodontic therapy targets a complex tissue system consisting of the tooth-pulp-periradicular complex. Conventionally, chemical antimicrobials are used within the root canals in combination with mechanical instrumentation to achieve "microbe-free" root canals before filling with an inert filling material. Commonly used irrigants include ethylenediaminetetraacetic acid (EDTA) and sodium hypochlorite (NaOCl), which are used for root canal debridement. However, these irrigants alone or in combination are often inadequate in achieving the desired treatment goals, highlighting the need for newer antimicrobials for root canal disinfection.

Therapeutic strategies for biofilms typically focus on destroying or inactivating resident bacteria within the biofilm structure or disrupting the biofilm structure while killing resident microbes. An ideal root canal irrigant should possess broad antimicrobial activity, dissolve necrotic pulp tissue, inactivate endotoxins, remove the smear layer, and be biocompatible with vital periapical tissues. However, to date, no single antimicrobial irrigant fulfills all these functions, necessitating the use of combinations of irrigants.

Current limitations in endodontic disinfection strategies stem from both the biofilm mode of growth within root canals and the anatomical complexities of root canal systems, dentin structure/composition, and factors associated with chemical disinfectants. Studies have shown that a significant portion of root canal surfaces remains untouched by instrumentation, and bacterial presence, mainly as biofilms, persists in complex anatomical sites even after instrumentation and irrigation procedures (Figure 10.3.).

Due to these limitations, advanced disinfection strategies are being developed and tested to achieve complete elimination of bacteria from the root canal system, including uninstrumented portions and anatomical complexities, without inducing adverse effects on dentin substrate and periradicular tissue. In the following sections, newer nanoparticles with significant potential for eliminating endodontic biofilms will be reviewed [1].

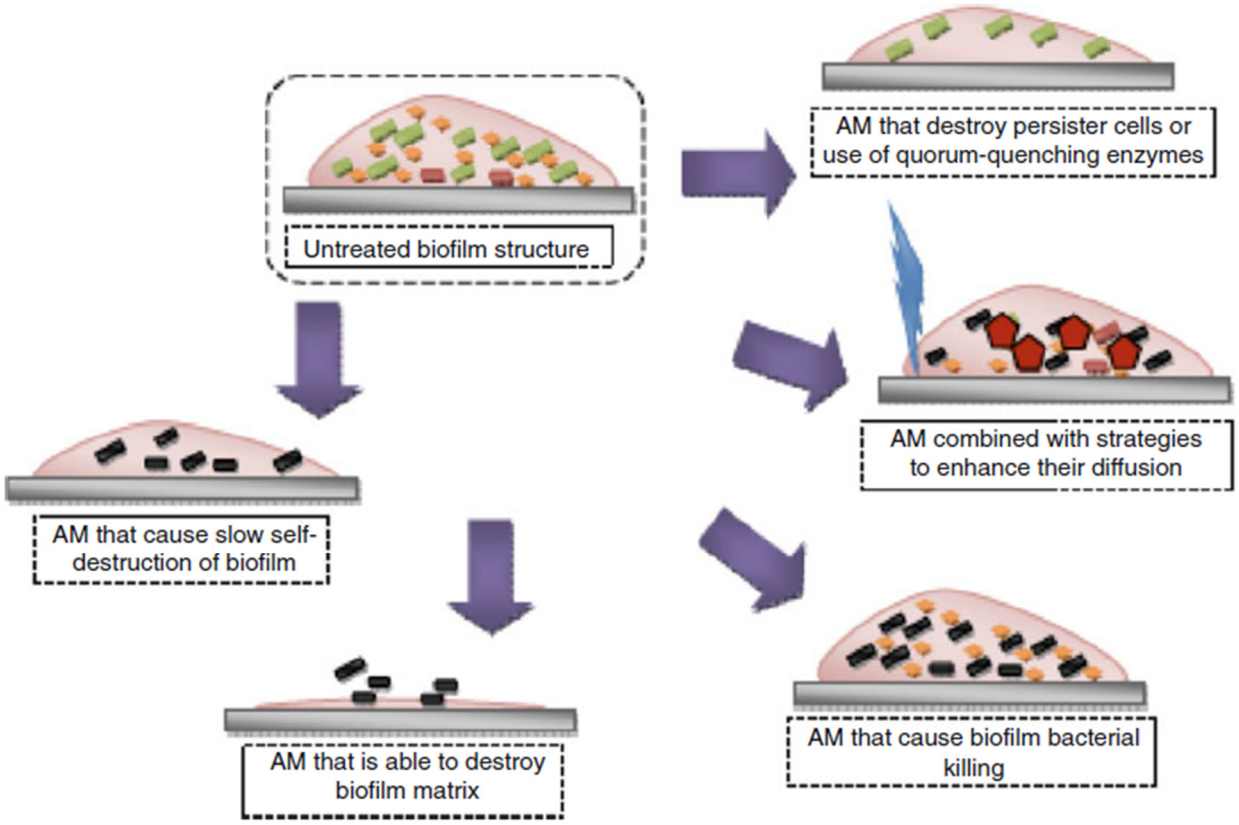


Figure 10.3. Schematic diagram showing different antibiofilm strategies. AM antimicrobial

10.1.5. Classification and Types of Antibacterial Nanoparticles

Nanomaterials can be classified based on their composition and various morphologies, including spheres, rods, tubes, and prisms. Nanoparticles designed for antibacterial purposes are currently under development, and Figure 10.4. presents a list of nanoparticles based on different compositions.

Many of these nanoparticles are still in the early stages of laboratory testing, aiming to enhance their effectiveness in combating bacterial infections. Figure 10.5. provides a compilation of literature relevant to the utilization of various nanoparticles for improving root canal disinfection.

Nanoparticles based on composition

Inorganic	**Metallic**	**Polymeric**	**Quantum dots**	**Functionalized With:**
Zinc oxide	Gold	Alginate	Cadmium sulfide	Drugs
Iron oxide	Silver	Chitosan	Cadmium selenide	Photosensitizers
Titanium dioxide	Iron			Antibodies
Cerium oxide	Copper			Proteins
Aluminum oxide	Magnesium			

Figure 10.4. Nanoparticles available based on the composition [1].

Author	Nanoparticles used	Bacteria tested	Observations
Waltimo et al. (2007)	Bioactive glass 4555	E. faecalis in planktonic	Micron to nano size increased the killing
Kishen et al. (2008)	ZnO Chitosan	E. faecalis in planktonic	CS-highest antibacterial Combination-highest leaching property
Waltimo et al. (2009)	Bioactive glass-Nano/Micron combination	3 weeks old E. faecalis biofilm in root canals	Nano BAG did not show any antibacterial efficacy
Mortazavi et al. (2010)	BAG of different sizes	Planktonic E. coli, P. aeruginosa, S. typhi, and S. aureus	Antibacterial activity decreased with decrease in size
Pagonis et al. (2010)	MB loaded PLGA	3 days old E. faecalis biofilm in root canals	Significant reduction of biofilm
Chogle et al. (2011)	C18 organoclay	E. faecalis in planktonic	Reduced apical microleakage when mixed with polymer
Shrestha et al. (2010)	ZnO Chitosan	E. faecalis in planktonic and biofilms	Total elimination of planktonic Significant reduction of biofilms Retained antibacterial property after aging
Shrestha and Kishen (2012)	Chitosan in the presence of tissue inhibitors	E. faecalis in planktonic	Pulp and BSA significantly inhibited the antibacterial effect
DaSilva et al. (2013)	Sealer incorporated with chitosan nanoparticles with/without canal surface treatment with different formulations of CS	E. faecalis 7 days in a chemostat-based biofilm fermentor	Inhibition of biofilm formation within the sealer-dentin interface Surface treatment with chitosan showed higher inhibition of biofilm formation
Abramovitz et al. (2013)	**Quaternary ammonium polyethyleneimine nanoparticles (QPEI NP) incorporated into standard TRMS**	**S. mutans and E. faecalis in planktonic form**	**Incorporation of 2% wt/wt QPEI NP significantly increased the sealing ability of TRMS**
Shrestha et al. (2013)	Rose bengal functionalized chitosan nanoparticles (CSRBnp)	E. faecalis in planktonic and biofilms	Photoactivation of CSRBnp resulted in reduced viability of biofilms and disruption of biofilm structure.
Shrestha (Kishen) et al. (2013)	Rose bengal functionalized chitosan nanoparticles (CSRBnp) in the presence of tissue inhibitors	E. faecalis in planktonic form	Pulp and BSA significantly inhibited the antibacterial effect

Shrestha (Kishen) et al. (2014	Photoactivated rose bengal functionalized chitosan nanoparticles (CSRBnp)	E. faecalis in planktonic and 21 days biofilms	CSRBnp displayed properties of both CS and RB in a photoactivable nano-structure that performed the dual function of targeted elimination of bacterial-biofilms
Shrestha and Kishen (2014)	Rose bengal functionalized chitosan nanoparticles (CSRBnp)	Multispecies biofilms (Streptococcus oralis. Prevotella intermedia, and Actinomyces naeslundii) grown on dentin sections for 21 days	CSRBnp showed complete disruption of multispecies biofilm with a reduction in viable bacteria and biofilm thickness.

Figure 10.5. List of literature available on the use of nanoparticles for antibacterial purpose to achieve root canal disinfection [1].

This includes studies investigating the efficacy of nanoparticles in eliminating biofilms and bacteria from the complex anatomy of root canals, contributing to the advancement of endodontic treatment strategies [1].

10.1.5.1. Chitosan Nanoparticles

Chitosan, derived from chitin, the second most abundant natural biopolymer found in crustaceans, has garnered significant interest in biomedicine due to its versatile properties. Structurally resembling cellulose, chitosan possesses reactive hydroxyl and amino groups, allowing for various chemical modifications. It can be synthesized into various forms such as powders, capsules, films, scaffolds, hydrogels, beads, and bandages. Particularly, chitosan nanoparticles (CS NPs) have been developed for applications in drug/gene delivery due to their favorable characteristics (Figure 10.6.).

The antibacterial properties of chitosan and its derivatives have been extensively studied, showcasing a broad range of antimicrobial activity, biocompatibility, and biodegradability. The exact mechanisms underlying its antibacterial action are still under investigation, with the most commonly proposed mechanism being contact-mediated killing. This involves electrostatic attraction between positively charged chitosan and negatively charged bacterial cell membranes, leading to altered cell wall permeability, cell rupture, and leakage of intracellular components.

Chitosan's antibacterial efficacy is influenced by factors such as degree of deacetylation (DD), molecular weight, chemical modifications, and environmental conditions. Higher DD results in increased amine groups per glucosamine unit, enhancing antibacterial activity. Gram-positive bacteria are generally more susceptible to chitosan compared to gram-negative ones. Chitosan nanoparticles have demonstrated efficacy in disinfecting and disrupting biofilm bacteria, with long-term retention of antibacterial properties even after aging (Figure 10.7.).

Overall, chitosan and its nanoparticles hold promise for enhancing root canal disinfection in endodontic treatment. Their biocompatibility, antibacterial activity, and ability to penetrate anatomical complexities make them potential candidates for improving the success rates of endodontic therapies [1].

10.1.5.2. Bioactive Glass Nanoparticles

Bioactive glass (BAG) has garnered interest in root canal disinfection due to its antibacterial properties. It typically consists of silicon dioxide (SiO_2), sodium oxide (Na_2O), calcium oxide (CaO), and phosphorus pentoxide (P_2O_5) at varying concentrations. Nanometric bioactive glass used in studies was found to be amorphous and ranged from 20 to 60 nm in size. The antimicrobial activity of BAG is primarily attributed to the increase in pH upon ion release in an aqueous environment,

along with osmotic effects and induced mineralization on the bacterial surface due to calcium/phosphorus precipitation. Several studies have investigated the antibacterial efficacy of BAG in root canal disinfection. However, comparisons with other disinfectants like calcium hydroxide have shown varying results.

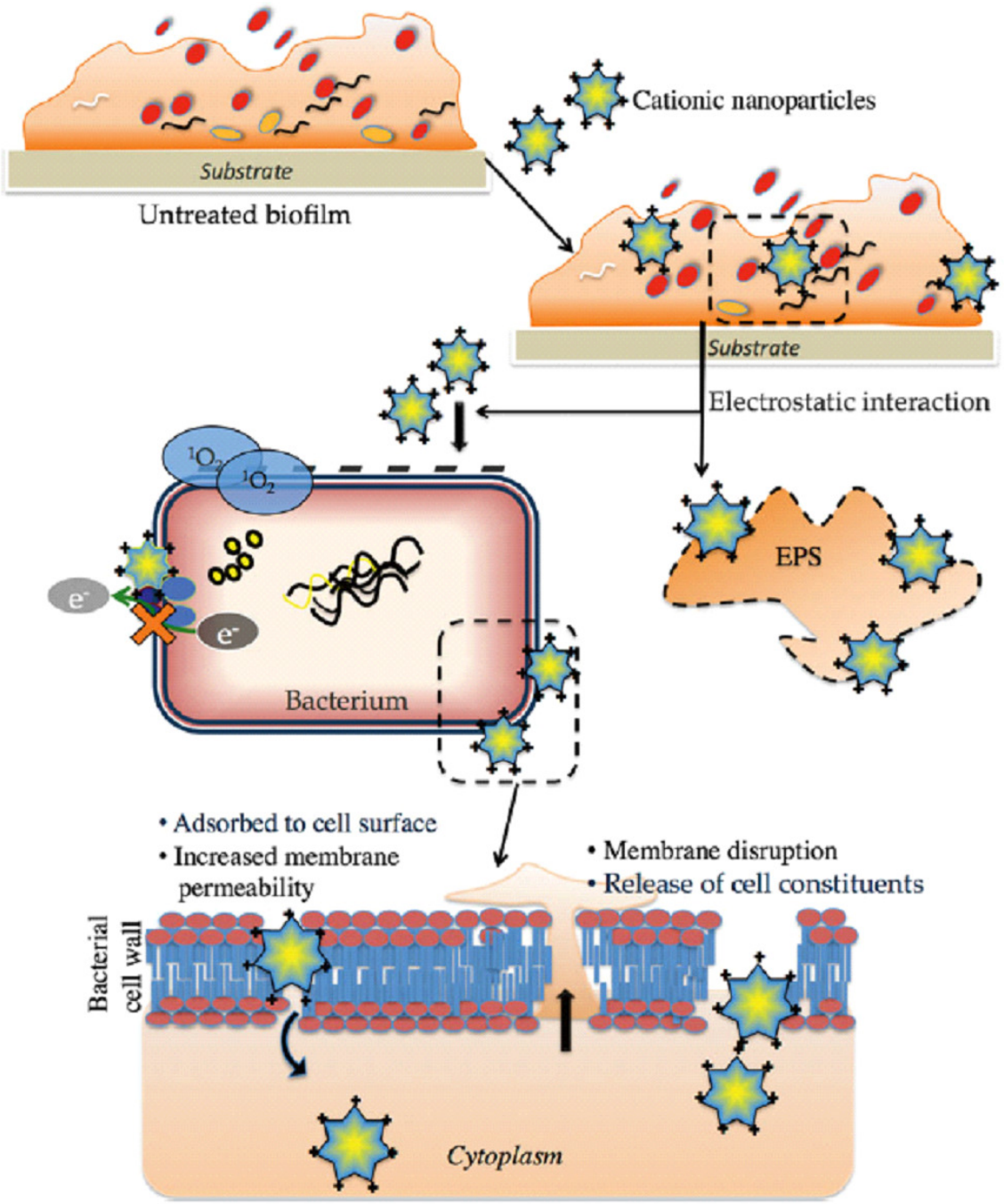


Figure 10.6. A schematic diagram illustrating the antibacterial mechanism of nanoparticles with positive charge (e.g. Chitosan). Mature bacterial biofilm consisting of abundant EPS and bacteria enclosed. When cationic nanoparticles are introduced for treatment of biofilms, it can interact with both EPS and bacterial cells. The initial electrostatic interaction between positively charged nanoparticles and negatively charged bacterial surface. Bacterial killing occurs upon contact mediated lipid peroxidation via production of reactive oxygen species (ROS). The membrane damage and increased permeability of unstable membrane eventually leads to ingress of nanoparticles into the cytoplasm and release of cytoplasmic constituents. EPS secreted by bacteria in biofilm may interact with the nanoparticles and prevent from interacting with bacteria and thus, reducing the antibacterial efficacy [1].

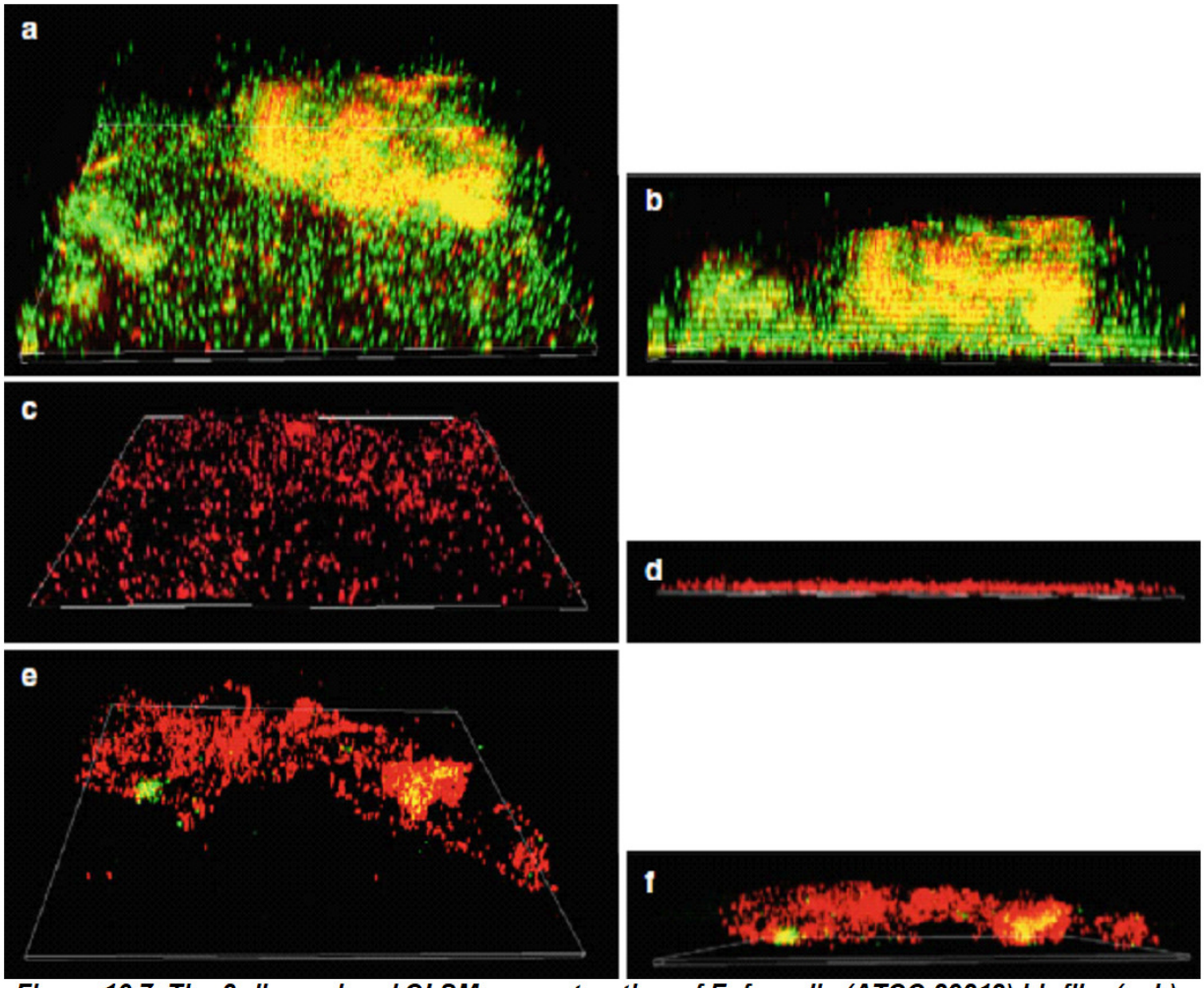


Figure 10.7. The 3-dimensional CLSM reconstruction of E. faecalis (ATCC 29212) biofilm (a, b) and after treatment with antibacterial ZnO-np (c, d) and CS-np (e, f). The number of live bacterial cells was reduced significantly, and the 3-dimensional structure was also disrupted. (b, d, and f show the sagittal sections of the biofilm structure) (original magnification)

While some studies found calcium hydroxide to be more effective in preventing residual bacterial growth, others suggested that the ideal preparation of BAG for root canal disinfection should combine high pH induction with continuous release of alkaline species. It was observed that nanometric BAG had a higher specific surface area but was less effective in eliminating biofilms compared to its micrometric counterpart.

This difference in efficacy with the transition from micron- to nano-sized BAG particles has been attributed to the significant increase in silica release and pH elevation observed with the nanometric version.

Overall, while bioactive glass holds promise as an antimicrobial agent for root canal disinfection, further research is needed to optimize its formulation and understand its interaction with bacterial biofilms in the complex environment of the root canal system.

10.1.5.3. Silver Nanoparticles

The use of silver compounds and nanoparticles is widespread, primarily due to their strong antibacterial properties. Historical records show that silver has been utilized for preventing infection in burn cases since the 1800s. Even before the advent of antibiotics, colloidal dispersions of silver were orally administered to prevent infections. In dentistry, silver and its nanoparticles have been investigated for various applications, including dental restorative materials, endodontic retrofill materials, dental implants, and caries inhibitory solutions.

The antibacterial activity of silver is attributed to its interaction with the sulfhydryl groups of proteins and DNA, leading to alterations in cellular processes such as hydrogen bonding, unwinding of DNA, and interference with cell wall synthesis and division. Silver nanoparticles destabilize bacterial membranes, increase permeability, and cause leakage of cell constituents. However, the cytotoxicity of silver ions has limited their widespread use, prompting research into developing silver nanoparticles with specific antibacterial activity and lower cytotoxicity.

Silver ions, when ionized in the presence of moisture, bind to tissue proteins and induce tissue changes. They bring about structural changes in bacterial cell walls and nuclear membranes, disrupting membrane barriers and resulting in cell death. Studies have evaluated the potential of silver nanoparticles for root canal disinfection, with promising results. For example, silver diamine fluoride has shown efficacy against E. faecalis biofilms and can penetrate dentinal tubules. However, concerns about toxicity remain a challenge.

The mode of application of silver nanoparticles affects their antibiofilm efficacy, with gels being more effective than solutions. Prolonged interaction between positively charged silver nanoparticles and negatively charged resident biofilm bacteria can lead to significant destruction of biofilm structure and bacterial killing. However, further experiments in well-characterized in vitro models or in vivo situations are needed to confirm the advantages of using silver nanoparticles for root canal disinfection.

Two main issues associated with the use of silver nanoparticles are the potential browning or blackening of dentin and toxicity toward mammalian cells. Studies have shown varying tissue responses to silver nanoparticles, with mild to moderate inflammatory responses observed. The toxicity concentrations of silver ions and nanoparticles differ, and their interaction with cells is influenced by factors such as size, structure, and the presence of proteins in biological media. Further research is necessary to understand and mitigate these concerns for the safe and effective use of silver nanoparticles in dentistry [1].

10.1.5.4. Nanoparticle-Incorporated Root Canal Sealers

Root canal filling plays a crucial role in preventing bacterial recontamination by sealing the prepared canal space. One of the desired properties of root canal sealers is their antibacterial activity, which can help eliminate remaining bacteria and prevent bacterial recolonization in case of leakage. However, common sealers typically possess antibacterial activity for only a short period after setting, highlighting the need for improved formulations.

Studies have shown that endodontic microorganisms have a high affinity for gutta-percha, a common root filling material, leading to bacterial adhesion and biofilm formation. This persistence of infection in root canals underscores the importance of long-term antibacterial properties in root canal sealers. Incorporating antibacterial nanoparticles into root canal sealers has been explored as a strategy to enhance their antibacterial efficacy.

For example, zinc oxide (ZnO)-based root canal sealers and resin-based sealers loaded with chitosan (CS) and ZnO nanoparticles have been investigated for their antimicrobial properties. These nanoparticle-loaded sealers have demonstrated improved direct and diffusible antibacterial effects compared to conventional sealers. Additionally, the application of CS nanoparticles has been shown to reduce the adherence of bacteria to root canal dentin.

The addition of nanoparticles has not been found to deteriorate the flow characteristics of root canal sealers. ZnO nanoparticle-loaded sealers exhibit better antibacterial properties and enhanced diffusion of antibacterial components, which is critical in the root canal environment. Similarly, root canal sealers incorporating CS nanoparticles, especially when combined with dentin surface treatments, have shown significant reductions in bacterial biofilms at the filling-dentin interface (Figure 10.8.).

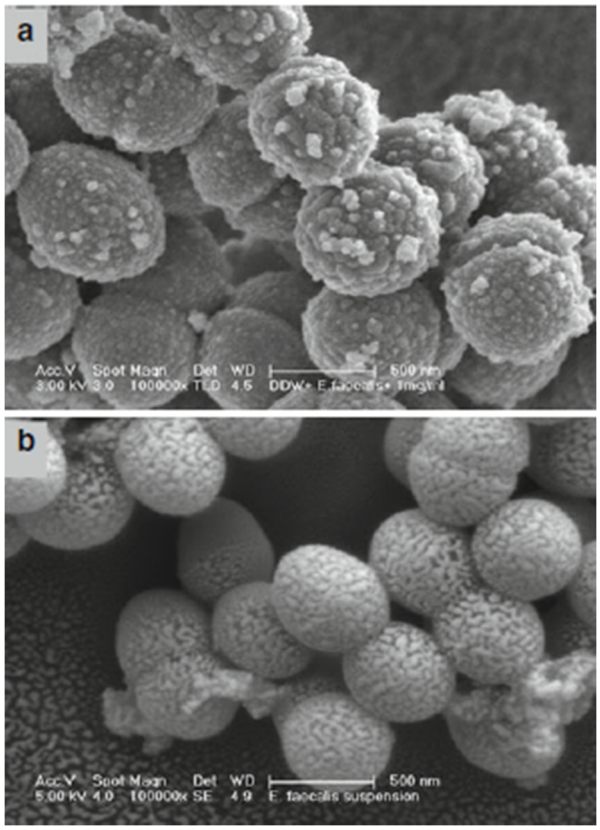


Figure 10.8. Determination of the antibacterial activity of QPEI nanoparticles in suspension. Scanning electron micrographs of E. faecalis. (a) In DDW with QPEI nanoparticles- depicting attached nanoparticles on bacterial membranes; (b) In DDW- depicting regular bacterial membranes [1].

Quaternary ammonium polyethylenimine (QAPEI) nanoparticles have also been utilized to improve the antibacterial efficacy of root canal sealers. Studies have demonstrated that incorporating QAPEI nanoparticles into sealers enhances their wettability and surface charge, leading to increased antibacterial efficacy. QAPEI nanoparticles exert bactericidal effects by adsorbing to and penetrating bacterial cell walls, disrupting cell membranes, and causing cell death.

Additionally, bioactive glass (BAG) nanoparticles have been recommended to promote closure of the interfacial gap between root canal walls and core filling materials. Combining BAG nanoparticles with polymers such as polyisoprene or polycaprolactone has been shown to create a hydroxyapatite interface, improving the sealing ability of the composite materials.

Overall, the incorporation of antibacterial nanoparticles into root canal sealers holds promise for enhancing their long-term antibacterial properties and improving the success rates of endodontic treatments. However, further research, including in vitro and in vivo studies, is needed to validate their efficacy and safety in clinical settings [1].

10.1.5.5. Nanoparticle Functionalization

Functionalization of nanoparticles involves modifying their surface properties with specific molecules to enhance their colloidal stability and tailor their application for targeted delivery. This process can alter surface composition, charge, and structure while preserving the bulk material properties. When biomolecules are conjugated with nanoparticles, it is termed biofunctionalization.

In a functionalized nanoparticle, the core substrate typically forms the matrix, with the core particle protected by inert material or organic molecules. Additional layers of linker molecules may be added for further functionalization, providing reactive groups for attaching various moieties such as biocompatibles, antibodies, or fluorophores, depending on the desired function.

Functionalized nanoparticles offer new possibilities for combating antimicrobial resistance. For instance, chitosan nanoparticles (CS-NPs) have been functionalized for protein, drug, and gene delivery applications. Modifications of chitosan nanocarriers with different ligands increase their recognition and uptake into cells through receptor-mediated endocytosis.

Labeling nanoparticles with fluorescent dyes like fluorescein isothiocyanate (FITC) allows tracking their interaction with tissues or cells. FITC can be covalently bound to chitosan nanoparticles, enabling visualization of their internalization into cells through endocytosis.

In antibacterial applications, CS-NPs are used as vehicles for delivering antibiotics, circumventing systemic side effects associated with antibiotic administration. Functionalization of chitosan micro/nanoparticles with tissue-specific molecules enables targeted antibacterial activities without harming host cells.

Chitosan's versatility in size and chemical modifications makes it advantageous for targeted antibacterial applications, especially in reaching anatomical complexities and dentinal tubules where bacterial biofilms persist. Moreover, chitosan's biocompatibility and biodegradability are crucial for in vivo applications (Figure 10.9.).

Functionalization of chitosan with photosensitizers can target bacteria over human cells, enhancing antibacterial activity. Photoactivation of photosensitizer-functionalized CS-NPs releases singlet oxygen, further potentiating their antibacterial effects.

Overall, bioactive functionalized nanoparticles offer multi-functionalities, addressing challenges related to antibiotics and bacterial resistance in various applications [1].

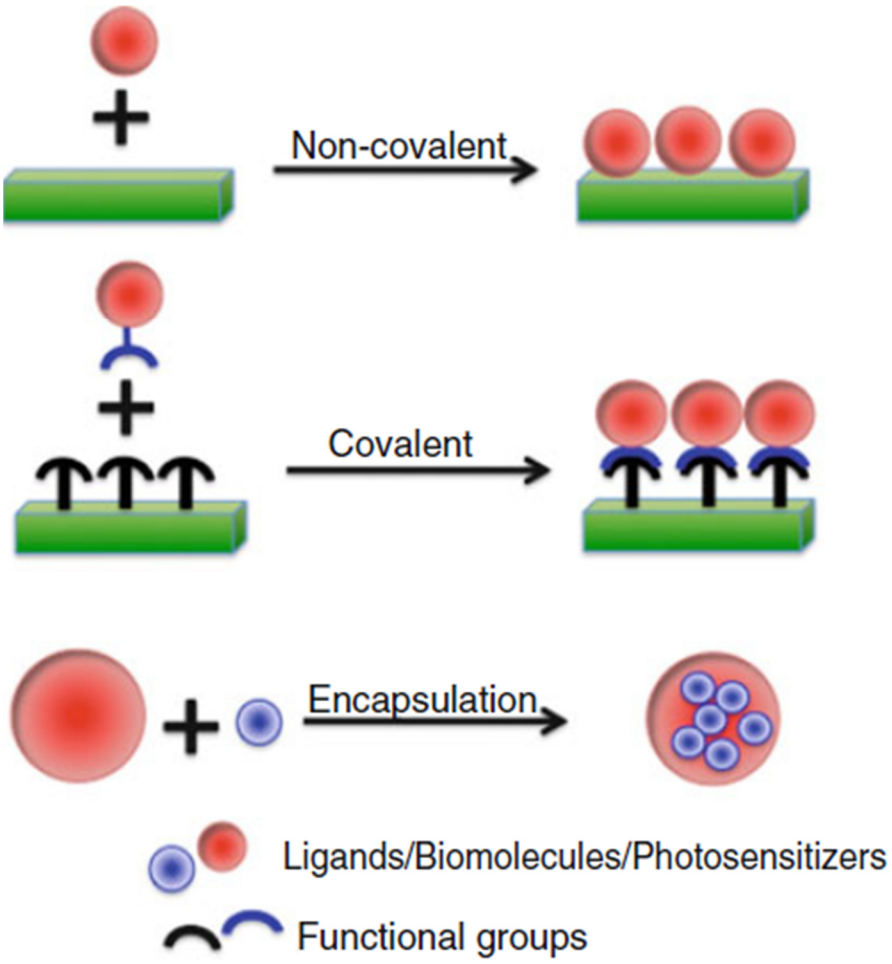


Figure 10.9. Surface modification or functionalization of nanoparticles through non-covalent, covalent and encapsulation approaches [1].

10.1.5.6. Nanoparticle Modification for Antimicrobial Photodynamic Therapy

Nanoparticle-based photosensitizers have emerged as promising tools to enhance the antimicrobial efficacy of photodynamic therapy (PDT). Functionalizing nanoparticles with photosensitizer molecules offer unique physicochemical properties, including ultrasmall sizes, large surface area/mass ratio, and increased reactivity. By utilizing bioactive nanoparticles for functionalization, the favorable functions and properties of the bioactive molecule can be leveraged effectively.

Certain metallic nanomaterials such as TiO2, ZnO, and fullerenes and their derivatives have shown the ability to generate singlet oxygen and induce bacterial elimination. Various strategies have been proposed to combine nanoparticles with photosensitizers, including supplementation, encapsulation, binding, or using nanoparticles themselves as photosensitizers. These combinations have been found to enhance antimicrobial PDT efficacy by increasing photosensitizer concentration, reducing efflux, allowing for targeting, improving stability, and enabling controlled release of reactive oxygen species (ROS).

For example, methylene blue-loaded poly(lactic-co-glycolic) acid (PLGA) nanoparticles exhibited significantly higher bacterial phototoxicity, enveloping bacterial cells with higher concentrations on the bacterial cell walls. Similarly, photosensitizer-bound polystyrene beads and Rose Bengal-bound silica nanoparticles showed improved bacterial elimination by binding to bacterial cell membranes and facilitating ROS generation upon light activation.

While synthetic polymers and liposomes have been used to conjugate photosensitizers, concerns about biocompatibility remain. Naturally occurring biopolymers like chitosan offer a solution to this issue due to their biocompatibility and chemical modifiability. Functionalized chitosan nanoparticles loaded with photosensitizers, such as chitosan-Rose Bengal nanoparticles (CSRBnp), have shown promising results. CSRBnp interacted effectively with bacteria and biofilms, leading to membrane damage and leakage of cellular constituents, resulting in significant bacterial elimination. Moreover, CSRBnp demonstrated lower cytotoxicity towards fibroblast cells and maintained antibacterial efficacy in the presence of biological fluids.

Overall, photosensitizer-functionalized chitosan nanoparticles hold great potential for the single-step treatment of infected root dentin by combining the antibacterial properties of chitosan with the photodynamic effects of photosensitizers. This approach offers a promising strategy for combating bacterial biofilms and preventing degradation of dentin matrix in infected root canals [1].

10.1.6. Concluding Remarks

For effective therapeutic efficacy using antibacterial nanoparticles, it is crucial to tailor the nanoparticles appropriately, considering the tissue-related factors at the site of infection and the chosen delivery method. Designing nanoparticles that meet all prerequisites is essential for managing infected tissue effectively.

- Antibacterial nanoparticle-based treatments have the potential to significantly improve antibacterial and antibiofilm efficacy. They offer distinct advantages when applied in dentistry and endodontics.
- Tailoring nanoparticles through functionalization allows for chemical modification, providing an opportunity to deliver therapeutic agents selectively to the site of infection to interact with and penetrate the biofilm and bacteria. This targeted antibacterial efficacy makes functionalized nanoparticles ideal for treating infections near host tissues.
- Nanoparticle functionalization can enhance drug efficacy by enabling the loading of more active bioactive molecules onto a single nanoparticle.
- Developing newer multifunctional nanoparticles and their modifications should be based on clinical requirements and involve collaboration among engineers, clinicians, and biologists.
- The concept of nanotechnology in healthcare should be embraced with both enthusiasm and caution for future development, ensuring that safety and efficacy are prioritized in all applications.

10.1.7. Photodynamic therapy

Biofilm disruption and disinfection of root canals are crucial steps in treating infected root canal systems to prevent the persistence of microbial infection and achieve endodontic success. Despite advancements in instrumental techniques and antiseptics, achieving total asepsis of the root canal is challenging. Antimicrobial photodynamic therapy (aPDT) has emerged as a promising approach, offering excellent experimental results and heralding a new era in endodontic disinfection [2, 3, 4].

One chlorophyll derivative, Zn(II)e6Me, has demonstrated adequate antimicrobial efficacy, particularly in the removal of mixed biofilms. PDT is considered an adjunctive, conservative, and non-selective method for eliminating bacteria. It aims to improve root canal disinfection without inducing bacterial resistance. The principle of PDT is effective not only against bacteria but also against other microorganisms such as viruses, fungi, and protozoa [5, 6, 7].

PDT involves the use of a photosensitizer and light of a specific wavelength. For example, toluidine blue at a 600-nm wavelength is commonly used. Effective destruction of oral biofilm has been demonstrated using methylene blue dye encapsulated within poly(D, L-lactide-co-glycolide) (PLGA) nanoparticles, which typically have diameters ranging from approximately 150 nm to 200 nm [8, 9].

10.2. Nanomaterials in endodontic instruments

The introduction of nickel-titanium (NiTi) alloys revolutionized endodontics, particularly with the automation of mechanical preparation using endodontic files. These files are instrumental in shaping the root canal during endodontic procedures. NiTi file systems were developed to reduce the likelihood of errors during endodontic procedures.

Despite their advantages such as high flexibility and increased resistance to torsional fracture compared to conventional stainless-steel instruments, NiTi files are prone to cycle fatigue and unexpected fracture, often without visible defects preceding the failure due to permanent deformation [10, 11].

The nickel-titanium alloy, known as Nitinol, was originally developed for the U.S. space program in 1963. Its use in dentistry began in 1971 for orthodontic wires due to its low modulus of elasticity, shape-memory effect, and flexibility. In endodontics, the fabrication of endodontic instruments from NiTi alloy was conceptualized by Civjan et al. in 1975. Handheld NiTi endodontic instruments were introduced in 1988 by Walia, Brantley, and Gerstein, initially made by machining orthodontic wire. Technological advancements later allowed for the production of NiTi instruments using machining processes with significant improvements in design and taper, diverging from the ISO standards set for manual instruments in 1958 [12, 13, 14].

Looking ahead, one future perspective involves coating NiTi files with nanoparticles to enhance resistance to cyclic fatigue and corrosion caused by endodontic irrigants. Coating NiTi files with cobalt and impregnated fullerene-like WS2 nanoparticles has been shown to significantly improve fatigue resistance and breakage time by reducing friction between the file and surrounding tissue. This innovation holds promise for improving the reliability and longevity of NiTi endodontic files [15].

10.3. Root canal sealers

Endodontic sealers play a crucial role in root canal obturation by sealing off the canal space and holding gutta-percha in place. The ideal properties of a sealer include ease of handling, non-toxicity, biocompatibility, absence of shrinkage upon setting, effective working time, hydrophilic properties, antibacterial action, and ease of retreatment [16].

Nanoparticle-based modifications are being utilized to enhance the physicochemical properties of endodontic sealers beyond just antibacterial efficacy. For example, the inclusion of bioactive glass and hydroxyapatite nanoparticles has been shown to enhance the bioactivity of epoxy resin-based sealers, as demonstrated by a study by Jerri Al-Bakhsh et al. in 2019 [17, 18].

Calcium hydroxide paste, a commonly used material in endodontics, can be enhanced by mixing it with silver nanoparticles, resulting in increased antibacterial action compared to using calcium hydroxide alone or in combination with chlorhexidine [19].

Zinc oxide nanoparticles, known for their antimicrobial properties, interact electrostatically with bacterial cell membranes, inhibiting permeability and leading to bacterial cell death [20].

Bio-ceramic-based nanomaterials, such as the Endo Sequence BC sealer, composed of calcium phosphate, calcium hydroxide, calcium silicates, zirconia, and a thickening agent, have improved physical properties due to nanoparticle incorporation. These nanoparticles facilitate material delivery, adapt to irregular dentin surfaces, provide excellent sealing, and enhance dimensional stability [21].

However, it's important to note that hydraulic calcium silicate-based cements, including bio-ceramic materials, may cause discoloration over time due to their interaction with blood. Oxide bismuth has been identified as an agent that can minimize this discoloration effect [22].

In comparison to mineral trioxide aggregate (MTA) cements, bio-ceramic materials offer advantages such as higher shear bond strength and cohesive fracture patterns. Biomaterials like Biodentine and TotalFill BC present suitable alternatives, allowing restorative procedures immediately after placement, depending on the specific cement used [23].

New developments in hydraulic calcium silicate-based cements aim to address the limitations of traditional MTA. For instance, additional hydrophobic bonding layers and variations in restoration time can affect bond performance and the ultra-morphological interface between composite adhesive restoration and hydraulic calcium silicate-based cements. These advancements enable a more conservative approach to pulp preservation and regeneration in endodontic treatment.

10.4. Pulp repair and regeneration

Regenerative endodontics represents a promising approach aimed at replacing damaged tooth structures, including dentin, root structures, and the pulp-dentin complex, through biologically based procedures. The ultimate goal is to physiologically restore the function and vitality of the tooth. Recent advancements in technology have transformed this theoretical concept into a practical reality [24, 25].

One key aspect of regenerative endodontics involves the use of nanoscale scaffold materials for tissue regeneration. Nanoscaffolds made from biodegradable materials such as collagen type I, fibronectin, and self-assembling polypeptide hydrogels have shown potential for promoting pulp tissue regeneration. Synthetic polymers like poly (l-lactic acid) (PLLA) in nano-form have also demonstrated promise in tissue engineering applications (Figure 10.10.).

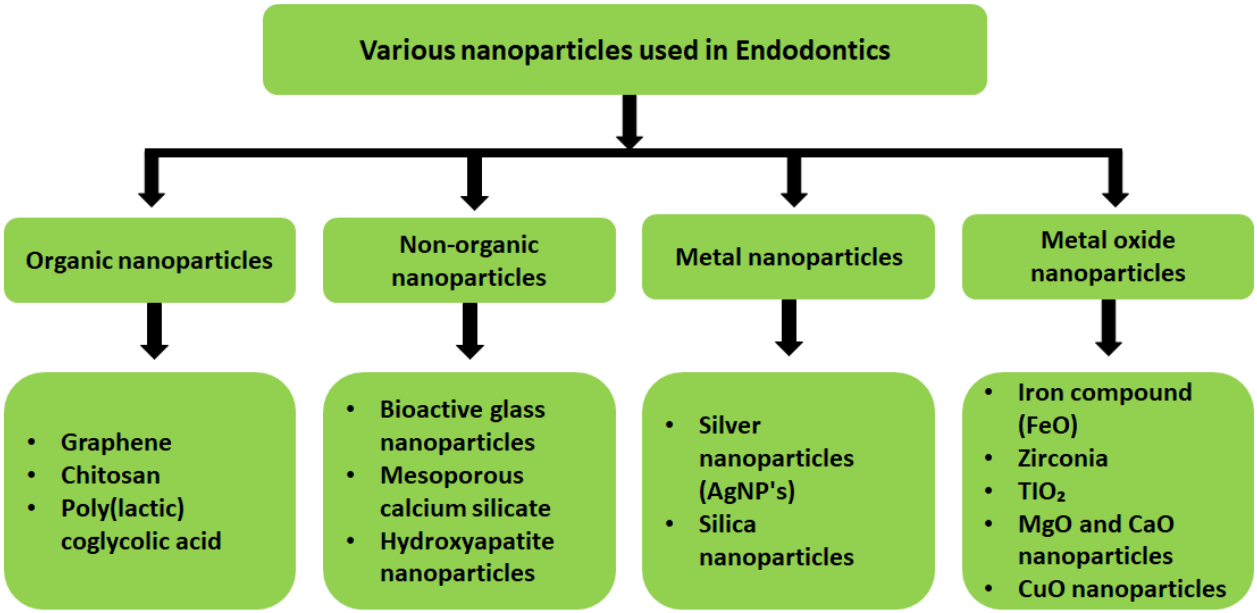


Figure 10.10. Variety of nanoparticles used in endodontology [24]

A notable advancement in this field is the development of a hierarchical growth factor-loaded nanofibrous microsphere scaffolding system by Xiangwei Li et al. This innovative system incorporates vascular endothelial growth factor (VEGF) encapsulated in heparin-conjugated gelatin nanospheres, which are then immobilized within nanofibers of an injectable PLLA microsphere. This hierarchical microsphere system not only protects VEGF from degradation but also provides controlled release, supporting the proliferation of dental pulp stem cells (DPSCs) and facilitating pulp tissue formation [26, 27].

Regenerative endodontic procedures (REPs) have shown excellent success rates in resolving periapical pathology and increasing the survival of immature teeth. Histologic studies from both animal models and human clinical cases provide valuable insights into the nature of newly formed tissues following REPs [28].

In conclusion, nanotechnology has made significant strides in the field of regenerative endodontics, bringing the regeneration of pulp tissue in pulp-less teeth closer to reality. Continued research and development in this area hold promise for further advancements and the widespread clinical application of regenerative endodontic techniques [29].

10.4.1. Organic nanoparticles

10.4.1.1. Graphene

Graphene, an allotrope of carbon, is renowned for being the thinnest material, forming a perfectly even crystal lattice structure without any structural dislocations. This remarkable material has found diverse applications, including in the field of biomedical science.

In particular, graphene nanoparticles (NPs) have shown promise in the diagnosis and detection of diseases, as well as in the development of antibacterial surfaces. Their unique properties make them suitable for various biomedical applications [30].

One derivative of graphene, known as graphene nanoplatelets, has exhibited notable antimicrobial properties in studies. For instance, research conducted by Rago et al. demonstrated the antimicrobial efficacy of graphene nanoplatelets against various microorganisms, particularly Streptococcus mutans. Scanning electron microscopy (SEM) images from this study revealed a strong mechanical bond between the graphene nanoplatelets and microbial cells. This interaction involved the shrinking and trapping of cells, ultimately resulting in the death of these microorganisms [31].

Overall, the antimicrobial properties of graphene nanoplatelets highlight their potential as a promising candidate for combating microbial infections and developing novel antibacterial materials in various biomedical applications.

10.4.1.2. Chitosan Nanoparticles (Cs-NPs)

Chitosan nanoparticles (Cs-NPs) have emerged as a prominent area of research in endodontics due to their promising properties and potential applications. Chitosan, a natural polysaccharide derived from the deacetylation of chitin, exhibits unique characteristics that make it suitable for various biomedical purposes. Chitin is abundantly found in the external skeletons of arthropods like crabs and shrimps, making chitosan readily available from natural sources [32, 33].

The mechanism of action of Cs-NPs primarily involves electrostatic interactions with bacterial cell membranes. This interaction disrupts the integrity of the cell membrane, leading to increased permeability and eventual cell death. Additionally, Cs-NPs have been shown to induce microleakage of intracellular components, further contributing to bacterial degradation [34, 35].

One of the notable advantages of Cs-NPs is their enhanced antibiofilm efficacy, making them effective against biofilm-forming bacteria. Moreover, Cs-NPs have demonstrated the ability to neutralize bacterial endotoxins, which are potent inflammatory mediators. This is achieved through the organized release of singlet oxygen species, which contribute to bacterial degradation and biofilm disruption [36, 37].

Cs-NPs are considered non-toxic to eukaryotic cells, making them suitable for usage as a finishing rinse in the irrigation of root canals. Their biocompatibility with human cells ensures

minimal adverse effects while effectively targeting bacterial pathogens within the root canal system [38].

Overall, the unique properties of chitosan nanoparticles, including their antibiofilm efficacy, ability to neutralize bacterial endotoxins, and biocompatibility, make them promising candidates for various applications in endodontics, particularly in root canal irrigation and disinfection procedures.

10.4.1.3. Poly (lactic) co-glycolic acid (PLGA)

PLGA (poly(lactic-co-glycolic acid)) is a biodegradable polymer widely utilized in various medical applications, including the dental industry. Its versatility and favorable properties make it suitable for the development of scaffolds, biofilms, membranes, microparticles, and nanoparticles [39].

One of the primary advantages of PLGA is its biocompatibility, meaning it is well-tolerated by biological systems without causing adverse reactions. Additionally, PLGA is biodegradable, meaning it can be broken down into harmless byproducts by the body over time. This property makes it ideal for use in biomedical applications where temporary support or drug delivery is needed [40].

PLGA microparticles have been extensively studied in dental applications, particularly in endodontic therapy. By encapsulating therapeutic agents such as antibiotics within PLGA microparticles, sustained and controlled release of the drug can be achieved. This targeted drug delivery system allows for efficient delivery of the drug directly to the site of infection, such as the root canal, while minimizing systemic side effects [41].

In endodontics, PLGA microparticles have been used to deliver antibiotics such as amoxicillin into the root canal. Amoxicillin is effective against Enterococcus faecalis, a microorganism commonly associated with endodontic failure and retreatment cases. By exceeding the concentration levels required for proper disinfection, PLGA microparticles loaded with amoxicillin offer a promising approach to combating E. faecalis infections within the root canal system.

Overall, PLGA-based drug delivery systems represent a valuable tool in endodontics, providing an effective means of delivering therapeutics to the site of infection while minimizing systemic side effects and improving patient outcomes.

10.4.2. Non-organic nanoparticles

10.4.2.1. Bioactive glass

Bioactive glass, developed by Hench et al. in 1960, consists of specific proportions of sodium oxide, calcium oxide, phosphorus pentoxide, and silicon dioxide. These components form the main composition of bioactive glass, with their sizes typically ranging from 20 to 60 nm [42, 43].

Bioactive glass, whether in micro- or nanoforms, has been utilized for disinfection of root canals due to its antibacterial properties. Several factors contribute to its antibacterial efficacy. First, when bioactive glass dissolves in water, it leads to an increase in pH, which can create an unfavorable environment for bacterial survival. Additionally, the deposition of calcium phosphate (Ca/P ions) on the surface of bacteria can initiate mineralization processes that interfere with bacterial function. Moreover, the increase in osmotic pressure, typically above 1%, can inhibit the growth of numerous bacteria, further contributing to its antimicrobial effect [44, 45].

In summary, bioactive glass demonstrates antibacterial properties in root canal disinfection by altering pH levels, promoting mineralization, and exerting osmotic effects, ultimately inhibiting bacterial growth and promoting a favorable environment for healing.

10.4.2.2. Mesoporous calcium silicate

The nanoparticles mentioned, with sizes ranging from 80 to 100 nm, possess a high specific surface area and pore volume ratio. Due to these properties, they are suitable for filling the apical third of root canals, as they exhibit high viscosity [46].

In addition to their viscosity, these nanoparticles offer several advantages in endodontics:

1. Drug delivery: Their high surface area-to-volume ratio allows for efficient loading and controlled release of drugs, facilitating targeted delivery within the root canal system.

2. Antibacterial efficiencies: These nanoparticles may possess inherent antibacterial properties or can be functionalized with antibacterial agents, enhancing their efficacy in eliminating bacteria from the root canal space.
3. Injectability: Their viscosity and rheological properties make them suitable for injection into narrow and complex root canal anatomy, ensuring thorough and complete filling.
4. Apatite mineralization: These nanoparticles may promote the formation of apatite minerals, aiding in the remineralization of dentin and potentially enhancing the sealing and stability of the root canal filling.
5. Osteo-stimulation: They may stimulate osteogenic activity, promoting bone formation and regeneration in periapical tissues, which is beneficial for the healing process after endodontic treatment [47].

Overall, these nanoparticles offer versatile properties that make them valuable tools in endodontics, contributing to improved treatment outcomes and long-term success.

10.4.2.3. Hydroxyapatite nanoparticles

Hydroxyapatite (HA) is indeed a highly valued biomaterial in the medical field due to its remarkable biocompatibility and its prevalence as the primary mineral component of bone and teeth. When scaled down to the nanoscale, forming nano-hydroxyapatite, its crystals typically range in size from 50 to 1000 nm [48].

Nano-hydroxyapatite offers several advantageous properties:

1. Biocompatibility: Nano-hydroxyapatite exhibits excellent compatibility with biological tissues, making it suitable for various medical applications without adverse reactions.
2. Similarity to Human Hard Tissues: Its composition closely resembles that of human hard tissues such as bone and teeth, enhancing its ability to integrate seamlessly into the body.
3. Antibacterial Properties: Nano-hydroxyapatite possesses inherent antibacterial properties, which can contribute to reducing the risk of infection in medical implants or dental applications.
4. Bioactivity: Nano-hydroxyapatite exhibits bioactive properties, meaning it can actively interact with biological tissues, promoting tissue regeneration and integration.

In dentistry, nano-hydroxyapatite serves multiple functions:

- Integration into Dentinal Tubules: Nano-hydroxyapatite can penetrate and seal dentinal tubules, preventing the exposure of dental nerves to external stimuli, which helps reduce dentin hypersensitivity.
- Dentin Hypersensitivity Reduction: By sealing dentinal tubules, nano-hydroxyapatite can effectively decrease dentin hypersensitivity, improving patient comfort.
- Biocompatibility in Periapical Healing: Nano-hydroxyapatite's biocompatibility makes it suitable for promoting periapical healing, reducing local or systemic inflammatory reactions, and facilitating tissue regeneration in the periapical region.

Overall, nano-hydroxyapatite holds great promise in various dental applications, including dentin tubule sealing, dentin hypersensitivity management, and periapical healing, owing to its exceptional biocompatibility, antibacterial properties, and bioactivity.

10.4.3. Metal nanoparticles

10.4.3.1. Silver nanoparticles (AgNP's)

Silver nanoparticles (AgNPs) exhibit significant biological activity, similar to other silver-containing products, primarily through the gradual release of silver ions via redox reactions in the presence of water. One of the key mechanisms of action of AgNPs involves the induction of reactive oxygen species (ROS) production, with hydroxyl radicals being the primary species responsible for oxidative damage [49, 50].

The effectiveness of AgNPs against bacteria stems from their ability to easily penetrate bacterial cell membranes, facilitated by their larger surface area and small size. This leads to rapid bactericidal action. Additionally, AgNPs demonstrate several desirable properties, including

biocompatibility, low bacterial resistance, low toxicity, and long-lasting antibacterial activity [51, 52].

Studies have shown that biologically produced silver nanoparticles exhibit effective antibacterial properties against specific bacteria such as Enterococcus faecalis. When utilized as an irrigating solution, AgNPs coated with polyvinyl alcohol (PVA) have demonstrated efficacy against various pathogens including Pseudomonas aeruginosa, Candida albicans, and Enterococcus faecalis [53, 54].

Furthermore, irrigating root canals with AgNPs solutions may impact the physical and structural properties of root dentine. Research suggests that incorporating an AgNPs-based irrigant as a final rinse in endodontic treatment can significantly enhance the fracture resistance of treated teeth compared to using traditional sodium hypochlorite (NaOCl) alone [55].

Overall, the multifaceted antimicrobial properties and favorable effects on dental structures make AgNPs a promising candidate for various endodontic applications, including irrigation solutions and treatments aimed at combating bacterial infections in root canals.

10.4.3.2. Silica nanoparticles

Silica nanoparticles have made a significant positive impact in the field of dentistry, particularly in conservative dentistry. These nanoparticles exhibit excellent biocompatibility and possess a large surface area, coupled with low levels of toxicity and density. As a result, they are widely utilized in various dental applications.

In conservative dentistry, silica nanoparticles are commonly employed as dental fillers in restorative materials. Their incorporation enhances the mechanical properties of these materials, such as strength and wear resistance, while maintaining biocompatibility with oral tissues. Additionally, silica nanoparticles contribute to the aesthetic properties of dental restorations by improving translucency and color stability.

Moreover, silica nanoparticles are utilized as a polishing agent in dental materials. Their ability to produce a smoother surface with lower roughness after polishing enhances the esthetic appearance of restorations and reduces the accumulation of plaque and bacteria, thereby contributing to improved oral health.

Overall, silica nanoparticles play a crucial role in conservative dentistry by enhancing the performance and aesthetics of dental materials while ensuring biocompatibility and safety for patients. Their widespread application underscores their importance in modern dental practice.

10.4.4. Metal oxide nanoparticles

10.4.4.1. Iron compound (FeOx)

Iron oxide nanoparticles, including magnetite (Fe_3O_4) and maghemite (γ-Fe_2O_3), are widely recognized for their important role in biology and the medicinal field. These nanoparticles are highly popular in biomedical science due to their biocompatibility and non-toxic properties to humans [56].

One of the key features of iron oxide nanoparticles is their superparamagnetic behavior at certain sizes. This property enables them to exhibit unique characteristics that make them suitable for various biomedical applications. Here are some of their notable applications:

Contrast Agents: Iron oxide nanoparticles are commonly used as contrast agents in magnetic resonance imaging (MRI). Their superparamagnetic properties allow them to generate strong contrast signals, making them valuable tools for visualizing anatomical structures and detecting abnormalities in medical imaging.

Drug Delivery Vehicles: Iron oxide nanoparticles can be functionalized or coated with specific molecules to serve as carriers for therapeutic agents, such as drugs or genes. Their small size and biocompatibility enable efficient delivery of these payloads to target tissues or cells, offering potential applications in targeted therapy and personalized medicine.

Thermal-Based Therapeutics: Iron oxide nanoparticles can also be utilized in thermal-based therapeutic approaches, such as magnetic hyperthermia. When exposed to an alternating magnetic

field, these nanoparticles generate heat through hysteresis losses, which can selectively induce hyperthermia and destroy cancer cells or pathogens while sparing healthy tissues [57].

Overall, iron oxide nanoparticles, particularly magnetite and maghemite, play a crucial role in various biomedical applications, ranging from medical imaging and drug delivery to therapeutic interventions. Their unique properties make them promising candidates for the development of innovative diagnostic and therapeutic strategies in biomedicine.

10.4.4.2. Magnesium halogen-containing nanoparticles

Magnesium-containing nanoparticles have been proposed as potential antimicrobial agents for combating endodontic pathogens, leveraging their known antibacterial properties against a wide range of microorganisms, including gram-positive and gram-negative bacteria, spores, and viruses [58]. These nanoparticles typically consist of either magnesium oxide nanoparticles or magnesium-halogen-containing nanoparticles, such as those containing chlorine, bromine, or fluorine [59, 60]. The primary mechanism by which magnesium-containing nanoparticles exert their antimicrobial effects involves their penetration into bacterial cells, leading to disruption of membrane potential. Once inside the bacterial cell, these nanoparticles can induce lipid peroxidation and bind to DNA, contributing to further damage and ultimately causing destruction of the bacterial cell [61].

Magnesium-containing nanoparticles hold promise as antimicrobial agents in endodontics, offering a potential strategy to combat microbial infections in root canals by disrupting essential bacterial functions and promoting cell death. Further research and development in this area may lead to the clinical application of these nanoparticles for improved endodontic therapy.

10.4.4.3. Zinc oxide nanoparticles (ZnONP)

Zinc oxide nanoparticles (ZnONPs) are utilized in endodontics due to their bactericidal properties, which operate through a mechanism akin to that of silver nanoparticles (AgNPs). Studies have demonstrated that an irrigant containing ZnO NPs effectively eradicated planktonic Enterococcus faecalis and disrupted biofilm matrices. Notably, the antibacterial activity of this solution remained effective even after a prolonged period of aging [62, 63]. Zinc oxide nanoparticles exhibit strong antibacterial efficacy, particularly in environments with elevated pH levels. The mechanism of action is similar to that of other nanoparticle types, involving an increase in permeability of the bacterial cell membrane, subsequent release of cytoplasmic contents, and ultimately, cell death. However, it's worth noting that ZnONPs may demonstrate reduced effectiveness against bacteria within biofilms compared to their planktonic counterparts. Despite this, their bactericidal properties make them valuable candidates for endodontic applications, particularly in combating microbial infections within root canals [64, 65, 66].

10.4.4.4. Magnesium oxide and Calcium oxide (MgO and CaO) nanoparticles

Magnesium oxide nanoparticles (MgO NPs) have demonstrated potent antimicrobial effects, making them valuable assets in endodontic practice. Studies have revealed that MgO NPs, along with calcium oxide (CaO) nanoparticles, exhibit efficacy against both Gram-positive and Gram-negative microorganisms. Specifically, MgO nanoparticles, when utilized at a concentration of 5 mg/L in combination with chitosan nanoparticles, have shown long-lasting effectiveness in eradicating Enterococcus faecalis [66, 67, 68].

Furthermore, metal oxides such as zinc oxide and magnesium oxide have been investigated for their antibacterial properties in various formulations. Incorporating MgO NPs into materials has been shown to significantly reduce the growth of bacteria like Staphylococcus aureus, highlighting the potential of MgO NPs in enhancing the antimicrobial properties of dental materials used in endodontics.

10.4.4.5. Cuprum oxide (CuO) nanoparticles

Copper oxide nanoparticles (CuO NPs) have shown effectiveness against both Gram-positive and Gram-negative bacteria by penetrating the bacterial cell membrane and disrupting vital enzymes.

Additionally, CuO NPs exhibit antifungal properties. However, their application in endodontics is limited, and further research is necessary to evaluate their efficacy [69, 70].

Research by Rai et al. explored the synthesis of gold nanoparticles using antibiotics, such as cefaclor, to enhance antimicrobial activity. The combined action of cefaclor, which inhibits peptidoglycan layer synthesis, and gold nanoparticles, which create openings in bacterial cell walls, leads to cell content leakage and eventual cell death [71, 72, 73]. Despite some limitations, such as low residence time in the bloodstream and susceptibility to proteases in an alkaline wound environment, antimicrobial peptides (AMPs) are emerging as alternatives to antibiotics due to the rise of multidrug-resistant bacteria. AMPs, like LL37 peptides, can be immobilized on the surface of medical devices, such as dental implants, to impart antimicrobial and angiogenic properties, often through conjugation with gold nanoparticles.

10.4.4.6. Titanium dioxide (TiO2) nanoparticles

Titanium dioxide (TiO2) nanoparticles have demonstrated safety for use in various medical and dental applications due to their biocompatibility, biosafety, and lack of allergic reactions with human tissues. They have a wide range of uses in medicine and dentistry, including applications such as bone grafting and dental implants. Moreover, TiO2 nanoparticles have garnered interest as antimicrobial agents in recent years [74].

10.4.5. Possible perils of endodontic nanotechnology

Indeed, nanoparticle-based endodontic therapies bring notable advantages, but they are not without drawbacks. One concern is the potential for cytotoxic effects on periapical and pulpal tissues. Additionally, the routes of entry into the human body for nanoparticles are diverse, including inhalation, dermal absorption, ingestion, and systemic administration. Because nanoparticles have dimensions similar to biological molecules, they can be readily absorbed by various organs and tissues, leading to potential accumulation in organs such as the lungs, liver, and reticuloendothelial system [75, 76, 77].

Moreover, environmental considerations must be considered. Nanoparticles used in endodontics may act as pollutants, accumulating in the environment. Toxic effects of nanoparticles are often concentration-dependent, and their bioaccumulation could result in systemic toxicity to living organisms exposed to them. These factors underscore the importance of careful assessment and regulation of nanoparticle use in endodontic therapies to mitigate potential adverse effects on both human health and the environment [78].

10.5. Conclusions

The increasing availability of nanoparticle-containing materials provides numerous options for their utilization in the medical field. In endodontics, the impact of nanoparticles is rapidly evolving, with applications ranging from infection diagnosis to regenerative procedures. Their unique properties, such as larger surface areas and enhanced reactivity, result in improved antibacterial actions compared to their bulk counterparts. This emergence of nanoendodontics suggests a promising future for the broader utilization of nanoparticles in dentistry. However, alongside their advantages, nanoparticles also present certain drawbacks. One major concern is their potential toxicity to humans and the environment, an aspect that warrants further investigation. Additionally, the synthesis of nanoparticles poses challenges, as they must be safe, environmentally friendly, and cost-effective.

To address these challenges and further enhance their properties and applications, additional clinical investigations are necessary. Research efforts should also focus on studying the potential risks associated with nanoparticles. The forecast of future papers in this field indicates a significant growth in research output, underscoring the importance of continued exploration and understanding of nanoparticle-based technologies in dentistry. Efforts to investigate the negative effects of nanoparticles on human health and the environment should be prioritized to ensure their safe and responsible use in clinical practice.

10.6. Quiz 10

1. Which of the following statements accurately describe the role of nanotechnology in endodontic disease management?

A) Nanotechnology enables efficient removal of biofilm bacteria from the root canal system.

B) Nanomaterial-based approaches offer distinct advantages over conventional methods in endodontics.

C) Nanotechnology facilitates tissue engineering-based approaches for repair or regeneration in previously infected teeth.

D) At the nanoscale, materials exhibit similar characteristics to their macro-scale counterparts.

E) The utilization of nanotechnology in endodontics has not shown promising opportunities for disease prevention, diagnosis, or treatment.

2. Which metallic nanoparticles exhibit antimicrobial properties?

A) Copper, gold, titanium, and zinc

B) Silver, aluminum, iron, and nickel

C) Platinum, palladium, rhodium, and iridium

D) Lead, mercury, cadmium, and arsenic

E) Sodium, potassium, calcium, and magnesium

3. What are the main challenges in achieving effective root canal treatment?

A) Lack of patient compliance and proper oral hygiene

B) Inadequate availability of dental equipment and instruments

C) Limited success rates of current treatment strategies

D) Difficulty in obtaining accurate diagnosis of endodontic diseases

E) Insufficient training and expertise among dental professionals

4. What are the main concerns associated with the use of silver nanoparticles in dentistry?

A) Limited antibacterial efficacy against biofilms

B) Risk of increased incidence of dental caries

C) Potential discoloration of dentin

D) Incompatibility with dental restorative materials

E) Reduced effectiveness in dental implants

5. What are potential applications of functionalized nanoparticles in combating antimicrobial resistance?

A) Protein delivery

B) Drug delivery

C) Gene delivery

D) Metal detection

E) Tissue regeneration

6. Which statements about antimicrobial photodynamic therapy (aPDT) are true?

A) It aims to improve root canal disinfection without inducing bacterial resistance.

B) One chlorophyll derivative, Zn(II)e6Me, has demonstrated adequate antimicrobial efficacy.

C) PDT is only effective against bacteria.

D) PDT involves the use of a photosensitizer and light of a specific wavelength.

E) Methylene blue dye is commonly used as a photosensitizer at a 600-nm wavelength.

7. Which factors contribute to the antibacterial efficacy of bioactive glass in root canal disinfection?

A) Increase in pH
B) Deposition of calcium phosphate on bacterial surfaces
C) Decrease in osmotic pressure
D) Increase in osmotic pressure
E) Promotion of bacterial growth

8. What are the advantages of PLGA (poly(lactic-co-glycolic acid)) in dental applications?

A) Non-biodegradable property
B) Biocompatibility
C) Low tolerance by biological systems
D) Rapid degradation in the body
E) Inefficient drug delivery system

9. What are the advantageous properties of nano-hydroxyapatite in dental applications?

A) Biocompatibility
B) Similarity to human soft tissues
C) Lack of antibacterial properties
D) Inactivity in promoting tissue regeneration
E) Incompatibility with dentinal tubules

10. Which statements about nanoparticles in antimicrobial strategies are true?

A) Copper oxide nanoparticles (CuO NPs) are effective against Gram-positive and Gram-negative bacteria.

B) Gold nanoparticles synthesized with antibiotics like cefaclor enhance antimicrobial activity by inhibiting cell wall synthesis.

C) Antimicrobial peptides (AMPs) are considered alternatives to antibiotics.

D) Gold nanoparticles conjugated with LL37 peptides impart antimicrobial properties to medical devices.

E) Further research is necessary to evaluate the efficacy of copper oxide nanoparticles in endodontics.

References

[1]. Anil Kishen, Nanotechnology in Endodontics, Current and Potential Clinical Applications, Springer Cham Heidelberg New York Dordrecht London, © Springer International Publishing Switzerland 2015, ISBN 978-3-319-13574-8 ISBN 978-3-319-13575-5 (eBook), DOI 10.1007/978-3-319-13575-5, Library of Congress Control Number: 2015935938.
[2]. Diogo, P.; Gonçalves, T.; Palma, P.; Santos, J.M. Photodynamic Antimicrobial Chemotherapy for Root Canal System Asepsis: A Narrative Literature Review. Int. J. Dent. 2015, 2015, 1–26, doi:10.1155/2015/269205.
[3]. Diogo, P.; Faustino, M.A.F.; Neves, M.G.P.M.S.; Palma, P.J.; Baptista, I.P.; Gonçalves, T.; Santos, J.M. An Insight into Advanced Approaches for Photosensitizer Optimization in Endodontics—A Critical Review. J. Funct. Biomater. 2019, 10, 44, doi:10.3390/jfb10040044.
[4]. Diogo, P.; Mota, M.; Fernandes, C.; Sequeira, D.; Palma, P.; Caramelo, F.; Neves, M.G.P.; Faustino, M.A.F.; Gonçalves, T.; Santos, J.M. Is the chlorophyll derivative Zn(II)e 6 Me a good photosensitizer to be used in root canal disinfection?. Photodiagnosis Photodyn. Ther. 2018, 22, 205–211, https://doi.org/10.1016/j.pdpdt.2018.04.009.
[5]. Dhole, A.E., Yarasu, R.B., Lata, D.B., Baraskar, S.S., Shaw, D., 2015. Mathematical modeling for the performance and emission parameters of dual-fuel diesel engine using producer gas as secondary fuel. Biomass Convers. Bioref. 5, 257–270. https://doi.org/ 10.1007/s13399-014-0142-6.]
[6]. Hamblin, M.R.; Hasan, T. Photodynamic therapy: A new antimicrobial approach to infectious disease? Photochem. Photobiol. Sci. 2004, 3, 436–450, https://doi.org/10.1039/b311900a.
[7]. Jori, G. Photodynamic Therapy of Microbial Infections: State of the Art and Perspectives. J. Environ. Pathol. Toxicol. Oncol. 2006, 25, 505–520, https://doi.org/10.1615/jenvironpatholtoxicoloncol.v25.i1- 2.320. [8]. Konopka, K.; Goslinski, T. Photodynamic Therapy in Dentistry. J. Dent. Res. 2007, 86, 694–707, https://doi.org/10.1177/154405910708600803.
[9]. Nagahara, A.; Mitani, A.; Fukuda, M.; Yamamoto, H.; Tahara, K.; Morita, I.; Ting, C.-C.; Watanabe, T.; Fujimura, T.; Osawa, K.; et al. Antimicrobial photodynamic therapy using a diode laser with a potential new photosensitizer, indocyanine green-loaded nanospheres, may be effective for the clearance of Porphyromonas gingivalis. J. Periodontal Res. 2013, 48, 591–599, https://doi.org/10.1111/jre.12042.
[10]. Palma, P.J.; Messias, A.; Cerqueira, A.R.; Tavares, L.D.; Caramelo, F.; Roseiro, L.; Santos, J.M. Cyclic fatigue resistance of three rotary file systems in a dynamic model after immersion in sodium hypochlorite. Odontology 2018, 107, 324–332, https://doi.org/10.1007/s10266-018-0401-2.
[11]. Auricchio, F.; Taylor, R.L.; Lubliner, J. Shape-memory alloys: macromodelling and numerical simulations of the superelastic behavior. Comput. Methods Appl. Mech. Eng. 1997, 146, 281–312, https://doi.org/10.1016/s0045-7825(96)01232-7.
[12]. Civjan, S.; Huget, E.F.; DeSimon, L.B. Potential Applications of Certain Nickel-Titanium (Nitinol) Alloys. J. Dent. Res. 1975, 54, 89–96, https://doi.org/10.1177/00220345750540014301.
[13]. Walia, H.; Brantley, W.A.; Gerstein, H. An initial investigation of the bending and torsional properties of nitinol root canal files. J. Endod. 1988, 14, 346–351, https://doi.org/10.1016/s0099-2399(88)80196- 1.
[14]. Thompson, S.A. An overview of nickel-titanium alloys used in dentistry. Int. Endod. J. 2000, 33, 297– 310, https://doi.org/10.1046/j.1365-2591.2000.00339.x.
[15]. Adini, A.R.; Feldman, Y.; Cohen, S.R.; Rapoport, L.; Moshkovich, A.; Redlich, M.; Moshonov, J.; Shay, B.; Tenne, R. Alleviating fatigue and failure of NiTi endodontic files by a coating containing inorganic fullerene-like WS2 nanoparticles. J. Mater. Res. 2011, 26, 1234–1242, https://doi.org/10.1557/jmr.2011.52.
[16]. Al-Bakhsh, B.A.J.; Shafiei, F.; Hashemian, A.; Shekofteh, K.; Bolhari, B.; Behroozibakhsh, M. In-vitro bioactivity evaluation and physical properties of an epoxy-based dental sealer reinforced with synthesized fluorine-substituted hydroxyapatite, hydroxyapatite and bioactive glass nanofillers. Bioact. Mater. 2019, 4, 322–333, https://doi.org/10.1016/j.bioactmat.2019.10.004.
[17]. Afkhami, F.; Akbari, S.; Chiniforush, N. Entrococcus faecalis Elimination in Root Canals Using Silver Nanoparticles, Photodynamic Therapy, Diode Laser, or Laser-activated Nanoparticles: An In Vitro Study. J. Endod. 2016, 43, 279–282, https://doi.org/10.1016/j.joen.2016.08.029.
[18] Reddy, K.M.; Feris, K.; Bell, J.; Wingett, D.G.; Hanley, C.; Punnoose, A. Selective toxicity of zinc oxide nanoparticles to prokaryotic and eukaryotic systems. Appl. Phys. Lett. 2007, 90, 213902– 2139023, https://doi.org/10.1063/1.2742324.
[19]. Chole, D.; Khan, I.; Kundoor, S.; Bakle, S.; Gandhi, N.; Deshpande, R. Nanotechnology: Conservative Dentistry and Endodontics. IOSR J. Dent. Med Sci. 2017, 16, 102–107, https://doi.org/10.9790/0853-160401102107.
[20]. Palma, P.J.; Marques, J.A.; Santos, J.; Falacho, R.I.; Sequeira, D.; Diogo, P.; Caramelo, F.; Ramos, J.C.; Santos, J.M. Tooth Discoloration after Regenerative Endodontic Procedures with Calcium Silicate-Based Cements—An Ex Vivo Study. Appl. Sci. 2020, 10, 5793, https://doi.org/10.3390/app10175793.
[21]. Camilleri, J.; Borg, J.; Damidot, D.; Salvadori, E.; Pilecki, P.; Zaslansky, P.; Darvell, B.W. Colour and chemical stability of bismuth oxide in dental materials with solutions used in routine clinical practice. PLOS ONE 2020, 15, e0240634, https://doi.org/10.1371/journal.pone.0240634.

[22]. Palma, P.J.; Marques, J.A.; Antunes, M.; Falacho, R.I.; Sequeira, D.; Roseiro, L.; Santos, J.M.; Ramos, J.C. Effect of restorative timing on shear bond strength of composite resin/calcium silicate–based cements adhesive interfaces. Clin. Oral Investig. 2020, 25, 3131–3139, https://doi.org/10.1007/s00784- 020-03640-7.
[23]. Xavier, M.T.; Costa, A.L.; Caramelo, F.J.; Palma, P.J.; Ramos, J.C. Evaluation of the Interfaces between Restorative and Regenerative Biomaterials Used in Vital Pulp Therapy. Materials 2021, 14, 5055, https://doi.org/10.3390/ma14175055.
[24]. Saoud, T.M.A.; Ricucci, D.; Lin, L.M.; Gaengler, P. Regeneration and Repair in Endodontics—A Special Issue of the Regenerative Endodontics—A New Era in Clinical Endodontics. Dent. J. 2016, 4, 3, https://doi.org/10.3390/dj4010003.
[25]. Cuculino L, Gutmann JL. Prospective nanotechnology applications in endodontics: a brief overview. Endodontic Practice Today. 2020 Apr 1;14(2).
[26]. Revathy CP, Deepak Baby, Sreedevi PV, Rajeev KG, Raihan KM, Veena MV Nanomodified Materials in Endodontics – A Game Changer!!! IOSR Journal of Dental and Medical Sciences (IOSR-JDMS). 2022;21(3):07-12. www.iosrjournals.org
[27]. Li, X.; Ma, C.; Xie, X.; Sun, H.; Liu, X. Pulp regeneration in a full-length human tooth root using a hierarchical nanofibrous microsphere system. Acta Biomater. 2016, 35, 57–67, https://doi.org/10.1016/j.actbio.2016.02.040.
[28]. Palma, P.J.; Ramos, J.C.; Martins, J.B.; Diogenes, A.; Figueiredo, M.H.; Ferreira, P.; Viegas, C.; Santos, J.M. Histologic Evaluation of Regenerative Endodontic Procedures with the Use of Chitosan Scaffolds in Immature Dog Teeth with Apical Periodontitis. J. Endod. 2017, 43, 1279–1287, https://doi.org/10.1016/j.joen.2017.03.005.
[29]. Palma, P.J.; Martins, J.; Diogo, P.; Sequeira, D.; Ramos, J.C.; Diogenes, A.; Santos, J.M. Does Apical Papilla Survive and Develop in Apical Periodontitis Presence after Regenerative Endodontic Procedures? Appl. Sci. 2019, 9, 3942, https://doi.org/10.3390/app9193942.
[30]. del Carpio-Perochena, A.; Kishen, A.; Shrestha, A.; Bramante, C.M. Antibacterial Properties Associated with Chitosan Nanoparticle Treatment on Root Dentin and 2 Types of Endodontic Sealers. J. Endod. 2015, 41, 1353–1358, https://doi.org/10.1016/j.joen.2015.03.020.
[31]. Rago, I.; Bregnocchi, A.; Zanni, E.; D'Aloia, A.G.; De Angelis, F.; Bossu, M.; De Bellis, G.; Polimeni, A.; Uccelletti, D.; Sarto, M.S. Antimicrobial activity of graphene nanoplatelets against Streptococcus mutans. In Proceedings of the IEEE International Conference on Nanotechnology, Rome, Italy, 27–30 July 2015; pp. 9–12.
[32]. Şenel, S.; Ikinci, G.; Kaş, S.; Yousefi-Rad, A.; Sargon, M.; Hıncal, A. Chitosan films and hydrogels of chlorhexidine gluconate for oral mucosal delivery. Int. J. Pharm. 2000, 193, 197–203, https://doi.org/10.1016/s0378-5173(99)00334-8.
[33]. Silva, P.V.; Guedes, D.F.C.; Nakadi, F.V.; Pécora, J.D.; Cruz□Filho, A.M. Chitosan: a new solution for removal of smear layer after root canal instrumentation. Int. Endod. J. 2012, 46, 332–338, https://doi.org/10.1111/j.1365-2591.2012.02119.x.
[34]. Rinaudo M. Chitin and chitosan: Properties and applications. Progress in polymer science. 2006 Jul 1;31(7):603-32.
[35]. Tyliszczak, B.; Drabczyk, A.; Kudłacik-Kramarczyk, S.; Sobczak-Kupiec, A. Sustainable Production of Chitosan. 2019, 45–60, https://doi.org/10.1007/978-3-030-11274-5_4.
[36]. Shrestha, A.; Zhilong, S.; Gee, N.K.; Kishen, A. Nanoparticulates for Antibiofilm Treatment and Effect of Aging on Its Antibacterial Activity. J. Endod. 2010, 36, 1030–1035, https://doi.org/10.1016/j.joen.2010.02.008.
[37]. Shrestha, A.; Kishen, A. Antibiofilm Efficacy of Photosensitizer-functionalized Bioactive Nanoparticles on Multispecies Biofilm. J. Endod. 2014, 40, 1604–1610, https://doi.org/10.1016/j.joen.2014.03.009.
[38]. Hussein, H.; Kishen, A. Antibiofilm and Immune Response of Engineered Bioactive Nanoparticles for Endodontic Disinfection. J. Clin. Med. 2020, 9, 730, https://doi.org/10.3390/jcm9030730.
[39]. Virlan, M.J.R.; Miricescu, D.; Totan, A.; Greabu, M.; Tanase, C.; Sabliov, C.M.; Caruntu, C.; Calenic, B. Current Uses of Poly (lactic-co-glycolic acid) in the Dental Field: A Comprehensive Review. J. Chem. 2015, 2015, 1–12, https://doi.org/10.1155/2015/525832.
[40]. Mundargi, R.C.; Babu, V.R.; Rangaswamy, V.; Patel, P.; Aminabhavi, T.M. Nano/micro technologies for delivering macromolecular therapeutics using poly(d,l-lactide-co-glycolide) and its derivatives. J. Control. Release 2008, 125, 193–209, https://doi.org/10.1016/j.jconrel.2007.09.013.
[41]. O Sousa, F.F.; Luzardo-Álvarez, A.; Perez-Estevez, A.; Seoane-Prado, R.; Blanco-Méndez, J. Development of a novel AMX-loaded PLGA/zein microsphere for root canal disinfection. Biomed. Mater. 2010, 5, 055008, https://doi.org/10.1088/1748-6041/5/5/055008.

[42]. Piotrowski, G.; Hench, L.L.; Allen, W.C.; Miller, G.J. Mechanical studies of the bone bioglass interfacial bond. J. Biomed. Mater. Res. 1975, 9, 47–61, https://doi.org/10.1002/jbm.820090408.
[43]. Palekar A, Garud S, Borse S, Deshpande Y, Palekar U, Biradar B. Nanoparticles and Its Implication in Endodontics–A Review. Annals of the Romanian Society for Cell Biology. 2020 Dec 30:826-32.
[44]. Stoor, P.; Söderling, E.; Salonen, J.I. Antibacterial effects of a bioactive glass paste on oral microorganisms. Acta Odontol. Scand. 1998, 56, 161–165, https://doi.org/10.1080/000163598422901. [45]. Zakrzewski, W.; Dobrzyński, M.; Zawadzka-Knefel, A.; Lubojański, A.; Dobrzyński, W.; Janecki, M.; Kurek, K.; Szymonowicz, M.; Wiglusz, R.J.; Rybak, Z. Nanomaterials Application in Endodontics. Materials 2021, 14, 5296, https://doi.org/10.3390/ma14185296.
[46]. Wu C, Chang J, Fan W. Bioactive mesoporous calcium–silicate nanoparticles with excellent mineralization ability, osteostimulation, drug-delivery and antibacterial properties for filling apex roots of teeth. Journal of Materials Chemistry. 2012;22(33):16801-9.
[47]. Raura, N.; Garg, A.; Arora, A.; Roma, M. Nanoparticle technology and its implications in endodontics: a review. Biomater. Res. 2020, 24, 1–8, https://doi.org/10.1186/s40824-020-00198-z.
[48]. Marica A, Sipos L, Iurcov R, Stefanescu T, Ciavoi G , Lucan A-I, Miere (Groza) F. Current use of nanoparticles in endodontics: a sytematic review Romanian Journal of Oral Rehabilitation. 2022;14(3):15-26.
[49]. Lee, Y.-J.; Kim, J.; Oh, J.; Bae, S.; Lee, S.; Hong, I.S.; Kim, S.-H. Ion-release kinetics and ecotoxicity effects of silver nanoparticles. Environ. Toxicol. Chem. 2011, 31, 155–159, https://doi.org/10.1002/etc.717.
[50]. Quinteros, M.A.; Viviana, C.A.; Onnainty, R.; Mary, V.S.; Theumer, M.G.; Granero, G.E.; Paraje, M.G.; Páez, P.L. Biosynthesized silver nanoparticles: Decoding their mechanism of action in Staphylococcus aureus and Escherichia coli. Int. J. Biochem. Cell Biol. 2018, 104, 87–93, https://doi.org/10.1016/j.biocel.2018.09.006.
[51]. Prabhu, S.; Poulose, E.K. Silver nanoparticles: mechanism of antimicrobial action, synthesis, medical applications, and toxicity effects. Int. Nano Lett. 2012, 2, 32, https://doi.org/10.1186/2228-5326-2-32.
[52]. Chávez-Andrade, G.M.; Tanomaru-Filho, M.; Bernardi, M.I.B.; Leonardo, R.D.T.; Faria, G.; Guerreiro-Tanomaru, J.M. Antimicrobial and biofilm anti-adhesion activities of silver nanoparticles and farnesol against endodontic microorganisms for possible application in root canal treatment. Arch. Oral Biol. 2019, 107, 104481, https://doi.org/10.1016/j.archoralbio.2019.104481.
[53]. Jowkar, Z.; Hamidi, S.A.; Shafiei, F.; Ghahramani, Y. The Effect of Silver, Zinc Oxide, and Titanium Dioxide Nanoparticles Used as Final Irrigation Solutions on the Fracture Resistance of Root-Filled Teeth. Clin. Cosmet. Investig. Dent. 2020, ume 12, 141–148, https://doi.org/10.2147/CCIDE.S253251.
[54]. Doozandeh, M.; Koohpeima, F. Shear Bond Strength of Self-Adhering Flowable Composite and Resinmodified Glass Ionomer to Two Pulp Capping Materials. Iran. Endod. J. 2017, 12, 83–86, https://doi.org/10.22037/IEJ.2017.17.
[55]. Suzuki, T.Y.U.; Gallego, J.; Assunção, W.G.; Briso, A.L.F.; dos Santos, P.H. Influence of silver nanoparticle solution on the mechanical properties of resin cements and intrarradicular dentin. PLOS ONE 2019, 14, e0217750, https://doi.org/10.1371/journal.pone.0217750.
[56]. Roig-Soriano, X.; Souto, E.B.; Elmsmari, F.; Garcia, M.L.; Espina, M.; Duran-Sindreu, F.; Sánchez-López, E.; Sánchez, J.A.G. Nanoparticles in Endodontics Disinfection: State of the Art. Pharmaceutics 2022, 14, 1519, https://doi.org/10.3390/pharmaceutics14071519.
[57]. Mitchell, M.J.; Billingsley, M.M.; Haley, R.M.; Wechsler, M.E.; Peppas, N.A.; Langer, R. Engineering precision nanoparticles for drug delivery. Nat. Rev. Drug Discov. 2020, 20, 101–124, https://doi.org/10.1038/s41573-020-0090-8.
[58]. Beyth, N.; Houri-Haddad, Y.; Domb, A.; Khan, W.; Hazan, R. Alternative Antimicrobial Approach: Nano-Antimicrobial Materials. Evid.-Based Complement. Altern. Med. 2015, 2015, 246012, doi:10.1155/2015/246012.
[59]. Pelgrift, R.Y.; Friedman, A.J. Nanotechnology as a therapeutic tool to combat microbial resistance. Adv. Drug Deliv. Rev. 2013, 65, 1803–1815, doi:10.1016/j.addr.2013.07.011.
[60]. Blecher, K.; Nasir, A.; Friedman, A. The growing role of nanotechnology in combating infectious disease. Virulence 2011, 2, 395–401, https://doi.org/10.4161/viru.2.5.17035.
[61]. Lellouche, J.; Kahana, E.; Elias, S.; Gedanken, A.; Banin, E. Antibiofilm activity of nanosized magnesium fluoride. Biomaterials 2009, 30, 5969–5978, https://doi.org/10.1016/j.biomaterials.2009.07.037.
[62]. Zaltsman, N.; Kesler-Shvero, D.; Weiss, E.I.; Beyth, N. Synthesis variants of quaternary ammonium polyethyleneimine nanoparticles and their antibacterial efficacy in dental materials. J. Appl. Biomater. Funct. Mater. 2016, 14, e205–11, https://doi.org/10.5301/jabfm.5000269.

[63]. Liu, Y.; He, L.; Mustapha, A.; Li, H.; Hu, Z.; Lin, M. Antibacterial activities of zinc oxide nanoparticles against Escherichia coli O157:H7. J. Appl. Microbiol. 2009, 107, 1193–1201, https://doi.org/10.1111/j.1365-2672.2009.04303.x.
[64]. Sirelkhatim, A.; Mahmud, S.; Seeni, A.; Kaus, N.H.M.; Ann, L.C.; Bakhori, S.K.M.; Hasan, H.; Mohamad, D. Review on Zinc Oxide Nanoparticles: Antibacterial Activity and Toxicity Mechanism. Nano-Micro Lett. 2015, 7, 219–242, https://doi.org/10.1007/s40820-015-0040-x.
[65]. Yamamoto, O. Influence of particle size on the antibacterial activity of zinc oxide. Int. J. Inorg. Mater. 2001, 3, 643–646, https://doi.org/10.1016/s1466-6049(01)00197-0.
[66]. Huang, Z.; Zheng, X.; Yan, D.; Yin, G.; Liao, X.; Kang, Y.; Yao, Y.; Huang, D.; Hao, B. Toxicological Effect of ZnO Nanoparticles Based on Bacteria. Langmuir 2008, 24, 4140–4144, https://doi.org/10.1021/la7035949.
[67]. Jowkar, Z.; Hamidi, S.A.; Shafiei, F.; Ghahramani, Y. The Effect of Silver, Zinc Oxide, and Titanium Dioxide Nanoparticles Used as Final Irrigation Solutions on the Fracture Resistance of Root-Filled Teeth. Clin. Cosmet. Investig. Dent. 2020, ume 12, 141–148, https://doi.org/10.2147/CCIDE.S253251.
[68]. Naguib, G.H.; Nassar, H.M.; Hamed, M.T. Antimicrobial properties of dental cements modified with zein-coated magnesium oxide nanoparticles. Bioact. Mater. 2021, 8, 49–56, https://doi.org/10.1016/j.bioactmat.2021.06.011.
[69]. Mahapatra, O.; Bhagat, M.; Gopalakrishnan, C.; Arunachalam, K.D. Ultrafine dispersed CuO nanoparticles and their antibacterial activity. J. Exp. Nanosci. 2008, 3, 185–193, https://doi.org/10.1080/17458080802395460.
[70]. Rai, A.; Prabhune, A.; Perry, C.C. Antibiotic mediated synthesis of gold nanoparticles with potent antimicrobial activity and their application in antimicrobial coatings. J. Mater. Chem. 2010, 20, 6789– 6798, https://doi.org/10.1039/c0jm00817f.
[71]. Shankar SS, Rai A, Ahmad A, Sastry M. Rapid synthesis of Au, Ag, and bimetallic Au core–Ag shell nanoparticles using Neem (Azadirachta indica) leaf broth. Journal of colloid and interface science. 2004 Jul 15;275(2):496-502.
[72]. Comune, M.; Rai, A.; Palma, P.; TondaTuro, C.; Ferreira, L. Antimicrobial and pro-angiogenic properties of soluble and nanoparticle-immobilized LL37 peptides. Biomater. Sci. 2021, 9, 8153–8159, https://doi.org/10.1039/d1bm01034d.
[73]. Rai, A.; Ferrão, R.; Palma, P.; Patricio, T.; Parreira, P.; Anes, E.; Tonda-Turo, C.; Martins, M.C.L.; Alves, N.; Ferreira, L. Antimicrobial peptide-based materials: opportunities and challenges. J. Mater. Chem. B 2022, 10, 2384–2429, https://doi.org/10.1039/d1tb02617h.
[74]. Mansoor, A.; Khurshid, Z.; Khan, M.T.; Mansoor, E.; Butt, F.A.; Jamal, A.; Palma, P.J. Medical and Dental Applications of Titania Nanoparticles: An Overview. Nanomaterials 2022, 12, 3670, https://doi.org/10.3390/nano12203670.
[75]. . Lu, X.; Zhu, T.; Chen, C.; Liu, Y. Right or Left: The Role of Nanoparticles in Pulmonary Diseases. Int. J. Mol. Sci. 2014, 15, 17577–17600, https://doi.org/10.3390/ijms151017577.
[76]. Gopee, N.V.; Roberts, D.W.; Webb, P.; Cozart, C.R.; Siitonen, P.H.; Warbritton, A.R.; Yu, W.W.; Colvin, V.L.; Walker, N.J.; Howard, P.C. Migration of Intradermally Injected Quantum Dots to Sentinel Organs in Mice. Toxicol. Sci. 2007, 98, 249–257, https://doi.org/10.1093/toxsci/kfm074.
[77]. Balasubramanian, S.K.; Jittiwat, J.; Manikandan, J.; Ong, C.-N.; Yu, L.E.; Ong, W.-Y. Biodistribution of gold nanoparticles and gene expression changes in the liver and spleen after intravenous administration in rats. Biomaterials 2010, 31, 2034–2042, https://doi.org/10.1016/j.biomaterials.2009.11.079. [78]. Dreher, K.L. Health and Environmental Impact of Nanotechnology: Toxicological Assessment of Manufactured Nanoparticles. Toxicol. Sci. 2003, 77, 3–5, https://doi.org/10.1093/toxsci/kfh041.

11. Nanoapplications in Preventive Dentistry

Nanotechnology encompasses the science of designing, synthesizing, characterizing, and applying materials and devices at the nanoscale. In dentistry, various approaches are employed to introduce both organic and inorganic nanoparticles. These nanoparticles have diverse applications in preventive dentistry, particularly in strategies aimed at managing biofilms, inhibiting demineralization, and promoting remineralization.

Researchers have explored the incorporation of different nanoparticles into various dental materials, including fissure sealants, bonding agents, dentifrices, mouthwashes, and glass ionomers. Both in vitro and in vivo studies have been conducted to evaluate the efficacy and safety of these nanoparticle-containing dental products.

11.1. Repair of enamel by using hydroxyapatite nanoparticles as the building blocks

Enamel damage caused by bacteria can lead to dental caries, and conventional treatments often involve filling the defects with artificial materials. However, secondary caries frequently develops at the interfaces between the tooth and these foreign materials.

Hydroxyapatite (HAP) is considered a model compound for enamel due to its chemical similarity, and remineralization using synthetic apatite or calcium phosphate is suggested in dental research. However, the complex structure of natural enamel makes it difficult to replicate, leading to poor adhesion and mechanical strength of the restorations. Recent studies suggest that the basic building blocks of enamel are nanoparticles of HAP, with dimensions ranging from 20 to 40 nm. These nanoparticles combine into self-assembled apatite during enamel formation.

A biomimetic approach is proposed, wherein the localized repair of enamel surface can be improved by using artificial HAP nanoparticles that closely resemble the natural building blocks of enamel. Unlike conventional HAP and amorphous calcium phosphate, artificial HAP nanoparticles with dimensions of 20 nm demonstrate enhanced biocompatibility with enamel. In vitro experiments show strong adsorption of nano HAP onto enamel surfaces, suggesting its potential for improving enamel repair. This biomimetic technique holds promise for more effective enamel restoration by utilizing nanoparticles that mimic the natural building blocks of enamel [1].

The nano HAP layer formed on the enamel surface not only aids in repairing damaged enamel but also serves to prevent demineralization of the hard tissue. Additionally, maintaining the mechanical strength of the restored enamel surface is crucial for its long-term durability and functionality. The in vitro results suggest that 20 nm sized HAP nanoparticles outperform any conventional restorative material used thus far, indicating their potential as a superior option for enamel repair. This suggests that the use of 20 nm sized HAP nanoparticles brings us closer to achieving perfect enamel repair.

The study involved the use of human molars obtained from the First Affiliated Hospital of Zhejiang University College of Medicine, with patient consent and approval from the hospital's ethical committee. The teeth were stored and prepared by sectioning and polishing, followed by demineralization using phosphoric acid. The enamel windows created had dimensions of 5 x 5 x 0.5 mm^3.

The 20 nm HAP nanoparticles were synthesized in the laboratory, while conventional HAP crystals were prepared using a suggested method. Amorphous calcium phosphate (ACP) was synthesized at room temperature. The morphologies and particle sizes of these materials were examined using transmission electron microscopy (TEM) [2].

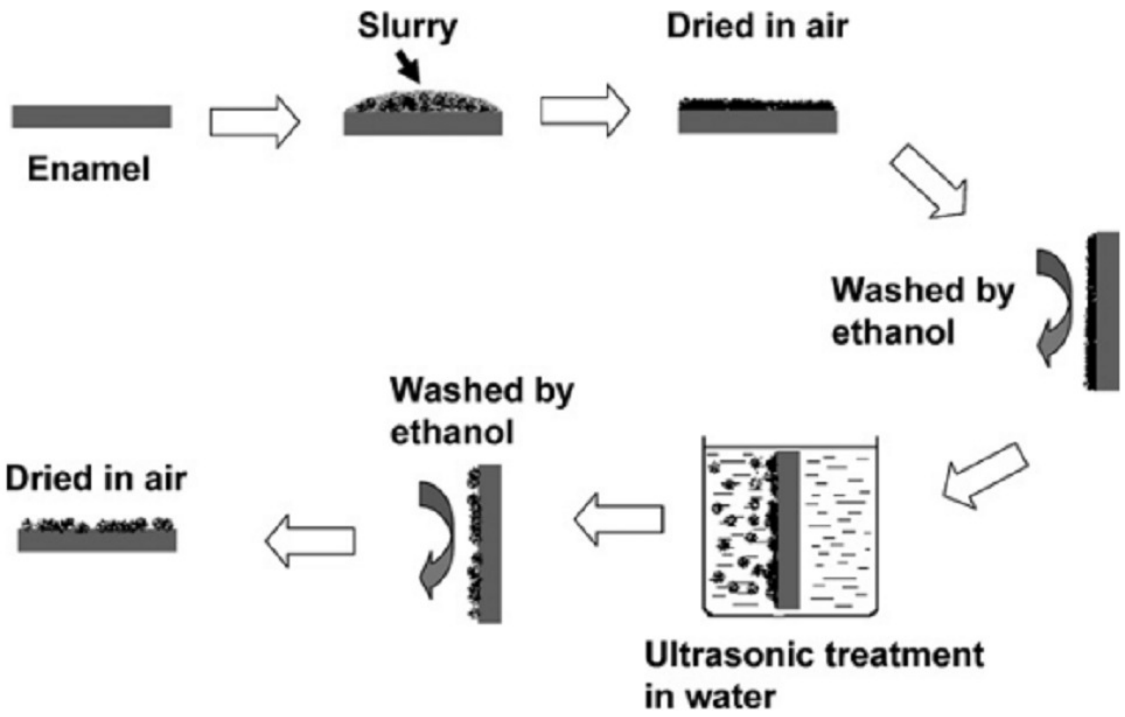


Figure 11.1. ***Treatment of the enamel window using different calcium phosphate materails [1].***

A slurry of calcium phosphate solid was applied onto the enamel surfaces and dried, followed by washing with ethanol to remove unabsorbed materials. The adsorption ability of the samples onto the enamel was estimated by subjecting the repaired windows to ultrasonication in distilled water. The enamel surfaces were then examined under scanning electron microscopy (SEM), and the quantitative examination of adsorbed particles was performed using a quartz crystal microbalance (QCM-D) [3].

Some enamel samples, with and without the coated nano HAP layer, were exposed to Rhodamine B solution for observation using confocal laser scanning microscopy (CLSM). Dissolution experiments were conducted by exposing the samples to a sodium chloride solution, with mass loss measured daily to estimate dissolution rates. Nanoindentation was performed using a multiple scanning probe microscope (SPM) with a diamond-tipped probe (Figure 11.1.).

11.1.1. Results and discussion

The transmission electron microscopy (TEM) images of the different artificial calcium phosphate materials revealed distinct morphologies. The nano HAP particles appeared grain-like with diameters of approximately 20 nm, while the particles of conventional HAP (cHAP) exhibited a typical rod-like morphology with lengths of hundreds of nanometres. The 20 nm ACP particles appeared sphere-like. Selected area electron diffraction (SAED) patterns confirmed the crystallinity of nano HAP and cHAP, while ACP showed no obvious diffraction pattern, indicating its amorphous nature.

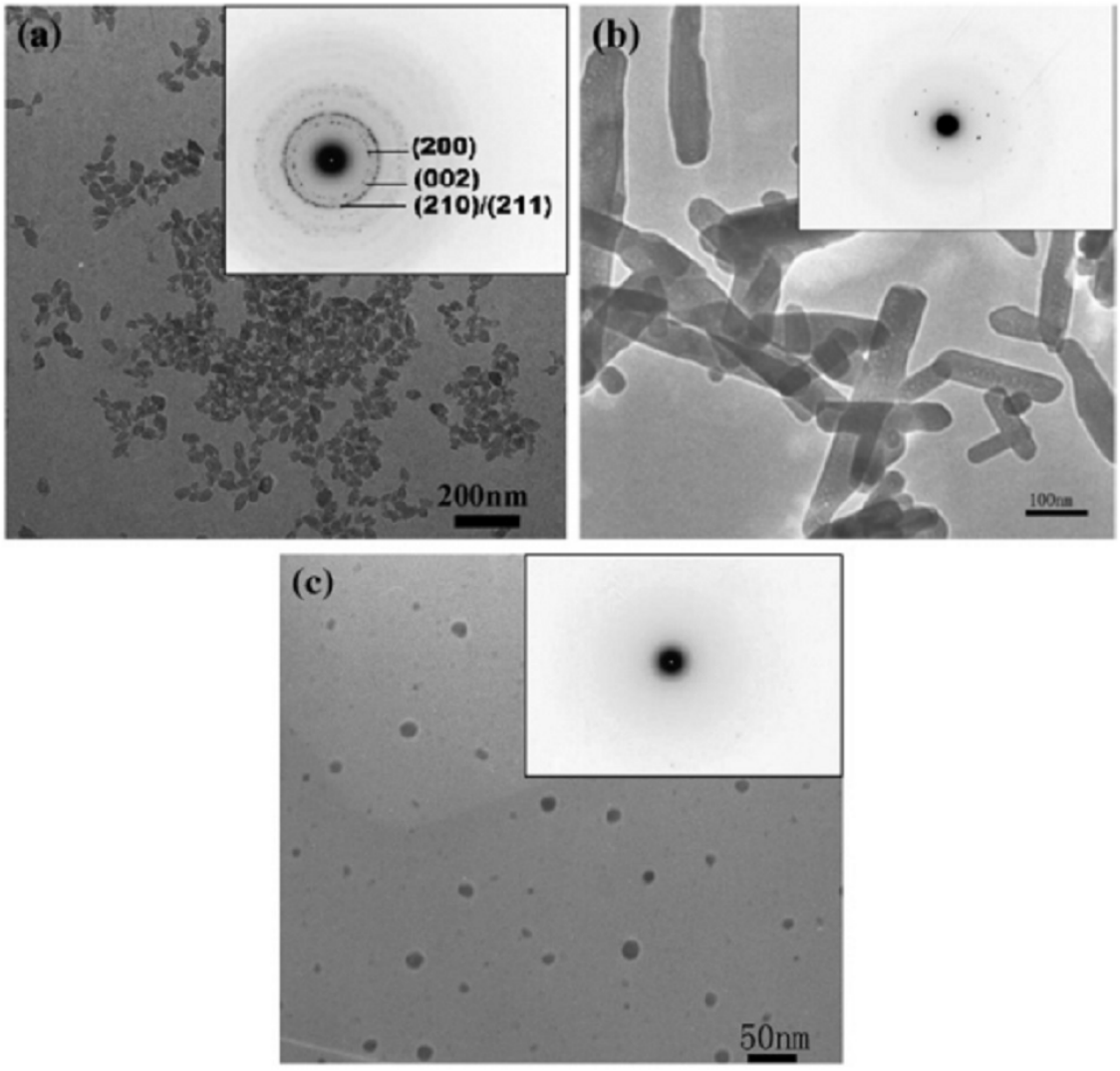


Figure 11.2. ***TEM and SAED results of nano HAP (a), cHAP (b) and ACP (c) [1].***

In the in vitro repair experiments, enamel windows obtained from human molars were treated with phosphoric acid to create an experimental model for the enamel surface. SEM images revealed the characteristic fish-scale 'keyhole' structure of native enamel, with needle-like apatite crystallites forming an organized structure on the enamel surface. Attempts at in situ remineralization using supersaturated calcium phosphate solution and ACP were unsuccessful in inducing enamel-structured HAP and resulted in weak adhesion of the newly formed calcium phosphates to the enamel surfaces [1].

When cHAP aqueous slurry was applied onto the enamel surface, the adsorption appeared easy, but the synthesized cHAP crystallites, despite being rod-like, aggregated randomly and did not form enamel-like structures by oriented assembling. The attachment of cHAP onto the enamel substrate was poor, with most crystallites readily detached from the enamel under ultrasonic conditions (Figure 11.2.).

Similarly, ACP exhibited even weaker attachment to the enamel surface compared to cHAP, with only a few particles adsorbing onto the enamel and most being washed out by ethanol. The attached ACP disappeared completely from the enamel surface after ultrasonic treatment, indicating extremely low affinity to enamel (Figure 11.3.).

Overall, neither cHAP nor ACP showed suitable properties for enamel repair, highlighting the limitations of these materials in promoting remineralization and repairing damaged enamel surfaces [1].

The experimental results demonstrate that the application of nano HAP (hydroxyapatite) effectively prevents enamel erosion and inhibits the formation of secondary caries. The fluorescence intensity analysis using confocal laser scanning microscopy (CLSM) shows a significant decrease in the penetration of the acidic solution into the enamel structure after surface treatment with nano HAP. This indicates that the nano HAP layer blocks the dissolution of enamel apatite, thereby inhibiting demineralization and subsequent caries formation.

Additionally, the nano HAP particles themselves exhibit resistance to dissolution in biological milieus, further contributing to the protection of enamel against erosion. Experimental observations confirm that the layer of nano HAP remains largely unchanged even after exposure to acidic solutions, while the natural enamel surface experiences notable demineralization. The mass loss measurements support these findings, with the nano HAP-coated enamel showing minimal mass loss compared to untreated enamel in acidic conditions (Figure 11.4.).

Furthermore, nanoidentation analysis reveals that the mechanical strength of the restored enamel surface with the nano HAP layer closely resembles that of natural enamel. The nano HAP-coated enamel exhibits similar hardness and elastic modulus values to natural enamel, indicating that the artificial repair maintains the mechanical integrity of the enamel surface.

These findings suggest that nano HAP holds promise as an effective agent for enamel repair, not only providing protection against erosion and caries formation but also preserving the mechanical strength of the restored enamel surface. The use of nano HAP offers a potential solution for addressing enamel defects and enhancing the longevity of dental restorations.

11.1.2. Conclusions

In conclusion, the resemblance between 20 nm HAP and the building blocks of enamel apatite enables effective adsorption of the artificial material onto the natural tissue. The presence of nano HAP reinforces the enamel structure, leading to the suppression of secondary caries formation and the preservation of enamel hardness.

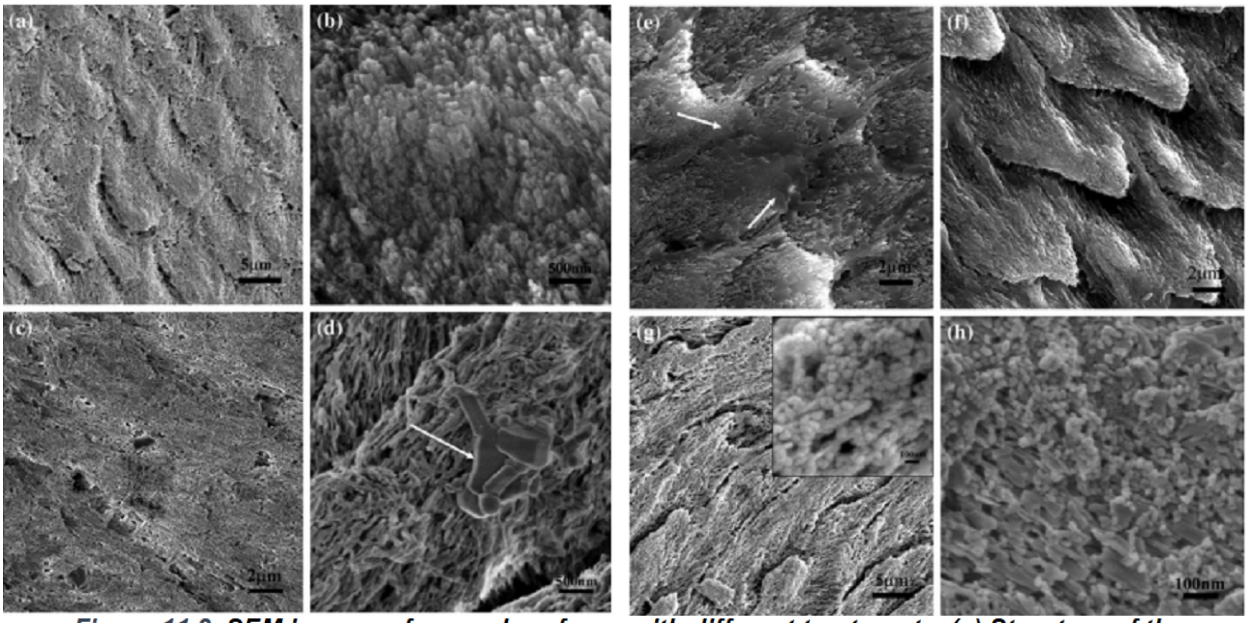


Figure 11.3. SEM images of enamel surfaces with different treatments. (a) Structure of the native enamel surface; (b) the oriented needle-like apatite crystals on the enamel surface; (c) adsorbed cHAP layer on enamel; (d) only a few cHAP crystallites (arrow) remain on the enamel surface after the ultrasonic treatment; (e) poor adsorption of ACP onto enamel (arrow); (f) all the attached ACP disappears from the enamel after the ultrasonic treatment; (g) enamel surface restored by nano HAP, the inset shows the 20 nm artificial HAP particles on enamel rods; (h) most nano HAP remains on the enamel rod after the ultrasonic treatment [1].

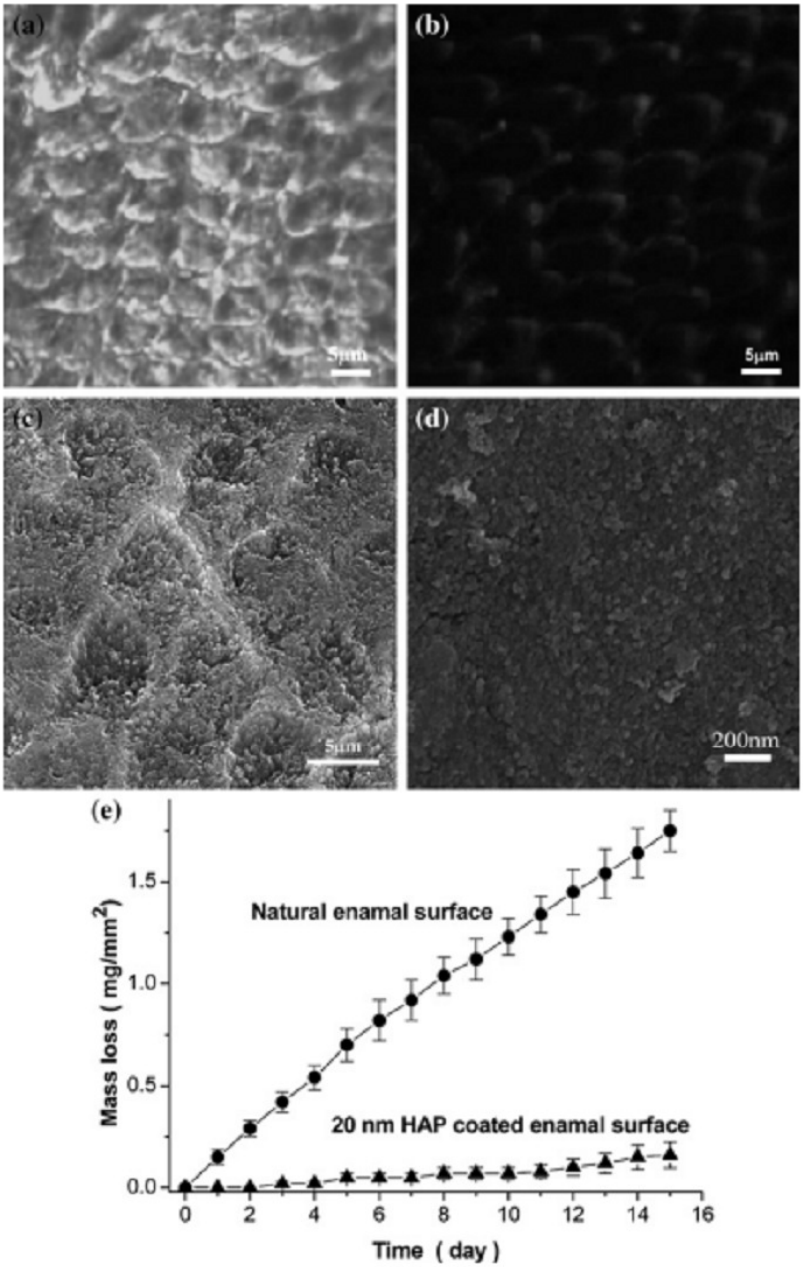


Figure 11.4. ***CLSM images of an enamel surface dyed by Rhodamine B: (a) original enamel surface; (b) enamel surface restored by nano HAP. SEM images of the enamel surface after the acidic treatment: (c) erosion of natural enamel; (d) dissolution of the enamel surface is not initiated, the layer of nano HAP stays unchanged in the acidic solution. (e) Dissolution curves (mass loss vs. time) [1].***

This approach holds promise for applications in dentistry by providing a straightforward yet efficient method for reconstructing tooth enamel affected by mineral loss.

Furthermore, the study underscores the importance of focusing on analogues of nano building blocks in biomineralization research. Despite the intricate morphology and structures of natural materials, emphasizing nano-scale counterparts may offer innovative solutions for enhancing tissue repair and regeneration in various biomedical applications [1].

11.2. Dentin Remineralization

In the context of dentin, its composition predominantly consists of collagen and minerals. Caries progression into dentin under pathological conditions results in the rapid dissolution of the dentin's mineral phase by acids. Subsequent exposure of collagen fibers to endogenous enzymes leads to their degradation, significantly compromising the mechanical properties of dentin.

Minerals within dentin can be classified into intrafibrillar and extrafibrillar categories. Intrafibrillar mineralization plays a crucial role in determining the mechanical properties of dentin at the nanoscale level. Inspired by nature's mechanisms of dentin biomineralization, bioinspired materials have achieved advancements in inducing intrafibrillar mineralization. These materials draw insights from non-collagenous proteins (NCPs), which play vital roles in regulating mineral formation and stabilizing precursors during biomineralization processes.

Material			Demineralization	Approach	Model	Performance
Peptides	8DSS peptide	8DSS peptide	37% phosphoric acid, 2 min	8DSS is coated on demineralized dentin by adding its solution: 1 mg-mL^{-1}, 1h	In vitro remineralization in artificial saliva for 3 weeks; in vitro cell experiment of human dental pulp cell	Good biocompatibility; good binding strength to dentin collagen; promote mineral regeneration and improve mechanical properties of demineralized dentin
			37% phosphoric acid, 15s		In vitro remineralization in artificial saliva for 4 weeks	Decrease dentin permeability, dentinal tubule occlusion
	DMP1-inspired peptides	DMP1-inspired peptides	14% EDTA, 10 d removal of non-collagenous proteins by the treatment of HCl and trypsin-EDTA	Immersion treatment in peptide solutions; 4%, 15 h	In vitro remineralization in wells supplied with calcium and phosphate buffer, for 2 weeks.	Bind to demineralized human dentin; stabilize nucleation clusters; promote remineralization in collagenase-challenged dentin matrices
	Amelogenin-inspired peptide	Amelogenin-inspired peptide	Demineralizing solution (2 mmol-L $CaCl_2$-$2H_2O$, 2 mmol-L KH_2PO 50 mmol-L sodium acetate, and 0.05 mol-L acetic acid), 3 d	Immersion treatment in peptide solution: 0.5 mg-mL^{-1}, overnight	In vitro remineralization in artificial saliva for 10 days	Increase mineral density, promote tensile strength, hardness, and modulus of remineralized dentin
PAMAM dendrimers	**PAMAM-COOH**	**PAMAM-COOH**	**37% phosphoric acid, 15 s; or 05 moll EDTA, 30 min, 4 mol-L guanidine chloride, 1h**	**Immersion treatment in PAMAM-PO,H, solution; 1.000 mg-mL^{-1}, 12 h**	**In vitro remineralization in artificial saliva; in vitro collagen mineralization; in vivo remineralization in the oral cavity of rats for 2 weeks**	**Promote intrafibrillar mineralization of demineralized dentin and collagen fibrils; induce remineralization in oral cavity, and promote the morphology and compactivity of newly generated minerals**
	PAMAM-POH	PAMAM-POH	0.5 M EDTA, 30 min, 4 mol-L guanidine chloride, 1h	Immersion treatment in PAMAM-PO,H, solution; 1.000 mg-mL^{-1}, 12 h	In vitro cell experiments of HepG2 cells; in vitro remineralization in artificial saliva; in vivo remineralization in the oral cavity of rats	Low cell cytotoxicity; promote mineral regeneration in vivo and in oral cavity, promote surface microhardness recovery

Polyelectrolytes-stabilized ACP	CaP-PILP	CaP-PILP	37% phosphoric acid, 20 s	CaP-PILP is added into remineralization solution	In vitro remineralization in remineralization solution for 10 days	Induce both intrafibrillar and extrafibrillar remineralization
	PAH-ACP	PAH-ACP	15% phosphoric acid, 15s	PAH-ACP loaded mesoporous silica nanoparticles are sprinkled onto dentin surface and embedded with a resin	In vitro remineralization for 3 months; in vitro cell experiment on osteogenic differentiation of hMSCs	Induce heavily mineralization; promote osteogenesis of hMSCs

Figure 11. 5. Representative biomineralization-inspired materials for dentin remineralization [4].

In the subsequent discussion, we delve into the biomineralization process of dentin and propose the requirements for biomineralization materials aimed at dentin remineralization. Additionally, we provide an overview of bioinspired materials used as analogs of NCPs for dentin remineralization, including protein-inspired peptides, poly(amidoamine) (PAMAM) dendrimers, and amorphous precursors stabilized by polyelectrolytes. Figure 11.5. summarizes the biological performances of some representative materials in this context [4].

The biomineralization process of dentin involves a series of tightly coordinated biological events. These events include odontoblast differentiation, formation of mantle dentin, mineralization of primary dentin, and the secretion of secondary and tertiary dentin. Odontoblasts play a central role in this process by producing and secreting unmineralized collagen, proteoglycans, and non-collagenous proteins (NCPs), which include dentin sialophosphoprotein and dentin matrix protein 1 (DMP1). NCPs contain abundant carboxylic acid and phosphate functional groups, making them favorable sites for mineral nucleation and subsequent crystallization. Despite constituting less than 10% of the organic matrix of dentin, NCPs actively promote and regulate the intrafibrillar mineralization of collagen fibrils.

The toughness of dentin is largely attributed to its structure, which closely resembles that of bone at the nanoscale. This structure is characterized by the highly organized arrangement of nanosized minerals within collagen fibrils. While dentin minerals can be classified as intrafibrillar and extrafibrillar based on their location, it is important to note that intrafibrillar minerals significantly contribute to the mechanical properties of dentin. Furthermore, intrafibrillar mineralization plays a crucial role in protecting collagen molecules from external challenges.

The main components of dentin and bone exhibit remarkable similarity, and their biomineralization processes share similarities as well. This similarity underscores the importance of understanding the biomineralization mechanisms of both tissues for advancing dental and bone tissue engineering strategies.

The requirements for biomineralization-inspired materials for dentin remineralization are crucial for the development of effective strategies to repair demineralized dentin. These requirements include:

1. Good biocompatibility: Since many of these materials are synthesized chemically, it is essential to ensure that they are biocompatible, meaning they do not cause harm or adverse reactions when in contact with biological tissues. Strict evaluation of biocompatibility is necessary to ensure the safety of these materials for clinical use.
2. Realization of both intrafibrillar and extrafibrillar mineralization: The mechanical properties and resistance to degradation of dentin depend significantly on the degree and pattern of mineralization. Therefore, remineralized dentin should ideally possess structures similar to native dentin, with minerals deposited both within the collagen fibrils (intrafibrillar mineralization) and in the spaces between fibrils (extrafibrillar mineralization). This comprehensive mineralization is essential for restoring the strength and durability of demineralized dentin.

3. Fast remineralization process in oral conditions: The remineralization process should occur rapidly under oral conditions, where the environment is dynamic and often acidic due to microbial activity and dietary factors. Rapid remineralization ensures timely repair of demineralized dentin and prevents further deterioration of tooth structure. Efficient remineralization methods are needed to counteract the effects of acid attack and promote the restoration of tooth integrity.

Addressing these requirements will be instrumental in developing effective biomineralization-inspired materials for dentin remineralization, ultimately improving the outcomes of dental treatments aimed at repairing and preserving tooth structure.

The 8DSS peptide, inspired by dentin phosphoprotein (DPP), has shown promising potential for dentin remineralization. Dentin phosphoprotein, which is highly acidic and contains repetitive units of Asp-Ser-Ser (DSS), plays a crucial role in regulating the nucleation and growth of hydroxyapatite (HAP), the main mineral component of dentin.

Studies have demonstrated that the 8DSS peptide can bind firmly with dentin collagen and induce mineral precipitation within the dentinal tubules and on the dentin surfaces. This remineralization process leads to significant improvements in the elastic modulus and hardness of demineralized dentin. Additionally, 8DSS treatment has been shown to effectively occlude dentinal tubules, reducing dentin permeability and alleviating dentin hypersensitivity.

However, it is noted that while 8DSS peptide shows promise in dentin remineralization and dentinal tubule occlusion, it has not yet achieved intrafibrillar mineralization of collagen fibrils. Achieving intrafibrillar mineralization would further enhance the mechanical properties and durability of remineralized dentin. Future studies may explore the stabilization effect of 8DSS on amorphous mineral precursors to potentially achieve intrafibrillar mineralization and further improve the efficacy of dentin remineralization therapies.

Peptides inspired by dentin matrix protein 1 (DMP1) have also shown promise in dentin remineralization efforts. DMP1, an acidic phosphoprotein found in dentin and bone, plays a crucial role in regulating the nucleation and growth of hydroxyapatite during biomineralization processes. Due to challenges in extracting and purifying natural DMP1, researchers have turned to small peptides inspired by DMP1 for dentin remineralization.

One such peptide, derived from the collagen-binding domain of DMP1, is the DSESSEEDR sequence, which exhibits strong collagen-binding ability. Researchers have combined this collagen-binding sequence with various functional peptide sequences, including calcium-binding peptides, to create synthetic peptides capable of binding demineralized dentin and promoting remineralization.

Additionally, peptides inspired by amelogenin, another protein present at the dentin-enamel boundary, have been explored for dentin remineralization. For example, the P26 peptide, derived from amelogenin, has been shown to stimulate interactions between collagen fibrils and amelogenin, facilitating the deposition of amorphous calcium phosphate (ACP) nanoparticles into collagen fibrils.

This peptide treatment resulted in remineralization of exposed collagen fibrils within dentinal tubules and significant improvements in the mineral density and mechanical properties of remineralized dentin.

Furthermore, inspired by cementum protein 1 (CEMP1), researchers have developed novel amphiphilic oligopeptides designed to mimic the polyelectrolyte nature of CEMP1. These peptides aim to regulate collagen mineralization in cementum and may have potential applications in dentin remineralization efforts.

Overall, peptides inspired by DMP1, amelogenin, and CEMP1 hold promise for dentin remineralization by facilitating interactions with collagen fibrils and promoting the deposition of mineral components, ultimately enhancing the mechanical properties and durability of remineralized dentin (Figure 11.6.).

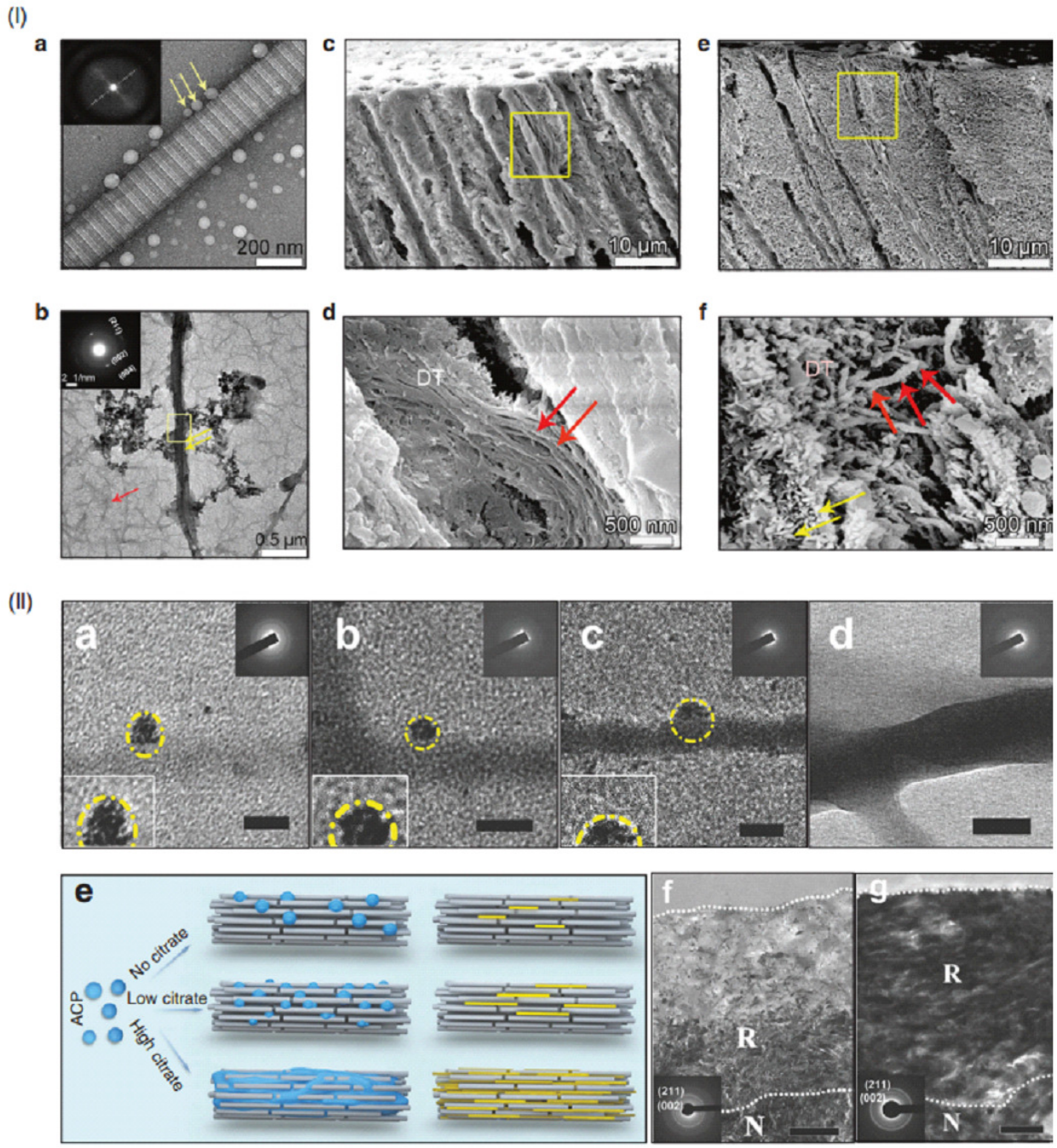


Figure 11.6. ***Schematics of biomineralization-inspired materials for dentin demineralization. (I) a TEM image of P26-collagen self-assembly. The assembled P26 peptides are dispersed nanospheres around the collagen fibril. b TEM image of collagen mineralization with P26 shows intrafibrillar mineralization and the inserted selected-area electron diffraction (SAED) image indicates the presence of HAP. Cross-sectional scanning electron microscopy (SEM) images of dentin after remineralization: c, d Control, and e, f with P26. By comparison, P26-treated dentin shows more apparent remineralization inside the dentinal tubules, which is reflected by a distinct string-of-beads morphology of the collagen fibrils. (II) a–d TEM images of ACP on collagen fibrils pretreated with different concentrations of citrate; a 0. b 25 × 10–3 M. c 50 × 10–3 M. d 100 × 10–3 M. These images indicate that citrate facilitates the infiltration of ACP into collagen fibrils. e Schematic of collagen mineralization via citrate pretreatment. Citrate decreases the contact angle and improves the wetting of ACP on collagen fibrils, and further promotes the degree of intrafibrillar mineralization. TEM images of remineralized dentin f without treatment and g with 100 × 10–3 M citrate treatment. By contrast, citrate significantly promotes dentin remineralization. Scale bars: 50 nm (a–d), and 1 μm (f, g) [4].***

Poly(amidoamine) (PAMAM) dendrimers have emerged as promising candidates for inducing dentin remineralization due to their well-defined structure and ability to mimic the functions of natural non-collagenous proteins (NCPs). PAMAM dendrimers possess distinct molecular structures consisting of a central core, branches, and terminal functional groups, which can be modified to tailor their properties for specific applications.

Studies have demonstrated that PAMAM dendrimers, such as those with carboxyl (COOH), amino (NH2), hydroxyl (OH), or phosphate (PO3H2) functional groups, can effectively promote dentin remineralization by regulating the crystallization behavior of calcium carbonate and calcium phosphate. These dendrimers have been shown to induce in situ remineralization of human dentin and intrafibrillar mineralization within collagen fibrils. Additionally, PAMAM dendrimers can be loaded with hydrophobic drugs to provide antibacterial activity alongside mineralization.

Despite these advancements, further research is needed to fully understand the interactions between PAMAM dendrimers and collagen fibrils, as well as their role in regulating mineral nucleation and growth in solution. Since the generation and terminal functional groups of PAMAM dendrimers can be altered, systematic studies are necessary to elucidate their specific mechanisms in dentin remineralization and optimize their use in dental applications. Overall, PAMAM dendrimers hold great potential for promoting dentin remineralization and addressing dental caries.

Amorphous calcium phosphate (ACP) precursor stabilized by polyelectrolytes has emerged as a promising strategy for inducing dentin remineralization. ACP is a transient phase during the formation of mineralized collagen in bone and dentin, but it is unstable and quickly transforms into more thermodynamically stable hydroxyapatite (HAP) without additives. However, polyelectrolytes, both anionic and cationic, have been studied for their ability to stabilize ACP and facilitate its infiltration into collagen fibrils, thereby promoting intrafibrillar mineralization.

Anionic polyelectrolytes, such as polyaspartic acid (PAsp) and polyacrylic acid (PAA), mimic the acidic nature of non-collagenous proteins (NCPs) found in dentin. These polyelectrolytes capture calcium ions and prevent premature crystallization of ACP. Studies have shown that ACP stabilized by anionic polyelectrolytes can induce intrafibrillar mineralization of collagen, leading to the remineralization of demineralized dentin. Additionally, molecules like L-glutamic acid, aspartic acid, citrate, and chondroitin sulfate have been introduced to enhance the crystallization kinetics or facilitate the penetration of ACP precursor into collagen fibrils, further promoting dentin remineralization.

Innovative strategies have also been developed for intrafibrillar mineralization, including the dual simulation of calcium phosphate-binding and collagen-binding motifs of NCPs. Poly(vinylphosphonic acid) (PVPA) and polyacrylic acid (PAA) have been used in combination to promote remineralization of demineralized dentin by recruiting ACP precursor into collagen fibrils. Cationic polyelectrolytes, such as polyallylamine hydrochloride (PAH), have also been shown to stabilize ACP and induce collagen mineralization. The mechanisms of polyelectrolyte-directed intrafibrillar mineralization are still under investigation, with new hypotheses proposed to explain their role in balancing electroneutrality and osmotic equilibrium during mineralization.

Overall, polyelectrolyte-stabilized ACP precursors represent a versatile and promising approach for promoting dentin remineralization, with potential applications in dental caries prevention and treatment. Further research is needed to optimize these strategies and understand their mechanisms fully.

11.3. Enamel Remineralization

Enamel, as the hardest tissue in the human body, plays a crucial role in food mastication. However, mature enamel lacks the ability to self-regenerate when subjected to significant mineral loss, such as dental caries and erosion. Despite the availability of commercial products and conventional treatment methods for enamel loss, regenerating the natural structure of enamel remains a considerable challenge. Drawing inspiration from the pathways and mechanisms of enamel biomineralization, some bioinspired materials have shown remarkable effectiveness in remineralizing and regenerating the structure of enamel.

The process of enamel biomineralization involves intricate biological events that result in the formation of enamel crystals. Understanding these processes is crucial for developing effective remineralization strategies. Key requirements for biomineralization-inspired materials for enamel remineralization include good biocompatibility, the ability to mimic both the intrafibrillar and extrafibrillar mineralization of enamel, and fast remineralization in oral conditions.

Several types of biomineralization-inspired materials have shown promise for enamel remineralization. Recombinant amelogenin, a protein involved in enamel formation, has been studied for its ability to promote enamel remineralization. Protein-inspired synthetic peptides, designed to mimic the functions of natural enamel proteins, have also demonstrated effectiveness in remineralizing enamel. Additionally, poly(amidoamine) (PAMAM) dendrimers and various inorganic materials have been investigated for their potential in enamel remineralization.

Overall, advancements in biomineralization-inspired materials offer promising avenues for the regeneration of enamel structure and the treatment of enamel loss. Further research and development in this field hold significant potential for improving dental health and addressing challenges associated with enamel damage.

The biomineralization of tooth enamel, also known as amelogenesis, is a highly regulated biological process consisting of several sequential stages. Two main functional stages are recognized: the secretory stage and the maturation stage.

During the secretory stage, specialized cells called ameloblasts are primarily responsible for producing enamel matrix proteins and proteinases. These proteins play crucial roles in controlling the shape and arrangement of the initially formed enamel crystals. This stage sets the foundation for the subsequent development of enamel structure.

In the maturation stage, there is a significant increase in the thickness and width of enamel crystals. This phase is characterized by a decrease in the abundance of proteins within the enamel matrix. As a result, the enamel becomes highly mineralized, comprising approximately 96% of mineral content along with a small proportion of residual biomacromolecules and water.

Two key issues that are integral to the biomineralization of enamel are:

1. **Structure Formation:** The arrangement and organization of enamel crystals during the secretory stage are critical for determining the structural integrity and strength of the enamel tissue. Proper alignment of the crystals ensures the formation of a dense and resilient enamel layer.
2. **Degree of Mineralization:** The degree of mineralization refers to the extent to which the enamel tissue is composed of mineral crystals. This parameter is influenced by various factors, including the activity of mineral-regulating proteins and the availability of calcium and phosphate ions during enamel formation. Achieving optimal mineralization is essential for imparting the enamel with its characteristic hardness and resistance to decay.

Understanding these key issues is essential for unraveling the intricacies of enamel biomineralization and developing strategies for promoting enamel remineralization and repair. Advances in this field hold significant promise for improving dental health and addressing enamel-related disorders (Figure 11.7.).

Material		Demineralization	Approach	Model	Performance
Proteins & peptides	Amelogenin with chitosan hydrogel	30% phosphoric acid, 30 s	The hydrogel is applied to enamel surface	In-vitro remineralization in artificial saliva, 7 days	Stabilize calcium phosphate clusters, stimulate needle-like crystals formation, and improve the bonding between enamel and newly grown layer
	shADP5 peptide	White spot lesion: daily cycling between demineralization and neutral solutions for 6 and 17.5 h, respectively	Immersion treatment in peptide solution; 0.8 mmol –L^{-1}, 10 min	In vitro remineralization in Ca^{2+}/PO_4^{3-} solution for 1 h	Facilitate the formation of dense layer of HAP crystals, and incorporate fluoride ions into the remineralized layer
	Peptide-7	37% phosphoric acid, 30 s	The peptide -7 solution is dropped on enamel surface; 2.5 mg mL^{-1}, 10 min	In vitro remineralization in artificial saliva for 8 days; in vivo remineralization in rats with caries	Strong affinity to HAP; induce the formation of compact crystal layer; excellent cariogenic prevention effect comparable to fluoride
	Oligopeptide amphiphile	**37% phosphoric acid, 60 s**	**The oligopeptide amphiphile is added into mineralization solution; 15 µg-mL^{-1}**	**In vitro remineralization in mineralization solution for 1 day or 20 days (1 mg-L^{-1} NaF is contained in the mineralization solution)**	**Induce the formation of ACP nanoparticles; improve the packing density of newly formed crystal layer of remineralized enamel**

	PTL/C-AMG	37% phosphoric acid, 50 s, or 5 min to remove the outermost prism-like enamel crystals	In vitro: immersion treatment in a PTL/C-AMG buffer; 10 min. In vivo: PTL/C-AMG buffer is injected into the oral cavity of rats	In vitro remineralization in artificial saliva for 1 week in vivo remineralization in rats oral cavity for 14 days	Induce regularly arranged enamel-like crystals with identical orientations, and restore mechanical strength to the level of natural enamel; induce enamel-like prisms in rats' oral cavity
PAMAM dendrimers	ALN-PAMAM-COOH PAMAM-PO_2H_2	37% phosphoric acid, 45 s	ALN-PAMAM-COOH is added onto enamel surface; 4 mg-mL^{-1} PAMAM-PO_2H_2 is added onto enamel surface; 1 mg-mL^{-1}	In vitro remineralization in artificial saliva for different periods; in vitro cell experiments of HepG2 cells, and L929 cells; in vivo remineralization in rats' oral cavity	Low cytotoxicity, strong binding on enamel and facilitate nanorod-like crystal formation; promote enamel remineralization in rats' oral cavity
Inorganic materials	Calcium phosphate ion clusters	37% phosphoric acid, 30 s or 10 min to remove the prism-less enamel	CPIC ethanol solution is dropped onto enamel	In vitro remineralization in modified simulated oral fluid for 48 h (15 mg L^{-1} F^- is	Induce epitaxial growth of enamel apatite, and recover hierarchical structure and
Inorganic materials	**Calcium phosphate ion clusters**	**37% phosphoric acid, 30 s or 10 min to remove the prism-less enamel**	**CPIC ethanol solution is dropped onto enamel surface; 2 mg-mL^{-1}**	**In vitro remineralization in modified simulated oral fluid for 48 h (15 mg L^{-1} F^- is involved in the mineralization solution)**	**Induce epitaxial growth of enamel apatite, and recover hierarchical structure and mechanical properties to those of natural enamel**

Amorphous ZrO2	35% phosphoric acid gel, 20 s	Amorphous ZrO2 layer is coated on enamel through in situ growth	N/A	Recover mechanical properties; prevent bacterial adhesion and proliferation

Figure 11.7. Representative biomineralization-inspired materials for enamel remineralization [4].

Amelogenin, the most crucial enamel matrix protein, plays a pivotal role in the formation of enamel, particularly in the organization of enamel rods, which are fundamental to enamel's exceptional mechanical properties.

During enamel formation, amelogenin undergoes extensive processing by enzymes after being secreted by ameloblasts. These proteolytic products of amelogenin are essential in regulating the mineralization of hydroxyapatite, the main mineral component of enamel.

One of the remarkable functions of amelogenin is its ability to self-assemble into nanoribbons. These nanoribbons serve as scaffolds that template the oriented growth of hydroxyapatite fibers. This templating process directed by amelogenin nanoribbons is crucial for the formation of enamel rods with precise shapes and alignments.

In summary, amelogenin orchestrates the formation of enamel rods through its self-assembly into nanoribbons, which guide the organized growth of hydroxyapatite fibers. This hierarchical organization at the nanoscale level is essential for the development of enamel's exquisite structural integrity and mechanical properties.

Proteins removal and enamel maturation play a critical role in achieving enamel with a high degree of mineralization during the maturation stage of enamel development. The cleavage and degradation of the proteinaceous matrix via proteolytic processes are essential for this process. Specifically, the occlusion of undegraded amelogenin inside enamel crystals, as demonstrated in studies, can lead to abnormalities in enamel crystal size, morphology, and crystallinity due to the lack of matrix metalloproteinase-20 (MMP-20) during amelogenesis.

For the remineralization of enamel, conventional substitutional materials such as amalgams, resins, and ceramics have limitations compared to native enamel in terms of chemical composition and crystal microstructures. These materials often do not provide the same level of performance and appearance as natural enamel, and they may also lead to issues such as secondary caries due to poor adhesion and fitting.

To address these challenges, researchers are turning to biomineralization-inspired materials for enamel remineralization. However, several key requirements must be met for these materials to be effective. Firstly, they must exhibit good biocompatibility to ensure their safety when in contact with the oral cavity or if ingested. Additionally, the newly regenerated enamel layer should seamlessly integrate with the original enamel, avoiding the risk of fracture at the repaired interfaces. Moreover, the regenerated enamel layer should mimic the structure of native enamel to maintain the mechanical properties of the repaired enamel. Finally, the remineralization process should occur rapidly under physiological conditions, avoiding the need for harsh operating conditions or extended application times.

Meeting these requirements will be essential for the development of effective biomineralization-inspired materials for enamel remineralization, ultimately bridging the gap between current restoration materials and the regeneration of natural enamel.

Amelogenin and its cleavage products play a crucial role in enamel formation, accounting for over 90% of the extracellular organic matrix during enamel development. Amelogenin exhibits intrinsic disorder and hydrophobicity, allowing it to self-assemble into various supramolecular structures, such as nanospheres, nanochains, and nanoribbons, which resemble the structures observed in natural enamel.

The ability of amelogenin to regulate apatite crystal formation has been utilized in the fabrication of biomaterials aimed at remineralizing enamel. Recombinant amelogenin has been introduced into mineralization solutions, where it modulates the growth of apatite crystals on substrates.

For instance, in one study, recombinant porcine amelogenin was combined with calcium phosphate to synthesize an enamel-mimicking nanocomposite coating. The self-assembly of amelogenin into nanochains facilitated the parallel arrangement of calcium phosphate crystals, resembling the organization found in natural enamel.

Another approach involves incorporating amelogenin into hydrogels, which can then be applied to the enamel surface. These hydrogels, such as amelogenin-containing chitosan (CS-AMEL) hydrogel, release amelogenin to regulate crystal growth. CS-AMEL hydrogel, for example, forms a tightly bound new layer on the enamel surface consisting of parallel nanocrystals aligned along the longitudinal direction.

However, the mechanical properties of the newly grown layer may be inferior to those of healthy enamel due to the occlusion of undegraded organic materials within the crystals. To address this issue, matrix metalloproteinase-20 (MMP-20) can be added to the hydrogel to prevent amelogenin occlusion during remineralization, thus producing biomaterials with properties more closely resembling natural enamel.

Overall, these approaches harness the biomineralization properties of amelogenin to fabricate biomaterials capable of remineralizing enamel and restoring its natural structure and properties.

Amelogenin and its cleavage by MMP-20 have been shown to play a critical role in enamel remineralization. MMP-20, when introduced into hydrogel-treated samples, enhances the degree of crystal orientation and crystallinity, leading to remarkable improvements in the mechanical properties of the induced hydroxyapatite (HAP) layer.

This innovative approach demonstrates the potential for improving the mechanical properties of repaired enamel by removing organic substances during the repair process.

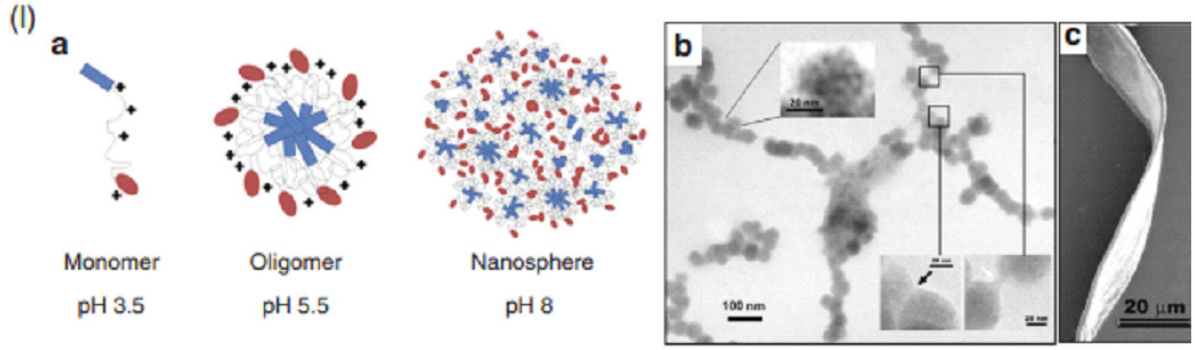
Amelogenin's unique ability to self-assemble, control crystal spacing, and bind to crystal surfaces stems from its separate functional domains, including the hydrophobic N-terminus, the central polyproline repeating domain, and the hydrophilic C-terminus.

Peptides inspired by amelogenin, such as leucine-rich amelogenin peptide (LRAP), have been used as substitutes for native amelogenin to regulate enamel remineralization. LRAP conserves critical sequences of native amelogenin and has been shown to self-assemble into nanospheres, regulate calcium phosphate mineralization, and promote crystal nucleation and growth.

Other bioinspired peptides, such as shorten human amelogenin-derived peptide 5 (shADP5) and QP5, have also demonstrated the ability to induce enamel remineralization by mimicking specific amino acid sequences of amelogenin.

Furthermore, peptides consisting of recombined domains of amelogenin, such as P26 and P32, have been synthesized and shown to self-assemble into nanospheres, regulate apatite nucleation, and induce multilayered aprismatic crystals.

These peptides offer advantages over full-length amelogenin, including reduced cost, enhanced design flexibility, and easier penetration into the enamel interior, making them promising candidates for enamel remineralization therapies (Figure 11.8.).



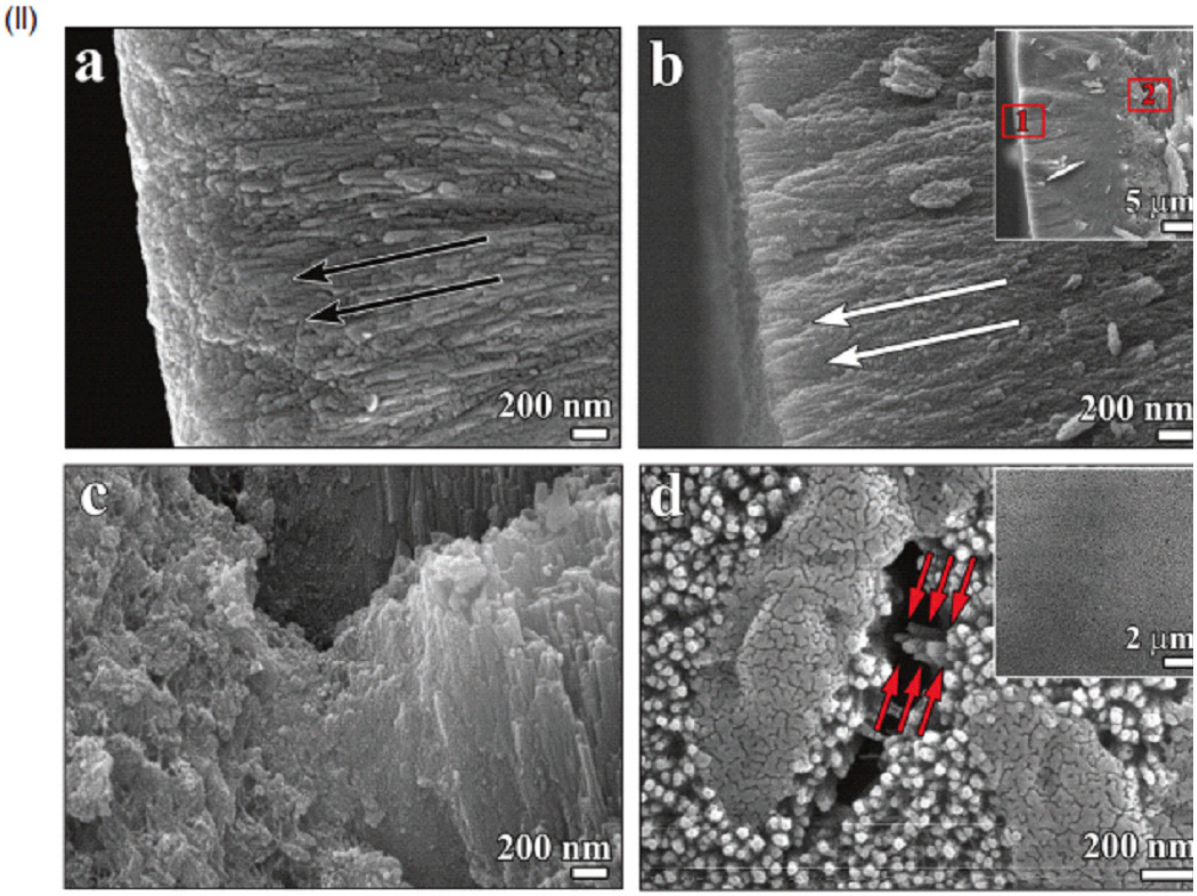


Figure 11.8. ***Schematics of amelogenin for enamel demineralization. (I) a Schematic of the formation of oligomer and nanosphere at different pH values. With the increase of pH, the amelogenin residues with positive charges are gradually deprotonated, thus the weak hydrophobic interactions lead to the formation of the nanospheres. b TEM images of the linear arrays of amelogenin nanospheres. c SEM image of a mature amelogenin ribbon showing well-defined edges. (II) a SEM images of native enamel, in which the arrows show the enamel orientation. b–d SEM images of newly formed crystal layer after the remineralization treatment with CS-AMEL hydrogel for 1 week. b Red rectangles 1 and 2 in the inserted image are selected regions in b, c. White arrows show the orientation of newly formed crystal layer. c The new layer is closely combined to the enamel surface. d Red arrows show the typical bundle of parallelly aligned crystals inside the new layer. The inserted image shows the homogenous surface of the new layer [4].***

Peptides inspired by salivary acquired pellicle (SAP) offer promising avenues for enamel remineralization. SAP is a thin layer on oral tissue surfaces composed of adsorbed proteins and glycoproteins, including phosphoproteins like statherin, histatin, and proline-rich proteins, which exhibit a high affinity for hydroxyapatite (HAP). Statherin, for instance, is a calcium-binding protein with a highly charged N-terminal fragment rich in acidic proline and tyrosine, known for its ability to prevent calcium phosphate precipitation.

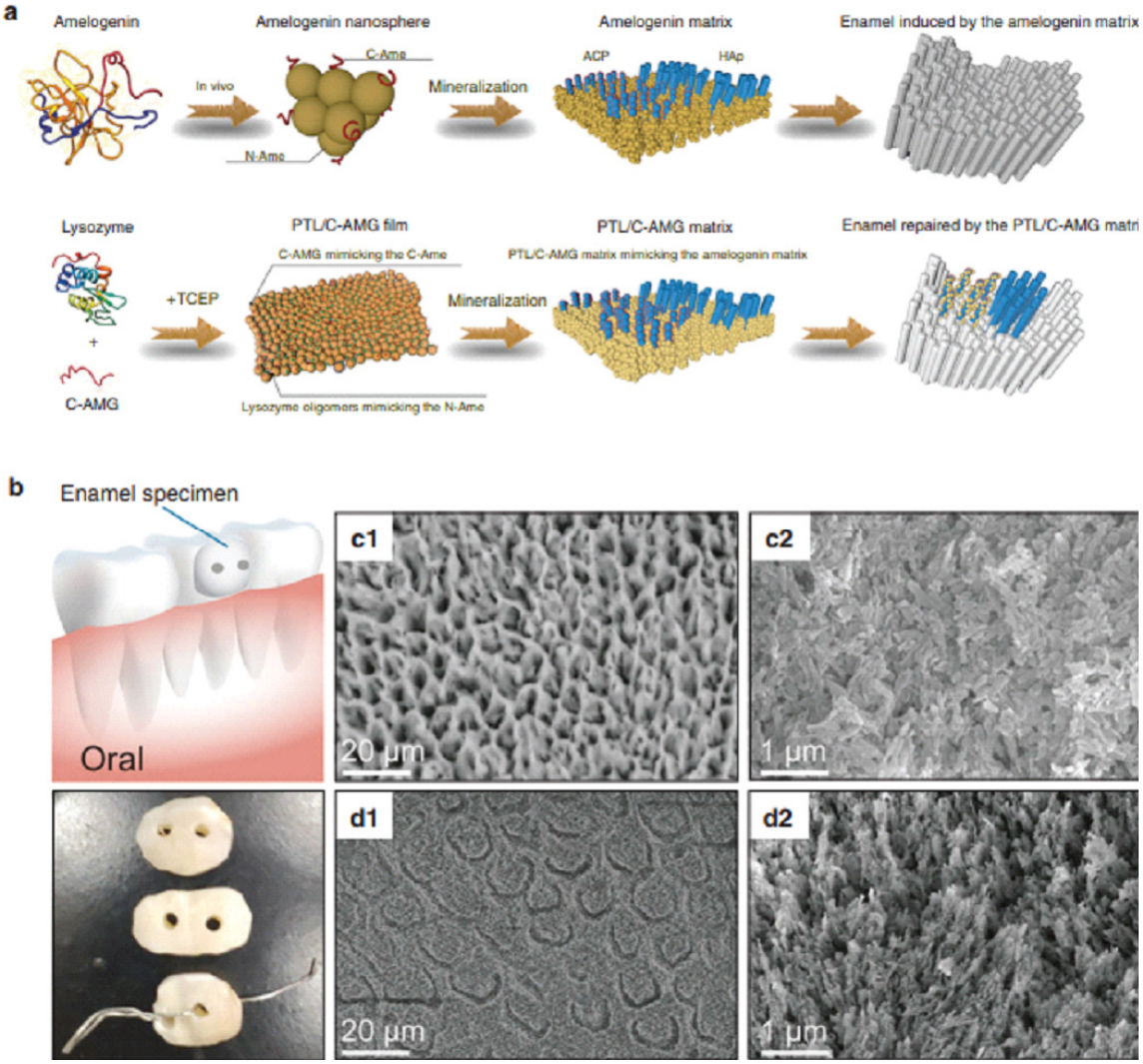
Inspired by statherin, small peptides have been designed, such as DDDDEEKFLRRIGRFG (SNA15), DpSpSEEKC, DDDEEK, and DDDEEKC, which exhibit strong binding affinity for HAP due to the conservation of the first six highly charged residues. For example, peptide-7 (DDDEEKC) was synthesized to mimic the six binding amino acids of statherin's N-terminus. Peptide-7 demonstrated robust adsorption onto HAP surfaces and induced the formation of a compact crystal layer on acid-etched enamel. Moreover, the crystals regenerated by peptide-7 exhibited properties similar to those induced by fluoride treatment and showed comparable remineralization capability to fluoride in in vivo studies. Further innovations have explored incorporating peptide-7 with oligomeric procyanidins, utilizing the cysteine residue of peptide-7 as a linkage, to confer bacteriostatic effects while inducing enamel remineralization. This dual-functionality material holds promise for resisting

bacteria and promoting enamel remineralization simultaneously. Future research in this area may focus on combining the HAP-binding capability of SAP-inspired peptides with other functional properties, such as anti-fouling properties, to broaden their applications in enamel remineralization and oral healthcare. Self-assembling peptides offer promising avenues for enamel remineralization by mimicking the abilities of extracellular matrix proteins to regulate hydroxyapatite (HAP) nucleation and growth. One extensively studied example is P11-4, a small peptide that exhibits pH-responsive self-assembly behavior through intermolecular hydrogen bonds. Treatment with P11-4 solution has been shown to increase net mineral deposition on caries-like lesions by promoting remineralization and inhibiting demineralization. P11-4 penetrates subsurface lesions and self-assembles into aggregates, promoting de novo HAP nucleation and growth. Due to its efficacy in reversing incipient carious lesions, P11-4 is commercially available in toothpaste form.

Another type of self-assembling peptide is peptide amphiphiles, which combine the bioactive functions of peptides with the physiochemical traits of surfactants. Peptide amphiphiles typically incorporate a hydrophobic alkyl chain with a peptide, enabling self-assembly through hydrophobic interactions, hydrogen bonds, and electrostatic interactions. While self-assembled peptide amphiphile nanofibers have been shown to direct HAP mineralization, there are fewer reports on their use in enamel remineralization.

Anionic self-assembling peptide amphiphiles, designed with a hydrophilic peptide tail derived from the C-terminal amelogenin, have successfully self-assembled into nanofibers with a well-defined helical twist. ACP nanoparticles were found to align along these nanofibers, leading to a higher packing density of the newly formed crystal layer during enamel remineralization.

Overall, self-assembling peptides, including P11-4 and peptide amphiphiles, hold promise for enamel remineralization by promoting the formation of densely packed crystal layers, thereby enhancing the mechanical properties and resistance to demineralization of enamel.



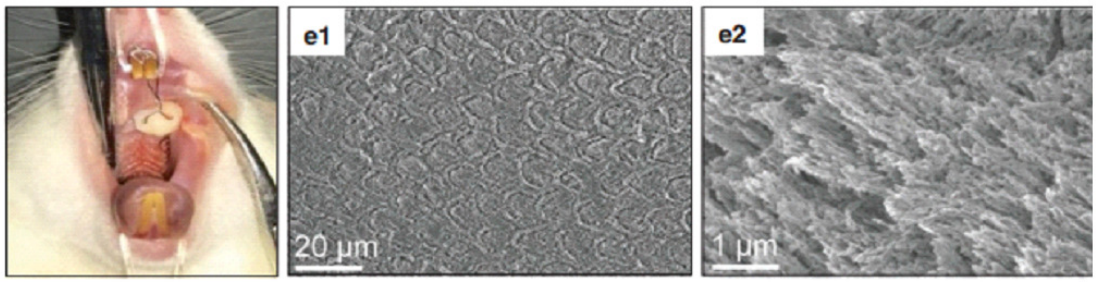


Figure 11.9. Schematic of PTL/C-AMG for enamel demineralization. a Schematic showing the similarity between amelogenin and PTL/C-AMG matrix in regulating the transition of ACP into HAP on enamel. b Schematic exhibiting the process of fixing demineralized enamel slices in the oral cavity of a rat. SEM images of c the untreated demineralized enamel, d demineralized enamel treated with fluoride, and e PTL/C-AMG film-treated demineralized enamel, after 2 weeks of remineralization in oral cavity. (c2), (d2), and (e2) are the corresponding high-magnification images of (c1), (d1), and (e1), respectively. The untreated group shows only incompact and irregular minerals. The fluoride group exhibits hollow cracks and irregular crystals. The PTL/C-AMG film group shows a "fish-scale" morphology that is similar to native enamel, and the newly formed crystals are highly oriented [4].

Several proteins and peptides, including dentin phosphophoryn (DPP), as well as peptides inspired by statherin, lysozyme, and tuftelin, have been explored for their potential in enamel remineralization.

DPP, despite not being present in tooth enamel, possesses a strong binding affinity toward calcium ions and hydroxyapatite (HAP). Peptides composed of multiple repetitive aspartic acid–serine–serine (DSS) segments, inspired by DPP, have been designed to inherit its functions. For example, 8DSS peptide has been shown to promote mineral deposition and enhance the surface roughness, hardness, and elastic modulus of demineralized enamel. Similarly, triplet repeats of asparagine–serine–serine (3NSS) peptides, derived from DSS peptides, have also demonstrated the ability to promote enamel remineralization.

Lysozyme, when induced to undergo a transition into β-sheet-rich amyloid-like aggregates, has been developed into phase-transited lysozyme (PTL), which resembles N-terminal amelogenin in its amyloid-like aggregation properties. Combining PTL with a synthesized peptide derived from amelogenin C-terminus (C-AMG) has shown promising results in inducing enamel-like crystal formation and improving mechanical properties during enamel remineralization.

Tuftelin, an acidic non-amelogenin protein found in tooth enamel, contains a domain that provides binding sites for calcium ions. A tuftelin-derived peptide (TDP), mimicking the calcium-binding domain of tuftelin, has been demonstrated to attract calcium and phosphate ions, significantly promoting the remineralization of initial carious lesions.

Overall, these proteins and peptides offer potential avenues for enamel remineralization, either through their direct effects on mineral deposition or by mimicking the properties of natural enamel proteins involved in mineralization processes. Further research is needed to fully understand their mechanisms of action and optimize their application in clinical settings.

Poly(amidoamine) (PAMAM) dendrimers have shown promise in controlling the shape and size of hydroxyapatite (HAP) crystals, akin to the functions of amelogenin, the protein involved in enamel formation. Studies have revealed that the surface groups, generations, and concentrations of PAMAM dendrimers can influence the morphology of HAP crystals. Carboxyl-terminated PAMAM dendrimers have been observed to hierarchically self-assemble into various structures, including nanospheres, nanochains, microfibers, and macroscopic aggregates. Similarly, phosphorylated dendronized PAMAMs have demonstrated self-assembly into ribbons or fibrils and induction of HAP deposition.

Several studies have focused on enamel regeneration facilitated by PAMAM dendrimers, leveraging their intrinsic similarities with amelogenin. For example, carboxyl-terminated PAMAM–alendronate conjugates have been synthesized to specifically bind to HAP surfaces, promoting the formation of nanorod-like crystals with high uniformity on acid-etched enamel. The structure of the newly grown crystals closely resembled native enamel, and microhardness was significantly restored

after mineralization. Similarly, phosphate-terminated dendrimers (PAMAM–PO3H2) have been shown to induce the formation of a fresh enamel-like layer on acid-etched enamel, indicating their potential for enamel remineralization.

These findings suggest the promising potential of PAMAM dendrimers in restoring acid-etched enamel, with opportunities for further enhancement through novel chemical modifications to their terminal functional groups. Continued research in this area could lead to the development of advanced strategies for enamel regeneration and remineralization (Figure 11.10.).

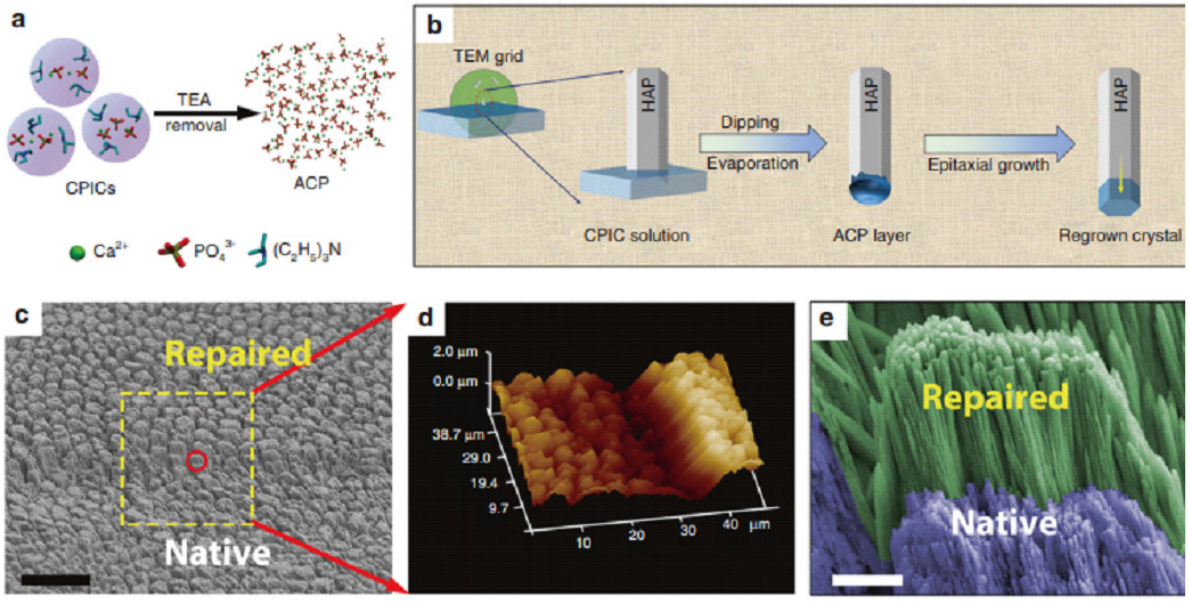


Figure 11.10. Schematics and characterizations of CPICs for enamel demineralization. a Schematic of ACP formation: ACP is formed when the stabilizer (TEA) is removed from CPICs. b Schematic of the epitaxial growth of crystalline HAP. The coating CPICs solution transforms into an amorphous frontier on the HAP surface, and then transforms into HAP. c SEM image exhibiting CPICs-repaired enamel and acid-etched enamel. The repaired enamel shows a similar morphology to that of native enamel. d 3D atomic force microscopy (AFM) image of repaired enamel indicates the formation of a new HAP layer. e High-magnification SEM image of the red circle in c, which shows the similar morphological texture between the repaired and native enamel. Scale bars: 20 μm (c), and 2 μm (e) [4].

Various calcium phosphate-based systems have been explored for their potential in enamel remineralization, leveraging the fundamental units of enamel crystals, calcium ions, and phosphate ions. Amorphous calcium phosphate (ACP) has been recognized as a crucial transient precursor in biomineralization, and efforts have been made to stabilize ACP using acidic macromolecules to fabricate bioinspired composite systems for enamel remineralization. However, the introduction of acidic macromolecules may pose challenges to the mechanical strength of repaired enamel, suggesting the need for alternative strategies utilizing degradable macromolecules to stabilize ACP.

Synthetic hydroxyapatite (HAP) has been explored as a potential solution for repairing demineralized enamel due to its chemical similarity to native enamel. However, conventional synthetic HAP often falls short in replicating the intricate structure of native enamel, resulting in less-than-optimal outcomes. In response, researchers have turned to 20 nm HAP, inspired by the nanoscale building blocks of enamel, which has demonstrated promising effects in strengthening acid-etched enamel without compromising its hardness. Furthermore, combining 20 nm HAP with glutamic acid has shown potential in promoting the regeneration of enamel-like structures under physiological conditions, although challenges persist in addressing the mechanical strength of repaired enamel.

While amorphous calcium phosphate (ACP) has shown promise in bioinspired mineralization, shortcomings remain in replicating the structure and mechanical resilience of native enamel. Efforts to induce epitaxial growth of enamel using foreign ACP phases have been impeded by oversized ACP nanoparticles. To overcome this, a novel approach based on calcium phosphate ion clusters (CPICs)

has been developed, employing small molecules to stabilize CPICs and create a mimetic biomineralization frontier for the epitaxial growth of enamel apatite crystals. This innovative strategy has demonstrated remarkable efficacy in repairing acid-etched enamel, yielding morphological texture and mechanical strength akin to native enamel, while also significantly reducing the time required for enamel repair.

The development of amorphous zirconium dioxide (ZrO2) ceramics for enamel repair represents another innovative approach inspired by the unique structure of the amorphous phase in natural enamel. This amorphous phase contributes to superior mechanical properties and acid resistance due to its lack of grain boundaries and dislocations, as well as its isotropic nature. Wei et al. devised a method to grow amorphous ZrO2 ceramics in situ for enamel repair, leveraging sequential nucleation, deposition, and growth processes. This approach resulted in the formation of a homogeneous layer of ZrO2 on acid-etched enamel, effectively restoring its mechanical properties to levels comparable to native enamel. Additionally, the amorphous ZrO2 layer exhibited high hydrophilicity, offering excellent antibacterial adhesion and proliferation capabilities.

However, it's worth noting that the in situ growth method of amorphous ZrO2 requires a high-temperature treatment process (80°C, 12 hours), presenting a significant limitation for its clinical application due to the potential risk of thermal damage to the tooth structure. Despite this limitation, the study underscores the potential of using amorphous ceramics for enamel restoration, paving the way for further exploration and refinement of techniques that could enable more practical and widespread clinical use.

The study of biomineralization pathways and mechanisms in vertebrate hard tissues offers valuable insights for the development of novel strategies and materials for tissue repair. By comprehending how biomacromolecules regulate mineral nucleation and growth, researchers have engineered a variety of bioinspired materials to mimic biomineralization processes for hard tissue repair.

These bioinspired approaches offer significant advantages over traditional methods, often utilizing synthetic analogs to natural biomacromolecules, which reduces costs and increases design flexibility. Moreover, these approaches frequently promote in situ tissue regeneration, avoiding complex procedures and harsh conditions associated with mimicking natural tissue structures directly.

Several bioinspired materials have already been commercialized and approved for clinical use in hard tissue repair, such as mineralized collagen, which mimics bone nanostructure and has shown efficacy in treating bone defects caused by various conditions. Despite these advancements, challenges persist, including incomplete evaluation of biological properties and repair effects of these materials, as well as the difficulty in replicating the structure and properties of native tissues.

Future efforts in this field should focus on understanding fundamental principles of biomineralization to conceive new tactics and materials for tissue repair. Reproducing the structure and properties of native tissues may require the use of multiple materials and fabrication methods. Incorporating antibacterial functions into bioinspired materials and combining them with growth factors, cells, or drugs may enhance repair outcomes. Finally, developing novel organic matrices as collagen alternatives could be a promising direction to address immunogenicity concerns associated with existing collagen products.

11.4. Recent Advances in Dental Hard Tissue Remineralization

Dental caries, a widespread disease affecting teeth, is characterized by demineralization and cavitation, leading to discomfort, pain, and functional limitations, along with compromised facial aesthetics.

The transmission of caries-causing bacteria, primarily Streptococcus mutans, often occurs from mothers or caregivers to children through salivary contact during the eruption of primary teeth, typically between 6 and 30 months of age, termed as a discrete window of infectivity. Caries is not a linear process but rather a cyclic event involving periods of demineralization and remineralization. When demineralization predominates, it leads to cavity formation.

During demineralization, minerals are lost from the lesion's advancing front beneath the enamel surface, driven by the transport of acid ions from plaque to the lesion and mineral ions from the lesion towards the plaque. Remineralization, a natural repair mechanism, occurs under near-neutral pH conditions, where calcium and phosphate ions are redeposited from saliva and plaque fluid into the caries lesion, forming larger and more acid-resistant hydroxyapatite (HAP) crystals.

The process of demineralization and remineralization is consistent across enamel, dentin, and root cementum; however, due to differences in their structures and the ratios of mineral to organic content, the characteristics and development of carious lesions vary among these tissues [5].

In the 1980s, fluoride was established as an effective agent for controlling caries lesions by promoting remineralization of demineralized enamel. Subsequent studies by Fazzi et al. in 1997 demonstrated that fluoride forms fluorapatite crystals by binding permanently to enamel crystals. This fluorapatite has reduced acid solubility, attributed to its lower carbonate content, as proven by Duggal et al. in 2001. However, concerns about the toxicity of high fluoride levels in dentifrices and systemic fluorides led to the development of non-toxic fluoride alternatives.

Casein phosphopeptides (CPPs) were first described as anticariogenic and anticalculus agents by Reynolds in 1993, followed by the introduction of amorphous calcium phosphate (ACP)-filled methacrylate composites in 1996. Enamelon toothpaste, is based on ACP technology and was commercially developed in 1999. By 2003, sugar-free chewing gums and mouth rinses containing CPP–ACP were available, showing effectiveness in remineralizing subsurface enamel lesions.

Sodium calcium phosphosilicate, also known as bioactive glass ceramic material, was introduced as a remineralizing agent capable of providing calcium, sodium, and phosphate ions to form hydroxyl carbonate apatite (HCA). "NovaMin" toothpaste, based on this formulation, was introduced by Dr. LenLitkowsky and Dr. Gary Hack. Recent research in remineralization has focused on biomimetic remineralization materials, initially proposed by Moradian in 2001.

Numerous types of remineralizing agents and techniques have been researched, many of which are used clinically with predictable positive results. Ideal remineralization materials should diffuse into the subsurface or deliver calcium and phosphate ions, without excess calcium or promoting calculus formation. They should also work at acidic pH levels and be effective in xerostomic patients, while enhancing saliva's remineralizing properties.

11.4.1. Fluoride

Soi et al. have identified four mechanisms of action of fluoride:

Inhibition of demineralization: Fluoride inhibits demineralization by forming fluorapatite crystals, which are more resistant to acid attack compared to hydroxyapatite (HAP) crystals found in enamel. This process reduces the dissolution of enamel minerals when exposed to acids.

Enhancement of remineralization: Fluoride speeds up the growth of new fluorapatite crystals during remineralization by facilitating the attraction and precipitation of calcium and phosphate ions. This promotes the repair of enamel lesions and strengthens tooth structure.

Inhibition of acid-producing bacteria: Fluoride interferes with the activity of acid-producing bacteria in the oral cavity by disrupting the production of phosphoenol pyruvate (PEP), a key intermediate in the glycolytic pathway of these bacteria. By reducing the acid production, fluoride helps to maintain a more neutral pH environment in the mouth, which is less conducive to enamel demineralization.

Retention on dental hard tissues and oral mucosa: Fluoride ions have the ability to adhere to dental hard tissues (such as enamel and dentin), oral mucosa, and dental plaque. This retention allows fluoride to exert its protective effects over time, decreasing demineralization and enhancing remineralization processes, thus contributing to overall oral health.

These mechanisms collectively contribute to the caries-preventive effects of fluoride, making it an important component of oral care products and preventive dental treatments [5].

11.4.2. Fluoride-containing Dentifrices

Toothpastes may incorporate fluoride in different chemical forms, such as:

- Sodium fluoride (NaF)
- Sodium monofluorophosphate (Na_2FPO_3)
- Amine fluoride ($C_{27}H_{60}F_2N_2O_3$)
- Stannous fluoride (SnF_2)

Each of these fluoride compounds plays a distinct role in oral care products. For instance, sodium fluoride is effective in directly supplying free fluoride ions.

Sodium monofluorophosphate is preferred when calcium-containing abrasives are used, as it releases fluoride ions that can form deposits on the mineral surface, such as CaF2 or CaF2-like compounds, in free or bound form.

Stannous fluoride provides both fluoride and stannous ions, with the latter acting as an antimicrobial agent.

Studies have shown the effectiveness of fluoride-containing toothpaste formulations in protecting enamel from erosive acid challenges. For example, Fowler et al. found that toothpaste formulations containing either 1426 ppm F as sodium fluoride or 1400 ppm F as amine fluoride significantly protected enamel from acid challenges compared to a placebo toothpaste with no fluoride.

In fluoride pastes containing zinc and amino acids, the amino acid prevents the formation of insoluble zinc fluoride, while the available zinc contributes to protection against erosion, reduces bacterial and biofilm, and enhances the polish of teeth.

Combining fluoride treatments with other oral care practices can further enhance remineralization. For instance, Pradubboon et al. demonstrated that using a 0.05% NaF mouth rinse in conjunction with twice-daily regular use of fluoride toothpaste effectively enhances the remineralization of incipient caries.

Light-activated fluoride (LAF) treatment is another method of fluoride delivery, where fluoride topical treatment is followed by exposure to intense monochromatic light sources, such as light-emitting diodes (LEDs) or halogen curing lights. Studies, such as the one by Mehta et al., have shown that single applications of light-curable fluoride varnishes, such as Clinpro T, can effectively prevent demineralization when combined with light activation [5].

11.4.3. Calcium Phosphate Compounds

Calcium phosphate, primarily in the form of hydroxyapatite (HA) crystals, plays a crucial role in dental health. It is a principal form of calcium found in various biological sources, including bovine milk and blood. The concentrations of calcium and phosphate in saliva and plaque are vital factors influencing the processes of tooth demineralization and remineralization.

Research suggests that maintaining an optimal calcium/phosphate ratio is essential for promoting enamel remineralization. At equal degrees of supersaturation, an optimal rate of enamel remineralization can be achieved with a calcium/phosphate ratio of 1.6. However, in plaque fluid, the calcium/phosphate ratio is typically around 0.3, indicating a lower concentration of calcium relative to phosphate.

Given the importance of calcium in enamel remineralization, providing additional calcium may help augment the process. By increasing the calcium supply, the balance between calcium and phosphate in the oral environment can be improved, potentially enhancing enamel remineralization and overall dental health [5].

11.4.4. β-TCP

The combination of tricalcium phosphate (TCP) with fluoride has been demonstrated to offer enhanced enamel remineralization and the formation of more acid-resistant mineral compared to fluoride alone. This combination is particularly effective when incorporated into toothpaste formulations.

When TCP is included in toothpaste formulations, it creates a protective barrier around the calcium, allowing it to coexist with fluoride ions.

During toothbrushing, this barrier interacts with saliva, causing it to dissolve and release calcium, phosphate, and fluoride ions. This released combination of ions can then contribute to enamel remineralization by providing essential mineral components and enhancing the effectiveness of fluoride in protecting against acid attacks and promoting remineralization.

Overall, the incorporation of TCP into toothpaste formulations provides a synergistic effect with fluoride, leading to improved enamel remineralization and greater resistance to acid challenges, thereby supporting better dental health outcomes [5].

11.4.5. Functionalized TCP

Functionalized tricalcium phosphate (TCP) is a calcium phosphate system with specific functional groups incorporated into its structure. When incorporated into a single-phase aqueous or non-aqueous topical fluoride formulation, functionalized TCP serves several purposes:

1. **Barrier Formation**: It creates a barrier that prevents premature interactions between TCP and fluoride within the formulation. This barrier ensures that the TCP remains stable until the product is applied to the teeth, maximizing its efficacy upon application.
2. **Targeted Delivery**: Functionalized TCP facilitates targeted delivery when applied to the teeth. The formulation allows for controlled release of TCP onto the tooth surface, ensuring that it reaches the desired areas for remineralization.

By combining the benefits of TCP with fluoride in a single formulation and providing controlled delivery to the teeth, functionalized TCP enhances the effectiveness of fluoride-based treatments for remineralization and dental health maintenance [5].

11.4.6. Dicalcium Phosphate Dihydrate (DCPD)

Dicalcium phosphate dehydrate (DCPD) serves as a precursor for apatite formation, particularly fluorapatite, in the presence of fluoride. When included in dentifrice formulations, DCPD has been shown to have several beneficial effects:

Increased Free Calcium Ions: DCPD inclusion leads to increased levels of free calcium ions in plaque fluid. This elevation in calcium ions persists for an extended period, up to 12 hours after brushing, when compared to conventional silica dentifrices. The presence of higher levels of calcium ions enhances the remineralization process by providing a ready source of calcium ions for enamel remineralization.

Fluorapatite Formation: DCPD readily turns into fluorapatite in the presence of fluoride. This conversion enhances the formation of fluorapatite crystals on the tooth surface, contributing to enamel remineralization and strengthening.

By promoting the release of free calcium ions and facilitating the formation of fluorapatite, DCPD inclusion in dentifrice formulations enhances their effectiveness in remineralizing enamel and improving dental health [5].

11.4.7. ACP

Amorphous calcium phosphate (ACP) serves as an initial solid phase that precipitates from a highly supersaturated calcium phosphate solution. It acts as a precursor to bioapatite and plays a crucial role as a transient phase in biomineralization processes.

The conversion of ACP to stable crystalline phases, such as octacalcium phosphate (OCP) or apatitic products, occurs through a series of steps. At physiological pH, this conversion process is described as follows:

Dissolution of ACP: Initially, ACP undergoes dissolution, leading to the release of calcium and phosphate ions into the surrounding environment.

Reprecipitation of Transient OCP Phase: The dissolved calcium and phosphate ions reprecipitate to form a transient solid phase known as octacalcium phosphate (OCP) through

nucleation and growth processes. This transient phase serves as an intermediate step in the conversion process.

Hydrolysis to Stable Apatite: The transient OCP phase subsequently undergoes hydrolysis into the thermodynamically more stable apatite phase through a topotactic reaction. This hydrolysis process involves the rearrangement of atoms within the crystal lattice, resulting in the formation of stable apatite crystals.

Overall, the conversion of ACP to apatite involves dissolution, reprecipitation of a transient OCP phase, and hydrolysis into stable apatite, ultimately contributing to the biomineralization and formation of mineralized tissues such as bone and tooth enamel [5].

11.4.8. ACP-filled Composites

Skrtic introduced a biologically active restorative material containing amorphous calcium phosphate (ACP) as a filler encapsulated in a polymer binder. This innovative material aims to stimulate the repair of tooth structure by releasing significant amounts of calcium and phosphate ions. As these ions are released, they diffuse into saliva and deposit onto tooth structures, forming an apatitic mineral similar to hydroxyapatite (HAP), which is naturally found in teeth and bone. This deposition process contributes to the remineralization and strengthening of the tooth.

Enamelon™ is a toothpaste formulation that contains unstabilized calcium and phosphate salts along with sodium fluoride. Studies have demonstrated that Enamelon™ is superior to conventional fluoride dentifrices in preventing root surface caries, particularly in patients undergoing radiotherapy. This highlights the effectiveness of incorporating calcium and phosphate ions alongside fluoride in dental products for enhanced caries prevention and tooth remineralization [5].

11.4.9. CPP–ACP

The protein nanotechnology developed by Eric Reynolds and colleagues involves casein phosphopeptide (CPP), a milk-derived protein, which can stabilize clusters of amorphous calcium phosphate (ACP) into CPP–ACP complexes. At neutral pH, the "acidic motif" in CPP is highly charged, allowing it to bind to minerals such as calcium, zinc, iron, manganese, and selenium. When CPP–ACP complexes are formed, they react to precipitate ACP material onto the tooth structure, thereby increasing calcium levels in plaque fluid.

GC Tooth Mousse Plus™ and MI Paste Plus™ are formulations containing CPP–ACP with added fluoride at a level of 900 ppm. The combination of CPP–ACP with fluoride provides additive effects in reducing caries experience. These formulations are available in various forms such as toothpaste, chewing gum, lozenges, and mouth rinses. Studies, including an in situ study conducted by Prestes et al., have demonstrated that chewing gum containing CPP–ACP significantly enhances mineral precipitation of initial enamel lesions, leading to remarkable microhardness recovery.

Reynolds et al. found that adding 2% CPP–ACP to a fluoride mouth rinse significantly increases fluoride incorporation into plaque. Additionally, Oliveira et al. demonstrated a greater protective effect against demineralization on smoother surfaces when CPP–ACP was combined with fluoride compared to CPP–ACP alone.

Other remineralization agents, such as chicken egg shell powder (CESP) solution with higher calcium content and calcium sucrose phosphate (ENAFIX), have also shown promising remineralization potential for enamel in in vitro studies. These agents contribute to the restoration of enamel mineral content and may offer additional options for enhancing enamel remineralization [5].

11.4.10. Bioactive Materials

This class of material prompts a positive reaction from the body, especially by encouraging attachment to host bone tissue and aiding in the development of a calcium phosphate layer on its surface. Bioglass (BG), a specific kind of bioactive material, is made up of calcium, sodium, phosphate, and silicate. Upon contact with body fluids, BG particles become reactive and form a layer of calcium phosphate on their surface.

Studies have demonstrated that BG particles can be deposited onto dentine surfaces. Subsequently, these particles induce the formation of carbonated hydroxyapatite (HAP)-like materials, which effectively occlude dentinal tubules. This process contributes to the restoration and protection of dentine, highlighting the potential of BG as a bioactive material for dental applications [5].

11.4.11. 45S5 BG

This bioactive glass, originally developed by Hench et al., consists of 45% SiO2, 24.5% Na2O, 24.5% CaO, and 6% P2O5 by weight. This material is very biocompatible and exhibits remarkable osteoconductivity, osteoinductivity, and controllable biodegradability. As the particle size decreases, the adhesive capacity onto the enamel surface increases, although the mechanical properties gradually decrease.

NovaMin™ is another bioactive glass formulation with the same composition as 45S5 BG, containing 45% SiO2, 24.5% Na2O, 24.5% CaO, and 6% P2O5. When applied to exposed dentin surfaces, NovaMin particles bind to the surface and form a protective layer of hydroxyl carbonate apatite (HCA), while also physically filling the open dentinal tubules. In aqueous environments such as saliva or water, the NovaMin particles release sodium ions, which elevate the local pH and facilitate the precipitation of ions to form the HCA layer [5].

11.4.12. Nanomaterials

Nanoparticles exhibit superior ion release profiles compared to microparticles. However, direct utilization of nanomaterials for tooth remineralization in the oral environment poses challenges.

Therefore, these materials are commonly incorporated into restorative materials, such as resin composites, as inorganic fillers. By doing so, nanoparticles can release calcium, phosphate, and fluoride ions, contributing to the remineralization of dental hard tissues.

This incorporation enhances the effectiveness of restorative materials in promoting tooth remineralization and improving overall oral health [5].

11.4.13. Calcium Fluoride Nanoparticles

Xu et al. demonstrated that incorporating nanoCaF2 into glass ionomer cements enhances cumulative fluoride release compared to traditional formulations.

This enhancement is attributed to the significantly higher surface area of CaF2 nanoparticles, which is approximately 20 times greater than that of conventional glass ionomer cements.

As a result, nanoCaF2 facilitates increased fluoride release, contributing to improved performance and effectiveness of the glass ionomer cement in preventing dental caries and promoting remineralization [5].

11.4.14. Calcium Phosphate-based Nanomaterials

The formulation incorporates nanoparticles of hydroxyapatite (HAP), tricalcium phosphate (TCP), and amorphous calcium phosphate (ACP) as sources to release calcium and phosphate ions. These ions work to increase the supersaturation of hydroxyapatite (HAP) within carious lesions, promoting remineralization and restoring the mineral content of the affected tooth structure. By utilizing nanoparticles of these calcium phosphate materials, the formulation can provide a higher surface area for ion release, enhancing its effectiveness in remineralizing dental lesions [5].

11.4.15. β-TCP (Ca3(PO4)2)

Functionalized β-TCP (fβ-TCP) refers to β-tricalcium phosphate that has been modified or enhanced with organic and/or inorganic materials to impart specific properties or functionalities. These modifications can be tailored to improve the material's performance in various applications, such as tissue engineering, drug delivery, and dental restoration.

Functionalization of β-TCP can involve the incorporation of biomolecules, polymers, or other substances onto its surface or within its structure. This process aims to enhance the material's biocompatibility, bioactivity, mechanical properties, or drug-loading capacity, among other characteristics.

For example, fβ-TCP may be functionalized with polymers to improve its handling properties and enhance its ability to adhere to surrounding tissues. Alternatively, biomolecules such as growth factors or cell adhesion peptides can be attached to fβ-TCP to promote cellular activity and tissue regeneration. Inorganic modifications, such as the addition of nanoparticles or surface coatings, can also be employed to confer antimicrobial properties or to modulate the material's degradation rate.

Overall, functionalized β-TCP offers a versatile platform for tailoring the properties of calcium phosphate-based biomaterials to suit specific biomedical applications [5].

11.4.16. NanoHAP Particles

Nano-sized hydroxyapatite (n-HAP) holds promise for biomimetic repair of tooth enamel due to its resemblance to the natural mineral constituent of enamel in morphology and crystal structure. Studies have shown that n-HAP particles, especially those with a size of around 20 nm, can effectively attach to demineralized enamel surfaces, inhibit further acid attack, and reduce dentinal hypersensitivity.

Research by Li et al. suggests that the dimensions of 20 nm n-HAP particles align well with nanodefects on the enamel surface caused by acidic erosion, allowing them to adhere strongly and provide protection. Additionally, commercially available nanoHAP pastes have been demonstrated to effectively reduce dentinal hypersensitivity over a period of 6 months when used as desensitizing agents.

Furthermore, comparisons between nanoHAP-containing and NovaMin-containing toothpastes have shown similar efficacy in occluding dentin tubules, indicating the potential of n-HAP in treating dentin hypersensitivity. However, it's important to note that the stability and mechanical properties of n-HAP may be inferior compared to natural enamel, and its clinical application may be limited by the time required for mineral formation, which can take several hours to days. Continued research and development are needed to address these limitations and fully realize the potential of n-HAP in clinical dentistry [5].

11.4.17. ACP Nanoparticles

ACP nanoparticles, characterized by their small spheroidal shape and nanoscale dimensions ranging from 40 to 100 nm, have garnered interest for their potential role in dental applications. These nanoparticles serve as a source of calcium and phosphate ions, which are crucial for remineralization of dental hard tissues.

Studies have incorporated ACP nanoparticles into various dental materials such as composite resins, ionomer cements, and adhesives. In particular, research utilizing in situ caries models of humans has demonstrated that nanocomposites containing nanoACP can effectively prevent demineralization at the restoration-enamel margins. Compared to control composites, these nanoACP-containing materials resulted in lesser enamel mineral loss, highlighting their potential in dental restoration.

Furthermore, in vitro studies conducted by Xu Zhang and colleagues have shown promising results regarding the remineralizing efficacy of treatments involving Pchitosan-ACP complexes. These treatments exhibited significantly higher remineralization rates compared to fluoride treatment, indicating the potential of ACP nanoparticles in promoting dental tissue remineralization and preventing caries progression.

Overall, the incorporation of ACP nanoparticles into dental materials holds promise for enhancing remineralization and protecting dental tissues from demineralization, thereby contributing to improved oral health outcomes. Continued research in this area may further elucidate the potential applications and benefits of nanoACP-based therapies in clinical dentistry [5].

11.4.18. Nanobioactive Glass Materials

The study by Sheng et al. demonstrated that nanoBG (nano-bioactive glass) particles have the ability to promote mineral formation on dentin surfaces, suggesting their potential application in enhancing dental remineralization processes. Additionally, the researchers found that the presence of nanoBG particles led to increased acid resistance of dentin.

These findings indicate that nanoBG particles have promising properties for dental applications, particularly in remineralization therapies aimed at repairing and strengthening dentin. By promoting mineral formation and enhancing acid resistance, nanoBG particles may contribute to the preservation and restoration of dental tissues, ultimately improving oral health outcomes.

Further research and clinical studies are warranted to explore the full potential of nanoBG particles in dental treatments and to determine their effectiveness and safety in various clinical scenarios [5].

11.4.19. Xylitol

Xylitol, a non-fermentable sugar alcohol, has garnered attention for its tooth-friendly properties and potential cariostatic effects. It functions by inhibiting the activity of Streptococcus mutans, a cariogenic bacteria, and reducing plaque's ability to produce acids and polysaccharides, thus exerting anticariogenic effects. Moreover, when consumed in the form of mints or gum, xylitol stimulates the production of alkaline and mineral-rich saliva, enhancing the buffering capacity against acids and providing minerals for remineralization of enamel.

However, the effectiveness of xylitol, especially when combined with fluoride, has been a subject of debate among researchers. Some studies, like the one by Milburn et al., have demonstrated that fluoride varnish containing xylitol-coated calcium and phosphate exhibits significant initial fluoride release, surpassing other varnishes. On the contrary, studies such as that by Brown et al. have failed to find any additional clinically relevant preventive effect of xylitol on caries in adults with sufficient fluoride exposure.

These contradictory reports underscore the need for further research to elucidate the potential synergistic effects of xylitol and fluoride in caries prevention. Additionally, more studies are required to better understand the optimal conditions and applications for maximizing the preventive benefits of xylitol in dental care [5].

11.4.20. Biomimetic Remineralization of the Dentin and Enamel

Research on remineralization has largely concentrated on the epitaxial growth of calcium and phosphate ions on pre-existing apatite seed crystallites. This mechanism indicates that remineralization might not occur in areas that lack seed crystallites, such as completely demineralized dentin which is devoid of these crystallites.

Conversely, biomimetic remineralization seeks to infuse demineralized dentin collagen with ACP (amorphous calcium phosphate) nanoprecursor particles that are stabilized by biomimetic analogs of non-collagenous proteins. This innovative approach to crystallization, which is particle-based, involves the sequestration of calcium and phosphate ions by biomimetic analogs of non-collagenous proteins. These ions form prenucleation clusters that evolve into larger, liquid-like ACP nanoparticles ranging from 10 to 50 nanometers in diameter.

These nanoparticles then infiltrate the intrafibrillar water compartments within collagen fibrils, initiating a process of self-assembly and crystallographic orientation to establish a metastable crystalline phase. Ultimately, these crystals merge to form single apatite crystallites within the interfibrillar spaces of collagen molecules, thus completing the remineralization process in a distinctly biomimetic fashion [5].

11.4.21. Polydopamines

The oxidative polymerization of dopamine in aqueous solutions results in the spontaneous formation of polydopamine, which mimics the adhesive properties of DOPA. Polydopamine exhibits

strong adhesion to various substrates under wet conditions. When applied to demineralized dentin, polydopamine-coated collagen fibers promote remineralization. This is because polydopamine binding to collagen fibers creates new nucleation sites that are favorable for the growth of hydroxyapatite crystals. Consequently, remineralization is facilitated in demineralized dentin treated with polydopamine [5].

11.4.22. PA

Proanthocyanidins (PA) are bioflavonoids that have a molecular structure consisting of a benzene-pyran-phenolic acid core. Grape seed extract (GSE), which is rich in PA, can create visually insoluble hydroxyapatite (HA) complexes when combined with a remineralizing solution at a pH of 7.4. Research by Cheng-fang Tan et al. noted an increase in microhardness, which was dependent on the concentration, after treating caries-like acid-etched demineralized dentine with PA-rich GSE. Furthermore, Epasinghe et al. showed in vitro that combining PA with CPP amorphous calcium fluoride phosphate (CPP-ACFP) had a synergistic effect on the remineralization of artificial root caries, leading to greater mineral deposition and increased hardness in artificial root caries lesions [5].

11.4.23. Self-assembling Peptide

Recent advancements in research have highlighted the efficacy of peptide treatments, demonstrating a combined effect of increased mineral gain and inhibition of mineral loss from the tooth. Specifically, β-sheet-forming peptides like P114 have emerged as promising candidates. These peptides have the ability to self-assemble into three-dimensional scaffolds under specific environmental conditions. Importantly, the anionic groups present in the side chains of P114 attract calcium ions (Ca++), facilitating the precipitation of hydroxyapatite (HAP) in situ. This mechanism promotes the nucleation of HAP, contributing to the remineralization of dental tissues [5].

11.4.24. Electric Field-induced Remineralization

Wu introduced a novel technique aimed at remineralizing completely demineralized dentin collagen matrix and accelerating the mineralization process. This technique, implemented in the absence of calcium phosphates and their analogs, involves the use of electrophoresis. Electrophoresis, a process that involves the movement of charged particles under the influence of an electric field, was leveraged to facilitate the incorporation of mineral ions into the demineralized collagen matrix. This innovative approach not only promotes remineralization but also reduces the time required for mineralization, offering potential benefits for dental tissue repair and restoration [5].

11.4.25. Polyamide

Poly(amidoamine) (PAMAM) dendrimers are synthetic molecules designed to mimic the self-assembly behavior of natural proteins like amelogenins. These dendrimers can form structures resembling those found in enamel in vitro and serve as organic templates for controlling the synthesis of hydroxyapatite (HAP) crystals, a key component of tooth enamel.

Chen et al. conducted research on PAMAM dendrimers modified with carboxylic acid groups (COOH) and their effect on the crystallization of HAP on etched enamel surfaces. They found that these dendrimers, acting as organic templates, induced the formation of HAP crystals on demineralized enamel surfaces. Notably, the resulting HAP crystals exhibited similar structure, orientation, and mineral phase as intact enamel, and this process occurred relatively quickly.

Overall, the use of PAMAM dendrimers holds promise for promoting enamel remineralization by facilitating the formation of HAP crystals with properties similar to natural enamel, potentially contributing to the development of effective dental remineralization therapies [5].

11.4.26. Theobromine

Theobromine, a compound found in cocoa and chocolate, is a member of the xanthine family. It has been studied for its potential to enhance the growth of enamel crystals, a key aspect of tooth remineralization.

Research conducted by Amaechi et al. compared the remineralizing effects of theobromine and sodium fluoride dentifrices. They observed a significantly higher mineral gain when using toothpaste containing both theobromine and fluoride compared to artificial saliva alone, suggesting the potential of theobromine in promoting enamel remineralization.

Similarly, Grace Syafira et al. demonstrated an increase in enamel microhardness following treatment with theobromine on the enamel surface. This suggests that theobromine may contribute to strengthening enamel.

However, it's worth noting that Abdillah Imron Nasution observed a greater increase in enamel surface hardness with fluoride application compared to theobromine. This indicates that while theobromine may have remineralizing properties, fluoride remains a more potent agent for enhancing enamel hardness.

Overall, theobromine shows promise as a natural compound for promoting enamel remineralization, but further research is needed to fully understand its effectiveness and potential benefits compared to fluoride and other remineralizing agents [5].

11.4.27. Arginine Bicarbonate

Arginine bicarbonate, an amino acid combined with particles of calcium carbonate, has been studied for its potential role in promoting enamel remineralization. This compound has demonstrated the ability to adhere to the mineral surface of enamel, releasing calcium and carbonate ions when dissolved.

The released calcium ions can then participate in the remineralization process, helping to rebuild the mineral structure of the enamel. Additionally, the release of carbonate ions may lead to a slight increase in local pH, which can contribute to a more favorable environment for remineralization.

Studies conducted by Yamashita et al. investigated the efficacy of arginine bicarbonate formulations in combination with fluoride for remineralizing demineralized enamel. Their research revealed that when used together with fluoride, arginine significantly enhanced fluoride uptake compared to fluoride alone. Furthermore, enamel lesions treated with arginine-containing toothpaste exhibited superior fluoride uptake compared to those treated with conventional fluoride toothpaste alone.

These findings suggest that arginine bicarbonate has the potential to enhance the remineralization process when used in conjunction with fluoride, making it a promising ingredient for oral care products aimed at promoting enamel health and preventing tooth decay. Further research may provide additional insights into its effectiveness and mechanisms of action in remineralization therapies [5].

11.4.28. Conclusion

The shift towards conservative approaches in restorative dentistry has led to a growing emphasis on remineralization procedures as an optimal method for regenerating lost tooth structure. Rather than resorting to traditional restorative treatments, such as fillings, preventive strategies focused on identifying, conserving, and non-restoratively treating incipient caries have become preferred options. This approach not only saves dental manpower and reduces expenses but also minimizes patient discomfort and suffering.

Initially, fluoride formulations were the primary materials used for remineralization, as they facilitated the rebuilding of hydroxyapatite (HAP) crystals by supplying essential ions that were lost from the lattice network. Over time, researchers have developed newer biomimetic remineralization products with the ability to create apatite crystals within completely demineralized collagen fibers.

These advanced materials and technologies hold promise for enhancing the remineralization process and restoring tooth structure.

In this review, various remineralization materials and technologies currently employed for remineralizing enamel and dentin are examined. It is anticipated that continued research in this field will lead to the development of even more effective products and technologies for clinical application, resulting in optimal responses and outcomes for patients. Through ongoing experimentation and innovation, the field of remineralization dentistry is poised to make significant advancements in preserving and restoring dental health [5].

11.5. Dental plaque-inspired versatile nanosystem for caries prevention and tooth restoration

Dental caries is currently one of the most widespread human diseases, affecting more than 3.5 billion people globally. Children and adults worldwide are significantly impacted, with 60-90% affected by this condition, leading to substantial financial costs and quality-of-life burdens. The consequences of tooth decay extend beyond oral health, with studies demonstrating that children with severe early childhood caries often experience poorer nutritional health compared to those without caries. Moreover, complications such as infection and sepsis resulting from untreated caries can lead to severe systemic consequences, including localized infections and, in rare cases, treatment-related deaths [6, 7, 8, 9, 10].

Dental caries is a multifactorial disease primarily caused by plaque formation and bacterial activity. Salivary proteins adhere to the tooth surface, providing a substrate for bacterial attachment and biofilm formation, ultimately leading to demineralization of dental hard tissues. Streptococcus mutans is a key cariogenic bacterium known for its ability to produce acidic environments within biofilms, which erode tooth enamel and initiate decay [11, 12, 13, 14, 15].

Traditional antimicrobials, typically broad-spectrum antibiotics, have limited efficacy against plaque biofilms due to their resistance and the buffering effect of saliva in the oral cavity, which limits the retention of drugs. Therefore, more effective strategies targeting the biological traits of acidic plaque biofilms are needed. Innovative approaches are required to combat dental caries effectively, considering the challenges posed by bacterial resistance and the unique environment of the oral cavity [16, 17, 18, 19].

11.5.1. Introduction

The recent development of intelligent stimuli-responsive nanomaterials has opened up new possibilities for targeted drug delivery in biomedical applications, including antibacterial adhesion and biofilm disruption. These nanosystems offer precise control over drug release, allowing for on-demand delivery to enhance bacterial targeting and minimize side effects and resistance. In the context of dental caries, bacteria-responsive nanomaterials hold promise for addressing the specific challenges posed by cariogenic plaque biofilms [20, 21, 22, 23].

The acidic microenvironment created by cariogenic plaque biofilms serves as a trigger for controlled drug release from intelligent nanosystems. These nanomaterials can exploit the pH fluctuations associated with caries, releasing antimicrobial agents specifically in acidic conditions while remaining inactive at near-neutral pH values, thus improving bacterial targeting and reducing off-target effects [24, 25, 26].

While antimicrobial and antiplaque properties are crucial, they are insufficient for fully restoring demineralized teeth. Current restorative therapies primarily focus on post-defect restoration and do not address the root causes of caries. New materials, such as polyacrylate acid (PAA) and casein phosphopeptide (CPP), show promise for dental remineralization but are limited by short-term drug release and the persistent presence of cariogenic biofilms [27, 28, 29, 30].

To address these limitations, the study proposes a dental plaque-inspired micellar multidrug delivery system (PMs@NaF) designed to provide intrinsic anti-caries and restorative properties in a bacteria-triggered manner. The system incorporates salivary-acquired peptide DpSpSEEK (SAP) for

selective adhesion to tooth enamel, enhancing drug efficacy and retention (Figure 11.11.). The self-assembled nanoparticle system can encapsulate multiple drugs and penetrate biofilm matrices, releasing antibacterial and restorative agents rapidly under acidic conditions [31, 32, 33, 34].

In preclinical studies using a rodent cariogenic model, topical treatment with PMs@NaF-SAP effectively inhibits biofilm formation and acid damage to tooth enamel, thereby preventing the occurrence and severity of caries. The therapeutic platform offers highly efficient biofilm disruption, enamel restoration, and on-demand drug release tailored to the pathological conditions induced by cariogenic bacteria. Importantly, this nanotherapy preserves oral microflora diversity and does not impact surrounding mucosal tissues, making it a promising candidate for clinical translation as a novel topical application to prevent dental caries and restore tooth defects [35, 36, 37].

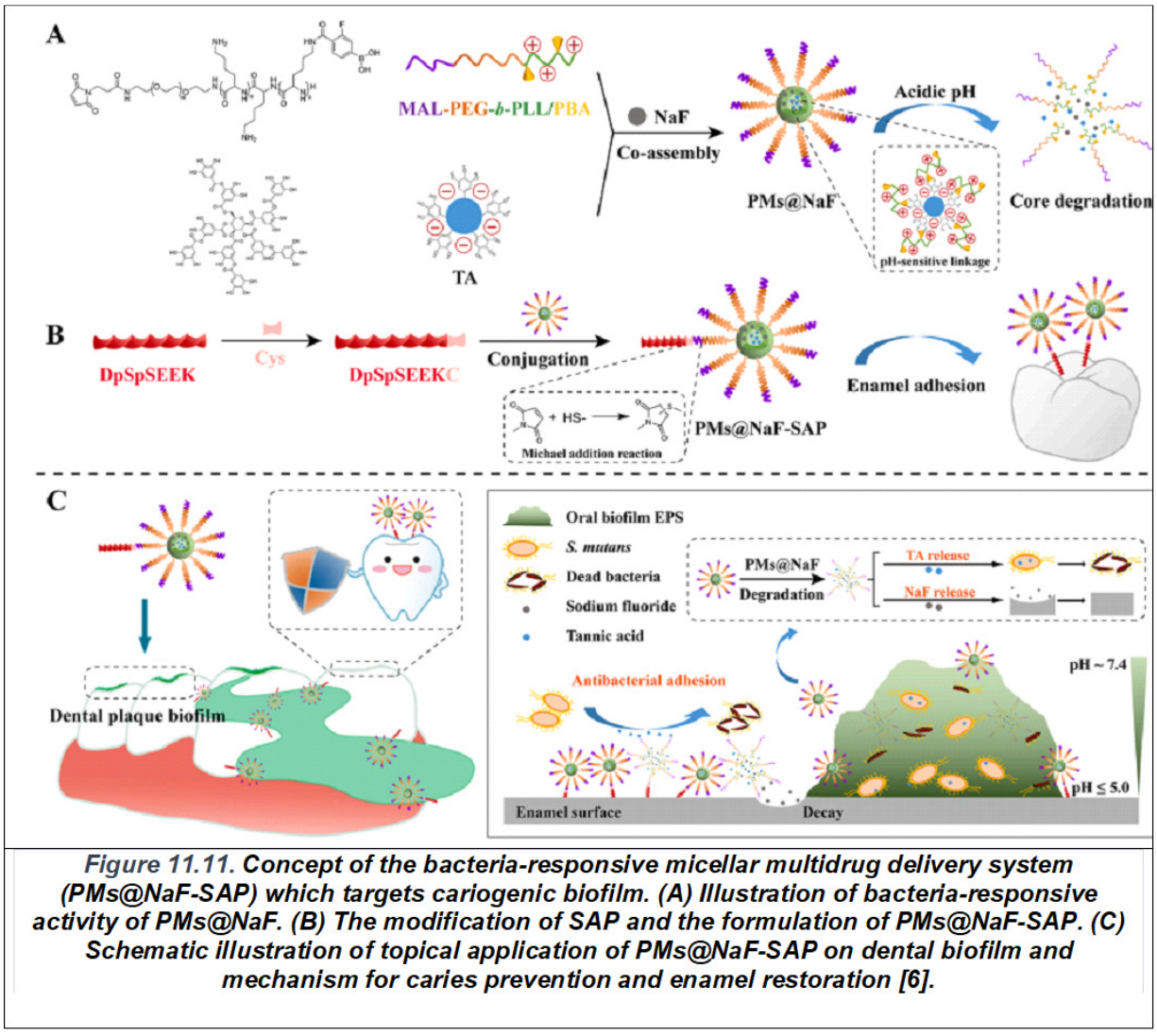


Figure 11.11. Concept of the bacteria-responsive micellar multidrug delivery system (PMs@NaF-SAP) which targets cariogenic biofilm. (A) Illustration of bacteria-responsive activity of PMs@NaF. (B) The modification of SAP and the formulation of PMs@NaF-SAP. (C) Schematic illustration of topical application of PMs@NaF-SAP on dental biofilm and mechanism for caries prevention and enamel restoration [6].

11.5.2. Process description

The chemicals and materials used in the study were obtained from reputable suppliers. Here is a brief description of each:

1. MAL-PEG-NH2: A polyethylene glycol (PEG) derivative functionalized with a maleimide (MAL) group and an amine (NH2) group, commonly used for bioconjugation and drug delivery applications.
2. ε-(benzyloxycarbonyl)-L-lysine N-carboxyanhydride: A lysine derivative used in peptide synthesis as a monomer for ring-opening polymerization.
3. Trifluoroacetic acid (CF3COOH): A strong organic acid commonly used for peptide cleavage and purification in solid-phase peptide synthesis.

4. N,N-Dimethylformamide (DMF): A common solvent used in organic synthesis, including peptide synthesis.
5. Trichloromethane (CHCl3): Also known as chloroform, it is a common solvent used in organic chemistry.
6. Hydrobromic acid (HBr): An inorganic acid used as a reagent in organic synthesis.
7. D-mannitol: A sugar alcohol used as a bulking agent or excipient in pharmaceutical formulations.
8. 3-fluoro-4-carboxy-phyenylboronic acid (FPBA): A boronic acid derivative often used in organic synthesis, including Suzuki coupling reactions.
9. 4-(4,6-dimethoxy-1,3,5-triazin-2-yl)-4-methylmorpholinium chloride n-hydrate: A coupling agent used in peptide synthesis for amide bond formation.
10. Tannic acid (TA): A polyphenolic compound with antioxidant properties, often used in dental and pharmaceutical applications.
11. Sodium fluoride (NaF): A common source of fluoride used in oral care products for its anti-caries properties.
12. Chlorhexidine (CHX): An antiseptic and disinfectant agent commonly used in dental and medical applications.
13. Triethylamine (TEA): A tertiary amine used as a base in organic synthesis reactions.
14. Peptide sequence DpSpSEEKC: A customized peptide sequence used in the study, likely designed for its specific interactions with dental enamel or biofilms.
15. S. mutans Ingbritt: A strain of Streptococcus mutans bacteria used in the study, commonly associated with dental caries.
16. Brain heart infusion (BHI) broth: A nutrient-rich medium used for culturing bacteria.
17. Mitis Salivarius Bacitricin Agar (MSBA) Base: A selective medium used for the isolation and identification of Streptococcus mutans and other oral streptococci.
18. CCK-8 assay reagent: A cell viability assay kit based on the colorimetric detection of metabolic activity.
19. LIVE/DEAD BacLightTM Bacterial Viability Kit L-7012: A fluorescence-based assay kit used to assess bacterial viability.

All chemicals were of analytical grade, ensuring high purity and reliability for use in the experiments [6].

11.5.2.1. Synthesis of polymer nanocarriers

The synthesis process involves several steps:

Synthesis of MAL-PEG-b-PLL/PBA:

1. **Polymerization Reaction:**
   - ε-(benzyloxycarbonyl)-L-lysine N-carboxyanhydride (Lys(Z)-NCA) is dissolved in DMF, followed by the addition of MAL-PEG-NH2. The mixture is stirred under dry argon at 35°C for 72 hours to initiate a polymerization reaction, resulting in MAL-PEG-b-PZLL.
2. **Precipitation and Purification:**
   - The solvent is evaporated, and the product is dissolved in CHCl3 and then precipitated in excess ether. The resulting MAL-PEG-b-PZLL is purified.
3. **Conversion to MAL-PEG-b-PLL:**
   - MAL-PEG-b-PZLL is dissolved in CF3COOH and added to HBr. After stirring at 0°C for 2 hours, the mixture is precipitated in cold ether, dissolved in DMF, and reprecipitated in excess ether to remove residual CF3COOH, yielding MAL-PEG-b-PLL.
4. **Preparation of MAL-PEG-b-PLL/PBA:**
   - MAL-PEG-b-PLL is dissolved in D-mannitol in a sodium bicarbonate solution, followed by the addition of FPBA in CH3OH and DMT-MM as a coupling agent. The mixture is stirred for 12 hours to conjugate FPBA and MAL-PEG-b-PLL by acylation. The resulting

solution is dialyzed against NaOH, HCl, and deionized water to obtain MAL-PEG-b-PLL/PBA, which is then freeze-dried.

Synthesis of PMs@NaF:

1. **Preparation of Micelle Solution:**
   - MAL-PEG-b-PLL/PBA is dissolved in deionized water, and NaF aqueous solution is added until the solute is completely dissolved.
2. **Addition of Tannic Acid (TA):**
   - TA dissolved in water is added dropwise to the solution, resulting in the formation of micelles. The solution is stirred for 4 hours at room temperature until micelles are formed, indicated by a change in solution color.
3. **Purification:**
   - The micelle suspension is purified by centrifugation using an ultrafiltration tube, obtaining the final product, PMs@NaF.

Synthesis of PMs (Control):

1. **Micelle Formation:**
   - MAL-PEG-b-PLL/PBA is dissolved in deionized water, followed by the addition of TA. The mixture is stirred for 4 hours to form micelles, similar to PMs@NaF.

Conjugation of PMs@NaF and Peptide Sequences (PMs@NaF-SAP):

1. **Modification of Peptide Sequence:**
   - The peptide sequence DpSpSEEK is modified with a cysteine at the end, forming DpSpSEEKC.
2. **Conjugation Reaction:**
   - DpSpSEEKC is added to the purified PMs@NaF solution in TEA (pH 8.0) and stirred vigorously for 2 hours at room temperature.
3. **Purification:**
   - The reaction mixture is purified by centrifugation using ultrafiltration tubes, yielding the final product, PMs@NaF-SAP, which is stored at 4°C before use [6].

11.5.2.2. Characterization of polymers

The experimental procedures for characterizing the synthesized materials are as follows:

1. Transmission Electron Microscopy (TEM):
   - Morphologies of MAL-PEG-b-PLL/PBA, PMs@NaF, and PMs@NaF-SAP are observed using TEM (JEM-100SX, Japan) to visualize their structures at the nanoscale.
2. Dynamic Light Scattering (DLS):
   - Particle size and zeta potential of the polymers are measured using DLS (Zetasizer Nano ZS90, Malvern Instruments, Malvern, UK) to determine their size distribution and surface charge.
3. Concentration Measurement:
   - Concentrations of each polymer are measured by lyophilization to determine the amount of material obtained.
4. Gel Permeation Chromatography (GPC):
   - Molecular weight and polydispersity index (PDI) of the samples are determined by GPC (Agilent PL-GPC50/Agilent 1260) to assess the molecular characteristics of the synthesized polymers.
5. Fourier Transform Infrared Spectroscopy (FTIR):
   - FTIR spectra of the samples are recorded using a Fourier transform infrared spectrometer (NICOLET 5700) to confirm the successful conjugation between PMs@NaF and SAP.

6. Proton Nuclear Magnetic Resonance Spectroscopy (1H NMR):
   - After dissolving in DMSO-d6, the 1H NMR spectra of MAL-PEG-b-PLL/PBA and PMs are recorded using a Bruker Avance spectrometer (Bruker AV II-400 MHz) to analyze their chemical structures and confirm the presence of specific functional groups [6].

11.5.2.3. In vitro drug loading and release

The experimental procedures for drug loading and in vitro pH-responsive drug release are outlined as follows:

Drug Loading

Measurement of Drug Loading Content (DLC) and Drug Loading Efficiency (DLE):

DLC and DLE of PMs@NaF and PMs@NaF-SAP are calculated using ion exchange chromatography (IEC) and high-performance liquid chromatography (HPLC).

The micellar solution is dissolved in ethanol to allow complete drug release from PMs.

The concentration of TA is quantified by HPLC at a detection wavelength of 276 nm.

Similarly, IEC measurements are performed to monitor the concentration of NaF.

DLC and DLE are calculated using the provided equations.

In vitro pH-Responsive Drug Release

Experimental Setup:

Drug release of PMs@NaF and PMs@NaF-SAP is investigated using the dialysis method.

PMs@NaF or PMs@NaF-SAP (2 mL) is transferred into a dialysis bag (MWCO 3500) and immersed into 15 mL of phosphate-buffered saline (PBS) at pH values of 5.0 and 7.4 with gentle shaking at 37°C.

Monitoring Drug Release:

At predetermined time points, samples of the release medium are collected for HPLC measurement of TA release at 276 nm.

Similarly, NaF release is measured under different pH conditions (pH 5.0, 6.5, and 7.4) using the same procedure.

Each experiment is performed in triplicate, and results are presented as the mean ± standard deviation (SD) [6].

11.5.2.4. Adsorbability of PMs@NaF-SAP on human enamel samples

The experimental procedures for specimen preparation and exploration of the adsorption capability of PMs@NaF-SAP on human enamel are described as follows:

Specimen Preparation

1. **Collection and Storage of Teeth:**
   - Non-carious human third molars that have been freshly extracted are gathered with the approval from the Ethics Committee.
   - Prior to specimen preparation, these teeth are preserved in a 0.1% thymol solution at a temperature of 4°C.
2. **Sectioning and Surface Preparation:**
   - After being separated from the roots, the crowns are cut using a low-speed, water-cooled diamond saw.
   - The crowns are then split longitudinally to expose the buccal and lingual surfaces.
   - The enamel surfaces are made flat and polished using SiC emery paper while being continuously rinsed with deionized water.
   - Acid-proof nail polish is applied to the other sides to isolate them from treatment.
3. **Ultrasonic Cleaning:**
   - Specimens are ultrasonically cleaned in deionized water for 15 minutes to eliminate any residues.
   - Before use, the samples are stored in deionized water at a temperature of 4°C.

Exploration of Adsorption Capability

1. **Visualization of Binding:**
   - Fam-labeled SAP is employed to observe the binding and localization of nanoparticles on the enamel surface.
   - Drops of PMs@NaF, Fam-labeled SAP, and PMs@NaF-SAP solutions are added to the surface of human enamel samples and incubated for 30 minutes with rocking in the dark at 37°C.
   - After incubation, samples are washed three times with PBS to eliminate any unbound materials and are then dried in a vacuum oven.
   - The enamel samples with adsorbed materials are examined using a confocal laser scanning microscope (CLSM).
2. **Testing Adsorption Time:**
   - Enamel working surfaces are treated with Fam-labeled PMs@NaF-SAP solution for 30 minutes, then rinsed three times with PBS.
   - The samples are then placed in equivalent PBS solutions and set on a rotator at 37°C in the dark.
   - Following incubation for various time intervals (0, 0.5, 1, 2, 3, 5, and 7 days), the samples are removed, freeze-dried, and analyzed using a confocal laser scanning microscope (CLSM).

These procedures allow for the exploration of the adsorption capability of PMs@NaF-SAP on human enamel and the visualization of nanoparticle binding over time [6].

11.5.2.5. In vitro antibacterial and antibiofilm experiments

Antibacterial Activity

S. mutans Growth Inhibition:

Actively growing S. mutans suspension is prepared and pipetted into 96-well plates along with PMs@NaF-SAP.

Plates are then incubated, and cell growth is measured at predetermined times using a microplate reader.

CHX and PBS with bacterial cells serve as positive and negative controls, respectively.

Biofilm Inhibition:

Overnight culture of S. mutans is subcultured to form biofilms in a 96-well plate.

PMs@NaF-SAP is added to the wells, followed by incubation.

Excess medium is discarded, and biofilm inhibition is determined by crystal violet staining.

Relative capacity of biofilm (%) is calculated, and CHX and BHIS with cells serve as controls.

Contact Angle Measurement

Hydroxyapatite discs are coated with PMs@NaF-SAP or ddH2O and dried.

Contact angle between deionized water and the surface is measured using a goniometer.

Analysis is based on three measurements per disc.

Antibacterial Adhesion Ability

Visualization and Quantification:

HA discs are coated with human entire saliva and treated with solutions.

After incubation and washing, discs are observed using CLSM to visualize penetration of PMs@NaF-SAP into biofilm.

Live/dead staining and CFU counting are performed to quantify bacterial adhesion.

In vitro Cariogenic Biofilm Model

HA discs coated with human entire saliva are seeded with S. mutans and incubated to establish biofilms.

Discs are then transferred, and the biofilm model is maintained until the end of the incubation period.

Cariogenic Biofilm Resistance

Biofilm-coated discs are topically treated with solutions and further incubated.

After incubation, discs are analyzed for antibiofilm effect using CLSM, CFU counting, and crystal violet staining.

16S rRNA PCR Analysis

qRT–PCR is used to measure the expression of S. mutans-specific genes in biofilms.

RNA is extracted, reverse transcribed, and quantitatively amplified.

Relative expression is calculated using 16S rRNA as a reference, and PCR results are analyzed [6].

11.5.2.6. PMs@NaF-SAP demineralization and remineralization assay

PMs@NaF-SAP Demineralization Assay

Simulation of Early Caries Lesions:

- Enamel windows of tooth slices are etched with phosphoric acid and washed.
- PMs@NaF-SAP, PMs@NaF, SAP, or deionized water is applied onto the enamel surface.
- Samples are rinsed and immersed in demineralization solution at 37°C for 5 hours.
- Enamel surface morphology is analyzed using FE-SEM and AFM.
- Concentrations of minerals Ca and P are measured using ICP–AES before and after treatment.
- Ca/P loss is calculated and statistically analyzed.
- XRD and EDS are used to characterize crystal texture and elemental composition of mineral loss.

PMs@NaF-SAP Remineralization Assay

Remineralization Process:

- Acid-etched enamel samples are treated with material solutions and rinsed.
- Tooth samples are immersed in remineralization solution for 24 hours.
- After incubation, samples are sonicated, washed, and air-dried.
- Enamel surface morphology is qualitatively analyzed by FE-SEM and AFM.
- Concentrations of minerals Ca and P are measured by ICP–AES.
- Ca/P gain is calculated and statistically analyzed.
- XRD and EDS are used to characterize crystal texture and elemental composition of mineral deposits.

Mechanical Property of PMs@NaF-SAP on Tooth Enamel

Measurement of Mechanical Properties:

- A Vicker's microhardness testing machine is employed to assess the surface microhardness (SMH) of enamel.
- A load of 50 g is applied for a duration of 10 seconds, with five indentations made on each sample.
- SMH values are recorded both before and after processes of artificial demineralization and remineralization.
- Calculations of surface hardness loss (% SHL) and surface microhardness recovery ratio (% SMHRR) are performed to evaluate the mineral loss and gain in the enamel, respectively.
- Atomic Force Microscopy (AFM) is utilized to examine changes in surface roughness of enamel following different treatments.

11.5.2.7. Cytotoxicity assay in vitro

Cytotoxicity Evaluation of PMs@NaF-SAP

Cell Culture:

- MC 3T3 cells are cultured in alpha-modified Eagle’s medium (α-MEM) with 10% heat-inactivated fetal bovine serum (FBS) and 1% penicillin–streptomycin at 37°C with 5% CO2 and 95% relative humidity.

CCK-8 Assay:

- MC 3T3 cells are seeded in a 96-well plate at a density of 5000 cells per well.
- After 24 hours of incubation, the medium is replaced with fresh medium containing PMs@NaF-SAP or CHX solution at various dilutions.
- Cells incubated with media serve as negative controls.
- After 24 hours of incubation with the test substances, CCK-8 solution is added to each well, and the cells are further incubated for 2 hours.
- Absorbance is measured at 450 nm using a microplate reader on Days 1, 2, and 3.
- The procedure is repeated with three wells per condition and three replicates.

Visualization of Cytoskeleton:

- The cytoskeleton of MC 3T3 cells is stained with FITC-phalloidin.
- Confocal laser scanning microscopy (CLSM) is performed to observe the morphology of cells exposed to medium containing PMs@NaF-SAP or CHX solution at various dilutions [6].

11.5.2.8. In vivo study

In Vivo Anti-Caries Efficacy of PMs@NaF-SAP

Animal Model and Experimental Setup:

- Female specific pathogen-free (SPF) Sprague Dawley (SD) rats aged 28 days were used.
- Rats were fed a cariogenic diet and 5% sucrose water to induce dental caries.
- Prior to infection, rats were prescreened for S. mutans.
- Teeth of all rats were topically inoculated with S. mutans for 7 days to induce infection.
- Rats were randomly divided into five treatment groups: distilled water (negative control), PMs@NaF, SAP, PMs@NaF-SAP, and CHX (positive control).
- Topical treatments were administered daily for 4 weeks using custom-made applicators.

Data Collection and Analysis:

- Weekly monitoring of rat weight and daily observation of physical appearances.
- Oral microbiota samples collected using sterile swabs at the end of the experiment.
- Teeth, gums, upper and lower jaws dissected and fixed in formalin (4%).
- Molars stained with murexide solution (0.4%) and prepared for caries scoring using Keyes' system.
- Caries scores determined by a calibrated examiner and two other examiners using a stereomicroscope.
- High-resolution microcomputed tomography (micro-CT) used to evaluate microarchitecture of molars and carious levels in teeth.

16 S rRNA Gene Amplicon Sequencing In Vivo

DNA Extraction and Sequencing:

- Dental microbiota samples are preserved at -80°C until it is time for DNA extraction.
- DNA extraction is carried out using the E.Z.N.A.™ Mag-Bind Soil DNA Kit.
- The extracted DNA is then sequenced at Sangon Biotech (Shanghai) Co., Ltd., utilizing primers that specifically target the V3 and V4 regions of the 16S rRNA gene.

Data Analysis:

- Sequences are clustered into operational taxonomic units (OTUs) with a 97% similarity threshold using Usearch.
- Statistical analyses and data processing are performed using R software, version 3.6.0.
- Richness, diversity, and bacterial taxon abundances are analyzed and compared using mothur.
- The differences in the relative abundance of bacterial taxa are evaluated using a t-test on the log-transformed relative abundances.

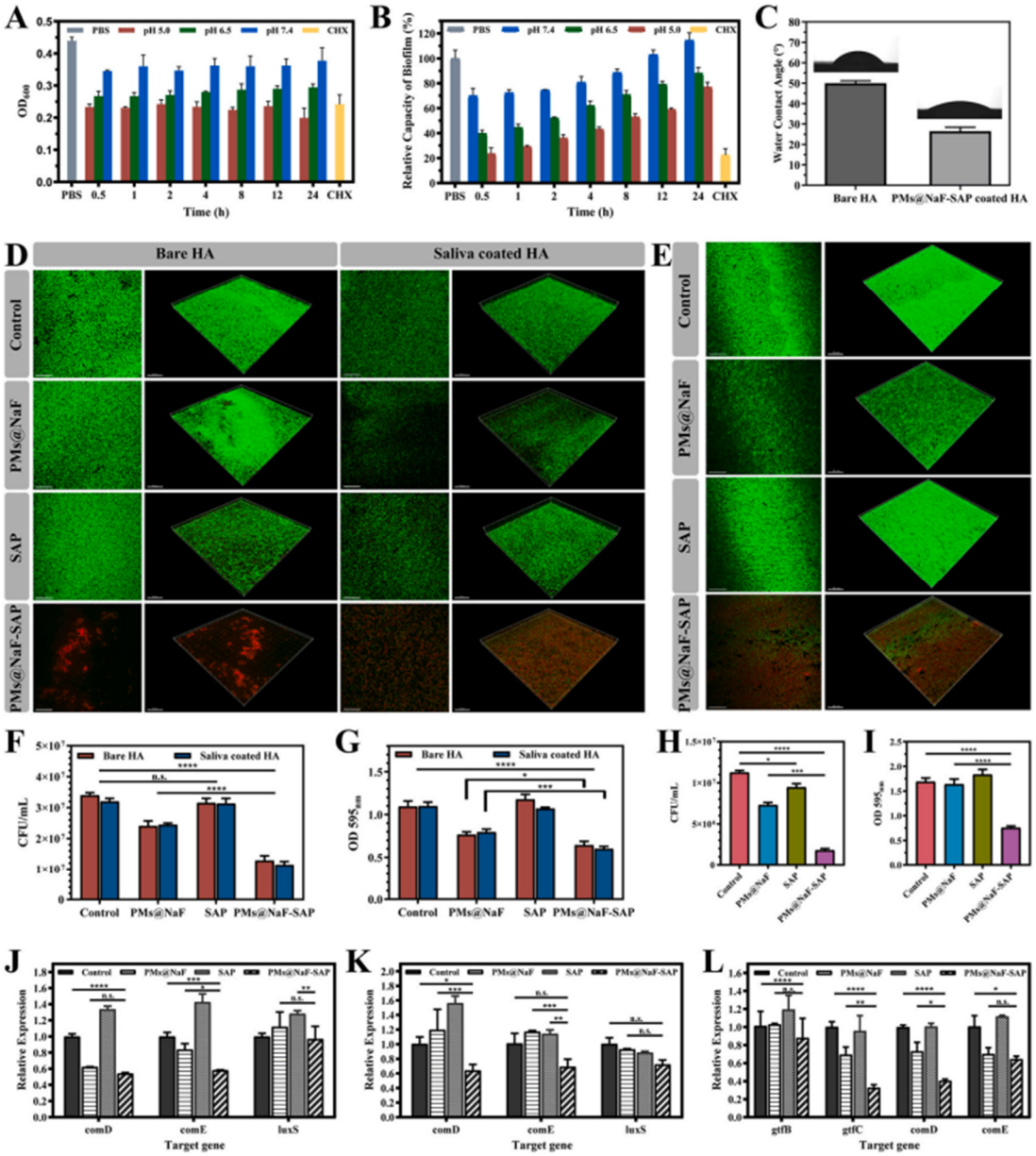


Figure 11.12. Antibacterial adhesion abilities and cariogenic biofilm resistance of topical PMs@NaF-SAP treatment in vitro. (A) OD600 value of S. mutans and (B) relative capacity of biofilm (%) as a function of incubation with PMs@NaF-SAP at pH 7.4, 6.5 or 5.0, with CHX as positive control and PBS as blank control. (C) Water contact angle (◦) of bare HA and PMs@NaF-SAP coated HA. (D) Adhesion of S. mutans on HA and sHA discs evaluated by CLSM (live cells are labeled in green by SYTO 9 and dead cells in red by propidium iodide, scale bar: 50 μm), (F) CFU counting and (G) crystal violet staining after pre-treated with sterile PBS (control), PMs@NaF, SAP or PMs@NaF-SAP solutions. (E) CLSM images (scale bar: 50 μm), (H) CFU counting and (I) crystal violet staining evaluating the penetration and antibiofilm activity of sterile PBS (control), PMs@NaF, SAP or PMs@NaF-SAP solution treating on the pre-established S. mutans biofilm. Relative expressions of genes related to S.mutans (J) on HA or (K) sHA when treated with sterile PBS (control), PMs@NaF, SAP or PMs@NaF-SAP in antibacterial adhesion assay and (L) in cariogenic biofilm resistance assay, respectively. Each experiment was performed in triplicate, and the data were presented as mean ± s.d. (n = 3). The quantitative data were subjected to Student's t-test for a pairwise comparison. *p < 0.5, **p < 0.01, ***p < 0.001, ****p < 0.0001 [6].

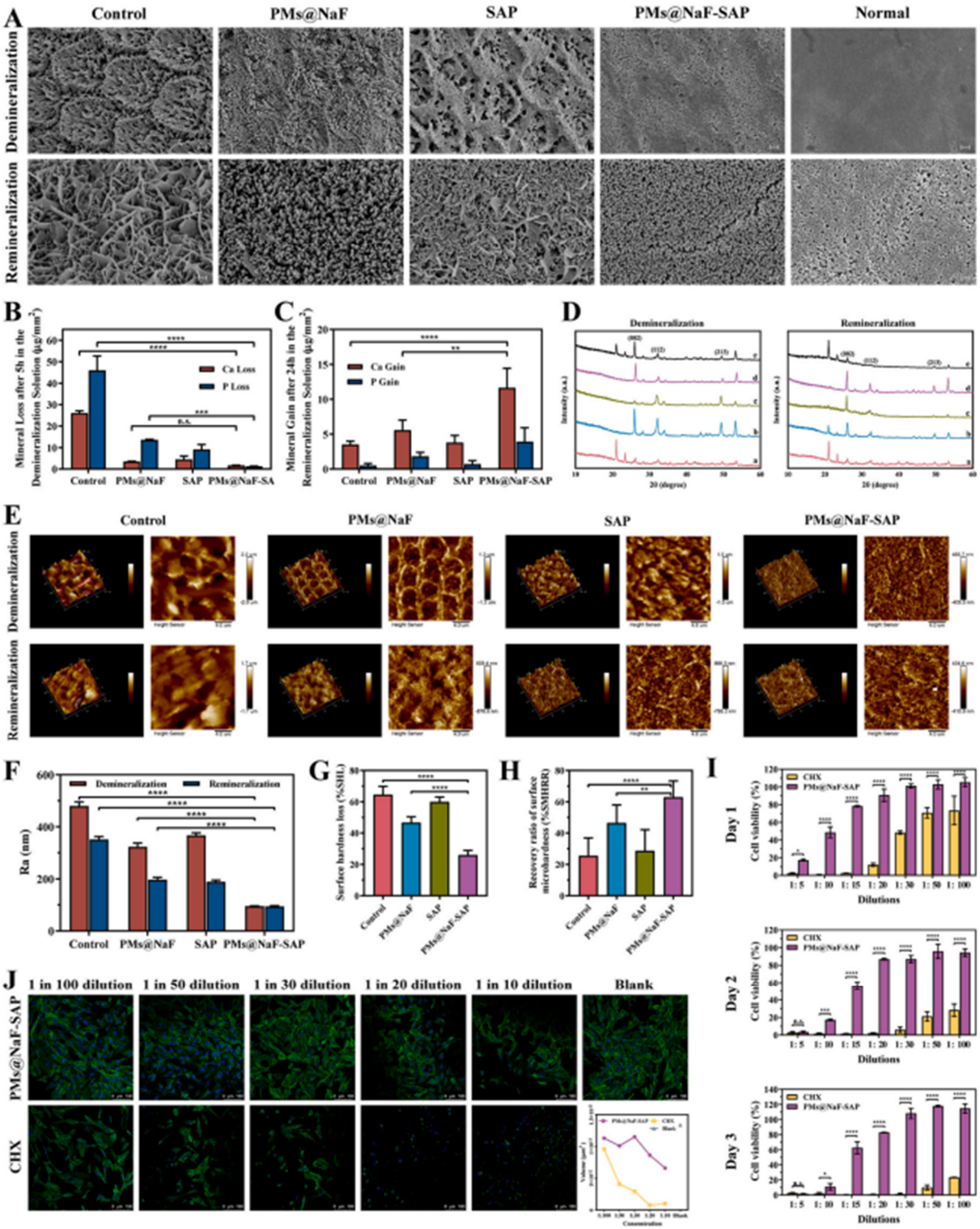


Figure 11.13. Demineralization and remineralization effects, mechanical recovery properties and cytotoxicity of PMs@NaF-SAP. (A) FE-SEM micrographs of the demineralization and remineralization surfaces in sterile PBS (control), PMs@NaF, SAP or PMs@NaF-SAP and normal enamel (scale bar: 1 μm). (B) Amount of Ca/P loss from enamel surfaces in demineralization solutions measured by ICP-AES after sterile PBS (control), PMs@NaF, SAP or PMs@NaF-SAP coating. The red bar denotes Ca loss and the blue bar indicates P loss. (C) Amount of Ca/P gain of enamel surfaces after 24 h in remineralization solutions by ICP-AES after sterile PBS (control), PMs@NaF, SAP or PMs@NaF-SAP coating. The red bar indicates the Ca gain and the blue bar denotes the P gain. (D) The XRD spectra for the mineral phase evolution on the demineralization or remineralization enamel window: the normal enamel (line a), sterile PBS coated (line b), PMs@NaF coated (line c), SAP coated (line d) and PMs@NaF-SAP coated (line e); (E) AFM images (scale bar: 4 μm) and (F) Ra of demineralization or remineralization surfaces in sterile PBS (control), PMs@NaF, SAP or PMs@NaF-SAP. (G) The % SHL of the four groups after demineralization. (H) The % SMHRR of the four groups after remineralization. (I) Cell viability of MC3T3 cells at various dilutions of medium containing PMs@NaF-SAP or CHX by CCK-8 assay. (J) Cytoskeletion staining and

fluorescence quantitative analysis of MC 3T3 cells at various dilutions of medium containing PMs@NaF-SAP or CHX, with cells untreated as the blank control (scale bar: 100 μm). Each experiment was performed in triplicate, and the data were presented as mean ± s.d. (n = 3). The quantitative data were subjected to Student's t-test for a pairwise comparison. *p < 0.5, **p < 0.01, ***p < 0.001, ****p < 0.0001 [6].

- Relative abundances, principal coordinate analysis (PCoA), and Anosim test used to assess differences between groups.

Histopathological Analysis

Tissue Collection and Staining:

- Gingival and palatal tissues collected and processed for hematoxylin and eosin (H&E) staining.

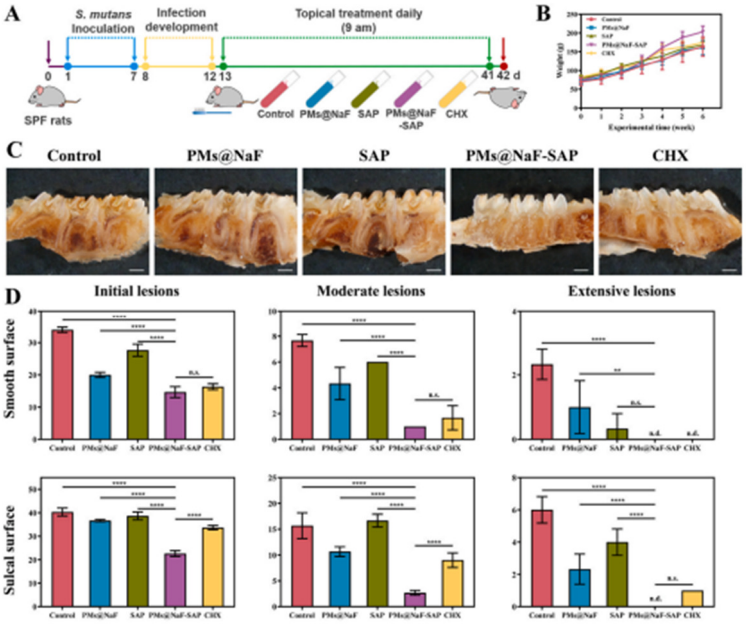
This comprehensive approach evaluates the in vivo anti-caries efficacy of PMs@NaF-SAP, encompassing microbiological, histopathological, and morphological analyses [6].

11.5.3. Conclusions

This research presents a cutting-edge, SAP-decorated bacterium-responsive, on-demand multidrug delivery system designed for both preventing dental caries and aiding in enamel restoration. This system leverages the acidic pH characteristic of cariogenic conditions as a trigger and uses MAL-modified PEG-b-PLL/PBA-sheddable micelles as nanocarriers. These micelles are loaded with the antibacterial drug TA and the restorative drug NaF. Furthermore, the bio-inspired peptide SAP DpSpSEEKC is attached to the micellar nanoparticles to facilitate specific binding to tooth surfaces.

The strong adherence of the peptide to enamel and the pH-sensitive boronate ester linkage between TA and PBA enable the PMs@NaF-SAP system to stick to tooth surfaces effectively. This adhesion withstands the buffering action of saliva in the oral environment and enhances the release of TA and NaF in response to the acidification of the oral microenvironment, particularly during caries formation. Both laboratory and clinical studies have verified that this sophisticated drug delivery system effectively adheres to bacterial surfaces and combats cariogenic biofilms, while also preventing enamel demineralization and enhancing remineralization. These capabilities help in averting tooth decay and facilitating enamel repair.

Moreover, cytotoxicity assays, analyses of the oral microbiome, and histological evaluations indicate that the nanosystem has minimal negative impact on cellular health, oral microbial diversity, and the tissues of the gums and palate. Offering distinct advantages over conventional antibiotics or restorative methods, this system provides targeted detection of cariogenic conditions, intelligent, on-demand drug release, and resilience to salivary buffering, all while preserving the diversity of the oral microbiota.



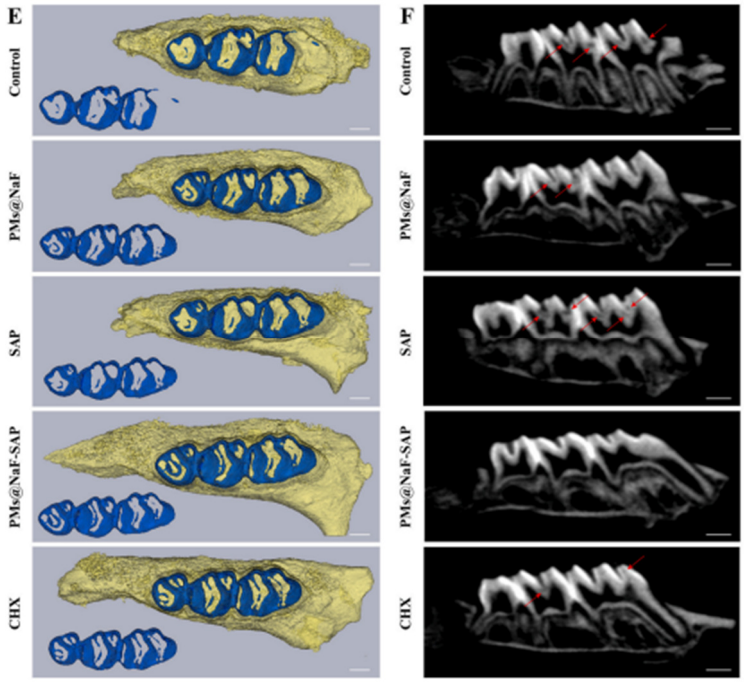
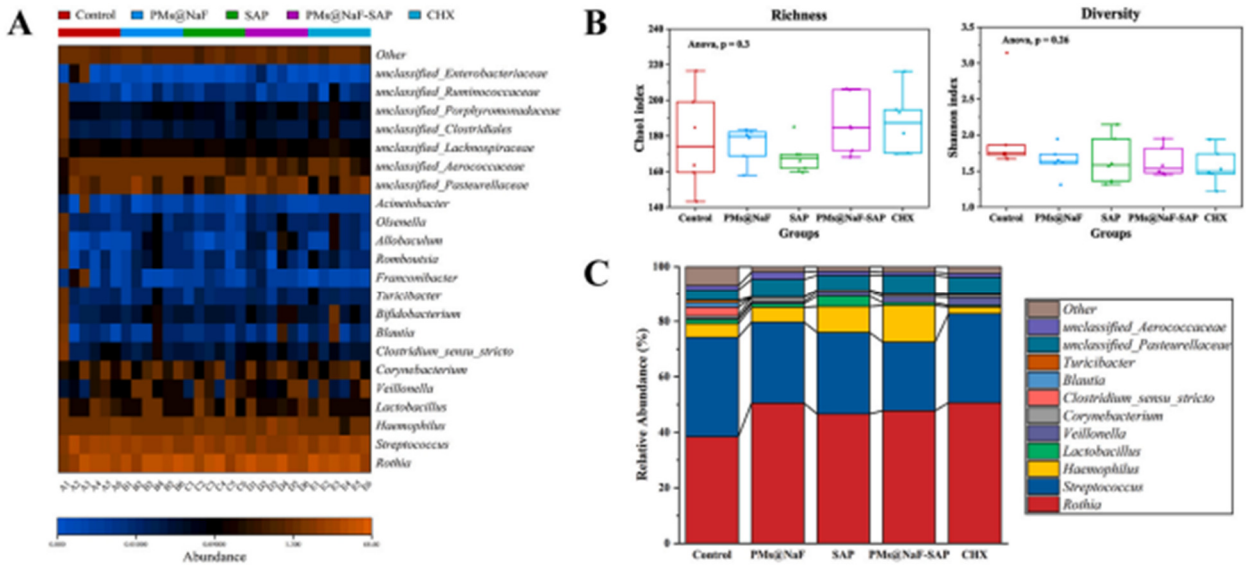


Figure 11.14. Therapeutic efficacy of topical PMs@NaF-SAP treatment against tooth decay in vivo as evaluated by Keyes' scoring and micro-CT analysis. In this model, tooth enamel progressively develops caries lesions (similar to those observed in humans), proceeding from initial lesions of demineralization to moderate lesions and on to extensive lesions characterized by enamel structure damage and cavitation. (A) Experimental design and treatment regimen of the animal model, the treatments (control, PMs@NaF, SAP, PMs@NaF-SAP and CHX) are represented in the centrifuge tubes. (B) Body weights of rats during the experimental period. (C) Images of rat teeth after treatment of the five groups (scale bar: 1 mm). (D) Caries onset and severity of smooth and sulcal surfaces. Caries scores are recorded as stages and extent of carious lesion severity according to Larson's modification of Keyes' scoring system. Data were presented as the mean ± s.d. (n = 6); ordinary oneway ANOVA, p value < 0.01, 0.001 and 0.0001 are indicated by **, *** and *, respectively; n.s. nonsignificant; n.d. nondetectable. (E) Threedimensional reconstruction of micro-CT images of maxillary molars in five groups, separated enamel (blue) by setting the density threshold above 4500 Hounsfield units (scale bar: 1 mm). (F) 2D scale sagittal images of the maxillary molars analyzed by micro-CT (red arrows, caries lesion sites, scale bar: 1 mm) [6].***



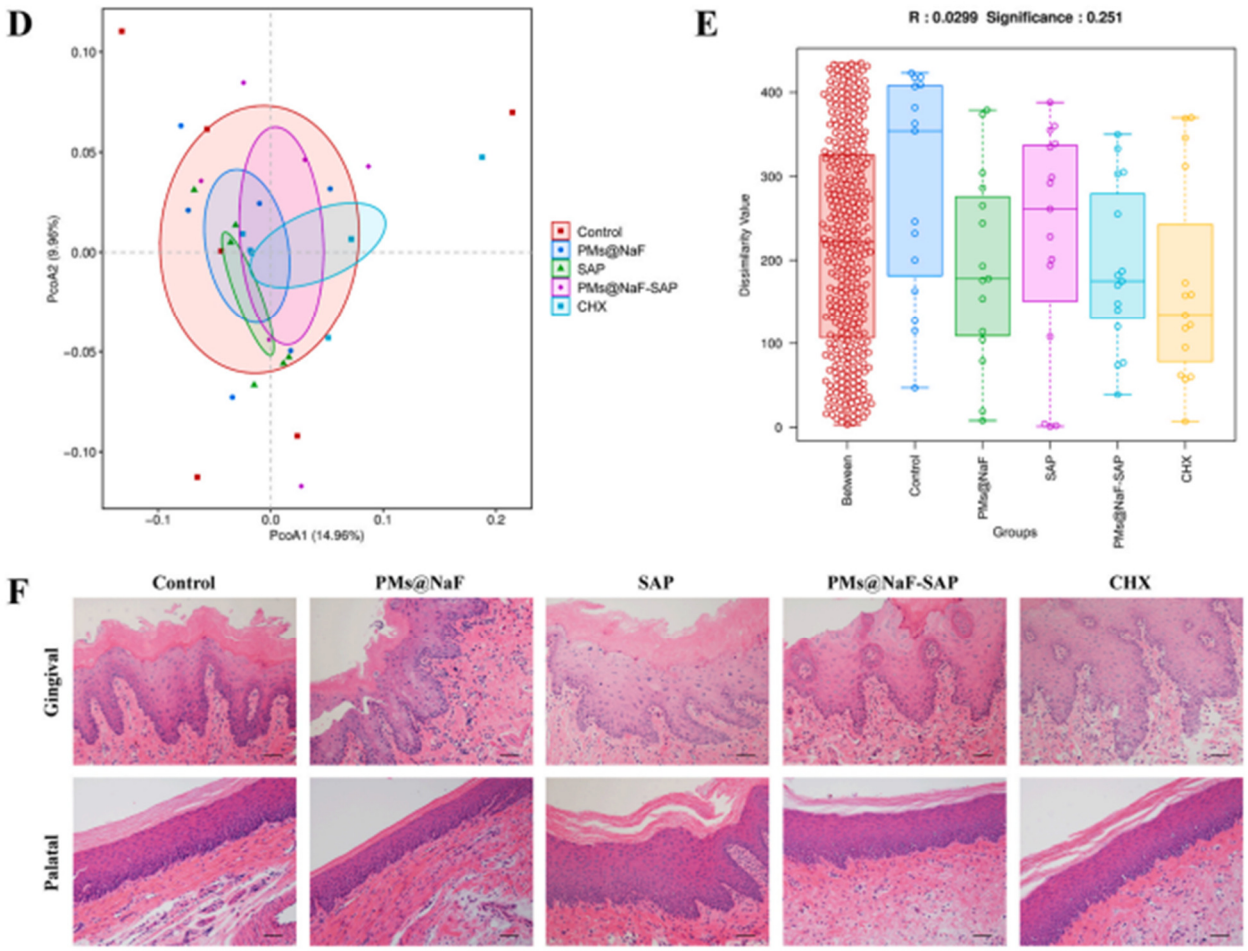


Figure 11.15. The effects of topical PMs@NaF-SAP treatment on oral microflora and soft tissue over 28 days are detailed through various analytical methods: (A) A heatmap illustrates the main bacterial types found across samples, categorized according to treatment. This visual representation helps identify which bacteria are prevalent in each treatment group, showing how the treatment influences the microbial composition. (B) The microbial diversity within the samples is assessed using the Chao 1 richness index and Shannon α-diversity index. The display includes whiskers that extend from the box to represent the upper and lower quartiles of data, offering insights into the microbial richness and diversity changes post-treatment. (C) This section compares the relative abundances of bacteria within different body sites of rodents for each treatment group. It highlights how the treatments affect local bacterial populations at specific sites. (D) A Weighted Unifrac Principal Coordinates Analysis (PCoA) plot is used to show the β-diversity among the groups. The analysis indicates that the bacterial composition in the PMs@NaF-SAP group is consistent between samples, suggesting a stabilizing effect of the treatment on microbial communities. (E) The Bray-Curtis Analysis of Similarities (ANOSIM) test, with an R value close to 0 and a p value greater than 0.05, demonstrates that there are no significant differences between and within groups based on their Bray–Curtis distances. This suggests that the treatment does not cause significant shifts in the microbial community structure compared to controls. (F) Histopathological examination of gingival and palatal tissues in rats treated with PMs@NaF-SAP shows similarities to the control group, with no significant tissue changes observed (scale bar: 50 μm).

Therefore, the topical application of PMs@NaF-SAP could expand the limited clinically available options for caries prevention and defect restoration therapy. Application to rodent caries models could facilitate the development of clinically effective mouthwash, spray, paint, or related anti-caries products. This system is expected not only to provide guidance and support for the innovation of existing post-defect restoration strategies but also to constitute significant progress in the construction and clinical transformation of smart controlled drug delivery in disease prevention and restoration (Figure 11.15.).

11.6. Quiz 11.

1. Which nanoparticles are commonly incorporated into dental materials for their preventive dentistry applications?
A) Silicon dioxide nanoparticles in dentifrices
B) Gold nanoparticles in mouthwashes
C) Silver nanoparticles in fissure sealants
D) Carbon nanotubes in electronic circuits
E) Titanium dioxide nanoparticles in bonding agents

2. What advantages do 20 nm hydroxyapatite (HAP) nanoparticles offer in enamel repair compared to conventional restorative materials?
A) Improved color matching with natural teeth
B) Enhanced biocompatibility and stronger adsorption onto enamel surfaces
C) Increased resistance to thermal changes
D) Better durability in high humidity environments
E) Superior mechanical strength and prevention of demineralization

3.What are the key findings from the enamel repair experiments using nano HAP?
A) Nano HAP prevents enamel erosion and caries.
B) cHAP and ACP strongly adhere to enamel.
C) Nano HAP resists dissolution, protecting enamel.
D) cHAP and ACP form enamel-like structures.
E) Nano HAP-restored enamel matches natural enamel strength.

4. What are essential requirements for dentin remineralization materials?
A) High thermal conductivity
B) Biocompatibility
C) Intrafibrillar and extrafibrillar mineralization
D) Rapid remineralization in oral conditions
E) Electric conductivity

5. What are the promising strategies for promoting dentin remineralization according to recent studies?
A) PAMAM dendrimers regulate calcium carbonate and phosphate crystallization, offering potential for remineralization and antibacterial applications.
B) Anionic polyelectrolytes like PAsp and PAA stabilize amorphous calcium phosphate (ACP), inducing intrafibrillar mineralization.
C) Cationic polyelectrolytes are ineffective in stabilizing ACP and promoting dentin remineralization.
D) Poly(vinylphosphonic acid) (PVPA) and polyacrylic acid (PAA) recruit ACP into collagen fibrils, enhancing remineralization.
E) Thermal treatment methods to strengthen dentin's mechanical properties.

6. What key insights do recent advancements in biomineralization-inspired materials for enamel remineralization reveal?
A) Recombinant amelogenin and synthetic peptides can mimic natural enamel proteins, promoting remineralization.
B) Only traditional dental treatments and commercial products are effective in regenerating enamel structure.
C) Poly(amidoamine) (PAMAM) dendrimers and inorganic materials have shown

potential in enamel remineralization.
D) Understanding the secretory and maturation stages of amelogenesis is irrelevant to developing remineralization strategies.
E) Fast remineralization in oral conditions is not a critical requirement for biomineralization-inspired materials.

7. How do SAP-inspired peptides and self-assembling peptides contribute to enamel remineralization?
A) SAP-inspired peptides like peptide-7 mimic the HAP-binding sites of statherin, promoting compact crystal layer formation on enamel.
B) Self-assembling peptides such as P11-4 and peptide amphiphiles direct HAP nucleation and growth, enhancing enamel's mechanical properties.
C) Peptide-7 combined with oligomeric procyanidins offers bacteriostatic effects alongside enamel remineralization.
D) SAP-inspired peptides decrease the mechanical strength of enamel by promoting loose crystal formation.
E) Self-assembling peptides are ineffective in reversing carious lesions and do not promote remineralization.

8. What are the four mechanisms by which fluoride acts to prevent dental caries according to Soi et al.?
A) Inhibits demineralization by forming fluorapatite crystals more resistant to acid than hydroxyapatite.
B) Enhances remineralization by accelerating fluorapatite crystal growth.
C) Interferes with acid-producing bacteria in the oral cavity to reduce acid production.
D) Retains on dental hard tissues and oral mucosa for prolonged protective effects.
E) Increases the mechanical strength of dental tissues directly without affecting mineral content.

9. How do ACP nanoparticles contribute to dental health according to recent research?
A) They increase the hardness of dental tissues without influencing mineral content.
B) NanoACP is incorporated into dental materials to prevent demineralization at restoration-enamel margins.
C) Pchitosan-ACP complexes show higher remineralization rates than fluoride treatments in vitro.
D) ACP nanoparticles are primarily used for cosmetic improvements in dentistry, such as whitening.
E) They serve as a direct source of calcium and phosphate ions for dental hard tissue remineralization.

10. What are the primary challenges in treating dental caries according to recent studies?
A) Ineffectiveness of traditional brushing methods in reducing plaque biofilms.
B) Limited efficacy of broad-spectrum antibiotics due to bacterial resistance and saliva buffering.
C) High cost and inaccessibility of professional dental care in remote areas.
D) Lack of public awareness about the importance of oral hygiene.
E) Streptococcus mutans' ability to produce acidic environments that demineralize dental hard tissues.

References

[1]. Anil Kishen, Nanotechnology in Endodontics, Current and Potential Clinical Applications, Springer Cham Heidelberg New York Dordrecht London, © Springer International Publishing Switzerland 2015, ISBN 978-3-319-13574-8 ISBN 978-3-319-13575-5 (eBook), DOI 10.1007/978-3-319-13575-5, Library of Congress Control Number: 2015935938.

[1]. Li, Li et al. Repair of enamel by using hydroxyapatite nanoparticles as the building blocks. Journal of Materials Chemistry, 18 (2008): 4079-4084.

[2]. J. Tao, H. Pan, Y. Zeng, X. Xu and R. Tang, J. Phys. Chem. B, 2007, 111, 13410.

[3]. M. S. Mohan and G. H. Nancollas, Arch. Oral Biol., 1970, 15, 731.

[4]. Tang, S., Dong, Z., Ke, X. et al. Advances in biomineralization-inspired materials for hard tissue repair. Int J Oral Sci 13, 42 (2021). https://doi.org/10.1038/s41368-021-00147-z.

[5]. Arifa MK, Ephraim R, et al. Recent Advances in Dental Hard Tissue Remineralization: A Review of Literature. Int J Clin Pediatr Dent 2019;12(2):139–144.

[6]. Yue Xu, Yuan You, Luyao Yi, Xiaoyi Wu, Yaning Zhao, Jian Yu, He Liu, Ya Shen, Jingmei Guo, Cui Huang, Dental plaque-inspired versatile nanosystem for caries prevention and tooth restoration, Bioactive Materials, Volume 20, 2023, Pages 418-433, ISSN 2452-199X, https://doi.org/10.1016/j.bioactmat.2022.06.010.

[7]. N.J. Kassebaum, A.G.C. Smith, E. Bernab´e, T.D. Fleming, A.E. Reynolds, T. Vos, C.J. L. Murray, W. Marcenes, Global, regional, and national prevalence, incidence, and disability-adjusted life years for oral conditions for 195 countries, 1990-2015: a systematic analysis for the global burden of diseases, injuries, and risk factors, J. Dent. Res. 96 (2017) 380–387, https://doi.org/10.1177/0022034517693566.

[8]. G.D.a.I.I.a.P. Collaborators, Global, regional, and national incidence, prevalence, and years lived with disability for 310 diseases and injuries 1990-2015: a systematic analysis for the Global Burden of Disease Study 2015, Lancet 388 (2016) 1545–1602, https://doi.org/10.1016/S0140-6736(16)31678-6.

[9]. P.E. Petersen, D. Bourgeois, H. Ogawa, S. Estupinan-Day, C. Ndiaye, The global burden of oral diseases and risks to oral health, Bull. World Health Organ. 83 (2005) 661–669.

[10]. N.J. Kassebaum, E. Bernab´e, M. Dahiya, B. Bhandari, C.J.L. Murray, W. Marcenes, Global burden of untreated caries: a systematic review and metaregression, J. Dent. Res. 94 (2015) 650–658, https://doi.org/10.1177/0022034515573272.

[11]. R.J. Schroth, J. Levi, E. Kliewer, J. Friel, M.E.K. Moffatt, Association between iron status, iron deficiency anaemia, and severe early childhood caries: a case-control study, BMC Pediatr. 13 (2013) 22, https://doi.org/10.1186/1471-2431-13-22. [7] R.J. Schroth, J.A. Levi, E.A. Sellers, J. Friel, E. Kliewer, M.E.K. Moffatt, Vitamin D status of children with severe early childhood caries: a case-control study, BMC Pediatr. 13 (2013) 174, https://doi.org/10.1186/1471-2431-13-174.

[12]. N. Pitts, B. Amaechi, R. Niederman, A.M. Acevedo, R. Vianna, C. Ganss, A. Ismail, E. Honkala, Global oral health inequalities: dental caries task group–research agenda, Adv. Dent. Res. 23 (2011) 211–220, https://doi.org/10.1177/0022034511402016.

[13]. N.B. Pitts, D.T. Zero, P.D. Marsh, K. Ekstrand, J.A. Weintraub, F. Ramos-Gomez, J. Tagami, S. Twetman, G. Tsakos, A. Ismail, Dental caries, Nat. Rev. Dis. Prim. 3 (2017), 17030, https://doi.org/10.1038/nrdp.2017.30.

[14]. W.H. Bowen, R.A. Burne, H. Wu, H. Koo, Oral biofilms: pathogens, matrix, and polymicrobial interactions in microenvironments, Trends Microbiol. 26 (2018) 229–242, https://doi.org/10.1016/j.tim.2017.09.008.

[15]. P.D. Marsh, D.J. Bradshaw, Dental plaque as a biofilm, J. Ind. Microbiol. 15 (1995) 169–175.

[16]. H.-C. Flemming, J. Wingender, The biofilm matrix, Nat. Rev. Microbiol. 8 (2010) 623–633, https://doi.org/10.1038/nrmicro2415.

[17]. J.L. del Pozo, R. Patel, The challenge of treating biofilm-associated bacterial infections, Clin. Pharmacol. Ther. 82 (2007) 204–209.

[18]. H. Koo, M.L. Falsetta, M.I. Klein, The exopolysaccharide matrix: a virulence determinant of cariogenic biofilm, J. Dent. Res. 92 (2013) 1065–1073, https://doi. org/10.1177/0022034513504218.

[19]. Y. He, B.W. Peterson, Y. Ren, H.C. van der Mei, H.J. Busscher, Antimicrobial penetration in a dual-species oral biofilm after noncontact brushing: an in vitro study, Clin. Oral Invest. 18 (2014) 1103–1109, https://doi.org/10.1007/s00784- 013-1097-x.

[20]. Y. Liang, Z. Li, Y. Huang, R. Yu, B. Guo, Dual-dynamic-bond cross-linked antibacterial adhesive hydrogel sealants with on-demand removability for post-wound-closure and infected wound healing, ACS Nano 15 (2021) 7078–7093, https://doi.org/10.1021/acsnano.1c00204.

[21]. X. Liao, X. Yu, H. Yu, J. Huang, B. Zhang, J. Xiao, Development of an anti-infective coating on the surface of intraosseous implants responsive to enzymes and bacteria, J. Nanobiotechnol. 19 (2021) 241, https://doi.org/10.1186/s12951-021-00985-3.

[22]. X. Wang, J. Wu, P. Li, L. Wang, J. Zhou, G. Zhang, X. Li, B. Hu, X. Xing, Microenvironment-responsive magnetic nanocomposites based on silver nanoparticles/gentamicin for enhanced biofilm disruption by magnetic field, ACS Appl. Mater. Interfaces 10 (2018) 34905–34915, https://doi.org/10.1021/acsami.8b10972.

[23]. P.C. Balaure, A.M. Grumezescu, Recent advances in surface nanoengineering for biofilm prevention and control. Part II: active, combined active and passive, and smart bacteria-responsive antibiofilm nanocoatings, Nanomaterials 10 (2020) 1527, https://doi.org/10.3390/nano10081527.
[24]. X. Kuang, V. Chen, X. Xu, Novel approaches to the control of oral microbial biofilms, 2018, BioMed Res. Int. (2018), 6498932, https://doi.org/10.1155/2018/ 6498932.
[25]. S. Fulaz, D. Hiebner, C.H.N. Barros, H. Devlin, S. Vitale, L. Quinn, E. Casey, Ratiometric imaging of the in situ pH distribution of biofilms by use of fluorescent mesoporous silica nanosensors, ACS Appl. Mater. Interfaces 11 (2019) 32679–32688, https://doi.org/10.1021/acsami.9b09978.
[26]. Z. Zhao, C. Ding, Y. Wang, H. Tan, J. Li, pH-Responsive polymeric nanocarriers for efficient killing of cariogenic bacteria in biofilms, Biomater. Sci. 7 (2019) 1643–1651, https://doi.org/10.1039/c8bm01640b. [27]. H. Koo, R.N. Allan, R.P. Howlin, P. Stoodley, L. Hall-Stoodley, Targeting microbial biofilms: current and prospective therapeutic strategies, Nat. Rev. Microbiol. 15 (2017) 740–755, https://doi.org/10.1038/nrmicro.2017.99.
[28]. J.D. Featherstone, S. Dom´ejean, The role of remineralizing and anticaries agents in caries management, Adv. Dent. Res. 24 (2012) 28–31, https://doi.org/10.1177/ 0022034512452885.
[29]. N. Philip, State of the art enamel remineralization systems: the next frontier in caries management, Caries Res. 53 (2019) 284–295, https://doi.org/10.1159/ 000493031.
[30]. J. He, J. Yang, M. Li, Y. Li, Y. Pang, J. Deng, X. Zhang, W. Liu, Polyzwitterion manipulates remineralization and antibiofilm functions against dental demineralization, ACS Nano 16 (2022) 3119–3134, https://doi.org/10.1021/ acsnano.1c10812.
[31]. S. Mai, Y.K. Kim, J. Kim, C.K.Y. Yiu, J. Ling, D.H. Pashley, F.R. Tay, In vitro remineralization of severely compromised bonded dentin, J. Dent. Res. 89 (2010) 405–410, https://doi.org/10.1177/0022034510363662.
[32]. T.T. Thula, F. Svedlund, D.E. Rodriguez, J. Podschun, L. Pendi, L.B. Gower, Mimicking the nanostructure of bone: comparison of polymeric process-directing agents, Polymers (Basel) 3 (2011) 10–35.
[33]. A. Hou, J. Luo, M. Zhang, J. Li, W. Chu, K. Liang, J. Yang, J. Li, Two-in-one strategy: a remineralizing and anti-adhesive coating against demineralized enamel, Int. J. Oral Sci. 12 (2020) 27, https://doi.org/10.1038/s41368-020-00097-y.
[34]. M.A.S. Melo, S.F.F. Guedes, H.H.K. Xu, L.K.A. Rodrigues, Nanotechnology-based restorative materials for dental caries management, Trends Biotechnol. 31 (2013) 459–467, https://doi.org/10.1016/j.tibtech.2013.05.010.
[35]. B.H. Clarkson, R.A.M. Exterkate, Noninvasive dentistry: a dream or reality? Caries Res. 49 (Suppl 1) (2015) 11–17, https://doi.org/10.1159/000380887.
[36]. P.E. Kolenbrander, J. London, Adhere today, here tomorrow: oral bacterial adherence, J. Bacteriol. 175 (1993) 3247–3252.
[37]. P.E. Kolenbrander, R.J. Palmer, S. Periasamy, N.S. Jakubovics, Oral multispecies biofilm development and the key role of cell-cell distance, Nat. Rev. Microbiol. 8 (2010) 471–480, https://doi.org/10.1038/nrmicro2381.

12. Nanoapplications in Odontotheraphy

The term "nano," derived from Greek, signifies "dwarf" and denotes extreme smallness. Nanotechnology primarily involves manipulating materials at the atomic or molecular level, encompassing processes like processing, separating, consolidating, and deforming materials at the scale of one atom or molecule [1].

Also referred to as molecular technology or molecular engineering, nanotechnology enables the production of materials and structures within the size range of 0.1–100 nm.

This cutting-edge technology has sparked significant advancements in dental materials, particularly in controlling oral biofilm formation through the biocidal, anti-adhesive, and drug delivery capabilities of nanoparticles [2].

Recent innovations include the incorporation of silver nanoparticles into denture materials and orthodontic adhesives to reduce bacterial and fungal adhesion to oral devices. In dental materials, inorganic fillers can be classified based on their size, ranging from macro fillers to nanofillers.

Particle size control can be achieved through either a top-down or bottom-up manufacturing approach. Top-down techniques involve conventional milling procedures to reduce particle size, typically not below 100 nm, while bottom-up approaches utilize direct molecular assembly to construct particles from atoms and molecular precursors into progressively larger structures [3].

The application of nanoparticles in restorative materials spans various areas, from developing highly translucent and polishable restorative composites to incorporating bioactive nanoparticles to combat secondary caries development. Specially formulated metal oxide nanoparticles exhibit potent antibacterial activity due to their significantly large surface area, enabling efficient contact with microorganism effluents. However, ensuring that the addition of active ingredients does not compromise the physical and mechanical properties or the setting/polymerization reaction of restorative materials is crucial [4].

A key challenge in nanotechnology application is preventing nanoparticle association, which often leads to agglomeration. Agglomeration, where particles weakly bond together, and aggregation, where particles are bonded by solid bridges, can significantly affect material properties. The zeta potential of nanoparticles, representing the electrostatic potential at the electric double layer surrounding a nanoparticle in solution, plays a crucial role in their tendency to agglomerate. Manufacturing processes impact the crystallinity, shape, and size of nanoparticles, with higher crystallinity associated with improved hardness and strength [5].

Despite the promising advancements in bionanotechnology, concerns regarding the biosafety of nanoparticles persist. Further investigation into the potential long-term effects of nanoparticle incorporation into materials used in the human body is necessary, particularly concerning their biocompatibility and potential adsorption by live tissue. While much of the current research relies on in vitro methodologies, addressing these concerns remains an ongoing endeavor [6].

12.1. Nanoparticles in Glass Ionomer Materials

Glass ionomer cements (GICs), also known as polyalkenoate cements, are water-based cements commonly used in dentistry. They derive their name from the interaction between silicate glass and polyacrylic acid, resulting in an acid-base reaction. The development of resin-modified glass ionomers has enhanced the mechanical and optical properties of GICs by replacing some water content with water-soluble methacrylate monomers, such as 2-hydroxyethyl methacrylate (HEMA). Unlike conventional GICs, resin-modified versions undergo an initial set through light-activated polymerization followed by a slower acid-based setting reaction [7, 8].

The photopolymerizable form of GIC has gained popularity due to its reduced water sensitivity, translucency, and ability to chemically bond to tooth structure. However, clinical challenges persist despite these advancements. While GIC is biocompatible and capable of fluoride ion release and uptake, its clinical implications for caries prevention and tooth remineralization remain uncertain [9].

Despite its unique properties, GIC has limitations as a restorative material. It exhibits low fracture toughness and high rates of occlusal wear compared to other restorative materials like amalgam and modern composite resin systems. Consequently, it is not recommended for permanent restorations in posterior teeth and is prone to early bulk fracture when subjected to tensile stress due to its brittleness [10].

The incorporation of nanoparticles into GIC compositions offers potential benefits. Nanoparticles, whether salt- or oxide-based, can react with the polyacrylic acid matrix to enhance the overall resistance of the material. Moreover, their significantly smaller size allows them to fill interstitial spaces, further strengthening the cement. Understanding the interaction between the matrix and filler is crucial for optimizing the mechanical properties of GICs [11].

12.1.1. Experimental Materials

To investigate the performance of nano-modified glass ionomer cements (GICs), a common approach is to add nanoparticles to the powder of commercial GICs and adjust the powder-to-liquid ratio accordingly. For instance, Prentice et al. (2006) examined the effects of adding ytterbium fluoride (YbF3) and barium sulfate (BaSO4) nanoparticles to a commercial GIC (Riva SC – SDI). While the addition of YbF3 was anticipated to enhance compressive strength similar to aluminum fluoride (AlF3), the results showed no improvement and even a decrease in strength with higher concentrations. Similarly, BaSO4 reduced compressive strength even at low concentrations due to differences in cation properties [12, 13, 14, 15].

Hydroxyapatite (HA), a calcium phosphate found in dental enamel, was investigated for its potential to improve mechanical properties. Mixing nanohydroxyapatite and nanofluorapatite (FA) with a commercial GIC resulted in better mechanical behavior compared to the control group. The addition of HA and FA affected the setting reaction mechanism and polysalt bridge formation, enhancing cement properties and bond strength to dentin [16, 17, 18].

Furthermore, titanium dioxide (TiO2) nanoparticles were added to a commercial GIC, resulting in improved mechanical performance overall. However, excessive TiO2 addition reduced strength due to insufficient bonding with polyacrylic acid. TiO2 also exhibited antibacterial properties, inhibiting bacterial growth and causing intracellular damage to infiltrated bacteria [19, 20, 21].

Another additive, chlorhexidine (CHX), in the form of nanoparticles (CHX-hexametaphosphate), was incorporated into GIC. Experimental GICs showed similar tensile strength compared to controls, with significant fluoride release observed, especially at higher CHX-HMP proportions. The addition of CHX-HMP altered the setting reaction, increasing fluoride mobility in the cement lattice [22, 23].

Overall, these studies highlight the potential of nanoparticle-modified GICs to improve mechanical properties and release beneficial agents like fluoride and antimicrobials. Further research is needed to fully understand and optimize the performance of these experimental materials [24].

12.1.2. Commercial Alternatives

The commercial resin-modified glass ionomer cement (GIC) Ketac Nano (3M ESPE) is marketed as containing aggregated 'nanoclusters' composed of spherical particles in the size range of 5–20 nm, along with non-agglomerated silica fillers and acid-reactive glass fillers in its powder. However, it's important to note that while these aggregates contain engineered nanoparticles, they are in the micro-size range, with some clusters reaching up to 5 μm. Therefore, a more accurate description would be "nano-filled clusters" or "clusters of nanoparticles" [25, 26, 27, 28].

When compared to conventional resin-modified GICs and restorative composites, Ketac Nano exhibits significantly higher roughness after biofilm degradation, indicating greater susceptibility to biomechanical degradation. However, its resistance to biomechanical degradation (biofilm + three-body abrasion) is about three times higher than other GICs, likely due to the removal of individual nano-sized particles from the matrix instead of the entire clusters [29, 30].

In terms of fluoride release, Ketac Nano demonstrates similar patterns to other resin-modified and conventional GICs, with a burst effect of fluoride release at shorter times. While smaller glass particles theoretically increase acid-based reactivity and fluoride release, Ketac Nano's filler content is lower than other resin-modified GICs, affecting both mechanical properties and fluoride uptake/release characteristics [31, 32].

Clinical evaluations have shown that Ketac Nano exhibits worse marginal staining and adaptation compared to other materials like Fuji II LC and Filtek Supreme after 1 year of clinical service. The micromechanical interaction between Ketac Nano and dentine/enamel is superficial, with no evidence of structural demineralization or hybridization [33, 34].

Another application of nanotechnology in GICs is the development of a nano-filled light-curing varnish (G-Coat Plus, GC Europe), applied onto highly viscous GICs (e.g., Fuji IX GP Extra) to provide surface protection during the early maturation phase. While EQUIA restorations have shown acceptable performance for small class I and II preparations, wear resistance and flexural strength may vary based on the presence of the nano-filled varnish [35, 36].

Despite its limitations, GICs remain an attractive option in public health systems due to their aesthetic properties, safety, and unique fluoride release characteristics. However, there is ongoing demand for further improvement to develop a more permanent restorative material [37].

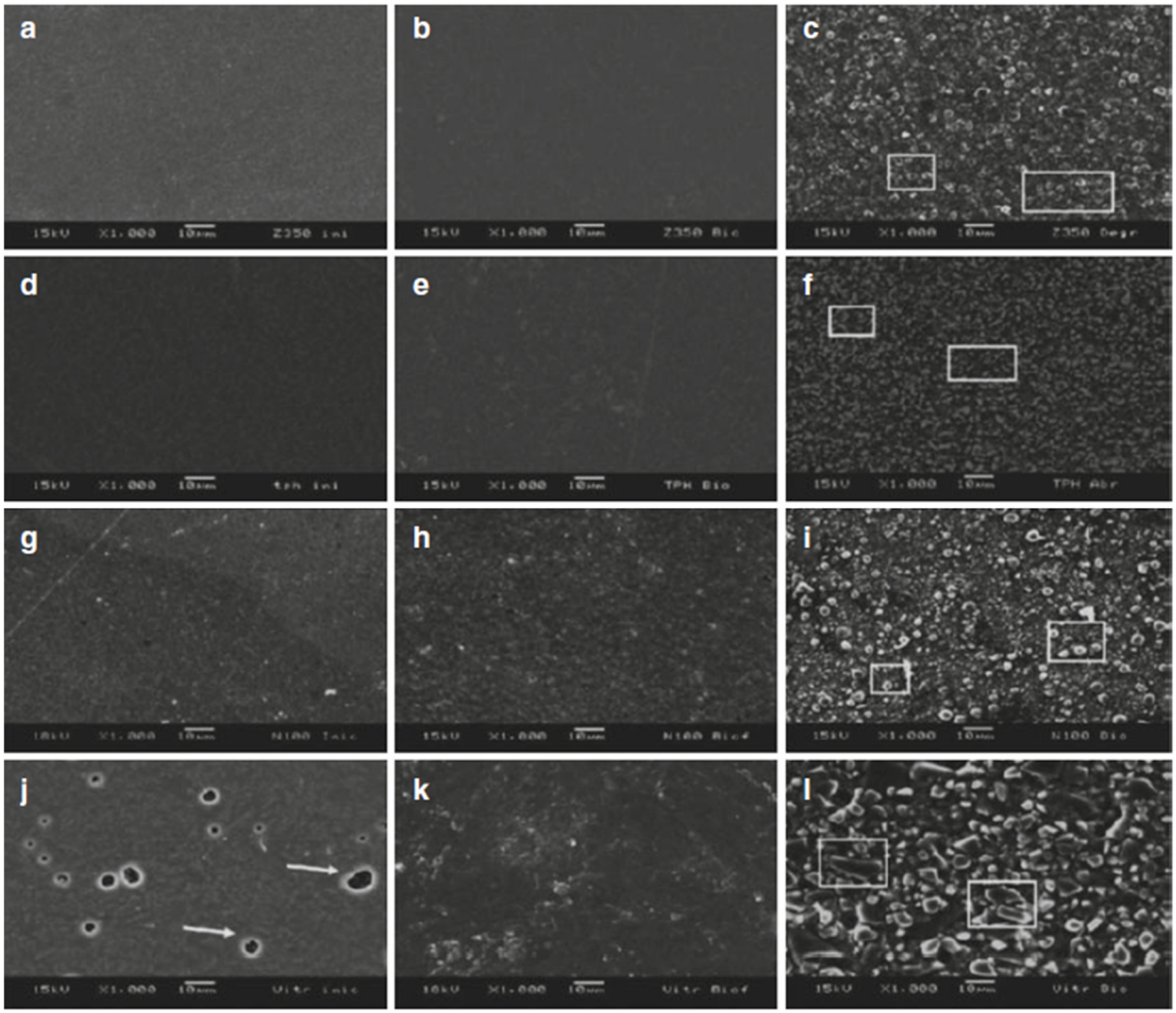


Figure 12.1. Scanning electron micrographs of microhybrid composites Filtek Z350 (a – c) and TPH Spectrum (d – f); nano- based Ketac N100 (g – i), and resin-modifi ed GIC Vitremer (j – l). The fi rst column shows the relative humidity storage groups (a , d , g , j), with porosities (small spherical and irregular shapes) indicated by arrows . The second column represents the S mutans biofi lm storage groups (b , e , h , k), with a severe degraded aspect of the matrix. The third column corresponds to biofi lm storage plus abrasion groups (c , f , i , l), with many exposed particles at the surface of materials [38].

12.2. Application of Nanoparticles in Resin-Based Materials

Composite materials, also known as resin composites, are composed of two or more constituent materials with significantly different properties that, when combined, create a material with unique characteristics. In restorative dentistry, these composites typically consist of an organic matrix, often Bis-GMA (bisphenol A-glycidyl methacrylate), combined with other monomers like TEGDMA (triethylene glycol dimethacrylate), HEMA (2-hydroxyethyl methacrylate), and UDMA (urethane dimethacrylate), as well as inorganic-organic fillers of various sizes. The surface treatment of these fillers with compounds like 3-methacryloxypropyl trimethoxy silane allows for covalent bonding between the inorganic filler particles and the organic resin matrix [38, 39, 40, 41, 42, 43, 44, 45].

Nanofillers used in dental composites include various materials such as silica, tantalum thoxide, zirconia-silica, alumina, nano-fibrillar silicate, and titanium oxide, among others. Dental composites containing filler particles smaller than 100 nm are often referred to as nanocomposites. However, the classification of these materials can be controversial, with some authors using terms like nanohybrids to describe composites containing a combination of nanoparticles, nano-filled clusters, and microparticles. The precise amount of nanofillers in these composites is often not reported by manufacturers or in research articles [46, 47, 48, 49, 50, 51, 52, 53, 54, 55, 56, 57, 58, 59, 60].

Challenges in developing dental nanocomposites include effectively dispersing nanoparticles in the resin to prevent agglomeration and achieving high filler loading levels to reduce polymerization shrinkage while maintaining good handling characteristics and cost-effectiveness. Additionally, understanding the impact of nanofiller size, morphology, composition, and hybridization on composite properties, as well as their long-term durability in vivo, is essential [61, 62, 63, 64, 65, 66, 67].

In restorative dentistry, achieving strong adhesion between the composite material and tooth structure is crucial to prevent issues like microleakage, secondary caries, postoperative sensitivity, and discoloration. The formation of a durable hybrid layer between the resin and dentin is critical for successful adhesion, but factors like collagen infiltration, resin penetration, and filler aggregation can influence its quality and longevity [68, 69, 70, 71, 72, 73, 74, 75, 76, 77].

Nanotechnology in adhesive systems aims to stimulate remineralization, improve mechanical properties, and develop bioactive adhesives capable of eliminating bacteria. However, no composite resin material has yet fully met the functional and aesthetic requirements for both posterior and anterior restorations, and the average longevity of composite restorations is approximately 4 years [78, 79].

Inorganic fillers incorporated into resin composites impact radiopacity, wear resistance, flexural modulus, and thermal expansion coefficient. By synergistically using releasing nanofillers and reinforcing fillers, nanocomposites with both stress-bearing and caries-inhibiting capabilities may be developed, offering a combination not currently available in dental materials [80, 81].

12.2.1. Dentin Bonding Systems

The incorporation of nanofillers into dentin bonding systems aims to stabilize the hybrid layer by improving its mechanical properties. However, nanofiller particles often agglomerate into clusters despite their supposed colloidal behavior, which can hinder resin penetration into demineralized dentin. This agglomeration occurs due to various factors such as the presence of residual solvent underneath the hybrid layer in self-etch techniques and the characteristics of the nanoparticles themselves [82, 83, 84, 85, 86].

While some studies suggest that nanofilled agglomerates are dispersed throughout the adhesive layer, others show that they collect on the top surface of the hybrid layer. The size and characteristics of nanoparticles, as well as the presence of additional substances like solvents, influence cluster formation. Despite efforts to use smaller nanofillers and modify adhesive

formulations, controversy remains regarding their ability to penetrate the restricted space of the hybrid layer effectively [87, 88, 89, 90, 91].

In recent developments, quaternary ammonium dimethacrylate (QADM) and nano-silver particles (nAg) have been incorporated into adhesive systems to confer antibacterial properties without compromising bond strength. This combination aims to combat residual bacteria in cavity preparations and at the tooth-restoration interface, contributing to long-term antibacterial effects [92, 93, 94, 95, 96, 97, 98, 99, 100, 101].

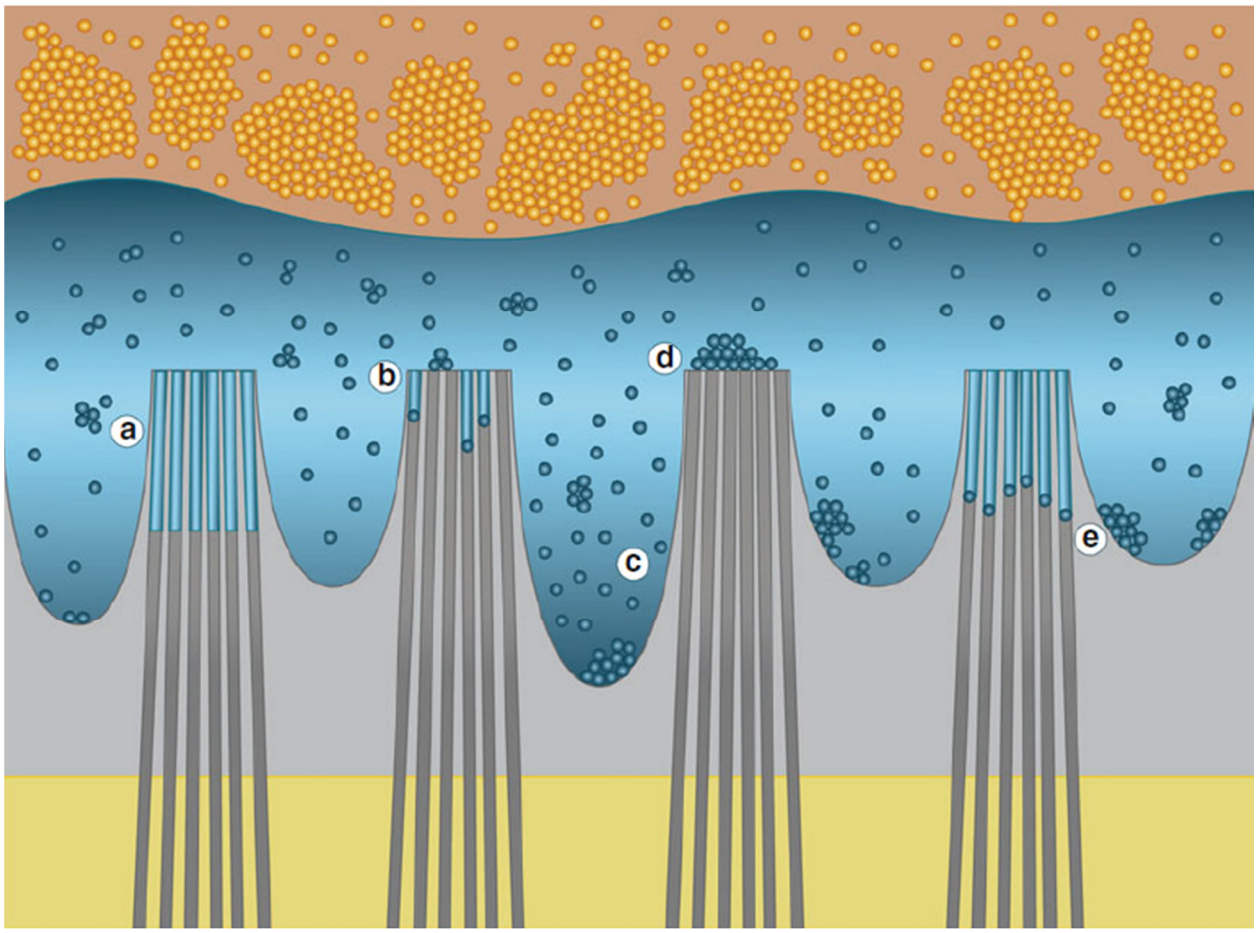


Figure 12.2. Schematic representation of the dentin/adhesive hybrid layer (orange composite resin, blue adhesive resin, gray demineralized dentin, yellow intact dentin) with the effect of different nanoparticles application: (A). Wagner et al. 2013: Hydrothermally-grown HA with smaller surface area are embedded within the adhesive and not deposited on top of the hybrid layer. (B) Besinis et al. 2012: Hydrophobic diluent combined with smaller nHA improves infi ltration ability of demineralized dentin. (C) Hoshika et al. 2010: Longer and denser resin tags obtained when CPN nanoparticles are added to the primer composition, by either improving monomer infi ltration or enhancing monomer conversion. (D) Lohbauer et al. 2010: Spherical zirconia nanoparticles are unable to penetrate the interfi brilar spaces, compromising hybrid layer formation. (E) Osorio et al. 2011: Zinc oxide nanoparticles infi ltrate the interfi brilar spaces and remain at the bottom of the hybrid layer, in contact with the demineralized dentin (Courtesy of Grace M De Souza and published with permission from University of Toronto).

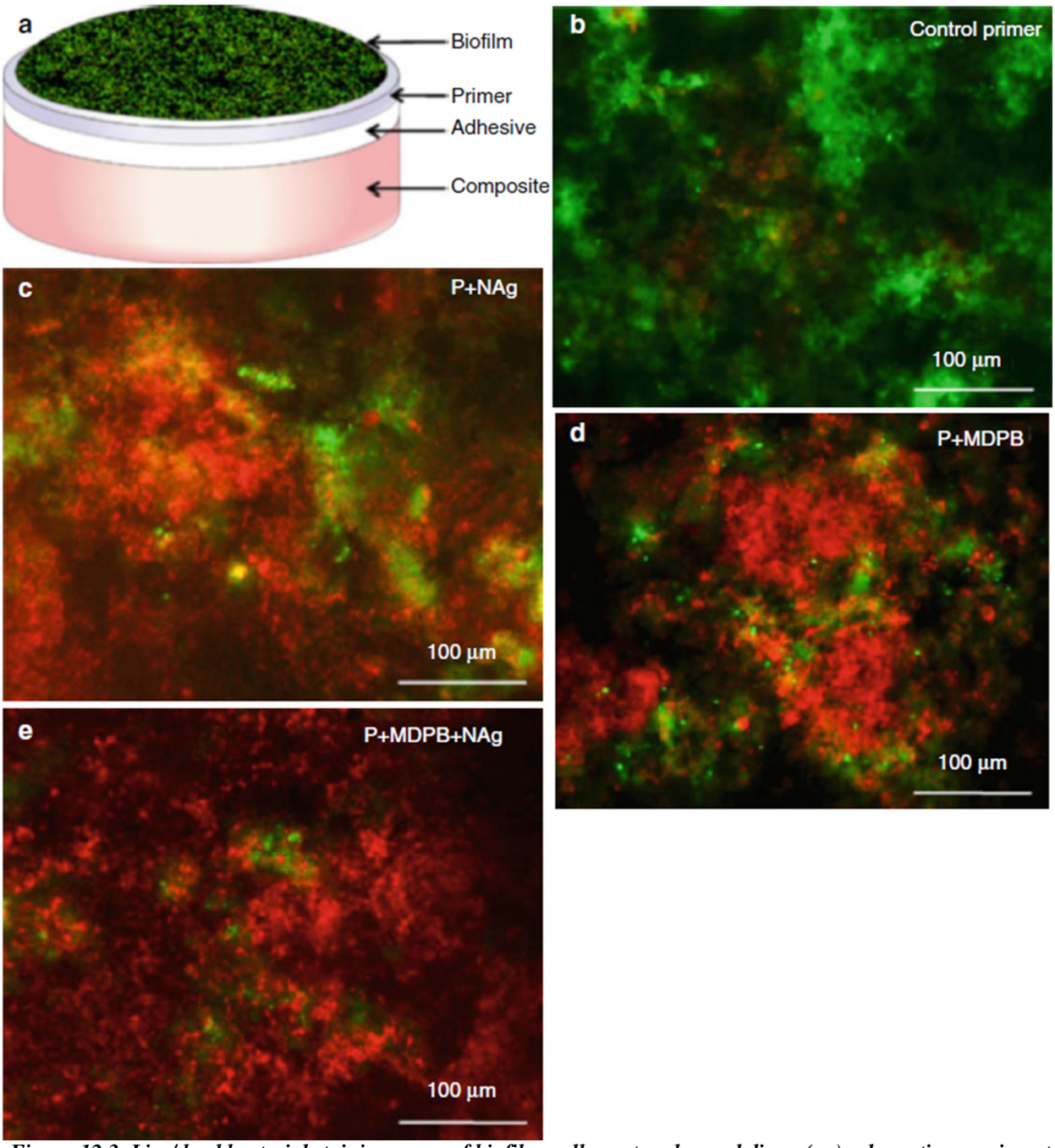


Figure 12.3. Live/dead bacterial staining assay of biofilms adherent on layered discs: (a) schematic experimental setup; (b – e) representative images of biofilms for control primer, P + nAg, P + MDPB, and P + MDPB + nAg. Live bacteria were stained green, and dead/compromised bacteria were stained red. Live and dead bacteria in close proximity of each other yielded yellow / orange colours [92].

Additionally, nanoparticles of amorphous calcium phosphate (nACP) have been utilized to remineralize tooth structure and reduce bacterial count at the adhesive interface. Novel experimental bonding agents containing nAg, QADM, and nACP have shown promising results in reducing biofilm viability and colony-forming units without affecting bond strength [102, 103, 104, 105, 106, 107, 108, 109, 110].

Other nanofillers such as colloidal platinum nanoparticles (CPN) and spherical zirconia nanoparticles have been investigated for their potential to enhance bond strength and mechanical properties of adhesive systems. Zinc-doped adhesives have also demonstrated therapeutic effects by inhibiting matrix metalloproteinase-induced collagen degradation in the hybrid layer [111, 112].

Polymeric nanogels have been explored for their ability to carry nanoparticles into demineralized dentin and improve adhesive properties. These nanogels restrict oxygen diffusion rates, enhance bond strength, and maintain stable mechanical properties after water storage [114].

Overall, incorporating bioactive and reinforcing nanofillers into dental adhesives shows promise in enhancing bond strength, mechanical properties, and antibacterial activity. However, challenges remain in optimizing the ratios and characteristics of nanoparticles to ensure stable material properties over time while reducing bacterial count on the restorative interface [115].

12.2.2. Restorative Composite Resins, Sealants and Luting Systems

This excerpt discusses the various strategies and materials used in the development of dental composites to enhance their mechanical properties, radiopacity, fluoride release, and antibacterial properties. Here's a summary of the key points:

1. Fillers and Manufacturing Techniques:
   - Dental composites typically contain a mixture of fillers to achieve desired properties like mechanical strength, radiopacity, and fluoride release.
   - Fillers include radiopaque glass, quartz, ceramics, sol-gel derived particles, and nanoparticles. Different manufacturing techniques yield fillers of varying sizes and shapes.
   - The sol-gel method produces nanoparticles with a large specific surface area, affecting resin matrix characteristics.
2. Antibacterial Properties:
   - Incorporating antibacterial agents like octyl alkylated quaternary ammonium poly (ethylene imine) (QA-PEI) particles has been investigated to develop antibacterial composites.
   - QA-PEI particles have demonstrated antibacterial effects against S. mutans and S. aureus, making them potential candidates for dental composites.
3. Remineralization Potential:
   - Amorphous calcium phosphate (ACP) and calcium fluoride nanoparticles (nCaF2) have shown potential for remineralizing tooth structure.
   - Composites containing these nanoparticles release ions like Ca and PO4, promoting remineralization while maintaining mechanical properties.
4. Nanoparticles and Antibacterial Effects:
   - Silver nanoparticles (nAg) added to composites inhibit bacterial growth and reduce bacterial adhesion.
   - Zinc oxide nanoparticles (nZnO) also exhibit antibacterial effects but may compromise the curing process due to their opacity.
5. Whiskers and Reinforcement:
   - Silicon carbide whiskers and nano-dicalcium phosphate anhydrous (nDCPA) can reinforce the resin matrix and promote ion release for remineralization.
6. Hydroxyapatite Nanocrystals (HAs):
   - HAs, resembling natural enamel crystallites, have been used to reduce bacterial adherence and enhance mechanical properties in composites.
7. Halloysite Nanotubes (HNTs):
   - HNTs, when incorporated into resin matrices, affect polymerization shrinkage and mechanical properties, but effective dispersion is still under investigation.
8. Nanoparticles in Luting Agents:
   - Incorporating nanoparticles in dental cements may improve mechanical properties but can compromise flexural strength and film thickness.

Overall, nanotechnology offers promising avenues for enhancing the clinical performance of resin-based dental materials, including improved antibacterial properties, remineralization potential, and mechanical strength. However, further research is needed to optimize material properties and manufacturing techniques for practical clinical applications.

12.2.2.1. Commercial Alternatives

Restorative materials face a formidable challenge in achieving a balance between strength, handling properties, and optical characteristics akin to natural tooth structure. Recent advancements in nanotechnology have led to the development of two novel resin composites: Filtek Supreme Standard (FSS) and Filtek Supreme Translucent (FST), both by 3M Espe. FSS incorporates zirconia-silica clusters and nanoparticles, while FST predominantly contains nanoparticles with a minor presence of silica clusters. These nanocomposites offer distinct advantages such as reduced stress concentration, enhanced damage tolerance, and unique fracture mechanisms owing to their spherical particle and cluster shapes [116].

Distinguishing resin composites with identical compositions under different brand names can lead to confusion. To streamline research correlations, Filtek composites from 3M Espe will be referenced as "Filtek DEB" (dentin-enamel-body) and "Filtek Translucent" [117, 118, 119].

Introduced in 1984, ormocers represent organic-inorganic polymeric hybrids aimed at boosting filler particle loading. Combining ormocers with nanoparticles yields materials with increased viscosity and reduced double-bond conversion, presenting potential benefits in dental applications [120, 121, 123, 124].

Nanocomposites exhibit crucial properties like polymerization shrinkage, water sorption, solubility, and mechanical strength, which are influenced by filler content and matrix composition. Despite challenges, nanocomposites demonstrate resilience to biomechanical degradation and surface roughness [125].

Clinical evaluations comparing various resin-based materials indicate comparable performance in terms of restoration longevity, secondary caries, and post-operative sensitivity over a two-year period. However, nanofill composites may exhibit heightened susceptibility to occlusal staining, warranting further investigation for long-term viability.

Nanotechnology holds promise for developing new sealant classes with enhanced antibacterial properties and fluoride release. Additionally, resin-based luting systems incorporating nanoparticles may enhance stress absorption and facilitate better control of film thickness in cemented restorations [126].

In conclusion, nanocomposites offer significant potential for enhancing the clinical performance of dental materials. Yet, further research and clinical studies are imperative to optimize their properties for long-term success in restorative dentistry.

12.2.3. Indirect Restorative Systems

Clinically unsuccessful restorations often follow a predictable sequence of events: (1) Cracks emerge beneath or near the occlusal contact area due to repeated occlusal forces in the presence of saliva; (2) These cracks lead to subcritical crack growth, causing fracture of the veneering porcelain; (3) Once cracks extend to the coping interface, the veneering porcelain chips, exposing the veneer-coping interface. Various strategies have been attempted to inhibit porcelain fracture and chipping, aiming to enhance the mechanical reliability of restorations [127, 128].

Particle size in indirect restorative materials significantly impacts microstructure and mechanical properties of ceramics. Ideally, powders should possess small, uniformly distributed particles. Nanocomposites, characterized by nanometer-sized secondary particles dispersed within ceramic matrix grains, offer promise in improving restoration reliability. However, challenges persist in fully harnessing nanoparticle technology due to issues like Ostwald ripening, which leads to larger grain sizes during traditional sintering techniques [129, 130, 131].

To address this, researchers have explored coating yttria-tetragonal zirconia polycrystal (Y-TZP) particles with alumina nanoparticles to control phase transformation and enhance mechanical properties. Additionally, zirconia-toughened alumina (ZTA) skeletons infiltrated with a thin glass film have shown improved bending strength and fracture toughness, attributed to zirconia's transformation-toughening mechanism [132].

Alternative stabilizers like cerium dioxide (CeO_2) in tetragonal zirconia polycrystal (Ce-TZP) aim to increase toughness and resistance to degradation. By optimizing nanoparticle distribution

within the matrix, materials with high strength and fracture toughness have been achieved [133, 134, 135].

Diatomite, a porous silicate structure, impregnated with zirconia nanoparticles has shown promise in reducing porosity and enhancing fracture toughness. Further research is needed to characterize the mechanical properties and clinical stability of these materials [136].

In the case of porcelain veneer layers, chipping remains a common issue. Strategies to increase toughness include incorporating silver nanoparticles into dental porcelain, resulting in higher hardness and toughness. However, significant color differences pose challenges, and further investigation into mechanical properties and optical characteristics is warranted [137].

In conclusion, advancements in nanoparticle technology hold promise for improving the mechanical reliability of dental restorations. However, ongoing research is essential to optimize material properties and ensure long-term clinical success.

12.3. Dental Adhesive Interfaces Reinforced with Magnetic Nanoparticles

Dental adhesives play a crucial role in various dental procedures, including the placement of direct composite restorations, cementing prosthetic restorations, and achieving a tight connection between restoration materials and tooth surfaces. To enhance the performance of these adhesives, two main directions of research are pursued [138, 139, 140,141, 142, 143, 144, 145].

Firstly, researchers aim to develop novel adhesive materials capable of providing a tighter and more durable connection between the tooth and the restoration material. One approach involves incorporating magnetic nanoparticles (MPs) into the adhesive formulation to optimize distribution and enhance adhesion. These nanoparticles have been extensively used in medicine and show promise in improving dental adhesive properties. Preliminary studies have demonstrated the potential of MPs in achieving a tighter connection compared to conventional methods. In this study, dental adhesives containing MPs are compared with conventional adhesives to assess their effectiveness in reducing interface widths [146, 147, 148, 149, 150, 151, 152, 153].

Secondly, researchers are exploring various techniques to analyze and assess microleakages at the tooth-restoration interface. These techniques include dye penetration, testing marginal integrity using radioactive isotopes or compressed air, electronic monitoring, and imaging assessments using techniques such as scanning electron microscopy (SEM), fluorescent microscopy, confocal microscopy, and optical coherence tomography (OCT). In this study, the efficiency of dental adhesives and procedures is evaluated using optical microscopy and micro-CT imaging methods. Micro-CT allows for a comprehensive volumetric evaluation, providing precise data for further analysis [154, 155, 156, 157, 158, 159, 160].

This study aims to address both research directions by developing improved dental adhesive materials and assessing their performance using advanced imaging techniques. By comparing microscopy and micro-CT results, researchers aim to determine the credibility of each method and utilize quantifiable micro-CT data to mathematically model adhesive properties. This approach not only facilitates comparison between different materials but also provides a methodology for studying adhesion phenomena in dentistry [161, 162, 163, 164, 165].

12.3.1. Materials and Methods

In this study, 20 teeth with class I and II cavities were utilized. The selected adhesive was Evetric Bond (Ivoclar Vivadent AG, Schaan, Principality of Liechtenstein), known for its ability to uniformly wet dental surfaces, resulting in the formation of a consistent film wherever applied. The samples were divided into four groups:

1. Group 1: Control group comprising "blank" samples treated with adhesive not containing magnetic nanoparticles (MPs).
2. Group 2: Samples treated with adhesive containing MPs.
3. Group 3: Samples treated with adhesive containing MPs, subjected to an active magnetic field for 5 minutes. This duration was selected to mimic the typical processing time for adhesive application in clinical settings, ensuring practical relevance.

4. Group 4: Samples treated with adhesive containing MPs, subjected to an active magnetic field for an extended duration of 10 minutes. This prolonged magnetization period was chosen to investigate any potential effects of doubling the magnetization time compared to Group 3, although such an extended period is not typical in clinical practice.

The adhesive materials used in Groups 2 to 4 were loaded with multicore-shell Fe3O4-SiO2 magnetic particles synthesized by encapsulating them with SiO2 colloidal stabilized multicore magnetite nanoparticle clusters. The Fe3O4 nanoparticles were synthesized through chemical coprecipitation of Iron (II) and Iron (III) chloride with NaOH. The resulting ~8 nm diameter Fe3O4 nanoparticles were sterically stabilized with oleic acid.

The ferrofluid containing oleic acid monolayer-coated magnetite nanoparticles dispersed in toluene was obtained from the Laboratory of Magnetic Fluids of the Romanian Academy–Timisoara Branch. Sodium lauryl sulfate (SLS) was used as a surfactant for clusters preparation, and Tetraethyl orthosilicate (TEOS), absolute ethanol, and ammonia solution were used for silica coverage.

The magnetic clusters (MCs) were prepared using the oil-in-water mini-emulsion method. Toluene-based ferrofluid (0.5 wt % Fe3O4) was added to an aqueous solution containing the surfactant. Ultrasonic homogenization was used to form stable mini-emulsions, followed by evaporation of toluene and washing with a methanol-water mixture (Figure 12.4.).

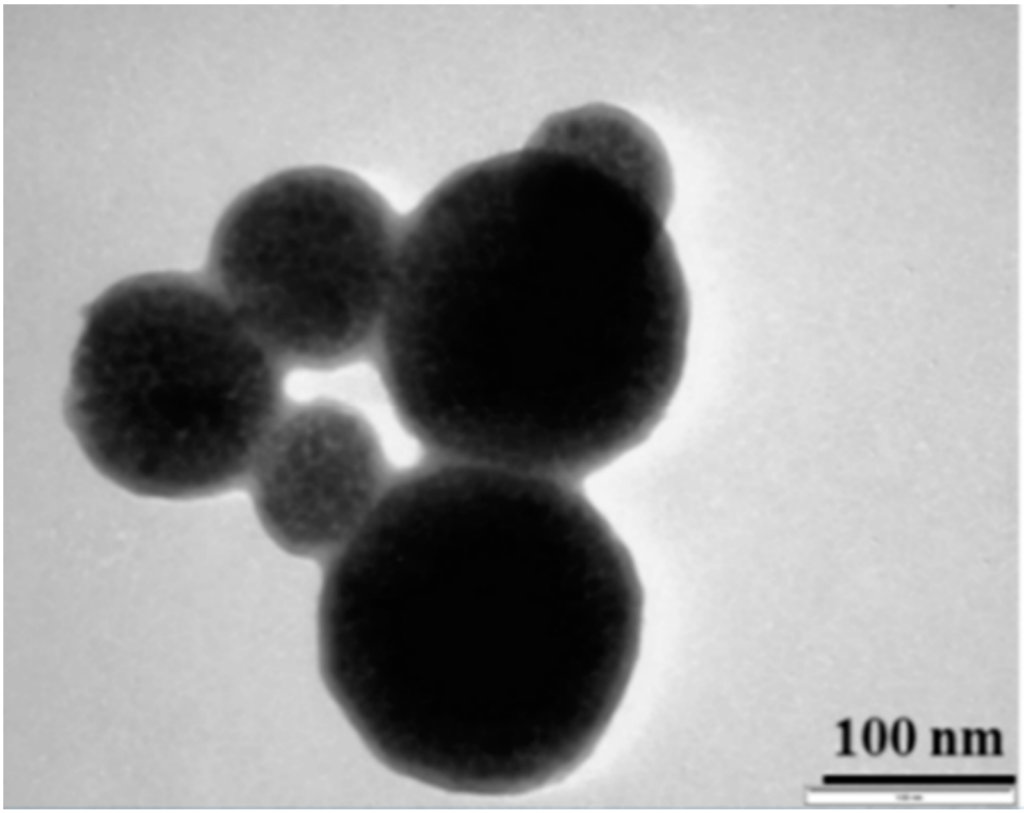


Figure 12.4. TEM image of manufactured multicore-shell Fe_3O_4-SiO_2 magnetic nanoparticles (MPs).

The prepared MCs were then coated with a SiO2 shell using the modified Stober method. An aqueous solution of ethanol and water was mixed with dry magnetic clusters, and TEOS and aqueous ammonia solution were added dropwise. The reaction mixture was stirred at room temperature, and the resulting Fe3O4-SiO2 product was separated, washed, and dried.

Transmission Electron Microscopy (TEM) analysis revealed spherical MPs with sizes ranging from 50 to 200 nm, a core diameter of ~8 nm, and a SiO2 shell thickness of approximately 20 nm. The MPs exhibited superparamagnetic behavior with a saturation magnetization of 21 emu/g. Energy-dispersive X-ray spectroscopy (EDAX) analysis was performed using a scanning electron microscope, confirming the elemental composition of the synthesized particles.

In the preparation of the samples for each group, various methods were employed, as outlined below. For Group 1, consisting of five 'blank' samples, the standard procedure for filling a tooth cavity was followed: demineralization of dentin for 15 seconds, followed by demineralization of enamel for 30 seconds using BlueEtch demineralizing gel. The demineralizing gel was then washed off, and the cavity was dried. Subsequently, the non-filled MPs adhesive was applied and dispersed with air, followed by polymerization for 20 seconds. The cavity was then filled with a radio-opaque flowable composite and polymerized for 40 seconds (Figure 12.5.).

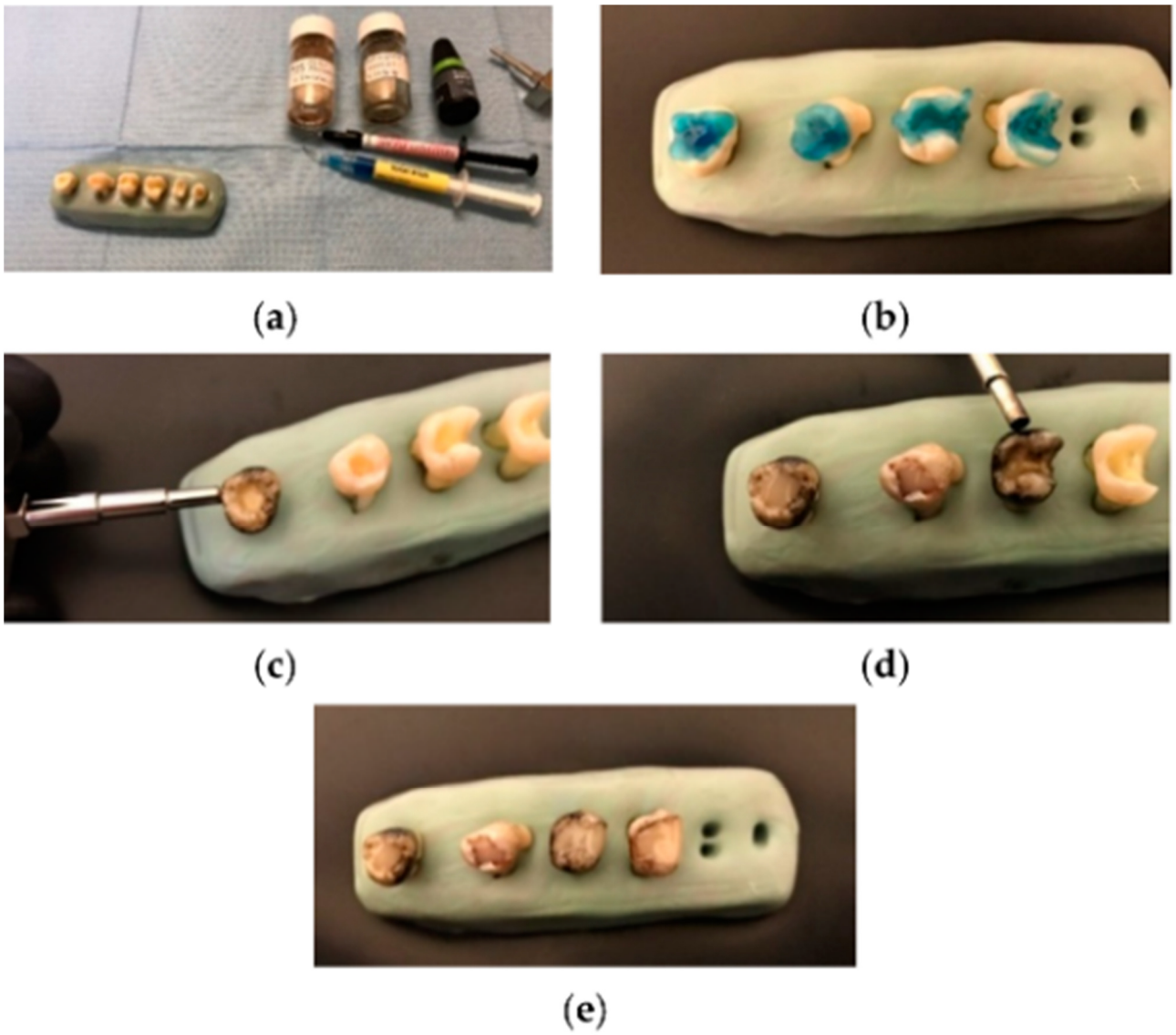


Figure 12.5. Processing of samples (examples): (a) study armamentarium and (b) etchant gel applied for 15 s on the dentin and for 30 s on the enamel; (c, d) application of the magnetic field on the dental adhesive (for 5 or 10 min, for Groups 3 and 4, respectively); (e) final samples with MPs fillings.

For Groups 2 to 4, the adhesive was mixed with the MPs specified in Section 2.1. In Group 2, the dental adhesive loaded with MPs was applied conventionally in five samples. In Groups 3 and 4, each of the five samples loaded with MPs had a magnetic field applied for 5 and 10 minutes, respectively, using a permanent magnet applicator. After applying the MPs-loaded adhesive, the cavities were filled with a fluid composite material (Figure 12.6.).

It is crucial to note that during the second step of this procedure, the permanent magnet applicator must be kept as close as possible to the adhesive doped with MPs, as the magnetic field induction decreases significantly with distance from the applicator tip.

For the first type of investigation, the samples were sliced, and their areas were evaluated using an A377 optical microscope with magnifications ranging from 20× to 800×, equipped with a 2MPX CMOS sensor and manual focus up to 40 mm.

For the second type of investigation, the scanning piece was positioned on the worktop of a Nikon XTH-450 micro-CT system. Scanning settings were configured, and actual scanning, reconstruction, and interpretation of the results were carried out. Micro-CT scanning was performed by rotating the samples 360 degrees around the center of rotation, with 1000 projections captured for each sample. The data were imported into Vg Studio Max software for 3D reconstructions, facilitating the analysis of the adhesive interface on dental surfaces.

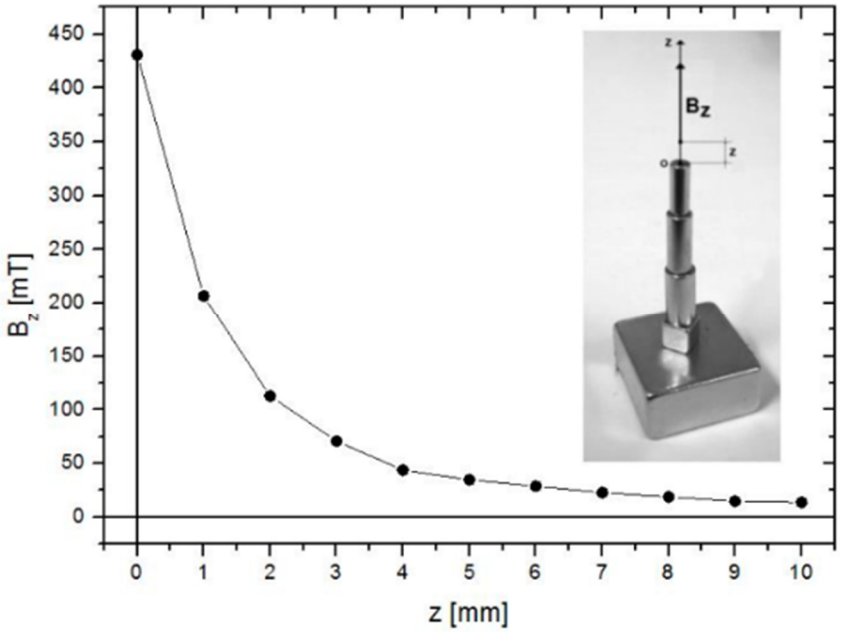


Figure 12.6. The induction of the magnetic field as a function of the distance z from the applicator tip.

12.3.2. Results

12.3.2.1. Optical Microscopy Analysis

The initial investigation, utilizing microscopy, is a common method for assessing the width/thickness of adhesive layers. Figure 4 provides examples of this investigation for a sample from each of the four considered groups. Direct measurements were conducted on sectioned samples at 10 characteristic points on each of the three surfaces of the teeth: vestibular, oral, and pulpal interfaces.

The microscopy analysis revealed the following results: (i) For Group 1, the adhesive layer width/thickness (w) ranged from 0.021 to 0.29 mm. (ii) In Group 2, w varied from 0.016 to 0.31 mm. (iii) Group 3 exhibited decreased values of w, ranging from 0.013 to 0.19 mm. (iv) Group 4 showed the smallest values of w, ranging from 0.011 to 0.039 mm (Figure 12.7.).

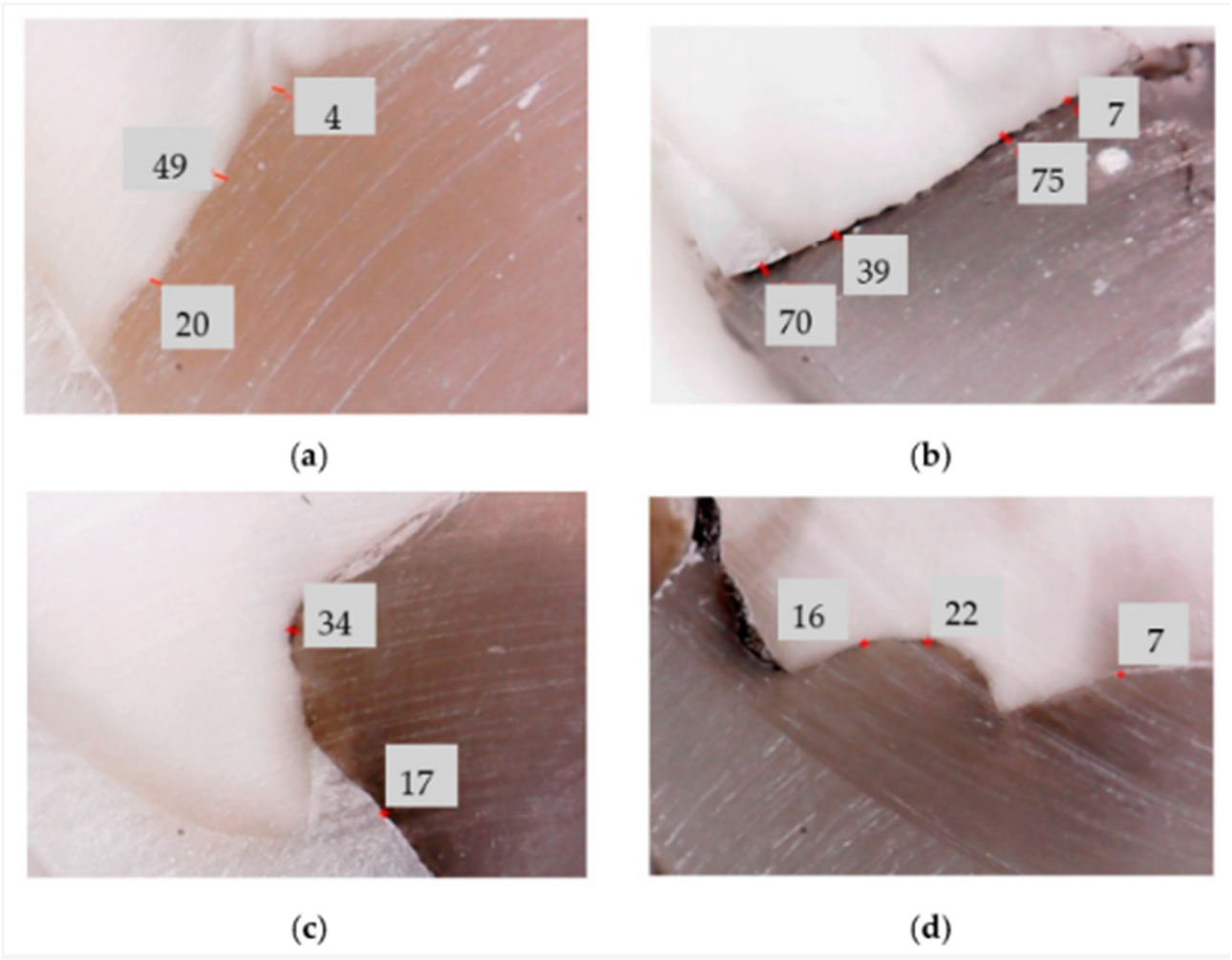


Figure 12.7. Example of a microscopy analysis of the width/thickness of the dental adhesive layer on a sample: (a) without MPs (from Group 1); (b) with MPs (from Group 2); (c) with MPs applied in a magnetic field for 5 min (from Group 3) and (d) for 10 min (from Group 4). The measured adhesive layer widths are provided in µm.

12.3.2.2. Micro-CT Analysis

The width/thickness of the adhesive layer obtained through micro-CT analysis ranged approximately between 0.018 and 0.40 mm (Table 1). Notably, the three areas analyzed using micro-CT yielded different results.

For Group 1 samples (non-loaded dental adhesives), the width (w) ranged between 0.02 and 0.4 mm. In Group 2 samples (adhesive loaded with MPs), w ranged between 0.017- and 0.4-mm. Group 3 samples (adhesives loaded with MPs and exposed to a magnetic field for 5 min) exhibited w ranging between 0.013 and 0.31 mm. Interestingly, the minimum width of the adhesive layer was found in Group 4 samples (adhesives loaded with MPs and exposed to a magnetic field for 10 min), with values between 0.011 and 0.032 mm.

Figure 12.8., 12.9., 12.10., 12.11., illustrate detailed micro-CT analyses for a sample from each of the four groups. These figures demonstrate similar results across all five samples in each group.

For Group 1 control teeth (Figure 12.8.), where dental adhesive was conventionally applied, surfaces exhibited w ranging from 0.01 to 0.4 mm, with the largest area of adhesive measuring approximately 0.1 mm in width.

In Group 2 samples (Figure 12.9.), where dental adhesive was loaded with MPs without exposure to a magnetic field, a similar range of w was observed. However, a slight decrease in adhesive thicknesses, particularly around 0.08 mm, was noticeable.

For Group 3 samples (Figure 12.10.), loaded with MPs and exposed to a magnetic field for 5 min, areas with increased adhesive thicknesses were substantially reduced, with predominant adhesive thicknesses ranging from 0.02 to 0.03 mm.

In Group 4 samples (Figure 12.11.), loaded with MPs and exposed to a magnetic field for 10 min, the adhesive layer thickness decreased across most areas. Predominantly, adhesive thicknesses ranged from 0.01 to 0.025 mm, with fewer areas exhibiting increased thickness compared to Group 3. These qualitative observations are complemented by quantitative analyses, demonstrating another advantage of micro-CT over microscopy—the ability to provide precise results for the entire volume of the dental adhesive layer.

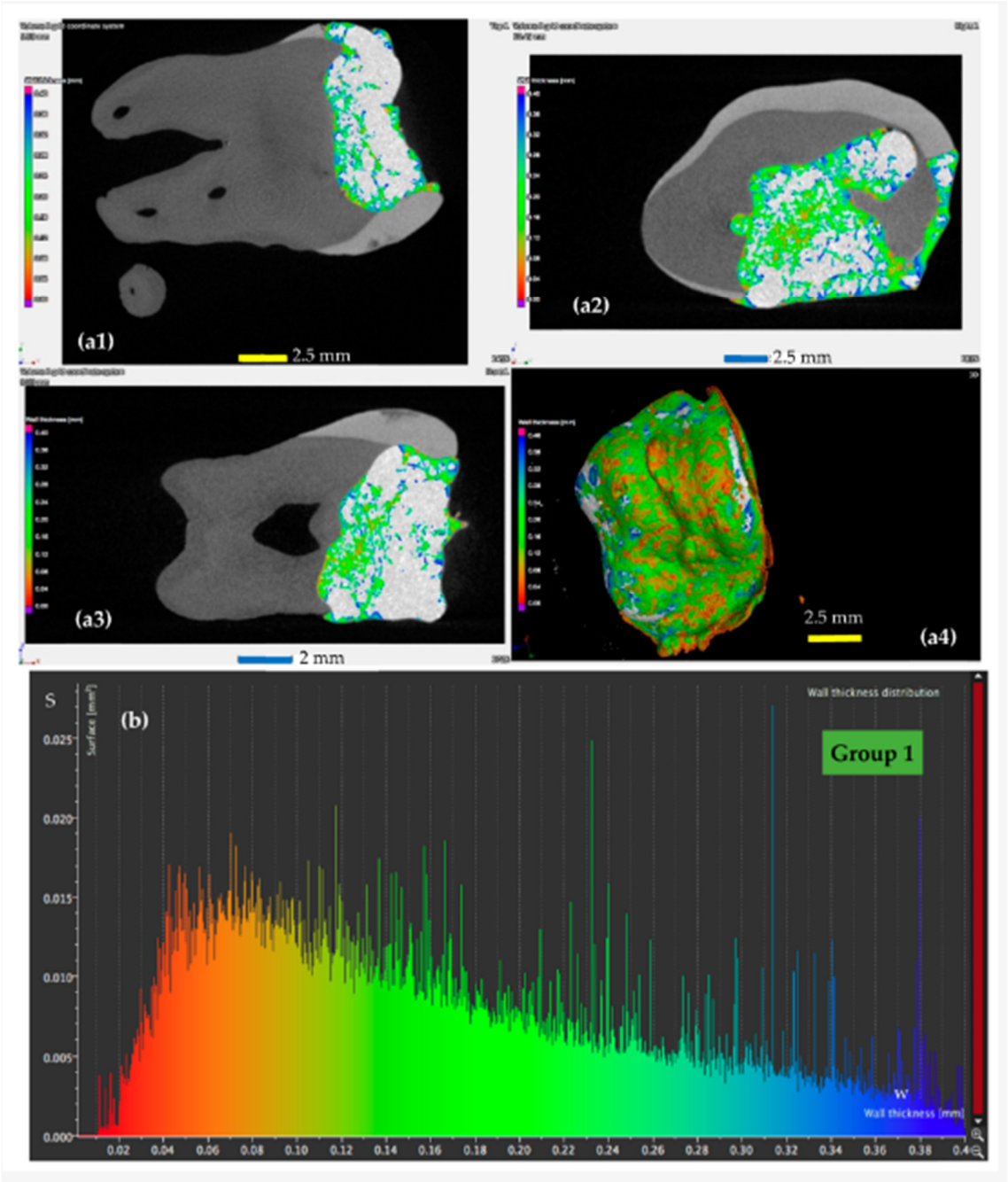


Figure 12.8. The results from a micro-CT investigation of a dental sample from Group 1, exploring various aspects of the dental layer and adhesive interface: (a) Micro-CT analysis of different interfaces in the Group 1 sample: (a1) Examines the vestibular interface, the tooth's external side facing the cheek, assessing how the dental adhesive interacts with this surface. (a2) Focuses on the oral interface, the side of the tooth facing into the oral cavity, to evaluate the adherence and effectiveness of the dental material in this area. (a3) Looks at the pulpal interface, the internal surface near the dental pulp, analyzing the penetration and bonding quality of the adhesive within the most

sensitive part of the tooth. (a4) Features a 3D reconstruction of the dental layer, providing a comprehensive visualization of the entire structure and distribution of the dental adhesive across different interfaces. (b) Analysis of the surface area of the dental adhesive layer (Area S) as it relates to its width/thickness ratio (denoted as w) for a Group 1 sample: This analysis seeks to understand how the physical dimensions of the adhesive layer, specifically its width and thickness, affect its surface area. Such insights are crucial for determining the optimal spread and thickness of the adhesive to ensure maximum coverage and effective bonding.

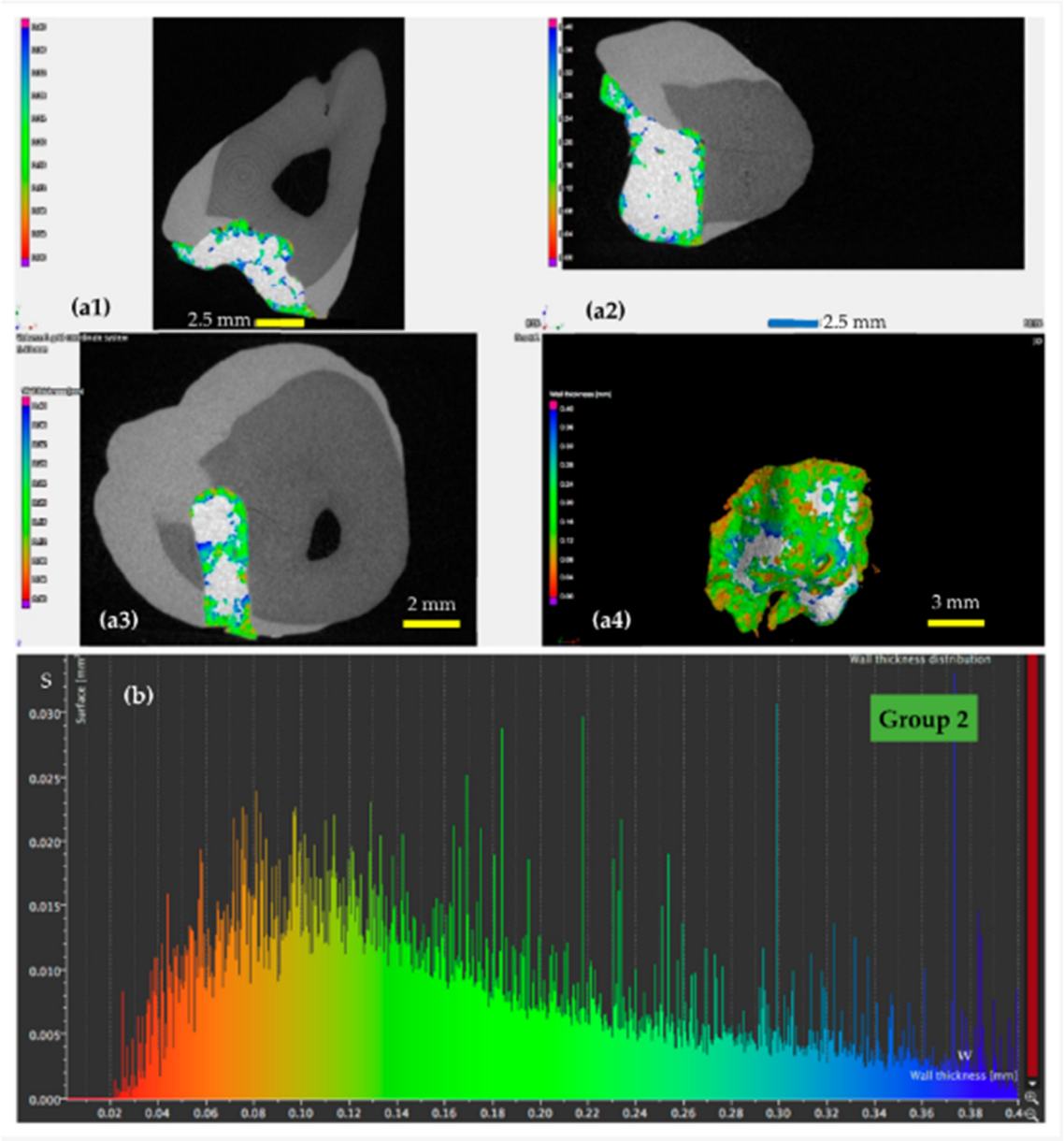


Figure 12.9. Findings from a micro-CT investigation focused on a dental sample from Group 2, providing a detailed analysis of the interfaces and adhesive layer dynamics: (a) The section features a micro-CT analysis of the different interfaces in the Group 2 dental sample: (a1) Assesses the vestibular interface, which is the external side of the tooth facing the cheek. This investigation helps understand the adhesive's coverage and bonding strength on the outermost surface of the tooth. (a2) Investigates the oral interface, the surface of the tooth that faces the interior of the oral cavity. This analysis evaluates how well the dental adhesive adheres to the areas exposed to the oral environment. (a3) Looks at the pulpal interface, the internal surface near the dental pulp. This part of the study examines the penetration and efficacy of the adhesive in the deeper, more sensitive layers of the tooth. (a4) Includes a 3D reconstruction of the dental layer, offering a holistic view of the adhesive's distribution and interaction with the tooth's structure across these various interfaces. (b) This segment explores the relationship between the surface area of the dental adhesive layer (Area S) and its width/thickness ratio (w) for a Group 2 sample: The analysis aims to determine how the dimensions of the adhesive layer influence its surface area, which is vital for optimizing the adhesive's effectiveness in terms of coverage and bonding capability.

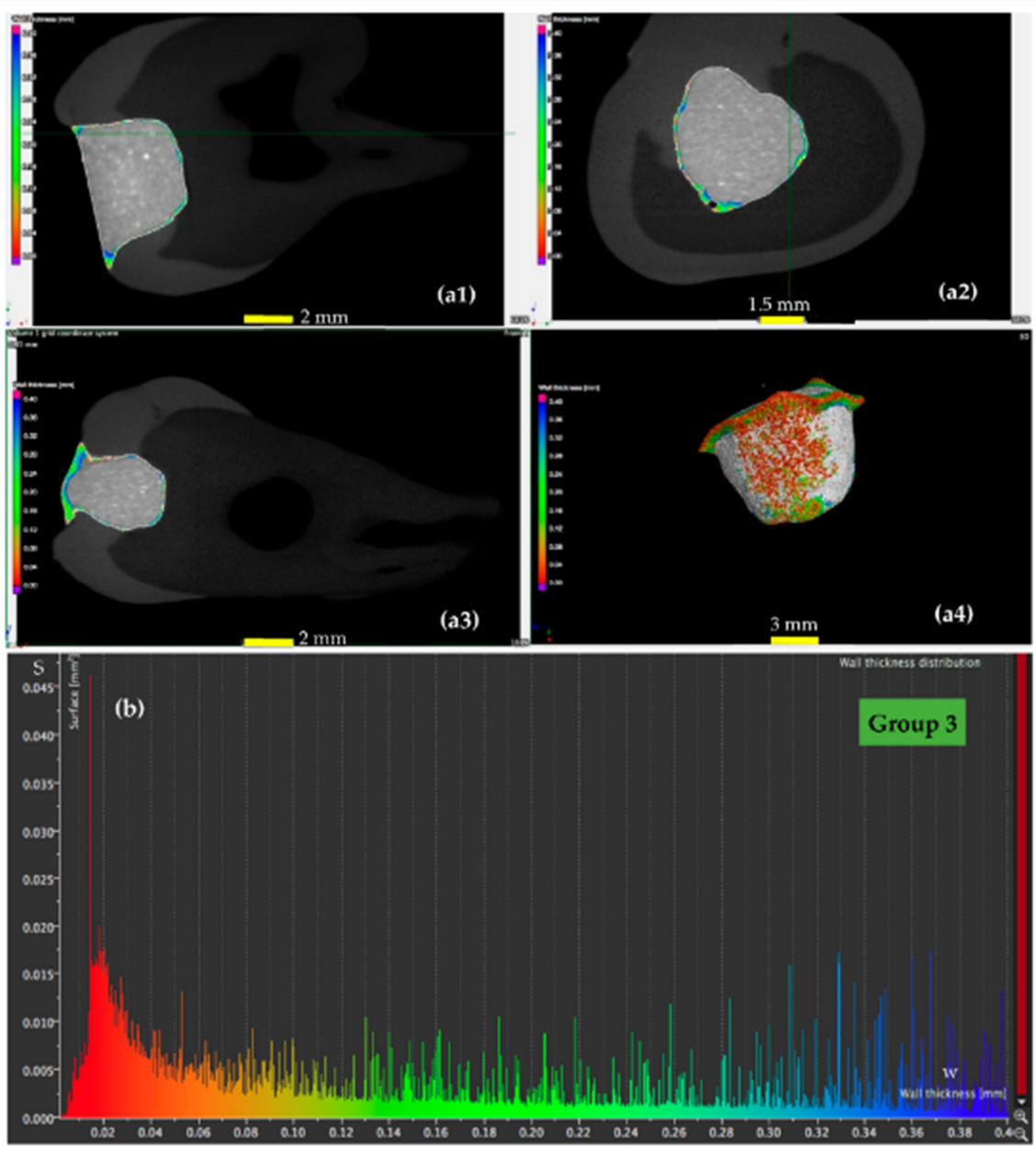


Figure 12.10. The results from a micro-CT investigation of a dental sample from Group 3, focusing on various tooth interfaces and the adhesive layer: (a) The micro-CT analysis covers different interfaces of the Group 3 dental sample: (a1) Examines the vestibular interface, which is the external side of the tooth facing the cheek. This study helps assess how the adhesive interacts with and adheres to the tooth's outer surface. (a2) Analyzes the oral interface, the side of the tooth facing the oral cavity. This evaluation looks at the effectiveness of the dental adhesive in areas exposed to oral environmental factors. (a3) Focuses on the pulpal interface, the inner surface near the dental pulp, examining the depth and quality of adhesive penetration and bonding within the tooth. (a4) Features a 3D reconstruction of the dental layer, providing an all-encompassing visual of the adhesive's distribution across these interfaces and its integration with the tooth structure. (b) This part discusses the relationship between the surface area of the dental adhesive layer (Area S) and its width/thickness ratio (denoted as w) in a Group 3 sample: This analysis aims to understand how the physical dimensions of the adhesive layer influence its overall surface area, crucial for optimizing the layer's spread, thickness, and bonding effectiveness.

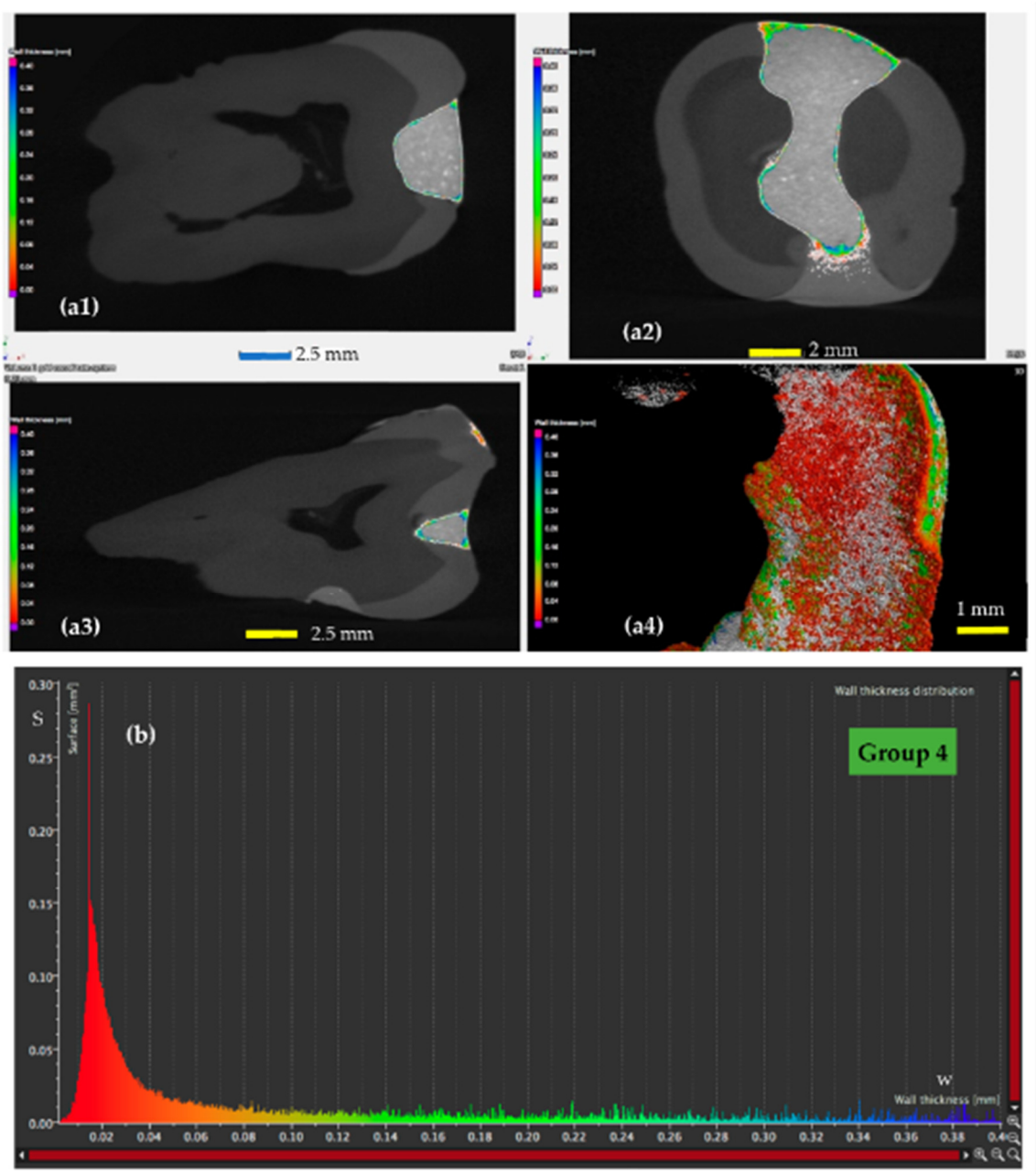


Figure 12.11. The analysis from a micro-CT study on a dental sample from Group 4, examining the interfaces and adhesive interactions within the tooth: (a) The micro-CT analysis includes detailed examinations of the various interfaces in the Group 4 sample: (a1) Studies the vestibular interface, the external side of the tooth that faces the cheek, assessing the coverage and bonding strength of the dental adhesive on this surface. (a2) Investigates the oral interface, the side of the tooth facing the oral cavity, to evaluate how effectively the dental adhesive adheres and performs in areas subjected to oral environmental conditions. (a3) Looks at the pulpal interface, the internal surface close to the dental pulp, examining the depth of adhesive penetration and the quality of bonding in the deeper layers of the tooth. (a4) Features a 3D reconstruction of the dental layer, providing a comprehensive visualization of how the adhesive is distributed across these interfaces and integrates with the overall tooth structure. (b) Discusses the relationship between the surface area of the dental adhesive layer (Area S) and its width/thickness ratio (denoted as w) in a Group 4 sample: This analysis is crucial for determining how the physical properties of the adhesive layer—specifically its width and thickness—affect its surface area, which is vital for achieving optimal adhesive coverage and bonding efficiency.

12.3.3. Conclusions

In this study, we introduced and evaluated a novel dental adhesive material loaded with magnetic nanoparticles (MPs), synthesized and characterized in our laboratory. Our findings demonstrate that incorporating MPs leads to a significant reduction in the width/thickness of the

adhesive layer, primarily due to the influence of a magnetic field on the Fe content of the nanoparticles. This reduction in width positively impacts the risk of microleakage at the dental interface. We observed that the best results in terms of adhesive layer thickness were achieved when MPs were incorporated into the adhesive and exposed to a magnetic field for an extended period. Therefore, it is advisable to prolong this exposure time to maximize the effectiveness of the adhesive—while ensuring patient comfort.

We found a notable agreement between the results obtained using the two measurement methods, optical microscopy and micro-CT, with microscopy being more accessible to users. However, micro-CT provided more precise results, allowing for a thorough comparison of adhesive layer thickness among the four experimental groups. Additionally, micro-CT facilitated mathematical modeling of the adhesive layer surfaces as a function of their widths, enabling the calculation and comparison of adhesive material volumes for each sample. This novel, quantitative, and accurate assessment methodology considers the entire volumetric distribution of the adhesive, representing a significant advancement in our understanding of adhesive behavior.

Future research in our group will focus on encapsulating the MPs to enhance the aesthetic properties of the adhesive. This will necessitate studying the mechanical properties and microleakage behavior of the resulting material, further advancing our understanding and application of dental adhesives.

12.4. Quiz 12.

1.Which of the following are potential benefits of incorporating nanoparticles into dental adhesive systems?
a). Enhanced antibacterial properties
b). Improved mechanical properties
c). Increased radiopacity
d). Enhanced antibacterial properties
e). Reduced polymerization shrinkage

2.What are common challenges in developing dental nanocomposites?
a). Achieving effective dispersion of nanoparticles
b). Maintaining high filler loading levels
c). Reducing polymerization shrinkage
d). Optimizing handling characteristics
e). Ensuring cost-effectiveness

3.Which nanoparticles have been utilized to enhance remineralization potential in dental composite materials?
a). Amorphus calcium phosphate (ACP)
b). Calcium fluoride nanoparticles (nCaF2)
c). Silver nanoparticles (nAg)
d). Zinc oxide nanoparticles (nZnO)
e). Silicon carbide whiskers

4.What properties can nanoparticles contribute to dental adhesives?
a). Increased bond strength
b). Improved resistance to microleakage
c). Enhanced antibacterial activity
d). Reduced polymerization shrinkage
e). Enhanced radiopacity

5.What challenges are associated with the use of nanoparticles in indirect restorative systems?
a). Controlling phase transformation
b). Enhancing fracture toughness
c). Addressing porosity
d). Achieving optimal particle distribution
e). Improving color matching

6.What are the potential advantages of using nanomodified glass ionomer (GICs) in dentistry?
a). Increased fracture toughness
b). Enhanced fluoride release
c). Improved wear resistance
d). Enhanced aesthetic properties
e). Reduced water sensitivity

7.Which nanoparticles have been investigated for their potential to improve mechanical properties in dental composite materials?
a). Titanium dioxide (TiO2)
b). Hydroxyapatite (HA)
c). Ytterbium fluoride (YbF3)
d). Barium sulfate (BaSO4)
e). Chlorhexidine (CHX)

8.What challenges are associated with the incorporation of nanoparticles into dental adhesive systems?
a). Achieving uniform dispersion of nanoparticles
b). Maintaining optimal handling characteristics
c). Preventing agglomeration of nanoparticles
d). Reducing filler loading levels
e). Enhancing polymerization shrinkage

9*. How do nanofillers contribute to the mechanical properties of dental composites?
a). By increasing polymerization shrinkage
b). By reducing wear resistance
c). By enhancing flexural strength
d). By decreasing radiopacity
e). By promoting microleakage

10*. Which commercial resin-modified glass ionomer cement (GIC) contains aggregated nanoclusters composed of spherical particles?
a). Ketac Nano
b). Riva SC
c). Fuji II LC
d). Filtek Supreme
e). Vitremer

References

[1]. Crisp S, Ferner AJ, Lewis BG, Wilson AD. Properties of improved glass-ionomer cement formulations. J Dent. 1975;3(3):125–30.
[2]. McLean JW, Nicholson JW, Wilson AD. Proposed nomenclature for glass-ionomer dental cements and related materials. Quintessence Int. 1994;25(9): 587–9.
[3]. McKinney JE, Antonucci JM, Rupp NW. Wear and microhardness of glass-ionomer cements. J Dent Res. 1987;66(6):1134–9.
[4]. Mitra SB, Oxman JD, Falsafi A, Ton TT. Fluoride release and recharge behavior of a nano-filled resin modified glass ionomer compared with that of other fluoride releasing materials. Am J Dent. 2011;24(6): 372–8.
[5]. Smith DC. Development of glass-ionomer cement systems. Biomaterials. 1998;19(6):467–78.
[6]. Sidhu SK, Sherriff M, Watson TF. In vivo changes in roughness of resin-modified glass ionomer materials. Dent Mater Off Publ AcadDent Mater. 1997; 13(3):208–13.
[7]. Goenka S, Balu R, Sampath Kumar TS. Effects of nanocrystalline calcium deficient hydroxyapatite incorporation in glass ionomer cements. J Mech Behav Biomed Mater. 2012; 7:69–76.
[8]. Rajabzadeh G, Salehi S, Nemati A, Tavakoli R, Solati Hashjin M. Enhancing glass ionomer cement features by using the HA/YSZ nanocomposite: a feed forward neural network modelling. J Mech Behav Biomed Mater. 2014; 29:317–27.
[9]. Randall RC, Wilson NH. Glass-ionomer restoratives: a systematic review of a secondary caries treatment effect. J Dent Res. 1999;78(2):628–37.
[10]. Wiegand A, Buchalla W, Attin T. Review on fluoride releasing restorative materials–fluoride release and uptake characteristics, antibacterial activity and influence on caries formation. Dent Mater Off Publ AcadDent Mater. 2007;23(3): 343–62.
[11]. Xie D, Brantley WA, Culbertson BM, Wang G. Mechanical properties and microstructures of glass-ionomer cements. Dent Mater Off Publ AcadDent Mater. 2000;16(2):129–38.
[12]. Shoji AK, H, Kentaro TGC. Fluor aluminosilicate glass powder for dental glass ionomer cement. 1988. US patent US 4775592 A. http://www.google.ca/ patents/US4775592.
[13]. Xu HH, Sun L, Weir MD, Antonucci JM, Takagi S, Chow LC, et al. Nano DCPA-whisker composites with high strength and Ca and PO (4) release. J Dent Res. 2006;85(8):722–7.
[14]. Xu HH, Moreau JL, Sun L, Chow LC. Novel CaF(2) nanocomposite with high strength and fluoride ion release. J Dent Res. 2010;89(7):739–45.
[15]. De Maeyer EA, Verbeeck RM, Vercruysse CW. Reactivity of fl uoride-containing calcium aluminosilicate glasses used in dental glass-ionomer cements. J Dent Res. 1998;77(12):2005–11.
[16]. Moshaverinia A, Ansari S, Moshaverinia M, Roohpour N, Darr JA, Rehman I. Effects of incorporation of hydroxyapatite and fluorapatite nano bioceramics into conventional glass ionomer cements (GIC). Acta Biomater. 2008;4(2):432–40.
[17]. Moshaverinia A, Ansari S, Movasaghi Z, Billington RW, Darr JA, Rehman IU. Modification of conventional glass-ionomer cements with N-vinylpyrrolidone containing polyacids, nanohydroxy and fluoroapatite to improve mechanical properties. Dent Mater Off Publ AcadDent Mater. 2008;24(10):1381–90.
[18]. Lee JJ, Lee YK, Choi BJ, Lee JH, Choi HJ, Son HK, et al. Physical properties of resin-reinforced glass ionomer cement modifi ed with micro and nanohydroxyapatite. J Nanosci Nanotechnol. 2010; 10(8):5270–6.
[19]. Siddharthan A, Seshadri SK, Sampath Kumar TS. Microwave accelerated synthesis of nanosized calcium deficient hydroxyapatite. J Mater Sci Mater Med. 2004;15(12):1279–84.
[20]. Fadeel B, Garcia-Bennett AE. Better safe than sorry: Understanding the toxicological properties of inorganic nanoparticles manufactured for biomedical applications. Adv Drug Deliv Rev. 2010;62(3): 362–74.
[21]. El-Negoly SA, El-Fallal AA, El-Sherbiny IM. A New Modification for Improving Shear Bond Strength and Other Mechanical Properties of Conventional Glass-ionomer Restorative Materials. J Adhes Dent. 2014;16(1):41–7.
[22]. Elsaka SE, Hamouda IM, Swain MV. Titanium dioxide nanoparticles addition to a conventional glassionomer restorative: infl uence on physical and antibacterial properties. J Dent. 2011;39(9):589–98.
[23]. Tsuang YH, Sun JS, Huang YC, Lu CH, Chang WH, Wang CC. Studies of photokilling of bacteria using titanium dioxide nanoparticles. Artif Organs. 2008; 32(2):167–74.
[24]. Hook ER, Owen OJ, Bellis CA, Holder JA, O'Sullivan DJ, Barbour ME. Development of a novel antimicrobial-releasing glass ionomer cement functionalized with chlorhexidine hexametaphosphate nanoparticles. J Nanobiotechnol. 2014; 12(1):3.
[25]. Clarkson BH, Feagin FF, McCurdy SP, Sheetz JH, Speirs R. Effects of phosphoprotein moieties on the remineralization of human root caries. Caries Res. 1991; 25:166–73.
[26]. McIntyre JM, Featherstone JD, Fu J. Studies of dental root surface caries. 1: comparison of natural and artificial root caries lesions. Aust Dent J. 2000; 45:24–30.
[27]. Nyvad B, Rejerskov O. Active root surface caries converted into inactive caries as a response to oral hygiene. Scand J Dent Res. 1986; 94:281–4.
[28]. ten Cate JM. Remineralization of deep enamel dentine caries lesions. Aust Dent J. 2008; 53:281–5.
[29]. Alauddin SS, Greenspan D, Anusavice KJ, Mecholsky J. In vitro human enamel remineralization using bioactive glass containing dentifrice. J Dent Res. 2005; 84:2546.

[30]. Cheng L, Weir MD, Xu HHK, Kraigsley AM, Lin NJ, Lin-Gibson S, Zhou X. Antibacterial and physical properties of calcium–phosphate and calcium–fluoride nanocomposites with chlorhexidine. Dent Mater. 2012;28(5):573–83.
[31]. Wefel JS. Effects of fluoride on caries development and progression using intra-oral models. J Dent Res. 1990; 69:626.
[32]. Ten Cate JM, Featherstone JDB. Mechanistic aspects of the interactions between fluoride and dental enamel. Crit Rev Oral Biol Med. 1991;2(3):283–96.
[33]. Stoodley P, Wefel J, Gieseke A, von Ohle C. Biofilm plaque and hydrodynamic effects on mass transfer, fluoride delivery and caries. J Am Dent Assoc. 2008;139(9):1182–90.
[34]. Kirsten GA, Takahashi MK, Rached RN, Giannini M, Souza EM. Microhardness of dentin underneath fluoride-releasing adhesive systems subjected to cariogenic challenge and fluoride therapy. J Dent. 2010;38(6):460–8.
[35]. Cenci MS, Tenuta LMA, Pereira-Cenci T, Del Bel Cury AA, Ten Cate JM, Cury JA. Effect of microleakage and fluoride on enamel-dentine demineralization around restorations. Caries Res. 2008;42(5):369–79.
[36]. Mousavinasab SM, Meyers I. Fluoride release and uptake by glass ionomer cements, compomers and giomers. Res J Biol Sci. 2009;4(5):609–16.
[37]. Xu HHK, Moreau JL, Sun L, Chow LC. Strength and fluoride release characteristics of a calcium fluoride based dental nanocomposite. Biomaterials. 2008;29(32):4261–7.
[38]. de Paula AB, Fucio SB, Ambrosano GM, Alonso RC, Sardi JC, Puppin-Rontani RM. Biodegradation and abrasive wear of nano restorative materials. Oper Dent. 2011;36(6):670–7.
[39]. Lammeier C, Li Y, Lunos S, Fok A, Rudney J, Jones RS. Infl uence of dental resin material composition on cross-polarization-optical coherence tomography imaging. J Biomed Opt. 2012;17(10): 106002.
[40]. Moszner N, Klapdohr S. Nanotechnology for dental composites. Int J of Nanotechnology. 2004;1(1/2): 130–56.
[41]. Klapdohr S, Moszner N. New inorganic components for dental fi lling composites. Monatshefte fur Chemie. 2005; 136:21–45.
[42]. Wilson KS, Zhang K, Antonucci JM. Systematic variation of interfacial phase reactivity in dental nanocomposites. Biomaterials. 2005;26(25): 5095–103.
[43]. Chen MH, Chen CR, Hsu SH, Sun SP, Su WF. Low shrinkage light curable nanocomposite for dental restorative material. Dent Mater Off Publ AcadDent Mater. 2006;22(2):138–45.
[44]. Furman B, Rawls HR, Wellinghoff S, Dixon H, Lankford J, Nicolella D. Metal-oxide nanoparticles for the reinforcement of dental restorative resins. Crit Rev Biomed Eng. 2000;28(3–4):439–43.
[45]. Wang Y, Lee JJ, Lloyd IK, Wilson Jr OC, Rosenblum M, Thompson V. High modulus nanopowder reinforced dimethacrylate matrix composites for dental cement applications. J Biomed Mater Res A. 2007; 82(3): 651–7.
[46]. Tian M, Gao Y, Liu Y, Liao Y, Hedin NE, Fong H. Fabrication and evaluation of Bis-GMA/TEGDMA dental resins/composites containing nano fibrillar silicate. Dent Mater Off Publ AcadDent Mater. 2008;24(2):235–43.
[47]. Xia Y, Zhang F, Xie H, Gu N. Nanoparticle reinforced resin-based dental composites. J Dent. 2008;36(6):450–5.
[48]. Zhang K, Melo MA, Cheng L, Weir MD, Bai Y, Xu HH. Effect of quaternary ammonium and silver nanoparticle-containing adhesives on dentin bond strength and dental plaque microcosm biofilms. Dent Mater Off Publ AcadDent Mater. 2012;28(8): 842–52.
[49]. Zhang K, Li F, Imazato S, Cheng L, Liu H, Arola DD, et al. Dual antibacterial agents of nano-silver and 12-methacryloyloxydodecylpyridinium bromide in dental adhesive to inhibit caries. J Biomed Mater Res B Appl Biomater. 2013;101(6):929–38.
[50]. Sideridou ID, Karabela MM, Vouvoudi E. Physical properties of current dental nanohybrid and nanofill light-cured resin composites. Dent Mater Off Publ AcadDent Mater. 2011;27(6):598–607.
[51]. Endo T, Finger WJ, Kanehira M, Utterodt A, Komatsu M. Surface texture and roughness of polished nanofill and nanohybrid resin composites. Dent Mater J. 2010;29(2):213–23.
[52]. Taha DG, Abdel-Samad AA, Mahmoud SH. Fracture resistance of maxillary premolars with class II MOD cavities restored with Ormocer, Nanofilled, and Nanoceramic composite restorative systems. Quintessence Int. 2011;42(7):579–87.
[53]. Tabatabaei MH, Sadrai S, Bassir SH, Veisy N, Dehghan S. Effect of food stimulated liquids and thermocycling on the monomer elution from a nanofilled composite. Open Dent J. 2013; 7:62–7.
[54]. Eren D, Bektas OO, Siso SH. Three different adhesives systems; three different bond strength test methods. Acta Odontol Scand. 2013;71(3–4):978–83.
[55]. Vanderlei A, Passos SP, Ozcan M, Bottino MA, Valandro LF. Durability of adhesion between feldspathic ceramic and resin cements: effect of adhesive resin, polymerization mode of resin cement, and aging. J Prosthodont Off J Am Coll Prosthodont. 2013;22(3):196–202.
[56]. Ernst CP, Brandenbusch M, Meyer G, Canbek K, Gottschalk F, Willershausen B. Two-year clinical performance of a nanofi ller vs a fi ne-particle hybrid resin composite. Clin Oral Investig. 2006;10(2): 119–25.
[57]. Polydorou O, Konig A, Hellwig E, Kummerer K. Long-term release of monomers from modern dental-composite materials. Eur J Oral Sci. 2009; 117(1): 68–75.
[58]. da Silva JM, da Rocha DM, Travassos AC, Fernandes Jr VV, Rodrigues JR. Effect of different finishing times on surface roughness and maintenance of polish in nanoparticle and microhybrid composite resins. Eur J Esthet Dent Off J Eur Acad Esthet Dent. 2010;5(3):288–98.

[59]. Feitosa VP, Fugolin AP, Correr AB, Correr-Sobrinho L, Consani S, Watson TF, et al. Effects of different photo-polymerization protocols on resin-dentine muTBS, mechanical properties and cross-link density of a nano-fi lled resin composite. J Dent. 2012; 40(10):802–9.
[60]. Egilmez F, Ergun G, Cekic-Nagas I, Vallittu PK, Lassila LV. Short- and long-term effects of additional post curing and polishing systems on the color change of dental nano-composites. Dent Mater J. 2013; 32(1):107–14.
[61]. Al Kheraif AA, Qasim SS, Ramakrishnaiah R, Ihtesham ur R. Effect of different beverages on the color stability and degree of conversion of nano and microhybrid composites. Dent Mater J. 2013; 32(2):326–31.
[62]. Takano T, Tasaka A, Yoshinari M, Sakurai K. Fatigue strength of Ce-TZP/Al2O3 nanocomposite with different surfaces. J Dent Res. 2012;91(8):800–4.
[63]. Fischer J, Stawarczyk B, Sailer I, Hammerle CHF. Shear bond strength between veneering ceramics and ceria-stabilized zirconia/alumina. J Prosthet Dent. 2010;103(5):267–74.
[64]. Xu HH, Weir MD, Sun L, Moreau JL, Takagi S, Chow LC, et al. Strong nanocomposites with Ca, PO (4), and F release for caries inhibition. J Dent Res. 2010;89(1):19–28.
[65]. Nakabayashi N, Kojima K, Masuhara E. The promotion of adhesion by the infiltration of monomers into tooth substrates. J Biomed Mater Res. 1982;16(3): 265–73.
[66]. Hosoya Y, Tay FR. Hardness, elasticity, and ultrastructure of bonded sound and caries-affected primary tooth dentin. J Biomed Mater Res B Appl Biomater. 2007;81(1):135–41.
[67]. Nakabayashi N, Nakamura M, Yasuda N. Hybrid layer as a dentin-bonding mechanism. J Esthet Dent. 1991;3(4):133–8.
[68]. Poitevin A, De Munck J, Van Landuyt K, Coutinho E, Peumans M, Lambrechts P, et al. Critical analysis of the infl uence of different parameters on the microtensile bond strength of adhesives to dentin. J Adhes Dent. 2008;10(1):7–16.
[69]. Breschi L, Mazzoni A, Ruggeri A, Cadenaro M, Di Lenarda R, De Stefano Dorigo E. Dental adhesion review: aging and stability of the bonded interface. Dent Mater Off Publ AcadDent Mater. 2008;24(1): 90–101.
[70]. Osorio R, Yamauti M, Osorio E, Roman JS, Toledano M. Zinc-doped dentin adhesive for collagen protection at the hybrid layer. Eur J Oral Sci. 2011;119(5): 401–10.
[71]. Sano H, Takatsu T, Ciucchi B, Horner JA, Matthews WG, Pashley DH. Nanoleakage: leakage within the hybrid layer. Oper Dent. 1995;20(1):18–25.
[72]. Hashimoto M, Tay FR, Ohno H, Sano H, Kaga M, Yiu C, et al. SEM and TEM analysis of water degradation of human dentinal collagen. J Biomed Res B Appl Biomater. 2003;66(1):287–98.
[73]. Hebling J, Pashley DH, Tjaderhane L, Tay FR. Chlorhexidine arrests subclinical degradation of dentin hybrid layers in vivo . J Dent Res. 2005;84(8): 741–6.
[74]. Spencer P, Wang Y. Adhesive phase separation at the dentin interface under wet bonding conditions. J Biomed Mater Res. 2002;62(3):447–56.
[75]. Kim JS, Cho BH, Lee IB, Um CM, Lim BS, Oh MH, et al. Effect of the hydrophilic nanofiller loading on the mechanical properties and the microtensile bond strength of an ethanol-based one-bottle dentin adhesive. J Biomed Mater Res B Appl Biomater. 2005; 72(2):284–91.
[76]. Lohbauer U, Wagner A, Belli R, Stoetzel C, Hilpert A, Kurland HD, et al. Zirconia nanoparticles prepared by laser vaporization as fi llers for dental adhesives. Acta Biomater. 2010;6(12):4539–46.
[77]. Osorio E, Toledano M, Yamauti M, Osorio R. Differential nanofi ller cluster formations in dental adhesive systems. Microsc Res Tech. 2012;75(6): 749–57.
[78]. Denehy GE. A direct approach to restore anterior teeth. Am J Dent. 2000;13(Spec No):55D–9.
[79]. Hickel R, Dasch W, Janda R, Tyas M, Anusavice K. New direct restorative materials. FDI Commission Project. Int Dent J. 1998;48(1):3–16.
[80]. Hosseinalipour M, Javadpour J, Rezaie H, Dadras T, Hayati AN. Investigation of mechanical properties of experimental Bis-GMA/TEGDMA dental composite resins containing various mass fractions of silica nanoparticles. J Prosthodont Off J Am Coll Prosthodont. 2010;19(2):112–7.
[81]. Xu HH, Moreau JL, Sun L, Chow LC. Nanocomposite containing amorphous calcium phosphate nanoparticles for caries inhibition. Dent Mater Off Publ AcadDent Mater. 2011;27(8):762–9.

[82]. Van Landuyt KL, Snauwaert J, De Munck J, Peumans M, Yoshida Y, Poitevin A, et al. Systematic review of the chemical composition of contemporary dental adhesives. Biomaterials. 2007;28(26): 3757–85.
[83]. Kasraei ShA M, Khamverdi Z, Khalegh Nejad S. Effect of nanofi ller addition to an experimental dentin adhesive on microtensile bond strength to human dentin. J Dent (Tehran). 2009; 6:91–6.
[84]. Osorio E, Toledano M, Aguilera FS, Tay FR, Osorio R. Ethanol wet-bonding technique sensitivity assessed by AFM. J Dent Res. 2010;89(11):1264–9.
[85]. Tay FR, Moulding KM, Pashley DH. Distribution of nanofillers from a simplified-step adhesive in acid conditioned dentin. J Adhes Dent. 1999;1(2): 103–17.
[86]. de Monredon-Senani S, Bonhomme C, Ribot F, Babonneau F. Covalent grafting of organoalkoxysilanes on silica surfaces in water-rich medium as evidenced by Si-29 NMR. J Sol-gel Sci Techn. 2009; 50(2): 152–7.
[87]. Cheng L, Weir MD, Zhang K, Xu SM, Chen Q, Zhou X, et al. Antibacterial nanocomposite with calcium

phosphate and quaternary ammonium. J Dent Res. 2012;91(5):460–6.
[88]. Cheng L, Weir MD, Xu HH, Antonucci JM, Kraigsley AM, Lin NJ, et al. Antibacterial amorphous calcium phosphate nanocomposites with a quaternary ammonium dimethacrylate and silver nanoparticles. Dent Mater Off Publ AcadDent Mater. 2012;28(5):561–72.
[89]. Li F, Weir MD, Chen J, Xu HH. Comparison of quaternary ammonium-containing with nano-silvercontaining adhesive in antibacterial properties and cytotoxicity. Dent Mater Off Publ AcadDent Mater. 2013;29(4):450–61.
[90]. Morones JR, Elechiguerra JL, Camacho A, Holt K, Kouri JB, Ramirez JT, et al. The bactericidal effect of silver nanoparticles. Nanotechnology. 2005; 16(10): 2346–53.
[91]. Zhang K, Cheng L, Imazato S, Antonucci JM, Lin NJ, Lin-Gibson S, et al. Effects of dual antibacterial agents MDPB and nano-silver in primer on microcosm biofilm, cytotoxicity and dentine bond properties. J Dent. 2013;41(5):464–74.
[92]. Cheng L, Zhang K, Weir MD, Liu H, Zhou X, Xu HH. Effects of antibacterial primers with quaternary ammonium and nano-silver on Streptococcus mutans impregnated in human dentin blocks. Dent Mater Off Publ AcadDent Mater. 2013;29(4): 462–72.
[93]. Skrtic D, Antonucci JM, Eanes ED, Eichmiller FC, Schumacher GE. Physicochemical evaluation of bioactive polymeric composites based on hybrid amorphous calcium phosphates. J Biomed Mater Res. 2000;53(4):381–91.
[94]. Melo MA, Cheng L, Zhang K, Weir MD, Rodrigues LK, Xu HH. Novel dental adhesives containing nanoparticles of silver and amorphous calcium phosphate. Dent Mater Off Publ AcadDent Mater. 2013; 29(2): 199–210.
[95]. Melo MA, Cheng L, Weir MD, Hsia RC, Rodrigues LK, Xu HH. Novel dental adhesive containing antibacterial agents and calcium phosphate nanoparticles. J Biomed Mater Res B Appl Biomater. 2013; 101(4):620–9.
[96]. Besinis A, van Noort R, Martin N. Infiltration of demineralized dentin with silica and hydroxyapatite nanoparticles. Dent Mater Off Publ AcadDent Mater. 2012;28(9):1012–23.
[97]. Cai YR, Tang RK. Calcium phosphate nanoparticles in biomineralization and biomaterials. J Mater Chem. 2008;18(32):3775–87.
[98]. Sadat-Shojai M, Atai M, Nodehi A, Khanlar LN. Hydroxyapatite nanorods as novel fillers for improving the properties of dental adhesives: Synthesis and application. Dent Mater Off Publ AcadDent Mater. 2010;26(5):471–82.
[99]. Earl JS, Wood DJ, Milne SJ. Nanoparticles for dentine tubule infi ltration: an in vitro study. J Nanosci Nanotechnol. 2009;9(11):6668–74.
[100]. Kajita M, Hikosaka K, Iitsuka M, Kanayama A, Toshima N, Miyamoto Y. Platinum nanoparticle is a useful scavenger of superoxide anion and hydrogen peroxide. Free Radic Res. 2007;41(6):615–26.
[101]. Salamanca-Buentello F, Persad DL, Court EB, Martin DK, Daar AS, Singer PA. Nanotechnology and the developing world. PLoS Med. 2005;2(5): e97.
[102]. Hoshika S, Nagano F, Tanaka T, Ikeda T, Wada T, Asakura K, et al. Effect of application time of colloidal platinum nanoparticles on the microtensile bond strength to dentin. Dent Mater J. 2010; 29(6):682–9.
[103]. Nagano F, Selimovic D, Noda M, Ikeda T, Tanaka T, Miyamoto Y, et al. Improved bond performance of a dental adhesive system using nano-technology. Bioed Mater Eng. 2009;19(2–3):249–57.
[104]. Hoshika S, Nagano F, Tanaka T, Wada T, Asakura K, Koshiro K, et al. Expansion of nanotechnology for dentistry: effect of colloidal platinum nanoparticles on dentin adhesion mediated by 4-META/MMATBB. J Adhes Dent. 2011;13(5):411–6.
[105] Toledano M, Sauro S, Cabello I, Watson T, Osorio R. A Zn-doped etch-and-rinse adhesive may improve the mechanical properties and the integrity at the bonded-dentin interface. Dent Mater Off Publ AcadDent Mater. 2013;29(8):e142–52.
[106]. Osorio R, Yamauti M, Osorio E, Ruiz-Requena ME, Pashley DH, Tay FR, et al. Zinc reduces collagen degradation in demineralized human dentin explants. J Dent. 2011;39(2):148–53.
[107]. de Souza AP, Gerlach RF, Line SR. Inhibition of human gingival gelatinases (MMP-2 and MMP-9) by metal salts. Dent Mater Off Publ AcadDent Mater. 2000;16(2):103–8.
[108]. Toledano M, Yamauti M, Ruiz-Requena ME, Osorio R. A ZnO-doped adhesive reduced collagen degradation favouring dentine remineralization. J Dent. 2012;40(9):756–65.
[109]. Sakharov DV, Lim C. Zn protein simulations including charge transfer and local polarization effects. J Am Chem Soc. 2005;127(13):4921–9.
[110]. Atai M, Solhi L, Nodehi A, Mirabedini SM, Kasraei S, Akbari K, et al. PMMA-grafted nanoclay as novel fi ller for dental adhesives. Dent Mater Off Publ AcadDent Mater. 2009;25(3):339–47.
[111]. Solhi L, Atai M, Nodehi A, Imani M. A novel dentin bonding system containing poly(methacrylic acid) grafted nanoclay: synthesis, characterization and properties. Dent Mater Off Publ AcadDent Mater. 2012;28(10):1041–50.
[112]. Solhi L, Atai M, Nodehi A, Imani M, Ghaemi A, Khosravi K. Poly(acrylic acid) grafted montmorillonite as novel fi llers for dental adhesives: synthesis, characterization and properties of the adhesive. Dent Mater Off Publ AcadDent Mater. 2012;28(4): 369–77.

[113]. Moraes RR, Garcia JW, Barros MD, Lewis SH, Pfeifer CS, Liu J, et al. Control of polymerization shrinkage and stress in nanogel-modifi ed monomer and composite materials. Dent Mater Off Publ AcadDent Mater. 2011;27(6):509–19.
[114]. Moraes RR, Garcia JW, Wilson ND, Lewis SH, Barros MD, Yang B, et al. Improved dental adhesive formulations based on reactive nanogel additives. J Dent Res. 2012;91(2):179–84.
[115]. Cheng YJ, Zeiger DN, Howarter JA, Zhang XR, Lin NJ, Antonucci JM, et al. In situ formation of silver nanoparticles in photocrosslinking polymers. J Biomed Mater Res B. 2011;97B(1):124–31.
[116]. Scherrer SS, Quinn JB, Quinn GD, Wiskott HW. Fractographic ceramic failure analysis using the replica technique. Dent Mater Off Publ AcadDent Mater. 2007;23(11):1397–404.
[117]. Ali SM. Prediction of the service life of dental porcelains by the measurements of post-indentation slow crack growth. Dent Mater J. 1993;12(1): 45–53.
[118]. Cesar PF, Soki FN, Yoshimura HN, Gonzaga CC, Styopkin V. Infl uence of leucite content on slow crack growth of dental porcelains. Dent Mater Off Publ AcadDent Mater. 2008;24(8):1114–22.
[119]. Zhu SM, Fahrenholtz WG, Hilmas GE. Influence of silicon carbide particle size on the microstructure and mechanical properties of zirconium diboridesilicon carbide ceramics. J Eur Ceram Soc. 2007; 27(4):2077–83.
[120]. Niihara K. New design concept of structural ceramic – ceramic nanocomposites. J Ceram Soc Jpn. 1991; 99:974–82.
[121]. Zhang J, Liao Y, Li W, Zhao Y, Zhang C. Microstructure and mechanical properties of glass-infiltrated Al2O3/ZrO2 nanocomposites. J Mater Sci Mater Med. 2012;23(2):239–44.
[122]. Allen AJ, Long GG, Kerch HM, Krueger S, Skandan G, Hahn H, et al. Sintering studies of nanophase ceramic oxides using small angle scattering. Ceram Int. 1996;22(4):275–80.
[123]. Chevalier J, Gremillard L, Deville S. Low temperature degradation of Zirconia and implications for biomedical implants. Annu Rev Mater Res. 2007; 37:1–32.
[124]. Yang SF, Yang LQ, Jin ZH, Guo TW, Wang L, Liu HC. New nano-sized Al2O3-BN coating 3Y-TZP ceramic composites for CAD/CAM-produced all ceramic dental restorations. Part I. Fabrication of powders. Nanomed Nanotechnol Biol Med. 2009; 5(2): 232–9.
[125]. Garvie RC, Hannink RH, Pascoe RT. Ceramic Steel. Nature. 1975;258(5537):703–4.
[126]. Tsukuma K, Shimada M. Strength, fracture toughness and vickers hardness of Ceo2-stabilized tetragonal Zro2 polycrystals (Ce-Tzp). J Mater Sci. 1985;20(4):1178–84.
[127]. Tsukuma K. Mechanical-properties and thermal stability of Ceo2 containing tetragonal zirconia polycrystals. Am Ceram Soc Bull. 1986;65(10): 1386–9.
[128]. Nawa M, Bamba N, Sekino T, Niihara K. The effect of TiO2 addition on strengthening and toughening in intragranular type of 12Ce-TZP/Al2O3 nanocomposites. J Eur Ceram Soc. 1998;18(3):209–19.
[129]. Nawa M, Nakamoto S, Sekino T, Niihara K. Tough and strong Ce-TZP/alumina nanocomposites doped with titania. Ceram Int. 1998;24(7):497–506.
[130]. Losic D, Mitchell JG, Voelcker NH. Diatomaceous lessons in nanotechnology and advanced materials. Adv Mater. 2009;21(29):2947–58.
[131]. Santoyo-Salazar J, Gonzalez G, Schabes-Retchkiman PS, Ascencio JA, Tartaj-Salvador J, Chavez-Carvayar JA. Synthesis and characterization of YSZ-Al2O3 nanostructured materials. J Nanosci Nanotechnol. 2006;6(7):2103–9.
[132]. Chevalier J, Taddei P, Gremillard L, Deville S, Fantozzi G, Bartolome JF, et al. Reliability assessment in advanced nanocomposite materials for orthopaedic applications. J Mech Behav Biomed Mater. 2011;4(3):303–14.
[133]. Silva NRFA, Bonfante EA, Rafferty BT, Zavanelli RA, Martins LL, Rekow ED, et al. Conventional and modified veneered zirconia vs. metalloceramic: fatigue and finite element analysis. J Prosthodont Implant Esthet Reconstruct Dent. 2012;21(6):433–9.
[134]. Kelly JR. Ceramics in restorative and prosthetic dentistry. Annu Rev Mater Sci. 1997; 27:443–68.
[135]. Theocharopoulos A, Chen X, Wilson RM, Hill R, Cattell MJ. Crystallization of high-strength nanoscale leucite glass-ceramics. Dent Mater. 2013; 29(11): 1149–57.
[136]. Chang J, Da Silva JD, Sakai M, Kristiansen J, Ishikawa-Nagai S. The optical effect of composite luting cement on all ceramic crowns. J Dent. 2009;37(12):937–43.
[137]. Uno M, Kurachi M, Wakamatsu N, Doi Y. Effects of adding silver nanoparticles on the toughening of dental porcelain. J Prosthet Dent. 2013;109(4): 241–7.

[138]. D'Arcangelo, C.; Vanini, L.; Casinelli, M.; Frascaria, M.; De Angelis, F.; Vadini, M.; D'Amario, M. Adhesive Cementation of Indirect Composite Inlays and Onlays: A Literature Review. Compendium 2015, 36, 570–577.
[139]. Ramakrishna, S.; Mayer, J.; Wintemantel, E.; Leong, K.W. Biomedical applications of polymer-composite materials: A review. Comp. Sci. Technol. 2001, 61, 1189–1224.
[140]. Pinzon, L.M.; Watanabe, L.G.; Reis, A.F.; Powers, J.M.; Marshall, S.J.; Marshall, G.W. Analysis of interfacial structure and bond strength of self-etch adhesive systems. Am. J. Dent. 2013, 26, 335–340.
[141]. Waldman, G.L.; Vaidyanathan, T.K.; Vaidyanathan, J. Microleakage and Resin-to-Dentin Interface Morphology of Pre-Etching versus Self-Etching Adhesive Systems. Open Dent. J. 2008, 2, 120–125.
[142]. Sezinando, A. Looking for the ideal adhesive—A review. Rev. Port. Estomatol. Med. Dentária Cir. Maxilofac. 2014, 55, 194–206.

[143]. Borges, M.A.P.; Matos, I.C.; Dias, K.R.H.C. Influence of Two Self-Etching Primer Systems on Enamel Adhesion. Braz. Dent. J. 2007, 18, 113–118.
[144]. Hilton, T.J. Can modern restorative procedures and materials reliably seal cavities? In vitro investigations. Part 2. Am. J. Dent. 2002, 4, 279–289.
[145]. Wu, W.; Cobb, E.; Dermann, K.; Rupp, W. Detecting margin leakage of dental composite restorations. J. Biomed. Mater. Res. 1983, 17, 37–43.
[146]. Mali, P.; Deshpande, S.; Singh, A. Microleakage of restorative materials: An in vitro study. J. Indian Soc. Pedod. Prev. Dent. 2006, 24, 15–18.
[147]. Carrera, C.A.; Lan, C.; Escobar-Sanabria, D.; Li, Y.; Rudney, J.; Aparicio, C.; Fok, A. The Use of Micro-CT with Image Segmentation to Quantify Leakage in Dental Restorations. Dent. Mater. 2015, 31, 382–390.
[148]. Kumar, M.; Lakshminarayanan, L. Methods of Detecting Microleakage. J. Conserv. Dent. 2004, 7, 79–88.
[149]. Ozel, E.; Tuna, E.B.; Firatli, E. The effects of cavity-filling techniques on microleakage in class II resin restorations prepared with Er: YAG laser and diamond bur: A scanning electron microscopy study. J. Scanning Microsc. 2016, 38, 389–395.
[150]. Milleding, P. Microleakage of indirect composite inlays. An in vitro comparison with the direct technique. Acta Odontol Scand. 1992, 50, 295–301.
[151]. Hasanreisoglu, U.; Sonmez, H.; Uctasli, S.; Wilson, H.J. Microleakage of direct and indirect inlay/onlay systems. J. Oral. Rehabil. 1996, 23, 66–71.
[152]. Soares, C.J.; Celiberto, L.; Dechichi, P.; Fonseca, R.B.; Martins, L.R.M. Marginal integrity and microleakage of direct and indirect composite inlays—SEM and stereomicroscopic evaluation. Braz. Oral. Res. 2005, 19, 295–301.
[153]. Otis, L.; Everett, M.J.; Sathyam, U.S.; Colston, B.W., Jr. Optical Coherence Tomography: A New Imaging Technology for Dentistry. J. Am. Dent. Assoc. 2000, 131, 511–514.
[154]. Turki, A.; Bakhsha, B.; Sadrb, A.; Shimadaa, Y.; Junji Tagamia, B.; Yasunori, S. Non-invasive quantification of resin–dentin interfacial gaps using optical coherence tomography: Validation against confocal microscopy. Dent. Mat. 2011, 27, 915–925.
[155]. Monteiro, G.Q.; Montes, M.A.; Gomes, A.S.; Mota, C.C.; Campello, S.L.; Freitas, A.Z. Marginal analysis of resin composite restorative systems using optical coherence tomography. Dent. Mater. 2011, 27, 213–223.
[156]. Hsieh, Y.-S.; Ho, Y.-C.; Lee, S.-Y.; Chuang, C.-C.; Tsai, J.; Lin, K.-F.; Sun, C.-W. Dental Optical Coherence Tomography. Sensors 2013, 13, 8928–8949.
[157]. Oancea, R.; Bradu, A.; Sinescu, C.; Negru, R.M.; Negrutiu, M.L.; Antoniac, I.; Duma, V.-F.; Podoleanu, A.G. Assessment of the sealant/tooth interface using optical coherence tomography. J Adhes. Sci. Technol. 2015, 29, 49–58.
[158]. Dsouza, R.; Subhash, H.; Neuhaus, K.; Kantamneni, R.; McNamara, P.M.; Hogan, J.; Wilson, C.; Leahy, M. Assessment of curing behavior of light-activated dental composites using intensity correlation based multiple reference optical coherence tomography. Lasers Surg. Med. 2016, 48, 77–82.
[159]. Canjau, S.; Todea, C.; Negrutiu, M.L.; Sinescu, C.; Topala, F.I.; Marcauteanu, C.; Manescu, A.; Duma, V.-F.; Bradu, A.; Podoleanu, A. Optical Coherence Tomography for Non-Invasive ex vivo Investigations in Dental Medicine—A Joint Group Experience (Review). Mod. Technol. Med. 2015, 7, 97–115.
[160]. Cavalu, S.; Fritea, L.; Brocks, M.; Barbaro, K.; Murvai, G.; Costea, T.O.; Antoniac, I.; Verona, C.; Romani, M.; Latini, A.; et al. Novel Hybrid Composites Based on PVA/SeTiO2 Nanoparticles and Natural Hydroxyapatite for Orthopedic Applications: Correlations between Structural, Morphological and Biocompatibility Properties. Materials 2020, 13, 2077.
[161]. Liu, X.; Chen, X.; Ren, J.; Zhang, C. TiO2-KH550 Nanoparticle-Reinforced PVA/xylan Composite Films with Multifunctional Properties. Materials 2018, 11, 1589.
[162]. Radwan-Pragłowska, J.; Janus, Ł.; Piątkowski, M.; Bogdał, D.; Matysek, D. 3D Hierarchical, Nanostructured Chitosan/PLA/HA Scaffolds Doped with TiO2/Au/Pt NPs with Tunable Properties for Guided Bone Tissue Engineering. Polymers 2020, 12, 792.
[163]. Chaitali, D.; Arup, G.; Manisha, A.; Ajay, G.; Madhuri, M. Improvement of anticancer drug release by cobalt ferrite magnetic nanoparticles through combined pH and temperature responsive technique. ChemPhysChem 2018, 19, 1–18.
[162]. Antoniac, I.; Cernea, A.; Petcu, C.; Laptoiu, D.; Tabaras, D.; Tecu, C.; Antoniac, A.; Gradinaru, S. Synthesis and Characterization of Coated Iron Oxide Nanoparticles Produced for Drug Delivery in Viscoelastic Solution. Rev. Chim. 2020, 71, 145–154.
[163]. Covaliu, C.I.; Jitaru, I.; Paraschiv, G.; Vasile, E.; Biri¸s, S.-S.; Diamandescu, L.; Ionita, V.; Iovu, H. Core-shell hybrid nanomaterials based on CoFe2O4 particles coated with PVP or PEG biopolymers for applications in biomedicine. Powder Technol. 2013, 237, 415–426.
[164]. Szunerits, S.; Nait Saada, T.; Meziane, D.; Boukherroub, R. Magneto-Optical Nanostructures for Viral Sensing. Nanomaterials 2020, 10, 1271.
[165]. AlKahtani, R.N. The implications and applications of nanotechnology in dentistry: A review. Saudi. Dent. J. 2018, 30, 107–116.

13. Nanoapplications in Periodontal Management

The periodontium consists of the tissues that invest and support the tooth, including the gingiva, periodontal ligament, cementum, and alveolar bone [1]. The health of the periodontium depends on the structural integrity and balance among these four key components. Changes in the morphology and functionality of the periodontium, often related to aging, are addressed through conventional treatments like scaling, root planing, and periodontal flap surgery. These procedures, coupled with appropriate post-operative care, are effective in managing progressive periodontal diseases [1].

Advancements in nanotechnology have introduced specialized nanoparticles designed to target oral tissues, including the periodontium. These nanoparticles, due to their nanometer-scale sizes, are particularly useful in diagnosing periodontal disorders through nano-scale biosensors. These sensors are capable of detecting specific substances in bodily fluids such as saliva, blood, and gingival crevicular fluid [2]. The applications of nanotechnology in dentistry extend to drug delivery, local anesthesia, and diagnostics.

A novel application involves nanorobots equipped with onboard computers, which can be controlled to perform precise dental treatments. These 'dentifrobots', which can be administered through mouth rinses or toothpaste, are designed to reside sub-occlusally and assist in daily oral care. They perform tasks such as inspecting both supragingival and subgingival areas, removing calculus, and converting organic molecules into non-offensive vapors [3]. Furthermore, these nanorobots are capable of differentiating between cell types by recognizing specific surface antigens through chemotactic sensors.

Once their tasks are completed, nanorobots can be safely expelled from the body via the excretory system or specialized scavenger systems [4]. This innovative use of nanoparticles and nanorobots offers transformative potentials in delivering bioactive chemicals and drugs, marking significant progress in oral healthcare.

Periodontal disease, encompassing gingivitis and periodontitis, represents an infectious condition involving various degenerative and inflammatory states of periodontal ligaments (PDLs), gingiva, alveolar bones, and cementum. Globally, they stand as significant causes of tooth loss and other oral health complications. For instance, in 2013, the prevalence of adult periodontal disease, defined by periodontal pockets deeper than 4 mm, was reported as 60% in the USA, 90% in China, and 45% in Japan, thereby escalating financial burdens for both patients and governments.

The etiology of periodontal disease primarily involves Gram-negative and anaerobic bacteria, fostering the formation of biofilms on teeth harboring over 1 × 10^10 bacteria/cm^3. Although more than 500 bacterial species have been identified in dental plaques, only a select few release toxins capable of eliciting a host inflammatory response, leading to the destruction of alveolar bone and connective. Consequently, with the deterioration of the periodontal apparatus, patients often experience tooth loss, resulting in diminished function and aesthetics. Moreover, periodontal disease exhibits associations with various other conditions such as atherosclerotic vascular disease, diabetes mellitus, and chronic nephritis.

Over the past few decades, diverse strategies have been employed in the treatment of periodontal disease. Initially, scaling and root planing (SRP) serve as the primary option for addressing periodontal inflammation, involving mechanical disruption of bacterial flora within biofilms (plaques). However, SRP has limitations in accessing bacteria deep within periodontal pockets and relies heavily on clinician skill. Hence, there's a need to develop advanced strategies for managing such prevalent diseases.

With advancements in material science and drug delivery techniques, various drug-loaded biomaterials have emerged, including hydrogels, films, micro/nanofibers, and particles, facilitating local drug delivery procedures to reduce and eliminate periodontal inflammation. For severely damaged or defective periodontal tissue that conventional treatments struggle to restore, periodontal regeneration holds significant promise in repairing damaged functional constructs. Biocompatible scaffolds derived from natural and synthetic polymers have been successfully employed for

periodontal tissue regeneration in vitro, with subsequent transplantation into damaged or missing sites. For instance, an alginate scaffold incorporated with human periodontal ligament fibroblasts (PDLf) and osteosarcoma (MG-63) cells demonstrated enhanced alkaline phosphatase (ALP) activity in PDL-like tissue constructs after 21 days of culture. Recently, a parallel and cross-aligned fibrous poly (lactic-co-glycolic acid) (PLGA) scaffold was fabricated to promote organized periodontal tissue regeneration in vitro.

The development of biomaterials tailored for drug and cell delivery and facilitating periodontal regeneration is pivotal in treating periodontal diseases. This review delves into multiple critical areas. Firstly, it examines the pathogenesis of periodontal disease, which encompasses plaque accumulation, immune responses, and the inflammatory processes triggered by bacterial activity. Understanding these mechanisms is crucial for developing targeted treatments. Secondly, the review discusses periodontal therapy, providing an overview of existing biomaterials used in the field of periodontal regenerative medicine. These materials are essential for restoring the integrity of periodontal tissues damaged by disease. Thirdly, it highlights the role of cutting-edge biomaterials specifically engineered for periodontal disease treatment and tissue regeneration. This section also covers the various methods used to fabricate these advanced materials, showcasing the technological progress in the field. Fourthly, the biological properties of these biomaterials are explored, including their biocompatibility, biodegradability, and immunogenicity. The review assesses how these properties impact their effectiveness and suitability in clinical applications, detailing current strategies for their use. Finally, the review concludes with remarks on the current state of the field and perspectives on the future of advanced biomaterials in periodontal disease treatment. It underscores ongoing research directions and potential innovations that could further enhance the efficacy of periodontal therapies. Overall, this review provides a comprehensive look at the advancements in biomaterials for periodontal regeneration, emphasizing their transformative potential in clinical settings.

13.1. Periodontal disease and their pathogenesis

Periodontal disease manifests as an infectious condition characterized by the degradation of tooth-supporting tissues due to inflammatory and immune responses provoked by bacteria residing in tooth-retained plaques. The formation of dental plaque involves three distinct stages. Initially, salivary proteins and glycoproteins adhere to the tooth surface, forming a thin non-cellular biofilm known as the acquired pellicle (Figure 13.1. A and B), providing specific receptors for bacteria, thus facilitating bacterial adhesion. Subsequently, various bacteria, such as Streptococcus, Bacillus, and Actinomyces, colonize continuously on the acquired pellicle in the oral cavity. Finally, different bacterial types on the acquired pellicle rapidly aggregate through specific receptor recognition, leading to dental plaque formation.

The onset of periodontal disease is triggered by a shift in oral bacterial colonization from Gram-negative to Gram-positive species like Tannerella forsythia, Aggregatibacter actinomycetemcomitans, Prevotella intermedia, and Porphyromonas gingivalis on the acquired pellicle. This transition is facilitated by antecedent commensal bacteria. Among these, P. gingivalis is recognized as the primary instigator of periodontal disease, employing various virulence factors such as lipopolysaccharide, fimbrae, and proteases (e.g., gingipains) to damage periodontal tissue and trigger host immune responses. Furthermore, matrix metalloproteinases (MMPs) secreted by fibroblasts, monocytes (MMP-1), and neutrophils (MMP-8) exhibit a nearly tenfold increase in concentration in individuals with severe periodontitis compared to healthy controls, leading to further degradation of periodontal tissues.

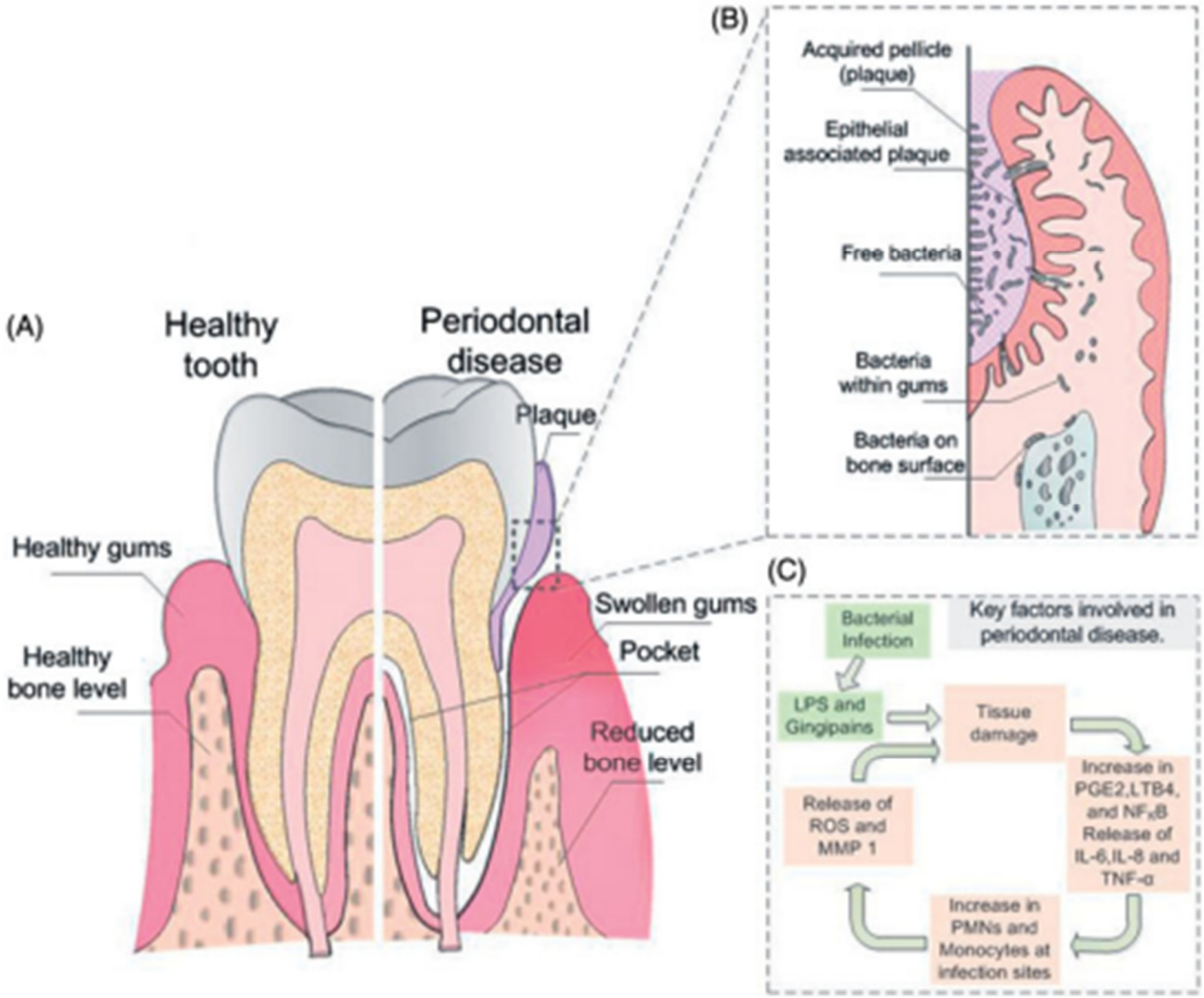


Figure 13.1. Schematics of mechanisms involved in periodontal diseases. (A) Profile of healthy tissues (left) and tissues suffering from periodontal diseases (right). (B) Bacterial invasion process during pathogenesis of periodontal disease. (C) Overview of key factors involved in periodontal disease. LPS, lipopolysaccharide; IL, interleukin; LTB4, leukotriene B4; MMP, matrix metalloproteinase; PGE2, prostaglandin E2; PMN, polymorphonuclearneutrophils; ROS, reactive oxygen species; TNF, tumor necrosis factor [5].

Another crucial factor in promoting periodontal disease is the host immune response to bacterial infection, particularly the magnitude and duration of inflammation. Initial responses to bacterial insult, including exposure to bacterial lipopolysaccharide, result in the secretion of pro-inflammatory cytokines such as interleukins (e.g., IL-8, IL-6, IL-1β) and tumor necrosis factor-alpha (TNF-α) (Figure 13.1. C). These cytokines play a pivotal role in recruiting host immune cells by acting as chemo attractants and stimulating the expression of intercellular adhesion molecules and vascular cell adhesion molecules, thereby enhancing margination and diapedesis processes. Such mechanisms significantly increase the population of polymorphonuclear neutrophils (PMNs) in the infected area, leading to elevated free radical-mediated damage to periodontal tissues and further augmenting pro-inflammatory cytokine release. Consequently, an auto-amplification scenario arises, as greater concentrations of immune cells in the infected area result in enhanced production and release of reactive oxygen species (ROS).

13.2. Current biological approaches for periodontal therapy

Periodontal treatment aims primarily to eliminate infected tissues caused by bacterial plaque and to regenerate lost or damaged periodontal tissues.

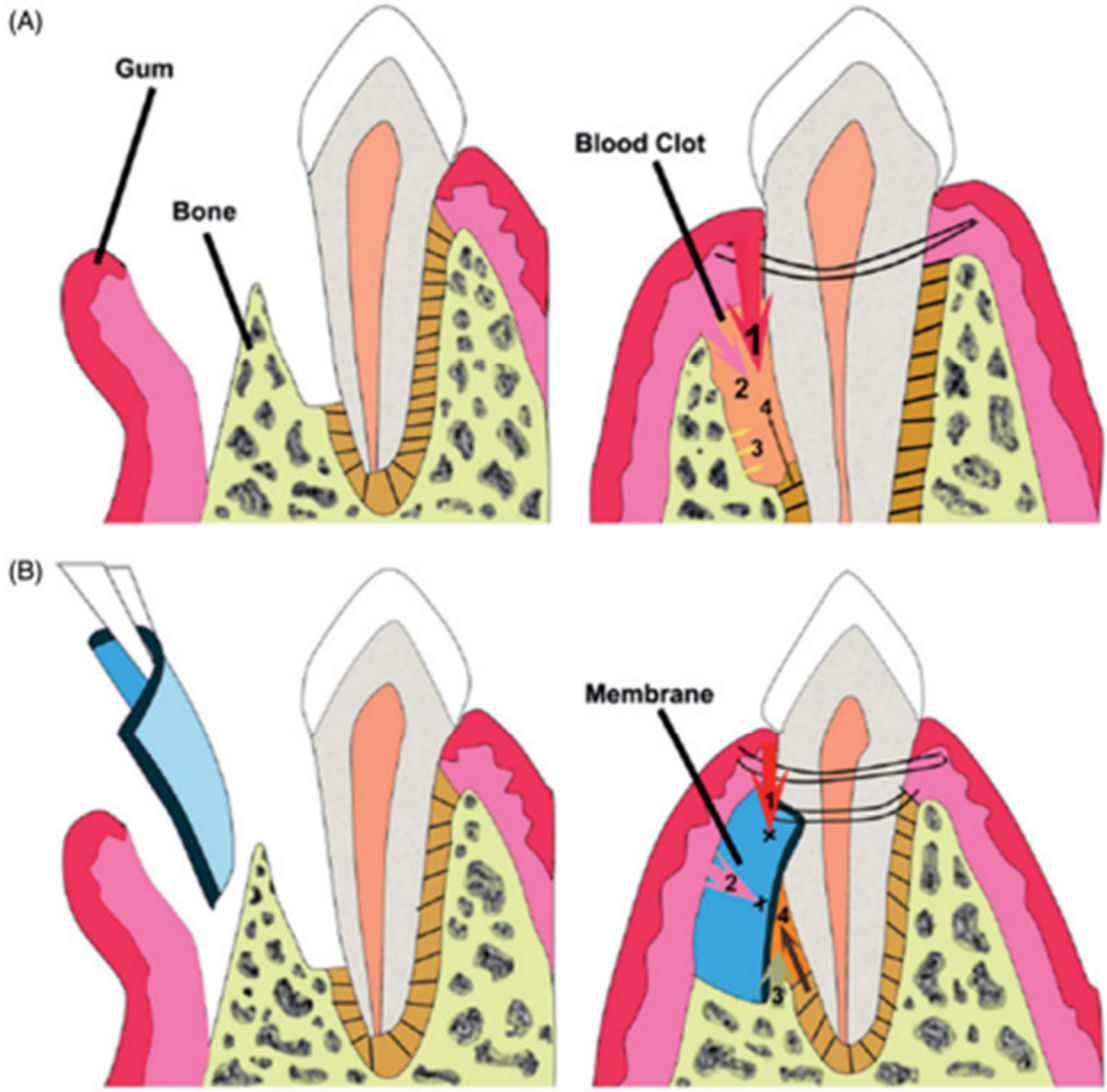


Figure 13.2. Schematic diagrams of several techniques commonly used in periodontal surgery (Chen et al., 2010). (A) OFD procedure involves lifting the gum up from the tooth and the surrounding bone, providing increased access for SRP. However, periodontal defects, if left empty after OFD, will be filled up with the first cell type to reach the area, i.e. epithelial cells (1) and fibroblasts (2), which will generate a core of fibroepithelial tissues that attach to the root surface, hence bone (3) and PDL (4) regeneration are cumbered. (B) GTR is a surgical procedure that utilizes a barrier membrane to be placed under the gum and over the remaining bone, to prevent epithelial downgrowth (1) and fibroblast trans-growth (2) into the wound space, thereby maintaining a space for true periodontal tissue regeneration (3 and 4) [5].

Over the last few decades, various treatment strategies, including scaling and root planning (SRP), open flap debridement (OFD), and guided tissue regeneration (GTR), have been developed and employed in periodontal therapy. While these approaches have demonstrated some effectiveness in promoting periodontal regeneration, several challenges persist (Figure 13.2.).

For example, the OFD strategy is instrumental in cleaning and detoxifying root surfaces, thereby facilitating the establishment of improved organization and structure in damaged periodontal tissues. However, if periodontal defects are left empty after OFD, they tend to be filled with the first cell type to reach the area, leading to the generation of fibro-epithelial tissues that attach to the root surface. Unfortunately, this attachment does not allow sufficient time for bone and periodontal ligament (PDL) regeneration to refill the pocket, hindering orderly and sequential regeneration of true hybrid periodontal tissues.

Similarly, the GTR strategy, aimed at creating a temporal and spatial space conducive to true periodontal regeneration, has shown promise in certain clinical therapies. However, quantitative analysis of clinical data following GTR suggests that this therapy achieves successful and predictable outcomes only in a few well-selected cases, such as narrow intrabony defects and class II mandibular

furcations. Moreover, patients often face the need for a second surgical procedure due to the limited biodegradability of barrier membranes used to prevent epithelial downgrowth and fibroblast trans-growth into the wound space.

Hence, there is an urgent need for the development of clinical approaches that can significantly enhance periodontal tissue repair and regeneration.

13.3. The role of biomaterials in periodontal therapy and regeneration

Tissue engineering and cell/drug delivery-based therapies have emerged as alternative approaches for regenerating various types of tissue damage, including periodontal tissue. These strategies involve utilizing functional supportive biomaterials, with or without growth factors, where cells are seeded and cultured to induce tissue regeneration. In the context of periodontal regeneration, a new generation of biomaterials and technologies is being developed to enhance cell recruitment, control cell behaviors, and regenerate complex tissue structures and functions. These advanced materials can possess superior properties such as biocompatibility, biodegradability, and appropriate mechanical properties, achieved by regulating their composition and microarchitecture.

Examples of polymers used for periodontal regeneration include synthetic materials like poly (lactic acid) (PLA), poly (glycolic acid) (PGA), their copolymers (e.g., PLGA), and polyethylene glycol (PEG)-based hydrogel systems; natural polymers such as collagen, agarose, and gelatin; and autologous materials like fibrin. A novel assembly approach known as "bottom-up" tissue remodeling focuses on fabricating microscale tissue building blocks (e.g., hydrogels) with specific microarchitectures and assembling these units to engineer larger tissue constructs from the bottom up, holding great promise for engineering periodontal tissue constructs with appropriate functions.

Various biomaterials including hydrogels, membranes, and micro/nanoparticles can also be utilized for drug/cell delivery systems. For instance, patient-derived fibrin hydrogel, serving as a biodegradable and controllable drug delivery system, has opened doors to personalized medicine currently applied in numerous medical and scientific fields. Thus, biomaterials play a critical role in supporting or carrying cells/drugs for periodontal tissue regeneration and therapy, with the potential to control infection and re-establish the periodontal apparatus.

The incorporation of biomaterials in regenerative medicine is believed to maximize the beneficial effects of cellular therapies while minimizing poor engraftment, improving persistence, and controlling cell/growth factor delivery for periodontal therapies and regeneration. Several evaluation criteria are adopted for assessing the performance of biomaterials aimed at periodontal regeneration and drug delivery, including in vitro and in vivo biostandards. In vitro evaluation considers cellular behavior such as viability, proliferation, migration, and differentiation to assess biocompatibility, alongside mechanical and structural characteristics resembling native tissues. Proper biodegradation rate and low inflammation during degradation are also desired. In vivo evaluation involves histologic and clinical (radiographic) aspects, analyzing biopsies from grafted sites for histomorphometry and immunohistochemical analyses, and clinical evaluation of treatment outcomes using universal indexes for periodontal disease diagnosis.

13.4. Advanced biomaterials developed for periodontal disease treatment

While various conventional procedures for treating periodontal disease are currently employed, they come with several limitations, including difficulty reaching deep pockets or furcation areas and a significant reliance on clinician skill [Herrera et al., 2012]. However, the emergence of advanced biomaterials such as membranes, hydrogels, micro/nanofibers, and particles hold promise in addressing these shortcomings. Additionally, these novel drug-loaded materials offer precise control over the rate of drug release. In this section, we will focus on four types of advanced biomaterials—hydrogels, micro/nanoparticles, films, and micro/nanofibers—that have been developed for the treatment of periodontal disease, as summarized in Figure 13.3. and Table 4.1.

Table 4.1. Advanced biomaterial-based strategies investigated for treatment of periodontal disease [5].

BIOMATERIALS	DELIVERY MODELS	THERAPEUTIC CELLS/DRUGS	ANIMAL MODEL	REFERENCES
COLLAGEN HYDROGEL CARRIER	Injectable delivery	Autologous cryopreserved BMMSCs	Dog's periodontal fenestration defects	Chen et al. (2007b) and Li et al. (2009)
CHITOSAN/ACS/HA HYDROGEL CARRIER		Human PDLfs	Rat's alveolar bone critical-sized defects (diameter 3 mm)	Pang et al. (2005)
SILK FIBROIN HYDROGEL SCAFFOLD		Nuclear matrix protein SATB2-modified iPSCs	Mouse's alveolar bone critical-sized defect (diameter 4 mm)	Ye et al. (2011)
PLGA/PCL MICROPARTICLES		Doxycycline Autologous BMMSCs	Dog's gingivitis	Liu et al. (2004)
GELATIN MICROPARTICLES			Rat's surgically created periodontal defects	Yang et al. (2010)
PEG/PLA NANOPARTICLES	Delivery of solid scaffolds	Minocycline	Dog's periodontitis	Yao et al. (2014).
CHITOSAN/PLGA FILMS		Tetracycline/meloxicam	Pig's periodontitis	Perugini et al. (2003)
TCP/HA SCAFFOLDS		Autologous PDLSCs	Miniature pig's experimental periodontitis lesions	Liu et al. (2008)
PCL/PGA/HA		Human PDLfs	Rat's PDL regeneration	Park et al. (2010)
PCL/6-TCP		PDLCs and osteoblasts	Rat's periodontal ligament and alveolar bone regeneration	Vaquette et al. (2012)

BMMSCS, BONE MARROW MESENCHYMAL STEM CELLS; IPSCS, INDUCED PLURIPOTENT STEM CELLS; PDLFS, PERIODONTAL LIGAMENT FIBROBLASTS; PDLSCS, PERIODONTAL LIGAMENT STEM CELLS.

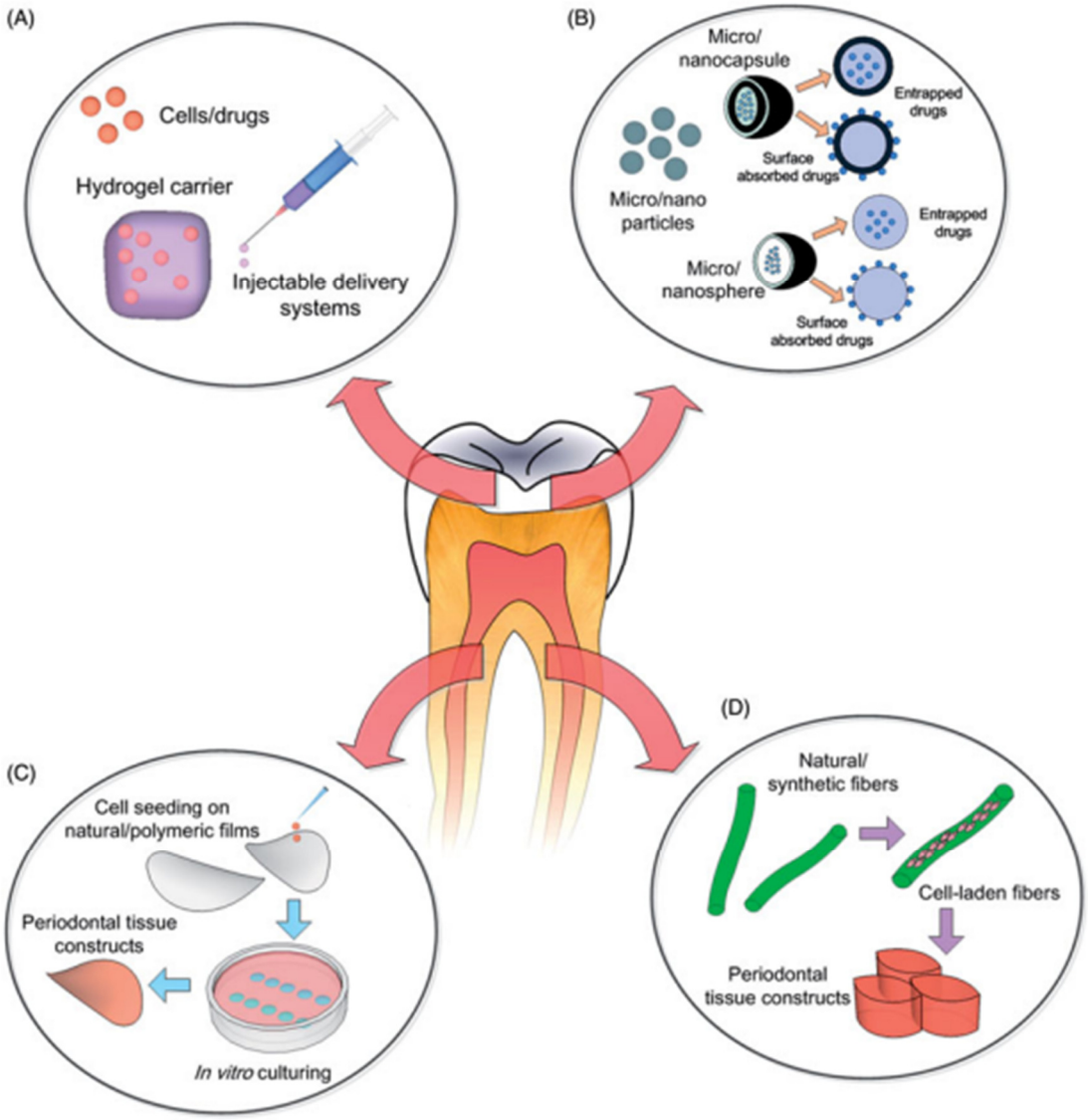


Figure 13.3. Schematic diagrams of developed biomaterials used for periodontal disease treatment. (A) Injectable hydrogels encapsulated with cells/drugs utilized for periodontal tissue repair. (B) Type of biodegradable micro/nanoparticles for the purpose of periodontal drug delivery. According to the structural organization, biodegradable micro/nanoparticles are classified as micro/nanocapsules, and micro/nanospheres. The drug molecules are either entrapped inside or adsorbed on the surface. (C) Natural/polymeric films seeded with PDL cells and in vitro cultured for periodontal tissue constructs. (D) Cells are seeded on natural/synthetic scaffolds and delivery of such scaffold-cell constructs for periodontal disease treatment [5].

13.4.1. Hydrogels

Hydrogels have emerged as three-dimensional, water-swollen, structurally similar materials to the extracellular matrix (ECM) in vivo at the nanoscale. These soft polymer materials possess tunable properties, including physical, chemical, and biocompatible characteristics. Considered as smart biomaterials, hydrogels have found widespread applications in biomedical engineering, particularly in tissue regeneration and cell/drug delivery systems.

A variety of hydrogels developed from natural and synthetic polymers have been utilized as carrier materials for drug/cell delivery. They offer structural integrity and cellular organization, acting as bio-adhesive drug depots, delivering bioactive substances and cells, and possessing unique swelling properties and structures. Additionally, hydrogel scaffolds comprising micro/nanoarchitectures such as pores and fibers can mimic the chemical and physical properties of natural ECM. These scaffolds have been successfully employed in periodontal tissue repair and regeneration.

In this context, we will discuss the advanced natural and synthetic hydrogels developed specifically for the treatment of periodontal disease.

13.4.1.1. Natural Hydrogels

Various hydrogels developed from natural polymers, including collagen, alginate, chitosan, gelatin, and fibrin, have been utilized as biocompatible and biodegradable matrix/scaffolds for regulating cellular events such as migration, proliferation, and differentiation, ultimately facilitating periodontal tissue regeneration.

Collagen, a typical natural polymer, comprises specific domain sequences, such as the Arg-Gly-Asp peptide (RGD), which serves as a cellular adhesive supporting site, retaining cell phenotype and guiding important cellular behaviors via integrin binding. For example, collagen hydrogel scaffolds with varying porosities (40%, 60%, 80%, and 90%), seeded with periodontal ligament cells (PDLCs), have been employed for periodontal ligament repair and regeneration. Studies have shown that samples with porosities higher than 80% successfully formed periodontal ligament-like tissues after 2 weeks of culture. This suggests that a collagen hydrogel sponge with a compact and interconnected porous structure, resembling the natural ECM porosity, can enhance cell proliferation and induce specific tissue formation.

Other natural hydrogels also hold promise for future periodontal tissue engineering. For instance, gelatin hydrogels encapsulated with dental bud cells have facilitated the regeneration of dentine-pulp complex with cementum and periodontal ligament in swine. Alginate hydrogels have been utilized for delivering bone marrow-derived mesenchymal stem cells (BMMSCs) to repair experimental alveolar bone defects in dogs and to promote in vivo bone regeneration in rats. Recently, chitosan hydrogels combined with beta-glycerophosphate (b-GP) and nanohydroxyapatite (HA) have been applied to improve osteogenic differentiation and generate alveolar bone-like structures after 2 weeks of culture.

While natural hydrogels are biocompatible, biodegradable, non-toxic, and non-antigenic biomaterials for delivering cells and remodeling periodontal-like tissues, their relatively fast degradation rate may pose a challenge to the regeneration of volume-stable tissues. One strategy to address this limitation is to combine these natural polymers to enhance their performance. For instance, collagen hydrogel composites have been prepared by mixing with one or two other natural polymers, such as chitosan, hyaluronic acid, and agarose, to decrease its in vivo degradation rate.

13.4.1.2. Synthetic hydrogels

The most extensively utilized synthetic hydrogels for periodontal disease treatment include polyethylene glycol (PEG), poly (lactic acid) (PLA), poly (glycolic acid) (PGA), and their copolymers such as PLGA. These synthetic hydrogels typically exhibit higher primary stability, mechanical properties, and are more amenable to forming micro/nanostructures compared to natural hydrogels.

For instance, PLGA-based hydrogels have been used to deliver cementoblasts in rodent periodontal fenestration models, where they demonstrated a marked ability to induce mineralization in periodontal wounds. By adjusting the ratio of PLA to PGA fractions in the PLGA hydrogel, the rate of hydrolysis-mediated degradation and the degree of hydrophobicity/hydrophilicity can be controlled to meet therapeutic criteria.

PEG hydrogels containing cell adhesive molecules like the RGD motif and substrates for MMPs as cross-linkers to polymer chains can serve as biomimetic hydrogel scaffolds. These hydrogel scaffolds promote cell invasion, regulate the release of BMPs, and facilitate the healing of dentoalveolar defects. PEG is often used to modify other polymers to meet the requirements of cell/drug delivery systems. For example, rapid degradation of fibrin can be slowed down by modification with PEG, creating a hybrid material for cell/drug delivery.

In recent studies, in situ forming hydrogel scaffolds composed of collagen and multi-branched PEG have been reported to effectively fill defects with complex geometries, adhere to adjacent tissues, and foster cell proliferation when used as cell carriers. Moreover, synthetic hydrogels like PEG hydrogels, composed of RGD and HA, have been employed as cellular matrices for cell-mediated gene delivery in guided bone regeneration, leading to increased bone formation in critical-sized defect models.

While synthetic hydrogels commonly exhibit lower degradation rates and better mechanical properties for forming stable tissue constructs compared to natural hydrogels, they may show less biocompatibility due to the lack of adhesion sites in the polymer networks. One approach to address this is to incorporate modified RGD ligands onto the polymer network or to combine synthetic hydrogels with other natural polymers suitable for cell adhesion. Additionally, the development of suitable controlled-release devices for bioactive molecules and alternative modes of delivery is necessary.

13. 4.2. Micro/nanoparticles

Micro/nanoparticles are considered smart vehicles for drug delivery, enhancing the therapeutic value of various water-soluble/insoluble medicinal drugs and bioactive molecules. These particles, typically ranging in size from 1 to 1000 nm, can improve solubility, bioavailability, and retention time of drugs, thus reducing patient expenses and the risk of toxicity.

Various synthetic and natural polymers, including PLA, PLGA, PCL, iron oxide, chitosan, and gelatin, have been investigated for the preparation of microparticles. These microparticles can be formulated as chips, part of dental paste formulations, or injected directly into the periodontal cavity. For instance, PLGA/PCL microparticles have been used to deliver tetracycline and histatins, achieving controlled delivery of drugs for up to 11 days in periodontal pockets (Figure 13.4.).

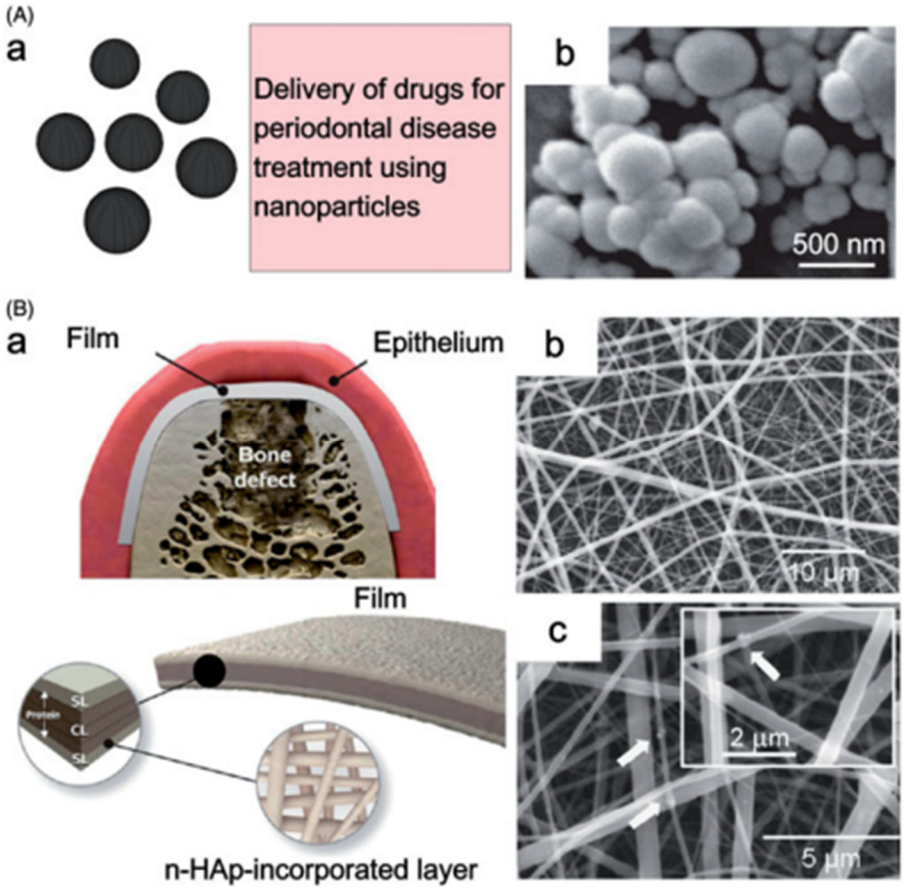


Figure 13.4. Periodontal disease treatment based on nanoparticles and films. (A) (a) Delivery of nanoparticles loaded with cells/drugs to periodontal intra-bony defects. (b) Scanning electron microscopy (SEM) images of fabricated MIN-loaded PLGA nanoparticles (Kashi et al., 2012). (B) (a) Schematic illustration of the spatially designed and functionally graded periodontal film. (b and c) Representative SEM micrographs of the individual electrospun layers embedded with n-HAp particles [5].

Despite their ease of fabrication and utilization for drug delivery, microparticles have limitations such as poor control over release rate, low dispersibility, and stability in aqueous media. Biodegradable nanoparticles (size range 10–1000 nm) have emerged as DDSs due to advances in

nanotechnology. Nanoencapsulation of drugs in nanoparticles increases efficacy, tolerability, specificity, and therapeutic index. Polymeric nanoparticles used for DDSs are synthesized using various approaches and offer advantages such as protection from premature degradation, enhanced absorption into tissues, improved bioavailability, and biocompatibility.

Synthetic nanoparticles, such as PEG-PLA nanoparticles encapsulating minocycline (MIN), have been developed for periodontal disease treatment. These nanoparticles maintain effective drug concentrations in the gingival crevice fluid for a longer time compared to conventional drug formulations, effectively suppressing symptoms of periodontitis. Similarly, PLGA nanoparticles encapsulating methylene blue (MB) have been fabricated for photodestruction of oral biofilms in combination with photodynamic therapy.

Innovative strategies involve entrapping chitosan nanoparticles loaded with tetracycline hydrochloride (TCH) into nano-fibrous networks for periodontal regeneration therapy. This integrated system, containing electrospun PCL fibers and TCH-loaded chitosan particles, promotes attachment and proliferation of human mesenchymal stem cells, indicating its potential for periodontal regeneration and treatment.

These advancements highlight the potential of micro/nanoparticles as effective carriers for drug delivery in periodontal disease treatment, offering controlled release, improved efficacy, and targeted therapy.

13.4.3. Films

Films are matrix networks frequently utilized for drug delivery systems (DDS), where drugs are dispersed throughout the polymer networks. These films can be prepared by direct milling or solvent casting methods. Films offer easy application within the oral cavity, such as onto the cheek mucosa or gingival surface, and drug release occurs via diffusion or matrix dissolution/erosion, depending on the properties of the polymer used.

One of the significant advantages of film-based DDS is the high controllability of drug release, allowing precise dosing with minimal invasion to the patient. This makes them stable, durable, and provides improved dosing accuracy. Film-based DDS not only ensures accurate drug administration but also enhances compliance, particularly beneficial for pediatric, elderly, and neurodegenerative disease patients.

Various polymers, including PLA, PLGA, collagen, alginate, and chitosan, have been investigated as film matrices for delivering drugs to the periodontal pocket. Several drugs have been incorporated into these films for treating periodontal disease, such as tetracycline, metronidazole, meloxicam, amoxicillin, and minocycline (MIN). For instance, Periochip, a commercialized film-based delivery system, contains chlorhexidine gluconate embedded in a biodegradable matrix of hydrolyzed gelatin cross-linked with glutaraldehyde, effectively inhibiting calculus and plaque development in human periodontitis models.

13.4.4. Micro/nanofibers

Fibers are another type of biomaterial utilized for periodontal drug delivery systems (DDS), consisting of one or more components encompassing drugs, proteins, and peptides with a polymer carrier in the form of homo-, bi-, or multi-component fibers. These fibers can be placed individually, packed into tablets, or enclosed in capsules. In fiber-based DDS, drugs are held within the fibers and released via a diffusion process.

Both natural and synthetic polymers, including collagen, alginate, chitosan, polyurethane, polypropylene, and cellulose acetate propionate, have been explored as fiber matrices for delivering drugs to periodontal pockets. Fiber-based DDS offers advantages such as improved drug loading capacity, ease of fabrication, applicability to target sites, tunable mechanical properties, better targeting, and enhanced adsorption.

In recent years, fibers have gained significant attention due to their suitability and adaptability in the drug delivery process. Various techniques, such as phase separation, melt fibrillation, electrospinning, gas jet, island in the sea, nanolithography, self-blowing, and melt blowing, are

employed to fabricate fibers. Drugs can be successfully encapsulated within fibers by incorporating them into the polymer solution used in processes like electrospinning.

A variety of drugs, including metronidazole, tetracycline, meloxicam, and minocycline (MIN), have been electrospun into fibers for periodontal drug delivery. The drug release behavior from fiber-based DDS mainly depends on factors such as the type and concentration of polymer, nature of the drug, and manufacturing equipment used.

An example of a commercialized fiber-based delivery system is Actisite, consisting of ethyl vinyl acetate fibers containing 25% tetracycline hydrochloride (TCH). Actisite fibers are placed circumferentially into periodontal pockets using an applicator and secured with cyanoacrylate adhesive, providing controlled release of the drug to the target site.

13.5. Biological properties of purpose-driven biomaterials

13.5.1. Biocompatibility and biodegradability

Biocompatibility and biodegradability are crucial characteristics for biomaterials used in regenerative medicine, including periodontal regeneration. However, it's important to understand that "biocompatibility/biodegradability" are not intrinsic properties of a material but depend on the biological microenvironment and tissue response.

For a material to be considered biocompatible and biodegradable, it should allow cells to adhere, function normally, migrate onto the surface or into the material matrix, proliferate, and eventually replace the material with their own extracellular matrix (ECM). Moreover, it should elicit a negligible immune reaction to prevent severe inflammatory responses or rejection by the body after implantation.

Natural polymers used for periodontal regeneration, such as collagen-based hydrogels and fibrin membranes, often exhibit superior biocompatibility and biodegradability due to their chemical and structural composition resembling native tissues. These materials support cell functions and tissue regeneration without adverse effects on neighboring tissues. However, their poor mechanical properties limit their applications in hard tissue regeneration like alveolar bone.

In contrast, synthetic biomaterials offer controllable physical properties, but they commonly lack inherent biocompatibility and biodegradability. Modifications, such as grafting short peptides like the Arg-Gly-Asp (RGD) tripeptide, can mitigate immunological responses and enhance cellular adhesion and proliferation on synthetic materials. Surface-immobilized ligands are also used to enhance biocompatibility and control stem cell differentiation.

Micro/nanoparticles used for drug delivery, such as Fe3O4 and g-Fe2O3 nanoparticles, must undergo metabolism to avoid accumulation in the body. These particles should be rapidly eliminated through pathways like the reticuloendothelial system (RES) and liver clearance. Particle size also influences clearance pathways, with smaller particles being eliminated renally, while larger ones are cleared by the liver or lymphatic drainage.

Further studies on the biodistribution and elimination of polymeric particles in vivo are necessary to advance their clinical applications in periodontal regeneration and other therapeutic areas.

13.5.2. Immunogenicity

The host immune response to biomaterial implantation or injection is a critical consideration for the long-term survival and function of biomaterials used in periodontal regeneration and therapy. After initial contact with tissue, proteins from blood and interstitial fluids are adsorbed onto the biomaterial surface, initiating a cascade of events that can lead to the formation of a transient provisional matrix and the onset of the inflammatory response.

For example, differences in protein displacement on hydrophilic and hydrophobic biomaterial surfaces can promote contact activation of factor XII, initiating the coagulation cascade. Thrombin, a main activator of platelets, can be released, leading to platelet activation and subsequent activation

of the coagulation process. Designing biomaterial surfaces to minimize the formation of such complexes and related immune responses is essential.

Various methods have been developed to enhance the immunomodulating properties of biomaterials used in periodontal regeneration and therapy. One approach is to apply artificial extracellular matrix (ECM) coatings on implanted biomaterials, as ECM proteins are potent regulators of immune cell activity. Modifying collagen matrices with glycosaminoglycans and proteoglycans, for example, has been shown to suppress the inflammatory response, which is crucial for periodontal regeneration and wound healing.

Another approach involves coupling anti-inflammatory factors and stem cells onto biomaterial surfaces. Incorporating periodontal ligament (PDL) stem cells and glucocorticoids into biomaterial membranes can reduce implant-associated inflammation, leading to improved outcomes in the inflammatory phase and reduced fibrous capsule formation in the later phase.

Overall, current approaches for designing advanced biomaterials with appropriate immunomodulatory properties focus on altering material surfaces through modification of physicochemical features or enhancement of biologically active sites to systematically target cell behavior. Biomaterials with artificial ECM coatings show promise in this regard.

13.6. Clinical strategies using purpose-driven biomaterials

13.6.1. Injectable delivery

The scope of cell-delivery systems for the treatment of periodontal disease has expanded significantly in recent years, offering new avenues for delivering therapeutics to patients. Injectable delivery systems, in particular, have emerged as promising approaches in regenerative medicine due to their unique advantages over traditional methods, including ease of application, localization and concentration of cells at the injection site, improved retention and distribution of cells, and support for cell proliferation and differentiation (Figure 13.5.).

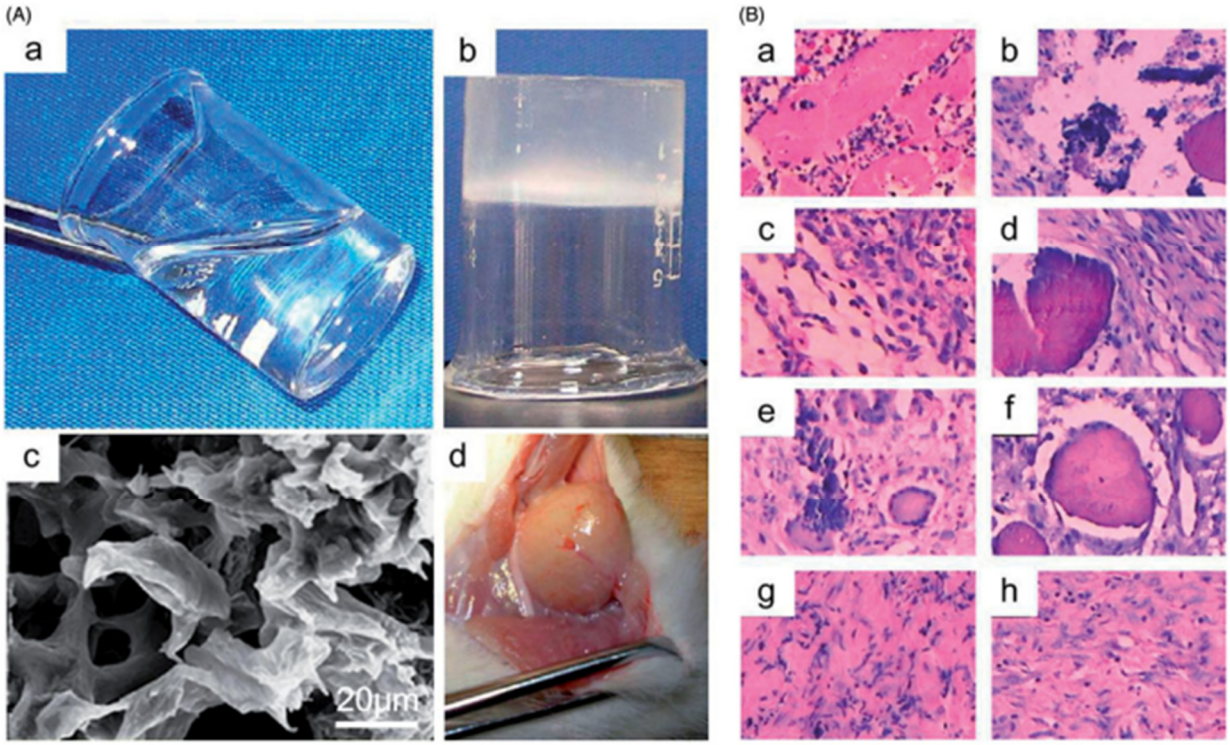


Figure 13.5. Injectable chitosan-based thermosensitive hydrogel developed for delivering cells and fibroblast growth factors for periodontal tissue repair (Ji et al., 2010). (A) (a and b) CS-HTCC/a,b-GP solution and CS-HTCC/a,b-GP hydrogel at 37 ——————————C. (c) SEM photomicrographs of the CS-HTCC/ a,b-GP thermosensitive hydrogel. (d) The CS-HTCC/GP aqueous solution formed a round gel-like plug at the injection site. (B) Light microscopy investigation of the inflammatory reaction after intramuscular injection of the CS-HTCC/GP thermosensitive hydrogel in rats. (a) After 3 days, tissues were swollen with signs of necrosis (arrow) appearing at

the local injection site. The leukocytes, principally neutrophils, (arrow) had infiltrated. (b) After 1 week, exudation and necrosis were observed. Granulation tissue encapsulated the gel (arrow) and necrotic tissue remained. Granulation tissue appeared and the number of neutrophils decreased along with inflammatory infiltration. (c and d) After 2 weeks, the number of lymphocytes and macrophages decreased, while the amount of collagen increased. (e and f) After 4 weeks, giant cells formed by the fusion of macrophages engulfed the injected gel. Giant cells surrounded the injected gel and engulfed the gel (arrow indicates the giant cells and the gel). (g) After 6 weeks, the number of cells and vessels decreased continuously and the amount of collagen accumulated progressively. (h) After 9 weeks, a large amount of collagen had formed [5].

Injectable hydrogel systems play a crucial role in delivering various cells and therapeutic agents for periodontal disease treatment and tissue repair. These hydrogels can encapsulate cells or drugs homogeneously and target diseased sites with minimal invasiveness. They undergo a solution-to-gelation phase transition after injection, facilitated by chemical or physical cross-linking mechanisms such as thermal gelation, pH-induced gelation, or ionic interactions.

Natural and synthetic polymers have been extensively explored for the development of injectable hydrogels, each offering unique advantages. Fibrin, for example, is widely used due to its biodegradability and support for cell infiltration and proliferation, leading to promising outcomes in bone regeneration for repairing alveolar bone defects. Other natural injectable hydrogels, including alginate, chitosan, agarose, and collagen, have also been developed by incorporating cells, drugs, and morphogens and initiating gelation through temperature or pH changes.

Recent studies have demonstrated the effectiveness of injectable hydrogels for periodontal disease therapy. For instance, chitosan-based thermosensitive hydrogels have shown excellent biocompatibility and potential as injectable local drug delivery vehicles and tissue engineering scaffolds for promoting periodontal regeneration. Similarly, alginate hydrogels encapsulated with dental pulp stem/progenitor cells have been effective for oro-maxillofacial bone tissue repair in clinical applications.

Despite their advantages, the widespread use of hydrogels as ideal biomaterials is limited by their bio-inertness and poor mechanical properties. However, recent advances in hydrogel synthesis have led to the development of mechanically robust hydrogels with suitable porous structures to support cell growth, elongation, and tissue penetration.

In conclusion, injectable hydrogel systems hold great promise for delivering cells and therapeutic agents in the treatment of periodontal disease, offering significant advantages in terms of application, localization, and support for tissue regeneration. Continued research efforts are focused on overcoming limitations and further optimizing the design and properties of injectable hydrogels for periodontal regeneration.

13.6.2. Delivery with solid scaffolds

Utilizing solid scaffolds seeded with cells represents another effective method for treating periodontal disease. These cell-scaffold constructs mimic tissue repair processes while maintaining structural integrity, offering potential benefits for tissue regeneration. For example, tricalcium phosphate/hydroxyapatite (TCP/HA) scaffolds seeded with cells have been used to create periodontal ligament (PDL)-like tissue constructs, which were subsequently implanted into periodontal defects in dogs for tissue repair. Additionally, HA/TCP scaffolds can serve as direct cell delivery scaffolds.

When designing solid scaffolds, it's essential to balance enhanced mechanical properties for alveolar bone regeneration with interconnecting porosity to facilitate nutrient supply and avoid adverse effects like tissue necrosis. Challenges arise in reconstructing large craniofacial and oral defects, particularly in regenerating complex osseous and ligamentous interfacial structures where the natural 3D shape of the tissue needs to be achieved.

Recent advancements include the development of multi-scale computational design and fabrication techniques for polymeric scaffolds targeting cell transplantation of genetically modified human cells to form human cementum-ligament-bone complexes. These scaffolds incorporate fiber-guiding structures to guide functionally oriented ligamentous fibers in vivo, resulting in predictably oriented fibrous architecture and better organization of the ligament interface.

Another innovation is the development of biphasic scaffolds consisting of bone and periodontal compartments, allowing simultaneous delivery of multiple cell types necessary for regenerating alveolar bone/PDL complex tissue constructs. In vitro studies have shown enhanced cell growth and extracellular matrix mineralization in the bone compartment of these scaffolds.

While advancements in cell-based research for periodontal bioengineering are promising, challenges remain in achieving spatial fibrous tissue organization, orchestrating the formation of multiple tissues, and achieving functional restoration of the tooth-supporting system using a single scaffold system in vivo. Continued research efforts are focused on designing and developing advanced medical devices that utilize multiple physical and geometric biomaterials to address these challenges (Figure 13.6.).

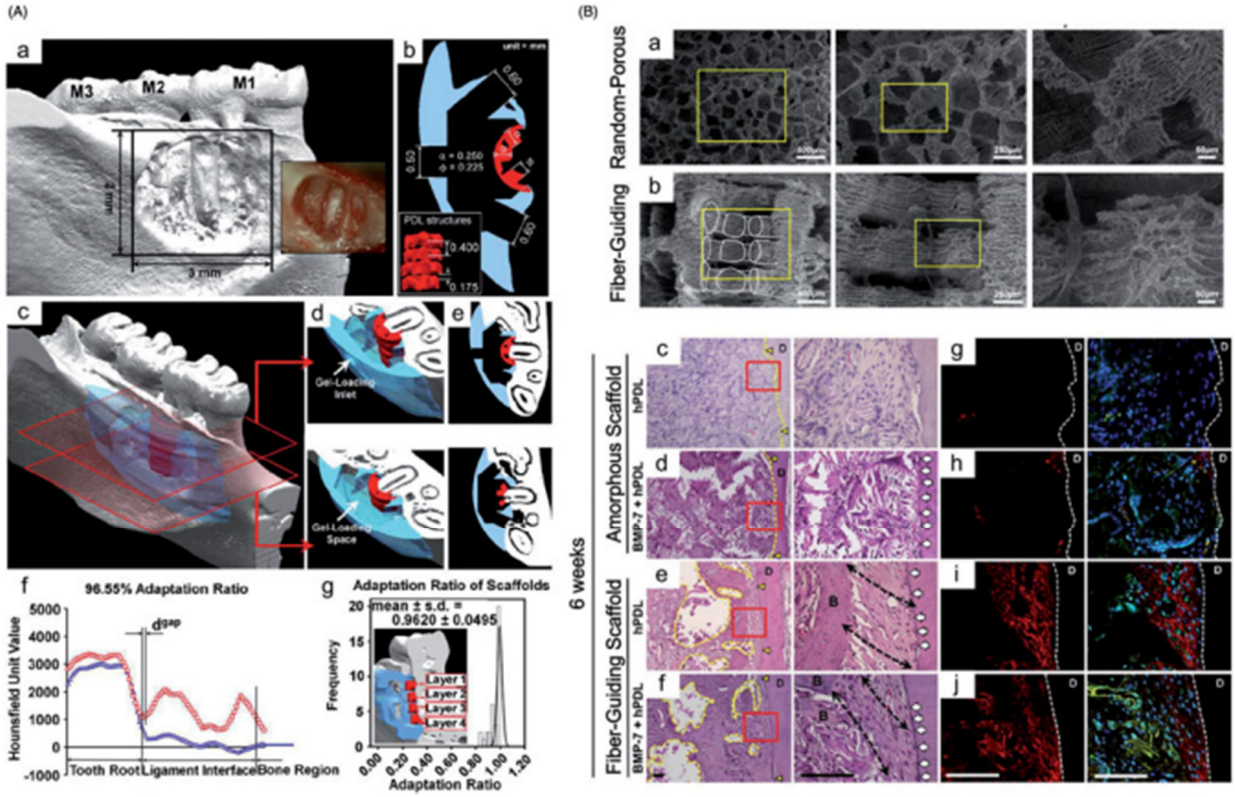


Figure 13.6. Periodontal bone-ligament tissue repair using fiber-guiding scaffolds (Park et al., 2012). (A) Surgically created periodontal osseous defect and fiber-guiding scaffold design based on the 3D medical image dataset. (a) The micro-computed tomographic (micro-CT) image shows the surgically created periodontal osseous defect on the buccal side of the mandible. (b) The customized fiber-guiding scaffold was designed. (c) The schematic figure using STL-generated files of micro-CT scanned mandibular images and designed customized defect-fit hybrid scaffolds to the osseous defects. (d) Cross-sectioned, 3D images provided computer-designed scaffold contact information to dentin surfaces with the indication of gel-loading inlet (top) and containing portion (bottom). (e) 2D digitized sectioned images of panel. (f) The adaptation ratio was assessed using BaSO4-stained scaffolds and the HU grayscale values from the micro-CT. (g) The adaptation ratio was calculated with three fiber-guiding scaffolds possessing four different layers, which had three ligament architectures on each layer (3D generated panel embedded in the graph). (B) (a) SEM images provided the micro/nanoporous internal architecture of random-porous scaffold with interconnectivity. (b) The microscopic architectures of the fiber-guiding scaffold with the microgrooved patterns and submicron pores. (c–j) Histology and immunofluorescence analysis of fibrous connective tissue formation and re-arrangement along the different topographic scaffolds. [5]

13.7. Challenges and future prospects

The emerging advanced biomaterials, including hydrogels, films, micro/nanofibers, and particles, offer significant potential for utilization as cell/drug carriers for local drug delivery and biomimetic scaffolds for periodontal disease treatment. Periodontal regeneration is a highly regulated biological process that requires precise control over sequence and timing to avoid impaired wound healing. Biomaterials play a crucial role in providing microenvironments for hybrid tissue regeneration and serving as carriers for drug delivery and release. Therefore, it's essential to consider the biological function of developed biomaterials, including biocompatibility, biodegradability, and

immunogenicity, during the material design process. Additionally, the mechanical properties of implanted biomaterials should be designed to mimic native tissues' properties to withstand in vivo strains and stresses experienced by the tissue under physiological loading after implantation. Characterizing the structural and material properties of the tissue is necessary to identify biomimetic parameters for biomaterial design, particularly for regenerating the soft tissue-to-bone interface.

Despite the high potential, several challenges need to be addressed before cell/drug delivery and periodontal regeneration become standard options for treating periodontal disease. Firstly, the large-scale expansion of cells for therapeutic transplantation requires protocols that do not rely on fetal bovine serum (FBS) as a nutritional supplement, as FBS carries the risk of transmitting viral and prion diseases. Secondly, the implantation of fabricated bone-PDL tissue-like constructs is prone to destruction due to the complex topologies of periodontitis, highlighting the need for tissue integration for functional restoration. Although some success has been reported, achieving bone and cementum formation with accompanying functional PDL tissues remains challenging. However, recent studies suggest that stem cells may offer promise in modulating immune responses and influencing endogenous tissue stem cells to enhance repair. Lastly, potential immune responses to exogenously implanted cell-biomaterial composites must be carefully examined before embarking on clinical trials.

While significant progress has been made through in vitro and pre-clinical animal studies, clinical studies in the field of periodontal disease treatment and regeneration are still emerging. A clear translational roadmap has yet to emerge, indicating that the field remains fragmented and further research is needed to address these challenges and advance towards clinical applications.

13.8. Quiz 13.

1. Which bacterial species are commonly associated with periodontal disease?
a) Streptococcus
b) Aggregatibacter actinomycetemcomitans
c) Porphyromonas gingivalis
d) Fusobacterium nucleatum
e) Prevotella intermedia

2. What are some virulence factors employed by Porphyromonas gingivalis?
a) Lipopolysaccharide (LPS)
b) Fimbrae
c) Proteases (gingipains)
d) Collagenase
e) Hyaluronidase

3. Which cytokines play a pivotal role in recruiting host immune cells during the initial response to bacterial insult in periodontal disease?
a) Interleukin-8 (IL-8)
b) Interleukin-6 (IL-6)
c) Interleukin-1β (IL-1β)
d) Tumor necrosis factor-alpha (TNF-α)
e) Leukotriene B4 (LTB4)

4. Which treatment strategies are commonly used in periodontal therapy?
a) Scaling and root planning (SRP)
b) Open flap debridement (OFD)
c) Guided tissue regeneration (GTR)
d) Antifungal therapy
e) Laser therapy

5. What are examples of natural polymers used for periodontal regeneration?
a) Collagen
b) Alginate
c) Chitosan
d) Poly (lactic acid) (PLA)
e) Polyethylene glycol (PEG)

6. Which advantages do synthetic hydrogels commonly exhibit over natural hydrogels for periodontal tissue regeneration?
a) Higher degradation rates
b) Better mechanical properties
c) Increased biocompatibility
d) Enhanced cell adhesion
e) Controlled drug release

7. What are critical considerations for the long-term survival and function of biomaterials used in periodontal regeneration and therapy?
a) Biocompatibility and biodegradability
b) Immunogenicity
c) Controlled drug release

d) Material stability
e) Mechanical properties

8*. Which bacterial species are commonly associated with the onset of periodontal disease?
a) Streptococcus mutans
b) Tannerella forsythia
c) Actinomyces naeslundii
d) Lactobacillus acidophilus
e) Veillonella parvula

9. What are some strategies used in periodontal therapy to eliminate infected tissues and promote regeneration?
a) Scaling and root planning (SRP)
b) Open flap debridement (OFD)
c) Bone grafting
d) Guided bone regeneration (GBR)
e) Enameloplasty

10. Which factors are involved in the formation of dental plaque?
a) Salivary proteins
b) Glycoproteins
c) Streptococcus
d) Actinomyces
e) Bacillus

References

[1]. Cho MI, Garant PR. Development and general structure of the periodontium.Periodontol 2000.2000;24:9–27.
[2]. Steigmann L, Maekawa S, Sima C, Travan S, Wang CW, Giannobile WV. Biosensor and lab-on-a-chip biomarker-identifying technologies for oral and periodontal diseases.Front Pharmacol.2020;11:588480.
[3]. Dalai DR, Gupta D, Bhaskar DJ, Singh N, Jain A, Jain A, et al. Nanorobot: a revolutionary tool in dentistry for next generation.J Contemp Dent.2014;4:106–112.
[4]. Piñón-Segundo E, Ganem-Quintanar A, Alonso-Pérez V, Quintanar-Guerrero D. Preparation and characterization of triclosan nanoparticles for periodontal treatment.Int J Pharm.2005;294:217–232.
[5]. Chen, Xi & Wu, Guofeng & Feng, Zhihong& Dong, Yan & Zhou, Wei & Li, Bei & Bai, Shizhu& Zhao, Yimin. (2015). Advanced biomaterials and their potential applications in the treatment of periodontal disease. Critical reviews in biotechnology. 36. 1-16. 10.3109/07388551.2015.1035693.

14. Nanorobots in Medicine and Dentistry

The potential of intelligent nano/micro-motors, active particles, and robots for performing intricate tasks and their integration into on-chip applications is substantial. Nanorobots (NBs) have garnered significant interest due to their adaptability to various environments and the attainment of necessary biocompatibility [1, 2, 3, 4, 5, 6, 7]. Recent advancements have seen the exploration of diverse NB designs, including helical structures, surface walkers, cilia, scaffolds, and biohybrids. Chemical propulsion mechanisms like self-electrophoresis, self-diffusiophoresis, and microbubble recoil have been developed, alongside alternative fuels such as carbon dioxide gas [8, 9, 10, 11, 12, 13, 14, 15].

NBs exhibit remarkable capabilities, generating motive forces at the nano-scale, converting chemical to mechanical energy efficiently, achieving ultrafast speeds, and navigating complex trajectories [16, 17, 18, 19, 20, 21, 22, 23]. They find application in various biomedical fields, such as cell delivery, minimally-invasive surgery, biosensing during motion, and pathogen isolation. Notably, slippery nano-propellers have penetrated the vitreous body of the eye without damage, while spermbots show promise in ovarian cancer treatment [24, 25, 26, 27, 28, 29, 30].

Fabricating NBs involves standard methods like electrochemical deposition, physical vapor deposition, rolled-up technology, layer-by-layer assembly, and biohybrid approaches [31, 32, 33, 34, 35, 36, 37]. However, conventional micromotors often lack the required biocompatibility and biodegradability for in vivo applications. Microfluidics presents a promising platform for controlled encapsulation and release of materials, enabling advancements like enzyme-powered vesicles and hydrogel microcapsules with catalytic cores. Integration with microfluidics and nanozymes opens new avenues for NB applications (Figure 14.1.).

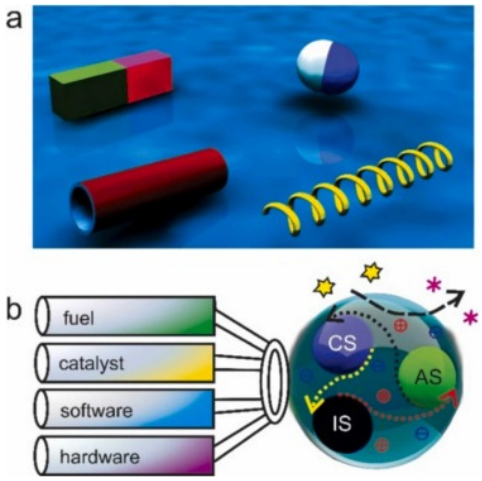


Figure 14.1. Scheme proposes next generation of NBs with integrative functions. (a) Schematic image of standard solid state-based nano- rod, tube, sphere, and helical structures. (b) Envisioned microfluidic method for integration of sub-systems to achieve intelligent NBs (CS: catalytic sub-system, AS: autonomous sub-system, IS: information sub-system).

Versatile methods for controlling NB motion include external fields (electrical, optical, magnetic, light, and ultrasound) and modulation of fuel concentration, composition, chemical gradients, and light sources. Specific programmable trajectories have been achieved using advanced soft computing techniques and optical resonance or light-driven mechanisms. Additionally, AI integration offers precise motion control and new directions for advanced applications in biomedical tasks [38, 39, 40, 41, 42, 43, 44, 45, 46, 47].

The future of NBs lies in advanced nano/micromachines with specific functions, including programmable DNA-based NBs for autonomous tasks like motion, sensing, and actuation. The exploration of self-catalyzing chemical reactions and non-equilibrium synthetic nanomaterials holds promise for mimicking biological functions like adaptation, self-healing, and self-replication. NBs find application across various sectors, including targeted disease treatments and diagnostics tools,

although safety considerations regarding motion, biocompatibility, and biodegradability remain crucial [49, 50].

This review discusses the next generation of NBs, emphasizing advanced fabrication methods, specific functions, and bio-applications. The intersection of nanomotors or nanorobots with microfluidics and reaction networks presents a novel interdisciplinary approach with potential applications in targeted drug delivery, environmental monitoring, and advanced manufacturing processes. The review aims to fill gaps in prior research by providing insights into this integration and its significance for future innovative applications [51, 52, 53].

14.1. Multiple fabrication techniques for micro/nanorobots

Numerous advanced fabrication methods have been employed to create classical nanorobots (NBs), including electrochemical deposition, physical vapor deposition, strain engineering nano/microtubes, and direct laser writing. However, the escalating demand for biocompatibility and precise manipulation has spurred the development of microfluidics for synthesizing micro/nanorobots. Microfluidics manipulates small fluid volumes within microscale channels to construct desired devices, offering advantages like biocompatibility, complex integration, and tailored chemical composition [54, 55, 56, 57].

Recent studies have reported various approaches for NB fabrication using microfluidics. For instance, Zhang et al. utilized a capillary glass device with an off-chip photopolymerization strategy to create droplet templates for NB preparation using three-phase immiscible flows (Figure 14.2.). By adjusting flow rates, control over droplet size and composition was achieved. Chen et al. developed glass capillary microfluidics for producing self-propelled Janus NBs, enhancing motor speed and fabrication precision. Feng et al. demonstrated a one-step microfluidic process for generating multiphase Janus NBs, exploiting phase separation methods. Additionally, electrochemical template-assisted methods have facilitated the synthesis of helical nano swimmers, offering insights into tailored catalytic performance [58, 59, 60, 61, 62, 63, 64, 65, 66, 67].

Fluidic, assembly, and physical methods have been combined to prepare NBs. For instance, Adams et al. utilized glass capillary microfluidics to functionalize toluene-filled microbubbles with silica nanoparticles, creating self-propelled bubble-bots. Meng et al. fabricated self-electrophoretic Janus NBs from single dispersed polystyrene microspheres using ion sputtering [68, 69, 70, 71, 72].

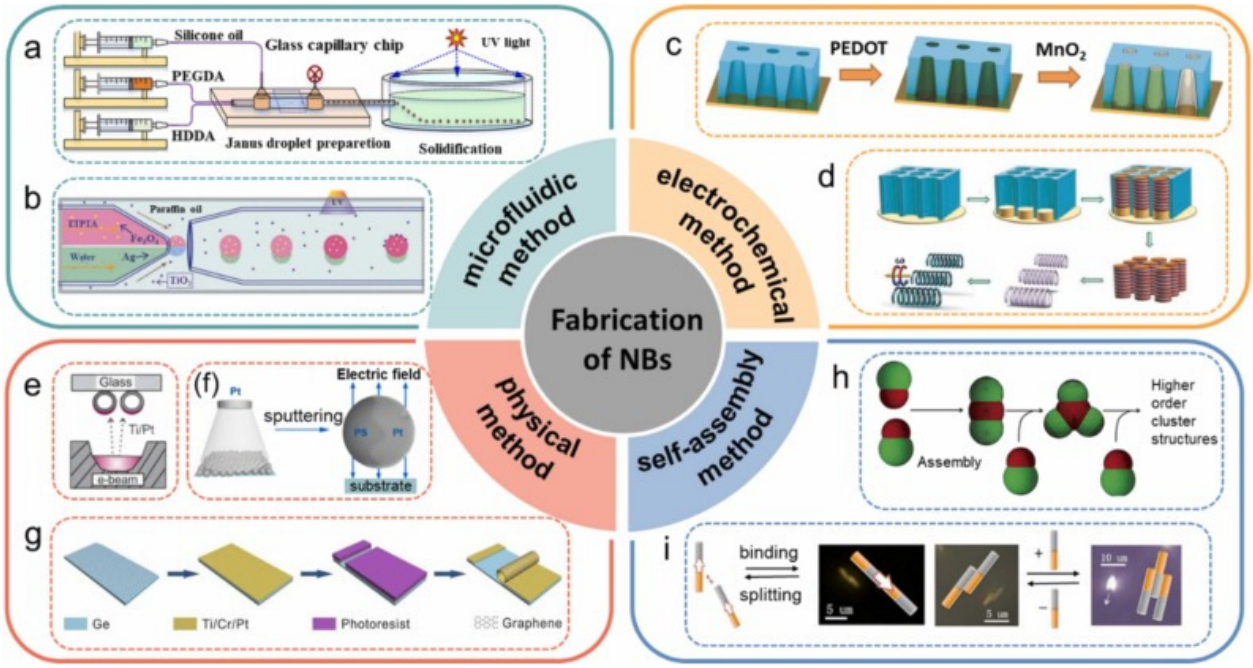


Figure 14.2. Fabrication methods of micro/-nanorobots. (a) Schematic of the microfluidic system used for generation of Janus microrobots. (b) The dispersed phase contains two phases: the water phase and the photocurable ETPTA oil phase. Yellow dots denote the ETPTA oil phase containing Fe3O4 nanoparticles with a size of 20 nm. The water phase contains modified Ag nanoparticles (50 nm) shown as red dots. The continuous phase is

paraffin oil mixed with TiO2nanoparticles (20 nm). Span 80 is the surfactant used to vary the interfacial tension between paraffin oil and water. (c) Schematic diagram of template-assisted electrodeposition procedures of PEDOT/MnO2 micromotors. (d) Schematic illustration of the template-based fabrication of helical magnetic nano swimmers. (e) Schematic image of electron-beam evaporation of Ti/Pt layers on SiO2 microbubbles in a vacuum. (f) Schematic diagram of Janus micromotors fabricated by ion sputtering. (g) Schematic image of the fabrication process of the rolled-up graphene/Ti/Cr/Pt tubular micromotor. (h) Dynamic self-assembly of electrophoretic nanomotors propelling as a cluster in fuel solutions. (i) 'Hard–soft' particles assembled to colloidal molecules to form higher order cluster structures.

Rolled-up nanotechnology, based on strain engineering, has also been employed to create tubular NBs. Mei's group pioneered bubble-propelled tubular NBs, subsequently adopted by others. Zhao et al. simplified the fabrication of rolled-up nanomembranes using magnetron sputtering [73, 74].

Self-assembly methods have yielded complex NB structures, as seen in the work of Skelhon et al., who reported self-assembled Janus microparticles. Wang et al. explored the self-assembly of Pt/Au nanorods, demonstrating assembly driven by self-induced electric fields [75, 76, 77].

Microfluidics, in particular, has emerged as a promising approach, offering rapid prototyping, high biocompatibility, and precise manipulation. Microfluidics can adjust NB geometry and functions by incorporating functional nanoparticles and manipulating fluid flow parameters. Keller et al. developed enzyme-driven gel NBs via high-throughput microfluidic droplet phase separation (Figure 14.3.). Zhu et al. used glass capillary microfluidics to fabricate hydrogel NBs with various structures and functionalities. Zou's group demonstrated a microfluidic method for generating multifunctional NBs with distinct cores, showcasing promising results in biomedical applications [78, 79, 80].

Furthermore, microfluidics has enabled continuous generation of helical microparticles and autonomous environment-adaptive microrobot swarm navigation through deep learning-based real-time distribution planning. This integration of intelligent algorithms with NBs holds promise for enhancing autonomy and adaptability in uncertain environments [81].

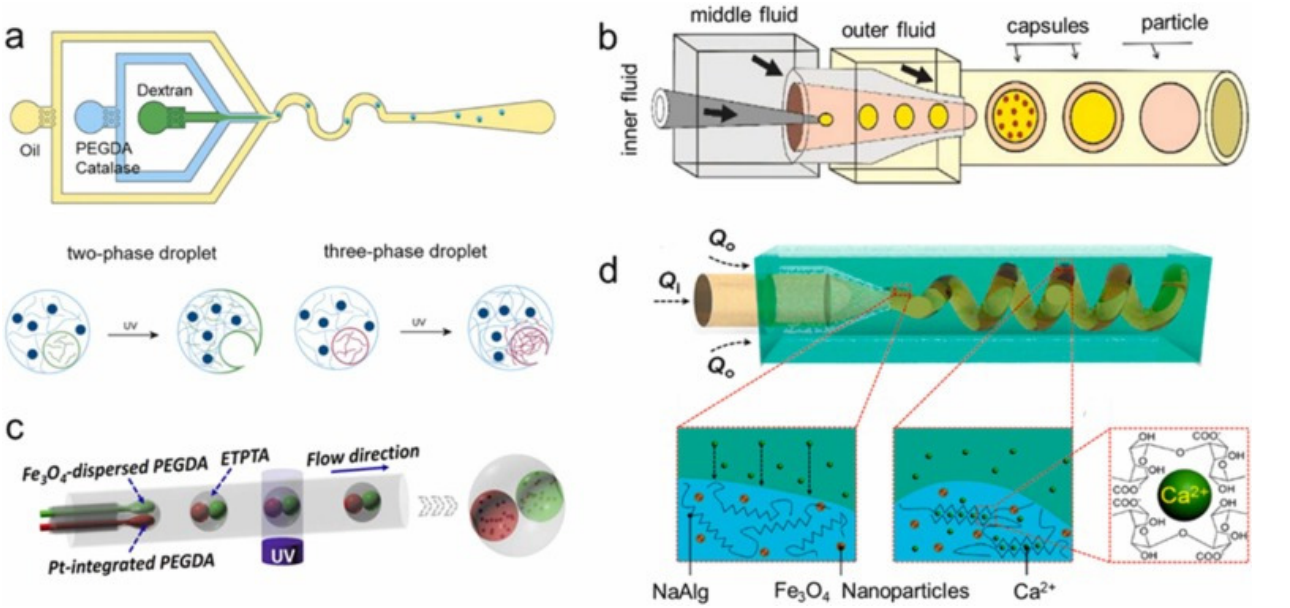


Figure 14.3. Microfluidic fabrication methods of micro/nanorobots. (a) A microfluidic chip is used to construct ATPS droplets, three inlets—oil,PEGDA, and dextran—and one outlet. At the first cross junction, an ATPS jet is formed, which is emulsified at the second cross-junction. (b) Schematic of microfluidic glass capillary device used for the generation of hydrogel particles. Capsules from complex emulsion drops and optical microscopy image of double emulsion drop formation in glass capillary microfluidic device. After generation, the double emulsions are irradiated withUV light(not shown) to photo-polymerize the shells of the microcapsules and particles. (c) Micromotor generation by the capillary microfluidic system with dual Inner injections and real-time microscope image of the microfluidic emulsification of the composite double emulsions with various numbers of cores. (d) for synthesizing magnetic helical Ca-Algmicrofibersvia interfacial cross-linking reactions and between alginateand Ca2+.

14.2. Smart motion control and intelligent collective behavior of micro/nanorobots

14.2. 1. Designs of collective behavior of micro/nanorobots

Various methods have been developed to control the motion of nanorobots (NBs), including magnetic fields, light, ultrasound, electric fields, electrochemical potential, and chemotaxis.

Figure 14.4(a) illustrates the diffusive chemotactic motion of catalase enzyme in the presence of hydrogen peroxide substrate. Enzymes are arranged in a co-flow configuration in a microfluidic channel, demonstrating elongated motion trajectories toward higher concentrations of hydrogen peroxide.

Figure14.4(b) showcases magnetic CNC/Fe3O4 nanomotors capable of effectively loading doxorubicin anticancer drugs using π–π stacking interactions. Magnetic fields serve as a versatile method to propel NBs, locate them near targeted cells, and release therapeutic agents, including via infrared light.

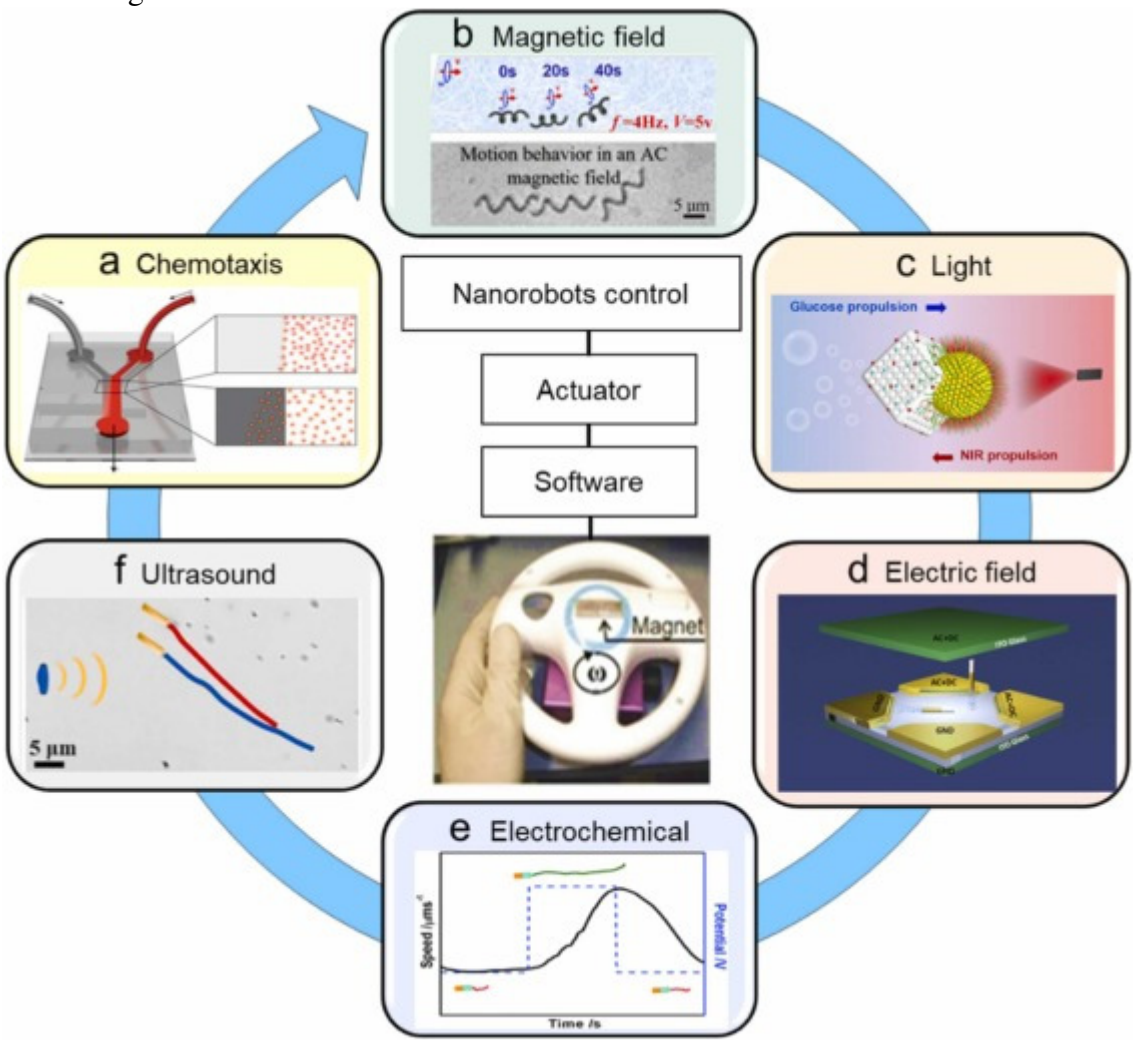


Figure 14.4. Concepts of various methods of motion control of NBs. (a) Study of non-biological chemotaxis observed for enzymes inmicrofluidic channelsco-laminar flows.(b) Magnetic field driven helical micromotor structures. (c)Near infrared light-driven propulsion in glucose fuel. (d) Electric field powered nanorod. (e) Modulation of NBs motion usingreference electrodeimmersed in the fluid, i.e.,electrochemical potential. (f) Ultrasound-powered method of nanorod-based NBs.

In Figure14.4(c), glucose-driven enzyme-based mesoporous Janus SiO2 @Au core@shell NBs are powered by near-infrared light. Glucose oxidase/catalase catalysts drive NBs using glucose, while thermophoretic/photothermal motive force is generated by illuminating the mesoporous structure with NIR light.

Figure 14.4(d) illustrates another approach to control motion using applied electric (E-) fields. Novel electrode architectures utilize AC and DC E-fields to achieve precise delivery of cargo payloads.

Figure 14.4(e) discusses an example of NB speed control, including switching power "on" and "off" using electrochemical potential. An Au-fiber working electrode placed close to the NBs controls the electrochemical reaction products generated at the surface of NBs.

Finally, Figure 14.4(f) demonstrates ultrasound-propelled Au nanowire-based NBs loaded with ovalbumin antigen for vaccine delivery. Ultrasound facilitates the effective internalization of NBs into the cytoplasm of antigen-targeting cells, offering high potential for enhancing immunity and immunotherapy.

Collective behaviors observed in nature, such as those seen in ant colonies, fish schools, and bird flocks, have inspired researchers to explore collective and swarming behaviors in nanorobots (NBs) [88]. Various strategies have been developed to induce the self-organization of dynamic NBs, utilizing either self-propulsion through chemical reactions or activation by external fields like magnetic, light, acoustic, or electrical fields [88], [89]. These collective behaviors offer numerous current and potential applications in environmental remediation and biomedical engineering, leveraging the cooperative interactions among nearby individuals and the substantial surface area coverage provided by the agents.

Magnetic field-driven micro robotic swarms offer a promising avenue for robotics control. For example, Xie et al. utilized alternating magnetic fields to program hematite colloidal particles in liquid, forming chain, vortex, and ribbon-like micro robotic swarms with the ability for rapid and reversible transformations between them, as depicted in Fig. 5(a) [90]. Dai et al. demonstrated light-controlled artificial NBs based on a Janus TiO2/Si nano-tree structure. Under ultraviolet illumination, these NBs exhibit phototactic swarming behavior when treated with 3-[2-(2-aminoethylamino)-ethylamino]-propyltrimethoxysilane (AEEA) or decorated with Pt NPs (positive phototaxis), or when grafted with 2-(4-chlorosulfonylphenyl)ethyltrimethoxysilane (CSPTMS) (negative phototaxis), as shown in Fig. 5(b) [91]. Additionally, Wu et al. employed a simple ion-exchange interaction between self-propelled ZnO nanorods and sulfonated polystyrene (PS) microbeads, resulting in collective behavior at a hierarchical scale. Through attractive osmosis, sulfonated PS microbeads approach ZnO nanorods and form tightly bonded core-shell clusters, leading to the formation of long stripes and larger-scale aggregations due to long-range and inter-cluster attractions, as illustrated in Figure 14.5(c) [92].

The acoustic gathering effect has been demonstrated in the formation of a micro swarm using liquid metal agents. Li et al. presented a reconfigurable dynamic assembly based on acoustically actuated eutectic gallium-indium alloy (EGaIn) liquid metal colloidal nanorobots (NBs) [93]. At a frequency of 730 kHz, various stripes of EGaIn colloidal motors were observed, gradually merging into larger striped patterns and self-organizing into flower-like patterns when the frequency was changed to 722 kHz. The swarm pattern dispersed again when the frequency was decreased to 680 kHz, as depicted in Fig. 6(a). Manipulating the frequency of the applied acoustic field further allowed for the movement of these EGaIn micro swarms. These collective movements are attributed to variations in the node planes resulting from changes in the frequency of the standing wave acoustic field [93].

Micro robotic swarms responsive to dual stimuli and controlled by hybrid external powers can adapt to more complex environments [94], [95]. Recently, the combination of acoustic power with light illumination was employed to induce the collective behaviors of Janus microrobots, as shown in Fig. 6(b) [94]. Driven by the acoustic field, the bowl-like TiO2/Au microrobot exhibits motion toward its exterior side, caused by the oscillating edges-generated second-order acoustic streaming flow [94]. This motion is independent of the position of the TiO2 and Au layers. In contrast, UV light-powered self-propelled motion is material-dependent, with the nanorobot exhibiting motion toward the TiO2 side. Due to the acoustic pressure gradient, two groups of Janus NBs gather at the low-pressure nodes, with the exterior side facing the center of the pattern. Upon turning on the UV light, the two patterns consisting of Janus NBs with reversed positions of TiO2 and Au layers exhibit different behaviors: pattern expansion and pattern contraction with the exterior layers of Au and TiO2, respectively.

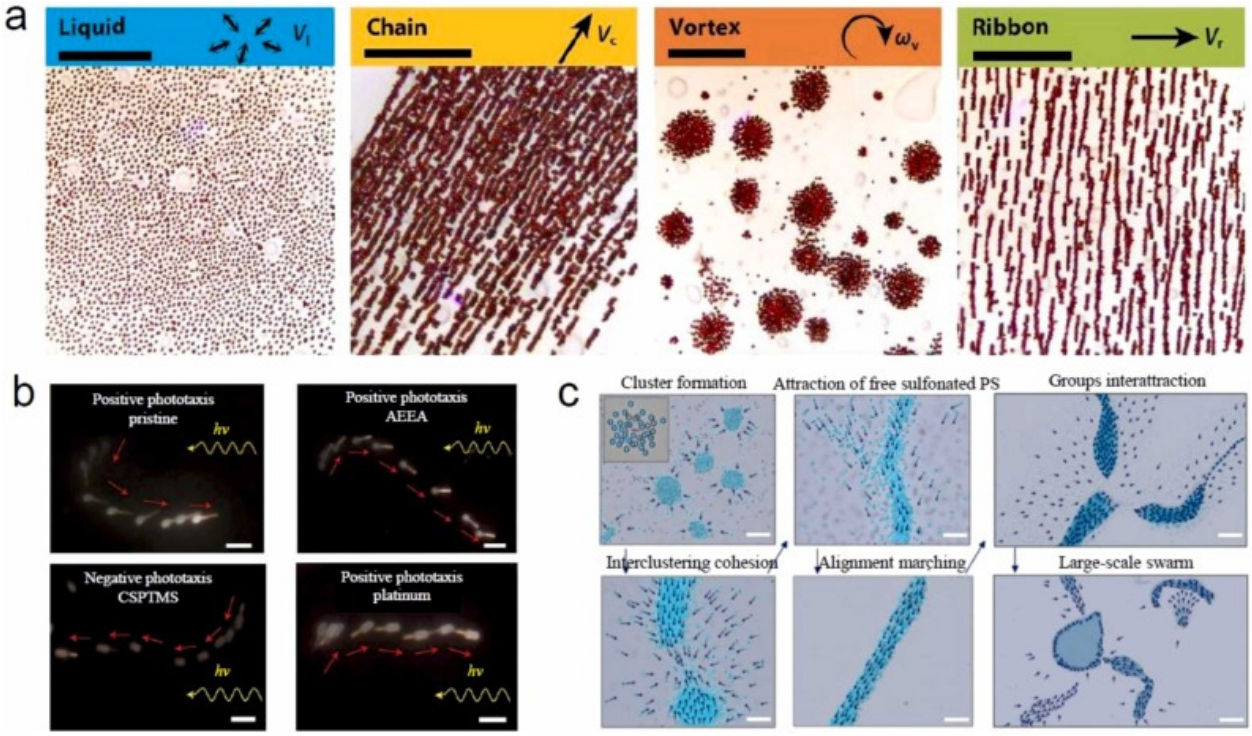


Figure 14.5. (a) Multimodal transformation ofhematitecolloidal particlesin liquid, chain, vortex, and ribbon-like swarm states. Scale bars: 50 µm. (b) Superimposed images of sequential frames. The Pristine and AEEA-treated nanotrees migrate in the tail-forward direction and exhibit positive phototaxis. The CSPTMS-treated nanotree migrates in the head-forward direction and exhibits negative phototaxis. The Pt-decorated nanotree migrates in the head-forward direction and exhibits positive phototaxis. Scale bars: 10 µm. (c) The emergence ofswarmingbehavior of ZnO-sulfonated PS mixture: sulfonated PS accumulate around theZnO nanorodand form clusters with it as the core (inset); cohesion of adjacent ZnO nanorod-sulfonated PS clusters via attractive osmosis; self-alignment of free sulfonated PS and ZnO nanorod-sulfonated PS clusters; alignment marching of clusters; further aggregation of ZnO nanorod-sulfonated PS clusters; large-scale swarming behavior of the ZnO-sulfonated PS mixture.

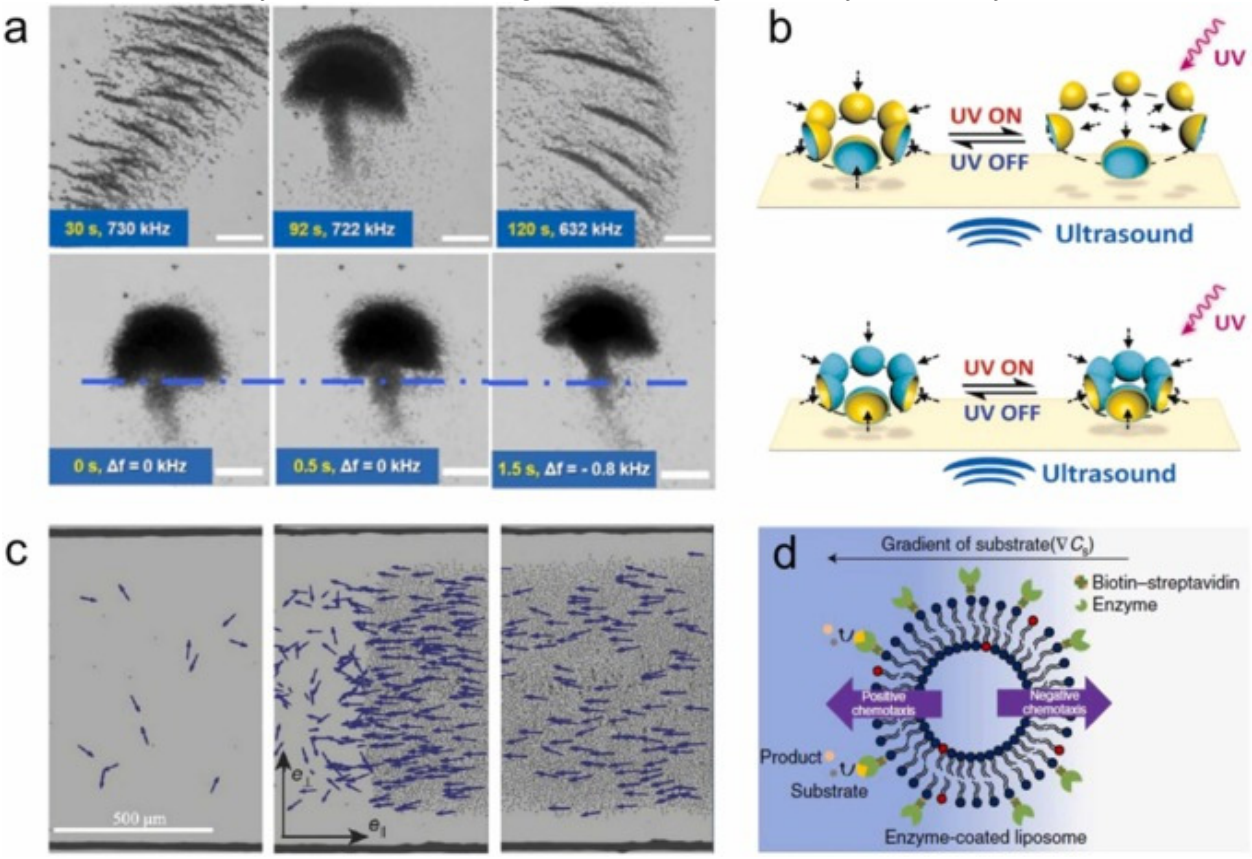


Figure 14.6. (a) Time-lapse images of formation and motion of acoustically triggered EGaIn colloidal swarm. (b) Structure-depended collective behavior for the microbowls in a hybrid source of UV light and an acoustic field.

The dispersion and compaction behaviors were formed for the resulting swarm of TiO2-Au microbowls and Au-TiO2 microbowls, respectively. Scale bar: 20 μm. Blue surfaces: TiO2, and yellow surfaces: Au. (c) Collective motion of rolling particles from isotropic gas to the propagating band and homogeneous polar liquid at increasing density. Scale bar: 500 μm.(d) Illustration of enzymatic propulsion or solute interactions driving the migration of enzyme-coated liposomes towards or away from the substrate. Egg LissRhod PE (the red-headed lipid) serves as a fluorescent marker, while DSPE-PEG (2000) biotin (the blue-headed lipid with attached enzyme) and L-phosphatidylcholine lipids (the blue-headed lipid) make up the rest of the liposomes.

Electric field-driven micro robotic swarms offer another avenue for robotics control. In Fig. 6(c), Bricard et al. applied an electric field to insulating particles immersed in a conducting fluid, resulting in the fluctuation of the charge distribution on the particle surface [96]. The electrostatic torque formed caused the particles to rotate randomly, displaying various collective states. At low area fractions, the rolling particles moved in random directions at the same speed, forming an isotropic gaseous phase. A clear transition to collective motion was observed by increasing the fraction above a critical value. A macroscopic fraction of the rollers self-organized, and its constituents cruised coherently in the same direction. Further increasing the particle fraction led to a homogeneous polar-liquid phase, in which the head of the propagating bands caught up with the tail of themselves. These results demonstrate that hydrodynamic interactions enable individual particles to perform directed collective motion [89], [96].

Chemotaxis offers another route for directional motion control. Somasundar et al. investigated the directional control of both positive and negative chemotaxis in liposomal protocells, as depicted in Fig. 6(d) [97]. The propulsion mechanism relies on the interaction of enzyme-catalysis-induced positive chemotaxis and solute-phospholipid-based negative chemotaxis. Thus, controlling the extent and direction of chemotaxis holds significant implications for developing cell mimics and delivery vehicles with motion reconfiguration capability under different environmental conditions [97].

To understand the mechanism for metabolon formation, Zhao et al. studied the coordinated movement of the first four enzymes of the glycolysis cycle using microfluidic and fluorescent spectroscopy techniques. The study suggested that each enzyme follows its substrate gradient generated by the previous enzymatic reaction. Even under conditions mimicking cytosolic crowding, the observed rate was similar to the previously reported rate of enzyme diffusion in living cells. Chemotaxis serves as the basis for organizing metabolic networks in the cytosol [98]. These studies suggest an opportunity for chemotaxis-based directionality control, paving the way for the development of synthetic micro- and nanomotors capable of achieving self-targeting and navigation in complex or microenvironments with responses to chemical gradients, integrating sensing, processing, and self-propelling functionalities.

14.3. Applications of collective behavior of micro/nanorobots

Dynamic micro swarm motion control enhances environmental remediation applications due to the high processing efficiency of collective working modes and the significant specific area coverage of agents [99], [100]. For instance, Zhang et al. developed a swarming biohybrid adsorbent (porous spore@Fe3O4) by growing magnetic nanoparticles on hydrothermally-treated fungi spores. This adsorbent efficiently removes heavy metal ions from contaminated water, as depicted in Figure 14.7(a) [101]. Enhanced adsorption capacity and shorter removal times were achieved through controllable magnetic collective motion compared to nonmotile counterparts [101]. Sun et al. demonstrated the cooperative behavior of micromagnetic submarines based on sunflower pollen grains (SPGs), applied for oil and microplastic removal [102]. The hollow micro submarines, when swarming at the oil-water interface under a magnetic field, facilitate capillary absorption of oil into their hydrophobic structure. Figure 14. 7(b) illustrates the formation of a vortex-like micro swarm under magnetic field application, accelerating absorption and cleaning more efficiently than static adsorption [102].

Wang et al. developed photocatalytic Au@Ni@TiO2-based micromotors, as shown in Figure 14.7(c), capable of efficiently collecting and transporting PS particles through phoretic interactions [103]. Park et al. demonstrated the removal of glyphosate from water samples using magnetite

nanoparticles (Fe3O4 NPs), as depicted in Figure 14.7(d) [104]. These Fe3O4 NPs, acting as catchers and carriers for magnetic removal, can be reused after thermal treatment, enabling cyclic use of the magnetic absorber [104]. Additionally, Hu et al. fabricated multilight-responsive micromotors Fe3O4 @poly(glycidyl methacrylate)/polystyrene (Fe3O4 @PGS), which can perform "chemistry-on-the-fly" tasks by harnessing catalytic efficiency and enzyme immobilization [105]. The swarming motion of these micromotors enhances mass exchange in treated solutions, accelerating reactions both in aqueous solutions and organic phases [105].

Moreover, Xie et al. demonstrated multiple collective modes within one colloidal system by programming hematite colloidal particles into various microrobotic swarms using alternating magnetic fields [90]. These reconfigurable microrobot swarms can adapt to environmental variations or multitasking requirements. For example, the colony-like vortex microrobot swarm can push PS microspheres, while the ribbon swarm can perform large-area manipulation, albeit with lesser carrying ability due to induced fluidic flow [90].

In the realm of biomedical applications, micro/nanoswarms hold promise. Law et al. demonstrated magnetic particle swarms for selective embolization to block blood flow inside targeted regions [106]. Sun et al. developed a magnetic microswarm platform for biofilm eradication, while Wang et al. showcased reconfigurable magnetic microswarms for thrombolysis under ultrasound imaging [107], [110]. Hoop et al. designed Ag-coated magnetic Pd nanocoils for targeted bacteria killing [108]. These examples underscore the potential of controlled NBs in biomedical applications, including drug delivery and in vivo imaging, as demonstrated by Hortelao et al. using PET-CT imaging techniques and Zhang et al. with dual-responsive biohybrid neutrophil-based microrobots ("neutrobots") for active cargo delivery to malignant glioma [70], [110].

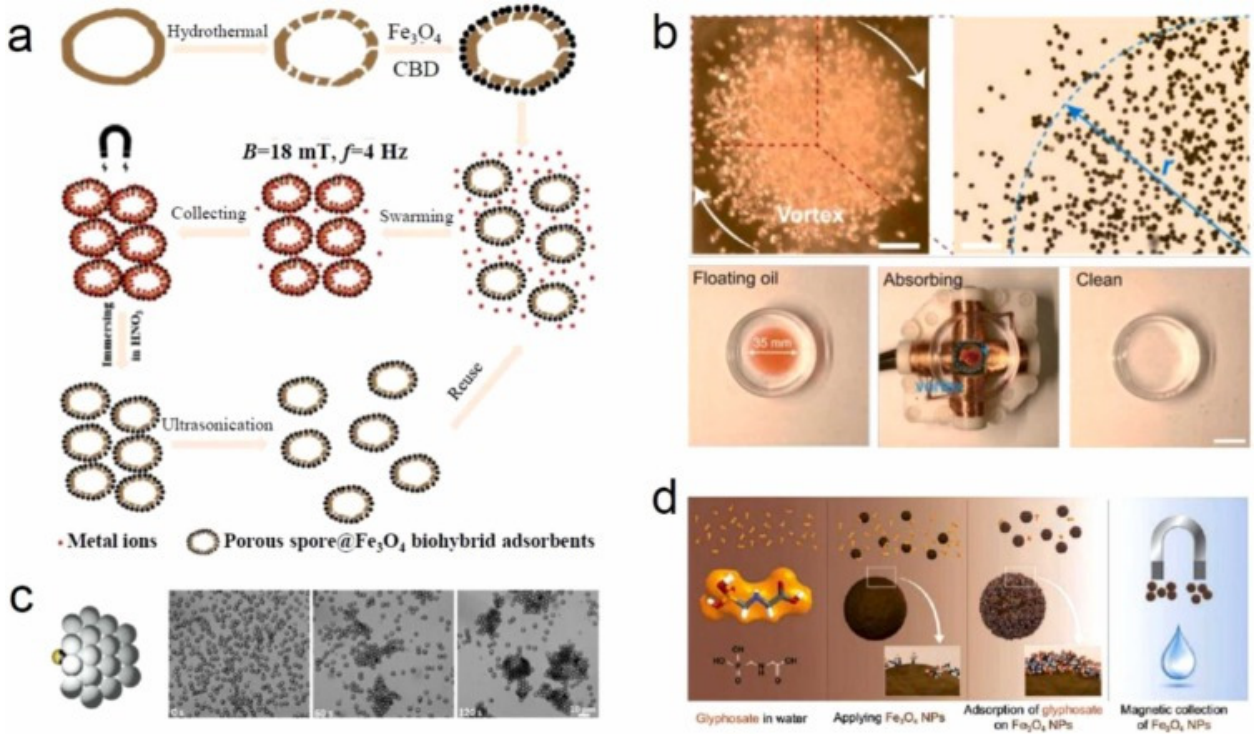


Figure 14.7. Environmental remediation of synthetic collective microrobots. (a) Reusable biohybrid adsorbents collectively removeheavy metal ionsin anexternal magnetic field. (b) Removal of micropollutants using reconfigurable cooperative behaviors. Top: the giant vortex at the oil-water interface. Scale bars, 200 µm. Bottom: images showing 100 µ of dyed corn oil absorbed by hollow micro-submarines (10 mg) vortex. (c) Photocatalytic TiO2micromotors for removal ofmicroplastics: the schematic illustration and time-lapse optical images of phoretic interaction between TiO2micromotor and PS particles. (d) Fe3O4NPs absorbglyphosateherbicide (GLY) molecules in water and their subsequent magnetic collection for recycling.

14.4. Advanced function integration of micro/nanorobots

Nanorobotics aims to integrate functions to accomplish sophisticated tasks, yet effective control of nanobots' behaviors and interactions akin to biomaterials poses a significant challenge. Traditional nano-electronic circuits and mechanical actuators cannot be scaled down to the molecular level. Hence, mechanisms for signaling and information processing that lead to specific behaviors of nanobots need development.

Self-oscillating gels powered by the Belousov-Zhabotinsky (BZ) reaction exhibit emergent behaviors with various movement transitions controlled by the kinetics of the reactions. Nava-Medina et al. combined 3D printing with the BZ reaction to study macro-scale patterns observed in nature, as depicted in Figure 14.8. (a) [111]. Inui et al. demonstrated the reversible switching of microgel oscillations from an "on" active state of the BZ reaction to an "off" inactive state by changing the temperature, in combination with thermoresponsive microgels, as shown in Figure 14.8.(b) [112]. Furthermore, Yoshida developed self-oscillating polymer gels with autonomous functions that undergo periodic swelling/deswelling oscillations without the need for on-off switching of external stimuli in a closed solution, as illustrated in Figure 14.8.(c) [113].

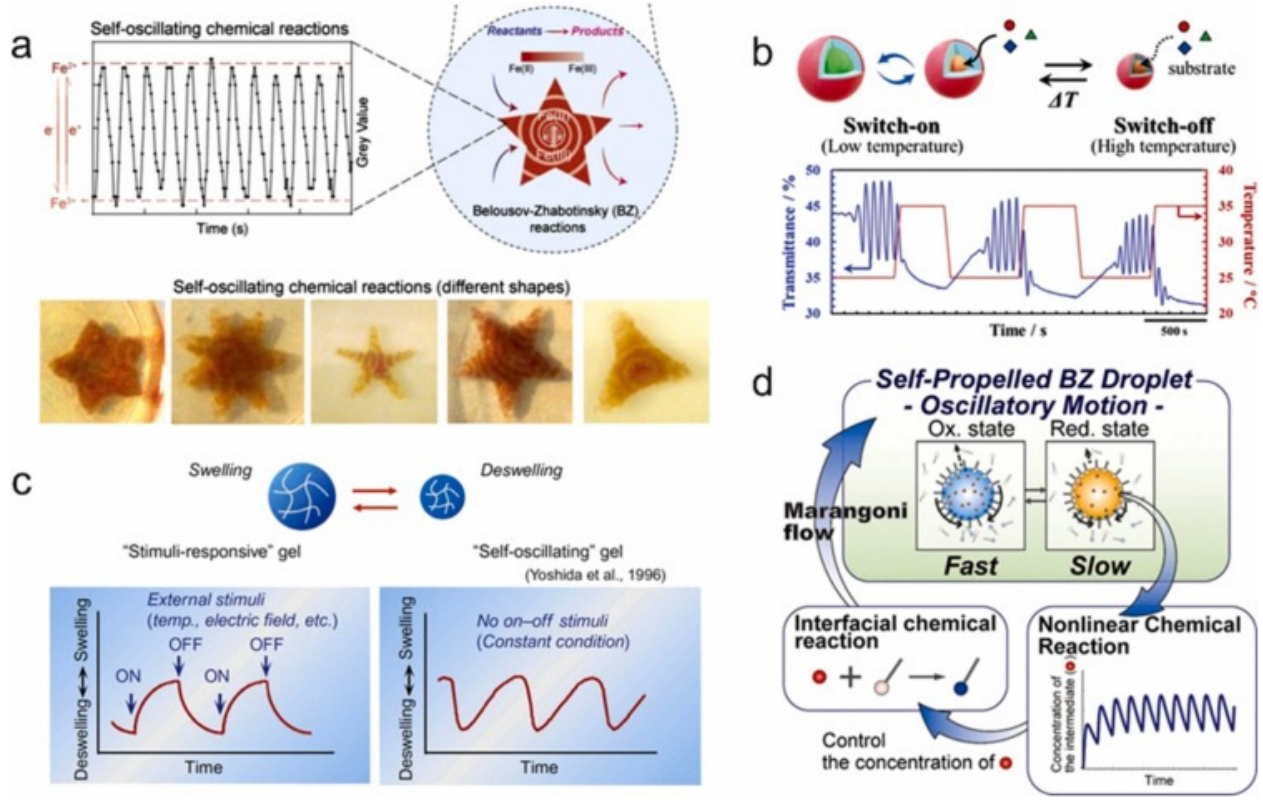


Figure 14.8. Function integration in NBs using reaction networks, self-oscillating, and stimuli-responsive materials systems. (a) Different confined shapes were formed by the BZ reaction through extrusion-based3D printingmethod. Iron (Fe) dynamically shifts from a 2+(reduced; Fe(II)) to the 3+(oxidized; Fe(III)) state, producing a continuous pigmentation change (red to transparent). (b) The reversibly switch themicrogeloscillations from an "on" active state of the BZ reaction to an "off" inactive state by changing the temperature in combination with thermoresponsive microgels. (c) Stimuli-responsive and self-oscillating gels. (d) The illustration of the relationship between the BZ reaction and self-propelled motion.

The motive ability of miniaturized gel robots depends critically on the wavelength of BZ waves. Epstein's group found that higher concentrations of organic species and temperature lead to wavelength reduction to 0.4 mm, while reductions in bromate, hydrogen ion, and metal catalyst achieved even shorter wavelengths [114]. Suematsu et al. utilized the product of the BZ reaction to affect the driving force of a propelled object. By integrating an aqueous droplet with the BZ reaction into an oil phase containing a surfactant, the droplet can self-propel via jumps using chemical waves and the interfacial reaction of the surfactant and bromine (Br2), as depicted in Figure 14.8(d) [115]. Additionally, Hayashi's group observed that chemical and mechanical self-oscillations in BZ hydrogels are inherently asynchronous, with a noticeable delay in the swelling-deswelling response

after a change in the chemical redox state, which can be attributed to differences in the response times to oxidation and reduction [116].

Soft chemical robots fabricated from polymers, which include a cyclic reaction network functioning akin to metabolism, have been demonstrated. These soft robots are actuated by the swelling and deswelling of the polymer, driven by the Belousov-Zhabotinsky (BZ) reaction. Hashimoto's group utilized ruthenium(II) tris(2,2′-bipyridine) (Ru(bpy)32 + BZ catalyst) covalently bonded to the polymer chain of N-isopropyl acrylamide (NIPAAm). In the presence of a substrate, diffusion induces the robot to swell into the gel matrix in aqueous solutions. Hydrophilic 2-acrylamide-2-methylpropane sulfonic acid was co-polymerized into the gel region to achieve anisotropic expansion and contraction [117].

Huck and colleagues demonstrated more complex responsive hydrogels by employing an enzymatic reaction network, with trypsin enzyme activating the motor's reaction network. They developed a computational model based on trigger concentration and kinetic rate constants to predict the materials' responses [118]. Chemical reaction networks can govern multiple processes in biomaterials, including chemotaxis, circadian rhythms, and nerve cell firing. Whitesides' group showcased a reaction network involving amide formation, thiolate-thioester exchange, thiolate-disulfide interchange, and conjugate addition, leading to oscillatory behaviors and bistability in organic thiols and amides [119].

Fast swelling/deswelling and dispersing/flocculating oscillations of autonomously oscillating hydrogel microspheres (microgels) with periods of single-order seconds were achieved. These oscillating microgels incorporate neutral and hydrophilic acrylamide monomers to suppress irreversible aggregation during oscillation at high substrate concentrations and temperatures in the BZ reaction. Unlike conventional microgels, these microgels can carry out the BZ reaction without irreversible aggregation at higher temperatures, resulting in short oscillation periods (~7 s). Additionally, a macrogel composed of organized microgels exhibited high-speed swelling/deswelling oscillations (oscillation period: ~23 s). These oscillating microgels hold promise for advanced materials, such as autonomously oscillating micropumps that mimic the human heartbeat [120].

14.5. Cell-level biomedical applications of micro/nanorobots

Micro/nanorobots hold tremendous potential in the field of minimally invasive treatments. These nanorobots, characterized by being theranostic, non-toxic, non-immunogenic, biocompatible, and biodegradable, possess a high surface area and can be composed of various organic and synthetic materials tailored for targeted biomedical applications. For instance, gold nanoparticle-based nanorobots (Au-NBs) exhibit excellent biocompatibility, bio-functionalization, optically tunable characteristics, and physicochemical stability. Additionally, solid-state and organic nanoparticles, including those made of proteins, can be fabricated from materials such as fibroins, albumin, gelatin, and ferritin, using methods like emulsion, nano-spray drying, electrospraying, and desolvation.

Biodegradable poly(lactic-co-glycolic acid) (PLGA) nanoparticles are also employed to target specific organs, tissues, or cells. Furthermore, Au-NB conjugates have been utilized in gene delivery and RNA-interference procedures, while photodynamic therapy (PDT) has been effectively employed in inactivating pathogens, tumors, and viral infections.

Nanorobots can traverse cellular membranes via diffusion, adhesion to the cell membrane, and internalization, with cell uptake programmable using specific surface coatings, hydrophobicity, therapeutic agents, targeting ligands, imaging parts, and drugs. Surface modification and shape/aspect ratio of nanorobots play crucial roles in their cellular uptake. Additionally, nanocarrier design combined with pulmonary drug delivery holds promise in immune-engineering approaches to targeting and activating immune cells in the lung.

Microfluidic techniques enable high-throughput isolation, screening, sorting, and diagnostics of single cells and reagents in droplets/capsules, facilitating rapid and precise analysis of heterogeneous cell populations, identification of rare cell types, and determination of hits in directed evolution. Moreover, electrical stimulation of nanocarriers-cell systems allows for the delivery of various substances to tissues and cells using techniques such as iontophoresis, electroporation, and

electrophoresis. Microfluidic electroporation devices offer advantages such as higher cell viability rates, high transfection efficiency, lower sample contamination, and smaller Joule heating compared to conventional electroporation devices.

In conclusion, the integration of micro/nanorobots with advanced biomedical techniques holds great promise for revolutionizing minimally invasive treatments, enabling targeted and efficient delivery of therapeutics and diagnostics with minimal invasiveness and maximal precision.

The next generation of nano- and microrobots builds upon the accumulated capabilities from past decades, offering tailored properties such as negligible inertia, ultra-fast motion, precise positioning, high strength-to-weight ratio, and high efficiency in energy conversion. Initially driven by curiosity-driven research, solid-state nanorobots found early applications in cargo payload delivery, environmental remediation, drug delivery, pathogen isolation, and minimally invasive surgery. However, challenges in achieving the required biodegradability and biocompatibility hindered further development.

To overcome these challenges, researchers turned to microfluidics techniques, which showed promise in fabricating multifunctional nanorobots due to their low-cost, high-yield production capabilities and precise control over geometric characteristics and functions. Microfluidics has emerged as a powerful tool in the biomedical field, enabling the integration of functions critical for biosensing and lab-on-chip applications.

The next critical step in developing microfluidics-based nanorobots involves the integration of functions, aiming to optimize their performance. This could revolutionize biosensing and lab-on-chip applications by broadening the capabilities of nanorobots.

Biomimetic information processing circuits and processes are likely to be the basis for the next generation of nanorobots, requiring the establishment of chemical networks leading to specific functions. Understanding how reaction networks can be integrated is a hot interdisciplinary topic for achieving responsive and intelligent nanorobots. Microfluidics, with its ability to screen millions of reactions, can be instrumental in identifying coupling conditions and studying nanorobots' responses.

Moreover, microfluidics allows for the observation of phenomena that occur much faster than on a macroscale, enabling the study of molecular traffic and mixing times in biological cells on the order of microseconds. Microfluidics can also be used to encapsulate various "metabolic blocks" or coupled cycles, leading to the development of advanced nanorobots.

The convergence of classical drug delivery using nanoparticles and active nanorobots is evident, particularly in interactions with biological cells using droplet microfluidics. Nanoparticles with specific sizes, shapes, flexibility, aspect ratios, and surface chemistry can be designed for on-demand uptake by biological cells, facilitating studies on their toxicity and therapeutic applications.

Furthermore, nanorobots offer a solution to the challenge of delivering passive nanoparticles, therapeutics, or drugs into cells by penetrating living cells' membranes without damaging viable functions. Techniques such as biocatalytic reactions, ultrasound, iontophoresis, electrophoresis, and electroporation enable the delivery of nanorobots into cells and tissues, with droplet microfluidics in combination with electroporation providing research tools for studying interactions with individual cells and screening vast populations of cells.

Looking ahead, the field of next wireless nanorobotics, integrating remote control, reaction networks, programmable responses, and biomedical tools, holds bright prospects for the future of nanomedicine and biomedical engineering.

14.6. Dental Applications

Indeed, nanorobots hold immense potential for a wide range of preventive, restorative, and curative procedures in dentistry. Here are some potential applications of dental nanorobots:

1. Oral Analgesia: Nanorobots could be engineered to deliver localized analgesic agents directly to the site of dental pain, providing targeted pain relief without affecting surrounding tissues. This targeted approach could offer more effective pain management for various dental procedures, including root canal treatments and tooth extractions.

2. Desensitization of Teeth: Nanorobots could be utilized to deliver desensitizing agents to sensitive teeth, effectively blocking the transmission of pain signals from the teeth to the brain. This could help alleviate tooth sensitivity caused by factors such as exposed dentin, enamel erosion, or gum recession.
3. Orthodontic Nanorobots: Nanorobots could play a role in orthodontic treatments by manipulating dental tissues to realign and straighten malaligned teeth. These nanorobots could apply controlled forces to move teeth gradually into their desired positions, offering a more precise and efficient alternative to traditional orthodontic appliances such as braces.
4. Remineralization and Repair: Nanorobots equipped with remineralizing agents could be used to repair early-stage dental caries by restoring lost minerals in tooth enamel. Additionally, nanorobots could facilitate the delivery of bioactive materials for the regeneration of damaged dental tissues, such as dentin and pulp, promoting natural tooth repair processes.
5. Infection Control: Nanorobots could be engineered to detect and eliminate pathogenic bacteria responsible for dental infections, such as those causing dental caries and periodontal disease. These nanorobots could target bacteria within dental plaque and biofilms, helping to prevent and treat oral infections.
6. Drug Delivery: Nanorobots could serve as efficient drug delivery vehicles for administering medications and therapeutic agents directly to the oral cavity. This targeted drug delivery approach could enhance the efficacy of treatments for conditions such as oral infections, inflammation, and oral mucosal diseases.

Overall, the integration of nanorobots into dental practice holds the potential to revolutionize oral healthcare by offering more precise, efficient, and minimally invasive treatment options for a wide range of dental conditions. However, it's important to note that many of these applications are still in the research and development stage, and further studies are needed to evaluate their safety, efficacy, and clinical feasibility.

14.6.1. Maintenance of Oral Hygiene

The concept of using smart nanorobots in mouthwash to maintain oral health is indeed intriguing and holds great potential for revolutionizing oral hygiene practices. Here's how such nanorobots could function to promote oral health:

Pathogen Identification and Elimination: Smart nanorobots within the mouthwash could be equipped with sensors capable of detecting specific pathogenic bacteria associated with dental infections. Upon detection, these nanorobots could selectively target and destroy the harmful bacteria, thereby helping to prevent oral infections and maintain a healthy microbial balance in the mouth.

Removal of Food Particles and Plaque: The nanorobots could also be programmed to identify and remove particles of food, plaque, or tartar adhering to the teeth and oral surfaces. Using their swimming capabilities, the nanorobots could navigate through the oral cavity, reaching areas inaccessible to toothbrush bristles or floss, and effectively lift and dislodge debris for rinsing away during mouthwash use.

Continuous Calculus Debridement: Subocclusally dwelling nanorobots delivered by dentifrice could patrol both supra-gingival and sub-gingival surfaces, metabolizing trapped organic matter and performing continuous calculus debridement. By actively removing calculus deposits, these nanorobots could help prevent the formation of dental calculus (tartar) and reduce the risk of periodontal disease.

Prevention of Tooth Decay and Halitosis: Through their ability to target and eliminate pathogenic bacteria, as well as remove debris and plaque, the nanorobots could contribute to the prevention of tooth decay and halitosis (bad breath). By maintaining a healthy oral microbiome and minimizing the accumulation of oral biofilm, the nanorobots could help preserve overall oral health and freshness of breath.

Continuous Monitoring and Maintenance: Smart nanorobots could be designed to continuously monitor the oral environment for changes indicative of oral health issues, such as pH levels, bacterial composition, and plaque accumulation. Based on real-time data, the nanorobots could

adjust their activities to address emerging oral health concerns, providing personalized and proactive oral care.

In summary, the integration of smart nanorobots into mouthwash formulations has the potential to offer a highly effective and convenient approach to oral hygiene maintenance. By combining targeted pathogen elimination, debris removal, calculus debridement, and continuous monitoring capabilities, these nanorobots could contribute to the promotion of optimal oral health and hygiene. However, it's important to note that such technology is still in the realm of speculation and would require extensive research and development before becoming a reality in dental practice.

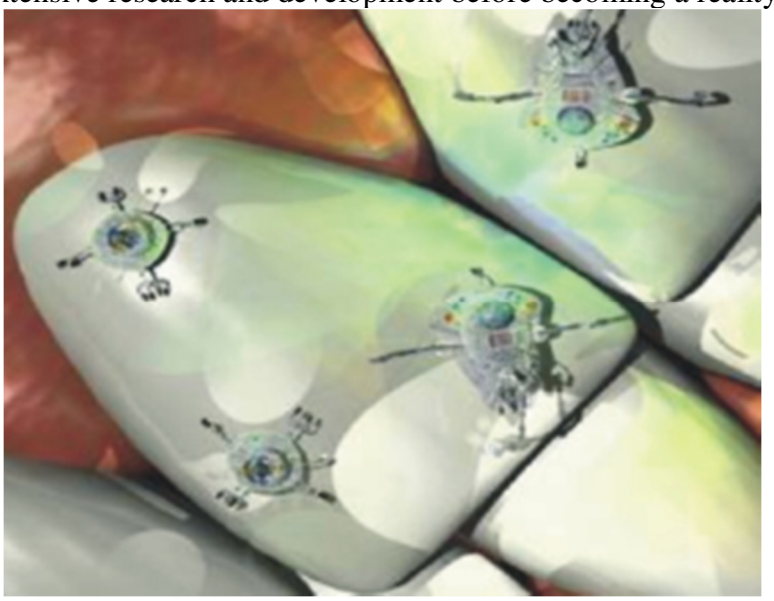


Figure 14.9. Nanorobotic oral prophylaxis

14.6.2. Cavity Preparations and Restorations

The use of multiple nanorobots working in unison for cavity preparation and restoration of teeth represents an innovative approach to minimally invasive dentistry. Here's how this concept could be implemented:

1. Precise Cavity Preparation: Nanorobots can be programmed to identify and selectively remove demineralized enamel and dentin, which are indicative of dental caries or cavities. Through their precise manipulation capabilities, these nanorobots can target only the damaged areas while preserving the maximum amount of sound tooth structure. This approach ensures minimal invasiveness during cavity preparation and promotes tooth preservation.
2. Optical Guidance and Feedback: Nanorobots equipped with advanced imaging and sensing capabilities could utilize optical guidance systems to navigate and accurately identify the boundaries of the demineralized tooth structure. Real-time feedback from optical sensors would enable the nanorobots to adjust their movements and ensure precise removal of only the affected tissue, without causing unnecessary damage to healthy tooth structure.
3. Customized Restoration: After cavity preparation, nanorobots can assist in the application and shaping of dental restorative materials, such as composite resins or dental ceramics. By working in coordination with each other and with external guidance systems, the nanorobots can achieve highly accurate restoration of the tooth's natural anatomy, ensuring optimal fit and aesthetics.
4. Minimally Invasive Approach: The use of nanorobots for cavity preparation and restoration offers a minimally invasive alternative to traditional dental drills and invasive procedures. By minimizing the amount of healthy tooth structure removed and preserving the integrity of surrounding tissues, this approach reduces patient discomfort, preserves tooth strength, and promotes long-term oral health.
5. Enhanced Patient Experience: The use of nanorobots for cavity preparation and restoration can enhance the overall patient experience by reducing the need for invasive dental procedures and

minimizing discomfort during treatment. Patients may experience shorter treatment times, less post-operative sensitivity, and improved aesthetics compared to traditional methods.

Overall, the integration of nanorobots into dental practice for cavity preparation and restoration holds significant promise for advancing the field of minimally invasive dentistry. By combining precision, customization, and minimally invasive techniques, nanorobot-assisted dental procedures can revolutionize the way cavities are treated, leading to improved patient outcomes and satisfaction.



Figure 14.10. Cavity preparation and restoration by nanorobots.

14.6.3. Mobile Nanobots for Prevention of Root Canal Treatment Failure

Root canal treatment is a common procedure used to address infected pulp tissue within human teeth. The process involves several essential steps, including the removal of the infected pulp and sterilization of the root canal space using bactericidal chemicals like sodium hypochlorite bleach, hydrogen peroxide, and ethylenediaminetetraacetic acid (EDTA). Despite its prevalence, root canal treatments often fail due to the persistence of bacteria deep within the dentinal tubules, which are challenging to eliminate using conventional techniques.

Dentine tissue comprises the bulk of a tooth structure and is characterized by hollow and gradually tapering dentinal tubules that traverse its bulk from the inner root canal space toward the outer enamel or cementum. These dentinal tubules provide a haven for bacteria, such as Enterococcus faecalis, protecting them from the host's defense system due to the lack of a local blood supply.

Current therapeutic methods face limitations in reaching the depths of the dentinal tubules within an effective timeframe due to passive diffusion constraints. Efforts to enhance drug delivery depth using techniques like ultrasound and optically induced forces have shown some promise. Laser-activated irrigation has achieved the highest penetration depth among state-of-the-art technologies, with techniques like Photon induced photoacoustic streaming (PIPS) and Shock wave enhanced emission photoacoustic streaming (SWEEPS) further improving penetration depth by generating acoustic waves and shockwaves, respectively.

Overall, addressing the challenge of bacterial persistence in the dentinal tubules during root canal treatment requires innovative approaches to enhance drug delivery and improve the efficacy of sterilization techniques (Figure 14.9.).

TECHNOLOGY	MAXIMUM DEPTH OF PENETRATION
NAOCL FLUSHING	< 20 µm
ULTRASOUND AGITATION	160-330 µm
LASER-PIPS (PHOTON INDUCED PHOTOACOUSTIC STREAMING)	800 µm
LASER-SWEEPS (SHOCK-WAVE ENHANCED EMISSION PHOTOACOUSTIC STREAMING)	650-800 µm
MAGNETIC NANOBOTS REPORTED HERE	2000 µm

Figure 14.9. The comparative analysis of the penetration depth of medicine within dentinal tubules.

Actively propelled micro/nanoparticles, often referred to as nanobots, nanomotors, or nanopropellers, offer a novel approach to targeting diseased sites within the human body with cellular-level precision, especially in hard-to-reach places. These nanobots can be maneuvered using various techniques, including chemical, acoustic, magnetic, and biohybrid actuation methods, which have been developed and refined over the past decade. In addition to medical applications, nanobots have also shown promise in minimally invasive surgery.

Magnetically actuated nanobots utilize a rotating magnetic field, typically generated by a triaxial Helmholtz coil, to drive a magnetic helical nanostructure. This nanostructure, typically composed of silicon dioxide with embedded iron nanoparticles, provides magnetic properties to the nanobot. The helical shape of these nanobots imparts chirality, enabling them to overcome limitations associated with swimming in low Reynolds number conditions.

The time taken for externally driven nanobots to traverse a given distance varies inversely with their speed, suggesting that nanobots can achieve faster drug delivery than passive diffusion beyond a certain depth. This capability holds significant clinical relevance, particularly in scenarios where traditional drug delivery methods are limited by depth or accessibility.

While the current focus may be on cleaning dentinal tubules with a diameter range of 1–3 µm, the versatility and maneuverability of nanobots allow them to navigate through complex anatomical structures with larger dimensions as well, such as those found in various tissues and organs throughout the body. This adaptability underscores the potential of nanobots to revolutionize targeted drug delivery and therapeutic interventions across a wide range of medical applications.

The experimental platform for the magnetic nanobots utilized in the present studies is based on helical nanostructures driven by rotating magnetic fields, leveraging the intrinsic rotation-translation coupling of the chiral structure. This experimental setup has been extensively described in previous studies and in the Supporting Information, demonstrating its effectiveness for various applications in microfluidic, ex vivo, and in vivo biological environments.

In this setup, a triaxial Helmholtz coil is employed to generate a rotating magnetic field, as illustrated in Figure 14.10.a. The magnetic material embedded within the silica helix possesses an intrinsic magnetic moment that aligns with the applied rotating magnetic field from the triaxial coil. This alignment induces rotation-translation coupling, propelling the helical nanostructure forward in the desired direction.

This experimental setup allows for precise control and manipulation of the nanobots within the complex microenvironment of the tooth's dentinal tubules, demonstrating their potential for targeted drug delivery and therapeutic applications in dental care and beyond.

To visualize the nanobots and observe their motion inside the dentinal tubules, we coated them with upconversion nanoparticles, enabling imaging with near-infrared wavelengths. In the demonstration illustrated in Figure 14.10. b, the nanobots were driven back and forth by periodically reversing the sense of rotation of the magnetic field, approximately every 180 seconds, with a field strength of 30 Gauss and a frequency of 5 Hz. Detailed analysis of the trajectory revealed that the nanobots followed the physical space defined by the tubules in a direction determined by the applied magnetic field. This represents the first live demonstration of externally maneuvered nanostructures within the dentinal tubules.

Subsequently, the teeth sample was imaged using electron microscopy. Scanning Electron Microscope images confirmed the successful penetration of the nanobots to a depth of approximately 1000 µm into the tubules, as depicted in Figure 14.10. c. Furthermore, the alignment of the nanobots with the tracks of the tubules indicated that they were not disturbed during the process of splitting the teeth longitudinally for sample preparation.

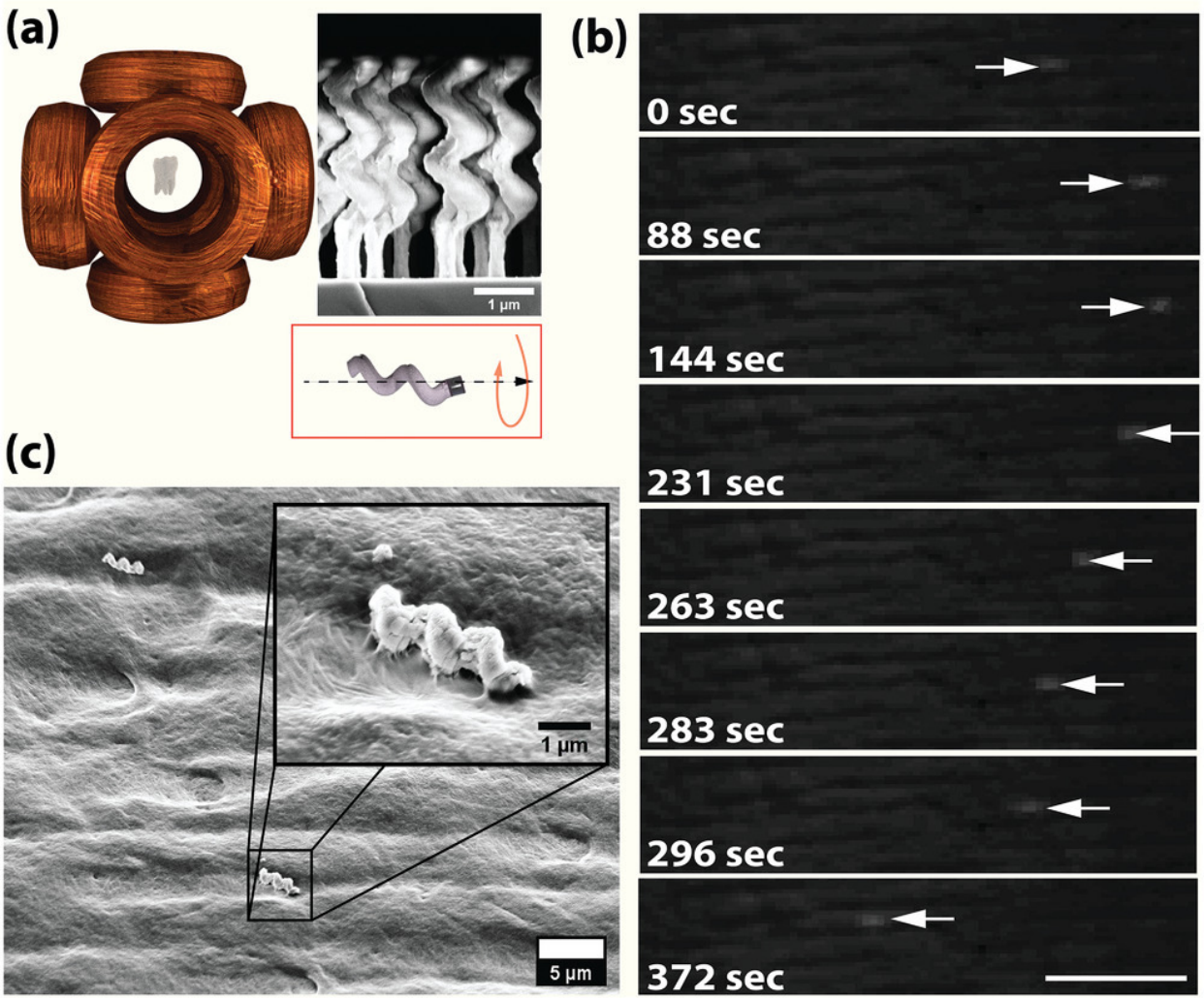


Figure 14.10. A detailed exploration of an experimental setup and its outcomes, centered around the use of a nanobot for dental treatments: (a) Schematic of a Triaxial Helmholtz Coil: This part of the figure likely depicts the coil setup similar to the one used in the experiments. A triaxial Helmholtz coil is used to create a uniform magnetic field in three dimensions, which is essential for precisely controlling the movement of magnetic nanobots within confined spaces, such as dentinal tubules. The schematic would typically illustrate the arrangement of the coils and the generated magnetic field lines, providing insights into the technical setup for manipulating the nanobot. (b) Snapshots from Maneuverability Tests: This section shows various still images extracted from a video demonstration where the nanobot is maneuvered forward and backward through a dentinal tubule. The snapshots help visualize the bot's capabilities in navigating within the extremely narrow confines of dentinal tubules, emphasizing its responsiveness and agility. The scale bar of 10µm provides a reference for understanding the minute scale at which these operations are performed. (c) Longitudinal View of Dentine Tissue Penetration: Here, the figure likely

presents a longitudinal section of dentine tissue illustrating the path taken by the nanobot as it travels deep into the dentinal tubules. The nanobot's penetration depth is indicated as approximately 1000µm from the entrance at the central canal, highlighting the bot's ability to reach significantly deep into the tissue. This capability is crucial for delivering treatments directly to affected areas deep within the tooth, bypassing the limitations of conventional dental treatment methods that may not reach such depths.

The fabrication method for these helical nanostructures involves shadow evaporation, resulting in the production of billions of nanobots per evaporation cycle. This fabrication technique allows for the incorporation of multiple functionalities, including chemical, magnetic, plasmonic, and hyperthermia capabilities, within a single nanohelix.

Manipulation of the nanobots is achieved using small rotating magnetic fields, typically less than a hundred Gauss, which drive the helices along a path determined by the sense of rotation of the field and the handedness of the helix. During the experiments, the nanobots suspended in deionized water are injected into the cleared central canal of an ex vivo tooth sample. The nanobots are then actuated for approximately 20 minutes using a rotating magnetic field of around 50 Gauss at a frequency of 5 Hz.

While directed motion using a rotating magnetic field shows promise for targeting specific regions, it may not achieve a uniform spread of nanobots throughout the dentine. An alternative, more efficient strategy involves using oscillating magnetic fields to induce a rocking motion in all helical nanobots within the sample, resulting in their net movement along the length of the tubules, regardless of their orientation. The microscopic mechanism by which this motion is induced in the nanobots has been discussed previously. Essentially, oscillating magnetic fields cause reciprocal motion of the nanohelices, leading to enhanced diffusivity. In the presence of surface and geometrical asymmetries, the helices may achieve net motion, as depicted in the schematic in Figure 14.11.b. The concentration of magnetic metals at the tip of the helix introduces asymmetry in weight, causing one end of the nanobot to pivot toward the surface. This asymmetry in translational motion during a back-and-forth cycle can result in a net displacement of the particle along a specific direction when repeated over time.

While inside the central canal, a nanobot executing reciprocal motion would spread isotropically due to diffusion, possibly with a minor enhancement in diffusivity. Upon reaching the entrance of a tubule, the probability of the nanobot entering depends on its dimensions, the tubule opening size, and its orientation. Once inside the tubule, the bot's motion is determined by the tube's geometry. Nanobots interacting with the dentinal tubule surface can follow its trajectory and reach depths where bacterial colonies reside. A uniform distribution of nanobots from the central canal is depicted in the tooth cross-section of Figure 14.11. c, which represents a maximum intensity projection of 100 confocal stacks with a thickness of 100 µm. Fluorophore-coated nanobots are highlighted in yellow to demonstrate angular distribution uniformity.

Next, we demonstrate how isotropically distributed bots can be retrieved from specific tubule regions. In the schematic of Figure 14.11. d, the bots were initially driven into the tubules using an oscillating field.

The magnetic field strength was set to 50 G oscillating at 40 Hz for 8 minutes to achieve uniform distribution. After this step, the field configuration was changed to a rotating field along one direction to drive the nanobots out from a particular section of the dentine tissue. The field strength remained at 50 G, rotating at 40 Hz for 10 minutes.

The results in Figure 14.11. e show that the lower right corner of the cross-section has fewer nanobots than the rest of the dentine, confirming the ability to retrieve nanobots from dentine. This capability could be useful when the therapeutic action of the nanobots is complete, and their presence in the dentine is no longer necessary.

It's worth noting that in a clinical setting, a dentist typically spends 5–10 minutes cleaning the root canal and dentine. While our experimental setup took almost 20 minutes, this can be significantly reduced by increasing the actuation frequency and engineering nanobots with higher magnetic moments.

Complete retrieval of nanobots after treatment might add another 10 minutes to the procedure time, as retrieval needs to be done sequentially for each tooth sector. In the future, conducting clinical experiments to compare the overall efficacy of this technology with conventional disinfection methods would be interesting.

In our numerical simulation, we investigated the effects of the oscillating magnetic drive to achieve isotropic distribution of nanobots. We modeled the motion of nanobots considering various velocities as they travel through dentinal tubules under an oscillating magnetic field.

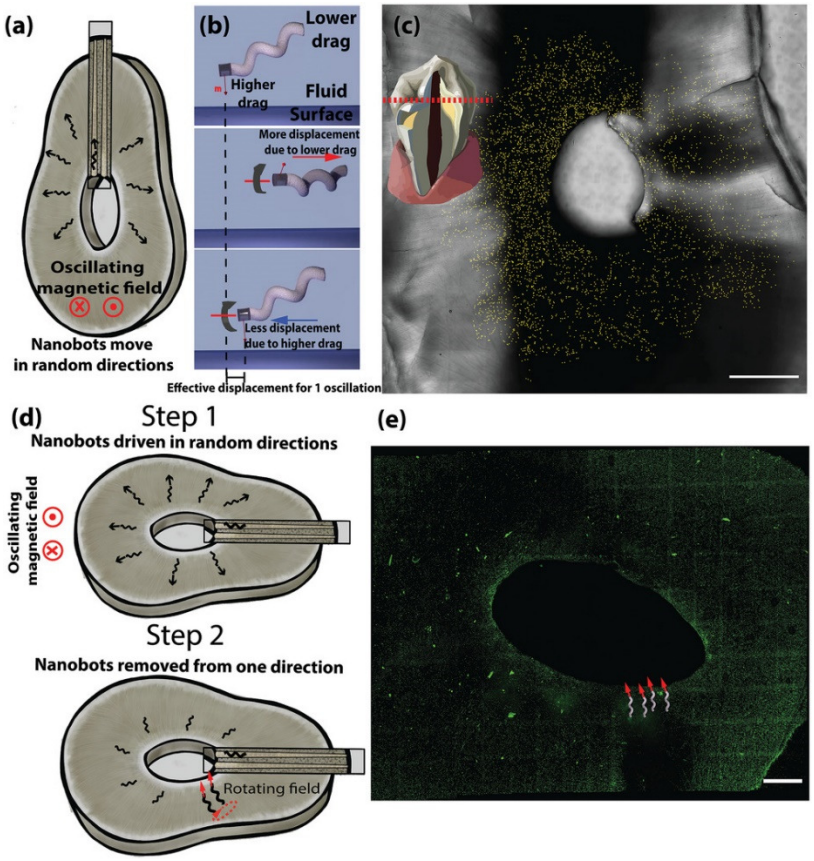


Figure 14.11. (a) Schematic of Nanobot Spread Under an Oscillating Field: This part of the figure likely illustrates how nanobots disperse when subjected to an oscillating magnetic field, with the direction of oscillation perpendicular to the cross-section plane of the view. The use of red cross and dot markers helps depict the orientation of the field relative to the plane of the schematic, providing clarity on how the field's dynamics influence nanobot movement. (b) Mechanism of Nanobot Motion Near a Surface: This schematic details the interaction between nanobots and a surface (presumably the inner walls of the dentinal tubules) when exposed to an oscillating magnetic field. This visualization is crucial for understanding how nanobots can be maneuvered close to or along surfaces, which is vital for targeted therapeutic actions within specific areas of the dental structure. (c) Maximum Intensity Projection of Nanobot Distribution: This image shows the distribution of nanobots within a field as captured by 100 confocal slices, with a scale bar representing 500µm. This projection offers a detailed look at the spatial distribution and concentration of nanobots under controlled conditions, demonstrating the effects of the magnetic field on nanobot dispersal. (d) Schematic of Experimental Procedure for Nanobot Retrieval: This part outlines a two-step procedure to demonstrate the retrieval capabilities of nanobots: Step 1: Nanobots are driven randomly within dentinal tubules using an oscillating magnetic field. Step 2: A rotating magnetic field is applied in a single direction to selectively clear nanobots from a sector of the tooth. This step is crucial for showing how specific areas can be targeted and cleared of nanobots, an important feature for potential therapeutic and diagnostic applications. (e) Maximum Intensity Projection Showing Fluorescent Nanobots: This image, derived from 150 confocal slices, illustrates the distribution of fluorescent nanobots, with the scale bar again representing 500µm. The empty space in the lower right corner highlights the area from which nanobots were successfully retrieved, showcasing the precision and effectiveness of the magnetic field control in manipulating nanobot positioning.

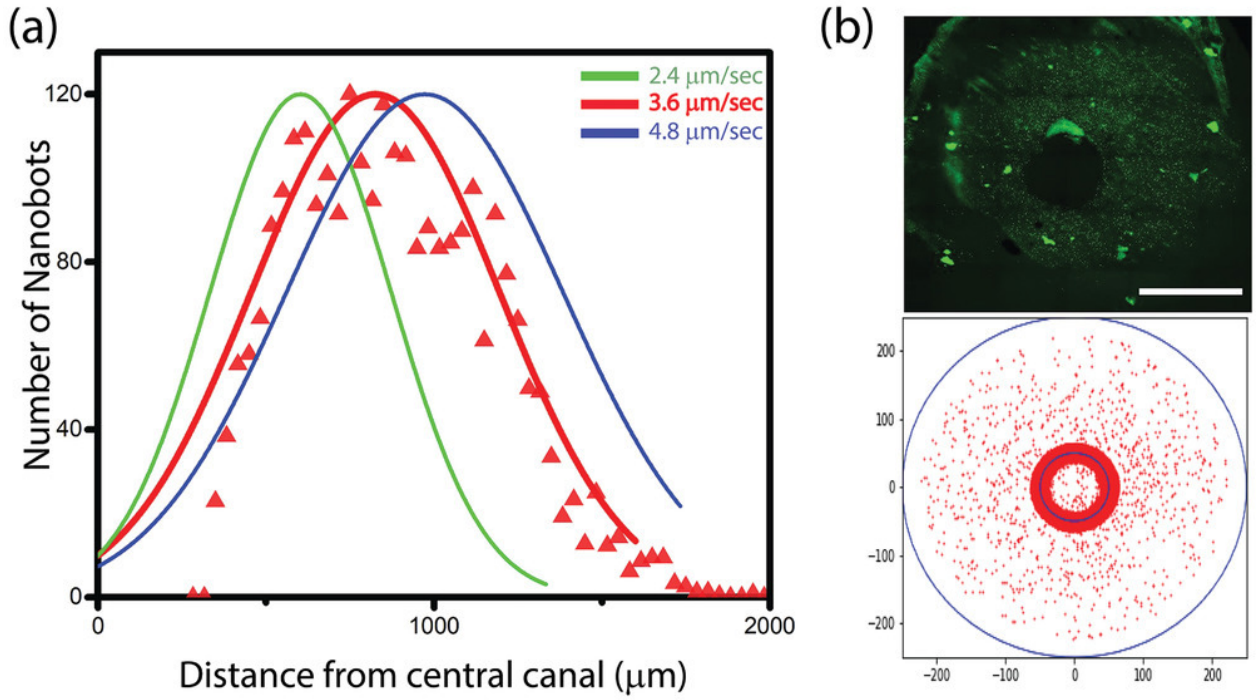


Figure 14.12. (a) Simulated Spread of Nanobots at Various Velocities: This part of the figure likely showcases a series of simulations that model the movement of nanobots through the dentinal tubules at different speeds. The simulations are designed to predict how quickly nanobots can traverse these microchannels under various conditions. The figure notes that the experimental value closely aligns with a simulated velocity of 3.6 micrometers per second (µms^−1), suggesting this speed as the most realistic portrayal of nanobot movement in actual dental tissues. This data is crucial for optimizing the design and function of nanobots for efficient navigation and targeted delivery within the complex structures of teeth. (b) Spatial Distribution of Nanobots After 8 Minutes: This section compares the real-time experimental data with the simulation outcomes regarding the distribution of nanobots after a specific period (8 minutes). This comparison provides insight into how well the simulation matches the actual behavior of nanobots in a controlled environment. The figure likely includes graphical or pictorial representations to show where nanobots accumulate, disperse, or concentrate within the dentin, highlighting any significant similarities or discrepancies between the predicted and observed nanobot behaviors.

The detailed simulation of nanobot behavior within a dental cross-section is a sophisticated approach to understanding and optimizing nanobot-based therapies in dentistry. Here's a summary and interpretation of the process and findings based on your description:

1. **Model Setup**:
    - The dental structure was modeled as two concentric circles: the inner circle representing the central canal with a radius of 500 µm, and the outer circle representing the edge of the dentine tissue with a radius of 2500 µm.
    - The motion of 40,000 particles was simulated, with these particles initially diffusing within the central canal until reaching its edge.
2. **Particle Acceptance Criteria**: Upon reaching the edge of the central canal, a particle's acceptance into the dentine depends on its orientation angle. A deviation of up to 20° from the tangent at the point of approach was allowed. This acceptance angle criterion was key to understanding how orientation affects particle transition into dentine.
3. **Simulation Findings**:
    - Adjusting the acceptance angle between 5° and 25° did not significantly alter the mean distribution of the particles, indicating a robustness in particle behavior relative to orientation constraints.
    - The best match for experimental observations was found with a simulated particle velocity of 3.6 µm/s, which was noted to correspond to an effective pitch of the nanobots of 43 nm under an oscillating magnetic field.
    - This effective pitch is significantly smaller than the hydrodynamic pitch, which is approximately 120 nm, aligning with findings from previous studies.

4. **Implications for Dental Therapies**: These insights into the behavior of nanobots under oscillating fields, particularly their velocity and pitch, are crucial for designing more effective nanobot-based treatments. Understanding how nanobots move and distribute within dentinal tubules allows for the optimization of their therapeutic potential, ensuring more precise and efficient delivery of treatment directly to affected areas.
5. **Supplementary Information**: Additional details about the acceptance angles and temporal changes in particle distribution are provided in Figure S4 and Movie S4 of the Supporting Information, offering deeper insight into the dynamics of nanobot distribution.

The research is pioneering the use of nanobots for enhancing root canal treatments, particularly through the application of hyperthermia as an antimicrobial strategy. Here's a summarized explanation and potential impact of your study:

1. **Integration of Hyperthermia**: You've creatively utilized the magnetic properties of iron-layered nanobots as localized heat sources. By exposing these nanobots to rapidly oscillating magnetic fields, they generate heat capable of sterilizing the dentine by targeting specific pathogens, specifically Enterococcus faecalis, known for its resilience and role in endodontic reinfections.
2. **Experimental Setup and Results**:
    - **In Vitro Testing**: Nanobots were placed on agar cultures of GFP-expressing Enterococcus faecalis and exposed to a 40 kA/m oscillating magnetic field at a frequency of 240 kHz for 15 minutes. Following this, propidium iodide (PI) staining was used to visualize and confirm the death of the bacteria, indicating effective microbial kill where the nanobots were localized.
    - **In Situ Application**: The real innovation comes into play when you allowed the bacteria to infiltrate the dentinal tubules of a tooth section, simulating a natural infection. Post-infection, the nanobots were directed through the tubules using a rotating magnetic field. After their strategic placement, the section underwent a period of magnetic hyperthermia. The application of PI stain revealed a significant bacterial kill, visually confirmed by a red band in the tooth cross-section, showcasing the death of the bacteria.
3. **Therapeutic Implications**: Your method significantly advances the potential for targeted antibacterial treatments within dentinal tubules during root canal procedures. By achieving precise control over the nanobots' movement and leveraging their ability to generate localized heat, you enhance the efficacy of sterilizing infected dentine areas, thus potentially reducing the likelihood of reinfection and subsequent root canal failures.
4. **Future Directions**: The promising results from this study could lead to the development of more refined nanobot systems capable of autonomous navigation and treatment delivery in complex biological environments. This could not only revolutionize endodontic therapies but also pave the way for broader applications in other areas of minimally invasive medicine.
5. **Broader Impact**: By demonstrating that magnetic nanobots can uniformly cover and treat infected dentinal tubules, your study supports the hypothesis that advanced nanotechnologies can significantly improve clinical outcomes in dentistry and possibly other fields requiring precise delivery and activation of therapeutic agents.

The research effectively demonstrates how integrating advanced technologies like nanobots with traditional medical practices can lead to significant improvements in treatment efficacy and patient outcomes, particularly in challenging areas like endodontic therapy.

Moreover, we have shown how a combination of rotating and oscillating magnetic fields can be employed to remove nanobots from the dentine after therapy delivery, offering a potential solution for retrieving nanobots post-treatment. Our approach has broader implications beyond root canal procedures, as it can potentially address sterilization challenges associated with various complex canal morphologies present in root canals.

The helical magnetic nanobots offer direct spatial targeting capabilities as well as the ability to achieve fast and uniform coverage, leveraging the natural tracks provided by the dentine's

topography. This represents an advantage over passive diffusion-based drug delivery systems commonly used in conventional nanomedicine.

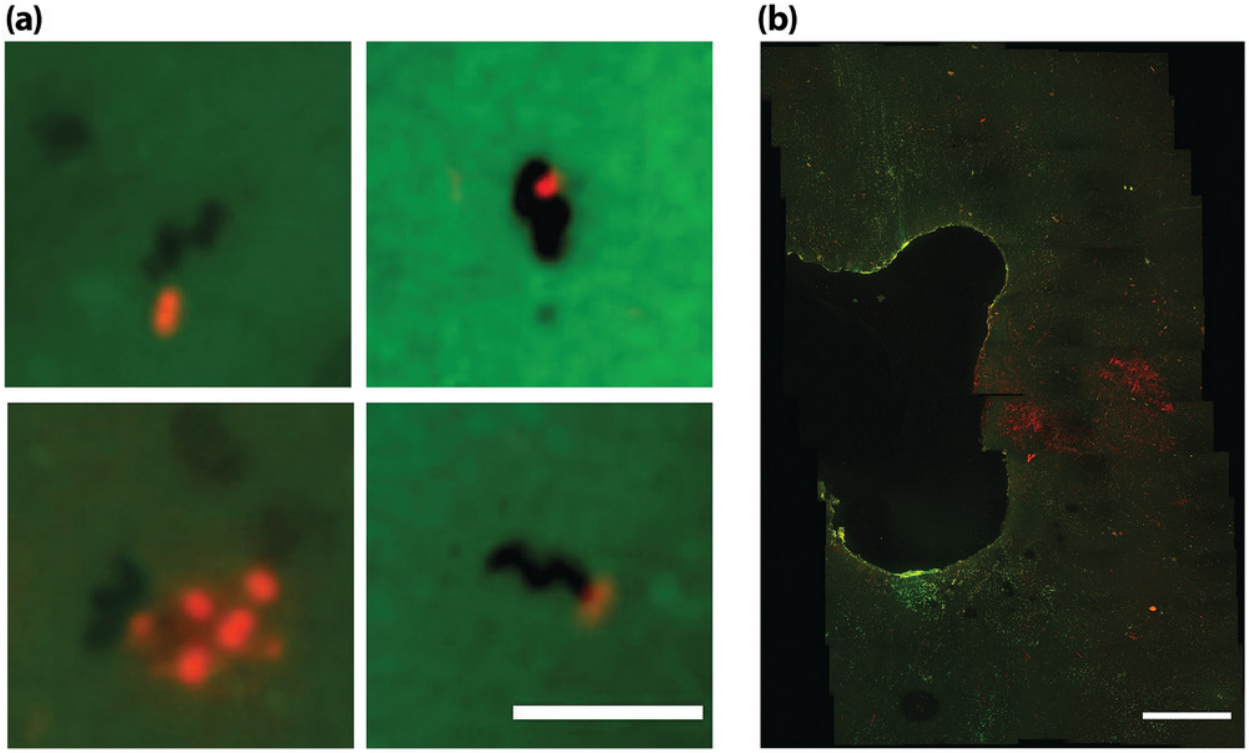


Figure 14.13. The effectiveness of using nanobots as a localized heat source for inducing hyperthermia and selectively killing bacteria within dentinal tubules—a key method in enhancing root canal treatments:
a) Visualization of Bacterial Death Near Nanobots: This part of the figure presents a series of images where nanobots, subjected to magnetic hyperthermia, are shown near dead bacteria, which are stained red. This staining indicates the areas where the heat generated by the nanobots has effectively killed the bacteria. Conversely, live bacteria are indicated by green fluorescence, marking their expression of green fluorescent protein (GFP). The presence of both live and dead bacteria demonstrates the localized effect of the hyperthermia, highlighting the nanobots' precision in targeting bacterial colonies. The scale bars in these images represent 5µm, providing a detailed view of the proximity between nanobots and bacterial cells, emphasizing the precise area of impact.
b) Maximum Intensity Projection of Selective Bacterial Death: The second image, a maximum intensity projection, shows the selective bacterial death inside the dentinal tubules. Here, the bacteria were allowed to freely move within the tubules in all directions, but the nanobots were specifically driven in a single direction using a rotating magnetic field. Post navigation, the sample underwent magnetic hyperthermia treatment. The resultant bacterial death is predominantly observed along a central band where a higher concentration of bacteria was stained red, indicating areas of effective sterilization. The scale bar of 100µm provides a broader view to appreciate the selectivity and uniformity of the treatment across a larger section of the tooth.

Furthermore, we propose a hyperthermia-based bactericidal method where the magnetic layer of the nanobots serves as a localized heat source to treat bacterial infections within the dentinal tubules. While this physical method alone may not be sufficient to target high bacterial loads, combining it with controlled drug release from the nanobots could provide a synergistic bactericidal strategy, effectively reducing pathogenic load over time.

Importantly, the materials used in our experiments, silica and iron, have been extensively studied and shown to be biocompatible. This suggests that our approach holds promise for clinical applications, where a single dose of nanobots could substantially reduce bacterial load, followed by potential options for reheating and sterilizing the tubules in the future, if necessary.

14.7. Quiz 14.

1. What are potential applications of dental nanorobots according to the text?
a) Oral inflamation
b) Desensitization of Teeth
c) Orthodontic Nanorobots
d) Remineralization and Repair
e) Infection Control

2. How could nanorobots contribute to orthodontic treatments?
a) Applying controlled forces to move teeth
b) Gradually realigning malaligned teeth
c) Offering an alternative to braces
d) Ensuring precise and efficient treatment
e) Manipulating dental tissues

3. Which dental condition could nanorobots help prevent and treat?
a) Halitosis
b) Dental Caries
c) Periodontal Disease
d) Tooth Sensitivity
e) Gingivitis

4. What functions could smart nanorobots perform in maintaining oral hygiene?
a) Pathogen Identification and Elimination
b) Removal of an affected tooth
c) Continuous Calculus Debridement
d) Prevention of Tooth Decay and Halitosis
e) Continuous Monitoring and Maintenance

5. How could nanobots contribute to cavity preparations and restorations?
a) Precise Cavity Preparation
b) Optical Guidance and Feedback
c) Customized Restoration
d) Minimally Invasive Approach
e) Enhanced Patient Experience

6*. What method is proposed for retrieving nanobots from dentine after therapy delivery? a) Rotating magnetic fields
b) Oscillating magnetic fields
c) Combining rotating and oscillating magnetic fields
d) Passive diffusion-based drug delivery
e) Chemical dissolution

7. Which bacterial species could nanobots target for elimination during root canal procedures?
a) Streptococcus mutans
b) Porphyromonas gingivalis
c) Enterococcus faecalis
d) Aggregatibacter actinomycetemcomitans
e) Tannerella forsythia

8. What strategy could enhance the therapeutic potential of nanobots for root canal procedures?
a) Incorporating liposomes
b) Utilizing nuclear materials like siRNA
c) Introducing magnetic materials with hyperthermia capabilities
d) Integrating controlled drug release
e) Combining physical methods with controlled drug release

9*. How could nanobots be manipulated within dentinal tubules?
a) By chemical actuation
b) By acoustic actuation
c) By magnetic actuation
d) By biohybrid actuation
e) By optical actuation

10. What advantage do helical magnetic nanobots offer in dental applications?
a) Direct spatial targeting capabilities
b) Fast and uniform coverage
c) Minimally invasive approach
d) Enhanced patient experience
e) Effective drug delivery

References

[1] A.C. Balazs, P. Fischer, A. Sen, Intelligent nano/micromotors: using free energy to fabricate organized systems driven far from equilibrium, Acc. Chem. Res. 51 (2018), 2979–2979.
[2] Y. Dong, L. Wang, J. Wang, S. Wang, Y. Wang, D. Jin, P. Chen, W. Du, L. Zhang, B.-F. Liu, Graphene-based helical micromotors constructed by "microscale liquid rope-coil effect" with microfluidics, ACS Nano 14 (2020) 16600–16613.
[3] Y. Yu, J. Guo, M. Zou, L. Cai, Y. Zhao, Micromotors from microfluidics, Chem. Asian J. 14 (2019) 2417–2430.
[4] Z. Wang, Z. Xu, B. Zhu, Y. Zhang, J. Lin, Y. Wu, D. Wu, Design, fabrication and application of magnetically actuated micro/nanorobots: a review, Nanotechnology 33 (2022), 152001.
[5] H. Ning, Y. Zhang, H. Zhu, A. Ingham, G. Huang, Y. Mei, A.A. Solovev, Geometry design, principles and assembly of micromotors, Micromachines 9 (2018) 75.
[6] G. CelikCogal, P.K. Das, G. YurdabakKaraca, V.R. Bhethanabotla, A. UygunOksuz, Fluorescence detection of miRNA-21 using Au/Pt bimetallic tubular micromotors driven by chemical and surface acoustic wave forces, ACS Appl. Bio Mater. 4 (2021) 7932–7941.
[7] Y. Yang, X. Arqu´e, T. Patino, ˜ V. Guillerm, P.-R. Blersch, J. P´erez-Carvajal, I. Imaz, D. Maspoch, S. S´ anchez, Enzyme-powered porous micromotors built from a hierarchical micro- and mesoporous UiO-type metal–organic framework, J. Am. Chem. Soc. 142 (2020) 20962–20967.
[8] Y. Zhang, H. Zhu, W. Qiu, Y. Zhou, G. Huang, Y. Mei, A.A. Solovev, Carbon dioxide bubble-propelled microengines in carbonated water and beverages, Chem. Commun. 54 (2018) 5692–5695.
[9] S. Naeem, F. Naeem, M. Manjare, F. Liao, V.A. Bolanos ˜ Quinones, ˜ G.S. Huang, Y. Li, J. Zhang, A.A. Solovev, Y.F. Mei, Tubular catalytic micromotors in transition from unidirectional bubble sequences to more complex bidirectional motion, Appl. Phys. Lett. 114 (2019), 033701.
[10] S. Sanchez, A.A. Solovev, S. Schulze, O.G. Schmidt, Controlled manipulation of multiple cells using catalytic microbots, Chem. Commun. 47 (2010) 698–700.
[11] M. Medina-Sanchez, ´ V. Magdanz, L. Schwarz, H. Xu, O.G. Schmidt, Spermbots: concept and applications, in: M. Mangan, M. Cutkosky, A. Mura, P.F.M. J. Verschure, T. Prescott, N. Lepora (Eds.), Biomimetic and Biohybrid Systems Lecture Notes in Computer Science, Springer International Publishing, 2017, pp. 579–588.
[12] W. Xi, A.A. Solovev, A.N. Ananth, D.H. Gracias, S. Sanchez, O.G. Schmidt, Rolledup magnetic microdrillers: towards remotely controlled minimally invasive surgery, Nanoscale 5 (2013) 1294–1297. [13] J. Wu, S. Balasubramanian, D. Kagan, K.M. Manesh, S. Campuzano, J. Wang, Motion-based DNA detection using catalytic nanomotors, Nat. Commun. 1 (2010) 36.
[14] S. Campuzano, J. Orozco, D. Kagan, M. Guix, W. Gao, S. Sattayasamitsathit, J. C. Claussen, A. Merkoçi, J. Wang, Bacterial isolation by lectin-modified microengines, Nano Lett 12 (2012) 396–401.
[15] Z. Wu, J. Troll, H.-H. Jeong, Q. Wei, M. Stang, F. Ziemssen, Z. Wang, M. Dong, S. Schnichels, T. Qiu, et al., A swarm of slippery micropropellers penetrates the vitreous body of the eye, Sci. Adv. 4 (2018), eaat4388.
[16] H. Xu, M. Medina-Sanchez, ´ W. Zhang, M.P.H. Seaton, D.R. Brison, R. J. Edmondson, S.S. Taylor, L. Nelson, K. Zeng, S. Bagley, et al., Human spermbots for patient-representative 3D ovarian cancer cell treatment, Nanoscale 12 (2020) 20467–20481.
[17] V. de la Asuncion-Nadal, ´ B. Jurado-S´ anchez, L. V´ azquez, A. Escarpa, Near infrared-light responsive WS2 microengines with high-performance electro- and photo-catalytic activities, Chem. Sci. 11 (2019) 132–140.
[18] J.A. Tejeda-Rodríguez, A. Núnez, ˜ F. Soto, V. García-Gradilla, R. Cadena-Nava, J. Wang, R. Vazquez-Duhalt, Virus-based nanomotors for cargo delivery, ChemNanoMat 5 (2019) 194–200.
[19] B. Zhang, G. Huang, L. Wang, T. Wang, L. Liu, Z. Di, X. Liu, Y. Mei, Rolled-up monolayer graphene tubular micromotors: enhanced performance and antibacterial property, Chem. Asian J. 14 (2019) 2479–2484.
[20] Y. Yuan, C. Gao, D. Wang, C. Zhou, B. Zhu, Q. He, Janus-micromotor-based on–off luminescence sensor for active TNT detection, Beilstein J. Nanotechnol. 10 (2019) 1324–1331.
[21] M. Sun, X. Fan, X. Meng, J. Song, W. Chen, L. Sun, H. Xie, Magnetic biohybrid micromotors with high maneuverability for efficient drug loading and targeted drug delivery, Nanoscale 11 (2019) 18382–18392. [22] F. Soto, E. Karshalev, F. Zhang, B. Esteban Fernandez de Avila, A. Nourhani, J. Wang, Smart materials for microrobots, Chem. Rev. 122 (2022) 5365–5403.
[23] J. Li, M. Pumera, 3D printing of functional microrobots, Chem. Soc. Rev. 50 (2021) 2794–2838.
[24] J. Sun, H. Tan, S. Lan, F. Peng, Y. Tu, Progress on the fabrication strategies of selfpropelled micro/nanomotors, JCIS Open 2 (2021), 100011.

[25] J. Ou, K. Liu, J. Jiang, D.A. Wilson, L. Liu, F. Wang, S. Wang, Y. Tu, F. Peng, Micro-/nanomotors toward biomedical applications: the recent progress in biocompatibility, Small 16 (2020), 1906184.
[26] X. Lin, B. Xu, H. Zhu, J. Liu, A. Solovev, Y. Mei, Requirement and development of hydrogel micromotors towards biomedical applications, Research 2020 (2020), 7659749, 2020/.
[27] S. Ghosh, F. Mohajerani, S. Son, D. Velegol, P.J. Butler, A. Sen, Motility of enzyme-powered vesicles, Nano Lett 19 (2019) 6019–6026.
[28] H. Zhu, S. Nawar, J.G. Werner, J. Liu, G. Huang, Y. Mei, D.A. Weitz, A.A. Solovev, Hydrogel micromotors with catalyst-containing liquid core and shell, J. Phys.: Condens. Matter 31 (2019), 214004.
[29] J. Mujtaba, J. Liu, K.K. Dey, T. Li, R. Chakraborty, K. Xu, D. Makarov, R. A. Barmin, D.A. Gorin, V.P. Tolstoy, et al., Micro-bio-chemo-mechanical-systems: micromotors, microfluidics, and nanozymes for biomedical applications, Adv. Mater. 33 (2021), 2007465.
[30] L.L.A. Adams, D. Lee, Y. Mei, D.A. Weitz, A.A. Solovev, Nanoparticle-shelled catalytic bubble micromotor, Adv. Mater. Interfaces 7 (2020), 1901583.
[31] Y. Liu, Y. Cheng, C. Zhao, H. Wang, Y. Zhao, Nanomotor-derived porous biomedical particles from droplet microfluidics, Adv. Sci. 9 (2022), 2104272.
[32] H. Liu, Y. Wang, H. Wang, M. Zhao, T. Tao, X. Zhang, J. Qin, A droplet microfluidic system to fabricate hybrid capsules enabling stem cell organoid engineering, Adv. Sci. 7 (2020), 1903739.
[33] Y. Feng, X. Chang, H. Liu, Y. Hu, T. Li, L. Li, Multi-response biocompatible Janus micromotor for ultrasonic imaging contrast enhancement, Appl. Mater. Today 23 (2021), 101026.
[34] Y. Yu, J. Guo, Y. Wang, C. Shao, Y. Wang, Y. Zhao, Bioinspired helical micromotors as dynamic cell microcarriers, ACS Appl. Mater. Interfaces 12 (2020) 16097–16103.
[35] T. Liu, L. Xie, C.-A.H. Price, J. Liu, Q. He, B. Kong, Controlled propulsion of micro/nanomotors: operational mechanisms, motion manipulation and potential biomedical applications, Chem. Soc. Rev. 51 (2022) 10083–10119.
[36] W.Z. Teo, M. Pumera, Motion control of micro-/nanomotors, Chem. Eur. J. 22 (2016) 14796–14804. [37] Q. Yang, L. Xu, W. Zhong, Q. Yan, Y. Gao, W. Hong, Y. She, G. Yang, Recent advances in motion control of micro/nanomotors, Adv. Intell. Syst. 2 (2020), 2000049.
[38] T.R. Kline, W.F. Paxton, T.E. Mallouk, A. Sen, Catalytic nanomotors: remotecontrolled autonomous movement of striped metallic nanorods, Angew. Chem. Int. Ed. 44 (2005) 744–746.
[39] M. Liu, L. Pan, H. Piao, H. Sun, X. Huang, C. Peng, Y. Liu, Magnetically actuated wormlike nanomotors for controlled cargo release, ACS Appl. Mater. Interfaces 7 (2015) 26017–26021.
[40] N. Kukreja, V.K. Sharma, Optimal path planning of mobile nanobots navigation control in human physiological systems using advanced soft computing technique, Mater. Today: Proc. 45 (2021) 3426–3430.
[41] J. Zheng, S.H. Lam, H. Huang, L. Shao, Recent progress in optical-resonanceassisted movement control of nanomotors, Adv. Intell. Syst. 2 (2020), 1900160.
[42] J. Wang, Z. Xiong, J. Zheng, X. Zhan, J. Tang, Light-driven micro/nanomotor for promising biomedical tools: principle, challenge, and prospect, Acc. Chem. Res. 51 (2018) 1957–1965.
[43] R. Dong, Y. Cai, Y. Yang, W. Gao, B. Ren, Photocatalytic micro/nanomotors: from construction to applications, Acc. Chem. Res. 51 (2018) 1940–1947.
[44] S. Yu, Y. Cai, Z. Wu, Q. He, Recent progress on motion control of swimming micro/nanorobots, VIEW 2 (2021), 20200113.
[45] H. Manoharan, Y. Teekaraman, R. Kuppusamy, A. Radhakrishnan, K. Hariprasath Venkatachalam, Acclimatization of nanorobots in medical applications using the artificial intelligence system with the data transfer approach, Wirel. Commun. Mob. Comput. 2022 (2022) 1–8.
[46] M. Wang, X. Li, F. He, J. Li, H.-H. Wang, Z. Nie, Advances in designer DNA nanorobots enabling programmable functions, ChemBioChem 23 (2022), e202200119.
[47] W. Xu, H. Qin, H. Tian, L. Liu, J. Gao, F. Peng, Y. Tu, Biohybrid micro/ nanomotors for biomedical applications, Appl. Mater. Today 27 (2022), 101482.
[48] M. Wan, T. Li, H. Chen, C. Mao, J. Shen, Biosafety, functionalities, and applications of biomedical micro/nanomotors, Angew. Chem. Int. Ed. 60 (2021) 13158–13176.
[49] H. Choi, J. Yi, S.H. Cho, S.K. Hahn, Multifunctional micro/nanomotors as an emerging platform for smart healthcare applications, Biomaterials 279 (2021), 121201.
[50] Y. Feng, M. An, Y. Liu, M.T. Sarwar, H. Yang, Advances in chemically powered micro/nanorobots for biological applications: a review, Adv. Funct. Mater. 33 (2023), 2209883.
[51] K. Hou, Y. Zhang, M. Bao, Y. Liu, J. Wang, C. Xin, Z. Wei, H. Zhang, Z. Wu, Z. Wang, Biosafety of micro/nanomotors towards medical application, Mater. Adv. 2 (2021) 3441–3458.

[52] C.C. Mayorga-Martinez, J. Vysko˘cil, F. Novotný, P. Bednar, D. Ruzek, O. Alduhaish, M. Pumera, Collective behavior of magnetic microrobots through immuno-sandwich assay: On-the-fly COVID-19 sensing, Appl. Mater. Today 26 (2022), 101337.
[53] K. Gentile, A. Somasundar, A. Bhide, A. Sen, Chemically powered synthetic "living" systems, Chemistry 6 (2020) 2174–2185.
[54] H. Wang, M. Pumera, Fabrication of micro/nanoscale motors, Chem. Rev. 115 (2015) 8704–8735.
[55] L. Hu, N. Wang, K. Tao, Catalytic micro/nanomotors: propulsion mechanisms, fabrication, control, and applications, in: T. Shabatina, V. Bochenkov (Eds.), Smart Nanosystems for Biomedicine, Optoelectronics and Catalysis, IntechOpen, 2020.
[56] K. Zhang, Y. Ren, T. Jiang, H. Jiang, Flexible fabrication of lipophilic-hydrophilic micromotors by off-chip photopolymerization of three-phase immiscible flow induced Janus droplet templates, Anal. Chim. Acta 1182 (2021), 338955.
[57] A. Chen, X. Ge, J. Chen, L. Zhang, J.-H. Xu, Multi-functional micromotor: microfluidic fabrication and water treatment application, Lab Chip 17 (2017) 4220–4224.
[58] Z. Feng, B. Zhou, X. Su, T. Wang, S. Guo, H. Yang, X. Sun, One-step fabrication of multiphasic Janus microparticles with programmed degradation properties based on a microfluidic chip, Mater. Des. 225 (2023), 111516.
[59] W. Liu, H. Ge, Z. Gu, X. Lu, J. Li, J. Wang, Electrochemical deposition tailors the catalytic performance of MnO2-based micromotors, Small 14 (2018), 1802771.
[60] J. Li, S. Sattayasamitsathit, R. Dong, W. Gao, R. Tam, X. Feng, S. Ai, J. Wang, Template electrosynthesis of tailored-made helical nanoswimmers, Nanoscale 6 (2014) 9415–9420.
[61] S. Meng, Y. Zhang, Y. Liu, Z. Zhang, K. Ma, X. Chen, Q. Gao, X. Ma, W. Wang, H. Feng, The effect of particle size on the dynamics of self-electrophoretic Janus micromotors, sputtering distribution, and rectifying voltage, JCIS Open 5 (2022), 100046.
[62] T.S. Skelhon, Y. Chen, S.A.F. Bon, Hierarchical self-assembly of 'hard–soft' Janus particles into colloidal molecules and larger supracolloidal structures, Soft Matter 10 (2014) 7730–7735.
[63] W. Wang, W. Duan, A. Sen, T.E. Mallouk, Catalytically powered dynamic assembly of rod-shaped nanomotors and passive tracer particles, Proc. Natl. Acad. Sci. U. S. A. 110 (2013) 17744–17749.
[64] Y. Mei, G. Huang, A.A. Solovev, E.B. Urena, ˜ I. Monch, ¨ F. Ding, T. Reindl, R.K. Y. Fu, P.K. Chu, O.G. Schmidt, Versatile approach for integrative and functionalized tubes by strain engineering of nanomembranes on polymers, Adv. Mater. 20 (2008) 4085–4090.
[65] A.A. Solovev, Y. Mei, E. BermúdezUrena, ˜ G. Huang, O.G. Schmidt, Catalytic microtubular jet engines self-propelled by accumulated gas bubbles, Small 5 (2009) 1688–1692.
[66] G. Zhao, A. Ambrosi, M. Pumera, Clean room-free rapid fabrication of roll-up selfpowered catalytic microengines, J. Mater. Chem. A 2 (2013) 1219–1223.
[67] Y. Wu, Z. Wu, X. Lin, Q. He, J. Li, Autonomous movement of controllable assembled janus capsule motors, ACS Nano 6 (2012) 10910–10916.
[68] Z. Wu, Y. Wu, W. He, X. Lin, J. Sun, Q. He, Self-propelled polymer-based multilayer nanorockets for transportation and drug release, Angew. Chem. Int. Ed. 52 (2013) 7000–7003.
[69] M. Urso, M. Ussia, M. Pumera, Smart micro- and nanorobots for water purification, Nat Rev Bioeng 1 (2023) 236–251.
[70] A.C. Hortelao, C. Simo, ´ M. Guix, S. Guallar-Garrido, E. Juli´ an, D. Vilela, L. Rejc, P. Ramos-Cabrer, U. Cossío, V. Gomez-Vallejo, ´ et al., Swarming behavior and in vivo monitoring of enzymatic nanomotors within the bladder, Sci. Robot. 6 (2021), eabd2823.
[71] V. Magdanz, S. Sanchez, O.G. Schmidt, Development of a sperm-flagella driven micro-bio-robot, Adv. Mater. 25 (2013) 6581–6588.
[72] S. Keller, S.P. Teora, G.X. Hu, M. Nijemeisland, D.A. Wilson, High-throughput design of biocompatible enzyme-based hydrogel microparticles with autonomous movement, Angew. Chem. Int. Ed. 57 (2018) 9814–9817.
[73] M. Zou, J. Wang, Y. Yu, L. Sun, H. Wang, H. Xu, Y. Zhao, Composite multifunctional micromotors from droplet microfluidics, ACS Appl. Mater. Interfaces 10 (2018) 34618–34624.
[74] M.-J. Tang, W. Wang, Z.-L. Li, Z.-M. Liu, Z.-Y. Guo, H.-Y. Tian, Z. Liu, X.-J. Ju, R. Xie, L.-Y. Chu, Controllable microfluidic fabrication of magnetic hybrid microswimmers with hollow helical structures, Ind. Eng. Chem. Res. 57 (2018) 9430–9438.
[75] X. Du, Q. Li, G. Wu, S. Chen, Multifunctional micro/nanoscale fibers based on microfluidic spinning technology, Adv. Mater. 31 (2019), 1903733.

[76] F. Qin, Y. Zhang, F. Peng, Fabrication of magnetically driven helical micro/ nanoscale motors and their functionalization for targeted drug delivery, ChemNanoMat 7 (2021) 415–428.
[77] M. Ren, W. Guo, H. Guo, X. Ren, Microfluidic fabrication of bubble-propelled micromotors for wastewater treatment, ACS Appl. Mater. Interfaces 11 (2019) 22761–22767.
[78] K.D. Seo, B.K. Kwak, S. Sanchez, D.S. Kim, Microfluidic-assisted fabrication of flexible and location traceable organo-motor, IEEE Trans. Nanobioscience 14 (2015) 298–304.
[79] Y. Yu, L. Shang, W. Gao, Z. Zhao, H. Wang, Y. Zhao, Microfluidic lithography of bioinspired helical micromotors, Angew. Chem. Int. Ed. 56 (2017) 12127–12131.
[80] H. Duan, M. Huo, Y. Fan, From animal collective behaviors to swarm robotic cooperation, Natl. Sci. Rev. 10 (2023), nwad040.
[81] L. Yang, J. Jiang, X. Gao, Q. Wang, Q. Dou, L. Zhang, Autonomous environmentadaptive microrobot swarm navigation enabled by deep learning-based real-time distribution planning, Nat. Mach. Intell. 4 (2022) 480–493.
[82] S. Sengupta, K.K. Dey, H.S. Muddana, T. Tabouillot, M.E. Ibele, P.J. Butler, A. Sen, Enzyme molecules as nanomotors, J. Am. Chem. Soc. 135 (2013) 1406–1414.
[83] Y. Sun, R. Pan, Y. Chen, Y. Wang, L. Sun, N. Wang, X. Ma, G.P. Wang, Efficient preparation of a magnetic helical carbon nanomotor for targeted anticancer drug delivery, ACS Nanosci. Au 3 (2023) 94–102.
[84] M. Liu, L. Chen, Z. Zhao, M. Liu, T. Zhao, Y. Ma, Q. Zhou, Y.S. Ibrahim, A. A. Elzatahry, X. Li, et al., Enzyme-based mesoporous nanomotors with nearinfrared optical brakes, J. Am. Chem. Soc. 144 (2022) 3892–3901.
[85] J. Guo, J.J. Gallegos, A.R. Tom, D. Fan, Electric-field-guided precision manipulation of catalytic nanomotors for cargo delivery and powering nanoelectromechanical devices, ACS Nano 12 (2018) 1179–1187.
[86] P. Calvo-Marzal, K.M. Manesh, D. Kagan, S. Balasubramanian, M. Cardona, G.- U. Flechsig, J. Posner, J. Wang, Electrochemically-triggered motion of catalytic nanomotors, Chem. Commun. (2009) 4509.
[87] J. Wang, X. Liu, Y. Qi, Z. Liu, Y. Cai, R. Dong, Ultrasound-propelled nanomotors for improving antigens cross-presentation and cellular immunity, Chem. Eng. J. 416 (2021), 129091.
[88] Z. Lin, C. Gao, M. Chen, X. Lin, Q. He, Collective motion and dynamic selfassembly of colloid motors, Curr. Opin. Colloid Interface Science 35 (2018) 51–58.
[89] Q. Wang, L. Zhang, External power-driven microrobotic swarm: from fundamental understanding to imaging-guided delivery, ACS Nano 15 (2021) 149–174.
[90] H. Xie, M. Sun, X. Fan, Z. Lin, W. Chen, L. Wang, L. Dong, Q. He, Reconfigurable magnetic microrobot swarm: multimode transformation, locomotion, and manipulation, Sci. Robot. 4 (2019), eaav8006.
[91] B. Dai, J. Wang, Z. Xiong, X. Zhan, W. Dai, C.-C. Li, S.-P. Feng, J. Tang, Programmable artificial phototactic microswimmer, Nat. Nanotechnol. 11 (2016) 1087–1092.
[92] C. Wu, J. Dai, X. Li, L. Gao, J. Wang, J. Liu, J. Zheng, X. Zhan, J. Chen, X. Cheng, et al., Ion-exchange enabled synthetic swarm, Nat. Nanotechnol. 16 (2021) 288–295.
[93] Z. Li, H. Zhang, D. Wang, C. Gao, M. Sun, Z. Wu, Q. He, Reconfigurable assembly of active liquid metal colloidal cluster, Angew. Chem. Int. Ed. 59 (2020) 19884–19888.
[94] S. Tang, F. Zhang, J. Zhao, W. Talaat, F. Soto, E. Karshalev, C. Chen, Z. Hu, X. Lu, J. Li, et al., Structure-dependent optical modulation of propulsion and collective behavior of acoustic/light-driven hybrid microbowls, Adv. Funct. Mater. 29 (2019), 1809003.
[95] Y. Gao, Z. Xiong, J. Wang, J. Tang, D. Li, Light hybrid micro/nano-robots: from propulsion to functional signals, Nano Res 15 (2022) 5355–5375.
[96] A. Bricard, J.-B. Caussin, N. Desreumaux, O. Dauchot, D. Bartolo, Emergence of macroscopic directed motion in populations of motile colloids, Nature 503 (2013) 95–98.
[97] A. Somasundar, S. Ghosh, F. Mohajerani, L.N. Massenburg, T. Yang, P.S. Cremer, D. Velegol, A. Sen, Positive and negative chemotaxis of enzyme-coated liposome motors, Nat. Nanotechnol. 14 (2019) 1129–1134.
[98] X. Zhao, A. Sen, Metabolon formation by chemotaxis. Methods in Enzymology, Elsevier, 2019, pp. 45–62.
[99] F. Ji, Y. Wu, M. Pumera, L. Zhang, Collective behaviors of active matter learning from natural taxes across scales, Adv. Mater. 35 (2023), 2203959.
[100] J. Parmar, D. Vilela, K. Villa, J. Wang, S. S´ anchez, Micro- and nanomotors as active environmental microcleaners and sensors, J. Am. Chem. Soc. 140 (2018) 9317–9331.
[101] Y. Zhang, K. Yan, F. Ji, L. Zhang, Enhanced removal of toxic heavy metals using swarming biohybrid adsorbents, Adv. Funct. Mater. 28 (2018), 1806340.

[102] M. Sun, W. Chen, X. Fan, C. Tian, L. Sun, H. Xie, Cooperative recyclable magnetic microsubmarines for oil and microplastics removal from water, Appl. Mater. Today 20 (2020), 100682.
[103] L. Wang, A. Kaeppler, D. Fischer, J. Simmchen, Photocatalytic TiO 2 micromotors for removal of microplastics and suspended matter, ACS Appl. Mater. Interfaces 11 (2019) 32937–32944.
[104] H. Park, A. May, L. Portilla, H. Dietrich, F. Münch, T. Rejek, M. Sarcletti, L. Banspach, D. Zahn, M. Halik, Magnetite nanoparticles as efficient materials for removal of glyphosate from water, Nat. Sustain. 3 (2019) 129–135.
[105] Y. Hu, W. Liu, Y. Sun, Multiwavelength phototactic micromotor with controllable swarming motion for "Chemistry-on-the-Fly", ACS Appl. Mater. Interfaces 12 (2020) 41495–41505.
[106] J. Law, X. Wang, M. Luo, L. Xin, X. Du, W. Dou, T. Wang, G. Shan, Y. Wang, P. Song, et al., Microrobotic swarms for selective embolization, Sci. Adv. 8 (2022), eabm5752.
[107] M. Sun, K.F. Chan, Z. Zhang, L. Wang, Q. Wang, S. Yang, S.M. Chan, P.W.Y. Chiu, J.J.Y. Sung, L. Zhang, Magnetic microswarm and fluoroscopy-guided platform for biofilm eradication in biliary stents, Adv. Mater. 34 (2022), 2201888.
[108] M. Hoop, Y. Shen, X.-Z. Chen, F. Mushtaq, L.M. Iuliano, M.S. Sakar, A. Petruska, M.J. Loessner, B.J. Nelson, S. Pan´e, Magnetically driven silver-coated nanocoils for efficient bacterial contact killing, Adv. Funct. Mater. 26 (2016) 1063–1069.
[109] Q. Wang, B. Wang, J. Yu, K. Schweizer, B.J. Nelson, L. Zhang, Reconfigurable magnetic microswarm for thrombolysis under ultrasound imaging. 2020 IEEE International Conference on Robotics and Automation ((ICRA)), IEEE,, 2020, pp. 10285–10291.
[110] H. Zhang, Z. Li, C. Gao, X. Fan, Y. Pang, T. Li, Z. Wu, H. Xie, Q. He, Dualresponsive biohybrid neutrobots for active target delivery, Sci. Robot. 6 (2021), eaaz9519.
[111] I.B. Nava-Medina, K.A. Gold, S.M. Cooper, K. Robinson, A. Jain, Z. Cheng, A. K. Gaharwar, Self-oscillating 3D printed hydrogel shapes, Adv. Mater. Technol. 6 (2021), 2100418, https://doi.org/10.1002/admt.202100418.
[112] K. Inui, T. Watanabe, H. Minato, S. Matsui, K. Ishikawa, R. Yoshida, D. Suzuki, The Belousov–Zhabotinsky reaction in thermoresponsive core–shell hydrogel microspheres with a Tris(2,2′-bipyridyl)ruthenium catalyst in the core, J. Phys. Chem. B 124 (2020) 3828–3835.
[113] R. Yoshida, 9 - Self-oscillating polymer gels as novel biomimetic materials, in: T. D. Ngo (Ed.), Biomimetic Technologies Woodhead Publishing Series in Electronic and Optical Materials., Woodhead Publishing, 2015, pp. 181–198.
[114] R. Teng, L. Ren, L. Yuan, L. Wang, Q. Gao, I.R. Epstein, Effect of reaction parameters on the wavelength of pulse waves in the belousov–zhabotinsky reaction–diffusion system, J. Phys. Chem. A 123 (2019) 9292–9297.
[115] N.J. Suematsu, Y. Mori, T. Amemiya, S. Nakata, Oscillation of speed of a selfpropelledBelousov–Zhabotinsky droplet, J. Phys. Chem. Lett. 7 (2016) 3424–3428.
[116] T. Geher-Herczegh, Z. Wang, T. Masuda, R. Yoshida, N. Vasudevan, Y. Hayashi, Delayed mechanical response to chemical kinetics in self-oscillating hydrogels driven by the Belousov–Zhabotinsky reaction, Macromolecules 54 (2021) 6430–6439.
[117] S. Maeda, Y. Hara, T. Sakai, R. Yoshida, S. Hashimoto, Self-walking gel, Adv. Mater. 19 (2007) 3480–3484.
[118] S.G.J. Postma, I.N. Vialshin, C.Y. Gerritsen, M. Bao, W.T.S. Huck, Preprogramming complex hydrogel responses using enzymatic reaction networks, Angew. Chem. Int. Ed. 56 (2017) 1794–1798.
[119] S.N. Semenov, L.J. Kraft, A. Ainla, M. Zhao, M. Baghbanzadeh, V.E. Campbell, K. Kang, J.M. Fox, G.M. Whitesides, Autocatalytic, bistable, oscillatory networks of biologically relevant organic reactions, Nature 537 (2016) 656–660.
[120] S. Matsui, K. Inui, Y. Kumai, R. Yoshida, D. Suzuki, Autonomously oscillating hydrogel microspheres with high-frequency swelling/deswelling and dispersing/ flocculating oscillations, ACS Biomater. Sci. Eng. 5 (2019) 5615–5622.